

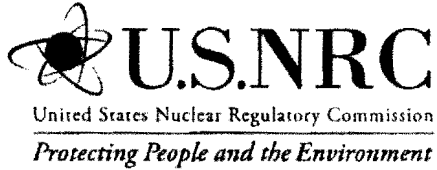
NUREG-XXXX, Vol. 3

Safety Evaluation Report Related to Disposal of High-Level Radioactive Wastes in a Geologic Repository at Yucca Mountain, Nevada

Volume 3: Repository Safety After
Permanent Closure

B/1

AVAILABILITY PAGE



NUREG-XXXX, Vol. 3

Safety Evaluation Report Related to Disposal of High-Level Radioactive Wastes in a Geologic Repository at Yucca Mountain, Nevada

**Volume 3: Repository Safety After
Permanent Closure**

Manuscript Completed: Month Year
Date Published: Month Year

**Office of Nuclear Material Safety and Safeguards
Division of High-Level Waste Repository Safety**

(Intentionally Left Blank)

NOTE TO READER: This volume is one of five volumes shown in the table below that comprise the Safety Evaluation Report (SER). Each of the volumes is published separately as it is completed; therefore, the volume number may not correspond to the chronological order of volume publication. The volume numbering, as well as the SER section numbering used within the chapters of a volume, is based on the Yucca Mountain Review Plan (YMRP)¹ the U.S. Nuclear Regulatory Commission (NRC) staff used to guide its review of the license application. Use of SER section numbers that correspond to the YMRP section numbers facilitated the NRC staff's writing of the SER, allowing the interested reader to easily find the applicable review methods and acceptance criteria within the YMRP. The following table provides the topics and SER sections for each volume. The table will help the reader locate SER sections cross-referenced among the volumes.

Chapter	SER Section	Title
Volume 1 General Information		
1	1.1	General Description
2	1.2	Proposed Schedules for Construction, Receipt, and Emplacement of Waste
3	1.3	Physical Protection Plan
4	1.4	Material Control and Accounting Program
5	1.5	Description of Site Characterization Work
Volume 2 Repository Safety Before Permanent Closure		
1	2.1.1.1	Site Description as it Pertains to Preclosure Safety Analysis
2	2.1.1.2	Description of Structures, Systems, Components, Equipment, and Operational Process Activities
3	2.1.1.3	Identification of Hazards and Initiating Events
4	2.1.1.4	Identification of Event Sequences
5	2.1.1.5	Consequence Analyses
6	2.1.1.6	Identification of Structures, Systems, and Components Important to Safety; and Measures to Ensure Availability of the Safety Systems
7	2.1.1.7	Design of Structures, Systems, and Components Important to Safety and Safety Controls
8	2.1.1.8	Meeting the 10 CFR Part 20 As Low As Is Reasonably Achievable Requirements for Normal Operations and Category 1 Event Sequences
9	2.1.2	Plans for Retrieval and Alternate Storage of Radioactive Wastes
10	2.1.3	Plans for Permanent Closure and Decontamination, or Decontamination and Dismantlement of Surface Facilities
Volume 3 Repository Safety After Permanent Closure		
1	2.2.1.1	System Description and Demonstration of Multiple Barriers
2	2.2.1.2.1	Scenario Analysis
3	2.2.1.2.2	Identification of Events with Probabilities Greater Than 10^{-8} Per Year
4	2.2.1.3.1	Degradation of Engineered Barriers
5	2.2.1.3.2	Mechanical Disruption of Engineered Barriers
6	2.2.1.3.3	Quantity and Chemistry of Water Contacting Engineered Barriers and Waste Forms
7	2.2.1.3.4	Radionuclide Release Rates and Solubility Limits
Volume 3 Repository Safety After Permanent Closure (continued)		

¹NRC. 2003. NUREG-1804, "Yucca Mountain Review Plan—Final Report." Rev. 2. Washington, DC: NRC.

Chapter	SER Section	Title
8	2.2.1.3.5	Climate and Infiltration
9	2.2.1.3.6	Unsaturated Zone Flow
10	2.2.1.3.7	Radionuclide Transport in the Unsaturated Zone
11	2.2.1.3.8	Flow Paths in the Saturated Zone
12	2.2.1.3.9	Radionuclide Transport in the Saturated Zone
13	2.2.1.3.10	Igneous Disruption of Waste Packages
14	2.2.1.3.12	Concentration of Radionuclides in Ground Water
15	2.2.1.3.13	Airborne Transportation and Redistribution of Radionuclides
16	2.2.1.3.14	Biosphere Characteristics
17	2.2.1.4.1	Demonstration of Compliance with the Postclosure Individual Protection Standard
18	2.2.1.4.2	Demonstration of Compliance with the Human Intrusion Standard
19	2.2.1.4.3	Demonstration of Compliance with the Separate Groundwater Protection Standards
20	2.5.4	Expert Elicitation
Volume 4 Administrative and Programmatic Requirements		
1	2.3	Research and Development Program to Resolve Safety Questions
2	2.4	Performance Confirmation Program
3	2.5.1	Quality Assurance Program
4	2.5.2	Records, Reports, Tests, and Inspections
5	2.5.3.1	Training and Certification of Personnel
6	2.5.3.2	U.S. Department of Energy Organizational Structure as it Pertains to Construction and Operation of Geologic Repository Operations Area
7	2.5.3.3	Personnel Qualifications and Training Requirements
8	2.5.5	Plans for Startup Activities and Testing
9	2.5.6	Plans for Conduct of Normal Activities, Including Maintenance, Surveillance, and Periodic Testing
10	2.5.7	Emergency Planning
11	2.5.8	Controls to Restrict Access and Regulate Land Uses
12	2.5.9	Uses of Geologic Repository Operations Area for Purposes Other Than Disposal of Radioactive Wastes
Volume 5 License Specifications		
1	2.5.10	License Specifications

ABSTRACT

This is Volume 3 of the NRC staff's "Safety Evaluation Report (SER) Related to Disposal of High-Level Radioactive Wastes in a Geologic Repository at Yucca Mountain, Nevada." Volume 3 presents certain results of the staff's review of DOE's Safety Analysis Report, provided in its June 3, 2008 license application, as updated by DOE in February 19, 2009, along with information provided in response to NRC staff's requests for information. In particular, SER Volume 3, documents the results of the staff's evaluation to determine if the proposed repository design will comply with the technical criteria and postclosure public health and environmental standards that apply after the proposed repository is permanently closed. (b)(5)

(b)(5)

(Intentionally Left Blank)

ACRONYMS AND ABBREVIATIONS	
AFM	active fracture model
AMR	Analysis and Model Report
APE	annual percentage of exceedence
BDCF	Biosphere Dose Conversion Factors
BSW	basic saturated water
BWR	boiling water reactor
CDSP	codisposal package
CFu	Crater Flat undifferentiated
CHn	Calico Hills nonwelded
CNWRA [®]	Center for Nuclear Waste Regulatory Analyses
CSNF	commercial spent nuclear fuel
DBGM	design basis ground motions
DOE	U.S. Department of Energy
DS	drip shield
DVRGFSM	Death Valley Regional Groundwater Flow System Model
EBS	Engineered Barrier System
ECRB	Enhanced Characterization of the Repository Block
EF	early failure
EPA	U.S. Environmental Protection Agency
EPRI	Electric Power Institute
ERMYN	Environmental Radiation Model for Yucca Mountain Nevada
ESF	Exploratory Studies Facility
EWDP	Early Warning Drilling Program
FEPs	features, events, and processes
GLUE	Generalized Likelihood Uncertainty Estimation
GROA	Geologic Repository Operation Area
GWSPD	Groundwater-specific discharge
HLW	high-level waste
IDPS	in-drift precipitates/salts model
ITWI	important to waste isolation
ITYM	Infiltration Tabulator for Yucca Mountain
LA	license application
MAI	mean annual infiltration
MAP	mean annual precipitation
MASSIF	Mass Accounting System for Soil Infiltration and Flow
MAT	mean annual temperature
MCO	multicanister overpack
MDEB	Mechanical Disruption of Engineered Barriers
MIC	microbially influenced corrosion
MSTHM	Multiscale Thermohydrological Model
NC-EWDP	Nye County Early Warning Drilling Program
NDE	nondestructive examination
NFC	near-field chemistry
NOAA	National Oceanic and Atmospheric Administration
NRC	U.S. Nuclear Regulatory Commission
OCED	Organisation for Economic Co-operation and Development
PCSA	probabilistic seismic safety analysis
PEST	parameter estimation program

ACRONYMS AND ABBREVIATIONS	
PFDHA	probabilistic fault displacement hazard assessment
PGA	peak ground accelerations
PGV	peak ground velocity
PSHA	probabilistic seismic hazard assessment
PTn	Paintbrush Tuff nonwelded
PVHA	probabilistic volcanic hazard assessment
PVHA-U	probabilistic volcanic hazard assessment-update
PWR	pressurized water reactor
QA	quality assurance
RAI	request for additional information
RB	repository block
RCA	radio chemical analysis
RMEI	reasonably maximally exposed individual
RMR	rock mass rating
RMS	root-mean-square
RST	residual stress threshold
RVT	random-vibration-theory
SA	spectral acceleration
SAR	Safety Analysis Report
SCA	Seismic Consequence Abstractions
SCC	stress corrosion cracks
SAW	simulated acidified water
SCW	simulated concentrated water
SDFR	slip-dissolution film-rupture
SDW	simulated dilute water
SEF	sorption enhancement factor
SER	Safety Evaluation Report
SIF	stress intensity factor
SNF	spent nuclear fuel
SSHAC	Senior Seismic Hazard Analysis Committee
SZ	saturated zone
SZEE	saturated zone flow and transport expert elicitation
TAD	transportation, aging, and disposal
TCw	Tiva Canyon welded
TEDE	Total Effective Dose Equivalent
TSPA	Total System Performance Assessment
TSPA-LA	Total System Performance Assessment-License Application
TSPA-SR	Total System Performance Assessment-Site Recommendation
TSw	Topopah Spring welded
UDL	upper subcritical limit
USGS	U.S. Geological Survey
UZ	unsaturated zone
Vs	shear wave velocity
WP	waste package
WRIP	water-rock interaction parameter
YMRP	Yucca Mountain Review Plan

EXECUTIVE SUMMARY

Background

On June 3, 2008, the U.S. Department of Energy (DOE or the applicant) a license application to the U.S. Nuclear Regulatory Commission (NRC) seeking authorization to begin construction of a geologic repository for high-level radioactive waste disposal at Yucca Mountain, Nevada.¹ The license application consists of general information and a Safety Analysis Report (SAR). This document, the NRC staff's Safety Evaluation Report (SER), Volume 3, presents certain results of staff's review of the SAR DOE provided in its June 3, 2008, license application and as updated on February 19, 2009.² The NRC staff also reviewed information DOE provided in response to NRC staff's requests for additional information. In particular, SER Volume 3 documents the results of the staff's evaluation to determine whether the proposed repository design for Yucca Mountain will comply with the technical criteria and postclosure public health and environmental standards that apply after the repository is permanently closed. These criteria and standards can be found in NRC's regulations at 10 CFR Part 63, Subparts E and L. In conducting its review of the license application, the NRC staff was guided by the review methods and acceptance criteria outlined in the Yucca Mountain Review Plan.³

Other portions of the NRC staff's safety review have been, or will be, documented elsewhere. SER Volume 1, NUREG-XXXX (NRC, 2010XX) contains the staff's evaluation of DOE's general information. SER Volume 2 will contain the staff's evaluation of DOE's compliance with preclosure safety objectives and requirements; SER Volume 4 will document the staff's evaluation of DOE's demonstration of compliance with administrative and programmatic requirements; and SER Volume 5 will document the staff's evaluation of the DOE's proposed probable subjects of license specification and will document the applicant's commitments, licensing specifications, and conditions. NRC will be able to determine if DOE has satisfied the requirements for a construction authorization for a geologic repository for high-level waste disposal at Yucca Mountain, Nevada, only after the NRC staff has completed all volumes of the SER. A decision to authorize construction will be effective only after a full public hearing has been conducted and the Commission has completed its review under 10 CFR 2.1023.

Technical Criteria and Postclosure Public Health and Environmental Standards

To decide whether to authorize construction of a geologic repository at the Yucca Mountain site, NRC must determine whether there is reasonable expectation that the types and amounts of radioactive material described in the license application can be disposed of without unreasonable risk to health and safety of the public. In arriving at that determination, NRC must consider, among other things, whether the site and design comply with the performance objectives and requirements contained in NRC's regulations at 10 CFR Part 63, Subparts E and L.

¹DOE. 2008. DOE/RW-0573, "Yucca Mountain Repository License Application." Rev. 0. ML081560400. Las Vegas, Nevada: DOE, Office of Civilian Radioactive Waste Management.

²DOE. 2009. DOE/RW-0573, "Yucca Mountain Repository License Application." Rev. 1. ML090700817. Las Vegas, Nevada: DOE, Office of Civilian Radioactive Waste Management.

³NRC. 2003. NUREG-1804, "Yucca Mountain Review Plan—Final Report." Rev. 2. Washington, DC: NRC.

Among the postclosure performance objectives is the requirement that the geologic repository include multiple barriers, both natural and man made, or engineered. After permanent closure, DOE must show that the natural and engineered barriers work together to keep radiologic exposures to a reasonably maximally exposed individual (RMEI)⁴ within specified limits, for up to a million years. DOE must also show that for 10,000 years, natural and engineered barriers work together to meet separate standards to protect groundwater resources in the vicinity of Yucca Mountain. And lastly, DOE must show that if people unwittingly drill into the repository without realizing the repository is there, natural and engineered barriers will work together to keep radiologic exposures within specified limits. DOE must show compliance with these objectives using a particular type of quantitative analysis called a performance assessment. This systematic set of projections and calculations must meet specific requirements laid out in NRC's regulations.

System Description and Demonstration of Multiple Barriers

NRC regulations specify that a geologic repository at Yucca Mountain must include multiple barriers, both natural and engineered. Barriers prevent or limit the movement of water or radioactive material and thus isolate waste. NRC imposes this requirement to ensure that the overall repository system is robust and not wholly dependent on any single barrier to ensure repository safety. NRC requires that DOE identify these barriers when it calculates how the repository will perform in the future. NRC also requires that DOE describe the capability of each barrier and provide the technical basis for its description. In its SAR for the proposed repository at Yucca Mountain, DOE identified three barriers: the Upper Natural Barrier, the Engineered Barrier System (EBS), and the Lower Natural Barrier. Each of these barriers includes multiple features that DOE described as important to waste isolation.

DOE expects that the Upper Natural Barrier will substantially reduce the amount of water that reaches the repository horizon. In semiarid environments, like that at Yucca Mountain, humidity and precipitation are low and surface evaporation rates are high. In addition, plant uptake and surface runoff can reduce further the amount of water available to move from the surface into the rock layers above the repository. In its SAR, DOE explained that during the first 10,000 years after the repository is closed, most of the water that does reach the depth of the repository is prevented from seeping into the repository and is diverted around waste emplacement tunnels, or drifts, because of thermal effects from the waste. After approximately 10,000 years, DOE concluded that the amount of heat generated from the waste will be low enough to allow water to seep into drifts and potentially contact the EBS.

DOE identified the primary purpose of the EBS as preventing or substantially reducing movement of water that actually contacts the waste, and of limiting movement of dissolved radionuclides away from the repository. DOE predicts that the walls of the waste emplacement drifts will degrade slowly over time. However, DOE expects that specific engineered features will mostly stay in place, will remain largely intact, and will continue to keep the waste substantially dry for very long time periods. If the repository is undisturbed by very large earthquakes or volcanoes, DOE projects that less than

⁴ A reasonably maximally exposed individual is an adult member of a hypothetical farming community assumed to reside 18 km (approximately 11 mi) south of the potential repository along the path of groundwater flow. He or she is assumed to have a diet and lifestyle representative of people who now live in Amargosa Valley, Nevada. DOE must assume this person drinks water contaminated with releases from the repository, eats crops irrigated with contaminated water, eats food products from livestock raised on contaminated feed and water, eats farmed fish raised in contaminated water, and inadvertently ingests and breathes resuspended soil, aerosols from evaporative coolers, and radon gas and its decay products.

0.01 percent of the waste will be exposed to water that seeps into the drifts during the first 10,000 years after the repository is closed.

In addition to the emplacement drifts, DOE expects other specific features to limit the flow of seepage water or dissolved radionuclides. These features include the drip shields, the waste packages, the waste forms and waste package internal components, and the emplacement pallet and invert. The drip shields divert seepage water away from the waste package. Likewise, as long as the waste packages remain intact, seepage water cannot reach or interact with the enclosed waste forms. Once waste packages begin to corrode, or form cracks, radionuclide releases from the packages are limited by, among other things, the rate at which the various waste forms deteriorate and the rate at which continuous liquid pathways can form through openings large enough to permit flow. DOE projects that most waste packages will remain intact for approximately 200,000 years after the repository is closed, unless large earthquakes or volcanoes occur and cause damage. Once the waste packages begin to leak, DOE expects that the internal components of the waste packages along with the emplacement pallet and invert materials will contribute to a physical and chemical environment around the waste that prevents or substantially reduces the movement of water and dissolved radionuclides away from the repository. DOE projects that the proposed EBS would limit radionuclide releases to the Lower Natural Barrier to less than 0.003 percent of the available inventory at 10,000 years and to not more than 7 percent of the available inventory at 1 million years after the repository is closed.

DOE concluded that the Lower Natural Barrier will impede the movement of most, but not all, radionuclides from the EBS to the accessible environment. Layers of unsaturated rock below the repository 300 m [approximately 1,000 ft] thick are expected to retard the flow of dissolved radionuclides on their way to the water table. Once in saturated rock or groundwater below the repository, water potentially contaminated with radionuclides from the repository must travel through 12–14 km [7–9 mi] of fractured volcanic rock and 4–6 km [2–4 mi] of saturated gravels and sands before reaching the human environment. DOE determined that the effectiveness of the Lower Natural Barrier in retaining specific individual radionuclides depends on the solubility, sorptive properties, and half-life of the specific radionuclide. DOE projects that the releases of solubility-limited, strongly sorbed nuclides are reduced by as much as 99 percent, while those of moderately soluble, low-sorption, long half-life nuclides are reduced by lesser amounts. Highly soluble, nonsorbing radionuclides, however, will not be retained and will move at roughly the same rate as the groundwater flow.

(b)(5)

Assessment of Repository Performance

A performance assessment is a systematic analysis that answers three questions: What can happen? How likely is it to happen? and What are the resulting consequences? The NRC staff reviewed the TSPA DOE provided in support of its license application for the proposed repository at Yucca Mountain. In conducting its review of DOE's TSPA of the repository, the staff evaluated DOE's system description, demonstration of multiple barriers, and associated supporting scientific and analytic methods to focus on those items most important to waste isolation. As part of its review, the staff evaluated whether DOE's TSPA of the Yucca Mountain repository complies with NRC's requirements for performance assessment at 10 CFR 63.114.

To answer the question "What can happen?" after a repository is closed at Yucca Mountain, DOE had to consider a wide range of specific features (e.g., geologic rock types, waste package materials), events (e.g., earthquakes, volcanic activity), and processes (e.g., corrosion of metal waste packages, sorption of radionuclides on rock surfaces), for possible inclusion in (or exclusion from) its evaluation. Once selected, DOE then used these features, events, and processes (FEPs) to postulate a range of credible, future scenarios. A scenario is a well-defined sequence of events and processes, which can be interpreted as an outline of one possible future condition of the repository system. Thus, scenario analysis identifies the possible ways in which the repository environment could evolve to develop a defensible representation of the system and estimate the range of credible potential consequences. After DOE selected appropriate FEPs and used them to postulate scenarios, DOE grouped similar scenarios into scenario classes and screened them for use in its performance assessment of the facility. The NRC staff's review of DOE's scenario analysis focused on its completeness and technical acceptability to verify that DOE did not overlook future conditions at the proposed repository that could significantly enhance or degrade its safety, as required by the regulations. To conduct this review, the staff used its own risk insights from previous performance assessments for the Yucca Mountain site, detailed process-level modeling efforts, laboratory and field experiments, and natural analog studies.

When addressing the question "How likely is it that these events will happen?," DOE assessed the likelihood that credible scenario classes could disrupt repository performance. A performance assessment used to demonstrate compliance with the individual protection standard for the Yucca Mountain repository must consider events that have at least 1 chance in 100 million of occurring. DOE included three disruptive event types for inclusion in its postclosure performance assessments: disruption by volcanic (i.e., igneous) events, disruptions by earthquake (i.e., seismic) events, and early failure of waste packages or drip shields.

To answer the question "What are the resulting consequences?" DOE made estimated projections called "model abstractions" to represent the performance of various parts of the repository system. Each model abstraction develops one or more numerical models that represent how specific FEPs interact and affect performance of repository systems. DOE also included potentially significant variations in site or design characteristics into the models, so that a range of potential outcomes would be calculated in the performance assessment.

To evaluate whether DOE's model abstractions adequately portrayed the expected consequences when implemented in the overall performance assessment, the NRC staff reviewed 13 separate categories of model abstractions. The NRC staff selected these abstractions from engineered, geosphere, and biosphere subsystems found to be most important to waste isolation on the basis of previous performance assessments, knowledge of site characteristics, and careful examination of DOE's proposed repository design. In its review,

the staff focused on those models of greatest risk significance to repository safety. For the postclosure period, "important to repository safety or waste isolation" means important to meeting the postclosure performance objectives in NRC's regulations as discussed previously.

For each model abstraction, the NRC staff determined whether the data DOE used appropriately represented site- and design-specific characteristics, including the variability and uncertainty in these characteristics. The NRC staff evaluated how DOE incorporated FEPs in the model abstractions and reviewed DOE's technical bases to support the inclusion or exclusion of these FEPs. In addition, the NRC staff reviewed the methods DOE used to develop the model abstractions, including how DOE represented model uncertainty. The staff's review also examined how DOE supported the use of its models in the performance assessment and how DOE considered the potential effects of alternative models.

(b)(5)

Compliance With Numerical Performance Objectives

NRC's regulations define how DOE must use its performance assessment to show compliance with specific numerical performance objectives. The first of these objectives is compliance with annual dose limits for the reasonably maximally exposed individual. DOE must use the performance assessment to (i) estimate the annual dose as a result of releases from the repository caused by all significant features, events and processes, weighted by their probability of occurrences; (ii) show that the average annual dose in any year during the initial 10,000 years is not greater than 0.15 mSv [15 mrem] per year; and (iii) show that the average annual dose after 10,000 years, up to 1 million years, is not greater than 1.0 mSv [100 mrem] per year.

DOE used its TSPA to represent the range of behavior of a repository at Yucca Mountain and to account for uncertainty in FEPs that could affect the evolution of the repository over the compliance period. DOE developed its analysis of repository performance by grouping scenario classes broadly as either nominal or disruptive. The nominal scenario class comprises those FEPs that are present under "normal" conditions (i.e., eventual infiltration of water, corrosion of waste packages, release of radionuclides, transport of radionuclides in groundwater). During the initial 10,000 years after repository closure, DOE's nominal scenario class does not result in any dose to the reasonably maximally exposed individual. Disruptive scenario classes, as noted earlier, include additional FEPs that account for the effects of specific events, such as earthquakes and volcanoes, which could disturb or alter the performance of the repository in ways not included under the nominal scenario class.

Disruptive events of sufficient magnitude have the potential to result in doses to the reasonably maximally exposed individual at any time during the compliance period. NRC's regulations provide, however, that the estimate of projected dose resulting from a disruptive event or

scenario class must be appropriately weighted by the probability that the disruptive event will occur. Therefore, a key component of the NRC staff's review of DOE's performance assessment is a determination that the probabilities and consequences of each of the scenario classes are appropriately included in the average annual dose calculations. The NRC staff must also determine that DOE's results provide a credible representation of repository performance and that the estimate of average annual dose complies with the regulatory limits and is statistically stable.

The NRC staff conducted confirmatory calculations to supplement and assist its review of DOE's TSPA. The confirmatory calculations provide both a quantitative understanding of the assessment and an understanding of whether there is a general consistency between submodels of the analysis and the overall results, including uncertainty. For example, the staff's confirmatory calculations examined whether the timing and extent of breaching of the waste packages corresponded and were consistent with the timing and magnitude of the average annual dose. The staff's confirmatory calculations were performed for selected time periods (i.e., 10,000; 100,000; 400,000; and 800,000 years) to provide the staff a perspective on the time-dependent nature of waste package failure, associated radioactive decay and release of specific radionuclides. In assessing the credibility of DOE's average annual dose curve for the groundwater pathway, the NRC staff conducted separate confirmatory calculations for (i) the amount of water entering failed waste packages, (ii) the release of radionuclides from the waste packages, (iii) transport of radionuclides through the unsaturated and saturated zones, (iv) effects of disruptive events, and (v) annual dose to the reasonably maximally exposed individual.

The staff's confirmatory calculations were based on the NRC staff's review of the DOE's TSPA calculation, including DOE's models and intermediate outputs. Thus NRC staff's confirmatory calculations address key quantitative attributes of the repository system to help evaluate overall performance. (b)(5)

(b)(5)

DOE presented the overall average annual dose curve due to releases from the repository over the entire compliance period in its SAR. The peak of the overall average annual dose curve is approximately 0.003 mSv [0.3 mrem] per year over the initial 10,000 years and is approximately 0.02 mSv [2 mrem] per year over the 1-million-year period after repository closure.

(b)(5)

As noted earlier, NRC's regulations provide a separate performance objective to protect groundwater resources in the vicinity of Yucca Mountain and specify the approach DOE must use to estimate the concentration of radionuclides in groundwater. NRC's groundwater

protection criteria provide different limits depending on the radionuclide and the type of associated radiation.⁵

NRC's regulations identify specific constraints for the performance assessment used to show compliance with the groundwater protection limits and identify how DOE must calculate a "representative volume" to estimate the concentration of radionuclides released from the repository system. The performance assessment for compliance with the groundwater protection limits is essentially the same as that used to show compliance with the individual protection limits, except that by regulation, unlikely events (i.e., most disruptive events) are not included in the assessment used for groundwater protection. As a result, the NRC staff's review of DOE's groundwater protection analysis focused on DOE's determination of the representative volume and compliance with the separate limits specified for groundwater protection.

DOE estimated the concentrations for the alpha activity (including background) would be 0.5 pCi/L with the largest contribution coming from natural background radiation already in the groundwater. The largest annual release from the repository of relevant alpha-emitting radionuclides into the representative volume from the repository was estimated to be more than 1,000 times less than background levels.

DOE estimated the dose from beta- and photon-emitting radionuclides would be 0.6 μ Sv [0.06 mrem] per year for the whole body and the largest dose to any organ would be 2.6 μ Sv [0.26 mrem] per year as a result of drinking 2 L [0.53 gal] of water per day assumed to be at peak estimated concentration levels of radionuclides released from the repository in the representative volume.

DOE estimated the concentration from the combined Ra-226 and Ra-228 (including background) would be 0.5 pCi/L with the largest contribution coming from natural background radiation already in the groundwater. The largest annual release from the repository of Ra-226 and Ra-228 into the representative volume from the repository was estimated to be almost 1 million times less than the background levels.

(b)(5)

To comply with the individual protection standards for human intrusion, DOE must determine the earliest time after disposal that waste packages would have degraded sufficiently such that an intrusion could occur without a driller recognizing it. DOE is required to assess the effects of a single intrusion that results from exploratory drilling for groundwater. DOE must assume that intruders drill a borehole directly through a degraded waste package into the uppermost aquifer underneath the repository using techniques and practices common to exploratory drilling in the

⁵ U.S. Environmental Protection Agency standards for Yucca Mountain at 40 CFR Part 197 provide separate limits for protection of groundwater resources. Radionuclides known as alpha emitters, such as Np-237, are treated as one group, and their combined concentration must not exceed 15 pCi/L (including background). Radionuclides known as beta- and photon-emitters (examples include I-129 and Tc-99) are treated as a second group, and their combined concentration must not result in a dose exceeding 0.04 mSv [4 mrem] per year to the whole body or to any organ. And lastly, the combined concentration of Ra-226 and Ra-228 must not exceed 5 pCi/L (including background radiation already present in groundwater at Yucca Mountain).

Yucca Mountain region today. DOE must assume that careful sealing of the borehole does not occur and, instead, natural degradation processes gradually modify the borehole. DOE must estimate doses using an exposure scenario where water enters the waste package, releases radionuclides, and transports them by way of the borehole to the saturated zone. DOE must show, using this prescribed scenario, that there is a reasonable expectation that the dose to a reasonably maximally exposed individual resulting from the intrusion event does not exceed 0.15 mSv [15 mrem] per year for 10,000 years after disposal and 1.0 mSv [100 mrem] per year after 10,000 years for as long as 1 million years.

DOE selected 200,000 years as a conservative assumption of the earliest time the waste packages could degrade enough so that an intrusion could occur without drillers recognizing it. DOE developed a separate performance assessment to evaluate the consequences of a postulated human intrusion event assumed to occur 200,000 years after permanent closure of the repository. DOE modified its performance assessment for individual protection to represent human intrusion in a manner consistent with NRC requirements. DOE's estimated dose due to releases from the repository is approximately 0.0001 mSv [0.01 mrem] per year shortly after the time of the intrusion.

(b)(5)

Summary Findings

(b)(5)

INTRODUCTION

On June 3, 2008, the U.S. Department of Energy (DOE or the applicant) submitted to the U.S. Nuclear Regulatory Commission (NRC) an application for authorization to begin construction of a geologic repository for high-level radioactive waste disposal at Yucca Mountain, Nevada. The license application consists of general information and a Safety Analysis Report (SAR). This document, the NRC staff's Safety Evaluation Report (SER), Volume 3, summarizes the results of the staff's review of the SAR DOE provided in its June 3, 2008, license application and as updated on February 19, 2009. In particular, this SER Volume 3 documents the results of staff's evaluation to determine whether the proposed repository design for Yucca Mountain will comply with the performance objectives and requirements that apply after the repository is permanently closed. These performance objectives and requirements can be found in NRC's regulations at 10 CFR Part 63, Subparts E and L.

Other portions of the NRC staff's safety review have been, or will be, documented elsewhere. SER Volume 1, NUREG-XXXX (NRC, 2010XX) contains the results of the staff's review of DOE's General Information. SER Volume 2 will contain the results of the staff's review and evaluation of DOE's compliance with preclosure safety objectives and requirements; SER Volume 4 will document the results of the staff's review and evaluation of DOE's demonstration of compliance with administrative and programmatic requirements; and SER Volume 5 will document commitments by the applicant and potential licensing specifications and conditions. In conducting its review of the entire license application, the NRC staff was guided by the review methods and acceptance criteria outlined in the Yucca Mountain Review Plan (YMRP)¹

Postclosure Performance Objectives and Requirements

To decide whether to authorize construction of a geologic repository at the Yucca Mountain site, the NRC must determine, among other things, whether there is reasonable expectation that the types and amounts of radioactive material described in the license application can be disposed of without unreasonable risk to the health and safety of the public. In arriving at that determination, the NRC staff will need to consider, among other things, whether the site and design comply with the performance objectives and requirements contained in 10 CFR Part 63, Subparts E and L, of NRC's regulations. Among the postclosure performance objectives is the requirement that the geologic repository include multiple barriers, both natural and man made, or engineered. After permanent closure, the applicant must show that the natural and engineered barriers work together to keep radiologic exposures to a reasonably maximally exposed individual (RMEI) within specified limits, for up to one-million years. The applicant must also demonstrate that for 10,000 years of undisturbed performance, natural and engineered barriers work together to control radioactive material releases to protect groundwater within specified limits. And lastly, the applicant must demonstrate that, in the event of an inadvertent human intrusion, natural and engineered barriers will work together to keep radiologic exposures to a reasonably maximally exposed individual within specified limits. Compliance with these objectives must be demonstrated with a particular type of quantitative analysis called a performance assessment. This systematic set of calculations and projections must meet specific requirements laid out in NRC's regulations.

¹NRC. 2003. NUREG-1804, "Yucca Mountain Review Plan—Final Report." Rev. 2. Washington, DC. NRC.

Risk-Informed, Performance-Based Review

The performance assessment quantifies repository performance as a means of demonstrating compliance with the postclosure performance objectives at 10 CFR 63.113. DOE's performance assessment is a systematic analysis that answers three basic questions that often are used to define risk: What can happen? How likely is it to happen? and What are the resulting consequences? The Yucca Mountain performance assessment is a sophisticated analysis that involves various complex considerations and evaluations. Examples include evolution of the natural environment, degradation of engineered barriers over the compliance period, and disruptive events, such as seismicity and igneous activity. Because the performance assessment encompasses such a broad range of issues, the staff used risk information throughout the review process to ensure that the review focused on those items most important to waste isolation. Section 2.2.1 of the YMRP provides guidance to the staff to apply risk information throughout the review of the performance assessment.

To support its risk-informed, performance-based review, the staff initially reviewed the DOE's demonstration of compliance with the multiple barriers requirement. DOE must identify the important barriers (engineered and natural) of the performance assessment, describe each barrier's capability, and provide the technical basis for that capability. This risk information describes the DOE's understanding of each barrier's capability to prevent or substantially delay the movement of water or radioactive materials. The result of the multiple barrier review is a staff understanding of each barrier's importance to waste isolation, which will influence the emphasis placed on the reviews conducted in SER Sections 2.2.1.2, "Scenario Analysis and Event Probability;" 2.2.1.3, "Model Abstraction;" and 2.2.1.4, "Demonstration of Compliance with the Postclosure Public Health and Environmental Standards." Particular parts of the NRC staff's review are emphasized on the basis of the risk insights (i.e., those attributes of the repository system most important to repository performance). Additionally, the NRC staff has considered independent risk insights from previous performance assessments conducted for the Yucca Mountain site, detailed process modeling efforts, laboratory and field experiments, and natural analog studies and has identified this information in this volume, as appropriate.

System Description and Demonstration of Multiple Barriers

NRC regulations specify that a geologic repository at Yucca Mountain must include multiple barriers, both natural and engineered. Barriers prevent or limit the movement of water or radioactive material. The NRC imposes this requirement to ensure that the overall repository system is robust and not wholly dependent on any single barrier to ensure repository safety. The NRC requires that DOE identify these barriers when it calculates how the repository will perform in the future. The NRC also requires that DOE describe the capability of each barrier and provide the technical basis for its description. In its SAR for the proposed repository at Yucca Mountain, DOE identified three barriers: the Upper Natural Barrier, the Engineered Barrier System (EBS), and the Lower Natural Barrier. The Upper Natural Barrier is composed of features above the repository (i.e., topography, surficial soils, and the unsaturated zone) that reduce the movement of water downward toward the repository, which in turn reduces the rate of movement of water from the radioactive waste in the repository to the accessible environment. The engineered barrier system includes different engineering features (e.g., emplacement drifts, drip shields, waste packages and its internal components, and emplacement pallets and inverters) that (i) enhance the performance of the waste package, preventing radionuclide releases while it is intact; (ii) limit radionuclide releases after the waste package is breached by limiting the amount of water that can contact the waste package; and

(iii) limit radionuclide release from the engineered barrier system through sorption processes. The Lower Natural Barrier is composed of features below the repository (i.e., unsaturated zone) and from the repository location to the compliance location (i.e., saturated zone) that reduce the rate of radionuclide movement from the repository to the compliance location through such processes as the slow movement of water and sorption of radionuclides onto mineral surfaces. Each of these barriers includes features that DOE described as important to waste isolation. The NRC staff review is provided in SER Section 2.2.1.1.

Assessing Compliance with the Postclosure Performance Objectives

A performance assessment is a systematic analysis that answers the three questions that define risk: What can happen? How likely is it to happen? and What are the resulting consequences? The NRC staff reviewed the Total System Performance Assessment (TSPA) analytic models and analyses DOE provided in support of its license application for the proposed repository at Yucca Mountain.

Scenario Analysis and Event Probability

To answer the question, "What can happen?" after a repository is closed at Yucca Mountain, DOE had to consider a wide range of specific features (e.g., geologic rock types, waste package materials), events (e.g., earthquakes, volcanic activity), and processes (e.g., corrosion of metal waste packages, sorption of radionuclides on rock surfaces) for possible inclusion in (or exclusion from) its TSPA model. Once selected, DOE then used these features, events, and processes (FEPs) to postulate a range of credible, future scenarios. A scenario is a well-defined sequence of events and processes, which can be interpreted as an outline of one possible future condition of the repository system. Thus, scenario analysis identifies the possible ways in which the repository environment could evolve so that a defensible representation of the system can be developed to estimate the range of credible potential consequences. After the features, events and processes are selected and used to postulate scenarios, similar scenarios are grouped into scenario classes, which are screened for use in the performance assessment model. The goal of scenario analysis is to ensure that no important aspect of the potential high-level waste repository is overlooked in the evaluation of its safety.

Consistent with this general guidance and the review areas in the YMRP Section 2.2.1.2.1, the NRC staff evaluates the applicant's scenario analysis in four separate SER sections (Sections 2.2.1.2.1.3.1 to 2.2.1.2.1.3.4). Section 2.2.1.2.1.3.1 contains the NRC staff's evaluation of both the applicant's methodology to develop a list of features, events and processes and DOE's list of the features, events and processes that it considered for inclusion in the performance assessment analyses. In Section 2.2.1.2.1.3.2, the NRC staff evaluates the DOE's screening of its list of features, events and processes, including the DOE's technical bases for the exclusion of features, events and processes from its performance assessment. DOE's formation of scenario classes and the exclusion of specific scenario classes in the DOE's performance assessment analyses are evaluated in Sections 2.2.1.2.1.3.3 and 2.2.1.2.1.3.4, respectively.

The NRC staff's evaluation of the applicant's methodology and conclusions on the probability of events included in the performance assessments is addressed in SER Section 2.2.1.2.2. That chapter is aimed at the second risk triplet question: How likely is it to happen?

Model Abstraction

The NRC staff's evaluation of the DOE's model abstractions focuses on the consequences of overall repository performance. In particular, the NRC staff's evaluation addresses the acceptability of the model abstractions in the DOE's TSPA to represent the performance (i.e., expected annual doses) of the Yucca Mountain repository.

The review of the model abstraction process begins with the review of the repository design and the data characterizing the geology and the performance of the design and proceeds through the development of models used in the performance assessment. The model abstraction review process ends with a review of how the abstracted models are implemented in the TSPA model (e.g., parameter ranges and distributions, integration with model abstractions for other parts of the repository system, representation of spatial and temporal scales, and whether the performance assessment model appropriately implements the abstracted model). For example, the review of parameter distributions will consider the relevant data, the corresponding uncertainty, and effects on repository performance (i.e., the dose to the reasonably maximally exposed individual). The potential for risk dilution—the lowering of the risk, or dose, from an unsupported parameter range and distribution—will also be part of this model abstraction review.

In many regulatory applications, a conservative approach can be used to decrease the need to collect additional information or to justify a simplified modeling approach. A conservative approach overestimates the dose to the reasonably maximally exposed individual. As such, a conservative approach may be used to demonstrate that the proposed repository meets the NRC regulations and provides adequate protection of public health and safety. Approaches designed to overestimate a specific aspect of repository performance (e.g., higher temperatures within the drifts) may be conservative with respect to temperature but could lead to nonconservative results with respect to dose. The TSPA is a complex analysis with many parameters, and DOE may use conservative assumptions to simplify its approaches and data collection needs. However, a technical basis that supports the selection of models and parameter ranges or distributions must be provided. The staff's evaluation of the adequacy of technical bases supporting models and parameter ranges or distributions will consider whether the approach results in calculated doses that would overestimate, rather than underestimate, the dose to the reasonably maximally exposed individual. In particular, the claim of conservatism as a basis for simplifying models and parameters should be carefully evaluated to verify that any simplifications are justified and do not unintentionally result in nonconservative results.

The intentional use of conservatism to manage uncertainty also has implications for the staff's efforts to risk inform its review. The staff will evaluate assertions that a given model or parameter distribution is conservative from the perspective of overall system performance (i.e., the dose to the reasonably maximally exposed individual). The staff used any available information to risk inform its review. For example, if DOE used an approach that overestimates a specific aspect of repository performance, then the staff would consider the effects of this approach on other parts of the TSPA model, overall repository performance, and the representation or sensitivity of important phenomena.

The NRC staff has separated the model abstraction review into the following 13 categories that are addressed in SER Sections 2.2.1.3.1 through 2.2.1.3.14:

1) Degradation of Engineered Barriers (SER Section 2.2.1.3.1)

This SER section provides the NRC staff's evaluation of the chemical degradation of the drip shields and waste packages emplaced in the repository drifts. Chemical degradation is primarily associated with the effect of corrosion processes on the metal surfaces of the drip shields and waste packages. The drip shields and the waste packages are engineered barriers, a subset of the engineered barrier system. The general functions of the engineered barrier system are to (i) prevent or significantly reduce the amount of water that contacts the waste, (ii) prevent or significantly reduce the rate at which radionuclides are released from the waste, and (iii) prevent or significantly reduce the rate at which radionuclides are released from the engineered barrier system to the Lower Natural Barrier. The engineered barrier system consists of the emplacement drifts, the drip shields, the waste packages, the naval spent nuclear fuel structure, the waste forms and waste package internal components, and emplacement pallets and inverters.

2) Mechanical Disruption of Engineered Barriers (SER Section 2.2.1.3.2)

This SER section provides the NRC staff's evaluation of the mechanical disruption of the drip shields and waste packages emplaced in the repository drifts. Mechanical disruption of engineered barrier system components generally results from external loads generated by accumulating rock rubble. Rubble accumulation can result from processes such as (i) degrading emplacement drifts due to thermal loads, (ii) time-dependent natural weakening of rocks, and (iii) effects of seismic events (vibratory ground motion or fault displacements). During seismic events, rubble loads on engineered barrier system components can increase as the accumulated rock rubble is shaken.

3) Quantity and Chemistry of Water Contacting Engineered Barriers and Waste Forms (SER Section 2.2.1.3.3)

This SER section provides the NRC staff's evaluation of (i) the chemistry of water entering the drifts, (ii) the chemistry of water in the drifts (tunnels), and (iii) the quantity of water in contact with the engineered barrier system. These three abstraction topics provide input needed to model the features and performance of the engineered barrier system (e.g., drip shields and waste packages). For example, in its license application, DOE relied on corrosion tests that were conducted on waste package and drip shield materials under a range of geochemical environments. The range of testing environments was deduced from a range of potential starting water compositions and from knowledge of near-field and in-drift processes that alter these compositions.

4) Radionuclide Release Rates and Solubility Limits (SER Section 2.2.1.3.4)

This SER section provides the NRC staff's evaluation of the processes that could result in water transport of radionuclides out of the engineered barrier system, including the waste packages and the emplacement inverters, and into the unsaturated zone (the rock mass directly below the repository horizon and above the water table). The engineered barrier system and the transport pathway within the drift (repository tunnel) are the initial barriers to radionuclide release. If a waste package is breached and water enters the waste package, the radionuclides contained in the package may be released from the engineered barrier system.

5) Climate and Infiltration (SER Section 2.2.1.3.5)

This SER section provides the NRC staff's evaluation of the representation of climate and infiltration. This evaluation considers the reduction of water flux from precipitation to net infiltration. Because of the generally vertical movement of percolating water through the unsaturated zone in the DOE's representation of the natural system, water entering the unsaturated zone at the ground surface (infiltration) is the only source for deep percolation water in the unsaturated zone at and below the proposed repository.

6) Flow Paths in the Unsaturated Zone (SER Section 2.2.1.3.6)

This SER section provides the NRC staff's evaluation of the abstraction of flow in that portion of the repository system above the water table (i.e., the unsaturated zone). Water percolating through the unsaturated zone above the repository (i.e., Upper Natural Barrier) may enter drifts, providing the means to interact with and potentially corrode the waste packages. Water percolating through the unsaturated zone below the repository (i.e., Lower Natural Barrier) also provides a flow pathway for transporting radionuclides downward to the water table. Once radionuclides pass below the water table, they may subsequently move laterally within the saturated zone to the accessible environment.

7) Radionuclide Transport in the Unsaturated Zone (SER Section 2.2.1.3.7)

This SER section provides the NRC staff's evaluation of the representation of radionuclide transport in the unsaturated zone. (b)(5)

(b)(5)

8) Flow Paths in the Saturated Zone (SER Section 2.2.1.3.8)

This SER section provides the NRC staff's evaluation of the representation of flow paths in the saturated zone (i.e., the direction and magnitude of water movement in the saturated zone). Flow paths in the saturated zone provide the pathway for releases of radionuclides to migrate from the saturated zone below the repository to the compliance location (approximately 18 km [11 mi] south of the repository). The magnitude (specific discharge) of water flow is used to determine the speed that water moves through the saturated zone to the compliance location.

9) Radionuclide Transport in the Saturated Zone (SER Section 2.2.1.3.9)

This SER section provides the NRC staff's evaluation of transport of radionuclides in the saturated zone. The NRC staff's technical review focuses on (i) how DOE represented the geological, hydrological, and geochemical features of the saturated zone in a framework for modeling the transport processes; (ii) how DOE integrated the saturated zone transport abstraction with other TSPA abstractions for performance

assessment calculations; and (iii) how DOE included and supported important transport processes in the saturated zone radionuclide transport abstraction.

10) Igneous Disruption of Waste Packages (SER Section 2.2.1.3.10)

This SER section provides the NRC staff's evaluation of models for the potential consequences of disruptive igneous activity at Yucca Mountain if basaltic magma rising through the Earth's crust intersects and enters a repository drift or drifts (DOE's igneous intrusion modeling case) or enters a drift and later erupts to the surface through one or more conduits (DOE's volcanic eruption modeling case). The proposed Yucca Mountain repository site lies in a region that has experienced sporadic volcanic events in the past few million years, such that the applicant previously determined the probability of future igneous activity at the site to exceed 1×10^{-8} per year. The NRC staff's technical review evaluates subsurface igneous processes (i.e., intrusion of magma into repository drifts, waste package damage, and formation of conduits to the surface), which involves entrainment of waste into the conduit and toward the surface. These processes control the amount of radionuclides that can be released during a potential igneous event.

11) Concentration of Radionuclides in Groundwater (SER Section 2.2.1.3.12)

This SER section provides the NRC staff's evaluation of the concentration of radionuclides in groundwater extracted by pumping and used in the annual water demand. Radionuclides transported through the saturated zone via groundwater to the compliance location may be available for extraction by a pumping well. The reasonably, maximally exposed individual is assumed to use well water with average concentrations of radionuclides and has an annual water demand of 3.7×10^9 L [3,000 acre-ft].

12) Airborne Transport and Redistribution of Radionuclides (SER Section 2.2.1.3.13)

This SER section reflects the NRC's staff evaluation of the volcanic ash exposure scenario and the groundwater exposure scenario. First, this SER section provides the NRC staff's evaluation of the airborne transport and deposition of radionuclides expelled by a potential future volcanic eruption and the subsequent redistribution of those radionuclides in soil. Second, this SER section evaluates redistribution of radionuclides in soil that arrive in the accessible environment through groundwater transport. This section addresses both airborne transport of radionuclides (YMRP Section 2.2.1.3.11) and redistribution of radionuclides in soil (YMRP Section 2.2.1.3.13).

13) Biosphere Characteristics (SER Section 2.2.1.3.14)

This SER section provides the NRC staff's evaluation of the model used to calculate biosphere transport and the annual dose to the reasonably, maximally exposed individual. The biosphere model calculates the transport of radionuclides within the biosphere through a variety of exposure pathways (e.g., soil, food, water, air) and applies dosimetry modeling to convert the reasonably, maximally exposed individual exposures into annual dose. Exposure pathways in the biosphere model are based on assumptions about residential and agricultural uses of the water and indoor and outdoor activities. These pathways include ingestion, inhalation, and direct exposure to radionuclides deposited to soil from irrigation. Ingestion pathways include drinking contaminated water, eating crops irrigated with contaminated water, eating food products produced from livestock raised on contaminated feed and water, eating farmed

fish raised in contaminated water, and inadvertently ingesting soil. Inhalation pathways include breathing resuspended soil, aerosols from evaporative coolers, and radon gas and its decay products.

Demonstration with the Numerical Limits for Postclosure Performance

DOE has conducted an analysis, through its TSPA, that evaluates repository behavior in terms of groundwater concentrations and annual dose due to potential releases from the repository. The performance assessment provides a method to evaluate the range of features (e.g., geologic rock types, waste package materials), events (e.g., earthquakes, igneous activity), and processes (e.g., corrosion of metal waste packages, sorption of radionuclides onto rock surfaces) that are relevant to the behavior of a Yucca Mountain repository. In determining whether DOE has demonstrated compliance with the numerical limits for postclosure performance (i.e., individual protection, separate limits for protection of groundwater, and human intrusion) the NRC staff review evaluates whether (i) the performance assessment includes the appropriate scenario classes (a set or combination of features, events and processes that are used in the performance assessment to represent a class or type of scenario, such as seismic activity), (ii) the representation of the scenario classes within the performance assessment is credible (e.g., the performance assessment results are consistent with the models, parameters, and assumptions that make up the performance assessment), and (iii) the annual dose the performance assessment estimates is less than the numerical limits set by the regulations.

The NRC staff has separated its review of the DOE's demonstration of compliance with the numerical limits for postclosure performance following three numerical limits that are addressed in SER Sections 2.2.1.4.1 through 2.2.1.4.3.

1) Postclosure Individual Protection Standards (SER Section 2.2.1.4.1)

This SER section provides the NRC staff's review of the calculation used to demonstrate compliance with the individual protection standards. 10 CFR 63.311 requires that the average annual dose must not exceed 0.15 mSv/yr [15 mrem/yr] during the initial 10,000 years after closure of the repository and not exceed 1.0 mSv/yr [100 mrem/yr] after 10,000 years up to 1 million years. The performance assessment used to demonstrate compliance with the individual protection standards considers both likely and unlikely events and all radiological exposure pathways.

2) Human Intrusion Standard (SER Section 2.2.1.4.2)

This SER section provides the NRC staff's review of the calculation used to demonstrate compliance with the human intrusion standard [i.e., exploratory drilling for groundwater results in a borehole penetrating a waste package in the repository—the timing of the intrusion is set to the earliest time after disposal that the waste packages would degrade sufficiently that a human intrusion could occur without the drillers recognizing it, per 10 CFR 63.321(a)]. 10 CFR 63.321(b) requires that the average annual dose must not exceed 0.15 mSv/yr [15 mrem/yr] during the initial 10,000 years after closure of the repository and not exceed 1.0 mSv/year [100 mrem/yr] after 10,000 years up to 1 million years. The performance assessment used to demonstrate compliance with the human intrusion standard considers likely events and all radiological exposure pathways.

3) Separate Groundwater Protection Standards (SER Section 2.2.1.4.3)

This SER section provides the NRC staff's review of the calculation used to demonstrate compliance with the separate standards for protection of groundwater—an important source of drinking water. The NRC's regulations provide separate standards to protect the groundwater resources in the vicinity of Yucca Mountain and specify the approach for estimating the concentration of radionuclides in groundwater. The groundwater protection standards provide for different limits depending on the radionuclide and the associated radiation. There are three distinct groups of radionuclides with the following limits: (i) radionuclides that are characterized as alpha emitters (e.g., Np-237) are grouped, and the combined concentration must be less than 15 pCi/L (this group explicitly excludes radon and uranium); (ii) radionuclides that are characterized as beta- and photon-emitting radionuclides (e.g., I-129, Tc-99) are grouped together, and the combined concentration cannot result in a dose exceeding 0.04 mSv [4 mrem] per year to the whole body or any organ, on the basis of drinking 2 L [0.53 gal] of water per day at the combined concentration; and (iii) the combined concentration of Ra-226 and Ra-228 cannot exceed a concentration of 5 pCi/L. The performance assessment used to demonstrate compliance with the separate groundwater protection standards considers likely events and the drinking water exposure pathway.

Expert Elicitation

This SER section provides the NRC staff's review of the three expert elicitations DOE used in support of its license application. Expert elicitations were conducted in the areas of seismic hazard (SAR Section 2.2.2.1), igneous activity (SAR Sections 1.1.6.2, 2.2.2.2, and 2.3.11), and saturated zone flow and transport (SAR Section 2.3.9.2).

Expert elicitation is a formal, structured, and well-documented process for obtaining the judgments of multiple experts. NRC routinely accepts, for review, expert judgments applicants use to evaluate and interpret the factual bases of license applications. Throughout the period of prelicensing interactions between the NRC and the DOE, the NRC staff has acknowledged that DOE could elect to use the subjective judgments of experts, or groups of experts, to interpret data and address technical issues and inherent uncertainties when assessing the long-term performance of a geologic repository. In its license application, DOE used the results of three formal expert elicitations to complement and supplement other sources of scientific and technical information such as data collection, analyses, and experimentation. In this context, the NRC staff has reviewed the DOE's use of expert elicitation, which includes a technical review of the results of these elicitations.

(Intentionally Left Blank)

FIGURES

Figure	Page
6-1 Potential Flow Pathways in the EBS	6-20

TABLES

Table	Page
1-1 Summary of Staff's Barrier Component Review.....	1-6
9-1 Quantitative Reduction in Flux From the Ground Surface to Water Entering the Drift Using Flux Averages Over the Repository Footprint.....	9-7
16-1 Exposure Pathways and Radionuclides Found To Be the Most Risk Significant in the DOE Performance Assessment for the 10,000-Year Simulation Period.....	16-4
16-2 Exposure Pathways and Radionuclides Found To Be the Most Risk Significant in the DOE Performance Assessment for the 1-Million-Year Simulation Period.....	16-5
17-1 Scenario Classes and Modeling Cases Included in the DOE's TSPA.....	17-8
17-2 DOE's Mean Values for the Seepage Rate Into Drifts.....	17-10
17-3 Percentage of CSNF and CDSP Waste Packages Breached for the Seismic Ground Motion Modeling Case in DOE's TSPA.....	17-11
17-4 Radionuclide Transport Times in the Unsaturated Zone for the Northern and Southern Repository Areas From DOE Breakthrough Curves.....	17-15
17-5 Summary of DOE Simulated Transport Times in the Saturated Zone Under Glacial-Transition Climate State.....	17-16
17-6 DOE Groundwater BDCF's.....	17-17
17-7 NRC Staff's Confirmatory Calculation Results of the Volume of Seepage Water Entering Patch Failures in the Waste Package for Seismic Ground Motion (Ruptures, Punctures, and General Corrosion) and Igneous Intrusion Modeling Cases for CSNF and CDSP Waste Packages.....	17-18
17-8 NRC Staff's Confirmatory Calculation Results for the Average Release Rates for Tc-99 (Seismic Ground Motion Modeling Case) for CSNF and CDSP Waste Packages.....	17-20
17-9 NRC Staff's Confirmatory Calculation Results for the Average Release Rates for Np-237 and Pu-242 in the Seismic Ground Motion Modeling Case for CSNF and CDSP Waste Packages.....	17-22
17-10 NRC Staff's Confirmatory Calculation Results for the Average Release Rates for Tc-99 in the Igneous Intrusive Modeling Case for CSNF and CDSP Waste Packages.....	17-23
17-11 NRC Staff's Confirmatory Calculation Results for the Average Release Rates for Np-237 and Pu-242 in the Igneous Intrusive Ground Motion Case for CSNF and CDSP Waste Packages.....	17-23
17-12 NRC Staff's Confirmatory Calculation Values for the Effectiveness (Expressed as a Percentage Reduction in Release) of the Unsaturated and Saturated Zones for Reducing Release Rates for Specific Radionuclides.....	17-24
17-13 NRC Staff's Confirmatory Calculation Results for the Average Dose Estimates for Tc-99 for the Seismic Ground Motion Modeling Case and Igneous Intrusive Modeling Case.....	17-25
17-14 NRC Staff's Confirmatory Calculation Results for the Annual Dose for Np-237 for the Seismic Ground Motion Modeling Case and Igneous Intrusive Modeling Case.....	17-26
17-15 NRC Staff's Confirmatory Calculation Results for the Annual Dose for Pu-242 for the Seismic Ground Motion Modeling Case and Igneous Intrusive Modeling Case.....	17-27

TABLES (continued)

Table	Page
17-16 NRC Staff's Confirmatory Calculation Results for Pu-239 and Am-241 Annual Dose for the Volcanic Eruption Modeling Case (Inhalation Pathway).....	17-30
17-17 NRC Staff's Confirmatory Calculation of Sr-90 and Cs-137 Annual Doses for the Volcanic Eruption Modeling Case (External Pathway)	17-31
17-18 NRC Staff's Confirmatory Calculation of Ra-226 Annual Dose for the Volcanic Eruption Modeling Case (External Pathway)	17-32
17-19 DOE Volcanic Eruption Modeling Case Short-term and Long-Term Inhalation BDCFs	17-33
17-20 DOE Volcanic Eruption Modeling Case Combined Ingestion, Radon, External BDCFs	17-33

(Intentionally Left Blank)

CONTENTS

Section	Page
ABSTRACT	v
ACRONYMS AND ABBREVIATIONS	vii
EXECUTIVE SUMMARY	ix
INTRODUCTION	xvii
FIGURES	xxvii
TABLES	xxviii
CHAPTER 1	1-1
2.2.1.1 System Description and Demonstration of Multiple Barriers	1-1
2.2.1.1.1 Introduction	1-1
2.2.1.1.2 Regulatory Requirements, Regulatory Guidance, and Acceptance Criteria	1-2
2.2.1.1.3 Technical Review	1-3
2.2.1.1.3.1 Identification of Barriers	1-4
2.2.1.1.3.2 Description and Technical Basis for Barrier Capability	1-4
2.2.1.1.3.2.1 Upper Natural Barrier: Topography and Surficial Soils	1-6
2.2.1.1.3.2.2 Upper Natural Barrier: Unsaturated Zone Above the Repository	1-8
2.2.1.1.3.2.3 EBS: Emplacement Drift	1-10
2.2.1.1.3.2.4 EBS: Drip Shield	1-11
2.2.1.1.3.2.5 EBS: Waste Packages	1-13
2.2.1.1.3.2.6 EBS: Waste Form and Waste Package Internal Components	1-15
2.2.1.1.3.2.7 EBS: Emplacement Pallet and Invert	1-18
2.2.1.1.3.2.8 Lower Natural Barrier: Unsaturated Zone Below the Repository	1-18
2.2.1.1.3.2.9 Lower Natural Barrier: Saturated Zone	1-21
2.2.1.1.4 Evaluation Findings	1-23
2.2.1.1.4.1 Identification of Barriers	1-23
2.2.1.1.4.2 Description of Barrier Capability to Isolate Waste	1-23
2.2.1.1.4.3 Technical Basis for Barrier Capability	1-24
2.2.1.1.4.4 Evaluation Findings	1-25
2.2.1.1.5 References	1-25
CHAPTER 2	2-1
2.2.1.2.1 Scenario Analysis	2-1
2.2.1.2.1.1 Introduction	2-1
2.2.1.2.1.2 Regulatory Requirements	2-2
2.2.1.2.1.3 Technical Review	2-3
2.2.1.2.1.3.1 Identification of a List of FEPs	2-4
2.2.1.2.1.3.2 Screening of the List of FEPs	2-6
2.2.1.2.1.3.3 Technical Review for Formation of Scenario Classes	2-66
2.2.1.2.1.3.4 Screening of Scenario Classes	2-68

CONTENTS (continued)

Section	Page
2.2.1.2.1.4 Evaluation Findings	2-70
2.2.1.2.1.5 References	2-71
CHAPTER 3	3-1
2.2.1.2.2 Identification of Events With Probabilities Greater Than 10^{-8} Per Year	3-1
2.2.1.2.2.1 Introduction.....	3-1
2.2.1.2.2.2 Regulatory Requirements	3-1
2.2.1.2.2.3 Technical Review	3-2
2.2.1.2.2.3.1 Technical Review for Igneous Event Probabilities	3-3
2.2.1.2.2.3.2 Technical Review for Seismic Event Probabilities	3-10
2.2.1.2.2.4 Technical Review of Early Waste Package and Drip Shield Failures Event Probabilities.....	3-18
2.2.1.2.2.5 Evaluation Findings	3-26
2.2.1.2.2.6 References	3-27
CHAPTER 4	4-1
2.2.1.3.1 Degradation of Engineered Barriers	4-1
2.2.1.3.1.1 Introduction.....	4-1
2.2.1.3.1.2 Regulatory Requirements	4-1
2.2.1.3.1.3 Technical Review	4-3
2.2.1.3.1.3.1 Drip Shield Degradation	4-3
2.2.1.3.1.3.1.1 Drip Shield General Corrosion	4-5
2.2.1.3.1.3.1.2 Drip Shield Early Failure	4-14
2.2.1.3.1.3.2 WP Degradation.....	4-16
2.2.1.3.1.3.2.1 General Corrosion of the WP Outer Barrier.....	4-22
2.2.1.3.1.3.2.2 Localized Corrosion of the WP Outer Barrier.....	4-32
2.2.1.3.1.3.2.3 SCC of the WP Outer Barrier	4-40
2.2.1.3.1.3.2.4 WP Early Failure	4-51
2.2.1.3.1.4 Evaluation Findings	4-53
2.2.1.3.1.5 References	4-54
CHAPTER 5	5-1
2.2.1.3.2 Mechanical Disruption of Engineered Barriers	5-1
2.2.1.3.2.1 Introduction.....	5-1
2.2.1.3.2.2 Regulatory Requirements	5-2
2.2.1.3.2.3 Seismic and Fault Displacement Inputs for Mechanical Disruption of Engineered Barriers	5-3
2.2.1.3.2.3.1 Seismic Site-Response Modeling.....	5-8
2.2.1.3.2.3.2 Fault Displacement Hazard Assessment	5-10
2.2.1.3.2.4 Fault Displacement Considerations in TSPA	5-11
2.2.1.3.2.5 Seismically Induced Drift Degradation	5-13
2.2.1.3.2.6 Drip Shield Structure/Mechanical Performance in the Context of Its Seepage Barrier Function.....	5-19
2.2.1.3.2.7 Waste Package Mechanical/Structural Performance	5-28

CONTENTS (continued)

Section	Page
2.2.1.3.2.8 Evaluation Findings	5-45
2.2.1.3.2.9 References	5-45
CHAPTER 6	6-1
2.2.1.3.3 Quantity and Chemistry of Water Contacting Engineered Barriers and Waste Forms	6-1
2.2.1.3.3.1 Introduction	6-1
2.2.1.3.3.2 Regulatory Requirements	6-1
2.2.1.3.3.3 Technical Review	6-3
2.2.1.3.3.3.1 Chemistry of Water Entering Drifts	6-3
2.2.1.3.3.3.2 Chemistry of Water in the Drifts	6-9
2.2.1.3.3.3.3 Quantity of Water in Contact With the EBS	6-18
2.2.1.3.3.4 Evaluation Findings	6-26
2.2.1.3.3.5 References	6-27
CHAPTER 7	7-1
2.2.1.3.4 Radionuclide Release Rates and Solubility Limits	7-1
2.2.1.3.4.1 Introduction	7-1
2.2.1.3.4.2 Regulatory Requirements	7-2
2.2.1.3.4.3 Technical Review	7-4
2.2.1.3.4.3.1 In-Package Chemical and Physical Environment	7-4
2.2.1.3.4.3.2 Waste Form Degradation	7-13
2.2.1.3.4.3.3 Concentration Limits	7-22
2.2.1.3.4.3.4 Availability and Effectiveness of Colloids	7-28
2.2.1.3.4.3.5 Engineered Barrier System Radionuclide Transport	7-37
2.2.1.3.4.4 Evaluation Findings	7-47
2.2.1.3.4.5 References	7-48
CHAPTER 8	8-1
2.2.1.3.5 Climate and Infiltration	8-1
2.2.1.3.5.1 Introduction	8-1
2.2.1.3.5.2 Regulatory Requirements	8-2
2.2.1.3.5.3 Technical Review	8-3
2.2.1.3.5.3.1 Identification of Features and Processes	8-3
2.2.1.3.5.3.2 Climate	8-5
2.2.1.3.5.3.2.1 Climate Change for the Next 10,000 Years	8-5
2.2.1.3.5.3.2.2 Local Spatial and Temporal Variation of Meteorological Conditions	8-11
2.2.1.3.5.3.3 Net Infiltration	8-14
2.2.1.3.5.4 Evaluation Findings	8-22
2.2.1.3.5.5 References	8-24
CHAPTER 9	9-1
2.2.1.3.6 Unsaturated Zone Flow	9-1
2.2.1.3.6.1 Introduction	9-1

CONTENTS (continued)

Section	Page
2.2.1.3.6.2 Regulatory Requirements	9-2
2.2.1.3.6.3 Technical Review	9-3
2.2.1.3.6.3.1 Integration Within the Unsaturated Zone	9-4
2.2.1.3.6.3.2 Ambient Mountain-Scale Flow Above the Repository	9-10
2.2.1.3.6.3.3 Thermohydrologic Effects of Water Emplacement	9-22
2.2.1.3.6.3.4 Ambient and Thermal Seepage Models	9-29
2.2.1.3.6.3.5 In-Drift Convection and Moisture Redistribution	9-40
2.2.1.3.6.3.5.1 In-Drift Heat Transfer and Convection	9-40
2.2.1.3.6.3.5.2 Moisture Redistribution and Condensation	9-42
2.2.1.3.6.3.6 Ambient Mountain-Scale Flow—Below the Repository	9-46
2.2.1.3.6.3.6.1 Flow Model Conceptualization	9-46
2.2.1.3.6.3.6.2 Flow Features Below Southern and Northern Portions of Repository	9-47
2.2.1.3.6.3.6.3 Adequacy of Flow Fields for Transport	9-53
2.2.1.3.6.3.6.4 Summary	9-54
2.2.1.3.6.4 Evaluation Findings	9-54
2.2.1.3.6.5 References	9-56
CHAPTER 10	10-1
2.2.1.3.7 Radionuclide Transport in the Unsaturated Zone	10-1
2.2.1.3.7.1 Introduction	10-1
2.2.1.3.7.2 Regulatory Requirements	10-1
2.2.1.3.7.3 Technical Review	10-3
2.2.1.3.7.3.1 System Description and Model Framework	10-3
2.2.1.3.7.3.1.1 Model Integration for the TSPA Code	10-4
2.2.1.3.7.3.1.2 EBS—UZ Boundary Condition	10-5
2.2.1.3.7.3.2 UZ Radionuclide Transport Processes	10-6
2.2.1.3.7.3.2.1 Advection and Dispersion	10-7
2.2.1.3.7.3.2.2 Sorption	10-8
2.2.1.3.7.3.2.3 Matrix Diffusion	10-11
2.2.1.3.7.3.2.4 Colloid-Associated Transport	10-14
2.2.1.3.7.3.2.5 Radionuclide Decay and Ingrowth	10-17
2.2.1.3.7.4 Evaluation Findings	10-17
2.2.1.3.7.5 References	10-18
CHAPTER 11	11-1
2.2.1.3.8 Flow Paths in the Saturated Zone	11-1
2.2.1.3.8.1 Introduction	11-1
2.2.1.3.8.2 Regulatory Requirements	11-2
2.2.1.3.8.3 Technical Review	11-3
2.2.1.3.8.3.1 System Description and Integration of Models Relevant to Flow Paths in the Saturated Zone	11-3

CONTENTS (continued)

Section	Page
2.2.1.3.8.3.2 Sufficiency of Baseline Data to Justify Models of Flow Paths in the Saturated Zone	11-7
2.2.1.3.8.3.3 Uncertainty in Data Used in Models of Flow Paths in the Saturated Zone	11-10
2.2.1.3.8.3.4 Uncertainty in Flow Paths in the Saturated Zone Models	11-14
2.2.1.3.8.3.5 Model Support Based on Comparison With Alternative Models or Other Information	11-17
2.2.1.3.8.4 Evaluation Findings	11-19
2.2.1.3.8.5 References	11-20
CHAPTER 12	12-1
2.2.1.3.9 Radionuclide Transport in the Saturated Zone	12-1
2.2.1.3.9.1 Introduction	12-1
2.2.1.3.9.2 Regulatory Requirements	12-1
2.2.1.3.9.3 Technical Review	12-3
2.2.1.3.9.3.1 Conceptual Model and Model Framework	12-3
2.2.1.3.9.3.1.1 Model Integration for TSPA-LA	12-6
2.2.1.3.9.3.1.2 UZ/SZ Boundary Condition	12-6
2.2.1.3.9.3.2 SZ Transport Processes	12-8
2.2.1.3.9.3.2.1 Advection and Dispersion	12-8
2.2.1.3.9.3.2.2 Sorption	12-10
2.2.1.3.9.3.2.3 Matrix Diffusion	12-15
2.2.1.3.9.3.2.4 Colloid-Associated Transport	12-17
2.2.1.3.9.3.2.5 Radionuclide Decay and Ingrowth	12-19
2.2.1.3.9.4 Evaluation Findings	12-22
2.2.1.3.9.5 References	12-22
CHAPTER 13	13-1
2.2.1.3.10 Igneous Disruption of Waste Packages	13-1
2.2.1.3.10.1 Introduction	13-1
2.2.1.3.10.2 Regulatory Requirements	13-2
2.2.1.3.10.3 Technical Review	13-4
2.2.1.3.10.3.1 General Approach by DOE	13-4
2.2.1.3.10.3.2 NRC Review of DOE Igneous Intrusion Modeling Case	13-6
2.2.1.3.10.3.3 NRC Review of DOE Volcanic Eruption Modeling Scenario	13-12
2.2.1.3.10.4 Evaluation Findings	13-18
2.2.1.3.10.5 References	13-19
CHAPTER 14	14-1
2.2.1.3.12 Concentration of Radionuclides in Groundwater	14-1
2.2.1.3.12.1 Introduction	14-1
2.2.1.3.12.2 Regulatory Requirements	14-1
2.2.1.3.12.3 Assessment of Well Water Concentration Estimates	14-1

CONTENTS (continued)

Section	Page
2.2.1.3.12.4 Evaluation Findings	14-2
2.2.1.3.12.5 References	14-2
CHAPTER 15.....	15-1
2.2.1.3.13 Airborne Transport and Redistribution of Radionuclides	15-1
2.2.1.3.13.1 Introduction.....	15-1
2.2.1.3.13.2 Regulatory Requirements	15-2
2.2.1.3.13.3 Technical Review	15-4
2.2.1.3.13.3.1 Assessment and Review of the Volcanic Ash Exposure Scenario	15-6
2.2.1.3.13.3.1.1 Airborne Transport Modeling	15-7
2.2.1.3.13.3.1.2 Tephra Redistribution in Fortymile Wash	15-16
2.2.1.3.13.2.1.3 Downward Migration of Radionuclides in Soil	15-25
2.2.1.3.13.3.2 Assessment and Review of Groundwater Exposure Scenarios	15-21
2.2.1.3.13.4 Evaluation Findings	15-36
2.2.1.3.13.5 References	15-37
CHAPTER 16.....	16-1
2.2.1.3.14 Biosphere Characteristics	16-1
2.2.1.3.14.1 Introduction.....	16-1
2.2.1.3.14.2 Regulatory Requirements	16-2
2.2.1.3.14.3 Technical Review	16-4
2.2.1.3.14.3.1 System Description and Model Integration	16-6
2.2.1.3.14.3.2 Assessment of Biosphere Transport Pathways	16-12
2.2.1.3.14.3.3 Assessment of Human Exposure	16-23
2.2.1.3.14.3.4 Assessment of Dosimetry.....	16-27
2.2.1.3.14.3.5 Assessment of Integrated Biosphere Modeling Results	16-29
2.2.1.3.14.4 Evaluation Findings	16-29
2.2.1.3.14.5 References	16-32
CHAPTER 17.....	17-1
2.2.1.4.1 Demonstration of Compliance With the Postclosure Public Health and Environmental Standards (Individual Protection)	17-1
2.2.1.4.1.1 Introduction.....	17-1
2.2.1.4.1.2 Regulatory Requirements	17-1
2.2.1.4.1.3 Technical Review	17-2
2.2.1.4.1.3.1 Introduction.....	17-2
2.2.1.4.1.3.2 Probabilities and Consequences of Scenario Classes	17-3
2.2.1.4.1.3.2.1 Summary of DOE Approach	17-3
2.2.1.4.1.3.2.2 NRC Staff Evaluation	17-6

CONTENTS (continued)

Section	Page
2.2.1.4.1.3.3 Credible Representation of Repository Performance	17-7
2.2.1.4.1.3.3.1 DOE's TSPA Calculation Related to Groundwater Releases	17-8
2.2.1.4.1.3.3.1.1 Summary of DOE Approach	17-8
2.2.1.4.1.3.3.1.1.1 Seepage of Water Into Drifts	17-8
2.2.1.4.1.3.3.1.1.2 Damage to Engineered Barriers (Drip Shield and Waste Package)	17-10
2.2.1.4.1.3.3.1.1.3 Seepage of Water Into Waste Packages	17-12
2.2.1.4.1.3.3.1.1.4 Release of Radionuclides From the Waste Package	17-13
2.2.1.4.1.3.3.1.1.5 Transport of Radionuclides in the Unsaturated and Saturated Zone	17-14
2.2.1.4.1.3.3.1.1.6 Annual Dose to the RMEI	17-16
2.2.1.4.1.3.3.1.2 NRC Staff Evaluation	17-17
2.2.1.4.1.3.3.2 Description and Understanding of TSPA Calculation for the Volcanic Eruption Modeling Case	17-28
2.2.1.4.1.3.3.2.1 Summary of DOE Approach	17-28
2.2.1.4.1.3.3.2.2 NRC Staff Evaluation	17-29
2.2.1.4.1.3.4 Average Annual Dose Limits Are Met and Statistically Stable	17-31
2.2.1.4.1.3.4.1 Summary of DOE Approach	17-31
2.2.1.4.1.3.4.2 NRC Staff Evaluation	17-34
2.2.1.4.1.4 Evaluation Findings	17-35
2.2.1.4.1.5 References	17-36
CHAPTER 18	18-1
2.2.1.4.2 Demonstration of Compliance With the Human Intrusion Standard	18-1
2.2.1.4.2.1 Introduction	18-1
2.2.1.4.2.2 Regulatory Requirements	18-1
2.2.1.4.2.3 Technical Review	18-2
2.2.1.4.2.3.1 Timing of Human Intrusion Event	18-3
2.2.1.4.2.3.2 Representation of Intrusion Event	18-5
2.2.1.4.2.3.3 Annual Dose to RMEI	18-9
2.2.1.4.2.4 Evaluation Findings	18-11
2.2.1.4.2.5 References	18-12
CHAPTER 19	19-1
2.2.1.4.3 Demonstration of Compliance With Separate Groundwater Protection Standards	19-1
2.2.1.4.3.1 Introduction	19-1
2.2.1.4.3.2 Regulatory Requirements	19-1
2.2.1.4.3.3 Technical Review	19-3
2.2.1.4.3.3.1 Representative Volume Location	19-3
2.2.1.4.3.3.2 Representative Volume Dimensions	19-4
2.2.1.4.3.3.3 Average Concentrations	19-6

CONTENTS (continued)

Section	Page
2.2.1.4.3.4 Evaluation Findings	19-8
2.2.1.4.3.5 References	19-8
CHAPTER 20.....	20-1
2.5.4 Expert Elicitation	20-1
2.5.4.1 Introduction.....	20-1
2.5.4.2 Regulatory Requirements	20-1
2.5.4.3 Technical Review	20-2
2.5.4.4 Evaluation Findings	20-7
2.5.4.5 References	20-7
CHAPTER 21.....	21-1
Conclusions	21-1
CHAPTER 22.....	22-2
Glossary	22-2
APPENDIX A—Commitments	
APPENDIX B—(b)(5) 	

CHAPTER 1

2.2.1.1 System Description and Demonstration of Multiple Barriers

2.2.1.1.1 Introduction

The performance objectives in 10 CFR Part 63 for the repository after permanent closure require that the geologic repository must include multiple barriers, consisting of both natural barriers and an engineered barrier system (EBS). Natural and engineered barriers isolate waste by preventing or substantially reducing the rate of movement of water or radionuclides from the Yucca Mountain repository to the accessible environment. A comprehensive description of the capabilities of natural and engineered barriers allows the staff's review of the applicant's performance assessment evaluation, documented in the rest of Volume 3 of this Safety Evaluation Report (SER), to focus on the most important aspects of repository performance. Therefore, this chapter evaluates the U.S. Department of Energy's (DOE) description of the capabilities of the barriers in the geologic repository. The technical basis for the barrier capability is evaluated in the chapters of Section 2.2.1.3 of this SER.

A system of multiple barriers is intended to ensure that the repository system is robust and is not wholly dependent on a single barrier. Such a system increases the resilience of the repository to unanticipated failures or external challenges. Therefore, the repository performance objectives in 10 CFR Part 63 require that a geologic repository contain both natural and engineered barriers.

Comment (b)(5)
(b)(5)

The NRC's evaluation of the applicant's overall compliance demonstration examines how all components of the repository system work together to protect public health and safety. The emphasis of the NRC staff's integrated review of the applicant's performance assessment calculation is not solely focused on the isolated performance of individual barriers, but rather on ensuring that the repository system is robust. Therefore, to increase the staff's understanding of integrated repository performance, the regulation requires the applicant to

- Identify the important barriers of the performance assessment evaluation
- Describe each barrier's capability
- Provide a technical basis for that capability which is based on and consistent with the performance assessment evaluation used to demonstrate compliance with the quantitative performance objectives

The required description of barrier capability provides risk information that helps the staff interpret the performance assessment results by describing how different elements of the performance assessment affect the overall performance of the system. This understanding can guide the NRC staff in the review of the technical bases for those aspects that are important, thereby allowing increased confidence that the postclosure performance objectives are met. The staff can therefore use this risk information to implement a risk-informed approach in its review of the applicant's performance assessment calculations.

The NRC staff's evaluation is based on information provided in the Safety Analysis Report (SAR) (DOE, 2008ab), as supplemented by DOE responses to the staff's requests for additional information (DOE, 2009an,bu). DOE provided a description of the barrier capabilities in SAR

Chapter 2.1. This description, supplemented by DOE's responses to the staff's requests for additional information, is used by the staff in its review of the technical bases for the performance assessment, as documented in the SER Chapters, Section 2.2.1.3. This SER chapter focuses on the adequacy of DOE's description of the barrier capabilities. As discussed in the staff's Yucca Mountain Review Plan (YMRP) Section 2.2.1 (NRC, 2003aa), the multiple barrier review focuses on each barrier's importance to waste isolation. Following the guidance in the YMRP Section 2.2.1, the staff evaluated the information required by 10 CFR 63.21(c)(1), (9), (10), (14), and (15).

2.2.1.1.2 Regulatory Requirements, Regulatory Guidance, and Acceptance Criteria

The regulatory requirements applicable to multiple barriers are found in 10 CFR 63.113(a) and 10 CFR 63.115(a–c). These require an applicant to

- Ensure that the geologic repository includes multiple barriers, consisting of both natural barriers and an EBS
- Identify those features of the repository that are considered barriers important to waste isolation (ITWI)
- Describe the capabilities of those barriers
- Provide a technical basis for the description of the capability that is based on and consistent with the technical basis for the performance assessment used to demonstrate compliance with 10 CFR 63.113(b) and (c)

Definitions and discussions of important terms and concepts, such as "barrier" and "ITWI," that supplement these requirements are located in 10 CFR 63.2 and 10 CFR 63.102(h). For example, 10 CFR 63.2 states that the term "barrier" means any material, structure, or feature that, for a period to be determined by NRC, prevents or substantially reduces the rate of movement of water or radionuclides from the Yucca Mountain repository to the accessible environment, or prevents the release or substantially reduces the release rate of radionuclides from the waste. Further information on the conceptual background of the multiple barrier requirements can be found in the statement of considerations for the proposed (64 FR 8647) and for the final (66 FR 55758) 10 CFR Part 63 rulemaking.

YMRP Section 2.2.1.1 provides guidance to the NRC staff on an acceptable review approach for meeting these requirements. Section 2.2.1.1 identifies three acceptance criteria that the applicant may use to demonstrate compliance with the requirements of 10 CFR 63.113(a) and 63.115(a–c):

- Identification of barriers is adequate.
- Description of barrier capability to isolate waste is acceptable
- Technical basis for barrier capability is adequately presented.

The following technical review is largely organized according to these three acceptance criteria. Because the description of the barrier capability and the technical basis for the barrier capability are interrelated, the review activities associated with these two acceptance criteria are discussed together in SER Section 2.2.1.1.3.2.

2.2.1.1.3 Technical Review

Summary of DOE License Application

DOE identified the barriers considered ITWI and summarized their capabilities and technical bases in SAR Section 2.1. This summary relies on more extensive information documented in SAR Sections 2.2 through 2.4. DOE documented the analyses that it used to identify and evaluate barrier capability in SNL (2008ad) report. The identification of the barriers, and the description of the capability of these barriers, is based on the scenario analysis summarized in SAR Section 2.2 that identifies and evaluates the features, events, and processes to be considered in the Total System Performance Assessment (TSPA) model. The TSPA is an abstracted model that quantitatively integrates inputs from the various supporting analytic models. DOE used this abstracted integrating model to demonstrate compliance with the postclosure performance standards.

DOE identified three barriers (upper natural, engineered, and lower natural) and provided the features or components that make up these barriers in SAR Section 2.1.1.

DOE summarized the capability of the barriers in SAR Section 2.1.2. For each barrier, DOE identified and provided a brief qualitative description of the key processes and events that influence the capability of each barrier component. DOE provided some of these descriptions at the level of individual barrier components (e.g., the waste package component of the EBS). DOE provided other descriptions at an aggregate level (e.g., the waste form, waste canisters, and waste package internals taken together). DOE then addressed

- The specific function of each barrier component and how the barrier component carries out its functions
- The time period over which the barrier functions and how DOE expects the capability of the barrier to evolve over time
- How uncertainty in the barrier capability has been accounted for in the performance assessment
- The impact of disruptive events on the barrier, if any
- A quantitative evaluation of the barrier capability to carry out its barrier functions

DOE summarized the technical basis for the description of barrier capability in SAR Section 2.1.3. DOE stated that the technical basis for the barrier capability is the same as the technical basis for the model used in the TSPA analyses. DOE also stated that the technical basis for the description of the barrier capability is provided in SAR Section 2.3. SAR Table 2.1-5 identified which TSPA model abstractions are associated with each barrier; SAR Section 2.1.3 identified the location of the technical basis for the description of the barrier capability for those abstractions. SAR Section 2.1.3 briefly summarized the technical basis for each TSPA model component. Each summary identified the subsection of SAR Section 2.3 where DOE described the technical basis of the model component in more detail.

2.2.1.1.3.1 Identification of Barriers

Summary of DOE Approach

In SAR Section 2.1.1, DOE identified three barriers (upper natural, engineered, and lower natural) and then provided the features or components that made up these barriers. SAR Table 2.1-1 indicates the safety classification (i.e., whether DOE considers the feature or component to be ITWI) of each feature or component. These barriers include ITWI features from the upper and lower natural barrier and ITWI components from the EBS. In DOE Enclosure 1 (2009an), DOE expanded SAR Table 2.1 to include

- The features, events, and processes considered important to barrier capability
- A qualitative discussion of how the stated barrier functions are attained
- For each barrier component considered ITWI, a quantitative summary of barrier capability based on information from the performance assessment analysis

NRC Staff's Evaluation

(b)(5)

(b)(5)

(b)(5) A barrier, as defined in 10 CFR 63.2, prevents or substantially reduces the rate of movement of water or radionuclides. (b)(5)

(b)(5)

2.2.1.1.3.2 Description and Technical Basis for Barrier Capability

NRC Staff's Review Process

The staff review of the description and technical basis for barrier capability is based on a list of 21 individual features presented in SAR Table 2.1-1. For purposes of evaluation, the staff consolidated these features to yield nine features as shown in Table 1-1. The staff reviewed the descriptions of the barrier capability of these nine features

To evaluate the description of the barrier capability, the staff reviewed how DOE

- Identified the safety classification and primary function of each barrier component

- Identified the characteristics and processes important to barrier capability, including both those that are potentially beneficial and those that are potentially harmful to barrier functions
- Described how the barrier component was represented in the performance assessment
- Described the qualitative and quantitative capabilities of each barrier component, consistent with the TSPA
- Characterized the time period over which the barrier functions and how DOE expects the barrier capability to change over time
- Accounted for the uncertainty in the description of the barrier capability

To evaluate the technical basis for the barrier capability, the staff reviewed the consistency between the descriptions of the barrier capability documented in SAR Section 2.1.2 and the technical bases summarized in SAR Section 2.1.3 and further documented in SAR Section 2.3. In addition, the staff reviewed the description of the performance confirmation plan to determine whether it was consistent with the descriptions of barrier capability. SER Section 2.4 contains the results of staff's review of the performance confirmation plan.

As an independent check, the staff also considered the insights gained from NRC Appendix D (2005aa), as updated (CNVRA and NRC, 2008aa), to determine whether DOE had omitted any features or processes that might contribute significantly to barrier capability in its description of barrier capability. In addition, the staff reviewed DOE's TSPA model described in SNL (2008ag) to assess consistency between the descriptions of barrier capability and how the TSPA model components actually represented the barrier capability.

The staff summarizes the results of the review of the individual barrier components, as identified in the second column of Table 1-1. In each of the following sections, the staff's evaluation

- Describes whether the barrier capability DOE described is consistent with the definition of a barrier
- Identifies the SAR sections where DOE described the capability of each barrier component and briefly summarizes the described capabilities
- Identifies and briefly summarizes where in the SAR DOE described the time period over which the barrier performs its stated function
- Briefly describes how DOE accounted for uncertainties in its characterization and modeling of the barriers
- Identifies where DOE summarized the technical basis for barrier capability, describes whether this technical basis is consistent with the technical basis for the performance assessment, and describes whether the technical basis is commensurate with the importance of each barrier's capability

Comment (b)(5)
(b)(5)

Table 1-1. Summary of Staff's Barrier Component Review

(b)(5)

2.2.1.1.3.2.1 Upper Natural Barrier: Topography and Surficial Soils

The staff reviewed DOE's description of the barrier capability of the topography and surface soils. DOE described the barrier capabilities of topography and surficial soils qualitatively in SAR Section 2.1.2.1.1 and quantitatively in SAR Section 2.1.2.1.6.1. DOE used net infiltration as a percentage of annual precipitation to quantify the barrier capability of topography and surficial soils. DOE supplemented this discussion in DOE Enclosure 1 (2009a) (b)(5)

(b)(5)

DOE's climate and infiltration analyses are summarized in SAR Tables 2.3.1-2, 2.3.1-3, and 2.3.1-4. DOE concluded that for approximately 10,000 years following closure of the repository, a limited amount of water would infiltrate into the unsaturated zone above the repository at Yucca Mountain. DOE attributed the low rate of infiltration to low precipitation that is substantially further reduced by high rates of evapotranspiration (e.g., uptake by plants,

surface evaporation) and surface runoff. Average net infiltration rate estimates range from about 3 to 17 percent of precipitation, depending upon the climate state and the infiltration scenario. For the post-10,000-year period, DOE has adopted a probabilistic distribution of deep percolation for a constant-in-time, long-term average climate for Yucca Mountain that is comparable to the probabilistic distribution NRC specified in 10 CFR 63.342(c)(2).

(b)(5)

DOE provided information in SAR Section 2.1.2.1.3 on the time period over which this upper natural barrier feature performs its intended function. DOE stated that the topography and surficial soils are not expected to change significantly in the 10,000 years following closure, but changes in climate and vegetation are expected to affect the barrier capability during this period. In SAR Tables 2.3.1-17 to 2.3.1-19 and DOE Enclosure 1 (2009a), DOE addressed when it expects different climate states to occur and provided infiltration rates under different climate scenarios. (b)(5)

(b)(5)

In SAR Section 2.1.2.1.4, DOE described sources of uncertainty that are considered in the climate and infiltration model. Sources of uncertainty include (i) the interpretation of the geologic record of past climates, (ii) the parameters describing evapotranspiration, (iii) the applicability of models, and (iv) the characteristics of the Yucca Mountain site. DOE also addressed the uncertainty in the barrier capability by describing results from its infiltration model demonstrating the probability of different infiltration scenarios (SAR Section 2.3.2.4.1.2.4.5 and Table 2.3.2-27). By adjusting these probability weights, based on deep subsurface observations of chloride and temperature (SAR 2.3.2.4.1.2.4.5 and Table 2.3.2-27). (b)(5)

(b)(5)

Comment (b)(5)

(b)(5)

In SAR Section 2.1.3.1, DOE summarized the technical basis of the barrier capability description of the upper natural barrier, which includes the topography and surficial soils component. In this discussion, DOE indicated which TSPA models it used to support the description of the barrier capability of the upper natural barrier. DOE based its description of the barrier capability of the topography and surficial soils on the climate and infiltration model described in SAR Section 2.3.1. SER Section 2.2.1.3.5 documents the staff's evaluation of the infiltration model that provides the technical basis for this capability. (b)(5)

(b)(5)

(b)(5)

(b)(5)

2.2.1.1.3.2.2 Upper Natural Barrier: Unsaturated Zone Above the Repository

The staff reviewed the DOE description of the barrier capability of the unsaturated zone above the repository. DOE described the capability of the unsaturated zone above the repository to prevent or substantially reduce seepage qualitatively in SAR Section 2.1.2.1.2 and quantitatively in SAR Section 2.1.2.1.6.2. DOE supplemented this description in DOE Enclosures 1 and 2 (2009an). (b)(5)

(b)(5)

In SAR Section 2.1.2.1.6.2, DOE explained that the average percolation flux at the depth of the repository is, at most, a few percent less than the average net infiltration near the surface above the repository. In other words, changes in the flow rate of water between the ground surface and the repository level are relatively small, indicating that there are no significant processes resulting in the diversion of water away from the emplacement drift location. However, DOE explained that capillary diversion of water at the host rock–air interface at the drift wall prevents much of the water flowing in the rock at the repository level from entering the drift as seepage (i.e., dripping). At some drift locations, all of the water is diverted around the drift, resulting in no drips at all; at others, only some of the water enters, and the remainder is diverted around the drift. In addition, the short duration, relatively higher flow rates resulting from infiltration following brief episodes of precipitation are spread out in time and space as they pass through the Paintbrush Tuff. This damping of episodic infiltration pulses by the Paintbrush Tuff results in water flow rates below the Paintbrush Tuff that are consistently lower than the peak flow rate during the infiltration pulse, but which are more nearly constant over time (i.e., steady-state fluxes below the Paintbrush Tuff). Because capillary diversion processes are more effective at low percolation flow rates, the damping of episodic infiltration pulses by the Paintbrush Tuff contributes to the effectiveness of the capillary barrier. DOE quantified the barrier capability of the unsaturated zone above the repository for each of the five percolation subregions for the climate states projected for the first 10,000 years after repository closure (SAR Section 2.1.2.1.2). DOE used an analysis based on the TSPA seepage models and inputs to demonstrate that average seepage rates range from less than 1 to about 17 percent of the percolation fluxes for intact drifts within the first 10,000 years following closure, as described in DOE Enclosure 3, Table 11 (2009an). In other words, DOE expects capillary forces to divert more than 80 percent of percolation flux away from the intact drifts for the initial 10,000 years after closure. DOE Enclosure 3, Table 5 (2009an) identified that the fraction of the repository experiencing dripping conditions (i.e., the seepage fraction) ranges from 10 to 70 percent. Results for the collapsed drift case, which is a likely scenario in the post-10,000-year period, are shown in DOE Enclosure 3, Table 11 (2009bo). These results indicated that mean seepage

percentage ranges from about 40 to 56 percent in the post-10,000-year period. In other words, DOE expects that capillary forces would divert at least 44 percent of percolation flux away from collapsed drifts. The post-10,000-year seepage fractions for the corresponding flow fields range from about 60 to 80 percent, as described in DOE Enclosure 3, Table 8 (2009bo).

(b)(5)

In SAR Section 2.1.2.1.3, DOE provided information on the time period over which this upper natural barrier feature performs its intended function. DOE stated that the unsaturated zone above the repository is not expected to change in the 10,000 years following closure and that changes in the barrier capability are due to changes in infiltration. SAR Figure 2.1-5 demonstrates how seepage changes as a function of time (b)(5)

(b)(5)

In SAR Section 2.1.2.1.4, DOE discussed sources of uncertainty in the barrier capability of the unsaturated zone above the repository. These primarily are associated with uncertainties in the models and the characteristics of the Yucca Mountain site. SAR Tables 2.1-6 through 2.1-9 demonstrate the range of uncertainty in seepage fractions. DOE also discussed these uncertainties in SAR Section 2.3.3.4.2 (b)(5)

(b)(5)

SAR Section 2.1.3.1 summarized the technical basis of the barrier capability of the upper natural barrier, which includes the unsaturated zone above the repository. In its discussion, DOE indicated which TSPA models it used to support the description of the barrier capability of the upper natural barrier. DOE based its description of the barrier capability of the unsaturated zone above the repository on the unsaturated zone flow model described in SAR Section 2.3.2 and on the seepage (ambient and thermal) models described in SAR Section 2.3.3. SER Section 2.2.1.3.6 documents the staff's evaluation of the technical basis for the unsaturated zone flow and seepage model abstractions that form the basis for this capability. (b)(5)

(b)(5)

(b)(5)

2.2.1.1.3.2.3 EBS: Emplacement Drift

The staff reviewed the DOE description of the barrier capability of the emplacement drift. DOE discussed the barrier capabilities of the emplacement drift in SAR Section 2.1.2.2 under the discussion titled "Emplacement Drift" and in DOE Enclosures 1 and 3 (2009an). DOE stated that the capability of the emplacement drift to prevent or substantially reduce the movement of water is associated with the capillary barrier discussed under the upper natural barrier. DOE associated the capability of the drift to prevent or reduce the rate of movement of radionuclides with the effect of temperature and water chemistry on various processes affecting the degradation of the other EBS components (e.g., drip shield, waste package, and waste form) and radionuclide transport. DOE Enclosures 1 and 3 (2009an) specifically identified and discussed the roles of individual processes in the capability of the emplacement drifts.

(b)(5)

(b)(5)

DOE discussed the time period over which the emplacement drift functions in SAR Section 2.1.2.2.3 and in DOE Enclosure 3 (2009an). DOE described the evolution of the mechanical stability of the drift and the in-drift environment and discussed how these changes affect the major processes associated with emplacement drift performance. (b)(5)

(b)(5)

In SER Section 2.2.1.3.2.3.2, the staff addresses the adequacy and uncertainty in the capabilities of the emplacement drift related to the mechanical integrity of the drift opening. DOE discussed the uncertainty in the performance of the emplacement drift in SAR Sections 2.1.2.2.4 and 2.3.4.4.8 and in DOE Enclosure 3 (2009a). DOE indicated that the uncertainties in the environmental conditions are a primary source of uncertainty in the performance of the EBS. In SAR Section 2.3.4.4.8, DOE discussed the sources and treatment of uncertainty in the evaluation of rockfall and demonstrated the effect of these uncertainties in SAR Figure 2.1-14.(b)(5)

(b)(5)

DOE summarized the technical basis of the EBS capability, which included the emplacement drift, in SAR Section 2.1.3.2. In its discussion, DOE indicated which TSPA models it used to support the description of the barrier capability of the EBS. DOE based its description of the barrier capability of the emplacement drift on three TSPA submodels: (i) the ambient and thermal seepage models described in SAR Section 2.3.3, (ii) the EBS mechanical degradation model described in SAR Section 2.3.4, and (iii) the in-drift chemical and physical environment model described in SAR Section 2.3.5. In SER Sections 2.2.1.3.2, 2.2.1.3.3, and 2.2.1.3.6, the NRC staff evaluates the adequacy of the technical bases used to support the barrier capability of the emplacement drift. (b)(5)

(b)(5)

(b)(5)

The following sections address the drip shield and waste package water diversion capabilities and the thermal and chemical effects on waste form degradation and radionuclide transport.

2.2.1.1.3.2.4 EBS: Drip Shield

The staff reviewed the description of the barrier capability of the drip shield. DOE discussed the capability of the drip shield to prevent or substantially reduce contact of seepage with the

waste package in SAR Section 2.1.2.2 under the discussion titled "Drip Shield," in SAR Section 2.1.2.2.1, and quantitatively in SAR Section 2.1.2.2.6. DOE supplemented its discussion in DOE Enclosure 1 (2009a). DOE addressed the drip shield's capability to prevent seepage water from contacting the waste package during the thermal period in SAR Section 2.1.2.2. (b)(5)

(b)(5)

DOE does not expect extensive drip shield failures before 100,000 years. General corrosion of the drip shield enhances the vulnerability of the drip shield to seismic events as the drip shield plates become thinner as a result of corrosion. DOE expects drip shields to fail between 200,000 and 300,000 years, when general corrosion has weakened the drip shield plates sufficiently that a seismic event can rupture them. DOE attributes the capability of the drip shield to divert water to corrosion-resistant materials coupled with a low probability of mechanical damage from seismic events and a relatively benign chemical environment during the thermal period.

(b)(5)

SAR Section 2.1.2.2.3 addressed the period over which the EBS, including the drip shield, performs its barrier function; DOE stated that the barrier capability of the drip shield and waste package is not impacted until sufficient corrosion has occurred to create breaches in the waste package. SAR Section 2.1.2.2.6 quantified the change in the effectiveness of the capability of the drip shield. (b)(5)

(b)(5)

DOE described the sources of uncertainty in the drip shield capability in SAR Section 2.1.2.2.4 and quantitatively demonstrated the effect of uncertainties in SAR Section 2.1.2.2.6. These include, for example, uncertainties in the environmental conditions affecting the drip shield. DOE described specific analyses of uncertainty in the model abstractions for drip shield degradation in SAR Sections 2.3.4.5 and 2.3.6.8. (b)(5)

(b)(5)

SAR Section 2.1.3.2 summarized the technical basis of the barrier capability of the EBS, which includes the drip shields. In its discussion, DOE identified which TSPA models it used to support the description of the barrier capability of the EBS. DOE based its description of the barrier capability of the drip shield on three TSPA submodels: (i) the mechanical damage model of the EBS features described in SAR Section 2.3.4.5, (ii) the general corrosion model described in SAR Section 2.3.6.8.1, and (iii) the early failure model described in SAR Section 2.3.6.8.4. In SAR Sections 2.2.1.3.1 and 2.2.1.3.2, the NRC staff evaluates the adequacy of the technical bases used to support the barrier capabilities of the drip shield. (b)(5)

(b)(5)

(b)(5)

Comment (b)(5)
(b)(5)

(b)(5)

2.2.1.1.3.2.5 EBS: Waste Packages

The staff reviewed the description of the barrier capability of the waste packages. DOE discussed the capability of the waste package to prevent or substantially reduce contact of seepage with the waste form in SAR Section 2.1.2.2 under the discussion titled "Waste Package," in SAR Sections 2.1.2.2.1 and 2.1.2.2.2, and quantitatively in SAR Section 2.1.2.2.6. DOE Enclosures 1 and 4 (2009an) supplemented this discussion. (b)(5)

(b)(5)

The staff notes that DOE also credited the barrier capability of the waste package for radionuclide transport through the engineered system. Specifically, the waste package inner vessel contains a large amount of stainless steel that corrodes after breach of the outer vessel. The corrosion products contain high sorption capabilities for some radionuclides. Although the ITWI component that DOE credits for this capability is the waste package inner vessel, DOE described the barrier capabilities associated with sorption to corrosion products as an aspect of the waste form and waste package internal components. SER Section 2.2.1.1.3.2.6 addresses the staff's evaluation of this barrier capability.

DOE attributed the capability of the waste package to divert water to corrosion-resistant materials coupled with a low probability of mechanical damage from seismic events and a relatively benign chemical environment. It discussed the incidence of waste package failure and concluded that extensive early failures of the waste packages are unlikely. DOE does not expect extensive waste package failures to occur until a seismic event capable of damaging the waste packages occurs. Although a model for localized corrosion is included in the TSPA analysis, DOE expects that the presence of the drip shields over the entire thermal period will prevent the occurrence of localized corrosion under the nominal or seismic scenarios. DOE indicated that waste package failures before approximately 200,000 years are primarily due to seismically induced stress corrosion cracking of codisposal waste packages containing DOE standard canisters and high-level waste. DOE attributed the higher resilience of the commercial spent nuclear fuel waste packages under seismic conditions, relative to the codisposal packages, to the damping provided by the massive transport, aging, and disposal canister containing the commercial spent fuel. Upon failure of the drip shield and filling of the drift with rubble, damage from further seismic events is unlikely. Subsequent failures are

largely associated with nominal processes affecting both commercial spent nuclear fuel waste packages and codisposal waste packages. Under nominal conditions, DOE expects approximately 50 percent of both the commercial spent nuclear fuel and codisposal waste packages to fail by stress corrosion cracking after 1 million years. The earliest general corrosion waste package failure (at the 95th percentile) is predicted to occur at 560,000 years. At 1 million years, about 10 percent of the waste packages are predicted to fail from general corrosion.

The ability of a breached waste package to prevent or reduce water flow is dependent upon the type and extent of the failure. DOE modeled stress corrosion crack breaches as allowing only diffusive release from the waste package. Larger breaches (primarily due to general corrosion and rarely due to rupture or puncture of the waste package during a seismic event) allow water flow, but a small breached area may limit the rate at which water may enter the waste package. DOE Enclosure 4 (2009an), based on the flux-splitting submodel documented in SAR Section 2.3.7.12.3.1, indicated that a waste package breached by general corrosion is still capable of significant water diversion provided that the breach area is limited to a small percentage of the waste package surface area

(b)(5)

SAR Section 2.1.2.2.3 addressed the period over which the EBS, including the waste package, performs its barrier function. DOE stated that the barrier capability of the drip shield and waste package is not impacted until sufficient corrosion has occurred to create breaches in the waste package. SAR Section 2.1.2.2.6 demonstrated the change in the effectiveness of the capability by providing time-dependent outputs of the waste package degradation model (b)(5)

(b)(5)

SAR Section 2.1.2.2.4 described the sources of uncertainty in the modeled performance of the EBS. These include, for example, uncertainties in the environmental conditions affecting the waste package, in the temperature dependence of the general corrosion rate, in the effect of microbially induced corrosion, and in the treatment of stress corrosion cracking and localized corrosion. DOE Enclosure 4 (2009an) also addresses the effects of uncertainty in corrosion processes on the ability of the waste package to divert water, noting that in most realizations, there is no breach of any waste package (b)(5)

(b)(5)

DOE summarized the technical basis of the barrier capability description of the EBS, which includes the waste packages, in SAR Section 2.1.3.2. DOE based its description of barrier capability of the waste package on six TSPA submodels: (i) the early failure model described in SAR Section 2.3.6.6.3, (ii) the general corrosion model described in SAR Section 2.3.6.3.3, (iii) the localized corrosion model described in SAR Section 2.3.6.4.3, (iv) the stress corrosion cracking model described in SAR Section 2.3.6.5.3, (v) the mechanical damage

model described in SAR Section 2.3.4.5, and (vi) the flux-splitting model described in SAR Section 2.3.7.12.3.1. SER Sections 2.2.1.3.1, 2.2.1.3.2, and 2.2.1.3.3 address the staff's evaluation of the adequacy of the technical bases used to support the barrier capability of the waste packages. (b)(5)

(b)(5)

(b)(5)

2.2.1.1.3.2.6 EBS: Waste Form and Waste Package Internal Components

The staff reviewed the description of the barrier capability of the waste form and waste package internal components. DOE provided a qualitative description of how the waste form and waste package internal components limit the release of radionuclides from a failed waste package in SAR Section 2.1.2.2 under the discussion titled "Waste Form and Waste Package Internals," in SAR Section 2.1.2.2.2, and in DOE Enclosures 1 and 5 (2009an). DOE described the performance of the waste package internal components quantitatively in SAR Section 2.1.2.2.6. DOE discussed the impacts of these processes in an aggregated fashion, using a metric that indicates the extent to which radionuclides are retained within the entire engineered system over time. Specifically, the approach identifies, for selected radionuclides, the decayed cumulative release from the engineered system (in other words, the amount of radionuclides existing within either the lower natural barrier or the accessible environment relative to the total inventory in the entire system). (b)(5)

(b)(5)

DOE attributed the barrier capability of the waste form and waste package internal components to a number of significant processes that can affect release rates. These processes include waste form degradation, precipitation and dissolution, colloid generation and stability, and sorption to and desorption from waste package internal components. These processes are in turn affected by the chemistry of the aqueous solution inside the failed waste packages as well as the water flow rate within the package. DOE described how these processes limit releases from the EBS and how these processes are associated with the different internal

components of the waste package in DOE Enclosure 5 (2009an). (b)(5)

(b)(5)

- DOE Enclosure 1 (2009an) provided a discussion and more specific association of processes with the safety classification of individual waste form and waste package internal components. For example, DOE explained that it considers the waste package inner vessel to be the dominant source of corrosion products for corrosion product sorption, and that corrosion of other internal components is not as significant and is therefore not considered ITWI.
- DOE provided specific information on the rate at which waste forms degrade in DOE Enclosure 5, Section 1.1 (2009an). DOE provided calculations based on TSPA input parameters that evaluate mean waste form lifetimes on the order of up to a few thousand years for spent fuel and tens to hundreds of thousands of years for high level waste glass waste forms, as identified in DOE Enclosure 5, Tables 1.1-1 and 1.1-2 (2009an). (b)(5)

(b)(5)

- DOE indicated in DOE Enclosure 5, Section 1.2 (2009an), on the basis of a selection of TSPA realizations, the effectiveness of the limited breach area associated with cracks for retaining radionuclides under diffusive release conditions and demonstrated that the effect of breach area on release is nuclide and breach area dependent. (b)(5)

(b)(5)

- DOE Enclosure 5, Sections 1.3 and 1.4 (2009an) indicated the effectiveness of solubility limits and sorption to corrosion products for limiting the releases from the waste package, on the basis of sensitivity analyses and selected realizations. DOE concluded that for the relatively insoluble, sorbing nuclides such as Np-237 and Pu-242, precipitation/dissolution processes are comparable in significance to sorption onto corrosion products.
- DOE addressed the significance of colloidal processes in DOE Enclosure 5, Section 1.5 (2009an). DOE does not identify transport facilitated by colloidal suspensions as significant to the barrier capability of the waste form and waste package internal components. DOE explained that colloids do not facilitate significant releases relative to dissolved forms of the same radionuclides.

(b)(5)

The time period over which the waste form and waste package internals limit the release of radionuclides is described in SAR Section 2.1.2.2.3, in which DOE described the degradation rates of the different waste forms. DOE supplemented this information in DOE Enclosure 5 (2009an), which identifies important processes controlling releases at different times in a

discussion of selected TSPA realizations and described how DOE expects the significance of various processes (e.g., solubility, radionuclide sorption) to change with time. SAR Section 2.1.2.2.6 demonstrated the change in the effectiveness of the capability by providing intermediate results from the TSPA that demonstrated the time-dependent performance of the EBS to retain selected radionuclides. (b)(5)

(b)(5)

DOE identified the sources of uncertainty in the barrier capabilities in SAR Section 2.1.2.2.4. These include, for example, uncertainties in the source term, in the evolution of in-package chemistry, in waste form degradation rates, and in radionuclide solubilities and sorption behaviors. In SAR Section 2.1.2.2.6, DOE demonstrated the effect of uncertainty on predictions of the ability of the waste form and waste package internals to limit the release of radionuclides from a failed waste package by showing uncertainty bounds on the amount of selected radionuclides retained within the EBS. (b)(5)

(b)(5)

DOE summarized the technical basis of the barrier capability description of the EBS, which included the waste form and waste package internal components, in SAR Section 2.1.3.2. DOE based its description of barrier capability of the waste form and waste package internal components on seven TSPA submodels: (i) the in-package water chemistry model described in SAR Section 2.3.7.5; (ii) three waste form degradation models described in SAR Sections 2.3.7.7, 2.3.7.8, and 2.3.7.9; (iii) the dissolved concentrations limits model described in SAR Section 2.3.7.10; (iv) the colloidal radionuclide availability model described in SAR Section 2.3.7.11; and (v) the EBS flow and transport model described in SAR Section 2.3.7.12. The staff's evaluation of the adequacy of these models in supporting the description of barrier capability is documented in SER Section 2.2.1.3.4. (b)(5)

(b)(5)

(b)(5)

2.2.1.1.3.2.7 EBS: Emplacement Pallet and Invert

DOE discussed the capabilities of the emplacement pallet and invert in SAR Section 2.1.2.2 and in DOE Enclosure 1 (2009an). DOE did not consider the emplacement pallet and invert to be ITWI, and DOE, therefore, did not provide a detailed description of their capabilities.

DOE identified a potential barrier capability of the emplacement pallet to reduce diffusive releases from the EBS by preventing contact between the waste package and invert, thereby reducing diffusive releases, but explained that this capability was not included in the TSPA. The staff notes that the mechanical integrity of the emplacement pallet affects the analyses of damage to waste packages during seismic events. The staff has separately evaluated DOE's assumptions about the potential mechanical stability of the emplacement pallet in SER Section 2.2.1.3.2.3.3.

DOE explained that the invert contributes to barrier capability because low diffusion rates and potential sorption of radionuclides in the crushed tuff ballast slow the release rate of radionuclides from the waste package to the unsaturated rock beneath the drift. However, DOE determined that the delaying effect in the invert is not significant over long time frames, so DOE classified the invert as not important to barrier capability. (b)(5)

(b)(5)

The staff reviewed DOE's description of barrier capability for the emplacement pallet and invert. Based upon examination of the EBS radionuclide transport abstraction described in SAR Section 2.3.7 and evaluated in SER Section 2.2.1.3.4, (b)(5)

(b)(5)

2.2.1.1.3.2.8 Lower Natural Barrier: Unsaturated Zone Below the Repository

The staff reviewed DOE's description of the barrier capability of the unsaturated zone below the repository. DOE identified the unsaturated zone beneath the repository as ITWI because it prevents or substantially reduces the rate of movement of radionuclides (SAR Table 2.1-1). DOE provided a qualitative description of the barrier capabilities of the unsaturated zone below the repository in SAR Section 2.1.2.3.1. In SAR Section 2.1.2.3.6 and in DOE Enclosures 1, 6, and 7 (2009an), DOE quantified the barrier capability with calculations of radionuclide travel times and reduction of radionuclide activity between the repository and the water table. (b)(5)

(b)(5)

Downward flow from the repository occurs primarily in well-connected fracture networks in the Topopah Spring welded tuff. Radionuclides leaving the emplacement drift invert will enter either the repository host rock matrix (primarily under nondripping conditions, where advective flows through the invert are negligible) or the fractures (primarily under dripping conditions, where advective flows through the invert are relatively high). In DOE's unsaturated zone transport abstraction (SAR Section 2.3.8), radionuclides may be retarded by sorption in the matrix but not in fractures. However, radionuclides can migrate from fractures to the rock matrix by matrix diffusion. DOE identified matrix diffusion, coupled with sorption in the matrix, as contributing

to barrier performance in the fracture-dominated flow paths. In the northern part of the repository area, radionuclide travel times through the lower unsaturated zone are fast because fracture-dominated flow from the repository host rock encounters a low-permeability, sparsely fractured rock unit, the zeolitic Calico Hills nonwelded tuff, and the flow is diverted laterally along the interface into transmissive faults that connect with the water table. In contrast, in the southern part of the repository area, the fracture-dominated flow from the repository host rock passes into the vitric Calico Hills nonwelded tuff, a permeable rock unit that is dominated by matrix flow conditions. Low flow velocities and the opportunity for sorption in the rock matrix result in long transport times through the unsaturated zone in the southern part of the repository area, particularly for radionuclides that can undergo sorption in the matrix.

DOE provided quantitative information on the barrier capability of the unsaturated zone below the repository in SAR Sections 2.1.2.3.6 and 2.3.8.5.4 and in DOE Enclosures 1, 6, and 7 (2009an). Using results from the TSPA-LA model with median parameter values, SAR Figures 2.3.8-43 through 2.3.8-49 indicate that the barrier performance of the lower unsaturated zone varies according to the location of the radionuclide release (i.e., northern or southern part of the repository area) and the mode of release from the repository drift into the unsaturated zone (i.e., into fractures or matrix). Because fracture flow dominates in the welded tuffs beneath the northern part and matrix flow dominates in the vitric Calico Hills tuff beneath the southern part of the repository, radionuclides released from a northern location will tend to reach the water table much faster than those released from a southern location. However, initial releases into the rock matrix will result in slow travel times regardless of release location. For example, DOE calculated that the median travel time of an unretarded tracer (Tc-99) through the lower unsaturated zone in the northern area is about 20 years for releases into fractures and about 5,000 years for releases into the matrix. For a southern release location, the calculated median travel times to the water table are slow regardless of whether releases are into fractures or the matrix, with either release mode resulting in a median arrival time of about 2,000 years (SAR Figure 2.3.8-49). Analyses documented in DOE Enclosures 1, 6, and 7 (2009an) showed that radioactive decay in the unsaturated zone coupled with a combination of matrix diffusion and sorption in the northern repository area and sorption in the vitric Calico Hills tuff layer in the southern repository area would substantially reduce releases of sorbing, short-lived radionuclides such as Cs-137. For longer lived radionuclides, DOE's analyses demonstrated that sorption slows but does not prevent their transport through the unsaturated zone. For example, DOE Enclosure 7, Tables 1-5 through 1-8 (2009an) indicated that the unsaturated zone beneath the repository (northern and southern areas combined) reduced the release of long-lived radionuclides such as Np-237 (weakly sorbing) and Pu-242 (moderately to strongly sorbing) from the EBS to the saturated zone by about 30–50 percent during the 10,000-year period and by about 5 to 30 percent over a million-year time frame.

(b)(5)

In SAR Section 2.1.2.3.3 and DOE Enclosure 7, Section 1.3 (2009an), DOE discussed the time period over which the unsaturated zone functions as a barrier. DOE stated that the hydrogeology and physical characteristics of the lower natural barrier, which includes the unsaturated zone below the repository, are not expected to significantly change within 10,000 years after closure. On the basis of the requirements of the proposed 10 CFR 63.342(c), DOE assumed that the intrinsic hydrologic, geologic, and geochemical characteristics of the lower natural barrier will not change significantly after 10,000 years

following closure but within the period of geologic stability. DOE expects changes in the unsaturated zone capability to be associated with projected increases in percolation and in the water table elevation due to changes in climate. DOE explained that sorption increases the barrier capability of the unsaturated zone below the repository because it slows the transport of sorbing radionuclides and allows for radioactive decay to reduce the total mass of radionuclides in the natural system. Information in DOE Enclosures 6 and 7 (2009an) demonstrated that the barrier capability of the unsaturated zone is more pronounced for the initial 10,000-year time frame than for a million-year time frame because sorption slows but does not prevent the release of long-lived sorbing radionuclides to the saturated zone. However, radioactive decay will reduce the total waste inventory by more than 90 percent within the first thousand years following disposal. (b)(5)

(b)(5)

DOE discussed and evaluated the uncertainties in the unsaturated zone in SAR Sections 2.1.2.3.4 and 2.3.8.5.5. DOE attributed the main uncertainties for barrier capability to (i) the variability of site characteristics and future climate and (ii) applicability of the models and assumptions used to estimate the performance of the repository system (SAR Section 2.1.2.3.4). Some examples of the uncertain characteristics included percolation flux, the extent of fracture-matrix interaction, matrix diffusion coefficients, and radionuclide distribution coefficients. DOE incorporated uncertainty in the TSPA unsaturated zone transport model by using sampled probabilistic distributions for parameter uncertainty and by using assumptions in models that would not overestimate performance. DOE demonstrated the impact of various uncertainties in SAR Figures 2.3.8-50 to 2.3.8-62. It supplemented this information with discussions of sensitivity analyses for various parameters in DOE Enclosure 7, Section 1.2 (2009an). These discussions included specific sources of uncertainty and indicated the performance impact of different sources of uncertainty. (b)(5)

(b)(5)

In SAR Section 2.1.3.3, DOE summarized the technical basis of the barrier capability description of the lower natural barrier, which includes the unsaturated zone below the repository. DOE based its description of barrier capability of the unsaturated zone below the repository on the unsaturated zone flow model described in SAR Section 2.2.2.4 and on the unsaturated zone transport model described in SAR Section 2.3.8. The staff documents its evaluation of the technical basis for the unsaturated zone flow model abstraction in SER Section 2.2.1.3.6 and for the unsaturated zone transport model abstraction in SER Section 2.2.1.3.7. (b)(5)

(b)(5)

(b)(5)

2.2.1.1.3.2.9 Lower Natural Barrier: Saturated Zone

The staff reviewed the description of the barrier capability of the saturated zone. DOE described the barrier capabilities of the saturated zone qualitatively in SAR Section 2.1.2.3.2 and used median transport times and reduction of radionuclide activity between the water table below the repository footprint and the accessible environment to quantify the barrier capability in SAR Section 2.1.2.3.6 and in DOE Enclosures 1, 6, and 7 (2009a). (b)(5)

(b)(5)

The saturated zone component of the lower natural barrier flows initially through approximately 12–14 km [7.4–8.7 mi] of fractured volcanic rocks. Beyond this distance, flow is predominantly within a saturated layer of alluvium. Flow in the fractured volcanic aquifers occurs primarily in the fractures. Hydraulic conductivities are much lower in the matrix of the volcanic tuffs than in the fractures, while the rock matrix is more porous than the fractures. These relative properties support exchange of radionuclides between the fractures and matrix through matrix diffusion. Hence, diffusion into the matrix followed by matrix sorption function to delay radionuclide transport to the accessible environment. After leaving the fractured volcanic aquifer, flow and transport occur in the intergranular pores of the alluvial sediments. Because of the low water velocity, the rate of radionuclide movement is slow, allowing more time for sorption onto the mineral surfaces to further delay radionuclide transport to the accessible environment. Dispersion of the radionuclides will tend to attenuate any abrupt changes in radionuclide concentrations as the nuclides travel through the saturated zone. The presence of colloids also affects the rate of movement of radionuclides in the saturated zone. Radionuclides embedded in or irreversibly sorbed onto colloids are retarded when the associated colloids are temporarily filtered from transport. Also, radionuclides that are sorbed reversibly to colloids are delayed by matrix diffusion in the volcanic aquifers and by sorption in the alluvial sediments.

DOE provided quantitative information on the barrier capability of the saturated zone in SAR Sections 2.1.2.3.6 and 2.3.9.3.4.1. SAR Figures 2.3.9-16 and 2.3.9-45 through 2.3.9-47 illustrated the combined effects of matrix diffusion and sorption in delaying radionuclide transport to the accessible environment. Median transport times ranged from about 10 to 10,000 years for nonsorbing radionuclides (e.g., Tc-99) and from 100 to 100,000 years for moderately sorbing radionuclides (e.g., Np-237). Median transport times generally exceeded 10,000 years for highly sorbing radionuclides (e.g., Pu-239). The median transport times for radionuclides irreversibly attached onto colloids ranged from 100 to 600,000 years. In DOE Enclosures 6 and 7 (2009a), DOE used TSPA-LA results to provide quantitative information on the barrier capability of the saturated zone in terms of reduction of radionuclide activity between the release from the unsaturated zone into the water table and the release into the accessible environment. DOE presented information on the performance of the saturated zone in Tables 1-5 through 1-8. This information indicated that DOE expects activities of soluble, short

half-life radionuclides (e.g., Cs-137 and Sr-90) to drop by 100 percent during transport to the accessible environment. For radionuclides with moderate to strong sorption and long half-life (e.g., Np-237 and Pu-242), DOE calculated the activities to drop by 70 to 98 percent during the 10,000-year period and by 20 to 50 percent during the post-10,000-year period over the transport time in the saturated zone to the accessible environment.

(b)(5)

DOE provided information on the time period over which the saturated zone performs its intended function in SAR Section 2.1.2.3.3 and DOE Enclosure 7, Section 1.3 (2009an). Additional information on the time period over which the saturated zone functions as a barrier is contained in SAR Section 2.3.9.3.4.1. DOE stated that the hydrogeology and physical characteristics of the lower natural barrier, which includes the saturated zone, are not expected to change in any significant way within 10,000 years after closure. On the basis of the requirements of 10 CFR 63.342(c), DOE assumed that the intrinsic hydrologic, geologic, and geochemical characteristics of the lower natural barrier will not change significantly after 10,000 years following closure but within the period of geologic stability. DOE addressed changes in the barrier function of the saturated zone by reference to an expected increase in groundwater recharge under projected wetter future climate conditions, resulting in a rise in the water table and increased groundwater flow. DOE did not expect these changes in groundwater flow to change the processes of sorption and matrix diffusion that control radionuclide transport to the accessible environment. DOE explained that sorption increases the barrier capability because it delays the release and allows for radioactive decay within the natural system to reduce the radionuclide mass in the system. Information in DOE Enclosures 6 and 7 (2009an) demonstrated that the barrier capability of the saturated zone is more pronounced for the initial 10,000-year time frame than for a million-year time frame. (b)(5)

(b)(5)

In SAR Section 2.1.2.3.4, DOE described the uncertainty in the barrier capability in terms of the conceptual and numerical models, observational data, and parameters used to represent water flow and radionuclide transport processes in the saturated zone. Some examples of the uncertain characteristics include groundwater-specific discharge, porosity, the spatial variation of aquifer properties, matrix diffusion coefficients, and radionuclide distribution coefficients. DOE incorporated parameter uncertainty in the TSPA saturated zone transport model through various probabilistic distributions. Effects of transport parameter uncertainty on radionuclide breakthrough at the accessible environment are presented in SAR Section 2.3.9.3.4.1 and SAR Figures 2.3.9-16 and 2.3.9-45 through 2.3.9-47. DOE also provided quantitative demonstrations of the impacts of barrier uncertainties on saturated zone flow processes in SAR Section 2.3.9.2.3.4. DOE supplemented this information with discussions of sensitivity analyses for various parameters in DOE Enclosure 7, Section 1.2 (2009an). These discussions included specific sources of uncertainty and indicated the performance impact of different

sources of uncertainty.

(b)(5)

(b)(5)

In SAR Section 2.1.3.3, DOE summarized the technical basis of the barrier capability description of the lower natural barrier, which includes the saturated zone. DOE based its description of barrier capability of the saturated zone on the saturated zone flow model described in SAR Section 2.3.9.2 and the saturated zone transport model described in SAR Section 2.3.9.3. The NRC staff's evaluation of the technical bases for these models are documented in SER Sections 2.2.1.3.8 and 2.2.1.3.9, respectively.

(b)(5)

(b)(5)

(b)(5)

2.2.1.1.4

Evaluation Findings

2.2.1.1.4.1

Identification of Barriers

DOE has identified specific features and components that are relied upon to achieve compliance with 10 CFR 63.113(b). DOE has linked these features and components to a description of their capability. These features and components include at least one from the engineered system and one from the natural system.

(b)(5)

(b)(5)

2.2.1.1.4.2

Description of Barrier Capability to Isolate Waste

Upper Natural Barrier

The staff reviewed the description of the barrier capabilities of the upper natural barrier. This barrier comprises two features: (i) the topography and surface soils at the repository location and (ii) the unsaturated zone above the repository.

(b)(5)

(b)(5)

(b)(5)

Engineered Barrier

The staff reviewed the description of the barrier capabilities of the EBS. This barrier comprises five features: (i) the emplacement drift, (ii) the drip shield, (iii) the waste package, (iv) the waste form and waste package internals, and (v) the emplacement pallet and invert. (b)(5)

(b)(5)

Lower Natural Barrier

The staff reviewed the description of the barrier capabilities of the lower natural barrier. This barrier comprises two features: the unsaturated zone below the repository and the saturated zone. (b)(5)

(b)(5)

2.2.1.1.4.3 Technical Basis for Barrier Capability

The SAR presents an overview of the technical bases for the models used to represent the performance of the barriers in the TSPA. This overview, summarized in SAR Section 2.1 and more fully documented in SAR Section 2.3, identifies the types of field investigations, laboratory studies, analog studies, literature surveys, and other technical approaches used to develop the conceptual TSPA model components. (b)(5)

(b)(5)

2.2.1.1.4.4 Evaluation Findings

(b)(5)

2.2.1.1.5 References

CNWRA and NRC. 2008aa. "Risk Insights Derived From Analyses of Model Updates in the Total-system Performance Assessment Version 5.1 Code." ML082240343. San Antonio, Texas: CNWRA.

DOE. 2009an. "Yucca Mountain—Response to Request for Additional Information Regarding License Application (Safety Analysis Report Section 2.1), Safety Evaluation Report Vol. 3, Chapter 2.2.1.1, Set 1." Letter (February 6) J.R. Williams to J.H. Sulima (NRC). ML090400455. Washington, DC: DOE, Office of Technical Management.

DOE. 2009bo. "Yucca Mountain—Response to Request for Additional Information Regarding License Application (Safety Analysis Report Sections 2.3.2 and 2.3.3), Safety Evaluation Report Vol. 3, Chapter 2.2.1.3.6, Set 1." Letter (June 1) J.R. Williams to J.H. Sulima (NRC). ML091530403. Washington, DC: DOE, Office of Technical Management.

DOE. 2009bu. "Yucca Mountain—Supplemental Response to Request for Additional Information Regarding License Application (Safety Analysis Report Section 2.1), Safety Evaluation Report Vol. 3, Chapter 2.2.1.1, Set 1." Letter (April 16) J.R. Williams to J.H. Sulima (NRC). ML091070088. Washington, DC: DOE, Office of Technical Management.

DOE. 2008ab. DOE/RW-0573, "Yucca Mountain Repository License Application." Rev. 0. ML081560400. Las Vegas, Nevada: DOE, Office of Civilian Radioactive Waste Management.

NRC. 2005aa. NUREG-1762, "Integrated Issue Resolution Status Report." Rev. 1. ML051360241. Washington, DC: NRC.

NRC. 2003aa. NUREG-1804, "Yucca Mountain Review Plan—Final Report." Rev. 2. Washington, DC. NRC.

SNL. 2008ad. "Postclosure Nuclear Safety Design Bases." ANL-WIS-MD-000024. Rev. 01. ACN 01, ERD 01, ERD 02. Las Vegas, Nevada: Sandia National Laboratories.

SNL. 2008ag. "Total System Performance Assessment Model/Analysis for the License Application." MDL-WIS-PA-000005. Rev. 00. AD 01, ERD 01, ERD 02, ERD 03, ERD 04. Las Vegas, Nevada: Sandia National Laboratories.

CHAPTER 2

2.2.1.2.1 Scenario Analysis

2.2.1.2.1.1 Introduction

This chapter provides the U.S. Nuclear Regulatory Commission (NRC) staff's evaluation of the U.S. Department of Energy's (DOE or the applicant) scenario analysis used in its performance assessment. The staff's evaluation is based on information in the Safety Analysis Report (SAR) (DOE, 2009av) as supplemented by the DOE responses to the staff's requests for additional information (RAIs) (DOE, 2009ab,ae,af,ah-aj,al,bv-bz,ca-ci,co,cq, 2010ad; ah).

A performance assessment is a systematic analysis that answers the following triplet risk questions: What can happen? How likely is it to happen? What are the resulting consequences? Scenario analysis answers the first question: What can happen? A scenario is a well-defined, connected sequence of features, events, and processes (FEPs) that can be interpreted as an outline of a possible future condition of the repository system. Thus, a scenario analysis identifies possible ways in which a geologic repository environment can evolve so that a defensible representation of the system can be developed to estimate consequences. The goal of scenario analysis is to ensure that no important aspect of the potential high-level waste repository is overlooked in the evaluation of its safety.

A scenario analysis is generally composed of four parts (Nuclear Energy Agency, 2001aa). First, a scenario analysis identifies FEPs relevant to the geologic repository system. Second, in a process known as screening, the scenario analysis evaluates and identifies FEPs for exclusion from or inclusion into the performance assessment calculations. Third, included FEPs are considered to form scenarios and scenario classes (i.e., related scenarios) from a reduced set of events. Fourth, the scenario classes are screened for implementation into the performance assessment.

Consistent with this general approach and the review areas in the Yucca Mountain Review Plan (YMRP) Section 2.2.1.2.1 (NRC, 2003aa), the staff evaluates the applicant's scenario analysis in four separate sections [Safety Evaluation Report (SER) Sections 2.2.1.2.1.3.1 to 2.2.1.2.1.3.4]. SER Section 2.2.1.2.1.3.1 evaluates both the applicant's methodology to develop a list of FEPs and its list of FEPs. In SER Section 2.2.1.2.1.3.2, the staff evaluates the applicant's screening of its list of FEPs, including the applicant's technical bases for the exclusion of FEPs. The applicant's formation of scenario classes and the exclusion of classes in the applicant's performance assessments are evaluated in SER Sections 2.2.1.2.1.3.3 and 2.2.1.2.1.3.4, respectively.

The staff's evaluation of the applicant's methodology and conclusions on the probability of events included in the performance assessments are presented in SER Section 2.2.1.2.2. That section is aimed at the second risk triplet question: How likely is it to happen? The staff's evaluation of the applicant's model abstraction is documented in SER Sections 2.2.1.3.1-2.2.1.3.14 and Sections 2.2.1.4.1-2.2.1.4.3. These sections focus on the included FEPs and the third risk triplet question (What can happen?) and present the staff's evaluation of the adequacy of assessment of consequences of included FEPs and scenario classes used in the applicant's performance assessments.

Comment (b)(5)

(b)(5)

2.2.1.2.1.2 Regulatory Requirements

A performance assessment is defined, in part, in 10 CFR 63.2 as an analysis that identifies the features, events, processes (except human intrusion), and sequences of events and processes (except human intrusion) that might affect the Yucca Mountain disposal system and their probabilities of occurring. A functional overview of the performance assessment used to demonstrate compliance with the postclosure performance objectives is presented in 10 CFR 63.102(j). 10 CFR 63.102(j) also identifies criteria for inclusion FEPs [those expected to materially affect compliance with 10 CFR 63.113(b) or be potentially adverse to performance] in the performance assessment. 10 CFR 63.102(j) identifies that events (event classes or scenario classes) that are very unlikely (less than 1 chance in 10,000 over 10,000 years) can be excluded from the analysis.

The postclosure performance objectives of 10 CFR 63.113 stipulate that a performance assessment must be used to demonstrate compliance with (i) the individual protection standard after permanent closure (10 CFR 63.311); (ii) the human intrusion standard (10 CFR 63.321 and 63.322); and (iii) the separate standards for protection of ground water (10 CFR 63.331). Requirements for any performance assessment used to demonstrate compliance with 10 CFR 63.113 for 10,000 years are presented in 10 CFR 63.114(a). 10 CFR 63.114(a)(4) requires that the performance assessment must consider only FEPs consistent with the limits on performance assessment specified at 10 CFR 63.342. 10 CFR 63.114(a)(5)–(6) requires the applicant to provide the technical basis for either inclusion or exclusion of FEPs and also defines criteria for inclusion of FEPs into the performance assessment [specific FEPs must be evaluated in detail if the magnitude and time of the resulting radiological exposures to the reasonably maximally exposed individual (RMEI), or radionuclide releases to the accessible environment, for 10,000 years after disposal, would be significantly changed by their omission]. 10 CFR 63.114(b) states that the performance assessment methods used to satisfy the requirements of paragraph (a) of that section are considered sufficient for the performance assessment for the period of time after 10,000 years and through the period of geologic stability.

10 CFR 63.113 also identifies that the performance assessments used to demonstrate compliance with the individual protection standard after permanent closure, the human intrusion standard, and the separate standards for protection of ground water must also meet the requirements of 10 CFR 63.342. The limits on performance assessments are defined in 10 CFR 63.342. According to 10 CFR 63.342(a), the performance assessment for 10,000 years after disposal to show compliance with 10 CFR 63.311(a)(1), 63.321(b)(1), and 63.331 shall not include FEPs with a chance of occurring of less than 10^{-8} per year. Also, 10 CFR 63.342(a) states that the performance assessments need not evaluate the impacts resulting from any FEPs or sequences of events and processes with a higher chance of occurring if the results of the performance assessments would not be changed significantly in the initial 10,000-year period after disposal. Thus, 10 CFR 63.342 defines the conditions for exclusion of FEPs on the basis of probability or consequence.

An additional basis for excluding FEPs in the performance assessments used to demonstrate compliance with 10 CFR 63.321(b)(1) and 63.331 during the first 10,000 years after disposal is provided in 10 CFR 63.342(b). For those performance assessments, 10 CFR 63.342(b) states that unlikely FEPs or sequences of events and processes (i.e., those that are estimated to have less than 1 chance in 100,000 per year of occurring and at least 1 chance in 100 million per year of occurring) can be excluded from the performance assessment. Also, 10 CFR 63.342(c) defines the approach to project the continued effects of FEPs beyond 10,000 years in the

Comment	(b)(5)
(b)(5)	

performance assessments models to show compliance with 10 CFR 63.311(a)(2) and 63.321(b)(2).

The cited regulations define criteria for excluding FEPs and scenario classes on the basis of probability or consequence from performance assessments used to demonstrate compliance with the standards. Guidance in YMRP Section 2.2.1.2.1.3, p. 2.2-9 identifies that specific FEPs and scenario classes can be excluded on the basis that they are specifically ruled out by regulation or are contrary to stated regulatory assumptions. For example, 10 CFR 63.305 defines the required characteristics of the reference biosphere, and FEPs that are contrary to definitions in 10 CFR 63.305 can be excluded.

Comment	(b)(5)
	(b)(5)

2.2.1.2.1.3 Technical Review

The applicant summarized in SAR Section 2.2.1 its five-step scenario analysis method used to develop a performance assessment model: (i) identification and classification of a list of FEPs, (ii) evaluation of the FEPs for inclusion or exclusion from the performance assessment model, (iii) formation of scenario classes, (iv) screening of scenario classes, and (v) definition of the implementation of scenario classes in the performance assessment model and documentation of the treatment of included FEPs. The first four steps are evaluated in this section. Step five is evaluated in SER Section 2.2.1.4.

The staff's evaluation of the scenario analysis follows the methodologies and acceptance criteria identified in YMRP Section 2.2.1.2.1. That guidance provides four criteria that DOE may use to demonstrate compliance with 10 CFR 63.114(a)(4)–(a)(6).

- The identification of a list of FEPs is adequate.
- Screening of the list of FEPs is appropriate.
- Formation of scenario classes using the reduced set of events is adequate.
- Screening of scenario classes is appropriate.

Additionally, YMRP Section 2.2.1 provides guidance to the staff on an acceptable process to apply risk information in its review of the DOE licensing application. Following the YMRP guidance, the staff considered DOE's risk information (derived from DOE's treatment of multiple barriers) and risk insights in SAR Section 2.4.2.2.1.2.

The level of detail of the staff's review on particular parts of the scenario analysis is based on the risk insights DOE developed, independent staff assessments, and precensuring interactions, as appropriate. Because the purpose of the first acceptance criterion in YMRP Section 2.2.1.2.1 is to ensure the completeness and comprehensiveness of the FEP list, the staff did not use risk information to limit its review of the applicant's identification of a list of FEPs (SER Section 2.2.1.2.1.3.1). In SER Section 2.2.1.2.1.3.2, the staff reviewed the applicant's screening of the list of FEPs following the second acceptance criterion in YMRP Section 2.2.1.2.1. The acceptance criterion includes the following three separate aspects: (i) all FEPs that are excluded are identified; (ii) justification for each excluded FEP is provided [an acceptable justification for excluding FEPs is that either the FEP is specifically excluded by regulation, probability of the FEP (generally an event) falls below the regulatory criterion, or omission of the FEP does not significantly change the magnitude and time of the resulting radiological exposures to the RMEI, or radionuclide releases to the accessible environment]; and (iii) an adequate technical basis for each excluded FEP is provided. In reviewing the technical basis for exclusion of FEPs, the staff focused in greater detail on items that were

deemed to have the largest impact on risk and used progressively less detail on items that were considered to have lower to negligible impact on risk. (b)(5)

(b)(5)

(b)(5)

The staff evaluated the technical bases of 222 excluded FEPs. In this chapter, in general, the FEPs discussed are those for which the staff issued RAI's to the applicant to supplement the technical bases for exclusion.

2.2.1.2.1.3.1 Identification of a List of FEP's

Identification of a list of FEPs is the initial step in the scenario analysis aimed at assembling a list that includes all FEPs with the potential to influence repository performance. This technical review of the identification of the list of FEPs follows the methodology established in YMRP Section 2.2.1.2.1, p. 2-2-7.

The applicant summarized the process to identify the list of FEPs in SAR Section 2.2.1.1.1 and in SNL (2008ac). DOE has published two major versions of the list of FEPs for the Yucca Mountain project: the Total System Performance Assessment-Site Recommendation (TSPA-SR) version and the Total System Performance Assessment-License Application (TSPA-LA) version. The applicant stated that the TSPA-SR FEP list was developed based on a Nuclear Energy Agency compilation of FEPs, supplemented with Yucca Mountain project literature, information in analysis reports, technical workshops, and reviews and resulted in a collection of 328 FEPs considered in TSPA-SR, as outlined in SNL p. 6-1 (2008ac).

DOE stated that the TSPA-SR FEP list was further refined to enhance classification strategies and to achieve consistent level of detail among FEPs, and that additional FEPs were identified on the basis of audits and technical information updates subsequent to the site recommendation, such as changes in design parameters. DOE stated that to verify comprehensiveness in the list of FEPs, an alternative list was developed using a top-down functional analysis of the repository (SNL, 2008ac). Each function was divided into smaller, more specialized functions until a level of detail was attained comparable to the existing list of FEPs. This alternative list was then compared to the TSPA-LA list to build confidence that the TSPA-LA list was indeed complete or to identify missing FEPs.

DOE stated that further analyses were applied to address changes in the regulations and in the design of the repository and disposal packages. The final count of FEPs is 374. The applicant stated that the iterative approach, including expanding on the existing FEP list, brainstorming, multiple reviews by subject matter experts, top-down elicitation from an independent classification scheme, and use of the Yucca Mountain project analyses support the conclusion that the TSPA-LA FEP list was complete, as described in SNL p. 6-4 (2008ac).

The staff evaluated the adequacy of the list of FEPs. The FEPs were classified by technical area, following a similar approach as in NRC Table 5.1.2.1-2 (2005aa). In numerous instances, the same FEP was classified as pertaining to several technical areas, to cover broad aspects, consequences, and couplings associated with that FEP. The objective of the split was to attain a thorough and integral review of the list of FEPs covering multiple technical perspectives and to facilitate identifying aspects potentially overlooked by the existing FEPs. The staff evaluated

the description of the scope for the individual FEPs, the screening decision of the individual FEPs, and the technical basis for excluding FEPs disposition for the included FEPs. The staff's review of the identification of the list of FEPs was based on knowledge gained reviewing the Yucca Mountain site and regional characterization data, including previous independent Yucca Mountain-related studies, and DOE's description of the modes of degradation, deterioration, and alteration of the engineered barriers. A previous staff review of DOE's identification of FEPs (Pickett and Leslie, 1999aa) was also considered. The staff also used available, internationally developed generic lists of FEPs (Nuclear Energy Agency, 1997ab) to determine the completeness of the DOE list of FEPs.

(b)(5)

The applicant further compared the TSPA-LA FEP list to a version of an international list of FEPs by the Nuclear Energy Agency, Organisation for Economic Co-operation and Development (OECD), Appendix D (Nuclear Energy Agency, 2000aa) to inquire about the completeness of the list of FEPs. The applicant documented the comparison in SNL Appendix F (2008ab) in tables mapping the license application FEPs into the OECD FEPs and vice versa.

(b)(5)

The applicant noted that the International FEP Database was updated in 2006 (Nuclear Energy Agency, 2006aa); however, the applicant concluded that the update did not present additional scope beyond the FEPs already addressed in the TSPA-LA FEP list (SAR p. 2-2-8) and SNL Appendix F (2008ab).

Staff's Findings

(b)(5)

(b)(5)

2.2.1.2.1.3.2 Screening of the List of FEP's

Screening of the list of FEPs is aimed at identifying FEPs that should be evaluated in detail in the performance assessment due to their clear potential to influence repository performance. The technical review of the screening of the list of FEPs follows the methodology established in YMRP Section 2.2.1.2.1, p. 2.2-7.

The applicant summarized the screening of FEPs in SAR Section 2.2.1.2. SAR Table 2.2-5 summarized the screening decision (included or excluded) for each FEP and the justification for exclusion. SAR Table 2.2-5 cited other SAR tables summarizing the technical basis for including the FEPs and also cited SNL (2008ab) as the document that detailed the technical basis for excluding FEPs. DOE developed criteria for exclusion on the basis of low probability, low consequence, or by regulation. The regulations define low probability as FEPs having less than a 1 in 10,000 chance of occurring within 10,000 years of disposal (10 CFR 63.342). Low consequence means that omission of FEPs would not result in significant adverse changes in the magnitude or timing of the radiological exposures to the RMEI or radionuclide releases to the accessible environment (10 CFR 63.114 and 10 CFR 63.342). By regulation means that FEPs can be excluded if they are inconsistent with the characteristics, concepts, and definitions specified in 10 CFR Part 63, as described in SNL Section 6.1 (2008ab).

The applicant supplemented the document SNL (2008ab) with Enclosure 1, Response Number 2, in DOE (2009cb) to provide a quantitative basis to argue that FEPs excluded on the basis of low probability had a probability below 1 in 10,000 in 10,000 years, as required by 10 CFR 63.342. The staff initially deemed a number of FEPs to lack adequate technical basis to support the applicant's exclusion conclusion. DOE supplemented the information (DOE, 2009ab,ae,af,ah,ai,aj,al,bv,bw,bx,by,bz,ca,cb,cc,cd,ce,cf,cg,ch,ci,co,cq, 2010ad,ah) in SNL (2008ab) to respond to RAIs. The staff reviewed the summary of the screening argument in SNL (2008ab), the supporting analyses referenced therein, and the DOE responses to RAIs (DOE, 2009ab,ae,af,ah-aj,al,bv-bz,ca-ci,co,cq, 2010ad,ah).

With respect to procedural safety controls or design configuration controls, the applicant stated that SAR Table 2.2-3 identified FEPs that relate to parameters requiring procedural safety controls or design configuration control to ensure that the TSPA-LA analysis basis is met. SAR Table 1.9-9 summarized the parameters requiring such controls. The applicant noted that the repository design (as defined in the included FEP 1.1.07.00.0A, Repository Design, and the controlled design parameters in SAR Table 2.2-3) was used to define the initial state or boundary conditions in the models and the analyses that are abstracted in the postclosure performance assessment. The applicant also stated in SAR Section 2.2.1.2 that controlled parameters and the repository design were used as a basis for describing other FEPs and as a basis for screening decisions of included and excluded FEPs. According to the applicant, SAR Table 1.9-9 presented design control parameters that describe the bases for the repository design.

Comment (b)(5)
(b)(5)

Staff's Findings

The staff used YMRP Section 2.2.1.2.1.3, Acceptance Criterion 2 to evaluate whether the screening of the list of FEPs is appropriate. This acceptance criterion evaluates (i) whether the applicant identified all FEPs that have been excluded, (ii) whether the applicant provided justification for exclusion of those FEPs, and (iii) whether the applicant provided adequate technical basis for exclusion of those FEPs.

(b)(5)

SAR Table 2.2-5 listed all of the FEPs the applicant considered, and it identified the excluded FEPs. (b)(5)

(b)(5)

With regard to point (iii) of YMRP Section 2.2.1.2.1.3, Acceptance Criterion 2, the staff's evaluation of the technical basis for the exclusion of FEPs is provided in the remainder of this section. The staff reviewed all of the screening arguments of the FEPs the applicant classified as excluded (a total of 222 FEPs). Only those (prior to the DOE RAI responses) FEPs identified as requiring additional information or clarification are discussed in this section. The discussed FEPs correspond to approximately 10 percent of the total number of excluded FEPs and are summarized later in this section under individual FEP headings. (b)(5)

(b)(5)

Example of Exclusion by Regulation

(b)(5)

Example of Exclusion by Probability

(b)(5)

(b)(5)

Example of Exclusion by Low Consequence

(b)(5)

Comment (b)(5)

(b)(5)

(b)(5)

(b)(5)

(b)(5)

FEP 1.1.01.01.0B Influx Through Holes Drilled In Drift Wall or Crown

The applicant excluded Influx Through Holes Drilled in Drift Wall or Crown on the basis of a low consequence argument as referenced in DOE Enclosure 2, Response Number 4, and Enclosure 7, Response Number 3, (2009cb) and SNL (2008ab). As defined by the applicant, this FEP addresses the potential of openings (or holes) that may be drilled through the drift walls or crown to promote flow or seepage into the drifts and onto the waste packages. These holes may be drilled for a variety of reasons including, but not limited to, rock bolt and ground support, monitoring and testing, or construction-related activities. For boreholes, FEPs 1.1.01.01.0B and 2.1.06.04.0A, Flow Through Rock Reinforcement Materials in EBS, according to the applicant's definitions, cover similar processes and features because open space will be present in boreholes regardless of whether rock bolts degrade.

The applicant stated in SAR Table 2.2-3, Parameters 01-15 and 01-16, and in SNL (2008ab) that boreholes into the walls of emplacement drifts will be drilled for ungrouted rock bolts and ground support. Using a modified version of the seepage model used for the performance assessment in BSC Sections 6.5 and 6.6.4 (2004be), DOE examined the potential for liquid water flowing into open rock bolt boreholes that extend vertically upwards from the drift crown.

The applicant concluded, supported by numerical simulations, that boreholes have only a minor effect on seepage, increasing the predicted seepage rates by less than 2 percent compared to seepage simulations without rock bolts. DOE based this result on the following considerations and assumptions: (i) an open borehole without grout acts as a capillary barrier to unsaturated flow; (ii) the cross-sectional area of the rock bolt borehole, onto which flow may be incident, is small; and (iii) water that may have seeped into the borehole can imbibe back into the rock matrix elsewhere along the borehole length. On the basis of this analysis, the applicant concluded that the presence of boreholes drilled in the drift wall or crown would not have a significant effect on seepage into drifts, and excluded the FEP Influx Through Holes Drilled in Drift Wall or Crown from the performance assessment model on the basis of low consequence.

Staff's Review

(b)(5)

(b)(5)

(b)(5)

DOE Enclosure 2,

Response Number 4, and Enclosure 7, Response Number 3, (2009cb) supplemented the screening argument and provided additional information on the relationship of field observations to flow in boreholes and seepage into drifts. The applicant framed the supplemental screening argument in terms of effects during thermal and ambient periods and relied on a total-system performance perspective; in particular, on the drip shield seepage barrier function. For the thermal period, DOE Enclosure 7, Response Number 3 (2009cb) pointed out the drip shield function of diverting water that has entered the drift. According to the applicant, the drip shields are expected to divert water during the thermal period and are expected to fail by general corrosion and cease to be a barrier against seepage well after the thermal pulse has dissipated and the system has returned to ambient conditions. DOE Enclosure 5, Response Number 7 (2009bo) referred to supplemental analyses showing that radionuclide releases are relatively

insensitive to the occurrence of seepage in the event of seismic damage to waste packages under intact drip shields.

DOE also analyzed other cases where the drip shield may fail during the thermal period (e.g., early failure, seismic fault displacement, and seismic ground motion modeling cases) and concluded that in none of those cases would borehole effects on seepage significantly alter the dose estimates. For the early failure case, the applicant referred to the low contribution of this case to the total mean dose and stated that changes in reflux would marginally affect the dose. For the fault displacement modeling case, the applicant stated that full collapse of the drift is generally associated with fault displacement, and thus, thermal reflux in open boreholes has a negligible effect on the mean annual dose from seismic fault displacement, as described in DOE Enclosure 7, Response Number 3 (2009cb). In the seismic modeling case, the applicant argued that the drip shield would fail only for large magnitude seismic events, which would be accompanied by large rockfall and borehole collapse. Therefore, thermal reflux in such boreholes would have a negligible effect on dose estimates, as detailed in DOE Enclosure 7, Response Number 3 (2009cb). (b)(5)

(b)(5)

(b)(5)

(b)(5)

According to the DOE model, seismic events would cause significant collapse of the host rock above drifts (e.g., SAR Figure 2.1-14) by the time drip shields are expected to fail by general corrosion (e.g., SAR Figure 2.1-11). (b)(5) In addition, the DOE abstraction for the igneous intrusion modeling case eliminates the seepage barrier capability of drifts. For the vapor flux through boreholes, DOE Enclosure 2, Response Number 4 (2009cb) argued that the magnitude of the vapor flux asymptotically decreases from the latter stages of the thermal period to the ambient period. (b)(5)

(b)(5)

(b)(5)

Using its condensation model, DOE stated that the magnitude of the condensation flux estimated for later times (after the thermal period) is much less than the estimated seepage flux derived from the seepage model. To provide confidence in the condensation flux estimate for early times, DOE stated that a conservative assumption of relative humidity at the drift wall of 100 percent was used in the condensation model. (b)(5)

(b)(5)

FEP 1.1.03.01.0A Error in Waste Emplacement

Comment (b)(5)

The applicant excluded Error in Waste Emplacement on the basis of low consequence (DOE, 2009af,av; SNL, 2008ab). This FEP, according to the applicant, refers to deviations from the

design or errors in waste emplacement that could affect long-term performance of the repository. The applicant identified two types of waste emplacement errors: the first concerns spacing of waste packages and the second concerns emplacement of a waste package on a fault. The applicant described controls that will be carried out to restrict by detection, evaluation, and mitigation the probability of both types of waste emplacement errors. These controls include controlled parameters and management controls. The applicant also assessed the potential consequences of undetected and unmitigated waste emplacement errors in DOE Enclosure 1, Response Number 1 (2009af). The applicant assessed the probability for waste package misplacement and violation of the thermal limits for the repository. The applicant estimated the mean number of misplaced waste packages to be less than one. The applicant compared the consequences of waste emplacement errors to the consequences of the waste package early failure modeling case and the seismic fault displacement modeling case; the applicant included both of these in the performance assessment.

Staff's Review

The staff reviewed the screening justification and the technical basis for excluding FEP 1.1.03.01.0A. The applicant provided an exclusion justification of low consequence in DOE Enclosure 1, Response Number 1 (2009af,cq). (b)(5)

(b)(5)

Comment (b)(5)
(b)(5)

(b)(5) The applicant identified that both the probability and consequence of waste emplacement error is less than that assessed in the waste package early failure model case. (b)(5)

(b)(5)

FEP 1.2.04.07.0B Ash Redistribution in Groundwater

The applicant excluded Ash Redistribution in Groundwater on the basis of low consequence. According to the applicant's definition of the FEP, during a volcanic eruption, magma may interact with waste packages, resulting in erupted deposits of volcanic ash contaminated with radionuclides. The applicant limited this FEP to the leaching of radionuclides from the ash and their subsequent transport in groundwater through the subsurface to the compliance boundary. The applicant considered other processes, such as ash remobilization by wind, in separate FEPs.

The DOE volcanic eruption model considers the mass and types of waste impacted by erupted magma (a maximum of seven damaged waste packages), the fraction of waste-containing magma that is incorporated into a tephra plume, and the fraction of the tephra plume that is deposited near the eruptive vent (i.e., in or near the repository footprint) (SNL, 2008ag). In contrast, the DOE igneous intrusion model assumes that (i) all waste packages in the repository are compromised by an igneous intrusion and (ii) the subsequent release of waste is not reduced by the amount that could be transported to the surface in an accompanying eruption (SNL, 2007ab). The applicant reasoned that because eruptive events are always associated with intrusive events, the potential dose consequences from radionuclides leached into groundwater from volcanic ash are small compared with the consequences of exposing the same inventory of radionuclides to seepage due to igneous intrusion (SNL, 2008ab). However, for the modeled fraction of volcanic ash that is deposited near the accessible environment boundary, the groundwater transport path is short compared to the transport path for radionuclides released from the repository. Short transport pathways to the accessible environment boundary have potential dose consequences for short-lived, high-activity radionuclides such as Cs-137, Sr-90, Am-241, and Pu-238, which have half-lives on the order of decades or hundreds of years. The short-lived radionuclides are important contributors to dose at early times in the volcanic eruption modeling case (e.g., SAR Figure 2.4-32).

In DOE Enclosure 1, Response Number 1 (2009ab), the applicant separately assessed the relative importance of leaching and groundwater transport of contaminated ash deposited near the accessible environment. The applicant's supporting calculation addressed differences in travel times depending on where the ash was deposited within the drainage basin of Fortymile Wash (i.e., very short flow paths for leaching of ash deposited near the accessible environment boundary and longer flow paths for ash deposited upstream). The transport calculation included the effects of radioactive decay and retardation of radionuclides and indicated that leaching of contaminated ash would not contribute significantly to mean annual dose compared to the volcanic eruption modeling case, as detailed in DOE Enclosure 1, Response Number 1, Figure 1 (2009ab).

Staff's Review

(b)(5)

(b)(5)

FEP 1.2.07.01.0A Erosion/Denudation

The applicant excluded the FEP 1.2.07.01.0A, Erosion/Denudation, from the performance assessment on the basis of low consequence. Erosion involves the transport of surficial material away from the site by mechanisms including glacial, fluvial, eolian, and chemical processes. As part of this FEP, the applicant also considered processes such as weathering, landsliding, and local uplift (BSC, 2008ab).

The applicant cited site characterization studies concluding erosion ranging from 0.4 to 2.7 cm [0.16 to 1.06 in] in 10,000 years for bedrock outcrops and 0.2 to 6 cm [0.08 to 2.4 in] in 10,000 years for unconsolidated material in hillslopes. The applicant concluded that the maximum expected erosion of 6 cm [2.4 in] in 10,000 years is consistent with existing surface irregularities and that erosion would be negligible compared with the minimum distance of 200 m [656.2 ft] from the ground surface to the repository emplacement areas (BSC, 2008ab). The applicant considered the effect of erosion on the extent of net infiltration and concluded it was negligible. Further, the applicant argued that the homogenizing action of the Paintbrush nonwelded hydrogeologic unit would buffer any localized change in net infiltration (BSC, 2008ab). The applicant stated that bedrock weathering could increase the soil thickness and decrease the net infiltration. Thus, disregarding weathering is a conservative approach. The applicant referred to site characterization studies to conclude that processes such as landslides and debris flows do not play a significant role in the erosional regime at Yucca Mountain.

The applicant argued that climatic conditions strongly influence erosional patterns, with deposition occurring during wetter periods and erosion occurring during drier periods. Because the 10,000-year period after closure is dominated by the glacial-transition climate (8,000 years of wetter climate), deposition is expected to be the dominant geomorphic process for the 10,000-year period after closure. The applicant stated that deposition leads to soil buildup, and thus, disregarding deposition is conservative. Another process affecting erosion is uplift, and the applicant stated that local rates of uplift are low, on the order of 0.01 mm/yr [3.94×10^{-4} in/yr].

Staff's Review

(b)(5)

Comment (b)(5)

(b)(5)

(b)(5)

FEP 1.2.10.01.0A Hydrologic Response to Seismic Activity

The applicant excluded Hydrologic Response to Seismic Activity on the basis of low consequence, according to DOE Enclosure 19, Response Number 19 (2009ab), DOE

(2009by,bz,ca), SNL (2008ab), and DOE Enclosure 6, Response Number 1 (2009cb). According to the applicant's definition of the FEP, seismic activity associated with fault movement may enhance existing or create new flow pathways or connections and barriers between stratigraphic units, or it may change the stress (and therefore fluid pressure) within the rock. These responses have the potential to change groundwater flow directions, water level, water chemistry, and temperature. Seismically induced changes to the local stress fields can cause a transient change in the water table elevations and lead to seismic pumping—a phenomenon the applicant defined as the temporary change in water table elevation resulting from fault movement and the opening and closing of fractures during an earthquake.

The low consequence screening argument is based on the applicant's conclusion that seismic events will result in relatively minor changes to the Yucca Mountain hydrologic system—changes that have no impact on repository performance. The applicant's rationale is based on implicit assumptions of how the repository will respond to seismic loads typical for relatively large-magnitude western U.S. earthquakes, observational evidence from recent earthquakes, and modeling results used to support the National Research Council study (National Research Council, 1992aa) on the effects of earthquakes on the water table at Yucca Mountain.

In SNL (2008ab), the applicant cited National Research Council Chapter 5 (1992aa), which indicates seismically induced water table rise ranges from a few centimeters to several tens of meters in response to seismic activity. The National Research Council study estimated that the maximum seismically induced water table rise over a 10,000-year period would be between 17 and 50 m [56 and 160 ft]. In addition, the applicant relied on the analyses in Kemeny and Cook (1992aa), who modeled transient reductions in the pore volume of bedrock resulting from the changes in shear stress along the seismogenic fault. On the basis of the information and analyses in the National Research Council Study (1992) and Kemeny and Cook (1992aa), the applicant concluded the maximum change in pore volume due to poroelastic effects will be equivalent to no more than a 50-m [160-ft] water table rise beneath the repository. The applicant also cited Gauthier, et al., pp. 163–164 (1996aa), who analyzed the potential effects of seismic activity resulting from three fault displacement types (normal, listric, and strike-slip) with 1-m [0.3-ft] displacement and 30-km [19-mi] rupture length. Gauthier, et al (1996aa) concluded that a strike-slip seismic event would cause a water table rise of 50 m [160 ft] within 1 hour and would return to steady-state conditions within 6 months. Other types and magnitudes of displacement were shown to cause smaller water table rises with similar transient durations.

The applicant also examined the effects of recent seismic events—the Landers–Big Bear–Little Skull Mountain earthquake sequence that occurred June 28–29, 1992, and the October 16, 1999, Hector Mine earthquake—on groundwater monitoring wells at Yucca Mountain and indicated that the water table rise observed at several Yucca Mountain vicinity monitoring wells ranged from 0.2 to 0.9 m [0.7 to 3 ft].

The applicant revised the rationale for excluding FEP 1.2.10.01.0A, Hydrologic Response to Seismic Activity, in supplemental documents DOE Enclosure 19, Response Number 19 (2009ab) and DOE (2009by,bz,ca). First, the applicant drew a distinction between two modeling types it used to evaluate water table rise from seismic activity in the Yucca Mountain area: the regional stress change model and the dislocation model. In making this distinction, the applicant emphasized the bounding nature of the regional stress change model; this model gave high values of predicted water table rise (higher than the dislocation model) that should be regarded as representative of the upper limits (bounds) of potential water table rise. The applicant attributed these high estimates of seismically induced water table rise to a series of simplifying

assumptions in the model. Using data from several studies since 1992, the applicant cited evidence to suggest that the dislocation model more realistically represents the actual magnitude of seismically induced water table rise. The applicant concluded that the water table rise values of the regional stress change model are overestimates of the seismically induced water table rise at Yucca Mountain.

Using the (bounding) regional stress change model and results from the Probabilistic Seismic Hazard Assessment (PSHA), the applicant performed calculations to evaluate the potential of local (to Yucca Mountain) faults as sources for future water table rise at Yucca Mountain. Using the likely seismic characteristics of faults as given in the PSHA, the applicant generated scenarios to calculate the values of maximum water table rise for each fault. Of 3,150 calculated scenarios, 13 generated water table rise exceeding 175 m [574 ft]. The applicant then calculated the probabilities that such events will occur using the PSHA hazard probabilities. Although some of the probabilities are greater than the 10^{-6} per year threshold, the applicant contended that because the regional stress change model overestimates water table rise, these results support excluding this FEP. Through the use of Probabilistic Fault Displacement Hazard Assessment results, the applicant estimated that slip events with a 10^{-6} per year probability of exceedence would produce water table rise values between 30 and 122 m [100 and 400 ft].

The applicant argued that water table rises of these magnitudes are not sufficient to reach the proposed repository, even in the case of future wetter climate conditions. The applicant estimated that the highest water table elevation beneath the repository footprint due to future wetter climate conditions would be limited to 850 m [2,790 ft] above sea level. This assumed water table elevation is generally consistent with results of a separate analysis by the applicant that used the saturated zone site-scale flow model. This separate analysis evaluated the potential effects of a future wetter climate on saturated zone flow and estimated future climate-induced water table elevations as high as 875 m [2,870 ft] above sea level (SNL, 2007ax) beneath northwestern portions of the repository. Given that the range of repository drift elevations falls between 1,040 and 1,100 m [3,400 and 3,610 ft] above sea level, the applicant concluded that water table depths under a future wetter climate would range between 187 and 250 m [620 and 820 ft] below the repository floor. Therefore, the additional transient water table rise due to a seismic event would remain below the repository drifts.

Staff's Review

(b)(5)

First, the applicant supported the poroelastic model and transient nature of any water-level changes due to an earthquake with observations from historical earthquakes, including earthquakes in the western United States and earthquakes in the vicinity of Yucca Mountain.

(b)(5)

(b)(5)

Comment (b)(5)

(b)(5)

(b)(5)

As the applicant documented in DOE (2009ca), recent observations of changes to water table elevations in unconfined aquifers from large earthquakes in Taiwan and Japan were substantially smaller than the changes in the hydraulic head of nearby confined aquifers. The applicant attributed differences in the reaction between confined and unconfined aquifers to the substantially smaller storability of confined aquifers.

(b)(5)

Comment (b)(5)

(b)(5)

FEP 1.4.01.00.0A Human Influences on Climate

The applicant excluded Human Influences on Climate on the basis of exclusion by regulation argument. The applicant stated that 10 CFR 63.305(b,c) excludes speculative prediction of changes to human behavior (SNL, 2008ab). The applicant stated that present and past human influences on climate (which are within the scope of the included FEP 1.3.01.00.0A, Climate Change) are implicitly included in estimates of modern climate used in the performance assessment (SNL, 2008ab) and, as such, are evaluated in SER Section 2.2.1.3.5.

(b)(5)

FEP 1.4.01.02.0A Greenhouse Gas Effects

The applicant excluded Greenhouse Gas Effects on climate on the basis of exclusion by regulation argument. The applicant constrained the scope of the FEP to future changes in human activities that may influence the concentrations of atmospheric gases. The applicant stated that 10 CFR 63.305(b,c) excludes speculative prediction of changes to human behavior (SNL, 2008ab). Present and past increases in greenhouse gases attributed to human activity are within the scope of the included FEP 1.3.01.00.0A, Climate Change. Those present and

past changes are implicitly included in estimates of modern climate used in the performance assessment (SNL, 2008ab) and, as such, are evaluated in SER Section 2.2.1.3.5. (b)(5)

(b)(5)

FEP 1.4.07.03.0A Recycling of Accumulated Radionuclides From Soils to Groundwater

The applicant excluded Recycling of Accumulated Radionuclides from Soil to Groundwater on the basis of a low consequence argument from a recycling model that estimated effects on the total system performance results (SNL, 2008ab). The applicant used this FEP to refer to the downward migration of contaminated irrigation water to the water table and the subsequent recapture and reuse (i.e., recycling) by irrigation wells within the contaminant plume that can potentially increase the concentration of radionuclides in the groundwater and dose to the RMEI. According to the applicant, this contaminant concentration through recycling can occur only when the infiltrating irrigation water is applied within the capture zone of a pumping well that is also capturing all or part of the contaminant plume.

The DOE screening analysis for radionuclide recycling in groundwater is based on a model that assumes a single hypothetical water supply well with an uninterrupted withdrawal rate of 3.715×10^9 L [3,000 acre-ft] per year from the center of a contaminant plume. Capture zone dimensions for this hypothetical well are computed based on the local-groundwater-specific discharge and saturated aquifer thicknesses upgradient and downgradient of the well. The applicant considered three mechanisms by which radionuclides can be lost from the recycling process: (i) irrigation water usage on fields located outside of the capture zone, (ii) residential water usage at locations outside of the capture zone, and (iii) erosion of soil from irrigated fields to locations outside of the recycling system. On the basis of current water usage in Amargosa Valley, about 90 percent of withdrawn water is used for irrigation. The applicant's screening analysis concludes that recycling could increase the total mean annual dose by approximately 7 to 11 percent for the seismic ground motion and igneous intrusion scenarios for the 1-million-year simulation period and by an average of 11 percent for the 10,000-year simulation period (SNL, 2008ab). On the basis of this result, the applicant excluded this FEP from the performance assessment.

Staff's Review

The staff reviewed the applicant's screening analysis (SNL, 2008ab) and consulted available literature relevant to irrigation practices, infiltration of irrigation water, and methods for determining capture zone geometry. The staff requested the applicant to provide a supplemental analysis to demonstrate the reasonableness of the three aspects of the applicant's screening analysis: (i) assumed capture zone geometry, (ii) assumed distances between the hypothetical pumping well and irrigated fields, and (iii) assumed instantaneous transport of recycled radionuclides through the unsaturated zone to the water table.

The assumed geometry of the capture zone for the hypothetical pumping well in the applicant's analysis (SNL, 2008ab) was based on an idealized system of a pumping well applied to a background of uniform, parallel groundwater flow lines. (b)(5)

(b)(5)

(b)(5)

The applicant provided a supplemental

analysis to show that the results of its screening analysis are not affected significantly when a converging flow field is considered, as identified in DOE Enclosure 2, Response Number 2 (2009af). (b)(5)

(b)(5)

(b)(5)

(b)(5) The applicant used a probabilistic distribution based on evidence of field locations in the Amargosa Valley community and considered a single hypothetical water supply well. (b)(5)

(b)(5)

(b)(5) The applicant supplemented its screening argument in DOE Enclosure 3, Response Number 3 (2009af) by explaining that the distances between irrigated fields and the well were not intended to represent actual distances. Rather, the screening analysis was a stylized approach constrained by requiring the pumping well to be at the location of highest concentration in the plume. The applicant provided a supplementary analysis in DOE Enclosure 3, Response Number 3 (2009af) based on a model in which the pumping wells within and adjacent to the plume are coincident with irrigated fields that vary in location and pumping duration during a 10,000-year simulation period. This supplemental analysis explicitly accounted for transport time of recycled irrigation water through the saturated zone before the water is potentially recaptured by other randomly located irrigation wells, as identified in DOE Enclosure 4, Response Number 4 (2009af). The analysis indicated that the average increase in radionuclide concentrations due to recycling of pumped water was 4.9 percent for nonsorbing radionuclides and negligible for sorbing radionuclides. This updated model does not use the steady-state approach involving a single well intersecting the highest concentration of the plume as in the original model in SNL (2008ab). The applicant concluded that the updated model is more reasonable and realistic, mimicking current practices.

To evaluate the case where the well intersects the highest concentration in the plume and irrigated fields are in proximity to the well, (b)(5)

(b)(5)

(b)(5)

FEP 2.1.03.02.0B Stress Corrosion Cracking (SCC) of Drip Shields

The applicant excluded Stress Corrosion Cracking (SCC) of Drip Shields from the performance assessment model on the basis of low consequence, as identified in DOE Enclosure 2, Response Number 2 (2009ab) and SNL (2008ab). The applicant used this FEP to consider consequences of SCC on drip shield materials. The applicant stated that the SCC of Titanium Grades 7 and 29 could occur when tensile stresses exceed a threshold tensile stress value of 80 percent and of 50 percent of the yield strength at a given temperature, respectively (SNL, 2007bb). The applicant stated that there are four possible sources of residual tensile stresses: (i) weld induced, (ii) caused by thermal expansion (i.e., thermal loading), (iii) plasticity induced caused by seismic events, and (iv) produced by rockfall and drift collapse. The applicant stated that an annealing process will be used to reduce weld-induced residual stresses below the threshold tensile stress {annealing by furnace heating at $593^{\circ}\text{C} \pm 10^{\circ}\text{C}$ [$1,100^{\circ}\text{F} \pm 50^{\circ}\text{F}$] for a minimum of 2 hours}.

Staff's Review

(b)(5)

(b)(5)

the applicant stated that drip shield connectors are designed to allow for thermal expansion with no effect on drip shield performance up to 300°C [572°F]. The thermal expansion coefficient of Titanium Grades 7 and 29 is $9.2 \times 10^{-6} \text{ K}^{-1}$ and $9.5 \times 10^{-6} \text{ K}^{-1}$, respectively (ASM International, 1994aa). (b)(5)

(b)(5)

The applicant considered that SCC may occur due to residual stresses caused by seismic events or due to stresses caused by rockfall and drift collapse. Under such conditions, through-wall cracks may form on the drip shield and seepage water may flow through those cracks. The applicant supplemented the screening argument in DOE Enclosure 2, Response Number 2 (2009ab), explaining that even if stress-corrosion cracks are assumed to penetrate the drip shield plates and remain open to water flow and if drift seepage flows through the cracks and contacts the waste package during the thermal period, the potential consequences to waste isolation are insignificant. The applicant provided an additional probabilistic analysis to compute the expected number of failed waste packages within 10,000 years on the basis of the assumption that (i) waste packages could be breached by localized corrosion as a result of seismic-induced residual-stress damage of the drip shield and (ii) stress corrosion cracks on the drip shield remain open for 10,000 years and seepage water flows through unplugged cracks. The probabilistic analysis in DOE Enclosure 2 (Number 2), Sections 1.2 and 1.5 (2009ab) estimated that the mean of the expected number of waste package failures due to advection through open stress corrosion cracks on drip shields is two to three orders of magnitude lower than the mean of the expected number of waste packages failed due to early failure of the drip shields or due to seismic fault displacement involving advective flow through the waste packages (the latter cases are included in the performance assessment model). The applicant

concluded that because the early failure drip shields and seismic fault displacement cases are not the major contributors to the mean annual dose in the performance assessment, as shown in SAR Figure 2.4-18 and DOE Enclosure 2, Response Number 2, Section 1.2 (2009ab), the inclusion of stress corrosion cracks on the drip shields would not significantly change the results of the performance assessment.

Staff's Review

(b)(5)

FEP 2.1.03.03.0B Localized Corrosion of Drip Shields

The applicant excluded Localized Corrosion of Drip Shields from the performance assessment model on the basis of low consequence (SNL, 2008ab). The applicant used this FEP to consider consequences of localized corrosion on drip shields. The applicant stated that it evaluated Titanium Grade 7 over all the anticipated ranges of pH, chloride concentration, and temperature relevant to the proposed repository. On the basis of available information, the applicant concluded that localized corrosion of Titanium Grade 7 is not expected to occur. Literature results suggest that the presence of fluoride ions can enhance the general corrosion rate of titanium alloys and possibly lead to localized corrosion. The applicant stated it examined localized corrosion of titanium alloys in fluoride-containing solutions and concluded that these types of solutions would rarely occur and that low fluoride concentration in combination with expected inhibiting species (such as nitrate, carbonate, and sulfate) is unlikely to lead to localized corrosion (SNL, 2008ab). The applicant noted that long-term corrosion tests of titanium alloys in repository-relevant environments up to 5 years did not indicate any evidence of localized corrosion. The applicant acknowledged that data on Titanium Grade 29 are sparse and that it is less resistant to localized corrosion. The applicant, therefore, postulated that localized corrosion may initiate on Titanium Grade 29. In other words, the applicant stated that existing information on localized corrosion on Titanium Grade 29 is not sufficient to rule out this process or support a notion that localized corrosion is of low probability. The applicant noted that the majority of the Titanium Grade 29 components except the side framework, however,

Comment	(b)(5)
(b)(5)	
(b)(5)	
(b)(5)	

would be located underneath the Titanium Grade 7 plates and would be exposed to benign environments. Therefore, the applicant concluded that the drip shield could experience localized corrosion only on the side framework. However, if these side frameworks collapsed, the applicant concluded that the drip shield would continue to function and protect the waste package against seepage through the Titanium Grade 7 plates (SNL, 2008ab). Therefore, the applicant excluded the FEP on the basis of low consequence.

Staff's Review

The staff reviewed the summary technical basis (SNL, 2008ab; BSC, 2004as). The staff examined the applicant's model assumptions and model support in the area related to localized corrosion of the drip shield. (b)(5)

(b)(5)

FEP 2.1.03.04.0B Hydride Cracking of Drip Shields

The applicant excluded Hydride Cracking of Drip Shields from the performance assessment model on the basis of low probability, as identified in DOE Enclosure 1, Response Number 2 (2009cb) and SNL (2008ab). According to the applicant's definition, this FEP refers to the absorption of hydrogen into the titanium drip shield materials to form mechanically weak hydrides, which could lead to the formation of cracks. The applicant noted that hydrogen absorption in titanium alloys could occur under repository conditions. The applicant evaluated hydride cracking by developing a model where hydrogen-induced cracking is assumed to occur if the absorbed hydrogen resulting from general corrosion of the drip shield into Titanium Grades 7 and 29 exceeds a critical hydrogen concentration (SNL, 2008ab). The applicant estimated that the amount of hydrogen uptake in 10,000 years would be below this critical hydrogen concentration. The applicant tracked the drip shield materials and thickness in SNL Design Control Parameter 07-04, Table 7-5 (2008ad).

The applicant also evaluated uphill diffusion along Titanium Grade 29 to Grade 7 welds, which could lead to locally elevated hydrogen concentrations near the welds. The applicant concluded in DOE Enclosure 8, Response Number 8 (2009ab) that the use of a filler metal (Titanium Grade 28) with a composition comparable to both welded components would eliminate this particular issue. By using Titanium Grade 28, is the applicant intended to provide a gradual aluminum concentration gradient to restrict hydride formation due to hydrogen redistribution. The applicant tracked the drip shield design including welds in SNL Table 7-5, Design Control Parameter 07-01 (2008ad) and the use of Titanium Grade 28 in

Comment (b)(5)

(b)(5)

(b)(5)

(b)(5)

(b)(5)

(b)(5)

Comment (b)(5)

(b)(5)

SNL Table 7-4, Design Control Parameter 07-12 (2008ad) as weld filler material for Titanium Grade 7 to Grade 29 welds.

The applicant concluded that, given the limited extent of hydrogen formation and the use of Titanium Grade 28 filler material on weld lines, Hydride Cracking of Drip Shields can be excluded from the performance assessment model (SNL, 2008ab)

Staff's Review

The staff reviewed the FEP screening technical basis in SNL (2008ab) and the DOE Enclosures 3-8, Response Numbers 3-8 (2009ab). The staff analyzed the applicant's model assumptions and model support in areas related to hydride cracking induced by hydrogen absorption resulting from general corrosion of the drip shield and hydrogen diffusion along dissimilar titanium welds. (b)(5)

(b)(5)

(b)(5)

The applicant argued that palladium and ruthenium played a beneficial role by increasing the critical hydrogen concentration value and decreasing the hydrogen absorption. (b)(5)

(b)(5)

(b)(5)

The applicant provided distributions of hydrogen in titanium due to uphill diffusion by a stress gradient in DOE Enclosure 7, Response Number 7 (2009ab) and due to uphill diffusion by aluminum concentration in SNL (2008ab). (b)(5)

(b)(5)

The applicant excluded Hydride Cracking of Drip Shields from the performance assessment model on the basis of low probability (SNL, 2008ab). The applicant updated the technical basis to show that the probability of hydride cracking of drip shields is less than 10^{-4} in 10,000 years, as detailed in DOE Enclosure 1, Response Number 2 (2009cb). The applicant argued that even with a high corrosion rate at a probability level of 2.5×10^{-5} (applied for 10,000 years), the hydrogen concentration would be below the critical hydrogen concentration for hydride cracking.

(b)(5)

FEP 2.1.03.10.0B Advection of Liquids and Solids Through Cracks in the Drip Shield

The applicant excluded the Advection of Liquids and Solids Through Cracks in the Drip Shield from the performance assessment model on the basis of low consequence, as described in DOE Enclosure 2, Response Number 2 (2009ab) and SNL (2008ab). According to the applicant's definition of the FEP, if cracks develop on the drip shield, water could flow through those cracks and contact the waste package. The applicant presented technical reasons for excluding the potential of advective flow of water through cracks in a drip shield. These involved (i) creep/stress relaxation in a drip shield (of Titanium Grade 7) could limit the development and penetration of stress corrosion cracks; (ii) a small damaged area (less than 0.5 percent) on the drip shield surface from seismic-induced rockfall could limit the surface area available for advective flow of seepage water; (iii) a low chance of large rockfall from lithophysal rock zone above the drip shield could cause sufficient stress corrosion cracks and denting of a drip shield; (iv) a low chance of large rock-block falls from the nonlithophysal rock zone above the drip shield could occur due to low probability of seismic events of sufficient magnitude; (v) potential filling and plugging of stress corrosion cracks by mineral precipitates and corrosion products could potentially limit the advective flow of water through a drip shield; (vi) a low chance of perfect alignment of tight and tortuous cracks on a drip shield surface could occur with impinging seepage drips from the drift wall; (vii) in the absence of drip shields, in less than 10 percent of the waste packages localized corrosion would be initiated [SNL Appendix O (2008ag)]; and (viii) if leakage through a crack-damaged drip shield caused a localized corrosion of the waste package, only a small flux {4 mL/yr [0.244 in³/yr]} would directly flow into the waste package, which would be insignificant from the repository performance standpoint (SNL, 2008ab). Therefore, DOE excluded the FEP from the performance assessment model on the basis of low consequence.

The applicant supplemented the screening argument with DOE Enclosure 2, Response Number 2 (2009ab) to argue that potential consequences to waste isolation are insignificant even if stress corrosion cracks are assumed to penetrate the drip shield plates and remain open to water flow and if drift seepage flows through the cracks and contacts the waste package during the thermal period. The applicant provided an additional probabilistic analysis in DOE Enclosure 2, Response Number 2, Sections 1.2 and 1.5 (2009ab) to compute the expected number of failed waste packages within 10,000 years on the basis of the assumption that (i) waste packages could be breached by localized corrosion as a result of seismic-induced, residual-stress damage to the drip shields and (ii) stress corrosion cracks on the drip shield remain open for 10,000 years and seepage water flows through unplugged stress corrosion cracks. DOE concluded that the additional number of failed waste packages would be too small to change dose estimates. In addition, the applicant stated in DOE Enclosure 2, Response Number 2, Sections 1.2 and 1.6 (2009ab) that volumetric flow through open (unplugged) cracks is expected to be smaller than volumetric seepage approaching drip shields and provided experimental evidence in DOE Enclosure 2, Response Number 2, Figure 1 (2009ab) to support this statement.

(b)(5)

FEP 2.1.06.04.0A Flow Through Rock Reinforcement Materials in EBS

The applicant excluded Flow Through Rock Reinforcement Materials in EBS on the basis of a low consequence argument in DOE Enclosure 2, Response Number 4, and Enclosure 7, Response Number 3, (2009cb) and SNL (2008ab). As defined by the applicant, this FEP

Comment (b)(5)

(b)(5)

(b)(5)

(b)(5)

(b)(5)

addresses the potential of groundwater flow to occur through the ground support materials such as wire mesh, rock bolts, grout, and liner. This FEP also evaluates the potential for ground support or its degradation products to enhance or decrease seepage (groundwater flow) into emplacement drifts, or to divert water flow within the drifts. In the performance assessment model, DOE assumes that seepage is not affected by any rock reinforcement materials. For boreholes, FEPs 1.1.01.01.0B, Influx Through Holes Drilled in Drift Wall or Crown, and 2.1.06.04.0A, as defined by the applicant, cover similar processes and features because open space will be present in boreholes regardless of whether rock bolts degrade.

DOE stated plans to employ friction-type carbon steel rock bolts with plates for use as temporary ground support during construction of the emplacement drifts, to be left in place between the rock and the permanent (Bernold-type sheets) ground support shown in SNL Design Parameter Number 01-15 (2008ad). The applicant stated in the screening argument that the seepage model indicates the presence of rock bolts does not lead to significant seepage enhancement. DOE supported this conclusion by assuming that (i) an open borehole without grout acts as a capillary barrier to unsaturated flow; (ii) a cross-sectional area of the rock bolt borehole, onto which flow may be incident, is small; and (iii) water that may have seeped into the borehole can imbibe back into the rock along its length (assumptions also related to FEP 1.1.01.01.0B, Influx Through Holes Drilled in Drift Wall or Crown). In addition, DOE indicated that the Bernold-type sheets, which are bolted to the drift walls and roof, may divert seepage. However, the applicant stated that this diversion may be limited as these sheets will be perforated and the supporting rock bolts will degrade as outlined in SNL Design Parameter 01-16 (2008ad). Therefore, DOE chose not to take credit for seepage diversion by the Bernold-type liner sheets for the period before the liner would fully corrode.

DOE stated that neither the rock bolts used as temporary ground support nor those holding the Bernold-type sheets will have a significant effect on the seepage flow rate. DOE also noted that the ground support system is expected to degrade as a result of drift degradation (BSC, 2004a). Therefore, the applicant argued that excluding the temporary ground support in the representation of seepage in the performance assessment model is a realistic representation of the system with respect to groundwater flow into the drift. DOE thus excluded Flow Through Rock Reinforcement Materials in the EBS from the performance assessment model.

The staff's evaluation for FEP 1.1.01.01.0B, Influx Through Holes Drilled in Drift Wall or Crown, discussed previously in this SER, also applies to the rock bolt aspect of FEP 2.1.06.04.0A. The basis for excluding the FEP in DOE Enclosure 2, Response Number 4, and Enclosure 7, Response Number 3 (2009cb) included the function of the drip shield, the effect on seepage rates caused by vapor flux, and the uncertainty of capillary diversion in boreholes. (b)(5)

(b)(5)

FEP 2.1.06.06.0B Oxygen Embrittlement of Drip Shields

The applicant excluded Oxygen Embrittlement of Drip Shields from the performance assessment model on the basis of low probability, as detailed in DOE Enclosure 9, Response Number 9 (2009ab) and SNL (2008ab). The applicant used this FEP to refer to oxygen embrittlement as a potential failure mechanism for the drip shields, resulting from diffusion of oxygen in titanium alloys. According to the applicant, oxygen embrittlement may affect mechanical properties of the drip shield materials. The applicant's screening argument considered oxygen diffusion data at 300 °C [572 °F] by Rogers, et al. (1988aa), who used single crystal, pure titanium to estimate the oxygen lattice diffusion coefficient in alpha-phase titanium. The applicant considered oxygen lattice diffusion data to estimate oxygen penetration depth for Titanium Grade 7 and concluded that any penetration depth would be minimal in 10,000 years. The applicant used 300 °C [572 °F] as the bounding drip shield temperature for analysis of oxygen embrittlement. The applicant stated that the 300 °C [572 °F] temperature selected for the analysis could only be exceeded in the case of a drift collapse and that the probability of conditions leading to drip shields exceeding 300 °C [572 °F] is about 1 in 10,000 within the first 10,000 years of disposal. Therefore, because of this low probability and minimal oxygen penetration that may occur in 10,000 years, oxygen embrittlement of the drip shields was deemed unlikely and this process was excluded from the performance assessment model on the basis of low probability.

The staff reviewed the screening rationale and the applicant's conclusion in DOE Enclosure 9, Response Number 9 (2009ab) and SNL (2008ab) that the penetration depth would be minimal in 10,000 years. The applicant cited the work of Liu and Welsch (1988aa) to support the statement that for alpha-phase titanium (e.g., Titanium Grade 7), oxygen diffusivity is independent of the form of the material (single crystal of polycrystalline) and that mass transport of oxygen is controlled by bulk diffusion through the alpha matrix (which is a slow process). For an alpha-beta alloy such as Titanium Grade 29, the applicant cited additional work by Liu and Welsch (1988ab) to support the statement that the properties of the alpha phase solely control the overall oxygen embrittlement. (b)(5)

(b)(5)

(b)(5)

The staff evaluates system temperature computations in SER

Section 2.2.1.3.6. (b)(5)

(b)(5)

FEP 2.1.07.02.0A Drift Collapse

DOE stated that degradation of waste emplacement drifts can occur from stresses that exceed the strength of the rock mass surrounding the drift. These stresses are attributed to several causes. One cause is excavation-induced stresses that are superimposed on the *in situ* (geostatic) stresses soon after the drifts are constructed. Another cause is thermally generated stresses. After waste emplacement, thermal stresses develop in the rocks from heat generated through radioactive decay of the emplaced waste. In addition, rocks under the influence of

Comment (b)(5)

(b)(5)

combined mechanical and thermal stresses may experience a gradual weakening with time. Occasional small seismic events and infrequent (low probability) large seismic events generate additional transient stresses in the rocks surrounding the emplacement drifts. Rocks can be expected to fail when any of the stresses, individually or in combination, exceed the rock strength. Such failures can cause a gradual accumulation of rubble on and around the engineered barriers as a result of a continuing but slow process of rockfall. Alternatively, rocks above the emplacement drift could collapse due to a combination of all the stresses that exceed the strength of the rock mass. (In this context, "rock mass strength" refers to the strength of the larger volume of rock around the waste emplacement drift whose behavior under stress is controlled by the presence of fractures, discontinuities, and cavities, as opposed to the strength of a small-sized intact rock core sample used in laboratory testing.) Both the gradual accumulation of rubble and instantaneous collapses of massive rocks may have undesirable consequences on the performance of the engineered barriers, depending on their magnitude (e.g., small, medium, or large amounts of rockfall).

DOE characterized the rock properties applied several analytical tools and numerical models to assess the long-term behavior of rocks under coupled natural and repository-induced processes as a function of time. Uncertainties in the long-term behavior of the rocks were incorporated in the analyses. The NRC staff used YMRP Section 2.2.1.2, Review Method 2, to evaluate the applicant's analyses. Specifically, the staff evaluated the applicant's analyses and calculations supporting its screening basis and its use of bounding or representative estimates for the consequences. The staff performed independent calculations using analytical tools and numerical models to scope potential issues and to verify or confirm the applicant's conclusions.

DOE considered seismically induced drift collapse in its performance assessment evaluation. This analysis is reviewed as a model abstraction in SER Section 2.2.1.3.2.3.2 and, hence, is not addressed in this subsection. However, DOE excluded drift collapse due to thermal loads and time-dependent weakening of rocks on the bases of low consequence. Under the excluded FEP evaluation, the applicant considered nonseismic drift collapse, specifically, the degradation of emplacement drifts that may result from the combination of excavation-induced rock stress and thermal loading in the absence of significant seismic events.

The applicant stated that drift degradation could occur rapidly if the stress change is large enough to cause instantaneous rock failure or gradually if the stress change is too small to cause rapid failure but large enough to weaken the rock with time. DOE summarized its basis for excluding nonseismic drift degradation in SAR Section 2.3.4.4.4 and in SNL (2008ab). DOE provided detailed supporting analyses in BSC (2004a). DOE also provided supplemental analyses and responses to NRC's RAI (DOE, 2009ae,cd,ce,cf,cg,eh). The applicant concluded that nonseismic drift degradation would cause only minor, localized rockfall that results in insignificant impact on the thermal and hydrologic conditions of the drift and minimal consequences to the EBS components.

In SAR Section 2.3.4.4.4, DOE addressed the analytic models it developed for lithophysal and nonlithophysal rock types in BSC Sections 6.3 and 6.4 (2004a). The predominant surroundings of the emplacement drifts consist of lithophysal rocks. Consequently, the staff focused its review for excluding nonseismic drift collapse on DOE's modeling of lithophysal rocks.

The applicant evaluated effects of post-excavation and thermal stresses in lithophysal rocks using a two-dimensional, drift-scale discontinuum Voronoi block model when applying the UDEC code to analyze the mechanical behavior of drifts for five rock-strength categories of lithophysal rock, as detailed in SAR Section 2.3.4.4.5 and BSC Section 6.4.2.1 (2004a).

Comment	(b)(5)
(b)(5)	

UDEC is a computer code used internationally by the rock mechanics and mining industries both as a research tool and a design tool. There are numerous, extensively peer-reviewed scientific papers and refereed journal articles on the use of UDEC code. In its implementation of the UDEC code, DOE chose the discontinuum Voronoi approach because the model allows computation of both the time-dependent stress-strain response of rock to thermal loading and the dynamic response of the rock mass under seismic events that can lead to rockfall. (Dynamic response under seismic events is discussed in SER Section 2.2.1.3.2.3.2.). The processes considered within the Voronoi domain are gravitational stresses, excavation-induced stresses, thermally induced stresses, and time-dependent strength degradation. Under the defined model domain and boundary conditions, the UDEC-Voronoi model is used to calculate mechanical response of the Voronoi domain to a set of imported temperature distributions that are updated at 45 discrete time steps to cover a 10,000-year period following repository closure.

On the basis of the staff's review of information provided in the SAR and supporting reference documents (b)(5)

(b)(5)

(b)(5)

The following subsections summarize DOE's approach and the NRC staff's evaluations for each of these aspects of the DOE technical basis and conclusions.

Characterization of Rock Mechanical and Thermal Properties

The Yucca Mountain site-specific geologic characterization of the rock units was accomplished by geologic mapping of the Topopah Spring Tuff, which was identified as the host rock. The Topopah Spring Tuff includes both lithophysal and nonlithophysal rock units. Approximately 15 percent of the emplacement block consists of nonlithophysal rocks that are hard, strong, fractured masses. The remaining 85 percent of the repository block consists of lithophysal rocks that are more deformable with lower compressive strength than the nonlithophysal units. DOE concluded that these two rock types require different rockfall analysis methods (SAR Section 2.3.4.4.2.1).

DOE performed laboratory and *in situ* testing to derive the mechanical and thermal properties of the lithophysal rocks used in its analysis. The mechanical and physical properties included elastic moduli, unconfined and triaxial compressive strength, tensile strength, density, porosity, normal and shear stiffness, and shear strength. The geometric rock fracture properties included dip and dip direction, spacing, length, surface roughness, and microstructure. These properties were obtained from laboratory tests of small- and large-diameter cores. The rock mass strength properties were established by *in-situ* measurements. Thermal properties measured

in the laboratory and *in situ* included thermal conductivity, thermal expansion coefficient, and heat capacity.

The applicant studied the time dependence of intact rock strength. These parameters (e.g., static-fatigue data at given environmental conditions of moisture and temperature) were used in the time-dependent drift degradation calculations to define the rate of strength decay as a function of stress state. The effects of sample size, anisotropy, and sample saturation were studied. DOE demonstrated that the unconfined compressive strength decreases with increases in sample size. DOE reported a maximum anisotropy of 10 percent in the average matrix moduli, which, according to DOE, is a second-order effect compared to the effect of lithophysae and fracturing on moduli and strength, as described in BSC Appendix E (2004a). The applicant also found that the variability in elastic and strength properties is not a function of lateral or vertical position within the repository host horizon, but primarily is a function of porosity of the samples (SAR Section 2.3.4.4.2.3.3.5). The applicant accounted for uncertainty in modeling the time dependence of intact rock strength by bounding the range of rock mechanical properties as a function of porosity, temperature, and saturation.

DOE stated that the major difference in fracture characteristics between the nonlithophysal and the lithophysal rocks is the trace, or fracture length. For the nonlithophysal rocks, the average fracture length is greater than or equal to 1 m [3.28 ft]; for the lithophysal rocks, fracture lengths average less than 1 m [3.28 ft]. (b)(5)

(b)(5)

The thermal properties of the lithophysal rocks were derived from laboratory and field measurements (SAR Section 2.3.4.4.2.3.6). To account for the uncertainty in the thermal properties, DOE used a coefficient for intact rock in the thermal-mechanical rockfall analysis, which DOE concludes leads to larger and, thus, conservative, thermally induced stresses (SAR Section 2.3.4.4.2.3.6.3).

A commercial discontinuum numerical modeling code (particle flow code PFC2D) was used to evaluate the effect of lithophysal size, shape, and distribution on the variability of the mechanical properties. This numerical analysis simulates the basic deformation and failure response mechanism of lithophysal tuff (BSC, 2004a). Bounding ranges for mechanical properties were established using this method. To determine rock-strength characteristics, DOE combined the PFC modeling results with the laboratory test data. The unconfined compressive strength was plotted as a function of the Young's modulus in BSC Appendix E (2004a). The analysis identified a lower bound strength cutoff at 10 MPa for lithophysal rocks. The sensitivity studies using stress analysis models found that instability would be expected to occur if the *in situ* rock strength was below about 10 MPa (SAR Section 2.3.4.4.2.3.7). DOE supported this conclusion with field observations from the existing Exploratory Studies Facility (ESF) and the Enhanced Characterization of the Repository Block (ECRB) cross-drift tunnels. Thus, this strength-Young's modulus plot is used as the basis for dividing the lithophysal rocks into five strength categories for rockfall modeling. DOE stated in BSC Section 6.4.1.2 (2004a) that the lowest ranges of strength categories with porosity greater than 20 percent likely underestimate the true rock-mass strength.

Staff's Review

The NRC staff reviewed the methods described in the SAR and (b)(5)

(b)(5)

(b)(5)

The staff reviewed the applicant's use of the PFC2D modeling code to simulate deformation and failure response mechanisms of lithophysal rocks. (b)(5)

(b)(5)

The staff questioned DOE about how uncertainties in stress-strain relationships for lithophysal rocks were characterized by the number of laboratory tests conducted, as outlined in DOE Enclosure 1, Response Number 4 (2009ce). In its response, DOE provided additional details on the stress-strain relationships for lithophysal rocks, which demonstrated that the tested rocks have a more ductile response (i.e., less prone to failure at peak stress) than the simulated rock mass in the UDEC models, as identified in DOE Enclosure 1, Response Number 4 (2009ce).

(b)(5)

Model Domain and Boundary Conditions

DOE used the NUFT thermo-hydrology continuum model to simulate the two-dimensional, drift-scale, thermal-hydrologic behavior and the FLAC 2-D continuum code to calculate thermally induced stresses. DOE used the UDEC 2-D discontinuum computer code for the drift stability analysis in lithophysal rock because the discontinuum approach best represented the highly fractured character of the lithophysal rock. In the UDEC lithophysal rockfall model, the region around the drift, where inelastic deformation is expected to occur, is discretized into discrete blocks using a mathematical relationship called a Voronoi tessellation. The Voronoi model was used to represent the random orientations of the rock blocks. DOE obtained the specified average dimension from the characterization of the rocks. In the UDEC model, the Voronoi block domain around the drift is bounded by large, continuous blocks with elastic properties. The temperature-time history from NUFT was mapped onto the UDEC grid blocks. To assess the repository edge effects and topographic influences on the temperature and thermal stress distributions, DOE performed coupled, three-dimensional (multiple drifts), regional- and drift-scale calculations using FLAC3D (three-dimensional continuum code).

A coupled three-dimensional regional- and drift-scale thermal-mechanical calculation was conducted to support the two-dimensional drift-scale calculation. The three-dimensional analysis was performed in two steps. First the regional scale thermal-mechanical calculation was used to calculate the temperature and stress changes on the entire mountain. Then the detailed local scale [also called large scale in BSC Appendix C (2004a)] thermal-mechanical analysis was performed such that the boundary conditions for temperature and stresses were obtained from the regional-scale calculation, as outlined in BSC Section 6.2 (2004a).

The temperatures and stresses calculated by the drift-scale model (NUFT-FLAC results), in which simplified rigid boundary conditions (zero displacement) are assumed for the vertical and bottom boundary planes, were compared with the coupled, three-dimensional, regional- and drift-scale model (FLAC3D results). The comparison demonstrated that the simplified rigid boundary condition used in the two-dimensional drift-scale model resulted in higher horizontal stresses compared to the three-dimensional regional model, especially at the repository edge where the confinement and temperatures are less than in the middle of the repository. Thus, DOE concluded in BSC Section 6.2 (2004a) that the two-dimensional model provides conservative conditions for use in the drift degradation analyses.

In the drift-scale calculation, a symmetric boundary condition is applied on a vertical plane halfway between the emplacement drifts. This modeling technique results in zero displacements (i.e., full confinement) perpendicular to the boundary and zero heat flux across the boundary, as described in BSC Section 6.2 (2004a). These boundaries account for the symmetry of mechanical behavior on either side of the vertical plane between parallel drifts, assuming that parallel drifts undergo similar thermal loads. The applicant compared the stresses calculated using these boundary conditions to stresses from the coupled regional and drift-scale calculations. On the basis of this comparison, DOE concluded in BSC Section 6.2 (2004a) the vertical boundary conditions in the UDEC–Voronoi model overestimate the thermal stress for drifts near the margins of the repository area.

The bottom boundary of the UDEC–Voronoi model is also fixed, which treats the underlying Earth's crust as a rigid body. The top of the model is assigned a constant-stress boundary condition, fixed at the estimated vertical *in situ* stress at a 300-m [984-ft] depth. In BSC Appendix W (2004a), DOE provided sensitivity analyses that show the calculated stresses at the drift walls are insensitive to extension of the model boundaries beyond the distances considered in the current models.

Staff's Review

The NRC staff reviewed the details of the applicant's numerical models and related calculations used to determine boundary conditions. (b)(5)

(b)(5)

To evaluate the acceptability of DOE's selection of boundary conditions, (b)(5)

(b)(5)

(b)(5)

(b)(5)

The staff reviewed the technical details of DOE's analyses, presented in BSC Appendix W (2004a), to determine whether the boundary conditions in DOE's model were appropriately selected. (b)(5)

(b)(5)

Initial Stress State and Temperature Inputs

The DOE model assesses the preexcavation *in-situ* stresses of 7 MPa vertical and 3.5 MPa horizontal for all simulations. The vertical component represents the stress at an overburden depth of 300 m [984 ft], and the horizontal component is simplified to be 3.5 MPa on the basis of an average horizontal-to-vertical stress ratio of 0.5, as identified in BSC Section 6.3.1.1 (2004a). To obtain the postexcavation equilibrium state as the initial condition for the thermal simulations, DOE performed a quasi-static simulation in which the preexcavation stresses are applied and the model is allowed to equilibrate, as detailed in BSC Section 6.4.2.2 (2004a). Once the initial postexcavation stress state is established, spatial temperature distributions are mapped onto the model grid blocks and updated for 45 discrete timesteps as a function of time over the 10,000-year simulation period following closure. The temperature inputs as a function of time are derived from the drift-scale model using the NUFT code, as outlined in BSC Appendix U (2004a), and interpolated onto the UDEC model grid. The UDEC-Voronoi model then computes changes in stress state with each update in temperature input.

Staff's Review

The staff reviewed DOE's evaluation of the initial stress state at the repository horizon.

(b)(5)

The staff reviewed the references DOE cited in BSC Section 6.3.1.1 (2004a) regarding measurements of *in-situ* horizontal stress at Yucca Mountain. (b)(5)

(b)(5)

DOE calculated the temperature inputs for the UDEC model using a detailed flow and transport code. (b)(5)

(b)(5)

Block Size and Shape in the Voronoi Domain

In DOE Enclosure 2, Response Number 1 (2009ae), DOE's evaluation of the rock types concluded that a relatively ductile and highly jointed rock mass will fail and separate from the main body preferentially along existing discontinuities, such as fractures, joints, and intersect lithophysal cavities, and crumble. In a brittle, nonlithophysal rock mass, new fractures are expected to penetrate intact rock blocks. Thus, DOE concluded in DOE Enclosure 2, Response Number 1 (2009ae) that thermal expansion of the Topopah Spring lower lithophysal tuff could result in movement along existing joints and deformation of lithophysal voids, whereas thermal expansion of the Topopah Spring nonlithophysal tuff could cause spalling of platy rock fragments from drift walls along newly created fractures.

To represent the lithophysal tuff, DOE used a Voronoi tessellation approach in the UDEC model to generate a series of model elements that represent random blocks of rock surrounding the drift opening, as described in BSC Section 6.4.2.1 (2004al). The interfaces between the blocks are intended to represent the approximate spacing and random nature of existing fractures and voids in the lithophysal rock. The blocks average 30 cm [11.8 in] in diameter and are relatively uniform in size, with the largest blocks being twice the size of the smallest blocks, as outlined in DOE Enclosure 2, Response Number 1 (2009ae). DOE concluded that an average 30-cm [11.8-in] block diameter is representative of the internal discontinuities (i.e., fractures and voids) within the lithophysal tuff. DOE conducted sensitivity analyses using average block sizes of 20 cm [7.9 in], as detailed in BSC Sections 6.4.2.3.1 and 7.6.7.1 (2004al); 10 cm [3.9 in], as outlined in DOE Enclosure 2, Response Number 1 (2009ae); and 4 cm [1.6 in], as identified in DOE Enclosure 1, Response Number 2 (2009ch). Although some realizations showed a small increase in the amount of fracturing and rockfall with decreasing average block size, DOE concluded these small increases are not significant with respect to EBS performance. DOE concluded that the results of the UDEC analyses are insensitive to variations in average block size from 4 to 30 cm [1.6 to 11.8 in].

Staff's Review

The staff reviewed DOE's technical basis used to represent lithophysal rock in the UDEC model. The staff evaluated DOE's conclusion in DOE Enclosure 2, Response Number 1 (2009ae) that yielding in heated lithophysal tuff should occur preferentially on existing structural discontinuities because the strength of the intact blocks is at least twice the strength of the discontinuous rock mass. (b)(5)

(b)(5)

(b)(5)

(b)(5)

DOE provided additional basis for its conclusions in DOE Enclosure 2, Response Number 1 (2009ae), describing that the presence of lithophysal voids creates a generally isotropic rock mass. How such voids randomized the potential effects of a strongly vertical anisotropy in the rock mass was addressed in DOE Enclosure 1, Response Number 2 (2009ch). The applicant stated that

visually apparent anisotropy does not affect damage and fracturing mechanics of the drift crown where the major principal stress and stress-induced fractures are normal to the subvertical fractures. (b)(5)

(b)(5)

(b)(5) The applicant also provided observations to demonstrate the random locations and shapes of the lithophysae and the close spacing and short trace lengths of fractures indicating that a homogeneous, isotropic model provides a reasonable model of the lithophysal unit. The size of the internal structure and spacing of fractures is much smaller than the size of a drift, and (b)(5)

(b)(5)

DOE Enclosure 4, Response Number 3 (2009ae) analyses showed that the crown of the heated drifts has an overstressed zone that is approximately tens of centimeters thick. This overstressed zone is spanned by only one to two Voronoi blocks in DOE's model. (b)(5)

(b)(5)

In DOE Enclosure 1, Response Number 2 (2009ch), DOE reduced the average size of the discretized blocks to 4 cm [1.6 in]. This sensitivity analysis simulated a larger number of small-scale fractures, resulting in minor rockfall, but leading to the same depth of fracturing as the models with larger block sizes. (b)(5)

(b)(5)

(b)(5) The applicant emphasized that the 20 to 30-cm [7.9 to 11.8-in] block sizes are appropriate because of the existing average spacing of the "preexisting" discontinuities in the rock. (b)(5)

(b)(5)

Model Calibration

In BSC Sections 7.6.3 and 7.6.4 (2004al), DOE described the approach used to calibrate the Young's modulus and unconfined compressive strength of the rock mass modeled to the expected characteristics of the lithophysal rock. Five rock-strength categories were considered in the calibration to represent the range of values for estimated Young's modulus in the lithophysal rock. For each of the five rock-strength categories considered, DOE used a mean value for unconfined compressive strength as indicated in SAR Figure 2.3.4-30. DOE then

adjusted four Voronoi block interface properties to achieve the calibration: (i) cohesion, (ii) friction angle, (iii) normal stiffness, and (iv) shear stiffness. The calibration was repeated iteratively until the UDEC model reasonably reproduced the mean unconfined compressive strength and mean Young's modulus for each rock-strength category. Separate calibrations were performed using different values of mean block size. A 30-cm [11.8-in] average block size was used for the screening analysis. Models with average block sizes of 20 cm [7.9 in] in BSC Sections 6.4.2.3.1 and 7.6.7.1 (BSC, 2004a) and 10 cm [3.9 in] in DOE Enclosure 2, Response Number 1 (2009ae) were developed for sensitivity analyses to ensure convergence of results.

A potentially important uncertainty in the DOE model is the representation of spatial variability in rock properties. DOE addressed this uncertainty by developing calibrated models for five different rock-strength categories, which are distinguished by different values of rock mass modulus. In conducting its calibration, DOE used the mean value of unconfined compressive strength as the calibration target for each selected value of rock mass modulus. DOE data, on the other hand, showed a range of potential values of unconfined compressive strength for a given value of rock mass modulus (SAR Figure 2.3.4-30). DOE stated (SAR p. 2.3.4-73) that a number of parametric studies were conducted in which the Young's modulus and strength parameters were varied to account for the reasonable bounding ranges of lithophysal and nonlithophysal rocks.

Staff's Review

The staff reviewed the results of DOE's analyses using the lower bound strength and Young's modulus for rock mass Categories 2, 3, 4, and 5, as outlined in DOE Enclosure 1, Response Number 3 (2009cd). (b)(5)

(b)(5)

The staff observed from DOE's analyses in DOE Enclosure 1, Response Number 3, Table 1 (2009cd) that the amount of rockfall at the crown area is the same for lithophysal rock Categories 2 to 5 for a range of lower bound unconfined compressive strength. DOE explained that rockfall is insensitive to the change of lower bound strength because the associated change of Young's modulus, which causes the ratios between lower bound strength and Young's modulus to vary by only a few percent as shown in DOE Enclosure 1, Response Number 3, Table 1 (2009cd). (b)(5)

(b)(5)

Model Results

The applicant conducted extensive modeling studies to estimate the timing and extent of thermal drift degradation. The following summarizes DOE's modeling results:

- The combined *in-situ* and thermal mechanical stress reached in the drift crown is about 7 MPa for Category 1 and about 37 MPa for Category 5 lithophysal rocks, respectively, as shown in BSC Figures 6-142 and 6-144 (2004a).
- These stress values can, in some conditions, slightly exceed the unconfined compressive strength of lithophysal rock.

- The elastic stress paths cover a time range of 10,000 years' variation of temperature.
- The amount of thermally induced rockfall is small for all five categories of lithophysal rocks.
- Basic rock mechanics principles show that the potential for the thermally induced rockfall process should cease at a short distance from the drift, where the confined strength of the rock is greater than the sum of mechanical and thermal stresses.

Staff's Review

(b)(5)

(b)(5)

(b)(5)

(b)(5) The UDEC-Voronoi model relies on accommodating some degree of rock stress by movement along the interfaces between adjacent blocks. When the applied stress exceeds the ability of the blocks to move, the interfaces can fail and blocks can separate from the modeled rock mass. (b)(5)

(b)(5)

(b)(5) In response, DOE provided supplemental analyses in DOE Enclosure 1, Response Number 2 (2009ch) that demonstrated failure patterns in models with 4-cm [1.6-in] average block sizes are comparable to failure patterns in models with larger block sizes. (b)(5)

(b)(5)

(b)(5)

In reviewing the UDEC–Voronoi model results, the staff (b)(5)

(b)(5)

(b)(5) DOE provided additional information in DOE Enclosure 2, Response Number 5 (2009ce) to show that although some part of the interface failed, some other parts of the interface retained sufficient strength to support the hanging block. Blocks also can remain intact if the geometry of adjacent blocks continues to support the block after an interface has failed, as shown in DOE Enclosure 2, Response Number 5 (2009ce). The staff reviewed the results of DOE's calculation (b)(5)

(b)(5)

(b)(5)

Model Support and Consistency With Available Observations

DOE supported the use of the UDEC–Voronoi model in the thermo-mechanical analyses through four investigations, as identified in BSC Section 7.6.5 (2004a) and SAR Section 2.3.4.4.5.3.2. DOE compared modeled failure mechanisms to large-core lithophysal sample failure mechanisms observed in the laboratory. DOE concluded that the UDEC model could simulate the observed patterns of fracturing due to (i) the axial splitting failure mode of lithophysal samples in unconfined compression tests and (ii) the measured strength and Young's modulus of the samples. Modeled drift-scale fracturing of the lower lithophysal tuff in the ECRB Cross-Drift also compared favorably to observations of stress-induced tunnel sidewall fracturing in the ECRB Cross-Drift.

DOE conducted detailed modeling of the Drift Scale Heater Test to determine whether the UDEC model could reasonably represent the spallation of nonlithophysal tuff observed during the test. Small amounts of spallation from the drift crown were observed during the heater tests.

Once the UDEC model was calibrated to appropriate Topopah Spring nonlithophysal tuff characteristics, the model was able to calculate small amounts of rockfall from the overstressed crown of the heated drift. DOE provided additional details of this analysis in DOE Enclosure 7, Response Number 6 (2009ae), including quantification and (b)(5)

(b)(5)

DOE used a continuum-based approach to model elastic and inelastic rock stress for a range of conditions representative of heated drifts, as described in BSC Section 7.6.5.4 (2004a). Although DOE does not consider continuum-based models as appropriate for calculating rockfall due to thermal-mechanical processes, as identified in BSC Section 7.4.1 (2004a), DOE concluded that both the continuum and the discontinuum (UDEC) models appropriately represent stress distributions prior to reaching the yielding point of the rock.

DOE supported the use of the calibrated rock-mass characteristics by comparing laboratory experiments of lithophysal rocks, as detailed in BSC Section 7.6.4 (2004a). DOE stated in BSC p. 7-61 (2004a) that the number and types of laboratory and *in-situ* experiments were insufficient to describe the complete constitutive behavior of the lithophysal tuff with a high level of confidence, particularly in the postpeak strain range and for confined conditions. Consistent with common engineering practice, DOE analyzed the continuum constitutive Mohr-Coulomb models ranging from perfectly plastic to perfectly brittle to bound the possible behavior of the lithophysal rock mass on damage and deformation. To accommodate the uncertainty represented by the limited characterization of the lithophysal tuff, DOE calibrated the UDEC-Voronoi model to give a more brittle stress-strain response than observed in tested samples, as described in BSC p. 7-38 (2004a). According to DOE, this approach enhanced the ability of rockfall to occur in the UDEC-Voronoi model, as identified in DOE Enclosure 6, Response Number 5 (2009ae).

Staff's Review

The staff reviewed the information DOE provided to support its use of the UDEC model in the thermal-mechanical analyses for drift stability. A key element of the UDEC-Voronoi model is the representation of postpeak strain. DOE presented several analyses showing calculated postpeak strains for simulated rock masses in BSC Section 7.6.4 (2004a). (b)(5)

(b)(5)

(b)(5)

In DOE Enclosure 1, Response Number 4 (2009ce), the staff requested additional information to determine if the six samples appropriately represent the range of strength characteristics needed to support the UDEC analyses in BSC Figure 7-16 (2004a).

In the response to an RAI related to the rock-mass categories [DOE Enclosure 1, Response Number 4 (2009ce)], the applicant stated that in modeling the rock mass responses, it applied a bounding approach to those five rock mass categories (lower bound relations between stiffness and strength cover and bound the loading response). This approach is meant to encompass the variability and uncertainties of the laboratory and field data. For postpeak response, the UDEC-Voronoi block model was calibrated to bound the brittleness of the lithophysal rock mass observed from the experimental data. This was achieved by bounding all test data in the axial

stress versus axial strain curve, as outlined in DOE Enclosure 1, Response Number 4 (2009ce).

(b)(5)

Treatment of Time-Dependent Failure

Time-dependent failure refers to the potential for rock to fail by gradual weakening under stresses less than the rock strength, if the rock is subjected to that stress for long periods of time. DOE considers the potential for time-dependent failure as a function of the ratio of applied stress to the rock strength. DOE evaluated the relationship of time to failure on the basis of two sets of test data for stress ratios ranging from about 0.8 to 1.0. A best linear fit between the stress ratio and the logarithm of time was calculated and used to extrapolate times to failure for stress ratios less than 0.8. For the extrapolated portion of this curve, predicted times to failure ranged from approximately 12 days (10^6 s) at a ratio of 0.8 to about 32,000 years (10^{12} s) at a ratio of 0.6. Below values of 0.55, no time-dependent failure is predicted. In BSC Appendix S (2004a), DOE supported the use of a linear fit approximation by comparison to a previous study of data from Lac du Bonnet granite and concluded that the linear fit is appropriate. DOE evaluated the uncertainty in the time-to-failure estimates by running the UDEC model for rock Categories 1, 2, and 5 using times to failure based on the Lac du Bonnet data.

In a response to a staff RAI, DOE Enclosure 3, Response Number 2 (2009ae) acknowledged uncertainty in the data used for the linear fit and cited observations from the ECRB and ESF as additional evidence that time to failure is not overestimated. DOE stated that stress ratios in the range of 0.58 to 1.0 are represented at unsupported drift spring-lines for a longer time (greater than 10 years) than is available from any experiment, and no significant degradation has occurred.

Staff's Review

The staff evaluated the extent to which time-to-failure estimates could affect predicted drift degradation, especially in the range of stress ratios between 0.6 and 0.7, for which time-to-failure data for tuff are not available but relatively long times to failure are predicted (i.e., 32 years for a ratio of 0.7 and to 32,000 years for a ratio of 0.6). There is uncertainty in these estimates because the data points are few and the correlation coefficient for the linear fit to the data is relatively low as shown in BSC Figure S-27 (2004a) (e.g., SAR Figure 2.3.4-44). Numerical analyses by DOE, shown in BSC Figures S-14 through S-21 (2004a), also suggested times to failure for this range of stress ratio could be on the order of a few days to a few years. In a response to the staff's earlier request for information on this topic in DOE Enclosure 4, Response Number 3 (2009ae), DOE cited observations from the ECRB and ESF tunnels, stating that these tunnels represent stress ratios between 0.58 and 1.0; however, significant rock failure has yet to occur.

In DOE Enclosure 1, Response Number 6 (2009cg), the applicant indicated that the uncertainty in time-dependent strength degradation of the lithophysal tuff was not represented in the thermo-mechanical calculations of drift stability, because the static-fatigue curve, based on the 1997 tuff data, bounds the potential for thermally induced drift degradation. Bounding was achieved by applying the Lac du Bonnet static-fatigue relationships for granite to the lithophysal tuff data. (b)(5)

(b)(5)

(b)(5)

The applicant also indicated that temperatures in the range between ambient and 200 °C [392 °F] have a small

effect on the tuff mechanical properties, including short-term strength and time to failure. The staff reviewed DOE's information (b)(5)

(b)(5)

Alternative Conceptual Models

The applicant considered alternative conceptual models that were based on assumptions and simplifications that differed from those of the base-case models discussed previously and described in BSC Section 6.7 (2004a). The conceptual models the applicant considered included continuum models. In a continuum model, the lithophysae and fractures are smeared into the elements of a continuous rock mass, where there is no slip between model elements. In the discontinuum model, lithophysae and fractures are represented by joints between the Voronoi blocks and slip can occur between these model elements. (b)(5)

(b)(5)

NRC Review of Alternative Conceptual Models

The staff reviewed the technical basis DOE provided in its evaluation of alternative conceptual models to the UDEC-Voronoi approach. As discussed in previous sections, (b)(5)

(b)(5)

(b)(5)

(b)(5)

Comment (b)(5)
(b)(5)

(b)(5)

Summary of DOE's Analysis and NRC Staff Review

DOE analyzed the thermally induced stresses causing instability of the waste emplacement drifts, compared the calculated stresses to the estimated strength of the rock mass, and estimated the timing and extent of potential drift degradation under anticipated loads (b)(5)

(b)(5)

(b)(5)

The NRC staff has reviewed the SAR, associated references (BSC, 2004a), and responses to the staff's RAI in its evaluation of DOE's exclusion of drift collapse due to thermal stresses and time-dependent rock weakening. (b)(5)

(b)(5)

DOE accounted for variability in rock types and a range of mechanical properties and strength characteristics, on the basis of laboratory tests and field investigations. DOE, in its design basis analysis (SAR), (b)(5)

(b)(5)

Staff Findings

The staff reviewed the models and results DOE used for screening out thermally induced drift degradation at the proposed Yucca Mountain repository using risk-informed, performance-based review methods described in the YMRP. (b)(5)

(b)(5)

FEP 2.1.07.05.0B Creep of Metallic Materials in the Drip Shield

The applicant excluded Creep of Metallic Materials in the Drip Shield from the performance assessment model on the basis of low consequence (SNL, 2008ab). Creep refers to time and temperature-dependent plastic (i.e., permanent) deformation of material caused by static loading. The applicant used the FEP Creep of Metallic Materials in the Drip Shield to consider creep as a potential degradation process affecting the drip shield. Due to the long duration of the regulatory period and the possibility of early drift collapse after the waste emplacement, the applicant noted the importance of the analysis of time-dependent deformation and the stability of the drip shield when nonuniformly loaded by the rock rubble mass.

DOE developed constitutive equations to express the amount of creep strain for Titanium Grades 7 and 29 as a function of temperature, applied stress, and time. DOE Enclosure 5, Response Number 6, Section 1.2.1 (2009af) assumed a drip shield temperature of 150 °C [302 °F] for the screening analysis. DOE stated that higher drip shield temperatures would only be reached in the event of near-complete drift collapse within the first few hundred years after repository closure and that, even for early drift collapse, the temperature will drop below 150 °C [302 °F] within 600 to 1,000 years after waste disposal. The applicant concluded that it was reasonable to assume a constant temperature of 150 °C [302 °F] for the screening analysis because the creep susceptibility of titanium alloys generally decreases with decreasing temperature and 150 °C [302 °F] is an overestimate of the drip shield temperature for most of the postclosure period.

In BSC Attachment I (2005an), the applicant used titanium creep data from the literature to derive creep equations for Titanium Grades 7 and 29 at 150 °C [302 °F]. Because there are limited creep data in the literature for titanium alloys for temperatures around 150 °C [302 °F], the applicant first derived equations to represent the creep behavior at room temperature, then rescaled those equations to a temperature of 150 °C [302 °F] using information about effects of temperature on creep kinetics. To derive the room temperature creep equation for Titanium Grade 7, DOE fitted a power-law-type equation to the 27-year creep data for Titanium Grade 2 from Drefahl, et al. (1985aa). The applicant used BSC Eq. (I-8) (2005an) to represent the room-temperature creep of Titanium Grade 7. To derive the room-temperature creep equation for Titanium Grade 29, DOE fitted a power-law-type equation to the 1,000-hour creep data for Titanium Grade 5 from Odegard and Thompson (1974aa). The applicant used BSC Eq. (I-19) (2005an) to represent the room-temperature creep of Titanium Grade 29. To rescale the room-temperature creep equations to represent the creep behavior at 150 °C [302 °F], DOE first accounted for the difference in yield stress at the respective temperatures, using BSC Eq. (I-7) (2005an). The applicant then rescaled the creep equations using BSC Eq. (I-12) (2005an) assuming an activation energy of 30 kJ/mol. In this manner, DOE derived BSC Eqs. (I-15) and (I-22) (2005an) to represent the creep behavior of Titanium Grades 7 and 29, respectively, at 150 °C [302 °F]. The applicant compared the creep strains the equations calculated to literature data for creep of titanium alloys at 150 °C [302 °F] (Kiessel and Sinnott, 1953aa; Odegard and Thompson, 1974aa). DOE stated that the equations used to represent the creep behavior of Titanium Grades 7 and 29 at 150 °C [302 °F] are acceptable because they predict greater creep strain than reported in the technical literature.

In the second part of the DOE creep analysis, DOE performed a finite element structural analysis of the drip shield, considering six potential loading scenarios derived from BSC (2004al) and using the constitutive creep equations to analyze the extent of drip shield creep. DOE assumed that creep will cause the drip shield to collapse when tertiary creep begins at any point on the drip shield. Tertiary creep refers to a rapid increase in creep strain rate associated with material instability, leading to rupture. The applicant assumed a tertiary creep threshold of 10 percent strain and concluded that this threshold is conservative because experimental observations (Drefahl, et al., 1985aa) indicated that the onset of tertiary creep in titanium alloys occurs at about 15 percent strain. On the basis of creep analyses cited in the FEP screening argument (SNL, 2008ab), the applicant concluded that the maximum strain is below the onset strain for tertiary creep. Therefore, creep would not impact the drip shield's ability to divert seepage and protect the waste package from anticipated loads. The applicant concluded that it is appropriate to exclude the FEP Creep of Metallic Materials in the Drip Shield from the performance assessment model on the basis of low consequence (SNL, 2008ab).

The staff reviewed the applicant's justification for assuming a constant temperature of 150 °C [302 °F] for the creep analysis. In BSC (2005an), DOE represented titanium creep as a thermally activated process, where the susceptibility to creep increases with increasing temperature. (b)(5)

(b)(5)

(b)(5) In BSC Assumption 3.2.4 (BSC, 2005an), however, the applicant stated that the drip shield temperature may exceed 150 °C [302 °F] for several hundred years in the event of early drift collapse. (b)(5)

(b)(5)

(b)(5) The applicant stated in DOE Enclosure 5, Response Number 6, Section 1.2.1 (2009af) that 300 °C [572 °F] is a reasonably bounding temperature because there is less than 10^{-4} probability that a drip shield will exceed this temperature for early drift collapse. Further, in DOE Enclosure 5, Response Number 6, Section 1.2.3 (2009af), DOE stated that the creep equations for 150 °C [302 °F], will not underestimate the extent of creep at 300 °C [572 °F] because above 150 °C [302 °F] creep becomes an athermal process (i.e., the susceptibility to creep does not increase with temperature). DOE attributed this behavior to the phenomenon of dynamic strain aging: a process whereby solute impurity atoms diffuse to areas of dislocations and impede dislocation motion. (b)(5)

(b)(5)

The staff reviewed the applicant's methodology to develop equations to represent the creep of Titanium Grades 7 and 29 at room temperature. With respect to Titanium Grade 7 (b)(5)

(b)(5)

(b)(5)

The staff reviewed the applicant's methodology to rescale the room-temperature creep equations for Titanium Grades 7 and 29 to 150 °C [302 °F]. In rescaling the room-temperature creep equations (b)(5)

(b)(5)

(b)(5) DOE's selected activation energy of 30 kJ/mol is lower than the activation energy of approximately 150 kJ/mol Kiessel and Sinnott (1953aa) and Stetina (1969aa) reported. In BSC (2005an), the applicant represented the creep strain temperature-dependence as an exponential function of the activation energy, such that a small change in the activation energy would yield a large change in the calculated creep strain. Therefore, the staff submitted an RAI to DOE requesting the applicant to address how its methodology for rescaling the room-temperature creep equations to 150 °C [302 °F] accounts for the uncertainty in the creep temperature dependence. In DOE Enclosure 6, Response Number 7 (2009af), the applicant stated that the activation energy for titanium creep depends on the rate-limiting deformation mechanism which, in turn, depends on a number of parameters including the alloy microstructure, phase composition, and strain rate. The applicant further stated that literature reports that give higher activation energy than used in its creep analysis do not provide sufficient information about the material and test conditions to support a direct comparison of the activation energies. (b)(5)

(b)(5)

The staff reviewed the information the applicant provided in DOE Enclosure 6, Response Number 7 (2009af). (b)(5)

(b)(5)

(b)(5) Further, DOE calculated greater creep strain at 99 and 204 °C [210 and 399.2 °F] than Kiessel and Sinnott (1953aa) measured for commercially pure titanium at these temperatures. (b)(5)

(b)(5)

(b)(5)

The staff reviewed the applicant's assumption that a creep strain of 10 percent anywhere on the drip shield will cause its collapse and that any strain smaller than that will not significantly affect the drip shield. (b)(5)

(b)(5)

The staff reviewed the applicant's finite difference structural analyses on creep deformation of the drip shield. (b)(5)

(b)(5)

FEP 2.1.09.03.0B Volume Increase of Corrosion Products Impacts Waste Package

The applicant excluded Volume Increase of Corrosion Products Impacts Waste Package from the performance assessment model on the basis of low consequence. In the FEP, the applicant considered volume increase of corrosion products (increase due to the higher molar volume of corrosion products than intact, uncorroded material) from the waste form, cladding, and waste package as a mechanism that could damage the waste package.

The applicant excluded the effect of volume increase of corrosion products on the basis of the following: (i) if the outer container is not breached, there will be negligible corrosion products; (ii) there are unlikely events leading to early waste package outer container failure; (iii) extended time (thousands of years) is needed for corrosion products to fill the space between the outer and inner containers before any significant stress buildup occurs; (iv) due to the higher Alloy 22 mechanical strength compared to the stainless steel strength, there is a higher likelihood for the inner stainless steel container to deform or crack if additional stresses develop due to the corrosion product buildup; and (v) extensive time is needed for the development of stresses needed to promote SCC on the waste package outer container.

The staff reviewed the summary technical basis in the FEP document (SNL, 2008ab) and DOE Enclosure 10, Response Number 10, and Enclosure 11, Response Number 11 (2009ab) on the screening argument. The applicant stated that prior to breach of the Alloy 22 waste package outer container, only dry oxidation by residual moisture is possible on the Alloy 22 inner surface or on the surface of the stainless steel inner container. The applicant concluded that the residual moisture in the waste package will not result in a large volume of corrosion products to cause mechanical damage to the Alloy 22 or stainless steel container. (b)(5)

(b)(5)

The applicant assessed that for significant corrosion of Alloy 22 inner surface and the stainless steel container, the Alloy 22 outer container must first be breached. The Alloy 22 general corrosion rates are low. SCC in the absence of weld flaws or seismic activity would not breach the outer container in 10,000 years after waste emplacement, according to the applicant. Combinations of large flaws and stresses are uncommon, and large magnitude seismic events capable to fail the waste packages within the first 10,000 years after waste emplacement are rare, according to the applicant. Nonetheless, to address the case of container failure due, for example, to seismic events, the applicant assumed failure of the outer container and conducted two analyses to estimate the magnitude and timing of stresses on the waste package outer container from the corrosion products from the inner vessel corrosion. The applicant performed analyses to show that stresses sufficient to enhance degradation of the outer container would not develop within 10,000 years after breach of the waste package outer container, as described in DOE Enclosure 10, Response Number 10 (2009ab).

In the applicant's assessment of the dependence of volume increase of corrosion products on outer container corrosion, the applicant considered information on Alloy 22 general corrosion rates. (b)(5)

(b)(5)

With regard to early failure, localized corrosion, or igneous intrusion model cases, the applicant stated that the performance assessment for these model cases does not take credit for the further presence of the waste package; thus, volume increase of corrosion products would not change the estimated consequences, as outlined in DOE Enclosure 10, Response Number 10 (2009ab).

On the basis of DOE Enclosure 10, Response Number 10, and Enclosure 11, Response Number 11 (2009ab) (b)(5)

(b)(5)

(b)(5)

The applicant estimated that the gap between the inner and outer containers would be filled with corrosion products after thousands of years (between 1,400 and 37,000 years) after breaching of the outer container (SNL, 2008ab). The time for stress buildup sufficient to cause SCC on the waste package outer container would exceed 10,000 years after the initial waste package breach, according to DOE Enclosure 10, Response Number 10 (2009ab). (b)(5)

(b)(5)

(b)(5)

the applicant argued that the extent of the area compromised by cracks is overestimated by the consideration of a crack distribution that fills a two-dimensional space, and consideration of a stress level equal to the yield strength of the material (as opposed to allowing the stress to relax when cracks form or grow), as detailed in DOE Enclosure 10, Response Number 10, and Enclosure 5, Response Number 5, respectively, (2009ab,c) and SNL Section 6.7.3 (2007bb). (b)(5)

(b)(5)

(b)(5)

FEP 2.1.09.28.0A Localized Corrosion on Waste Package Outer Surface Due to Deliquescence

The applicant excluded Localized Corrosion on Waste Package Outer Surface Due to Deliquescence on the basis of low consequence (SNL, 2008ab). In the FEP, the applicant considered that moisture from air could be absorbed by salts in dust deposited on the waste package, even at low relative humidity; this moisture could dissolve the salts and create concentrated aqueous solutions or brine. According to the applicant, these brines could promote localized corrosion of the waste package outer surface.

The applicant's analysis penetration of the Alloy 22 waste package outer barrier by localized corrosion induced by dust deliquescence brines was based on the following five questions from SNL, pp. 6-705 to 6-710 (2008ab)

1. Can multiple-salt deliquescent brines form at elevated temperature?
2. If deliquescent brines form at elevated temperature, will they persist?
3. If deliquescent brines persist, will they be corrosive?
4. If deliquescent brines are potentially corrosive, will they initiate localized corrosion?
5. Once initiated, will localized corrosion penetrate the waste package?

In SNL (2008ab), the applicant stated that the answers to those questions are (1) yes, (2) sometimes, (3) not expected, (4) no, and (5) no, respectively. Because all of the questions must be answered affirmatively for outer container penetration to be possible, the applicant concluded that localized corrosion was unlikely. In summary, the applicant concluded that brines formed by dust deliquescence are not expected to be aggressive; the amount of brine volume that will be distributed on the waste package will be extremely small and will not support the initiation of localized corrosion; and several processes will stifle localized corrosion limiting, penetration of the waste package outer container (SNL, 2008ab). Accordingly, the applicant excluded Localized Corrosion on Waste Package Outer Surface Due to Deliquescence from the performance assessment model.

Staff's Review

The staff reviewed the technical basis in the FEP document (SNL, 2008ab), BSC (2005aa), SNL (2007a), and the analysis to supplement the screening argument in DOE Enclosures 12 to 15, Response Numbers 12 to 15 (2009ab). The staff reviewed the screening rationale.

(b)(5)

(b)(5)

FEP 2.1.11.06.0A Thermal Sensitization of Waste Packages

The applicant excluded Thermal Sensitization of Waste Packages from the performance assessment model on the basis of low consequence (SNL, 2008ab). According to the applicant's definition of the FEP, phase changes in waste package materials could result from long-term storage under repository thermal conditions, phase changes could affect the corrosion resistance and mechanical properties of waste package materials. The applicant described a model for long-term thermal aging and phase stability of Alloy 22 based on experimental measurements and theoretical calculations (BSC, 2004ab; DOE, 2009av). The phase stability studies included tetrahedrally close-packed phase precipitation in the base metal and in the welded regions, and long-range ordering reactions. The applicant conducted thermodynamic and kinetic modeling to predict the rate of precipitation of tetrahedrally close-packed phases and long-range ordering in Alloy 22 using the Thermo-Calc and DICTRA software and databases. The applicant assessed validity of the aging and phase stability model and the databases in BSC (2004ab) and DOE Enclosure 16, Response Number 16, and Enclosure 17, Response Number 17 (2009ab). According to the calculated time-temperature-transformation diagrams for the formation of P, σ , and ordered phases in Alloy 22 base metal, the applicant stated that precipitation of these phases greater than 2 percent transformation rate will not occur under the repository conditions. According to the applicant, the planned solution annealing and quenching conditions for the waste package outer container are sufficient to prevent phase instability in Alloy 22. The applicant compared the model results to the extent of tetrahedrally close-packed phase precipitation obtained from short-term aging experiments at temperature ranges exceeding those expected in the repository and the extent of long-range ordering from microhardness measurements. On the basis of these results, the applicant concluded that

insignificant aging and phase instability would occur in Alloy 22 under conditions that bound repository temperatures the applicant estimated.

The applicant also evaluated the effects of welding and thermal aging on the corrosion rate and localized corrosion resistance of Alloy 22 in the mill-annealed, as-welded, and as-welded plus thermally aged conditions (SNL, 2007ab,al). On the basis of the results of short-term electrochemical tests, the applicant stated that thermal aging and phase instability do not adversely affect the corrosion resistance of Alloy 22. In summary, the applicant concluded that, on the basis of the model predictions and experimental evidence, long-term thermal aging is insignificant and phase instability is not expected to adversely affect the corrosion resistance of the waste package outer container. Therefore, the applicant excluded the FEP from the performance assessment model on the basis of low consequence. On the basis of the aging and phase stability analysis, the applicant also imposed a restricted Alloy 22 composition range, which has a narrower range of chemical compositions for Cr, Mo, Fe, and W compared to the composition limits specified in the standard ASTM B 575-04 (ASTM International, 2004aa). According to the applicant, the design properties for Alloy 22 are in compliance with the ASME SB-575 specification (American Society of Mechanical Engineers, 2001aa).

Staff's Review

The staff reviewed the applicant's technical basis for excluding the FEP and its model assumptions and model support in areas related to long-term thermal aging and phase stability of Alloy 22, as detailed in DOE Enclosure 16, Response Number 16, and Enclosure 17, Response Number 17 (2009ab) and BSC (2004ab). (b)(5)

(b)(5)

FEP 2.2.07.05.0A Flow in the UZ [Unsaturated Zone] From Episodic Infiltration

The applicant excluded Flow in the UZ from Episodic Infiltration from the performance assessment model on the basis of low consequence, as identified in SNL (2008ab), DOE Enclosure 8, Response Number 5 (2009cb), DOE (2009cc), and DOE Enclosure 5, Response Number 7 (2009bo). This FEP refers to the influence of episodic flow on radionuclide transport in the unsaturated zone; specifically, transient flow arising from episodic infiltration events. DOE stated that episodic flow through and below the repository horizon is expected to be strongly attenuated by the overlying Paintbrush Tuff nonwelded (PTn) hydrogeologic unit.

Comment (b)(5)
(b)(5)

The applicant stated that periods of high precipitation and water percolation are expected to occur during future rain storms, and also that the porous rock matrix in the PTn unit is expected to strongly attenuate episodic percolation fluxes. DOE described the PTn unit as ranging from approximately 21 m [70 ft] to over 120 m [400 ft] within the repository area. The applicant stated that flow attenuation by the PTn is predicted to yield steady flow below the PTn in the unsaturated zone, except for volumetrically insignificant rapid flow through preferential pathways in the PTn. DOE asserted that transient flow below the PTn may occur in the southern part of Solitario Canyon because the PTn is completely offset by the Solitario Canyon Fault. However, episodic flow is not expected to significantly affect performance, because the emplacement drifts would be located away from Solitario Canyon in the affected area.

DOE based the assessment of episodic flow attenuation on two transient, one-dimensional simulations reported in SNL Section 6.9(a) (2007bf). DOE observed that the maximum flux below the PTn for these two simulations was around 17 mm/yr [0.67 in/yr], compared to the overall percolation flux uncertainty for the post-10,000-year period of 51 mm/yr [2 in/yr]. DOE supported its analysis by citing other studies considering one-, two-, and three-dimensional simulations, all using earlier estimates for PTn parameters. DOE stated that the other studies, in general, show similar damping of percolation flux by the PTn matrix.

DOE further supported the assessment of episodic flow attenuation in the PTn using results from (i) a water-release test within the PTn (in Alcove 4), (ii) line surveys of fracture minerals in tunnels below the PTn, (iii) inferred stagnation of a wetting pulse below the channel of Pagany Wash, and (iv) inferred long residence times in the PTn on the basis of C-14 observations from boreholes.

DOE considered Cl-36 observations from tunnels below the PTn, some of which have a radioisotope signature indicating that a portion of the *in-situ* waters infiltrated during or subsequent to the period of nuclear device testing from 1954 through 1970. DOE concluded that high observed concentrations of Cl-36 in some samples taken from the ESF tunnel possible indicate relatively small amounts of fracture flow penetrating as fast pathways, either steady or transient, through fault zones between the ground surface and the repository elevation. DOE used flow and transport models to examine the Cl-36 observations, concluding that the quantity of water penetrating the PTn as a result of fast pathways is approximately 1 percent of total infiltration, and characterized this quantity as negligible with respect to repository performance.

DOE also considered tritium data from boreholes and tunnels below the PTn. DOE concluded that some observations of tritium below the PTn within the ESF and ECRB tunnels, and from five boreholes, also have a bomb-pulse or post-bomb-pulse radioisotope signature. DOE's analysis of the data led to the following conclusions: (i) all of the elevated tritium observations from the ESF are associated with faults, (ii) the elevated observations in the boreholes may be associated with lateral flow from faults, and (iii) most elevated tritium observations from the ECRB are not associated with faults but may be associated with fast and focused (but not necessarily episodic) flow pathways.

DOE concluded that the PTn will attenuate episodic flow, resulting in approximately steady-state flow in the repository host rock and below, and the volume of flow that could lead to episodic flow in the repository host rock is small. Therefore, the applicant excluded the FEP Flow in the UZ from Episodic Infiltration from the performance assessment model.

Staff's Review

(b)(5)

(b)(5)

(b)(5) DOE considered increased seepage into emplacement drifts to be the largest performance consequence that would arise from episodic flow, but expects that any additional seepage would be small relative to the difference in percolation flux considered during calibration of infiltration uncertainty. In SER Section 2.2.1.3.6.3.2, the staff considers episodic flow in the larger context of DOE's representation of the spatial and temporal variability of ambient percolation flux above and through the proposed repository horizon during performance assessment. In its review of information related to flow above the repository horizon (SER Section 2.2.1.3.6.3.2), (b)(5)

(b)(5)

FEP 2.2.08.03.0A Geochemical Interactions and Evolution in the SZ [Saturated Zone]

The applicant excluded Geochemical Interactions and Evolution in the SZ on the basis of low consequence, as outlined in SNL (2008ab) and DOE Enclosure 1, Response Number 44 (2009ai). According to the FEP definition by the applicant, groundwater chemistry and other characteristics may change over time as a result of disposal system evolution or from mixing with other waters. Geochemical interactions may lead to dissolution and precipitation of minerals along the groundwater flow path, affecting groundwater flow, rock properties, and sorption of radionuclides (SNL, 2008ab).

In DOE Enclosure 1, Response Number 44 (2009ai), the applicant further examined natural groundwater geochemical variations in the immediate vicinity and down gradient from Yucca Mountain as a function of space and time. The applicant stated in DOE Enclosure 1, Response Number 44 (2009ai) that chemical compositions exhibit spatial variability that may be related to mixing of waters. The staff evaluates the acceptability of the applicant's model abstractions of flow paths in the saturated zone in SER Section 2.2.1.3.8. The applicant stated that temporal changes in properties that may affect radionuclide sorption such as pH, temperature, and major ion chemistry are gradual and fall within the range of groundwater chemistries it considered in developing the transport parameter (sorption coefficients or K_d)

values used in the saturated zone transport model of the performance assessment (SAR Section 2.3.9.3).

In its model abstraction for radionuclide transport through the saturated zone, the applicant assumed oxidizing conditions along the flow paths through the tuff and alluvium. The applicant stated in DOE Enclosure 1, Response Number 44 (2009ai) that redox potential has a strong effect on the transport of redox-sensitive radionuclides. The applicant also stated that other groundwater conditions such as reducing zones that may affect radionuclide sorption are localized in extent and unlikely to be changed at a larger scale for at least 10,000 years after repository closure. To support this statement, the applicant reasoned that (i) there is sufficient pyrite in reducing hydrogeological units of the saturated zone to sustain those reducing conditions, (ii) the long residence time of water in the saturated zone causes its oxidation state to be largely determined by water-rock interactions, and (iii) no current mechanism is known to support the concept that reducing zones will become more extensive along the saturated zone path (SNL, 2008ab). For these reasons, the applicant excluded Geochemical Interactions and Evolution in the SZ from the performance assessment model on the basis of low consequence (SNL, 2008ab).

The applicant also presented performance assessment calculations that indicated the radionuclides that contribute the most to the calculate mean annual dose during the first 10,000 years after repository closure are nonsorbing, and that radionuclides whose sorption is most affected by changes in these geochemical parameters (Pu-239 and -240, Np-237, and Se-79) only constitute about 20 percent of the total mean annual dose during the first 10,000 years after repository closure. The applicant also indicated that for the igneous intrusion modeling case, the release rates of plutonium and neptunium are only slightly sensitive to K_d values in volcanic rocks, but not sensitive to K_d values in the alluvium (DOE, 2009ai).

Staff's Review

The staff reviewed the model assumptions and field and laboratory data the applicant used to support its screening argument, as identified in SNL (2008ab) and DOE Enclosure 1, Response Number 44 (2009ai). To address uncertainty associated with natural variations in pH, temperature, and major ion chemistry, the applicant considered a range in aqueous water chemistries in developing parameter distributions for the model abstraction of radionuclide transport through the saturated zone for the performance assessment (SAR Section 2.3.9.3).

(b)(5)

FEP 2.2.08.03.0B Geochemical Interactions and Evolution in the UZ

The applicant excluded Geochemical Interactions and Evolution in the UZ on the basis of low consequence following SNL (2008ab) and DOE Enclosure 18, Response Number 18 (2009ab)

According to the applicant's definition of the FEP, the geochemical environment of the unsaturated zone may evolve over time in response to thermal and chemical perturbations introduced by the repository system. Precipitation or dissolution of minerals or changes in groundwater chemistry may affect the flow and composition of seepage into drifts or the transport of radionuclides in the near-field environment (SNL, 2008ab). In the screening argument, the applicant considered (i) how elevated temperatures would affect geochemical interactions between water and rock in the vicinity of the emplacement drifts and (ii) how changes in water chemistry due to reactions with repository construction materials would subsequently affect flow and transport properties in the unsaturated zone (SNL, 2008ab). The applicant also considered how geochemical interactions between waste package effluent and the solids and ambient waters might affect radionuclide transport in the crushed tuff invert and in the unsaturated rock beneath the repository drift, as detailed in DOE Enclosure 18, Response Number 18 (2009ab).

The applicant cited model analyses of geochemical interactions that estimated how drift seepage chemistry and near-field flow properties would be affected by changes in temperature, pH, redox potential, ionic strength and other compositional variables, time dependency, precipitation or dissolution, and resaturation times, as described in SNL (2007ai) and SNL Section 7.1.2.2 (2007ak). The applicant determined that the expected changes would be limited to small changes near the drift wall or, at a larger scale, within the range of variation that is already considered in the performance assessment. The applicant reasoned that there would be little potential for cementitious materials in the repository to affect radionuclide transport by forming an alkaline cement leachate plume because (i) of the minor amount of cementitious material to be used in construction of the repository, none will be used in the waste emplacement drifts themselves and (ii) high pH conditions in an alkaline cement leachate plume would be rapidly neutralized in the unsaturated zone by reaction with ambient carbon dioxide. As a result, the applicant concluded there would be little opportunity for the cement leachate to interact chemically with radionuclides or to affect radionuclide transport pathways by precipitation of calcite.

The applicant also concluded that there would be little potential for evolved waste package fluids to cause more than minor changes in unsaturated zone fluid compositions. The applicant cited the description of waste package chemistry (SAR Section 2.3.7.5.3.1) in stating that the main chemical factors in the effluent that affect radionuclide solubility will generally overlap the expected ranges of composition of the ambient unsaturated zone waters, as identified in DOE Enclosure 18, Response Number 18 (2009ab). Any change in effluent composition by reaction with the main chemical components of the engineered materials (iron, chromium, nickel) will be limited by the formation of low-solubility corrosion products inside the waste package. The applicant reasoned that the waste package effluent may become concentrated by evaporation or consumption of water by degradation reactions, but upon exiting the waste package, the mixing of effluent with ambient waters in the invert and unsaturated zone would quickly dilute the effluent, resulting in no significant changes in bulk water chemistry in the unsaturated zone.

Staff's Review

(b)(5)

(b)(5)

FEP 2.2.08.04.0A Re-Dissolution of Precipitates Directs More Corrosive Fluids to Waste Packages:

The applicant excluded Re-Dissolution of Precipitates Directs More Corrosive Fluids to Waste Packages on the basis of low consequence. According to the applicant's definition of the FEP, the heat generated by radioactive decay inside the waste packages is expected to dry out the rock surrounding the emplacement drifts. Evaporation of the pore waters will leave behind precipitates that may plug pores. The redissolution of these precipitates, following the thermal pulse, may produce pore waters with corrosive chemistries, which could reach the waste packages when gravity-driven flow conditions resume (SNL, 2008ab).

The applicant expects rewetting of the host rock around the drifts to occur as the temperature drops below the boiling point of water. Initially, the applicant explained, precipitates could dissolve and form brines. During the initial stages of rewetting, redissolution of precipitated minerals may temporarily concentrate chloride and other soluble components relative to ambient solutions. As rewetting continues, the applicant expects the brines to become diluted and pore waters to return to ambient compositions. The applicant argued that the drip shield is expected to perform its diversion function during the time when the transient changes in pore water composition could occur, preventing potentially corrosive waters from contacting waste packages (SNL, 2008ab).

In addition to the undisturbed repository performance, the applicant also evaluated this FEP in the event of early drip shield failure and seismic events. In the event of early drip shield failure, the applicant assumed that a waste package under a compromised drip shield and at a seepage location would fail by localized corrosion, thus no additional failures would occur as a result of compositional changes due to redissolution of precipitates. In the event of a seismic event prior to rewetting and redissolution of precipitates, the applicant argued that the frequency and extent of drip shield failure would be insignificant in 10,000 years. The applicant also excluded FEP 2.1.03.10.0B, Advection of Liquids and Solids Through Cracks in the Drip Shield, on the basis of low consequence, as described in SNL (2008ab) and DOE Enclosure 2, Response Number 2 (2009ab). In that FEP, the applicant analyzed, in the screening argument, scenarios allowing for water infiltrating failed drip shields and contacting the waste packages and concluded that those scenarios would not change the magnitude of the dose estimates, as identified in SNL (2008ab) and DOE Enclosure 2, Response Number 2 (2009ab).

Staff's Review

(b)(5)

Comment: (b)(5)
(b)(5)

(b)(5)

FEP 2.2.09.01.0B Microbial Activity in the UZ

Comment (b)(5)
(b)(5)

The applicant excluded Microbial Activity in the UZ on the basis of low consequence (SNL, 2008ab; DOE, 2009ci). According to the applicant's definition of the FEP, microbial activity may affect radionuclide sorption processes in the unsaturated zone by changing groundwater pH and redox conditions, by adding complexing agents to the water, or by changing the valence state of certain radionuclides by biotransformation. In addition, a microbe suspended in water may act as a biocolloid, facilitating the transport of radionuclides in the unsaturated zone by sorbing to the microbe itself. The applicant also considered that increased microbial activity associated with condensation in the unsaturated zone during the early thermal period could affect the chemistry of water entering the drifts as seepage (DOE, 2009ci).

In the screening argument, the applicant cited information provided in another excluded FEP 2.1.10.01.0A, Microbial Activity in EBS (SNL, 2008ab), and in a supporting report, BSC Section 6 (2004aq), that evaluated the potential impact of microbial activity on drift chemistry. The applicant stated in BSC Section 6.3 (2004aq) that although laboratory analyses have identified a diverse microbial population in Yucca Mountain tuff samples, the microbes are largely dormant under ambient conditions due primarily to constraints on the availability of nutrients and water in the unsaturated tuffs, as identified in BSC Section 6.4 (2004aq). The applicant stated that any variation in radionuclide sorption coefficients that might be caused by changes in water chemistry due to microbial activity are within the existing range of the sorption coefficient distributions used in the performance assessment calculations. Similarly, the applicant reasoned that the uncertain, small concentration of biocolloids in Yucca Mountain groundwaters is encompassed by the wide range of concentration values for naturally occurring colloids that is already sampled for radionuclide transport calculations. The applicant also noted that the uncertainty distributions specified for the sorption coefficients in the performance assessment calculations implicitly included the effects of naturally occurring microbial activity because the applicant developed the radionuclide K_d distributions from sorption experiments on the basis of the chemistry of Yucca Mountain water samples, as described in FEP 2.2.09.01.0B (SNL, 2008ab).

Staff's Review

The staff has reviewed the adequacy of the applicant's sorption-related and colloid-associated unsaturated zone transport parameters in SER Section 2.2.1.3.7 and (b)(5)

(b)(5)

For perturbed conditions in the unsaturated zone during the repository's early thermal period, the applicant stated that microbial activity associated with water vapor condensation in the near-field rock beyond the dryout zone would not significantly affect seepage chemistry for three main reasons (DOE, 2009ci). First, a change from ambient to warmer temperatures in the near-field rocks would not increase the availability of already scarce nutrients in the rock, so the nutrient limitation on microbial activity would persist. Second, the applicant estimated from modeling calculations that even for ambient conditions, the relative humidity of the densely

welded Topopah Spring tuff at the repository horizon is already at the upper end of conditions that support optimal microbial activity in the matrix pore spaces, as outlined in DOE Enclosure 2, Response Number 2 (2009ck). As a result, the applicant reasoned that an increase in microbial activity in the condensation zone would be limited primarily to water that condensed in fractures. Third, the applicant stated that for the near-field environment as a whole, any increased microbial activity in the condensation zone would be offset by reduced microbial activity in the dryout zone during the same period.

The staff reviewed the applicant's screening arguments for microbial activity during the thermal period in the context of the applicant's thermohydrologic models for Yucca Mountain, as described in SNL Section 6.1 (2008aj); site characterization data for the densely welded Topopah Spring tuff, described in BSC Section 7.2 (2004bi); Yucca Mountain field tests and interpretations of fracture flow and transport processes in BSC Section 7.6.3.1 (2004bi) and BSC Section 6.2.4 (2006aa); and observations of increased microbial activity in fractures during an unsaturated zone infiltration and transport experiment at Yucca Mountain, explained in BSC Section 6.1.2 (2006aa). (b)(5)

(b)(5)

The applicant's exclusion argument for increased microbial activity in the unsaturated zone during the thermal period identified the scarcity of nutrients in the rocks as one of the main factors limiting microbial activity. (b)(5)

(b)(5)

The applicant stated that despite the limited availability of nutrients, the increased availability of water in fractures may contribute to an increase in microbial activity in the condensation zone. The technical basis for the applicant's statement is supported by observations from a Yucca Mountain large-scale unsaturated zone field experiment, the Large Plot Test, which reported in BSC Section 6.1.2 (2006aa) the growth of biofilms (slime layers excreted by certain microbes at solid-water interfaces) in fractures on a wetted floor in the subsurface at Yucca Mountain. (b)(5)

(b)(5)

(b)(5)

The applicant also stated an increase in microbial activity in the condensation zone would be offset by restricted microbial activity in the dryout zone, so there would be no net increase in microbial activity during the thermal period. (b)(5)

(b)(5)

(b)(5)

FEP 2.2.10.09.0A Thermal-chemical Alteration of the Topopah Spring Basal Vitrophyre

The applicant excluded Thermal-chemical Alteration of the Topopah Spring Basal Vitrophyre on the basis of low consequence. According to the applicant's information, the Topopah Spring basal vitrophyre is a glassy, densely welded tuff that forms the lowermost part of the Topopah Spring tuff hydrogeologic unit (SAR General Information Volume, Figure 5-30). The applicant used the FEP to examine the possibility that temperatures elevated by repository heating might cause the volcanic glass in the vitrophyre to alter to zeolites and clay minerals, potentially changing permeability, sorption characteristics, and flow paths in the basal vitrophyre (SNL, 2008ab).

In the screening argument, the applicant stated that although heat from the repository will locally increase temperatures in the unsaturated zone for hundreds to several thousand years, the potential for any thermo-chemical alteration of the vitrophyre would be of limited spatial extent and of short duration compared to the previous alteration history of the Topopah Spring tuff. The applicant cited fluid inclusion and isotope studies of fracture minerals in the Topopah Spring tuff units to support the screening argument. The studies identified that regionally elevated temperatures {above 80 °C [176 °F]} occurred in the tuffs at least 10 million years ago, followed by gradual cooling over several million years to near-ambient conditions. Despite its long exposure to the elevated temperatures, the basal vitrophyre remained largely unaltered. The applicant reasoned that, by comparison, the relatively brief and spatially limited postclosure thermal pulse from the repository will only minimally alter the vitrophyre to secondary minerals, so that any effects on the sorptive or hydrologic properties of the unit would be of limited consequence.

Staff's Review

The staff examined the applicant's cited modeling studies, empirical data, and glass alteration rates (SNL, 2008ab) that supported the applicant's representation of the past thermal history of the Topopah Spring tuff units and that supported the applicant's thermal model predictions for

repository heating (b)(5)

(b)(5)

Screening of Criticality Events

The applicant classified criticality events as FEPs and excluded all of the criticality FEPs from the performance assessment model (SAR Table 2.2-5; SNL, 2008ab) on the basis of low probability. In addition, arguments to screen out criticality as an event class were provided in SAR Section 2.2.1.4.1. The applicant's arguments for excluding criticality as FEPs (SNL, 2008ab) or event class (SAR Section 2.2.1.4.1) are evaluated in this SER section.

The applicant's criticality evaluation consisted of a probability analysis based on initiating events, location, and state of degradation. The criticality analysis classified the waste forms by type—commercial spent nuclear fuel (CSNF), high-level waste glass, and DOE spent nuclear fuel (SNF)—which were further subdivided, in some cases. The criticality FEPs listed in SNL (2008ab) encompass FEPs 2.1.14.15.0A through 2.1.14.26.0A and 2.2.14.09.0A through 2.2.14.12.0A.

The NRC staff reviewed the information provided in the application, including the cited references, and (b)(5)

(b)(5)

(b)(5)

Comment (b)(5)

(b)(5)

(b)(5)

Moderator Intrusion

In its criticality analysis, the applicant considered various reactivity control mechanisms within a waste package to ensure that all probable configurations remain subcritical. The applicant assumed that failed waste packages would be flooded (SNL, 2008ai), so that the probability of criticality would be overestimated. The applicant conservatively assumed that enough water is available to act as a neutron moderator in the criticality calculations whenever any breach of the package is calculated—even for cracks on the waste package too small to permit liquid infiltration. No credit is taken for only partial filling of the waste package, nor for the drip shield's diversion of liquid from the package (DOE, 2009bx). In the nominal modeling case, DOE estimates that the waste packages would not be breached in 10,000 years (e.g., SAR

Figure 2.1-10). However, other modeling cases (early failure, seismic ground motion, seismic fault displacement, and igneous intrusion) account for failure of the waste package within 10,000 years (e.g., SAR Figure 2.4-18). Unbreached waste packages do not allow ingress of water (neutron moderator) and thus do not pose a criticality concern. Thus, criticality events could only occur within 10,000 years for the early failure and seismic scenarios.

NRC Review

(b)(5)

(b)(5) The staff reviewed documents with analyses supporting screening arguments for excluding criticality events from the performance assessment analysis (SNL, 2008aa,ab,ad,ae,al) and supplemental analyses (DOE, 2009ai,aj,al,bv,co). DOE assumed that given a postulated breach of the spent fuel package, no matter how small a breach, the waste package would fill with enough water to support criticality (i.e., the availability of water was not assumed to be a limiting factor for criticality). (b)(5)

(b)(5)

(b)(5)

(b)(5) The staff reviewed the conditions the applicant identified as necessary for in-package criticality, as well as the methodology used to identify these conditions. The total probability of criticality is dependent on the probability to attain those necessary conditions (e.g., waste package failure, moderator intrusion, configuration changes, package/absorber degradation, and fuel characterization). The applicant stated that a criticality event was possible only after a waste package breach and under the following conditions: (i) accidentally loading a fuel assembly with higher reactivity than permissible into the waste package (a mistake referred to as a misload) or (ii) manufacturing errors resulting in missing neutron absorber material. (b)(5)

(b)(5)

For the classified naval SNF postclosure criticality analysis, the applicant relied on the low probability of breach of a U.S. Navy canister to exclude criticality events for the naval canisters. The applicant analyzed breached waste packages with naval SNF that were fully flooded with water. The analysis credited the design of the naval canister internals with preventing the rearrangement of the fuel into a more reactive configuration than the design basis configuration.

(b)(5)

(b)(5) The applicant determined that a breach of a U.S. Navy canister in 10,000 years was unlikely. Nonetheless, the applicant modeled a fully flooded U.S. Navy canister configuration with the most reactive geometric rearrangement physically possible (b)(5)

(b)(5)

Degraded Fuel Conditions

The applicant's design basis configuration model incorporates some rearrangement and degradation of fuel and neutron absorbers to overestimate the probability of a criticality event. The applicant concluded that under such configurations, a criticality event could occur only if the waste package was misloaded or if a manufacturing error resulted in missing neutron absorbers, as identified in FEP 2.1 14 15 0A (SNL, 2008ab). The NRC staff discusses these two events: misloaded fuel assemblies and missing neutron absorbers in the following sections.

Misloaded Fuel

The applicant developed loading curves for CSNF using SNL Figures 6-32 and 6-33 (2008aa) and SAR Figures 2.2-7 and 2.2-8 to define "acceptable" and "underburnt" assemblies that could be loaded into waste packages based on minimum burnup, as a function of initial fuel assembly enrichment. The applicant considered assemblies above the loading curve acceptable, while those below the loading curve were considered underburnt, in the sense that a canister filled with underburnt assemblies could become critical (exceed the critical limit as shown in SAR Table 2.2-11) if flooded without additional criticality control mechanisms. These underburnt assemblies comprise the potential misload inventory. The applicant stated that the underburnt assemblies would have to be loaded into canisters with additional reactivity control mechanisms and further analyzed to ensure subcriticality (SAR Section 2.2.1.4.1.1.3). (b)(5)

(b)(5)

The waste package configuration used to compute the loading curves was selected to bound degraded configurations that were not explicitly evaluated in the screening argument [e.g., the conversion of UO_2 into schoepite, as described in SNL Sections 6.1.3 and 6.2.5 (2008aa)]. The applicant considered it safe (i.e., criticality events are not expected) to load canisters with spent fuel whose burnup exceeds the minimum burnup defined by the loading curve for the initial enrichment of the fuel. The applicant implemented these bounding analyses to provide confidence that waste package configurations not explicitly analyzed are less reactive than those that were analyzed and used to generate the loading curve.

The applicant defined a misload as the process of loading, by mistake, a fuel assembly into a canister without enough criticality prevention controls for that fuel assembly (specifically for CSNF, when an assembly from the misload inventory is loaded into a canister). The applicant assumed that a misload may cause a criticality event if the misloaded assembly is significantly more reactive than accounted for in the waste package design. The applicant assumed misloads result from operator error and used representative human reliability data and prototype loading procedures to estimate the probability of misloads, because actual data and procedures are not available (DOE, 2003aa).

The applicant assumed that misloads will not occur for DOE SNF, because the physical differences in fuel types allow operators to easily distinguish spent fuel types and in some cases physically prevent misloads [SNL, 2008ab; FEP 2.1.14.15.0A, In-package Criticality (Intact Configuration)]. The applicant did not consider misleading naval SNF feasible, because naval SNF has already been loaded offsite according to well-defined quality assurance procedures, which apply to relatively few canisters. A CSNF misload would occur if an underburned assembly is loaded; however, a criticality event would only be possible if the other assemblies were not burned enough to compensate for the underburned assembly.

Staff Review

The NRC staff reviewed the applicant's determination of the misload probability. The applicant modeled all the misloads as random human error in the selection of fuel assemblies to be loaded, because human error is the dominant cause of misloads. This calculation resulted in a combined misload probability of 1.18×10^{-5} per canister. This is the probability that the operator will misload a single assembly into a canister.

The applicant also calculated an additional probability related to misloads: the probability that a criticality event would occur given one assembly has been misloaded. To calculate this probability, the applicant assumed that misloaded assemblies would be positioned in the center (i.e., along the axis) of the waste package. (b)(5)

(b)(5)

(b)(5) In DOE Enclosure 13, Response Number 22 (2009aj), the applicant supplemented the analysis by performing a sensitivity study that assumed a criticality event resulted whenever a misload occurred. This analysis computed an overall probability of criticality of 5.76×10^{-5} in 10,000 years. (b)(5)

(b)(5)

Neutron Absorbers

To model the effects of missing neutron absorbers, the applicant reduced the amount of absorber in the models. It assumed that loss of absorber results from manufacturing error or corrosion of neutron absorber materials. For the corrosion of the absorber plates in the transportation, aging, and disposal (TAD) canister, the applicant assumed that after 10,000 years, 6 mm [0.24 in] out of the initial 11 mm [0.43 in] of borated stainless steel would remain in place. In response to the staff's RAs on use of average corrosion values in DOE Enclosure 1, Response Number 5, and Enclosure 2, Response Number 6 (2009bv) and in SAR Section 1.5.1.1.1.2.2.2, the applicant indicated that the 5 mm [0.2 in] material thinning was based on a borated stainless steel corrosion rate of 250 nm/yr [0.01 mil/yr]. This corrosion rate is about nine times the average corrosion rate on 304B4 borated stainless steel Lister, et al. (2007aa) measured. Lister, et al. (2007aa) measured the corrosion rate at 60 °C [140 °F] in an aerated simulated in-package solution and determined an average value of 27 nm/yr [0.001 mil/yr] with a standard deviation of 10.1 nm/yr [4×10^{-4} mil/yr]. Although some boron would remain in the steel as separate chromium boride particles left behind as insoluble

products during corrosion, this remaining boron was not credited in the applicant's criticality models. In its criticality models with SCALE and MCNP, the applicant modeled 75 percent of the boron that exists in the stainless steel as per the guidance in NUREG-1567 (NRC, 2000ab).

The applicant assumed that if a manufacturing error resulted in neutron absorbers not being installed or too little absorber material being installed, a criticality event could occur. The applicant used a surrogate analysis to model the probability of this error occurring as the probability of a material selection error multiplied by the probability that an independent inspection does not detect it to derive a mean value of 1.25×10^{-7} per canister. The applicant considered representative reliability data and prototype manufacturing procedures to develop an overestimate of the probability of misloading the neutron absorber plates.

The naval waste packages use hafnium—a strong thermal neutron absorber that is extremely corrosion resistant—as a neutron absorber. For the absorbers considered in the DOE SNF canisters, the applicant evaluated the solubility, retention, and distribution of the neutron absorbers in DOE Enclosure 5, Response Number 8 (2009cb). The applicant has not yet completed the design of the neutron-absorbing shot that will be added to some waste forms (waste forms the applicant referred to as DOE1, DOE5, and DOE8). The applicant stated in DOE Enclosure 5, Response Number 8 (2009cb) that due to its high corrosion resistance, $GdPO_4$ is the most likely form of neutron absorber.

Staff Review

(b)(5)

(b)(5)

The information in Fix, et al. (2004aa), BSC Tables 6-4 and 6-7 (2004ae), and SNL (2007am) indicated that the corrosion rates of borated stainless steels were higher than for unborated 304 and 316 stainless steels. BSC (2004ae) also indicated that the corrosion rate of borated 304 stainless steel with 1.5 percent boron was about 14 times higher than that with 0.3 percent boron in boiling freshwater. The corrosion rates of borated stainless steel ranged from tens of nanometers per year (Lister, et al., 2007aa) to tens of micrometers per year in BSC Table 6-7 (2004ae), depending on simulated environmental conditions.

(b)(5)

(b)(5)

(b)(5)

(b)(5)

(b)(5)

(b)(5)

Burnup Credit

In the probability of criticality analysis for the CSNF, the applicant accounted for the change in reactivity caused by changes in fuel composition that resulted from irradiation in a reactor and radioactive decay. This is referred to as burnup credit. To compute the change in reactivity, the applicant modeled CSNF fuel as being composed of 29 principal isotopes (SAR Table 2.2-9) considered to be the most relevant and concluded in DOE Section 6 (2004ab) that increasing the burnup of CSNF decreases its reactivity. The applicant used reactor records to determine the burnup of the fuel (SAR Section 2.2.1.4.1 1.4.1) and a computer model to generate the isotopic composition for a given burnup and enrichment. The applicant accounted for the

uncertainties in the reactor records by using a burnup that is 5 percent less than reported. This adjustment bounded the highest reactor record uncertainty identified in AREVA 2004, which was 4.2%. This uncertainty is the difference between the calculated and measured values of burnup to determine the uncertainty in the reactor records. Measured burnup was determined with calibrated in-core instrumentation. Calculated burnup was determined using analytic methods of the reactor core power distribution. Uncertainties in the isotopic composition were accounted for by using modeling parameters that would conservatively overestimate the chance of criticality (SAR Section 2.2.1.4.1.1.2.4.1). Burnup credit for CSNF assemblies was limited to 50 GWd/MTU (DOE, 2009bx). The applicant used a decay time for the isotopic composition of 5 years to bound the increase in reactivity caused by Pu-240 decay. The applicant attempted to validate the isotopic model by comparing the results of the model to the results of radiochemical assays that measured the amount of some or all of the principal isotopes in small samples of CSNF (DOE, 2004ab).

Staff Review

The NRC staff reviewed the applicant's use and justification of boiling water reactor (BWR) burnup credit (b)(5)

(b)(5)

(b)(5)

(b)(5)

(b)(5)

Criticality Code Validation

An important aspect in assessing criticality code validation is the applicability of the selected benchmark experiments, which must be similar in form and composition to the systems to be evaluated. The applicant described the benchmarks used for the criticality code validation, and determination of the lower bound tolerance limits for CSNF and DOE SNF, in DOE (2004aa) and Radulescu, et al. (2007aa). The applicant included in the criticality model document (DOE, 2004aa) analyses for the various types of commercial and DOE SNF. The applicant updated its validation methodology and benchmarks for CSNF in Radulescu, et al. (2007aa), during which several benchmarks used in the criticality model were excluded because they were no longer considered applicable. The applicant has not yet updated the benchmark selection and validation for DOE SNF with the new methodology used in Radulescu, et al. (2007aa).

Staff Review

(b)(5)

(b)(5)

The staff reviewed the applicant's documentation on criticality models, calculations, and results. (b)(5)

(b)(5)

(b)(5)

(b)(5)

The applicant considered code validation and conservatism in modeling parameters when assessing the proposed margin of subcriticality of zero. (b)(5)

(b)(5)

The NRC reviewed the applicant's justification for a margin of subcriticality of zero. (b)(5)

(b)(5)

(b)(5)

In DOE Enclosure 15 (Question Number 35), Table 1 (2009aj) and the related discussion, the applicant showed that, with the exception of some fuel in DOE SNF Group 3, the DOE SNF has at least a margin of 0.02. (b)(5)

(b)(5)

Staff's Findings

(b)(5)

The NRC staff

(b)(5)

(b)(5)

2.2.1.2.1.3.3 Technical Review for Formation of Scenario Classes

Summary of the DOE License Application on Formation of Scenario Classes

The applicant described the approach to the definition of event class and scenario class formation in SAR Section 2.2.1.3. The applicant cited 10 CFR 63.102(j) as a basis to define an event class as consisting of all possible initiating events that are caused by a common natural process. The applicant extended the definition to allow event classes to represent the aggregation of initiating events with a common characteristic, either natural or man-made. The applicant stated that the objective of scenario class development is to define a limited set of scenario classes that could be analyzed qualitatively while still covering the range of possible future states of the repository system (SAR Section 2.2.1.3, p. 2.2-22), and that the implemented classification allowed for workable consequence analyses.

SAR Section 2.2.1.3.1 presented the scenario class formation for the computations to address compliance with (i) the individual protection standard after permanent closure and (ii) separate standards for protecting the ground water. On the basis of the probabilities in

SAR Section 2.2.2 (which were evaluated in the SER Section 2.2.1.2.2), the applicant retained the following events—seismic, igneous, and early waste package and drip shield failure—and developed general scenario classes from these retained events. The applicant defined the nominal scenario as the scenario that does not include any of these events, but that accounts for all other included FEPs. The applicant stated that the broad event classes (seismic, igneous, and early waste package and drip shield failure) are independent but not mutually exclusive. To define mutually exclusive classes that encompass a complete span of possible future states of the repository system, the applicant considered a total of eight independent combinations from the three events and the nominal scenario, and summarized those combinations in the diagram in SAR Figure 2.2-3. The applicant concluded that these eight scenario class combinations cover all of the possibilities of damaging events or processes that could affect a waste package during the timeframe of the analysis (e.g., a waste package could be damaged by both an early failure event and a seismic event). The applicant did not explicitly implement these eight mutually exclusive scenario classes and their probabilities for the computation of aggregated consequence estimates. The applicant introduced simplifications (SAR Section 2.4.2.1) and derived consequence estimates on the basis of the three broad scenario classes (seismic, igneous, and early waste package and drip shield failure), the nominal scenario class, and their probabilities.

The applicant discussed scenario class formation for the human protection standard in SAR Section 2.2.1.3.2 and referred to 10 CFR 63.322 to define assumptions to support the development of the scenario.

Staff Evaluation of Formation of Scenario Classes

The staff evaluated the formation of scenario classes for performance assessments to demonstrate compliance with the individual protection standard and separate standards for protection of ground water by evaluating whether they cover the full range of potential future states of the repository system. (b)(5)

(b)(5)

Comment (b)(5)

(b)(5)

(b)(5)

(b)(5)

Comment: (b)(5)

(b)(5)

With respect to the scenario class formation for human intrusion, DOE referred to 10 CFR 63.322 to define assumptions for the analysis to demonstrate compliance with individual protection standards for human intrusion (10 CFR 63.321). (b)(5)

(b)(5)

Evaluation Findings

(b)(5)

2.2.1.2.1.3.4 Screening of Scenario Classes

Summary of the DOE License Application on Screening of Scenario Classes

In SAR Section 2.2.1.4, DOE described step 4 (screening for scenario classes) of the scenario analysis (SAR Section 2.2.1). DOE provided justifications for excluding scenario classes from the performance assessment analyses on the basis of probability or consistency with the regulations (10 CFR 63.311, 10 CFR 63.321, and 10 CFR 63.331).

The applicant included the following four scenario classes for the performance assessment to demonstrate compliance with the individual protection standard (10 CFR 63.311): nominal, early failure, seismic, and igneous scenario classes. The applicant asserted that all of these scenario classes have a probability greater than 10^{-4} in 10,000 years.

For the performance assessment to demonstrate compliance with separate ground water protection standards (10 CFR 63.311), the applicant excluded the igneous scenario class on the basis that its probability is less than 0.1 in 10,000 years.

The applicant excluded the human intrusion scenario class from the performance assessments to demonstrate compliance with individual protection and separate ground water protection standards on the basis that it is explicitly ruled out by the regulation.

Staff Evaluation of Screening of Scenario Classes

DOE screened scenario classes on the basis of probability, consequences, or consistency with regulations. Accordingly, the staff's review of the applicant's exclusion of scenarios classes on the basis of low probability used the results of the staff's evaluation documented in SER.

Section 2.2.1.2.2. In addition, the staff reviewed whether the scenario classes that DOE ruled out by regulation were identified and justified.

In SAR Section 2.2.1.3 DOE defined scenario classes referred to as nominal, early failure, seismic, igneous scenario, and human intrusion, which were used as the starting point for the screening of scenario classes. As described in SER Section 2.2.1.2.1.3.3, (b)(5)

(b)(5)

In SAR Section 2.2.1.3.1, DOE stated that, on the basis of probabilities described in SAR Section 2.2.2, seismic, igneous, and early waste package and drip shield failure were retained in the formation of scenario classes used in the performance assessments. The staff reviewed the DOE basis for estimating these event probabilities in SER Section 2.2.1.2.2.3 (b)(5)

(b)(5)

DOE included the nominal, early failure, seismic, and igneous scenarios in the performance assessment to demonstrate compliance with individual protection standards. The human intrusion scenario was analyzed separately in conformance with 10 CFR 63.311(a), (b)(5)

(b)(5)

DOE included the nominal, early failure, and seismic scenarios in the performance assessment to demonstrate compliance with separate ground water protection standards and excluded the igneous and human intrusion scenarios. (b)(5)

(b)(5)

In 10 CFR 63.342(b), unlikely events are defined as those estimated to have a chance less than 1 in 100,000 per year of occurring (equivalent to a probability less than 0.1 in 10,000 years). On the basis of the staff's evaluation in SER Section 2.2.1.2.2, the (b)(5)

(b)(5)

(b)(5)

For compliance with individual protection standards (10 CFR 63.311), DOE included nominal, early failure, seismic, and igneous scenario classes from the performance assessment, and the staff (b)(5)

(b)(5)

(b)(5)

For compliance with the separate standards for ground water protection (10 CFR 63.331), DOE excluded the igneous scenario class from the performance assessment model, and the staff

(b)(5)

(b)(5)

For compliance with 10 CFR 63.311 and 63.331, DOE excluded the human intrusion scenario from the performance assessments, and the staff

(b)(5)

(b)(5)

2.2.1.2.1.4

Evaluation Findings

(b)(5)

2.2.1.2.1.5 References

Aiyanger, A.K., B.W. Neuberger, P.G. Oberson, and S. Ankem. 2005aa. "The Effect of Stress Level and Grain Size on the Ambient Temperature Creep Deformation Behavior of an Alpha Ti-1.6 Wt Pct V Alloy." *Metallurgical and Materials Transactions A*. Vol. 36A. pp. 637–644.

American Society of Mechanical Engineers. 2001aa. *ASME Boiler and Pressure Vessel Code*. New York City, New York: American Society of Mechanical Engineers.

Ankem, S., C.A. Greene, and S. Singh. 1994aa. "Time Dependent Twinning During Ambient Temperature Creep of Alpha-Ti-Mn Alloys." *Scripta Metallurgica*. Vol. 30. pp. 803–808.

AREVA 2004. "Reactor Record Uncertainty Determination." 32-5041666-02, Rev 02. ACC: DOC. 20040623.0002.ML092310715. ML092310716. 5/26/04.

ASM International. 2003aa. *ASM Handbook: Heat Treating*. Vol. 4. Metal Park, Ohio: ASM International.

ASM International. 1994aa. *Materials Properties Handbook: Titanium Alloys*. Metal Park, Ohio: ASM International.

ASTM International. 2004aa. "Standard Specification for Low-Carbon Nickel-Molybdenum-Chromium, Low-Carbon Nickel-Chromium-Molybdenum, Low-Carbon Nickel-Chromium-Molybdenum-Copper, Low-Carbon Nickel-Chromium-Molybdenum-Tantalum, and Low-Carbon Nickel-Chromium-Molybdenum-Tungsten Alloy Plate, Sheet, and Strip." B 475-04: Annual Book of ASTM Standards. Vol. 02.04. West Conshohocken, Pennsylvania: ASTM International.

Beavers, J.A. and C.L. Durr. 1991aa. NUREG/CR-5598, "Immersion Studies on Candidate Container Alloys for the Tuff Repository." Washington, DC: NRC.

Beavers, J.A., N.G. Thompson, and C.L. Durr. 1992aa. NUREG/CR-5709, "Pitting, Galvanic, and Long-Term Corrosion Studies on Candidate Container Alloys for the Tuff Repository." Washington, DC: NRC.

Brossia, C.S. and G.A. Cragnolino. 2000aa. "Effects of Environmental, Electrochemical, and Metallurgical Variables on the Passive and Localized Dissolution of Ti Grate 7." CORROSION 2000. Paper No. 00211. Houston, Texas: NACE International.

BSC. 2008ab. "Canister Receipt and Closure Facility Event Sequence Development Analysis." 060-PSA-CR00-00100-000. Rev. 00A. CACN 001. Las Vegas, Nevada: Bechtel SAIC Company, LLC.

BSC. 2007be. "Subsurface Geotechnical Parameters Report." ANL-SSD-GE-000001. Rev. 00. Las Vegas, Nevada: Bechtel SAIC Company, LLC.

BSC. 2006aa. "Analysis of Alcove 8/Niche 3 Flow and Transport Tests." ANL-NBS-HS-000056. Rev. 00. ACN 01. Las Vegas, Nevada: Bechtel SAIC Company, LLC.

BSC. 2005aa. "Analysis of Dust Deliquescence for FEP Screening." ANL-EBS-MD-000074. Rev. 01. AD 01, ACN 001, ACN 002. Las Vegas, Nevada: Bechtel SAIC Company, LLC.

BSC. 2005an. "Creep Deformation of the Drip Shield." CAL-WIS-AC-000004. Rev. 00A. Las Vegas, Nevada: Bechtel SAIC Company, LLC.

BSC. 2004ab. "Aging and Phase Stability of Waste Package Outer Barrier." ANL-EBS-MD-000002. Rev. 02. Las Vegas, Nevada: Bechtel SAIC Company, LLC.

BSC. 2004ae. "Aqueous Corrosion Rates for Waste Package Materials." ANL-DSD-MD-000001. Rev. 01. ACN 001, ERD 01, ERD 02. Las Vegas, Nevada: Bechtel SAIC Company, LLC.

BSC. 2004al. "Drift Degradation Analysis." ANL-EBS-MD-000027. Rev. 03. ACN 001, ACN 002, ACN 003, ERD 01. Las Vegas, Nevada: Bechtel SAIC Company, LLC.

BSC. 2004aq. "Evaluation of Potential Impacts of Microbial Activity on Drift Chemistry." ANL-EBS-MD-000038. Rev. 01. ACN 01, ACN 02, ERD 01, ERD 02. Las Vegas, Nevada: Bechtel SAIC Company, LLC.

BSC. 2004as. "General Corrosion and Localized Corrosion of the Drip Shield." ANL-EBS-MD-000004. Rev. 02. AD 01, ACN 01, ACN 02, ERD 01. Las Vegas, Nevada: Bechtel SAIC Company, LLC.

BSC. 2004be. "Seepage Model for PA Including Drift Collapse." MDL-NBS-HS-000002. Rev. 3. ACN 001. Las Vegas, Nevada: Bechtel SAIC Company, LLC.

BSC. 2004bi. "Yucca Mountain Site Description." TDR-CRW-GS-000001. Rev. 02 ICN 01, ERD 01, ERD 02. Las Vegas, Nevada: Bechtel SAIC Company, LLC.

Dean, J.C. and R.W. Tayloe, Jr. 2001aa. NUREG/CR-6698, "Guide for Validation of Nuclear Criticality Safety Calculational Methodology." Washington, DC: NRC.

DOE. 2010ad. "Yucca Mountain—Supplemental Response to Request for Additional Information Regarding License Application (Safety Analysis Report Section 2.2.1.2), Safety Evaluation Report Vol. 3, Chapter 2.2.1.2.1, Set 4." Letter (January 20) J.R. Williams to J.H. Sulima (NRC). ML100210164. Washington, DC: DOE, Office of Technical Management.

DOE. 2010ah. "Yucca Mountain—Supplemental Response to Request for Additional Information Regarding License Application (Safety Analysis Report Section 2.2.1.2), Safety Evaluation Report Vol. 3, Chapter 2.2.1.2.1, Set 4." Letter (January 7) J.R. Williams to J.H. Sulima (NRC). ML100110028. Washington, DC: DOE, Office of Technical Management.

DOE. 2009ab. "Yucca Mountain—Response to Request for Additional Information Regarding License Application (Safety Analysis Report Section 2.2, Table 2.2-5), Safety Evaluation Report Vol. 3, Chapter 2.2.1.2.1, Set 2." Letter (February 23) J.R. Williams to J.H. Sulima (NRC). ML090550101. Washington, DC: DOE, Office of Technical Management.

DOE. 2009ae. "Yucca Mountain—Response to Request for Additional Information Regarding License Application (Safety Analysis Report Section 2.2), Safety Evaluation Report Vol. 3, Chapter 2.2.1.2.1, Set 1." Letter (January 23) J.R. Williams to J.H. Sulima (NRC). ML090260710. Washington, DC: DOE, Office of Technical Management.

DOE. 2009af. "Yucca Mountain—Response to Request for Additional Information Regarding License Application (Safety Analysis Report Section 2.2, Table 2.2-5), Safety Evaluation Report Vol. 3, Chapter 2.2.1.2.1, Set 3." Letter (March 4) J.R. Williams to J.H. Sulima (NRC). ML091830594. Washington, DC: DOE, Office of Technical Management.

DOE. 2009ah. "Yucca Mountain—Response to Request for Additional Information Regarding License Application (Safety Analysis Report Section 2.2, Table 2.2-5), Safety Evaluation Report Vol. 3, Chapter 2.2.1.2.1, Set 2." Letter (March 3) J.R. Williams to J.H. Sulima (NRC). ML090860902. Washington, DC: DOE, Office of Technical Management.

DOE. 2009ai. "Yucca Mountain—Response to Request for Additional Information Regarding License Application (Safety Analysis Report Section 2.2.1.2), Safety Evaluation Report, Vol. 3, Chapter 2.2.1.2.1, Set 4." Letter (March 23) J.R. Williams to J.H. Sulima (NRC). ML090830357. Washington, DC: DOE, Office of Technical Management.

DOE. 2009aj. "Yucca Mountain—Response to Request for Additional Information Regarding License Application (Safety Analysis Report Section 2.2.1.2), Safety Evaluation Report, Vol. 3, Chapter 2.2.1.2.1, Set 4." Letter (March 24) J.R. Williams to J.H. Sulima (NRC). ML090840280. Washington, DC: DOE, Office of Technical Management.

DOE. 2009al. "Yucca Mountain—Response to Request for Additional Information Regarding License Application (Safety Analysis Report Section 2.2.1.2), Safety Evaluation Report Vol. 3, Chapter 2.2.1.2.1, Set 4." Letter (March 26) J.R. Williams to J.H. Sulima (NRC). ML090860424. Washington, DC: DOE, Office of Technical Management.

DOE. 2009av. DOE/RW-0573, "Yucca Mountain Repository License Application." Rev. 1. ML090700817. Las Vegas, Nevada: DOE, Office of Civilian Radioactive Waste Management.

DOE. 2009bo. "Yucca Mountain—Response to Request for Additional Information Regarding License Application (Safety Analysis Report Sections 2.3.2 and 2.3.3), Safety Evaluation Report Vol. 3, Chapter 2.2.1.3.6, Set 1." Letter (June 1) J.R. Williams to J.H. Sulima (NRC). ML091530403. Washington, DC: DOE, Office of Technical Management.

DOE. 2009bv. "Yucca Mountain—Response to Request for Additional Information Regarding License Application (Safety Analysis Report Section 2.2.1.2), Safety Evaluation Report Vol. 3, Chapter 2.2.1.2.1, Set 4." Letter (March 25) J.R. Williams to J.H. Sulima (NRC). ML090900069. Washington, DC: DOE, Office of Technical Management.

DOE. 2009bw. "Yucca Mountain—Response to Request for Additional Information Regarding License Application (Safety Analysis Report Section 2.2.1.2), Safety Evaluation Report Vol. 3, Chapter 2.2.1.2.1, Set 4." Letter (October 26) J.R. Williams to J.H. Sulima (NRC). ML093070154. Washington, DC: DOE, Office of Technical Management.

DOE. 2009bx. "Yucca Mountain—Supplemental Response to Request for Additional Information Regarding License Application (Safety Analysis Report Section 2.2.1.2), Safety Evaluation Report Vol. 3, Chapter 2.2.1.2.1, Set 4." Letter (December 15) J.R. Williams to J.H. Sulima (NRC). ML093500245. Washington, DC: DOE, Office of Technical Management.

DOE. 2009by. "Yucca Mountain—Supplemental Response to Request for Additional Information Regarding License Application (Safety Analysis Report Section 2.2, Table 2.2-5), Safety Evaluation Report Vol. 3, Chapter 2.2.1.2.1, Set 2." Letter (June 4) J.R. Williams to J.H. Sulima (NRC). ML091560538. Washington, DC: DOE, Office of Technical Management.

DOE. 2009bz. "Yucca Mountain—Supplemental Response to Request for Additional Information Regarding License Application (Safety Analysis Report Section 2.2, Table 2.2-5), Safety Evaluation Report Vol. 3, Chapter 2.2.1.2.1, Set 2." Letter (June 25) J.R. Williams to J.H. Sulima (NRC). ML091760913. Washington, DC: DOE, Office of Technical Management.

DOE. 2009ca. "Yucca Mountain—Supplemental Response to Request for Additional Information Regarding License Application (Safety Analysis Report Section 2.2, Table 2.2-5), Safety Evaluation Report Vol. 3, Chapter 2.2.1.2.1, Set 2." Letter (July 31) J.R. Williams to J.H. Sulima (NRC). ML092150623. Washington, DC: DOE, Office of Technical Management.

DOE. 2009cb. "Yucca Mountain—Response to Request for Additional Information Regarding License Application (Safety Analysis Report Section 2.2, Table 2.2-5), Safety Evaluation Report Vol. 3, Chapter 2.2.1.2.1, Set 5." Letter (June 5) J.R. Williams to J.H. Sulima (NRC). ML091590581. Washington, DC: DOE, Office of Technical Management.

DOE. 2009cc. "Yucca Mountain—Supplemental Response to Request for Additional Information Regarding License Application (Safety Analysis Report Section 2.2, Table 2.2-5), Safety Evaluation Report Vol. 3, Chapter 2.2.1.2.1, Set 5." Letter (August 12) J.R. Williams to J.H. Sulima (NRC). ML092250006. Washington, DC: DOE, Office of Technical Management.

DOE. 2009cd. "Yucca Mountain—Response to Request for Additional Information Regarding License Application (Safety Analysis Report Section 2.2, Table 2.2-5), Safety Evaluation Report Vol. 3, Chapter 2.2.1.2.1, Set 6." Letter (November 5) J.R. Williams to J.H. Sulima (NRC). ML093090335. Washington, DC: DOE, Office of Technical Management.

DOE. 2009ce. "Yucca Mountain—Response to Request for Additional Information Regarding License Application (Safety Analysis Report Section 2.2, Table 2.2-5), Safety Evaluation Report Vol. 3, Chapter 2.2.1.2.1, Set 6." Letter (November 17) J.R. Williams to J.H. Sulima (NRC). ML093220119. Washington, DC: DOE, Office of Technical Management.

DOE. 2009cf. "Yucca Mountain—Response to Request for Additional Information Regarding License Application (Safety Analysis Report Section 2.2, Table 2.2-5), Safety Evaluation Report Vol. 3, Chapter 2.2.1.2.1, Set 6." Letter (November 24) J.R. Williams to J.H. Sulima (NRC). ML093360134. Washington, DC: DOE, Office of Technical Management.

DOE. 2009cg. "Yucca Mountain—Response to Request for Additional Information Regarding License Application (Safety Analysis Report Section 2.2, Table 2.2-5), Safety Evaluation Report Vol. 3, Chapter 2.2.1.2.1, Set 6." Letter (December 3) J.R. Williams to J.H. Sulima (NRC). ML093380138. Washington, DC: DOE, Office of Technical Management.

DOE. 2009ch. "Yucca Mountain—Response to Request for Additional Information Regarding License Application (Safety Analysis Report Section 2.2, Table 2.2-5), Safety Evaluation Report Vol. 3, Chapter 2.2.1.2.1, Set 6." Letter (December 4) J.R. Williams to J.H. Sulima (NRC). ML093410044. Washington, DC: DOE, Office of Technical Management.

DOE. 2009ci. "Yucca Mountain—Response to Request for Additional Information Regarding License Application (Safety Analysis Report Section 2.2, Table 2.2-5), Safety Evaluation Report Vol. 3, Chapter 2.2.1.2.1, Set 7." Letter (October 30) J.R. Williams to J.H. Sulima (NRC). ML093060134. Washington, DC: DOE, Office of Technical Management.

DOE. 2009cj. "Yucca Mountain—Response to Request for Additional Information Regarding License Application (Safety Analysis Report Section 2.3.6.8), Safety Evaluation Report Vol. 3, Chapter 2.2.1.3.1, Set 3." Letter (May 7) J.R. Williams to J.H. Sulima (NRC). ML091280184. ML091280185. Washington, DC: DOE, Office of Technical Management.

DOE. 2009ck. "Yucca Mountain—Response to Request for Additional Information Regarding License Application (Safety Analysis Report Section 2.3.5), Safety Evaluation Report Vol. 3, Chapter 2.2.1.3.3, Set 1." Letter (April 30) J.R. Williams to J.H. Sulima (NRC). ML091210691. Washington, DC: DOE, Office of Technical Management.

DOE. 2009co. "Yucca Mountain—Response to Request for Additional Information Regarding License Application (Safety Analysis Report Section 2.2.1.2), Safety Evaluation Report Vol. 3, Chapter 2.2.1.2.1, Set 4." Letter (August 11) J.R. Williams to J.H. Sulima (NRC). ML092310639. Washington, DC: DOE, Office of Technical Management.

DOE. 2009cq. "Yucca Mountain—Supplemental Response to Request for Additional Information Regarding License Application (Safety Analysis Report Section 2.2, Table 2.2-5), Safety Evaluation Report Vol. 3, Chapter 2.2.1.2.1, Set 3." Letter (December 4) J.R. Williams to J.H. Sulima (NRC). ML093410044. Washington, DC: DOE, Office of Technical Management.

DOE. 2004aa. "Criticality Model." CAL-DSO-NU-000003. Rev. 00A. ECN 1. Las Vegas, Nevada: DOE, Office of Civilian Radioactive Waste Management.

DOE. 2004ab. "Isotopic Model for Commercial SNF Burnup Credit." CAL-DSU-NU-000007. Rev. 00B. ECN 1. Las Vegas, Nevada: DOE, Office of Civilian Radioactive Waste Management.

DOE. 2003aa. "Commercial Spent Nuclear Fuel Waste Package Misload Analysis." CAL-WHS-MD-000003. Rev. 00A. ECN 1. Las Vegas, Nevada: DOE, Office of Civilian Radioactive Waste Management.

Drefahl, K., P. Wincierz, U. Zwicker, and P. Delarbre. 1985aa. "The 230,000 h Creep Properties of Titanium Produced From Electrolytic and Sponge Material and TiAl6V4 Alloy at 20 °C." Proceedings from the 5th International Conference on Titanium, Congress-Center, Munich, Germany. pp. 2,387–2,394.

Dunn, D.S., Y.-M. Pan, L. Yang, and G.A. Cragnolino. 2006aa. "Localized Corrosion Susceptibility of Alloy 22 in Chloride Solutions: Part 2—Effect of Fabrication Processes." *Corrosion*. Vol. 62, No. 1. pp. 3–12.

Fix, D.V., J.C. Estill, L.L. Wong, and R.B. Rebak. 2004aa. "General and Localized Corrosion of Austenitic and Borated Stainless Steels in Simulated Concentrated Ground Waters." Proceedings of the 2004 ASME/JSME Pressure Vessel and Piping Conference: Transportation, Storage, and Disposal of Radioactive Materials Report No. PVP-Vol. 483. San Diego, California.

Gauthier, J.H., M.L. Wilson, D.J. Borns, and B.W. Arnold. 1996aa. "Impacts of Seismic Activity on Long-Term Repository Yucca Mountain." Proceedings of the American Nuclear Society Topical Meeting on Methods of Seismic Hazards Evaluation: Focus '95, September 18–20, 1995, Las Vegas, Nevada. pp. 159–168.

Glass, R.S., G.E. Overturf, R.E. Garrison, and R.D. McCright. 1984aa. "Electrochemical Determination of the Corrosion Behavior of Candidate Alloys Proposed for Containment of High Level Nuclear Waste in Tuff." Report UCID-20174. Livermore, California: Lawrence Livermore National Laboratory.

Green, R.T., C. Manepally, R.W. Fedors, and M.M. Roberts. 2008aa. "Examination of Thermal Refluxing in *In-Situ* Heater Tests." San Antonio, Texas: CNWRA

He, X. D.S. Dunn, and A.A. Csontos. 2007ab. "Corrosion of Similar and Dissimilar Metal Crevices in the Engineered Barrier System of a Potential Nuclear Waste Repository." *Electrochimica Acta*. Vol. 52. pp. 7,556–7,569.

Jaeger, J.C., N.G.W. Cook, and R.W. Zimmerman. 2007aa. *Fundamentals of Rock Mechanics*. 4th Edition. Malden, Massachusetts: Blackwell Publishing.

Kaiser, P.K., M.S. Diederichs, C.D. Martin, J. Sharp, and W. Steiner. 2000aa. "Underground Works in Hard Rock Tunnelling and Mining." Proceeding of GeoEng 2000, Melbourne, Australia. Lancaster, Pennsylvania: Technomic Publishing Company. pp. 841–926.

Kemeny J.M. and N.G.W. Cook. 1992aa. "Water Table Change Due to a Normal Faulting Earthquake." *Section 6: Demonstration of a Risk-Based Approach to High-Level Waste Repository Evaluation—Phase 2*. EPRI-TR-100384. Palo Alto, California: Electric Power Research Institute.

Kiessel, W.R. and M.J. Sinnott. 1953aa. "Creep Properties of Commercially Pure Titanium." *Journal of Metals*. Vol. 5. pp. 331–337.

Lin C., B. Leslie, R. Codell, H. Arit, and T. Ahn. 2003aa. "Potential Importance of Fluoride to Performance of the Drip Shield." Proceedings of the American Nuclear Society 10th International High-Level Radioactive Waste Management Conference, March 30–April 2, 2003, Las Vegas, Nevada

Lister, T., R. Mizia, A. Erickson, and S. Birk. 2007aa. "Electrochemical Corrosion Testing of Borated Stainless Steel Alloys." INL/EXT-07-12633. Rev. 1. Idaho Falls, Idaho: Idaho National Laboratory.

Lister T., R. Mizia, A. Erickson, and T. Trowbridge. 2007ab. "Electrochemical Corrosion Testing of Neutron Absorber Materials." INL/EXT-06-11772. Rev. 1. Idaho Falls, Idaho: Idaho National Laboratory.

Liu, Z. and G. Welsch. 1988aa. "Literature Survey on Diffusivities of Oxygen, Aluminum, and Vanadium in Alpha Titanium, Beta Titanium, and Rutile." *Metallurgical Transactions A*. Vol. 19A, No. 4. pp.121–125.

Liu, Z. and G. Welsch. 1988ab. "Effects of Oxygen and Heat Treatment on the Mechanical Properties of Alpha and Beta Titanium Alloys." *Metallurgical Transactions A*. Vol. 19a, No. 3 pp. 527–542.

Manepally, C., K. Bradbury, S. Colton, C. Dinwiddie, R. Green, R. McGinnis, D. Sims, K. Smart, and G. Walter. 2007aa. "The Nature of Flow in the Faulted and Fractured Paintbrush Nonwelded Hydrogeologic Unit." San Antonio, Texas: CNWRA.

McCright, R.D., W.G. Halsey, and R.A. Van Konynenburg. 1987aa. "Progress Report on the Results of Testing Advanced Conceptual Design Metal Barrier Materials Under Relevant Environmental Conditions for a Tuff Repository." Report No. UCID–21044. Livermore, California: Lawrence Livermore National Laboratory.

Miller, W.H., R.T. Chem, and E.A. Starke. 1987aa. "Microstructure, Creep and Tensile Deformation in Ti-6Al-2Nb-1Ta-0.8Mo." *Metallurgical Transactions A*. Vol. 18a. pp. 1,451–1,468.

Mintz, T. and X. He. 2009aa. "Modeling of Hydrogen Uphill Diffusion in Dissimilar Titanium Welds." Proceedings of the CORROSION 2009 Conference. Paper No. 09430. Houston, Texas: NACE International.

Moskalenko, V.A. and V.A. Puptsova. 1972aa. "Thermal Activation Parameters of the Plastic Deformation of Single Crystals of α -Titanium." *Fizika Metallov i Metallovedenie*. Vol. 34. pp. 1,264–1,269.

National Research Council. 1992aa. *Ground Water at Yucca Mountain: How High Can It Rise?* Washington, DC: National Academies Press.

NRC. 2005aa. NUREG–1762, "Integrated Issue Resolution Status Report." Rev. 1. Washington, DC: NRC.

NRC. 2005ac. Regulatory Guide 3.71, "Nuclear Criticality Safety Standards for Fuel and Material Facilities." Rev. 1. Washington, DC: NRC.

NRC. 2003aa. NUREG–1804, "Yucca Mountain Review Plan—Final Report." Rev. 2. Washington, DC: NRC.

NRC. 2000ab. NUREG–1567, "Standard Review Plan for Spent Fuel Dry Storage Facilities." Washington, DC: NRC, Spent Fuel Project Office.

Nuclear Energy Agency. 2006aa. "The NEA International FEP Database, Version 2.1." Issy-les-Moulineaux, France: Organisation for Economic Cooperation and Development, Nuclear Energy Agency.

Nuclear Energy Agency. 2001aa. "Scenario Development Methods and Practice: An Evaluation Based on the NEA Workshop on Scenario Development, Madrid, May 1999." Paris, France: Organisation for Economic cooperation and Development, Nuclear Energy Agency.

Nuclear Energy Agency. 2000aa. "Features, Events, and Processes (FEPs) for Geologic Disposal of Radioactive Waste: An International Database." Paris France: Organisation for Economic Co-operation and Development, Nuclear Energy Agency.

Nuclear Energy Agency. 1997ab. "Safety Assessment of Radioactive Waste Repositories: An International Database of Features, Events, and Processes." Ver. 3. SAM-J012-R1. Paris, France: Organisation for Economic Co-operation and Development, Nuclear Energy Agency.

Odegard, B.C. and A.W. Thompson. 1974aa. "Low Temperature Creep of Ti-6Al-4V." *Metallurgical Transactions A*. Vol. 5A. pp. 1,207–1,213.

Ofoegbu, G., R. Fedors, C. Grossman, S. Hsiung, L. Ibarra, C. Manepally, J. Myers, M. Nataraja, O. Pensado, K. Smart, and D. Wyrick. 2007aa. "Summary of Current Understanding of Drift Degradation and Its Effects on Performance at a Potential Yucca Mountain Repository." Rev. 1. CNWRA 2006-02 ML071030115. San Antonio, Texas: CNWRA.

Orava, R.N. 1967aa. "On the Deformation Mechanisms in Alpha-Titanium Below 0.4 T_M ." *Scripta Metallurgical*. Vol. 1. pp. 153–156.

Pan, Y.-M., D.S. Dunn, and G.A. Cragolino. 2005aa. "Topologically Close-Packed Phase Precipitation and Thermal Stability in Alloy 22." *Metallurgical and Materials Transactions*. Vol. 36A. pp. 1,143–1,151.

Parks, C.V., J.C. Wagner, D.E. Mueller, and I.C. Gauld. 2007aa. "Full Burnup Credit in Transport and Storage Casks—Benefits and Implementation." *Radwaste Solutions*. Vol. 14. pp. 32–41.

Perfect, D.L., C.C. Faunt, W.C. Steinkampf, and A.K. Turner. 1995aa. "Hydrochemical Data Base for the Death Valley Region, California and Nevada." USGS Open-File Report 94-305. Denver, Colorado: U.S. Geological Survey.

Pickett, D.A. and B.W. Leslie. 1999aa. "An Audit of the DOE Treatment of Features, Events, and Processes at Yucca Mountain, Nevada, With Emphasis on the Evolution of the Near-Field Environment." San Antonio, Texas: CNWRA.

Radulescu, G., D.E. Mueller, S. Goluoglu, D.F. Hollenbach, and P.B. Fox. 2007aa. "Range of Applicability and Bias Determination for Postclosure Criticality of Commercial Spent Nuclear Fuel." ACC: LLR.20071120.0179. ML092310677. Oak Ridge, Tennessee: Oak Ridge National Laboratory.

Rogers, J.W., Jr., K.L. Erickson, D.N. Belton, R.W. Springer, T.N. Taylor, and J.G. Berry. 1988aa. "Low Temperature Diffusion of Oxygen in Titanium and Titanium Oxide Films." *Applied Surface Science*. Vol. 35, No. 1. pp. 137–152.

Salve, R. and T.J. Kneafsey. 2005aa. "Vapor-Phase Transport in the Near-Drift Environmental at Yucca Mountain." *Water Resources Research*. Vol. 41. W01012. Washington, DC: American Geophysical Union.

SNL. 2008aa. "CSNF Loading Curve Sensitivity Analysis." ANL-EBS-NU-000010. Rev. 00. Las Vegas, Nevada: Sandia National Laboratories.

SNL. 2008ab. "Features, Events, and Processes for the Total System Performance Assessment: Analyses." ANL-WIS-MD-000027. Rev. 00. ACN 01, ERD 01, ERD 02. Las Vegas, Nevada: Sandia National Laboratories.

SNL. 2008ac. "Features, Events, and Processes for the Total System Performance Assessment: Methods." ANL-WIS-MD-000026. Rev. 00. Las Vegas, Nevada: Sandia National Laboratories.

SNL. 2008ad. "Postclosure Nuclear Safety Design Bases." ANL-WIS-MD-000024. Rev. 01. ACN 01, ERD 01, ERD 02. Las Vegas, Nevada: Sandia National Laboratories.

SNL. 2008ae. "Screening Analysis of Criticality Features, Events, and Processes for License Application." ANL-DSO-NU-000001. Rev. 00. ACN 01, ERD 01, ERD 02. Las Vegas, Nevada: Sandia National Laboratories.

SNL. 2008ag. "Total System Performance Assessment Model/Analysis for the License Application." MDL-WIS-PA-000005. Rev. 00. AD 01, ERD 01, ERD 02, ERD 03, ERD 04. Las Vegas, Nevada: Sandia National Laboratories.

SNL. 2008aj. "Multiscale Thermohydrologic Model." ANL-EBS-MD-000049. Rev. 03. ADD 02. Las Vegas, Nevada: Sandia National Laboratories.

SNL. 2008al. "Waste Package Flooding Probability Evaluation." CAL-DN0-NU-000002. Rev. 00C. AD 01. Las Vegas, Nevada: Sandia National Laboratories.

SNL. 2007ab. "Atmospheric Dispersal and Deposition of Tephra From a Potential Volcanic Eruption at Yucca Mountain, Nevada." MDL-MGR-GS-000002. Rev. 03. ERD 01. Las Vegas, Nevada: Sandia National Laboratories.

SNL. 2007ai. "Drift-Scale THC Seepage Model." MDL-NBS-HS-000001. Rev. 05. ERD 01. Las Vegas, Nevada: Sandia National Laboratories.

SNL. 2007ak. "Engineered Barrier System: Physical and Chemical Environment." ANL-EBS-MD-000033. Rev. 06. ERD 01. Las Vegas, Nevada: Sandia National Laboratories.

SNL. 2007al. "General Corrosion and Localized Corrosion of Waste Package Outer Barrier." ANL-EBS-MD-000003. Rev. 03. ACN 01, ERD 01. Las Vegas, Nevada: Sandia National Laboratories.

SNL. 2007am. "Geochemistry Model Validation Report: Material Degradation and Release Model." ANL-EBS-GS-000001. Rev. 02. Las Vegas, Nevada: Sandia National Laboratories.

SNL. 2007ax. "Saturated Zone Site-Scale Flow Model." MDL-NBS-HS-000011. Rev. 03. ACN 01, ERD 01, ERD 02. ERD 03. Las Vegas, Nevada: Sandia National Laboratories.

SNL. 2007bb. "Stress Corrosion Cracking of Waste Package Outer Barrier and Drip Shield Materials." ANL-EBS-MD-000005. Rev. 04. ERD 01, ERD 02. Las Vegas, Nevada: Sandia National Laboratories.

SNL. 2007bf. "UZ Flow Models and Submodels." MDL-NBS-HS-000006. Rev. 03. ACN 01, ERD 01, ERD 02, ERD 03. Las Vegas, Nevada: Sandia National Laboratories.

Stetina, K. 1980aa. "Creep of Titanium Between 30 °C and 300 °C." Proceedings of the International Conference on Engineering Aspects of Creep, September 1980, University of Sheffield, England. Paper No. C194/80. London, England: Institute of Mechanical Engineers.

Stetina, K. 1969aa. "Comments on 'On the Deformation Mechanisms in Alpha-Titanium Below 0.4 T_M.'" *Scripta Metallurgica*. Vol. 3. pp. 57–58.

Stonestrom, D.A., D.E. Prudic, R.J. Lacznia, K.C. Akstin, R.A. Boyd, and K.K. Henkelman. 2003aa. "Estimates of Deep Percolation Beneath Native Vegetation, Irrigated Fields, and the Amargosa-River Channel, Amargosa Desert, Nye County, Nevada." USGS Open-Field Report 03-104. Denver, Colorado: U.S. Geological Survey.

Teper, B. 1991aa. "Activities Aimed at Qualification of a HLW Disposal Canister." Proceedings of the Second Annual International Conference on High-Level Radioactive Waste Management, Las Vegas, Nevada, April 1991. La Grange Park, Illinois: American Nuclear Society.

Thompson, A.W. and B.C. Odegard. 1973aa. "The Influence of Microstructure on Low Temperature Creep of Ti-5Al-2.5Sn." *Metallurgical Transactions*. Vol. 4. pp. 899–908.

Turner, D.R. and R.T. Pabalan. 1999aa. "Abstraction of Mechanistic Sorption Model Results for Performance Assessment Calculations at Yucca Mountain, Nevada." *Waste Management*. Vol. 19. pp. 375–388.

Waiting, D.J., J.A. Stamatakis, D.A. Ferrill, D.W. Sims, A.P. Morris, P.S. Justus, and K.I. Abou-Bakr. 2003aa. "Methodologies for the Evaluation of Faulting at Yucca Mountain, Nevada." Proceedings of the 10th International High-Level Radioactive Waste Management Conference, Las Vegas, Nevada, March 30–April 2, 2003. La Grange Park, Illinois: American Nuclear Society. pp. 377–387.

Zeyfang, R., R. Martin, and H. Conrad. 1971aa. "Low Temperature Creep of Titanium." *Materials Science and Engineering*. Vol. 8. pp. 134–140.

CHAPTER 3

2.2.1.2.2 Identification of Events With Probabilities Greater Than 10^{-8} Per Year

2.2.1.2.2.1 Introduction

This chapter evaluates the U.S. Department of Energy's (DOE) information on event probability used in its performance assessments evaluations. The U.S. Nuclear Regulatory Commission (NRC) staff's evaluation is based on information provided in the Safety Analysis Report (SAR) (DOE, 2008ab), as supplemented by the DOE responses to the staff's requests for additional information (RAIs) (DOE, 2009aa–ad,aq,bd).

A performance assessment is a systematic analysis that answers the following triplet risk questions: What can happen? How likely is it to happen? What are the consequences? Scenario analysis answers the first question: What can happen? The staff's evaluation of the DOE scenario analysis is documented in its Safety Evaluation Report (SER) Section 2.2.1.2.1. One result from the scenario analysis is the identification of the events to be included in the performance assessment calculation used to demonstrate compliance with the postclosure performance objectives. This chapter addresses the second question: How likely is it that these events will happen?

A performance assessment evaluation that is used to demonstrate compliance with the individual protection standard for the proposed Yucca Mountain repository must consider events that have at least 1 chance in 100 million per years of occurring. To address this requirement, DOE identified and described those events that exceeded this probability threshold. Performance assessments are also used to demonstrate compliance with the human intrusion and groundwater protection standards. These performance assessments have different considerations for event probabilities than those required for the individual protection standard. The DOE approach for quantifying the event probabilities and the technical basis for determining the probability estimates assigned to each event type are addressed in this chapter.

2.2.1.2.2.2 Regulatory Requirements

A performance assessment evaluation is required, per 10 CFR 63.113, to demonstrate compliance with the postclosure individual protection standard, human intrusion standard, and the groundwater protection standard. 10 CFR 63.114, 63.303, 63.305, 63.312, and 63.342 identify the regulatory standards. For demonstrating compliance with the human intrusion standard (10 CFR 63.321 and 63.222), the requirements for the performance assessment are stipulated in 10 CFR 63.114, 63.303, 63.305, 63.312, and 63.342. The requirements for the performance assessment used for demonstrating compliance with the groundwater protection standard limit (10 CFR 63.331) are identified in 10 CFR 63.114, 63.303, 63.332, and 63.342.

This chapter of the SER documents the staff's review and findings on whether DOE complied with the requirements of 10 CFR 63.114(a)(4) and 63.114(b). 10 CFR 63.114(a)(4) states, "consider only features, events, and processes (FEPs) consistent with the limits on performance assessment specified at 10 CFR 63.342." 10 CFR 63.342(a) requires that a performance assessment used to show compliance with 10 CFR 63.311(a)(1), 10 CFR 63.321(b)(1), and 10 CFR 63.331 not consider very unlikely events (i.e., those that are estimated to have a less than 1 chance in 100 million per year of occurring). Further, 10 CFR 63.342(b) establishes that

compliance with 10 CFR 63.321(b)(1) and 10 CFR 63.331 shall exclude unlikely events (i.e., those events that are estimated to have an annual probability of occurring between 1 in 100,000 and 1 in 100 million). 10 CFR 63.114(b) stipulates that the performance assessment methods used to satisfy the requirements of 10 CFR 63.114(a) are considered sufficient for the performance assessment for the period of time after 10,000 years and through the period of geologic stability.

The NRC staff has followed the review guidance provided in the Yucca Mountain Review Plan (YMRP) (NRC, 2003aa). YMRP Section 2.2.1.2.2 identifies the following five criteria that the staff may consider in its evaluation:

1. Events are adequately defined.
2. Probability estimates for future events are supported by appropriate technical bases.
3. Probability model support is adequate.
4. Probability model parameters have been adequately established.
5. Uncertainty in event probability is adequately evaluated.

Additionally, YMRP Section 2.2.1 provides guidance to the staff on an acceptable process to apply risk information in its review of the DOE licensing application. Following the YMRP guidance, the staff considered DOE's risk information (derived from DOE's treatment of multiple barriers) and risk insights that are identified in SAR Section 2.4.2.2.1.2. The level of detail of the staff's review on particular parts of the application is based on the risk insights DOE developed and independent staff assessments, as appropriate. Accordingly, the staff used a graded approach in its review per the guidance identified in YMRP Section 2.2.1.2.2.

2.2.1.2.2.3 Technical Review

In SAR Section 2.2.2, DOE considered events for inclusion into the postclosure performance assessments. Initial considerations included five event types: igneous events, seismic events, early failure events, criticality events, and human intrusion events. As described in SAR Section 2.2.1.2.1, DOE screened out the individual criticality FEPs and DOE determined that the probability of the nuclear criticality event class has less than 1 chance in 100 million per year of occurring.

As described in SAR Section 2.2.2, DOE analyzed the human intrusion event in its performance assessment evaluation to demonstrate compliance with 10 CFR 63.321, consistent with the regulatory requirements of 10 CFR 63.322. 10 CFR 63.102(l) does not specify a probability for the human intrusion event, but requires a separate analysis subject to the specific requirements of 10 CFR 63.321, 63.322, and 63.342. Because no probability value is required, the YMRP Acceptance Criteria 2 through 5 are not applicable. DOE defined the human intrusion event in SAR Section 2.2.2.4.1 and in SAR Table 2.2-6.

The staff reviewed the DOE's definition of the human intrusion event to determine whether the event definition is unambiguous and consistent with the regulatory requirements. (b)(5)

(b)(5)

(b)(5)

DOE also incorporated, as part of the technical basis and approach for including the FEP, the regulatory requirement (10 CFR 63.321) for determining the

earliest time after disposal that the waste package would degrade sufficiently that human intrusion could occur without recognition by the drillers. (b)(5)

(b)(5) The staff's evaluation of the performance assessment DOE used to demonstrate compliance with the human intrusion standard (10 CFR 63.321 and 63.222) is documented in SER Section 2.2.1.4.2.

DOE retained igneous activity, seismic activity, and early failure events in its performance assessment evaluation to demonstrate compliance with the individual protection standard at 10 CFR 63.311. The staff's evaluations of DOE information for igneous events, seismic events, and early failure events are documented in SER Sections 2.2.1.2.2.3.1, 2.2.1.2.2.3.2, and 2.2.1.2.2.3.3, respectively.

2.2.1.2.2.3.1 Technical Review for Igneous Event Probabilities

This section presents the staff's evaluation of information DOE presented to estimate the probability of future igneous events. The staff reviewed SAR Sections 2.1 and 2.4; SAR Sections 1.1.6, 2.2.2.2, and 2.3.11; and material provided in response to NRC staff's RAI (DOE, 2009aa) and the references cited therein. The DOE's description of past igneous activity in the Yucca Mountain region (SAR Sections 1.1.6 and 2.3.11) and the overall approach for treatment of igneous events in the license application are summarized next.

DOE indicated that periods of igneous activity have resulted in the eruption of basalt magmas in the Yucca Mountain region during the last 11 million years and identified that the risk to the repository from future igneous activity could come from rising basalt magmas. The age and location of basaltic rocks that formed during at least six volcanic events in the last 5 million years, within approximately 50 km [31.1 mi] of the repository, are provided in SAR Figure 1.1-152. In presenting information on the location of volcanism in the Yucca Mountain region, DOE described the geologic and geophysical techniques it used to characterize past activities. DOE indicated that basalts in the Yucca Mountain region appear to be products of partial melting of lower lithospheric mantle material, but acknowledged that there is a poor understanding of the exact mechanism of mantle melting. DOE characterized the basaltic volcanism in the Crater Flat volcanic field, which is in close proximity to Yucca Mountain, as having a relatively long lifetime with a small volume of erupted material (SAR Section 1.1.6.1.1).

DOE included igneous events within the igneous event scenario class (SAR Section 2.2.1.3.1). The DOE's Total System Performance Assessment (TSPA) evaluation divides the igneous event scenario class into separate modeling cases for intrusive events and extrusive events (SAR Section 2.4.1.2.3). Intrusive events involve the rise of molten rock (i.e., magma) from deep in the Earth with the magma intersecting the repository drifts (tunnels). DOE made the assumption that if magma flows into drifts, it damages the barrier capabilities of the drip shields and waste packages and allows subsequent radionuclide release through the hydrologic (water) transport pathway (SAR Section 2.3.11.3). The applicant viewed extrusive events as an extension of intrusive events: after the magma has entered a repository drift and reached the surface, a conduit may develop from which most of the magma erupts, producing a volcano. Of the intrusive igneous events that intersect the repository footprint, DOE only considered a subset of these events to develop a conduit within the repository and form a volcano at the surface. DOE further assumed that only in some cases will waste packages be intersected by this conduit and release their contents into the rising magma. The magma and incorporated waste is then explosively erupted (expelled) from the surface volcano and transported by airborne dispersion for some distance downwind of the vent (SAR Section 2.3.11.4). Thus, the probabilities of intrusive and extrusive (volcanic eruptive) igneous events that may disperse

waste and radionuclides into the environment, either in the subsurface or via atmospheric transport, are different (SAR Section 2.4.1.2.3). To assess the probability of a future igneous event intersecting the repository, DOE conducted a probabilistic volcanic hazard assessment (PVHA) using an elicitation process consisting of recognized experts (SAR Section 5.4).

Risk Perspective

If an igneous event occurred at the proposed repository, the igneous intrusion modeling case would constitute most of the calculated dose for the first 1,000 years following closure, as shown in SAR Figure 2.4-18(a), and is approximately half the calculated dose for the seismic ground motion modeling case in the ensuing 9,000 years. For the first 10,000 years, SAR Figure 2.4-18(a) indicated that the mean annual dose from igneous intrusion for the first 10,000 years after permanent closure is at least approximately 100 times lower than the dose limit. Moreover, DOE indicated that for the post-10,000-year period, the igneous intrusion modeling case and seismic ground motion modeling case provide approximately equal contributions to the total mean annual dose to the reasonably maximally exposed individual for the last 300,000 years of the time period, and that each modeling case is about 100 times lower than the dose limit. This statement (in SAR Section 2.1) is supported by the results presented in SAR Figure 2.4-18(b).

In SAR Section 2.4.2.2.1.2.3, DOE provided the probability-weighted consequences of igneous activity (intrusive and extrusive) using the probability distribution from the PVHA. DOE identified that the probability-weighted igneous intrusive dose is estimated to be less than 0.1 mrem for the 10,000-year period and less than 0.5 mrem for the post-10,000-year time period (SAR Section 2.4.2.2.1.2.3.1). The DOE estimates for probability-weighted igneous extrusive (volcanic eruptive) dose are about 10^{-4} mrem for the 10,000-year period and less than 6×10^{-5} mrem for the post-10,000-year time period (SAR Section 2.4.2.2.1.2.3.2).

(b)(5)

(b)(5)

For igneous intrusive events, DOE assumed that all waste packages will fail (approximately 11,000), whereas for an igneous extrusive event, DOE estimated only a few waste packages (<10) will result in radionuclide release (SAR Section 2.3.11.4.2.1).

Summary of the DOE License Application on Igneous Event Probability

DOE evaluated the risk of future igneous activity, in part, by considering the probability that a future igneous event could intersect the repository. To quantify the probability of future igneous activity at the proposed Yucca Mountain repository, DOE conducted an expert elicitation review (PVHA) (CRWMS M&O, 1996aa). This expert elicitation review resulted in a quantification of the mean annual probability, and its associated uncertainty distribution, of intersection of the repository by a future basaltic dike (an igneous intrusion) and its associated uncertainty distribution.

In SAR Sections 2.2.2.2.1–2.2.2.2.5, DOE described the probability of a future igneous event intersecting the repository, the technical basis for the probability estimate, the probability model support including alternative estimates of the intersection probability, the probability model parameters, and the uncertainties associated with the probability estimate, respectively.

Subsequent to the PVHA, DOE conducted an aeromagnetic survey and drilling program to increase confidence in site characterization results related to igneous activity. As described in

Comment (b)(5)

(b)(5)

SER Section 2.5.4, DOE updated the PVHA (CRWMS M&O, 1996aa) in a study known as probabilistic volcanic hazard assessment-update (PVHA-U) (SNL, 2008ah). In SAR Section 5.4.1 (DOE, 2009av), DOE stated that the PVHA-U was conducted in a manner that is consistent with NUREG-1563 (NRC, 1996aa) and past practices. The average annual probability for an intrusive igneous event calculated in the PVHA-U is approximately twice as high as calculated in the original PVHA (Boyle, 2008aa). DOE stated that the difference between these two event probability distributions would not significantly affect the estimates of repository performance over either 10,000 years or 1 million years, and in SAR Section 5.4.1, DOE further stated that the PVHA-U results are confirmatory of the original PVHA technical basis (DOE, 2009av; also see Boyle, 2008aa).

Staff Evaluation of Igneous Event Probability

The staff reviewed DOE's igneous event probability in SAR Sections 2.2.2.2.2, 2.2.2.2.4, and 2.2.2.2.5. (b)(5)

(b)(5)

Event Definition

In SAR Section 2.2.2.2.1.1, DOE stated that the output of the PVHA is the annual frequency of intersection of the proposed repository by an intrusive basaltic dike [CRWMS M&O, Section 4.2, Figure 4-32 (1996aa)]. The PVHA expert elicitation program computed the mean annual probability of intersection of the proposed repository by an igneous basaltic dike as 1.5×10^{-8} per year (CRWMS M&O, 1996aa). The PVHA results increased only slightly when these probability estimates were recalculated to reflect postelicitation changes to the size, shape, and location of the proposed repository footprint (BSC, 2004af); the recalculated mean annual probability from PVHA thus became 1.7×10^{-8} per year (SAR Section 2.2.2.1.2). In the TSPA, DOE sampled a distribution of probability values for the likelihood of intrusive intersection with a mean value of 1.7×10^{-8} per year and computed the 5th and 95th percentiles of the uncertainty distribution at 7.4×10^{-10} and 5.5×10^{-8} , respectively.

DOE also calculated the proportion of the intersections that include development of a conduit (i.e., an eruption through the repository). It incorporated information from the PVHA and model calculations that are supported by information obtained from studies of analog volcanoes with exposed intrusive rocks from depths of 200–300 m [656–984 ft] (SNL, 2007ae). DOE subsequently calculated that 28 percent of intrusive events would develop a volcanic conduit within the repository footprint (SAR Sections 2.2.2.2.1.3 and 2.3.11.4.2.1). This fraction was determined by considering that a conduit can form at any location on a dike that intersects the repository and thus may not necessarily form within the footprint and by considering several other factors (SER Section 2.3.11.4.2.1.3). This conditional probability is for a conduit that develops within the repository. DOE then applied a second conditional probability of 0.29 (SAR Section 2.3.11.4.2.1) to represent the fraction of conduits that may intersect a drift containing waste packages and eject the waste contents through a volcanic vent (SAR Section 2.3.11.4.2.1).

Some PVHA panel members (CRWMS M&O, 1996aa) used event definitions for igneous events that included characteristics of both intrusive and extrusive events. For example, recurrence rates for intrusive events often were determined by interpreting the number of volcanic vents associated with a single event. However, the dike lengths used to represent these recurrence rates in probability models were independent of the relevant vent counts. See, for example, the discussion by McBirney in CRWMS M&O Appendix E (1996aa) that gave 90 percent weight to the 12-km [7.5-mi]-long chain of Quaternary Crater Flat volcanoes as representing a single event, but gave 90 percent weight that the dike supporting this event is less than 5 km [3.1 mi] {the dike must be at least 12 km [7.5 mi] long to feed the chain of volcanoes}. These inconsistencies in event definitions were resolved in the PVHA-U (SNL, 2008ah), which used consistent definitions for intrusive and extrusive (volcanic) igneous event probabilities.

The probability of an intrusive disruption of the repository differed between PVHA and PVHA-U by a factor of 1.8 (1.7×10^{-8} versus 3.1×10^{-8} per year, respectively). The event definition for the extrusive (volcanic) case in PVHA-U was the formation of a conduit within the repository that would support an (explosive) eruption column; thus it was different and more specific than the PVHA conditional probability of a conduit forming. The probability of an eruptive conduit event developing within the repository differed between PVHA and PVHA-U by a factor of 2.5 (4.8×10^{-9} versus 1.2×10^{-8} per year, respectively). However, the two values are not directly comparable for the reason stated previously (Boyle, 2008aa) (b)(5)

(b)(5)

(b)(5)

Further information and review of the intrusive and extrusive (volcanic) igneous scenarios are provided by DOE in SAR Section 2.3.11 and by the staff's evaluation in SER Section 2.2.1.3.10.

(b)(5)

Comment (b)(5)

(b)(5)

(b)(5)

Probability Model Support

In describing the geologic basis for the PVHA (SAR Section 2.2.2.3.1), DOE indicated that the PVHA combined multiple alternative conceptual models into a single distribution that captured the uncertainty in the expert panel's conceptual models for the physical behavior of volcanism in the Yucca Mountain region. DOE also stated that for regional volcanism, no single conceptual model is appropriate because the underlying physical processes that control the precise timing and location of volcanic events within a particular region remain uncertain (BSC, 2004af). To support the PVHA, DOE provided its elicitation panel with a variety of published information on igneous features, tectonics, and geophysical characteristics of the Yucca Mountain region

(see CRWMS M&O, 1996aa). The PVHA panel concluded that basaltic volcanism in the Yucca Mountain region resulted from complex interactions in the lithospheric mantle that produced episodes of small-volume basaltic magma. Because these mantle processes were viewed as uncertain, the PVHA panel members did not explicitly include mantle processes in their probability models.

DOE has also indicated that past volcanic activity has occurred in the tectonically active Yucca Mountain region and could continue into the future with a very small probability of occurrence. During the period from 14 to 10 million years ago, major explosive eruptions involving rhyolite magma from volcanic centers lying roughly 20–40 km [12–25 mi] north of the repository site formed large caldera volcanoes and deposited the volcanic ash-flow tuffs of the region, some of which are the host rocks for the proposed repository. There has been a sufficient time gap since caldera-forming volcanic activity ended about 8 million years ago (BSC, 2004bi) for DOE to conclude that the chance of a recurrence within the repository lifetime is less than 1 in 10,000 during 10,000 years (SAR Sections 2.2.2.2.1 and 2.3.11.2.1.1; see also Detournay, et al., 2003aa). (b)(5)

(b)(5)

(b)(5)

To support the PVHA probability estimates developed prior to 2002, DOE characterized known basaltic igneous features within approximately 80.5 km [50 mi] of the Yucca Mountain site (BSC, 2004af). These investigations provided the location, age, and basic characteristics necessary to support probability estimates in the PVHA. DOE also conducted geophysical investigations and borehole drilling to further characterize buried igneous features in the Yucca Mountain region (O'Leary, et al., 2002aa; Perry, et al., 2005aa). This new information was considered in the PVHA-U (SNL, 2008ah). The staff reviewed the information in these documents and (b)(5)

(b)(5)

(b)(5)

Comment (b)(5)

Comment (b)(5)

(b)(5)

(b)(5)

(b)(5)

(b)(5)

DOE discussed alternative estimates of the annual probability of an intrusive event intersecting the repository footprint (SAR Section 2.2.2.2.3.2). Both the staff and the State of Nevada independently sponsored the development of these published models (SAR Table 2.2-18). Some of these models use methods and data developed after the 1996 PVHA elicitation. Annual probability estimates for these published models range from 3×10^{-10} to 3×10^{-7} . DOE stated that these values cluster at slightly greater than 10^{-8} per year (SAR Section 2.2.2.2.3.2) and concluded that the apparent clustering near 10^{-8} per year provides confidence that the PVHA probability estimate is robust. (b)(5)

(b)(5)

In the discussion of probability model support (SAR Section 2.2.2.2.3.2), DOE did not address published models by Ho and Smith (1997aa) and Ho, et al. (2006aa). The staff requested additional information from DOE to address these published probability estimates. In its response to the staff, DOE concluded that the calculations in Ho and Smith (1997aa) were performed as sensitivity analyses, which included parameter ranges selected from either expert knowledge or for "mathematical convenience," as stated in Ho and Smith, p. 621 (1997aa). DOE stated that the probability model approach developed in Ho and Smith (1997aa) was captured in the range of probability estimates Ho and Smith (1998aa) presented subsequently. The staff reviewed the information in the DOE response and (b)(5)

(b)(5)

As an independent confirmatory estimate, the staff examined whether the DOE's probability model results are consistent with past patterns of basaltic igneous events in the Yucca Mountain region that are younger than approximately 11 million years old in the Yucca Mountain region.

(b)(5)

(b)(5)

As shown in BSC (2004af), during the past approximately 11 million years, about 20 basaltic igneous events have occurred in the Crater Flat–Amargosa Valley area. These events are the basic event data used in most probability models for Yucca Mountain (CRWMS M&O, 1996aa; SAR Section 2.2.2.2.1.3).

(b)(5)

Comment (b)(5)

(b)(5)

(b)(5)

(b)(5)

Comment (b)(5)

(b)(5)

Comment (b)(5)

(b)(5)

(b)(5)

(b)(5)

Findings

On the basis of the information DOE provided, the staff's evaluation of the PVHA expert elicitation process in SER Section 2.5.4, and the preceding review, staff reached the following findings.

(b)(5)

(b)(5)

(b)(5)

Evaluation Findings

(b)(5)

2.2.1.2.2.3.2 Technical Review for Seismic Event Probabilities

This section reviews and evaluates information DOE presented to estimate the probability of seismic ground motion and fault displacement at the proposed repository site. This technical review of seismic event probabilities follows the review guidance provided in the YMRP Sections 2.2.1 and 2.2.1.2.2. As part of its technical review, the staff reviewed SAR Sections 2.2.2.1 and 2.3.4 and additional information provided in response to the staff's RAI in DOE Enclosure 19 (2009ab) and DOE Enclosures 6, 7, and 8 (2009aq) and the references cited therein.

Risk Perspective

As described in SER Section 2.2.1.2.2.3.1, DOE indicated that the seismic ground motion modeling case dominates the mean annual dose for the first 10,000 years after permanent closure and that the mean annual dose from seismic ground motion is about 100 times smaller than the dose limit. As shown in SAR Figure 2.4-18(a), the seismic ground motion modeling case constitutes most of the calculated dose after the first 2,000 years following closure. For the first 10,000 years, SAR Figure 2.4-18(a) indicates mean annual dose from seismic ground motion for the first 10,000 years after permanent closure is at least approximately 100 times lower than the dose limit. Moreover, DOE indicated that for the post-10,000-year period, the igneous intrusion modeling case and seismic ground motion modeling case provide approximately equal contributions to the total mean annual dose to the reasonably maximally exposed individual for the last 300,000 years of the time period, and that the calculated dose in each modeling case is about 100 times lower than the dose limit.

Summary of DOE License Application on Seismic Event Probability

SAR Section 2.2.2.1 described the DOE's overall approach to developing a seismic hazard assessment for Yucca Mountain, including fault displacement hazards. This overall approach involves the following three general steps.

1. DOE conducted an expert elicitation program in the late 1990s to develop a probabilistic seismic hazard assessment (PSHA) for Yucca Mountain. This assessment included a probabilistic fault displacement hazard assessment (PFDHA) (CRWMS M&O, 1998aa; BSC, 2004bp). The PSHA was developed for a reference bedrock outcrop, specified as a free-field site condition with a mean shear wave velocity (V_s) of 1,900 m/sec [6,233 ft/sec] and located adjacent to Yucca Mountain. This value was derived from a shear wave velocity profile of Yucca Mountain with the top 300 m [984 ft] of tuff and alluvium removed, as provided in Schneider, et al., Section 5 (1996aa).
2. DOE conditioned the PSHA ground motion results to constrain the large low-probability ground motions to ground motion levels that, according to DOE, are more consistent with observed geologic and seismic conditions at Yucca Mountain, as provided in BSC, ACN02 (2005aj).
3. DOE modified the conditioned PSHA results, using site-response modeling, to account for site-specific rock material properties of the tuff in and beneath the emplacement drifts and the site-specific rock and soil material properties of the strata beneath the Geologic Repository Operation Area (GROA). DOE used the results of the site response to develop inputs for preclosure seismic design and the preclosure seismic safety analysis as well as inputs to its postclosure TSPA calculation, as provided in BSC (2005aj) and BSC, ACN 02 (2008bl).

DOE applied these three steps equally to the preclosure seismic design and safety analyses as well as to its postclosure performance assessment. Moreover, many of the geological and geophysical data, conceptual and process models, and supporting technical analyses to support the DOE's conclusions in the SAR are common to the preclosure seismic design and safety analyses and postclosure performance assessment calculations. The staff documented its evaluation of Step 1 in SER Section 2.5.4. The staff's evaluation of those aspects of the DOE's seismic hazard assessment (Steps 2 and 3) that are pertinent to postclosure performance assessment, including evaluations needed to address the five event probability acceptance criteria in the YMRP, is documented in this SER chapter.

DOE PSHA Expert Elicitation

DOE conducted an expert elicitation on PSHA in the late 1990s (CRWMS M&O, 1998aa; BSC, 2004bp) based on the methodology described in the Yucca Mountain Site Characterization Project (DOE, 1997aa). DOE stated that its PSHA methodology followed the guidance of the DOE-NRC-Electric Power Research Institute-sponsored Senior Seismic Hazard Analysis Committee (Budnitz, et al., 1997aa). On SAR p. 2.2-67, DOE concluded that the methodology used for the PSHA expert elicitation is consistent with the NRC expert elicitation guidance, which is described in NUREG-1563 (NRC, 1996aa).

To conduct the PSHA, DOE convened two panels of experts. The first expert panel consisted of six, three-member teams of geologists and geophysicists (seismic source teams) who developed probabilistic distributions to characterize relevant potential seismic sources in the

Yucca Mountain region. These distributions included location and activity rates for fault sources, spatial distributions and activity rates for background sources, distributions of moment magnitude and maximum magnitude, and site-to-source distances. The second panel consisted of seven seismology experts (ground motion experts) who developed probabilistic point estimates of ground motion for a suite of earthquake magnitudes, distances, fault geometries, and faulting styles. These point estimates incorporated random and unknown uncertainties that were specific to the regional crustal conditions of the western Basin and Range. The ground motion attenuation point estimates were then fitted to yield the ground motion attenuation equations used in the PSHA. The two expert panels were supported by technical teams from DOE, the U.S. Geological Survey, and Risk Engineering Inc., who provided the experts with relevant data and information; facilitated the formal elicitation, including a series of workshops designed to accomplish the elicitation process; and integrated the hazard results.

The resulting ground motion hazard curves express increasing levels of ground motion as a function of the annual probability that the ground motion will be exceeded. These curves include estimates of uncertainty (see SAR Figure 2.2-9; for example, PSHA curves). The SAR provided PSHA findings on horizontal and vertical components of peak acceleration (defined at 100 Hz); spectral accelerations at frequencies of 0.3, 0.5, 1, 2, 5, 10, and 20 Hz; and peak ground velocity (PGV).

The staff's review of the PSHA finds that DOE's expert elicitation process followed the NRC guidance provided in NUREG-1563 to quantify probabilistic seismic hazards (e.g., Cornell, 1968aa; McGuire, 1976aa). The staff's review of the PSHA expert elicitation process is documented in SER Section 2.5.4. The basic elements of this process are (i) identification of seismic sources such as active faults or seismic zones; (ii) characterization of each of the seismic sources in terms of their activity, recurrence rates for various earthquake magnitudes, and maximum magnitude; (iii) ground motion attenuation relationships to model the distribution of ground motions that will be experienced at the site when a given magnitude earthquake occurs at a particular source; and (iv) incorporation of the inputs into a logic tree to integrate the seismic source characterization and ground motion attenuation relationships, including associated uncertainties. Each logic tree pathway represents one expert's weighted interpretations of the seismic hazard at the site. The computation of the hazard for all possible pathways results in a distribution of hazard curves that is representative of the seismic hazard at a site, including variability and uncertainty.

(b)(5)

Probabilistic Fault Displacement Hazard Assessment

The seismic source teams also developed a PFDHA as part of the PSHA. DOE used results from the PFDHA in its preclosure analysis to assess how surface fault displacements within the GROA could potentially affect preclosure safety and repository design. The NRC staff's

evaluation of DOE's preclosure fault displacement analysis is described in SER Volume 2, Section 2.1.1.1.3.5. To assess the postclosure performance, DOE relied on the PFDHA results to support the TSPA analyses of mechanical degradation of engineered barrier systems. In SAR Section 2.3.4, DOE described how the information from the PFDHA was used to develop the fault displacement abstraction and to generate inputs to the TSPA. The staff's evaluation of the DOE's analysis of postclosure fault displacement effects on engineered barriers is described in SER Section 2.2.1.3.2.3.3.

In the PFDHA, the experts derived probabilistic fault displacement hazard curves for nine demonstration points at or near Yucca Mountain (SAR Table 2.2-15 and Figure 2.2-12). These demonstration points represent a range of faulting and related fault deformation conditions in the subsurface and near the proposed surface facility sites in the GROA, including large block bounding faults such as the Solitario Canyon Fault, smaller mapped faults within the repository footprint such as the Ghost Dance Fault, unmapped minor faults near the larger faults, fractured tuff, and intact tuff. The fault displacement hazard curves (e.g., SAR Figure 2.2-13) are analogous to seismic hazard curves, in which increasing levels of fault displacements are computed as a function of the annual probability that those displacements will be exceeded.

For the largest mapped faults at Yucca Mountain (i.e., those that form the boundary of the major fault block that comprises the Yucca Mountain geologic features), the probabilistic fault displacement hazard curves were largely based on the same detailed paleoseismic and earthquake data used to characterize these faults as potential seismic sources (CRWMS M&O, 1998ab). However, for smaller faults and fractures that were not part of the seismic source characterization, there were no established techniques available to the experts. Because of the complexity of Yucca Mountain fault analyses, the experts relied on both available information and expert judgment to develop conceptual models of distributed faulting and estimated the probabilities of secondary faulting in the repository (Youngs, et al., 2003aa, CRWMS M&O, 1998ab).

The PFDHA experts derived these curves using two different methods, which DOE referred to as the displacement approach and earthquake approach. The displacement approach uses fault-specific data, such as cumulative displacement, fault length, paleoseismic data from trenches, and historic seismicity. The earthquake approach relates the frequency of the fault slip events to the frequency of earthquakes on the fault as defined in the seismic source models developed for the corresponding seismic hazard analysis.

For the displacement approach, the experts relied on direct observations of faulting, deriving the two required parameters directly from paleoseismic displacement and recurrence rate data, geologically derived slip rate data, or scaling relationships that relate displacement to fault length and cumulative fault displacement. For the earthquake approach, the experts used earthquake recurrence models from the seismic hazard analysis. For this approach, the experts assessed three probabilities:

1. The probability that an earthquake will occur. The experts derived the probability that an earthquake will occur from the frequency distribution of earthquakes for each source (fault or area) used on the seismic hazard assessment and based on geologic, historical seismic, or paleoseismic data.
2. The probability that this earthquake will produce surface rupture on the fault generating the earthquake (the primary fault where the earthquake occurs). The expert teams determined the probability of surface rupture by a statistical regression of historical

earthquake and surface rupture data from the Basin and Range and focal depth calculations. In the focal depth calculations, the size and shape of the fault rupture for each earthquake (generally considered circular or elliptical) was estimated from empirical scaling relationships (e.g., Wells and Coppersmith, 1994aa). Depending on focal depth, the experts determined the surface displacement (if any) along the fault. Because the maximum surface displacement of a fault may not coincide with the demonstration point, an additional variable that randomized the rupture along the fault length was also introduced.

3. The probability that the earthquake will produce distributed surface displacement on other faults, primary or secondary. The experts determined the probability of distributed faulting by using a statistical best fit to data from Basin and Range historical ruptures in which distributed faulting was mapped after the earthquake (e.g., Pezzopane and Dawson, 1996aa) or by using slip tendency analysis (Morris, et al., 1996aa).

(b)(5)

(b)(5)

Conditioning of Low Probability Ground Motions

Since completion of the PSHA in 1998, several studies and reports, including ones from the staff (NRC, 1999aa), the Nuclear Waste Technical Review Board Panel on Natural Systems and Panel on Engineered Systems (Coradini, 2003aa), and DOE itself (e.g., BSC, 2004bj), questioned whether the very large ground motions the PSHA predicted at low annual exceedance probabilities (below $\sim 10^{-6}$ /yr) were physically realistic. For example, strong motion recordings of acceleration and velocity that DOE scaled to the unbounded PSHA curve at 10^{-7} annual exceedance probability yield peak ground acceleration (PGA) as high as 20 g [~ 640 ft/s²] and PGVs up to 1,800 cm/sec [~ 60 ft/s] (BSC, 2004bj). These values were based on extrapolating the expert elicitation results and are well beyond the limits of any recorded earthquake accelerations and velocities. That includes the largest recorded earthquakes worldwide. These large ground motions also are deemed physically unrealizable (e.g., Kana, et al., 1991aa) because they require a combination of earthquake stress drop, rock strain, and fault rupture propagation that cannot be sustained without wholesale fracturing of the bedrock.

In the past, probabilistic seismic hazard curves were used to estimate ground motions with annual exceedance probability to 10^{-4} or 10^{-5} (typical annual exceedance probability values for nuclear power plant design and safe shutdown earthquakes). For Yucca Mountain, however, the seismic hazard curves are extrapolated to estimate ground motions with annual exceedance probabilities as low as 10^{-8} . At these low probabilities, the seismic hazard estimates are driven

by the tails of the untruncated lognormal distributions of the input ground motion attenuation models (e.g., Bommer, et al., 2004aa).

To account for these large ground motions, DOE conditioned, or reduced the hazard using two approaches. The first approach used geological observations at the repository level to develop a limiting distribution on shear strains experienced at Yucca Mountain (BSC, 2005aj). The shear-strain threshold distribution was then related to the distribution of horizontal PGV through ground motion site-response modeling. To develop the shear strain threshold distribution, laboratory rock mechanics data, corroborated by numerical modeling, were used. The shear-strain levels to initiate unobserved stress-induced failure of lithophysal deposition of the Topopah Spring Tuff were derived. The site-response calculation used the random-vibration-theory (RVT)-based equivalent-linear model to compute the mean motions: strains for the deaggregation earthquakes that dominate the contribution of ground motion hazard of the specified annual probability of exceedance (APE). Lately, this approach has been (i) generalized to other than horizontal PGV; (ii) modified to use the inferred shear-strain threshold at the repository waste emplacement level to determine the level of ground motion not experienced at the reference rock outcrop, rather than at the waste emplacement level; (iii) refined to include variability in shear-strain levels and integration over the entire hazard curve; and (iv) updated to incorporate additional geotechnical data on site tuff and alluvium properties in the site-response part of the approach (BSC, 2008bl)

The second approach used expert judgment (BSC, 2008bl) to develop a distribution of extreme stress drop in the Yucca Mountain vicinity, which results in strong motion far exceeding the recorded data. The distribution is based on available data (stress drop measurements and apparent stress from laboratory experiments) and interpretations. It is used in the RVT method for point sources to develop distributions of PGV and PGA at the reference rock outcrop. The extreme stress drop is characterized by a lognormal distribution with a median value of 400 bars and σ_{ln} of 0.6 (mean of 480 bars). This distribution is discretized to three values of 150, 400, and 1,100 bars with the weighting factors of 0.2, 0.6, and 0.2, respectively. This distribution is mapped into a distribution of extreme ground motion for the reference rock outcrop through the RVT site-response modeling.

The unconditioned hazard curve, which is the APE as a function of ground motion, is convolved with the distribution of extreme ground motion for the reference rock outcrop to produce the conditioned ground motion hazard of the same rock outcrop. SAR Section 1.1.5.2.5.1 stated that the conditioning is done using combined shear-strain-threshold and extreme-stress-drop approaches. (b)(5)

(b)(5)

(b)(5)

SAR Figures 1.1-79 and 1.1-80 compare the unconditioned and conditioned PGA and PGV mean hazard curves for the reference rock outcrop.

Staff Evaluation of the DOE License Application

On the basis of the information DOE provided, the staff's evaluation of the PSHA expert elicitation process in SER Section 2.5.4, and the preceding review, staff reached the following conclusions.

(b)(5)

(b)(5)

(b)(5)

(b)(5)

(b)(5) During the expert elicitation process, the seismic source teams considered a range of information provided by DOE, the U.S. Geological Survey, other project-specific Yucca Mountain studies, and information published in the scientific literature. This information included data and models for the geologic and seismotectonic setting, seismic sources, historical and instrumented seismicity, earthquake recurrence, maximum magnitude, and ground motion attenuation. Detailed evaluations of this information are provided in NUREG-1762, (NRC, 2005aa). (b)(5)

(b)(5)

(b)(5)

(b)(5)

(b)(5) Both the seismic source and ground motion characterization panels provided inputs to the PSHA. The panels considered a wide variety of geological, geophysical, and seismological information. The DOE's PSHA report (CRWMS M&O, 1998ab) documents how the experts considered this information. (b)(5)

(b)(5)

(b)(5)

(b)(5) DOE provided an example of a partial logic tree for one of the seismic source teams in SAR Figure 2.2-21. The experts developed these probabilistic inputs to the PSHA by assessing the information the technical support teams provided. (b)(5)

(b)(5)

(b)(5) Each expert or team of experts documented its rationale for the input parameters in the DOE's PSHA report (CRWMS M&O, 1998ab).

(b)(5)

(b)(5) Each expert or team of experts documented its rationale for the uncertainty in parameters in the DOE's PSHA report (CRWMS M&O, 1998ab).

(b)(5)

Evaluation Findings

(b)(5)

2.2.1.2.2.4 Technical Review of Early Waste Package and Drip Shield Failures Event Probabilities

This section reviews and evaluates information DOE presented to estimate the probability of early failure of waste packages and the drip shield at the proposed repository site. This technical review of early failure event probabilities follows the review guidance provided in YMRP Sections 2.2.1 and 2.2.1.2.2. As part of the technical review, the staff reviewed SAR Sections 2.2.2.3, 2.3.6.6, and 2.3.6.8.4, and additional information provided in response to RAIs (DOE, 2009ac,ad) and the references cited therein.

Summary of the DOE Information

In SAR Section 2.2.2.3.1, DOE defined early failure of a waste package or drip shield as through-wall penetration of the barrier caused by the presence of a manufacturing- or handling-induced defects at a time earlier than would be expected for a nondefective barrier.

The DOE's approach for early failure probability calculations is to quantify errors in manufacturing or handling of waste packages or drip shields, respectively, and to quantify the potential that the error goes undetected prior to emplacement. In such instances, the defective waste package or drip shield is assumed to experience early failure.

DOE first systematically identified the types of errors or defects that could lead to early failure of the waste package and drip shield, respectively. It reviewed the technical literature for empirical data of similar systems and components (i.e., industrial analogues). DOE identified five industrial analogues, which can generally be described as welded metallic containers: (i) boilers and pressure vessels, (ii) nuclear fuel rods, (iii) underground storage tanks, (iv) radioactive cesium capsules, and (v) dry storage casks for spent nuclear fuel (SNF). For these analogues, DOE obtained qualitative and quantitative information on the types of manufacturing and handling errors that may occur, and their associated frequency for the occurrence, as identified in SNL Section 6.1 (2007aa).

SAR Table 2.3.6-21 identifies the specific types of defects and their occurrence rates for these analogues. From these industrial analogues, DOE developed a list of 13 generic errors or defects that could lead to early failure of welded metallic containers (SAR Section 2.3.6.6.2.1).

Given that the industrial analogues are only partly analogous to the waste package and drip shield in terms of manufacturing techniques, intended safety function, and operating environment, DOE determined that only some of the generic defects applicable to welded metallic containers are applicable to the waste package and drip shield, as identified in SNL Section 6.1.6 (2007aa). DOE screened out those defects not applicable to the waste package and drip shield (SAR Sections 2.3.6.6.3.1 and 2.3.6.8.4.3.1). DOE considered that weld flaws, particularly in the waste package closure weld, could affect the performance of the waste package, but would not necessarily lead to early failure. It considered weld flaws as potential initiation sites for stress corrosion cracking. SAR Section 2.3.6.5 addressed weld flaws and is evaluated in SER Section 2.2.1.3.1.3.3.

For the waste package, DOE identified six types of defects or errors that could lead to early failure (SAR Section 2.3.6.6.3.1). For the drip shield, DOE identified four types of defects or errors that could lead to early failure (SAR Section 2.3.6.8.4.3.2). Those defects were further analyzed.

DOE developed event trees to identify event sequences that could lead to undetected defects or errors in the waste package and drip shield, respectively, as identified in SNL Sections 6.3 and 6.4 (2007aa). The event sequences generally consist of an equipment or process failure event, followed by human errors event(s), where the equipment or process failure is undetected or uncorrected. To quantify the probabilities for the respective event sequences, each basic event in the sequences was assigned a probability distribution. For the equipment or process failure events, the probability distribution was based on data that were generated from similar components or processes at nuclear power plants (e.g., Babcock and Wilcox, 1979aa; Blanton and Eide, 1993aa). For human reliability data, the probability distributions were taken from data for nuclear power plant activities (Swain and Guttman, 1983aa; Benhardt, et al., 1994aa)

DOE used Monte Carlo simulations to analyze the event trees and calculate the probability distributions for event sequences that could lead to undetected errors or defects in the waste package or drip shield, respectively. DOE described end state probabilities for event sequences as lognormal distributions. DOE grouped probability distributions for all of the event sequences that could lead to the presence of an undetected defect in the waste package to calculate the overall probability that the waste package contains at least one undetected defect (i.e., the waste package early failure probability). DOE followed the same process for the drip shield to calculate the overall probability that the drip shield contains at least one undetected defect (i.e., the drip shield early failure probability). DOE described the early failure probability for the waste package as a lognormal distribution with a mean of 1.13×10^{-4} per waste package and an error factor of 8.17 (SAR Section 2.3.6.6.3.2.7). DOE described the early failure probability for the drip shield as a lognormal distribution with a mean of 2.21×10^{-6} per drip shield and an error factor of 14 (SAR Section 2.3.6.8.4.3.2.5).

DOE compared its probability estimates for early failure of the waste package and drip shield, respectively, with the defect-related failure rates for the industrial analogues. The failure rates for the industrial analogues for pressure vessels, nuclear fuel rods, underground storage tanks, and radioactive cesium capsules DOE cited ranged from 10^{-6} to 10^{-4} per component (SAR Table 2.3.6-21). DOE did not identify any cases of SNF casks that failed due to undetected defects after entering service.

The probability estimates for early failure of the waste package and drip shield as described in SAR Section 2.4.1.2.3 and reviewed by the staff in SER Section 2.2.1.4.1 are implemented in TSPA in the Early Failure Scenario Class. The staff review of the implementation of the model abstraction for early failure is documented in SER Section 2.2.1.3.1.3.6.

Staff's Evaluation of DOE Information

(b)(5)	Early
failure clearly refers to through-wall penetration of the waste package or drip shield at a time earlier than the design life because of undetected manufacturing- or handling-induced defects. Early failure is clearly distinguished from other events and processes that could lead to through-wall penetration (e.g., corrosion, tensile rupture) (b)(5)	
(b)(5)	

The staff reviewed the DOE's assumption that the early failure probabilities for the waste package and drip shield, respectively, are equivalent to the probabilities that there are undetected manufacturing- or handling-induced defects in the respective barriers. (b)(5)

(b)(5)

(b)(5)

The staff reviewed the DOE's use of industrial analogues to identify the generic types of defects or errors that, if undetected, could lead to early failure. (b)(5)

(b)(5)

The staff reviewed the DOE's decision to screen some of the generic errors and defects from the early failure analyses. (b)(5)

- DOE screened out improper weld-flux material from the early failure analyses for the waste package because weld flaws were evaluated as stress corrosion cracking initiation sites in SAR Section 2.3.6.5. (b)(5)

(b)(5)

- DOE screened out weld flaws from the drip shield early failure analysis because SAR Section 1.3.4.7 stated that the drip shield will be fully stress relieved, thus preventing stress corrosion crack initiation from weld flaws. (b)(5)

(b)(5)

- DOE screened out poor joint design from further analyses for the waste package and drip shield, respectively, because controls specified in SAR Section 1.9.2 required extensive development and testing of waste package and drip shield joints. (b)(5)

(b)(5)

- DOE screened out missing welds from further analyses for the waste package and drip shield, respectively, because controls specified in SAR Section 1.9.2 require extensive inspection and nondestructive examination of the welds. (b)(5)

(b)(5)

(b)(5)

- DOE screened out mislocated welds from further analyses for the waste package and drip shield, respectively, because controls specified in SAR Section 1.9.2 require extensive inspection and nondestructive examination of the welds. (b)(5)

(b)(5)

- DOE screened out surface contaminants (e.g., material that could enhance the corrosion rate) from further analyses for the waste package and drip shield, because controls specified in SAR Section 1.9.2 require that fabrication and handling processes will limit the type and amount of surface contamination. (b)(5)

(b)(5)

- DOE screened out improper low-plasticity burnishing from the drip shield early failure analysis because the drip shield is not low-plasticity burnished. The staff reviewed the description of the drip shield design in SAR Section 1.3.4.7 and (b)(5)

(b)(5)

- DOE screened out handling damage from early failure analysis for the drip shield because the high strength-to-weight ratio of titanium makes it resilient to scratches and denting from handling-induced impacts. (b)(5)

(b)(5)

(b)(5)

- DOE screened out emplacement error from the early failure analysis for the waste package. (b)(5)

(b)(5) The staff's review of the DOE screening evaluation for this FEP is found in SER Section 2.2.1.2.1.

- DOE did not screen out administrative or operational errors, but did not count them as distinct errors. Rather, DOE implicitly incorporated such errors (e.g., failure to follow a written procedure) into the analyses of the defects that were not screened out.

(b)(5)

The staff reviewed the event trees and event sequences DOE used to calculate the probabilities for the errors that could cause early failure. The staff reviewed the extent to which DOE identified key processes involved with waste package and drip shield handling and manufacturing, and whether the event sequences were appropriate and realistic to estimate the undetected defect (i.e., early failure) probabilities. The staff makes the following specific conclusions on the DOE event trees and event sequences used to calculate probabilities.

- The staff reviewed the DOE event tree for waste package fabrication with improper base metal selection, which is shown in SNL Figure 6-9 (2007aa). In response to the staff's RAI (DOE 2009bd), DOE stated that the composition of the base metal will be certified by the supplier and independently checked upon receipt at the fabrication facility. (b)(5)

(b)(5)

- The staff reviewed the DOE event sequence for waste package fabrication with improper weld filler material selection, which is shown in SNL Figure 6-14 (2007aa). In response to the staff's RAI (DOE 2009bd), DOE stated that the composition of the weld filler metal will be certified by the supplier and independently checked upon receipt at the fabrication facility. (b)(5)

(b)(5)

- The staff reviewed the DOE event sequence for waste package fabrication with improper heat treatment for waste package outer shell, which is shown in SNL Figure 6-10 (2007aa). In SNL Section 6.3.3 (2007aa), DOE stated that the critical steps during heat treatment are moving the heated shell from the furnace to the quench tank and the subsequent quench. (b)(5)

(b)(5)

- The staff reviewed the DOE event sequence for waste package fabrication with improperly heat-treated outer lid, which is shown in SNL Figure 6-11 (2007aa). In SNL Section 6.3.4 (2007aa), DOE stated that the critical steps during heat treatment are moving the heated lid from the furnace to the quench tank and the subsequent quench. (b)(5)

(b)(5)

- The staff reviewed DOE's event sequence for waste package fabrication with improper low-plasticity burnishing of the closure weld, which is shown in SNL Figure 6-12 (2007aa). In SNL Section 6.3.5 (2007aa), DOE stated that burnishing will be performed by a dedicated, automated system, with subsequent inspection to assure that the appropriate procedures were followed. (b)(5)

(b)(5)

- The staff reviewed the DOE event sequence for improper handling of the waste package, which is shown in SNL Figure 6-13 (2007aa). In SAR Section 2.3.6.6.3.2.5, DOE defined damage as visible gouging or denting of the waste package surface between receipt and drip shield installation that could jeopardize the performance of the outer barrier. Because handling procedures have not been fully developed, DOE assumed that the waste package could be damaged by any one of eight generic events, each of which is analogous to fuel assembly handling at nuclear power plants. In response to the staff's RAI (DOE, 2009bd), DOE stated that this comparison is appropriate because fuel assemblies are handled in tightly controlled conditions similar to those expected at the repository. (b)(5)

(b)(5)

- The staff reviewed the DOE event sequence for drip shield fabrication with out-of-specification base metal, which is shown in SNL Figure 6-16 (2007aa). In response to the staff's RAI (DOE, 2009bd), DOE stated that the composition of the base metal will be certified by the supplier and independently checked upon receipt at the fabrication facility. (b)(5)

(b)(5)

- The staff reviewed the DOE event sequence for drip shield fabrication with out-of-specification weld filler metal, which is shown in SNL Figure 6-18 (2007aa). In response to the staff's RAI (DOE 2009bd), DOE stated that the composition of the base metal will be certified by the supplier and independently checked upon receipt at

the fabrication facility (b)(5)
(b)(5)

- The staff reviewed the DOE event sequence for drip shield fabrication with improper heat treatment, which is shown in SNL Figure 6-17 (2007aa). In SNL Section 6.4.2 (2007aa), DOE stated that the drip shield temperature during heat treatment will be monitored by calibrated thermocouples in contact with the material, and that the drip shield will be subject to a post-heat-treatment inspection to ensure that the heat-treatment procedure was properly followed. (b)(5)

(b)(5)

- The staff reviewed the DOE event sequence for improper drip shield installation, which is shown in SNL (2007aa) Figure 6-19. In SNL Section 6.4.4 (2007aa), DOE stated that drip shields will be visually inspected at the surface facilities, that emplacement activities will be monitored by camera, and that the inspections will be independently checked and documented. (b)(5)

(b)(5)

(b)(5)

The Postclosure Design Control Parameters require that drip shield handling and emplacement be monitored by appropriate equipment, including an alarm, with an operator and independent inspector verifying proper installation.

(b)(5)

(b)(5)

Comment (b)(5)
(b)(5)

In SAR Sections 2.3.6.6.4.2 and 2.3.6.8.4.2, DOE compared its probability estimates for early failure of the waste package and drip shield, respectively, with the defect-related failure rates for the industrial analogues. For pressure vessels, nuclear fuel rods, underground storage tanks, and radioactive cesium capsules, the failure rates DOE cited are in the range of 10^{-6} to 10^{-4} per component (SAR Table 2.3.6-21), which is consistent with the calculated early failure rates for the waste package and drip shield. DOE did not identify any cases of SNF casks that failed after entering service.

(b)(5)

(b)(5)

In particular, the waste package, drip shield, and industrial analogues are (i) metallic, (ii) cut from sheet and formed into a cylindrical-type shape, (iii) welded, (iv) heat treated, and (v) closed/sealed (i.e., intended to act as a container or barrier).

(b)(5)

(b)(5)

DOE developed event sequences to calculate the probabilities for undetected errors or defects (i.e., the early failure probabilities) in the waste package and drip shield, respectively. The event sequences generally consist of an equipment or process failure (e.g., probability that a motorized valve fails to open on demand), followed by human error(s), where the equipment or process failure is undetected (e.g., probability that the responsible technician does not detect the failure of the valve to open) or uncorrected. Each event in the event sequences was assigned a probability distribution that was obtained from external data sources, as identified in SNL Section 4.1 (2007aa).

The external data used to establish the probability distributions for key processes and events in waste package and drip shield manufacturing and handling come from nuclear power plant activities. For the equipment or process failure events, DOE used reliability data that were generated from similar components or activities at nuclear power plants (e.g., Babcock and Wilcox, 1979aa; Blanton and Eide, 1993aa). For human error events, the probability distributions for these events were taken from nuclear power plant human reliability analyses (Swain and Guttman, 1983aa; Benhardt, et al., 1994aa).

The staff reviewed the external data to determine whether it is reasonable and appropriate to use such data to quantify the reliability of events and processes associated with manufacturing and handling of the waste package and drip shield. (b)(5)

(b)(5)

DOE represented each basic event in an event sequence that can lead to an undetected defect (i.e., early failure) by a lognormal distribution. For the human error events, the external human reliability data DOE cited specify lognormal distributions with particular mean values and error factors. For equipment or process failure events, the reliability data DOE cited typically specify only point (mean) values. As a result, DOE assigned an error factor to the probability data given in the literature as point (mean) values, as identified in SNL Section 5.3 (2007aa). DOE assumed that this point (mean) value is the mean of an unspecified probability distribution and that it is therefore appropriate to characterize the reliability with any reasonable, probability distribution. DOE used the lognormal distribution to be consistent with the human reliability data.

DOE used Monte Carlo simulations to calculate the probability distributions for the end states of the event sequences that could lead to early failure. Because the probability distributions for the basic events in the sequences may have different error factors, DOE stated that the mean value of the probability distribution for the end state of the sequence is not just a simple product of the mean of each basic event in the sequence, as identified in SNL Section 6.5.1 (2007aa). The probability distributions for all of the event sequences that could lead to an undetected defect in the waste package were combined to give the overall probability that the waste package has at least one undetected defect, which is assumed to be equivalent to the waste package early failure probability. The same was done for the drip shield. DOE ran 90,000 realizations to obtain the probability distributions for early failure of the waste package and drip shield, respectively, as identified in SNL (2007aa) Section 6.5.1

The staff reviewed the treatment of uncertainty in the early failure probability calculations (b)(5)

(b)(5)

The staff identifies that the probability distributions and values DOE provided for the probabilities of waste package and drip shield early failure are lognormal distributions, with a mean of 1.13×10^{-4} per waste package and an error factor of 8.17 (SAR Section 2.3.6.6.3.2.7) and a lognormal distribution with a mean of 2.21×10^{-6} per drip shield and an error factor of 14 (SAR Section 2.3.6.8.4.3.2.5) for the waste package and drip shields (b)(5)

(b)(5)

Evaluation Findings

The staff has reviewed the information in the SAR and other information submitted in support of the license application and has (b)(5)

(b)(5)

2.2.1.2.2.5 Evaluation Findings

The staff reviewed the SAR and other information submitted to support the license application and (b)(5)

(b)(5)

2.2.1.2.2.6 References

Babcock and Wilcox. 1979aa. "Records Investigation Report Related to Off-Chemistry Welds in Material Surveillance Specimens and Response to IE Bulletin 78-12 and 78-12A—Supplement." Mt. Vernon, Indiana: Babcock and Wilcox.

Benhardt, H.C., S.A. Eide, J.E. Held, L.M. Olsen, and R.E. Vail. 1994aa. "Savannah River Site Human Error Data Base Development for Nonreactor Nuclear Facilities." WSRC-TR-93-581. Aiken, South Carolina: Savannah River Site, Westinghouse Savannah River Company.

Blanton, C.H. and S.A. Eide. 1993aa. "Savannah River Site Generic Data Base Development (U)." WSRC-TR-93-262. Aiken, South Carolina: Westinghouse Savannah River Company.

Bommer, J.J., N.A. Abrahamson, F.O. Strasser, A. Pecker, P.-Y. Bard, H. Bungum, F. Cotton, D. Fäh, F. Sabetta, F. Scherbaum, and J. Struder. 2004aa. "The Challenge of Defining Upper Bounds on Earthquake Ground Motions." *Seismological Research Letters*. Vol. 75. pp. 82–95.

Boyle, W.J. 2008aa. "Transmittal of Report: Probabilistic Volcanic Hazard Analysis Update (PVHA-U) for Yucca Mountain, Nevada." Letter (October 17) to Director, DHLWRS, NRC. Las Vegas, Nevada: DOE, Office of Civilian Radioactive Waste Management.

BSC. 2008bi. "Supplemental Earthquake Ground Motion Input for a Geologic Repository at Yucca Mountain, NV." MDL-MGR-GS-000007. Rev. 00. ACN 01, ACN 02. Las Vegas, Nevada: Bechtel SAIC Company, LLC.

BSC. 2005aj. "Peak Ground Velocities for Seismic Events at Yucca Mountain, Nevada." ANL-MGR-GS-000004. Rev. 00. ACN 01, ACN 02. Las Vegas, Nevada: Bechtel SAIC Company, LLC.

BSC. 2004af. "Characterize Framework for Igneous Activity at Yucca Mountain, Nevada." ANL-MGR-GS-000001. Rev. 02. ACN 01, ERD 01. Las Vegas, Nevada: Bechtel SAIC Company, LLC.

BSC. 2004bi. "Yucca Mountain Site Description." TDR-CRW-GS-000001. Rev. 02 ICN 01, ERD 01, ERD 02. Las Vegas, Nevada: Bechtel SAIC Company, LLC.

BSC. 2004bj. "Technical Basis Document No. 14: Low Probability Seismic Events." Rev. 1. MOL 20000510.0175. Las Vegas, Nevada: Bechtel SAIC Company, LLC.

BSC. 2004bp. "Characterize Framework for Seismicity and Structural Deformation at Yucca Mountain, Nevada." ANL-CRW-GS-000003. Rev. 00. MOL20000510.0175. DOC20040223.0007. Las Vegas Nevada: Bechtel SAIC Company, LLC.

Budnitz, R.J., G. Apostolakis, D.M. Boore, L.S. Cluff, K.J. Coppersmith, C.A. Cornell, and P.A. Morris. 1997aa. NUREG/CR-6372, "Recommendations for Probabilistic Seismic Hazard Analysis: Guidance on Uncertainty and Use of Experts—Main Report." Vol. 1. Washington, DC: NRC.

Coraddini, M.L. 2003aa. "Board Comments on February 24, 2003 Panel Meeting on Seismic Issues." Letter (June 27) to Dr. Margaret S.Y. Chu, DOE, Office of Civilian Radioactive Waste Management. Washington, DC: United States Nuclear Waste Technical Review Board.

Cornell, C.A. 1968aa. "Engineering Seismic Risk Analysis." *Bulletin of the Seismological Society of America*. Vol. 58. pp. 1,583–1,606.

Cornell, C.A. and G. Toro. 1992aa. *Techniques for Determining Probabilities for Geologic Events and Processes*. R.L. Hunter and C.J. Mann, eds. New York City, New York: Oxford University Press.

Costa, F. 2008aa. "Residence Times of Silicic Magmas Associated With Calderas." *Developments in Volcanology, Vol. 10. Caldera Volcanism: Analysis, Modeling, and Response*. J. Gottsmann and J. Marti, eds. Amsterdam, The Netherlands: Elsevier. pp. 1–55.

CRWMS M&O. 1998aa. "Probabilistic Seismic Hazard Analyses for Fault Displacement and Vibratory Ground Motion at Yucca Mountain, Nevada." WBS 1.2.3.2.8.3.6. Las Vegas, Nevada: CRWMS M&O.

CRWMS M&O. 1998ab. "Synthesis of Volcanism Studies for the Yucca Mountain Site Characterization Project." 3781MR1. MOL 19981207 0393. Las Vegas, Nevada: CRWMS M&O.

CRWMS M&O. 1996aa. "Probabilistic Volcanic Hazard Analysis for Yucca Mountain, Nevada." BA0000000–01717–2200–00082. Rev. 0. Las Vegas, Nevada: CRWMS M&O.

Detournay, E., L.G. Mastin, J.R.A. Pearson, A.M. Rubin, and F.J. Spera. 2003aa. "Final Report of the Igneous Consequences Peer Review Panel." DN2000219072. MOL20031014-0097. Las Vegas, Nevada: Bechtel SAIC Company, LLC.

DOE. 2009aa. "Yucca Mountain—Response to Request for Additional Information Regarding License Application (Safety Analysis Report Section 2.2.2.2), Safety Evaluation Report Vol. 3, Chapter 2.2.1.2.2, Set 2." Letter (January 27) J.R. Williams to J.H. Sulima (NRC). ML090280281. Las Vegas, Nevada: DOE, Office of Civilian Radioactive Waste Management.

DOE. 2009ab. "Yucca Mountain—Response to Request for Additional Information Regarding License Application (Safety Analysis Report Section 2.2, Table 2.2-5), Safety Evaluation Report Vol. 3, Chapter 2.2.1.2.1, Set 2." Letter (February 23) J.R. Williams to J.H. Sulima (NRC). ML090550099. Las Vegas, Nevada: DOE, Office of Civilian Radioactive Waste Management.

DOE. 2009ac. "Yucca Mountain—Response to Request for Additional Information Regarding License Application (Safety Analysis Report Sections 2.3.6.6, 2.3.6.8.4, and 2.2.2.3), Safety Evaluation Report Volume 3, Chapter 2.2.1.2.2, Set 2." Letter (January 9) J.R. Williams to J.H. Sulima (NRC). ML090120301. Las Vegas, Nevada: DOE, Office of Civilian Radioactive Waste Management.

DOE. 2009ad. "Yucca Mountain—Response to Request for Additional Information Regarding License Application (Safety Analysis Report Sections 2.3.6.6, 2.3.6.8.4, and 2.2.2.3), Safety Evaluation Report Vol. 3, Chapter 2.2.1.2.2, Set 2." Letter (January 16) J.R. Williams to J.H. Sulima (NRC). ML090210465. Las Vegas, Nevada: DOE, Office of Civilian Radioactive Waste Management.

DOE. 2009aq. "Yucca Mountain—Response to Request for Additional Information Regarding License Application (Safety Analysis Report Sections 1.1.10, 1.2.2, 1.1.5.2, and 1.1.5.3), Safety Evaluation Report Vol. 2, Chapter 2.1.1.1, Set 1." Letter (January 12) J.R. Williams to C. Jacobs (NRC). Enclosures (10). ML090270750. Las Vegas, Nevada: DOE, Office of Civilian Radioactive Waste Management.

DOE. 2009av. DOE/RW-0573, "Safety Analysis Report Yucca Mountain Repository License Application." Rev. 01. Las Vegas, Nevada: DOE, Office of Civilian Radioactive Waste Management.

DOE. 2009bd. "Yucca Mountain—Response to Request for Additional Information Regarding License Application (Safety Analysis Report Section 2.2.2.2), Safety Evaluation Report Vol. 3, Chapter 2.2.1.2.2, Set 3." Letter (July 20) J.R. Williams to J.H. Sulima (NRC). ML092010472. Las Vegas, Nevada: DOE, Office of Civilian Radioactive Waste Management.

DOE. 2008ab. DOE/RW-0573, "Safety Analysis Report Yucca Mountain Repository License Application." Rev. 0. Las Vegas, Nevada: DOE, Office of Civilian Radioactive Waste Management.

DOE. 1997aa. "Topical Report YMP/TR-002-NP: Methodology To Assess Fault Displacement and Vibratory Ground Motion Hazards at Yucca Mountain." Rev. 1. Las Vegas, Nevada: DOE, Office of Civilian Radioactive Waste Management.

Fleck, R.J., B.D. Turrin, D.A. Sawyer, R.G. Warren, D.E. Champion, M.R. Hudson, and S.A. Minor. 1996aa. "Age and Character of Basaltic Rocks of the Yucca Mountain Region, Southern Nevada." *Journal of Geophysical Research*. Vol. 101, No. B4. pp. 8,205–8,227.

Hill, B.E. and C.B. Connor. 2000aa. "Technical Basis for Resolution of the Igneous Activity Key Technical Issue." San Antonio, Texas: CNWRA.

Hill, B.E. and J.A. Stamatakos. 2002aa. "Evaluation of Geophysical Information Used To Detect and Characterize Buried Volcanic Features in the Yucca Mountain Region." San Antonio, Texas: CNWRA.

Ho, C.H. and E.I. Smith. 1998aa. "A Spatial-Temporal/3-D Model for Volcanic Hazard Assessment: Application to the Yucca Mountain Region, Nevada." *Mathematical Geology*. Vol. 30, No. 5. pp. 497–510.

Ho, C.H. and E.I. Smith. 1997aa. "Volcanic Hazard Assessment Incorporating Expert Knowledge: Application to the Yucca Mountain Region, Nevada, U.S.A." *Mathematical Geology*. Vol. 29. pp. 615–627.

Ho, C.H., E.I. Smith, and D.L. Keenan. 2006aa. "Hazard Area and Probability of Volcanic Disruption of the Proposed High-Level Radioactive Waste Repository at Yucca Mountain, Nevada, USA." *Bulletin of Volcanology*. Vol. 69. pp. 117–123.

Kana, D.D., B.H.G. Brady, B.W. Vanzant, and P.K. Nair. 1991aa. NUREG/CR-5440, "Critical Assessment of Seismic and Geotechnical Literature Related to a High-Level Nuclear Waste Underground Repository." Washington DC: NRC.

Keefer, W.R., J.W. Whitney, and E.M. Taylor. 2004aa. "Quaternary Paleoseismology and Stratigraphy of the Yucca Mountain Area, Nevada." U.S. Geological Survey Professional Paper 1689. Denver, Colorado: U.S. Geological Survey.

Magsino, S.L., C.B. Connor, B.E. Hill, J.A. Stamatakis, P.C. LaFemina, D.A. Sims, and R.H. Martin. 1998aa. "CNWRA Ground Magnetic Surveys in the Yucca Mountain Region, Nevada (1996-1997)." CNWRA 98-001. San Antonio, Texas: CNWRA.

McGuire, R.K. 1976aa. "FORTRAN Computer Program for Seismic Risk Analysis." U.S. Geological Survey Open-File Report 76-67. Reston, Virginia: U.S. Geological Survey.

Morris, A.P., D.A. Ferrill, and D.B. Henderson. 1996aa. "Slip-Tendency Analysis and Fault Reactivation." *Geology*. Vol. 24. pp. 275-278.

NRC. 2005aa. NUREG-1762, "Integrated Issue Resolution Status Report." Rev. 1. Washington, DC: NRC.

NRC. 2003aa. NUREG-1804, "Yucca Mountain Review Plan—Final Report." Rev. 2. Washington, DC: NRC.

NRC. 2002aa. "Consolidated Safety Evaluation Report Concerning the Private Fuel Storage Facility." ML020850233. Docket No. 72-22. Washington, DC: NRC.

NRC. 1999aa. "Issue Resolution Status Report, Key Technical Issue: Structural Deformation and Seismicity." Rev. 2. Washington, DC: NRC.

NRC. 1996aa. NUREG-1563, "Branch Technical Position on the Use of Expert Elicitation in the High-Level Radioactive Waste Program." Washington, DC: NRC.

O'Leary, D.W., E.A. Mankinen, R.J. Blakely, V.E. Langenheim, and D.A. Ponce. 2002aa. "Aeromagnetic Expression of Buried Basaltic Volcanoes Near Yucca Mountain, Nevada." U.S. Geological Survey Open-File Report 02-020. Denver, Colorado: U.S. Geological Survey.

Perry, F.V., A.H. Cogbill, and R.E. Kelley. 2005aa. "Uncovering Buried Volcanoes at Yucca Mountain." *Eos, Transactions, American Geophysical Union*. Vol. 86, No. 47. pp. 485-488.

Pezzopane, S.K. and T.E. Dawson. 1996aa. "Fault Displacement Hazard: A Summary of Issues and Information in Seismotectonic Framework and Characterization of Faulting at Yucca Mountain, Nevada." J.W. Whitney, report coord. U.S. Geological Survey Milestone Report 3GSH100M, Chapter 9. MOL 19970129.0041. Denver, Colorado: U.S. Geological Survey.

Private Fuel Storage Limited Liability Company. 2001aa. "Safety Analysis Report for the Private Fuel Storage Facility." Rev. 22. Docket No. 72-22. LaCrosse, Wisconsin: Private Fuel Storage Limited Liability Company.

Sawyer, D.A., R.J. Fleck, M.A. Lanphere, R.G. Warren, D.E. Broxton, and M.R. Hudson. 1994aa. "Episodic Caldera Volcanism in the Miocene Southwestern Nevada Volcanic Field: Revised Stratigraphic Framework, $^{40}\text{Ar}/^{39}\text{Ar}$ Geochronology, and Implications for Magmatism and Extension." *Geological Society of America Bulletin*. Vol. 106, No. 10. pp. 1,304–1,318.

Schneider, J.F., N.A. Abrahamson, and T.C. Hanks. 1996aa. "Ground Motion Modeling of Scenario Earthquakes at Yucca Mountain: Final Report for Activity 8.3.1.17.3.3." MOL.19980617.0477. Las Vegas, Nevada: Yucca Mountain Project.

Smith, E.I., D.L. Keenan, and T. Plank. 2002aa. "Episodic Volcanism and Hot Mantle: Implications for Volcanic Hazard Studies at the Proposed Nuclear Waste Repository at Yucca Mountain, Nevada." *GSA Today*. Vol. 12, No. 4. pp. 4–11.

SNL. 2008ag. "Total System Performance Assessment Model/Analysis for the License Application." MDL-WIS-PA-000005. Rev. 00. AD 01, ERD 01, ERD 02, ERD 03, ERD 04. Las Vegas, Nevada: Sandia National Laboratories.

SNL. 2008ah. "Probabilistic Volcanic Hazard Analysis Update (PVHA-U) for Yucca Mountain, Nevada." Rev. 01. Las Vegas, Nevada: Sandia National Laboratories.

SNL. 2007aa. "Analysis of Mechanisms for Early Waste Package/Drip Shield Failure." ANL-EBS-MD-000076. Rev. 00. ACN 01, ERD 01, ERD 02. Las Vegas, Nevada: Sandia National Laboratories.

SNL. 2007ae. "Characterize Eruptive Processes at Yucca Mountain, Nevada." ANL-MGR-GS-000002. Rev. 03. ERD 01, ERD 02. Las Vegas, Nevada: Sandia National Laboratories.

Spudich, P., W.B. Joyner, A.G. Lindh, D.M. Boore, B.M. Margaris, and J.B. Fletcher. 1999aa. "SEA99: A Revised Ground Motion Prediction Relation for Use in Extensional Tectonic Regimes." *Bulletin of the Seismological Society of America*. Vol. 89, No. 5. pp. 1,156–1,170.

Stamatakis, J.A., S. Biswas, and M. Silver. 2007aa. "Supplemental Evaluation of Geophysical Information Used To Detect and Characterize Buried Volcanic Features in the Yucca Mountain Region." San Antonio, Texas: CNWRA.

Stamatakis, J.A., C.B. Connor, and R.H. Martin. 1997ab. "Quaternary Basin Evolution and Basaltic Volcanism of Crater Flat, Nevada, From Detailed Ground Magnetic Surveys of the Little Cones." *Journal of Geology*. Vol. 105. pp. 318–330.

Swain, A.D. and H.E. Guttmann. 1983aa. NUREG/CR-1278, "Handbook of Human Reliability Analysis With Emphasis on Nuclear Power Plant Applications Final Report." Washington, DC: NRC.

Wells, D.L. and K.J. Coppersmith. 1994aa. "New Empirical Relationships Among Magnitude, Rupture Length, Rupture Width, Rupture Area, and Surface Displacement." *Bulletin of the Seismological Society of America*. Vol. 84. pp. 974–1,002.

Youngs, R.R., W.J. Arabasz, R.E. Anderson, A.R. Ramelli, J.P. Ake, D.B. Slemmons, J.P. McCalpin, D.I. Doser, C.J. Fridrich, F.H. Swan, III, A.M. Rogers, J.C. Yount, L.W. Anderson, K.D. Smith, R.L. Bruhn, P.L. Knuepfer, R.B. Smith, C.M. dePolo,

D.W. O'Leary, K.J. Coppersmith, S.K. Pezzopane, D.P. Schwartz, J.W. Whitney, S.S. Olig, and G.R. Toro. 2003aa. "A Methodology for Probabilistic Fault Displacement Hazard Analyses (PFDHA)." *Earthquake Spectra*. Vol. 19, No. 1. pp. 191–219.

CHAPTER 4

2.2.1.3.1 Degradation of Engineered Barriers

2.2.1.3.1.1 Introduction

This chapter addresses the chemical degradation of the drip shield and waste packages (WPs) stored in the repository drifts. The drip shield and the WPs are engineered barriers, a subset of the Engineered Barrier System (EBS). The general functions of the EBS are to (i) prevent or significantly reduce the amount of water that contacts the waste, (ii) prevent or significantly reduce the rate at which radionuclides are released from the waste, and (iii) prevent or significantly reduce the rate at which radionuclides are released from the EBS to the Lower Natural Barrier [Safety Analysis Report (SAR) Section 2.1.1.2 (DOE, 2009ab)]. The EBS consists of the emplacement drift, the drip shield, the WP, the naval spent nuclear fuel structure, the waste form and WP internals [e.g., transportation, aging, and disposal canisters], the WP pallet, and invert features (SAR Figure 2.1-7).

In the postclosure performance assessment, the U.S. Department of Energy (DOE) evaluated whether the ability of EBS components to perform their barrier functions could be compromised by features, events, and processes (FEPs) that degrade their physical structure. In particular, DOE considered that the EBS components were subject to mechanical degradation caused by seismic ground motion (SAR Section 2.3.4). The staff's review of DOE's Total System Performance Assessment (TSPA) models for mechanical degradation of the EBS is found in SER Section 2.2.1.3.2. The other class of EBS degradation that DOE considered in the postclosure performance assessment was chemical degradation, or corrosion, caused by reactions between the EBS materials and the environment. In SAR Section 2.3.6, DOE described the TSPA model abstractions for chemical degradation of the drip shield and the WP outer barrier. This chapter reviews DOE's TSPA model abstractions for chemical degradation of the drip shield and the WP outer barrier.

2.2.1.3.1.2 Regulatory Requirements

Model abstractions used in the applicant's postclosure performance assessment must meet the regulatory requirements given in 10 CFR 63.114 (Requirements for Performance Assessment) and 63.342 (Limits on Performance Assessment), to support the predictions of compliance for 63.113 (Performance Objectives for the Geologic Repository after Permanent Closure). Specific compliance with 63.113 is reviewed in SER Section 2.2.1.4.1.

The requirements for performance assessment in 10 CFR 63.114 require the applicant to

- Include appropriate data related to the geology, hydrology, and geochemistry of the surface and subsurface from the site and the region surrounding Yucca Mountain
- Account for uncertainty and variability in the parameter values used to model degradation of engineered barriers
- Consider alternative conceptual models for degradation of engineered barriers
- Provide technical bases for the inclusion of FEPs affecting degradation of engineered barriers, including effects of deterioration or alteration processes of engineered barriers

that would adversely affect performance of the natural barriers, consistent with the limits on performance assessment in 10 CFR 63.342

- Provide technical basis for the models of degradation of engineered barriers that in turn provide input or otherwise affect other models and abstractions

10 CFR 63.114(a) considers performance assessment for the initial 10,000 years following permanent closure. 10 CFR 63.114(b) and 63.342 consider the performance assessment methods for the time from 10,000 years through the period of geologic stability, defined in 10 CFR 63.302 as 1 million years following disposal. These sections require that through the period of geologic stability, with specific limitations, the applicant

- Use performance assessment methods consistent with the performance assessment methods used to demonstrate compliance for the initial 10,000 years following permanent closure
- Include in the performance assessment those FEPs used in the performance assessment for the initial 10,000 year period

For this model abstraction of degradation of engineered barriers, 10 CFR 63.342(c)(3) further provides that DOE must assess the effects of general corrosion on engineered barriers, and may use a constant representative rate throughout the period of geologic stability, or a distribution of rates correlated to other parameters. DOE elected to use a distribution of corrosion rates in its SAR, thus this method is reviewed for the post-10,000-yr period.

The U.S. Nuclear Regulatory Commission (NRC) staff review of the license application (LA) follows the guidance laid out in the Yucca Mountain Review Plan (YMRP), NUREG-1804, Section 2.2.1.3.1, Degradation of Engineered Barriers (NRC, 2003aa), as supplemented by additional guidance for the period beyond 10,000 years after permanent closure (NRC, 2009ab). The acceptance criteria in the YMRP generically follow 10 CFR 63.114(a). Following the guidance, the NRC staff review of the applicant's abstraction of the degradation of engineered barriers considered five criteria

- System description and model integration are adequate.
- Data are sufficient for model justification.
- Data uncertainty is characterized and propagated through the abstraction.
- Model uncertainty is characterized and propagated through the abstraction.
- Model abstraction output is supported by objective comparisons

Because 10 CFR Part 63 specifies the use of a risk-informed approach for the review of a LA, the guidance provided by the YMRP as supplemented by NRC (2009ab) is followed to the extent reasonable for aspects of the degradation of engineered barriers important to repository performance. Whereas NRC staff considered all five criteria in their review of information provided by DOE, only aspects that substantively affect results of the performance assessment, as judged by NRC staff, are discussed in this chapter. NRC staff's judgment is based both on risk information provided by DOE, and staff's knowledge, experience, and independent analyses.

Requirements for DOE's evaluation of the degradation of the drip shield and WP engineered barriers in the postclosure performance are specified in 10 CFR 63.21(c)(3), (9), (15), and

(19) 10 CFR 63.114(a)(1), (2), (3), (5), (6), and (7) and 63.114(b), as implemented by 10 CFR 63.342 (Limits on Performance Assessments). 10 CFR 63.114(b) stipulates that the performance assessment methods used to satisfy the requirements of 10 CFR 63.114(a) are considered sufficient for the performance assessment for the period of time after 10,000 years and through the period of geologic stability. In general the applicant is required to

- Include information on the design of the EBS used to define parameters and conceptual models used in the performance assessment
- Account, and provide a technical basis, for uncertainties and variabilities used in the performance assessment
- Consider and evaluate alternative conceptual models that are consistent with currently available data and scientific understanding
- Provide a technical basis for including or excluding degradation processes from the performance assessment, and evaluate those processes that would significantly change the timing or magnitude of exposures to the reasonably maximally exposed individual if they were excluded

NRC staff's evaluation of DOE's compliance with these requirements follows the review methodologies established in the YMRP Section 2.2.1.3.1. From a risk-informed perspective, the NRC staff evaluated whether DOE satisfied the following criteria

- System description and model integration are adequate
- Data are sufficient for model justification
- Data uncertainty is characterized and propagated through the model abstraction
- Model uncertainty is characterized and propagated through the model abstraction
- Model abstraction output is supported by objective comparisons

2.2.1.3.1.3 Technical Review

DOE's models for chemical degradation of the EBS focus on the drip shield and the WP outer barrier, respectively. Consistent with the YMRP guidance, the staff performed a risk-informed, performance-based review, focusing on those aspects of the DOE models for chemical degradation of the drip shield and the WP that are most important to the calculations of barrier capability. DOE concluded that seepage flux is the primary source of water that may react with the EBS components (SAR Section 2.3.7.12.1). In the DOE model for flow of seepage water through the EBS, the water must first pass through the drip shield and then through the WP before contacting and mobilizing the waste form. As such, this chapter first concentrates on DOE's models for chemical degradation of the drip shield and then addresses DOE's models for chemical degradation of the WP

2.2.1.3.1.3.1 Drip Shield Degradation

The drip shield, which DOE described in SAR Section 1.3.4.7, is an engineered metal barrier designed to divert water that enters the drift and prevent it from contacting the WP. DOE stated that the drip shield will be fabricated from Titanium Grade 7 (UNS R52400). Titanium Grade 7 is a commercially pure titanium alloy with the addition of a small amount of palladium (approximately 0.2 weight percent) to enhance its corrosion resistance. The drip shield

<p>Comment(b)(5)</p> <p>(b)(5)</p>

structural supports will be fabricated from Titanium Grade 29 (UNS R56404), which is a titanium alloy composed of approximately 6 weight percent aluminum and 4 weight percent vanadium for strength, plus approximately 0.1 weight percent ruthenium for corrosion resistance.

In developing the postclosure performance assessment analysis, DOE evaluated a number of FEPs (in SAR Table 2.2-5) related to chemical degradation of the drip shield, including

- General corrosion of the drip shields (FEP 2.1.03.01.0B)
- Stress corrosion cracking (SCC) of the drip shields (FEP 2.1.03.02.0B)
- Localized corrosion of the drip shields (FEP 2.1.03.03.0B)
- Hydride cracking of the drip shields (FEP 2.1.03.04.0B)
- Microbially influenced corrosion (MIC) of the drip shields (FEP 2.1.03.05.0B)
- Early failure of the drip shields (FEP 2.1.03.08.0B)
- Oxygen embrittlement of the drip shields (FEP 2.1.06.06.0B)
- Creep of metallic materials in the drip shield (FEP 2.1.07.05.0B)
- Localized corrosion on drip shield surfaces due to deliquescence (FEP 2.1.09.28.0B)
- Thermal sensitization of the drip shields (FEP 2.1.11.06.0B)

With the exception of general corrosion and early failure of drip shields, these FEPs were screened out from the performance assessment on the basis of low consequence or low probability (SAR Table 2.2-5). The NRC staff's evaluation of DOE's bases for excluding these FEPs from the performance assessment is addressed in SER Section 2.2.1.2.1.

With respect to the FEPs that are included in the performance assessment, DOE described general corrosion of the drip shield as the uniform thinning of both the Titanium Grade 7 drip shield plates and the Titanium Grade 29 structural supports (SAR Section 2.3.6.8.1.1). In SAR Section 2.2.2.3, DOE defined drip shield early failure as through-wall penetration caused by manufacturing- and handling-induced defects, at a time earlier than would be expected for a nondefective drip shield.

In the TSPA analysis, DOE calculated that conditions in the drift (e.g., temperature, pH, seepage water chemistry) may support localized corrosion of the WP if the drip shield fails and allows seepage water to contact the WP within approximately 12,000 years after repository closure, as detailed in DOE Enclosure 11 (2009cl). The TSPA, however, also calculates that few drip shields fail within 12,000 years after repository closure. Therefore, the probability of WP breach by localized corrosion is low in the DOE model. Following 12,000 years after repository closure, DOE calculated that there is a low probability for conditions in the drift to support localized corrosion of the WP even if the drip shield fails and allows seepage water to contact the WP.

Other than for localized corrosion, the integrity of the drip shield does not have a significant effect on the DOE model abstractions for chemical degradation of the WP. In the TSPA Nominal Modeling Case, DOE's models for general corrosion and SCC of the WP conservatively assume aqueous degradation conditions, even for the intact drip shield. In the Seismic Ground Motion Modeling Case in the TSPA analysis, the presence of the drip shield does have some effect on SCC of the WP because DOE calculated that the WP under an intact drip shield will have a greater likelihood of being damaged under low-probability seismic ground motion events than it would under the assumption of a failed drip shield condition. This is because an intact drip shield permits unobstructed free movement of the WP, thereby potentially causing damage as WPs strike one another (SAR Section 2.3.4.5). Under a

collapsed drip shield event, WPs are constrained from significant movement and unable to strike or bump into each other. Consequently, a WP under an intact drip shield is more susceptible to SCC if a low probability seismic event occurs that imparts the required energy for the WPs to strike each other. Nevertheless, DOE calculated that the probability of a seismic ground motion with sufficient magnitude to damage the WP is so low, even in the Seismic Ground Motion Modeling Case, that the presence of the drip shield has an insignificant effect on the postclosure performance assessment beyond 12,000 years after repository closure, as described in DOE Enclosure 5 (2009cn).

The staff's reviews of the DOE model abstractions for general corrosion and early failure of the drip shield are presented in the following sections. Because the presence of the drip shield is important for the DOE calculations that localized corrosion of the WP is unlikely within 12,000 years after repository closure, the staff focused on those aspects of the models which were most important to the DOE calculations of the drip shield lifetime.

2.2.1.3.1.3.1.1 Drip Shield General Corrosion

In SAR Section 2.3.6.8.1, DOE described the model for general corrosion of the drip shield that was implemented in the TSPA. The drip shield is constructed of titanium alloys that are assumed to be highly corrosion resistant because of their passivity. Passivity refers to a state in which metals and alloys lose their chemical reactivity under certain environmental conditions. The passive state is generally attributed to the presence of a thin, protective oxide film on the metal surface. Because the maintenance of the passive state is important to the corrosion performance of the drip shield, the staff first the drip shield's long-term passive film stability in the repository conditions. Staff then reviewed the model abstraction used to calculate the drip shield general corrosion rate in the TSPA.

Drip Shield's Long-Term Passive Film Stability

Comment	(b)(5)
	(b)(5)

In BSC Section 1.1 (2004as), DOE presented literature references (Pourbaix, 1974; Schutz and Thomas, 1987aa) which indicated that the passive films on titanium alloys are stable over wide ranges of chemical potential and pH, and that, should the passive film rupture, titanium has a strong tendency for repassivation in the type of oxidizing conditions that are expected in the repository. DOE, however, also cited literature references (e.g., Lorenzo de Mele and Cortizo, 2000aa; Brossia, et al., 2001aa; Brossia and Cragolino, 2000aa, 2001ab, 2004aa; Pulvirenti, et al., 2002aa, 2003aa) which indicated that dissolved fluoride in brine solutions can increase the general corrosion rates for titanium alloys and possibly compromise the stability of the passive film. Therefore, DOE evaluated the uncertainty in long-term drip shield passive film persistence associated with possible passive film degradation by fluoride-bearing seepage water brines, as described in BSC Section 6.5.7 (2004as).

In BSC Section 6.5.7.2 (2004as), DOE reviewed and analyzed passive film instability. They cited literature references that described the onset of localized corrosion on titanium specimens that were exposed to fluoride shortly after the passive film was manually removed by polishing (e.g., Brossia and Cragolino, 2000aa, 2001ab; Brossia, et al., 2001aa). When the specimens were in an oxidizing environment, for as little as 4 days prior to fluoride exposure the specimens exhibited resistance to fluoride attack (Lorenzo de Mele and Cortizo, 2000aa). DOE stated that it expects the drip shield to have an extended period of dry thermal oxidation between the time the repository is closed and the time at which seepage water may fall onto the drip shield, as described in BSC Section 6.5.7 (2004as). Even for thermally oxidized Titanium Grade 7 specimens, however, passive film instability in fluoride-rich solution with low pH (~4) has been

observed (Lian, et al., 2005aa). However, DOE concluded that such conditions are not representative of the environment expected in the repository, as outlined on SNL p. 6-408 (2008ac). DOE expects that even if seepage water brines in the repository contain fluoride, high concentrations of other species will also be present that will suppress or neutralize any fluoride attack. In this regard, DOE identified studies of alloys with similar composition to Titanium Grade 7 in environments with temperatures up to 177 °C [351 °F], pH as low as 1, and fluoride, along with other species such as calcium, magnesium chloride, and silicate (Thomas and Bomberger, 1983aa; Schutz and Grauman, 1986aa). The studies showed that the titanium had a high passive film persistence, which was attributed to calcium reducing the fluoride ion solubility by precipitation of calcium fluoride, as well as the displacement of fluoride from absorption on the passive film by other species. Moreover, DOE presented its own test results in BSC Section 6.5 (2004as) in which Titanium Grade 7 specimens showed no evidence of passive film instability after 5 years' exposure to SCW, which contained approximately fluoride, as well as chloride, silica, sulfate, nitrate, and bicarbonate (composition given in SAR Table 2.3.6-1). Therefore, DOE concluded that the drip shield passive film will be stable during the postclosure period given the expected composition of seepage water brines, as described on SNL p. 6-410 (2008ac).

NRC Staff's Review

The NRC staff reviewed DOE's assessment of drip shield passivity. On the basis of information DOE provided in BSC Section 6.5.7 (2004as) (b)(5)

(b)(5)

Drip Shield General Corrosion Conceptual Model

In SAR Section 2.3.6.8.1, DOE described the conceptual model for general corrosion of the drip shield that was implemented in the TSPA. In the DOE model, corrosion begins at the time of repository closure and progresses at a constant rate over time. DOE assumed aqueous conditions in the drift and also that the general corrosion rate is independent of in-drift environmental conditions (e.g., temperature, relative humidity).

The NRC staff requested DOE's technical basis for assuming that the general corrosion rate of the drip shield is independent of temperature. In DOE Enclosure 3 (2009cn), DOE stated that at the start of the general corrosion process the corrosion rates of titanium alloys are temperature dependent. However, over time, the corrosion rates at different temperatures tend to converge. DOE observed a noticeable trend of increasing corrosion rate with increasing temperature for Titanium Grade 7 specimens tested in the range of 50 to 110 °C [122 to 230 °F] after 4 weeks exposure, but DOE also observed that the corrosion rate was less temperature dependent after 8 weeks (Hua and Gordon, 2004aa). Further, DOE referenced 3-year corrosion tests of titanium plus 0.2 weight percent palladium, which has nearly the same composition as Titanium Grade 7 in the temperature range of 90 to 200 °C [194 to 392 °F] in a pH 4.9 chloride-sulfate brine (Smailos and Köster, 1987aa). DOE concluded that the corrosion rates initially showed some temperature dependence, but were effectively identical within 3 years as shown in Smailos and Köster Figure 1 (1987aa).

NRC Staff's Review

The NRC staff reviewed DOE's conceptual model for general corrosion of the drip shield (b)(5)

(b)(5)

In addition, the NRC staff reviewed the DOE assumption that the general corrosion rate is independent of temperature. (b)(5)

(b)(5)

Long-Term Corrosion Test Data

The corrosion rates for Titanium Grades 7 and 29 that were sampled in the TSPA were based on data from weight-loss corrosion tests at the Long-Term Corrosion Test Facility (SAR Section 2.3.6.8.1.2.1). The following summarizes the staff's review of DOE's data implemented in the TSPA analysis.

Titanium Grade 7

The corrosion rate for Titanium Grade 7 that was sampled in the TSPA was based on 2.5-year tests of Titanium Grade 7 crevice and weight-loss specimens with wrought (base metal-type)

and as-welded metallurgical conditions (SAR Section 2.3.6.8.1.2.1). Some specimens were fully immersed in solution (i.e., aqueous phase), whereas others were in the saturated vapor above the aqueous phase. DOE exposed the test specimens to different solutions, including simulated acidified water (SAW), simulated dilute water (SDW), and SCW, the compositions of which are given in SAR Table 2.3.6-1. The tests were performed at temperatures of 60 and 90 °C [140 and 194 °F]. DOE measured the material weight loss during the test period and used these data to calculate the general corrosion rates, following American Society of Testing and Materials (ASTM) G1-90 (ASTM International, 1999aa). DOE observed that the corrosion rates of crevice specimens were lower than those of weight-loss specimens (SAR Figure 2.3.6-44). Therefore, DOE chose to use only the data from the weight-loss specimens in the model abstraction because it will calculate a higher corrosion rate in the TSPA. For the weight-loss specimens, DOE did not observe a significant difference in corrosion rates between wrought and as-welded materials, but did observe that the corrosion rates depended upon the chemistry of the test solution. In particular, the corrosion rates for specimens tested in the SCW aqueous phase were as high as 50 nm/yr [1.97×10^{-6} in/yr], whereas the corrosion rates for the specimens tested in the aqueous and vapor phases of SAW and SDW, as well as for specimens tested in SCW vapor phase, were below 20 nm/yr [7.87×10^{-7} in/yr] as shown in BSC Figures 6.6[a] and 6.7[a] (2004as).

In the TSPA analysis, DOE considered that corrosion occurs simultaneously on the inner surface and the outer surface of the Titanium Grade 7 drip shield plates, with different corrosion rates for the respective surfaces. DOE assumed the outer surface of the plate corroded faster than the inner surface because the outer surface is expected to be exposed to a more aggressive environment, including dust and dripping seepage water, as detailed in BSC Section 6.1.6[a] (2007as). DOE used the data from the most aggressive test condition, obtained from the SCW aqueous phase, to derive the distribution from which the outer surface corrosion rate was sampled in the TSPA model. In aqueous SCW, DOE measured higher corrosion rates for Titanium Grade 7 at 90 °C [194 °F] than at 60 °C [140 °F] as shown in BSC Figure 6.6[a] (2004as). DOE did not, however, consider temperature dependence for the titanium general corrosion rate. Instead, DOE elected to use only the data from the 90 °C [194 °F] tests because these gave a higher corrosion rate. These data ("Aggressive Condition" in SAR Figure 2.3.6-46) have a mean corrosion rate of 46.1 nm/yr [1.81×10^{-6} in/yr]. For the general corrosion rate on the underside of the drip shield plates, DOE used the data from specimens tested at 60 and 90 °C [140 and 194 °F] in the aqueous and vapor phases of the SAW and the SDW, respectively, as well as specimens tested at 60 and 90 °C [140 and 194 °F] in the SCW vapor phase, as detailed in BSC Section 6.1.7(a) (2004as). These data ("Benign Condition" in SAR Figure 2.3.6-46) have a mean corrosion rate of 5.1 nm/yr [2.01×10^{-7} in/yr].

DOE considered uncertainty in the measured corrosion rates, which it attributed to difficulties in cleaning and weighing corrosion specimens, particularly given the very small weight losses associated with low corrosion rates, as well as randomness in the general corrosion processes, as described in BSC Section 6.1.6.1[a] (2004as). DOE determined that the corrosion rate for the outside of the drip shield plates is best represented by a normal distribution, the mean of which is sampled from a *t*-distribution, described in SNL Table 6.3.5-3 (2008ag). The *t*-distribution is a broader normal distribution DOE used given that this set of corrosion rate data only has six data points. The mean of the *t*-distribution is approximately 46.1 nm/yr [1.81×10^{-6} in/yr], with 2.5th and 97.5th percentile values of approximately 43.0 and 49.1 nm/yr [1.69×10^{-6} in/yr and 1.93×10^{-6} in/yr], respectively, as detailed in BSC Section 6.1.6.2[a] (2004as). The variability distributions for the general corrosion rate on the outside of the drip shield plates were shown in BSC Figure 6-11[a] (2004as). For the inside of the drip shield plates, DOE determined that the general corrosion rate is best represented by a

gamma distribution, the mean of which is sampled from a normal distribution, described in SNL Table 6.3.5-3 (2008ag). The mean of the normal distribution is approximately 5.1 nm/yr [2.01×10^{-7} in/yr], with 2.5th and 97.5th percentile values of approximately 3.5 nm/yr and 6.8 nm/yr [1.38×10^{-7} in/yr and 2.68×10^{-7} in/yr], respectively, as outlined in BSC Section 6.1.7.2[a] (2004as). The variability distributions for the general corrosion rate on the inside of the drip shield plates were shown in BSC Figure 6-19[a] (2004as).

DOE compared the corrosion rate the TSPA code calculated to independently reported corrosion rates for analogous alloys in environments similar to or more aggressive than those expected in Yucca Mountain, as detailed in SAR Section 2.3.6.8.1.5 and BSC Section 7.2.1[a] (2004as). DOE concluded that the TSPA calculated corrosion rates are consistent with corrosion rates measured by Smailos and Köster (1987aa) for titanium plus 0.2 weight percent palladium in the temperature range of 90 to 200 °C [194 to 392 °F] in a pH 4.9 chloride-sulfate brine.

In response to the NRC staff's request for additional information (RAI) on how the experimental uncertainties associated with sample cleaning, weighing, and measuring were incorporated into the sampled corrosion rate distributions, DOE (2009cn) stated that subsequent examination of corrosion test specimens revealed that posttest specimen cleaning did not adequately remove a residual oxide film. This resulted in under-measurements of specimen weight loss and, in turn, an underestimation of the general corrosion rates for the inside and outside of the drip shield plates. To assess the effect of the incomplete specimen cleaning procedure on corrosion rate uncertainties, DOE conducted cross section analyses of the chemically cleaned posttest specimens. DOE estimated that the general corrosion rates for Titanium Grade 7, presented in SAR Section 2.3.6.8.1, were underestimated by, at most, a factor of two. Consequently, DOE conducted a sensitivity analysis in which it considered corrosion rates up to four times those given in SAR Section 2.3.6.8.1. This shortened the drip shield framework and plate lifetime compared to those calculated in the TSPA model. DOE stated that this sensitivity analysis showed that corrosion rates of up to four times higher than those given in SAR Section 2.3.6.8.1 resulted in negligible differences in the expected dose curves, as shown in DOE Enclosure 5, Figure 2 (2009cn). Therefore, DOE concluded that the data presented in SAR Section 2.3.6.8.1 were acceptable to use in the TSPA model because unquantified experimental uncertainties had negligible impact on the postclosure performance assessment. Nevertheless, DOE committed to update the LA to incorporate the analysis provided in the response to DOE Enclosure 1 (2009cn).

DOE responded, in DOE Enclosure 4 (2009cn), to the NRC staff's RAI for justification that the immersion test conditions in simulated brines to determine general corrosion rates are adequate to model the corrosion behavior of the drip shield, considering that some passive alloys may be more susceptible to corrosion in dripping conditions than in immersion conditions (e.g., Lee and Solomon, 2006aa). DOE stated that the temperatures at which dripping effects on corrosion behavior have been observed in other passive alloys are greater than the temperatures expected for the drip shield in dripping conditions. Moreover, DOE stated that data in the technical literature indicate that titanium alloys are highly resistant to dripping effects because of their tenacious passive film (Schutz, 2005aa). Therefore, DOE concluded that the immersion tests in the simulated brines were adequate to model the corrosion behavior of the drip shield in the repository because they accounted for potential dripping conditions.

NRC Staff's Review

The NRC staff reviewed the information DOE provided in SAR Section 2.3.6.8.1 and DOE (2009c) (b)(5)

- With regard to the material conditions (b)(5)

(b)(5)

- With respect to the corrosion test solutions (b)(5)

(b)(5)

- With regard to the testing conditions, DOE used immersion corrosion tests to represent corrosion behavior, including potential dripping conditions in the drift (b)(5)

(b)(5)

In addition, the staff evaluated DOE's experimental procedures for cleaning, weighing, and measuring the corrosion rates of the test specimens. (b)(5)

(b)(5)

(b)(5)

In the TSPA, the sum of the mean general corrosion rates for the inside and outside of the Titanium Grade 7 drip shield plates is approximately 51.2 nm/yr [2.06×10^{-6} in/yr]. (b)(5)

(b)(5)

(b)(5)

(b)(5)

Titanium Grade 29

The corrosion rate for Titanium Grade 29 that was applied in the TSPA analysis was based on 42-day weight-loss measurements of Titanium Grades 7 and 29 specimens in solutions that DOE stated were representative of seepage water and deliquescent brines expected in the repository [SAR Section 2.3.6.8.1.3 and BSC Section 6.2.1[a] (2004as)]. The compositions of the brines are given in BSC Table 6-7[a] (2004as). For tests at 120 and 150 °C [248 and 302 °F], DOE calculated the ratios of the corrosion rates of Titanium Grade 29 to those of Titanium Grade 7. For a given test environment, DOE calculated that the corrosion rate of Titanium Grade 29 could be a factor of one to seven times higher than that of Titanium Grade 7 (SAR Figure 2.3.6-48). From these data, DOE developed a discrete probability distribution function summarized in BSC Table 6-8[a] (2004as), which gave the ratio for the corrosion rate of Titanium Grade 29 to that of Titanium Grade 7. To calculate the corrosion rate for the Titanium Grade 29 structural supports in the TSPA model, DOE sampled the ratio from this probability distribution function and multiplied the sampled ratio by the corrosion rate on the outside of the Titanium Grade 7 plate (i.e., under aggressive conditions).

In BSC Section 6.2[a] (2004as), DOE acknowledged that it did not have long-term general corrosion data for Titanium Grade 29. DOE stated, however, that the passive films for both Titanium Grade 7 and Grade 29 are likely to be predominantly titanium oxide. DOE also stated that data show that the passive behavior for the respective alloys is the same for the range of brines expected in the repository (Andresen and Kim, 2006aa). Therefore, DOE concluded that the corrosion processes for Titanium Grades 7 and 29 are similar and that comparing the corrosion rates of the respective alloys in short-term tests is an adequate basis for calculating the long-term corrosion rate for Titanium Grade 29.

In response to the staff's RAIs that requested DOE to assess additional uncertainties associated with the comparative corrosion tests, DOE reanalyzed the comparative corrosion data (DOE, 2009cm). DOE determined that the weight loss for the respective alloys was measured by a

weighing balance that had uncertainty larger than most of the measured weight change values. DOE concluded that it was unable to make a meaningful distinction between actual material weight loss and measurement uncertainty. Further, DOE stated that for the same tests, corrosion rates were also measured by electrochemical impedance spectroscopy and linear polarization resistance (Andresen and Kim, 2006aa), with negligible difference for the respective alloys. On the basis of this reanalysis, DOE determined that, because there was no measurable difference between the corrosion rates for the respective alloys in the 42-day tests, the corrosion rate ratio described in SAR Section 2.3.6.8.1.3 was not needed. DOE decided to follow an alternative approach in which the corrosion rates for the Titanium Grade 29 structural supports are the same as the corrosion rate for the outer surface of the Titanium Grade 7 plate. DOE stated that this approach is justified because the corrosion rates measured by electrochemical impedance spectroscopy and linear polarization resistance for the respective alloys in the 42-day tests were nominally identical (Andresen and Kim, 2006aa). DOE also referenced Schutz (2005aa), which showed that the corrosion rates of Titanium Grades 7 and 29 are similar when exposed in a chloride solution with pH greater than 1, as shown in BSC Figure 6-22[a] (2004as).

In addition, DOE (2009cm) performed a sensitivity analysis using the TSPA model that compared the approach described in SAR Section 2.3.6.8.1.3 (in which the ratio for the corrosion rate of Titanium Grade 29 to that of Titanium Grade 7 was sampled from a probability distribution function with a value in the range of approximately one to seven) to the new approach, in which the corrosion rate of Titanium Grade 29 is assumed to be equivalent to that of Titanium Grade 7. The analysis revealed that the drip shield structural framework failure time occurred later for the new approach, as shown in DOE Figure 1 (2009cm). The analysis also showed that, in the event of a seismic ground motion, the new approach gives a median dose that is about 25 percent higher between 80,000 and 300,000 years after repository closure, due to increased probability of WP damage, as shown in DOE Figure 2 (2009cm). DOE stated that the mean expected dose was nearly the same for the respective approaches because the contribution of the seismic ground motion modeling case to the total mean annual dose is small during this time period. Therefore, DOE concluded that the data presented in SAR Section 2.3.6.8.1 were acceptable to use in the TSPA calculation, because unquantified experimental uncertainties had a negligible effect on the results from the postclosure performance assessment calculation. Nevertheless, DOE committed to update the LA to incorporate the analysis provided in DOE (2009cm).

NRC Staff's Review

The NRC staff reviewed the DOE approach to calculate the general corrosion rate of Titanium Grade 29. (b)(5)

(b)(5)

(b)(5)

Abstraction and Integration

For the Nominal Modeling Case in the TSPA analysis, DOE implemented the model abstraction for general corrosion of the drip shield in the WP and Drip Shield (DS) Degradation Submodel, as described in SNL Section 6.3.5.1 (2008ag), in which the drip shields were distributed in the five percolation subregions. The WP and DS Degradation Submodel considers only general corrosion breach of the Titanium Grade 7 plates. DOE concluded that the drip shield would protect the WP against seepage if the drip shield plates are intact, even if the drip shield supports collapsed and the sidewall buckled (SAR Section 2.3.4.5.3.1). For each realization, DOE sampled one general corrosion rate for the outside of the drip shield plates (under the aggressive condition) and one for the inside of the drip shield plates (under the benign condition) from the respective distributions given in SNL Table 6.3.5-3 (2008ag). The corrosion rates were applied to all drip shields, regardless of the percolation subregion, such that all drip shields in a given realization failed at the same time. The output of the WP and DS Degradation Submodel was the fraction of drip shields in each percolation subregion breached by general corrosion as a function of time. This output was provided to the Waste Form Degradation and Mobilization Model Component and the EBS Flow and EBS Transport Submodels.

SAR Figures 2.1-8 and 2.4-24 showed the distribution of calculated failure times for the Titanium Grade 7 drip shield plates in the Nominal Modeling Case, on the basis of the model described in SAR Section 2.3.6.8.1. DOE's analyses calculated that most drip shield failures occur between 260,000 and 340,000 years after repository closure. DOE Enclosure 5, Figure 1 (2009cn) showed a modified distribution of failure times considering both a higher corrosion rate (based on additional uncertainties associated with specimen cleaning) and lower corrosion rate (based on potential decrease in corrosion rate over time). The modified distribution shows that most drip shield plate failures occur between 80,000 and 500,000 years after repository closure. In either case, there is negligible probability of drip shield plate breach by nominal processes within 12,000 years after repository closure, the time period during which DOE calculates that the WP is susceptible to localized corrosion if contacted by seepage water.

For the Seismic Ground Motion Modeling Case in the TSPA analysis, DOE also implemented the WP and DS Degradation Submodel to calculate the timing and magnitude of drip shield plate breach by general corrosion, as outlined in SNL Section 6.6.1 (2008ag). Both the Titanium Grades 7 and 29 corrosion rates are sampled in this modeling case. The Titanium Grade 7 corrosion rate was sampled in the same manner as in the Nominal Modeling Case. For Titanium Grade 29 structural supports, DOE sampled the ratio of the corrosion rate of Titanium Grade 29 to that of Titanium Grade 7 once per realization from the discrete probability distribution function summarized in BSC Table 6-8[a] (2004as). The ratio was applied to all drip shields in a realization. SAR Figures 2.1-11 and 2.4-24 showed the distribution of failure times for the Titanium Grade 7 drip shield plates in the Seismic Ground Motion Modeling Case. Most plate failures occur between 100,000 and 300,000 years after repository closure. There is

negligible probability of drip shield breach within 12,000 years after repository closure. For the Titanium Grade 29 structural supports, DOE calculated that most drip shield frameworks failed between 20,000 and 170,000 years after repository closure, using the model described in SAR Section 2.3.6.8.1 and DOE Enclosure 2, Figure 1 (2009cm). For the alternative approach, in which DOE assumed equivalent corrosion rates for the structural supports and the plate, DOE calculated that most frameworks failed between about 80,000 and 170,000 years after repository closure, as shown in DOE Enclosure 2, Figure 1 (2009cm).

NRC Staff's Review

The NRC staff reviewed the implementation and integration of the model abstraction for general corrosion of the drip shield used in the postclosure performance assessment calculation. (b)(5)

(b)(5)

NRC Summary of Evaluation Findings for General Corrosion of the Drip Shield

The staff reviewed the DOE model abstraction for general corrosion of the drip shield that was implemented in the TSPA code. (b)(5)

(b)(5)

2.2.1.3.1.3.1.2 Drip Shield Early Failure

In SAR Section 2.3.6.8.4, DOE described how it developed the probability distribution for early failure of the drip shield that was sampled in the TSPA code. DOE assumed that a drip shield underwent early failure if it was emplaced in the repository with an undetected manufacturing- or handling-induced defect. On the basis of the processes associated with drip shield manufacturing and handling, DOE concluded that the probability of a drip shield early failure is best represented in the TSPA by a lognormal distribution with a median of 4.30×10^{-7} per drip shield and an error factor of 14, as shown in SNL Table 7-1 (2007aa). The staff reviewed the adequacy of this probability distribution in SER Section 2.2.1.2.2.3. The implementation of this probability distribution is addressed in this section.

Drip Shield Early Failure Conceptual Model

In DOE's conceptual model for early drip shield failure, a drip shield with an undetected manufacturing- or handling-induced defect completely fails (i.e., is removed as a barrier to the flow of water) at the time of repository closure (SAR Section 2.3.6.8.4.4.1). DOE selected this representation because there are uncertainties associated with the timing and extent of breach for defective drip shields and a completely degraded drip shield at the time of repository closure will not underestimate the timing and magnitude of radionuclide releases, as described in SNL

Comment (b)(5)

(b)(5)

Section 6.5.2 (2007aa). DOE concluded that this is a conservative representation of the early failed drip shield because the most likely consequence of improper drip shield manufacturing or handling would be SCC. DOE excluded drip shield SCC from the performance assessment because even if cracking occurred, the cracks would not affect the drip shield performance, because advective flow through cracks in the drip shield is also excluded from the performance assessment (SAR Section 2.3.6.8.3).

NRC Staff's Review

The staff reviewed DOE's conceptual model for drip shield early failure, as described in SAR Section 2.3.6.8.4. (b)(5)

(b)(5)

Abstraction and Integration

The model abstraction for early failure of the drip shield was implemented in the TSPA calculation in the Drip Shield Early Failure Modeling Case, as described in SAR Section 2.4.2.1.5.2 and SNL Section 6.4.1 (2008ag). This modeling case uses most of the same modeling components and submodels as were implemented in the Nominal Modeling Case. In the Nominal Modeling Case, however, the WP and DS Degradation Submodel calculates the WP and drip shield breached areas as a function of time and passes this to the EBS Flow and Transport Submodels and the Waste Form Degradation and Mobilization Model Components. In the Drip Shield Early Failure Modeling Case, the WP and DS Degradation Submodel was replaced with the drip shield early failure mode, which simulated early failure by removing a selected drip shield as a barrier to seepage at the time of repository closure.

In the Drip Shield Early Failure Modeling Case, the underlying WP immediately experienced initiation of localized corrosion if the early failed drip shield was in seepage conditions. If the early failed drip shield was not in seepage conditions, the underlying WP did not experience initiation of localized corrosion. In the TSPA model, DOE calculated the dose consequence of a drip shield early failure in each of the five percolation subregions for both commercial spent nuclear fuel (CSNF)-type and codisposal (CDSP)-type WPs. DOE then calculated the expected dose using the early failure probability [sampled from the distribution given in SNL Table 7-1 (2007aa)], the distribution for the WP type, and the seepage fraction for each percolation bin.

DOE calculated that there is approximately 98.3 percent probability of no drip shield early failures, approximately 1.6 percent probability of one drip shield early failure, and approximately 0.1 percent probability of two or more drip shield early failures, as shown in SNL Table 6.4-1 (2008ag). Drip shield early failure makes a negligibly small contribution to DOE's calculated mean annual dose during the first 10,000 years following closure (less than 10^{-3} mrem [10^{-8} Sv]), with a declining contribution thereafter (SAR Figure 2.4-18).

NRC Staff's Review

The staff reviewed the implementation of the drip shield early failure model in the TSPA calculation, as described in SNL Section 6.4.1 (2008ag). (b)(5)

(b)(5)

NRC Summary of Evaluation Findings for Drip Shield Early Failure

The staff reviewed the DOE model abstraction for early failure of the drip shield that was implemented in the TSPA code. (b)(5)

(b)(5)

2.2.1.3.1.3.2 WP Degradation

In SAR Section 1.5.2, DOE stated that WPs are relied upon to limit water contacting the waste form and to prevent the mobilization of radionuclides. The WP will have an outer barrier that is fabricated from a material that is expected to be corrosion resistant in the range of environmental conditions expected in the repository (SAR Section 2.3.6.1). In particular, the WP outer barrier will be fabricated from Alloy 22 (UNS N06022), which is a nickel-chromium-molybdenum alloy.

In developing the postclosure performance assessment, DOE evaluated a number of FEPs in SAR Table 2.2-5 related to chemical degradation of the WP. These FEPs include

- General corrosion of WPs (FEP 2.1.03.01.0A)
- SCC of WPs (FEP 2.1.03.02.0A)
- Localized corrosion of WPs (FEP 2.1.03.03.0A)
- Hydride cracking of WPs (FEP 2.1.03.04.0A)
- MIC of WPs (FEP 2.1.03.05.0A)
- Internal corrosion of WPs prior to breach (FEP 2.1.03.06.0A)
- Early failure of WPs (FEP 2.1.03.08.0A)
- Creep of metallic materials in WPs (FEP 2.1.07.05.0A)
- Localized corrosion on WPs outer surface due to deliquescence (FEP 2.1.09.28.0A)
- Thermal sensitization of WPs (FEP 2.1.11.06.0A)

DOE included general corrosion, SCC, localized corrosion, MIC, and early failure in the postclosure performance assessment. The other FEPs were screened from the performance assessment on the basis of low consequence or low probability (SAR Table 2.2-5). The NRC staff's evaluation of DOE's bases for excluding these FEPs from the performance assessment is found in SER Section 2.2.1.2.1.3.

In the TSPA analysis, DOE calculated that, due to its corrosion resistance, the WP will significantly reduce the amount of water contacting the waste form for hundreds of thousands of years after repository closure (SAR Section 2.1.2.2.6). Because of the importance of the WP in the postclosure performance assessment, the staff reviewed the DOE model abstractions for

WP chemical degradation. In the context of these reviews, the staff recognized that DOE attributed the high corrosion resistance of Alloy 22, in part, to the presence of its passive film. In the event of deterioration or loss of WP passivity, the time to WP breach may be sooner and the size of the breached area may be larger than DOE calculated in the TSPA code. As such, DOE stated that long-term persistence of the passive film on Alloy 22 is one of the key issues that determine the long-term performance of the WP in the repository, as described in SNL Section 6.4.1.1 (2007a). In NRC Appendix D, Section 4.3.1 (2005aa), NRC also identified the long-term persistence of the passive film on the WP outer barrier as being of high significance to risk for waste isolation.

Therefore, the staff first reviewed the DOE approach support the assumption of Alloy 22 passive film stability in the repository conditions. This is followed by the detailed review of DOE's model abstractions for chemical degradation of the WP, including general corrosion, MIC, localized corrosion, SCC, and early failure.

Passivity of Alloy 22

Comment	(b)(5)
	(b)(5)

In SAR Section 2.3.6.3.1 and SNL (2007a), DOE indicated that the stability of the Alloy 22 passive film depends primarily upon its physical and chemical properties, including microstructure, composition, and thickness. On Alloy 22 corrosion specimens, DOE investigated these passive film properties with various surface analytic techniques, including Auger electron spectroscopy, transmission electron microscopy, x-ray photoelectron spectroscopy, and electron energy loss spectroscopy (Orme, 2005aa). DOE performed short-term polarization tests, exposing Alloy 22 samples at 90 °C [194 °F] to solutions with a range of chemical compositions that DOE assumed were similar to, or more aggressive than, those expected in the repository (Orme, 2005aa). The solutions used in short-term polarization tests were either buffered 1 M NaCl solutions or multi-ionic solutions, including SAW, SCW, and basic saturated water (BSW) (compositions given in SAR Table 2.3.6-1). To assess the long-term passive film behavior, DOE examined 5-year U-bend samples of Alloy 22 exposed to SAW, SCW, and SDW at 90 °C [194 °F] (Orme, 2005aa).

For both short- and long-term tests, DOE observed a thin, adherent passive oxide film on the surface of Alloy 22 corrosion specimens. The film typically had thickness in the range of 2 to 7 nm [7.87×10^{-8} to 2.76×10^{-7} in] and tended to be rich in chromium (III) oxides (Cr_2O_3 and/or NiCr_2O_4). In the solutions of acidic and near-neutral pH, a thick outer layer was also observed on the top of the inner chromium-rich oxide layer (Orme, 2005aa). The outer layer was porous and consisted mostly of nickel oxide and the oxides of some other alloying elements, including iron, tungsten, and molybdenum. In BSW (pH ~12–13), DOE observed a thick silica deposit on Alloy 22 specimens (Orme, 2005aa), which DOE concluded arose from dissolution of test cell glassware or precipitation of silica from the test solution. In the case of 5-year U-bend samples exposed to SAW, SCW, and SDW, all of the immersed samples had 100 to 5,000 nm [3.94×10^{-6} to 1.97×10^{-4} in] thick carbon and iron deposits on their surfaces. DOE determined the deposits are formed as leachates from either the walls of the test tanks or other metals in the tanks (Orme, 2005aa). Oil from the mill processing is also considered to be included in the deposits. DOE stated that, underneath these deposits, the passive film was still close to 5 nm [1.97×10^{-7} in] thick after 5 years' exposure. The presence of chromium-rich oxide passive film on the Alloy 22 surface was also observed at high temperatures (in the range of 120 to 220 °C [248 to 428 °F] in NaCl–NaNO₃–KNO₃ solutions (Orme, 2005aa; Dixit, et al., 2006aa).

To support the assessment of long-term passive film stability, DOE performed thermodynamic modeling with the EQ3/6 program (Orme, 2005aa). DOE concluded that this demonstrated

that chromium -rich oxides are stable on Alloy 22, which is consistent with empirical observation of passive film chemistry. Although the tests that DOE used to characterize the passive film of Alloy 22 were for a period of, at most, 5 years, DOE referenced the point defect film growth model, which states that the passive film on Alloy 22 will maintain steady-state thickness as the porous outer layer dissolves and the compact chromium-rich oxide inner layer is continuously regenerated.

After the LA was submitted, DOE examined some 5- and 9.5-year Alloy 22 specimens from the Long-Term Corrosion Test Facility (SNL, 2009aa,ab). DOE identified thick organic deposits on some specimens. In DOE (2009d; 2010ae), DOE responded to the NRC staff's RAI requesting an evaluation of the effects of the carbon deposits on the DOE's assessment of long-term passivity and corrosion behavior. In the response, DOE stated that the organic deposits on the Alloy 22 specimens most likely originated from lubricant or grease from mechanical equipment in the corrosion test facility. DOE did not identify evidence of either increased general corrosion rate or localized corrosion attack on the specimens. For these specimens, DOE measured a corrosion rate of 3 to 5 nm/yr [1.18×10^{-7} to 1.97×10^{-7} in] in SCW at 60 °C [140 °F] after 9.5 years. DOE determined that this corrosion rate was consistent with that of uncontaminated specimens, as well as the WP corrosion rate used in the TSPA model. Therefore, DOE concluded that the organic deposits did not affect the assessment of long-term passivity or corrosion behavior.

NRC Staff's Review

The NRC staff reviewed the DOE approach to establish the stability of the WP passive film in repository conditions. (b)(5)

(b)(5)

In regard to the organic deposits on the corrosion specimens, the staff reviewed the DOE reports (SNL, 2009aa,ab)(b)(5)

(b)(5)

The staff also reviewed the DOE's use of thermodynamic modeling and the point defect film growth model to support the assessment of the WP passive film stability. (b)(5)

(b)(5)

Though in the LA, DOE provided information to support the WP passive film stability in repository conditions, the NRC staff identified three primary technical issues for which additional information from DOE was required. These issues involved passive film degradation by (i) anodic sulfur segregation, (ii) dripping seepage water, and (iii) silica deposits on the WP. The staff's reviews of these technical issues are presented next

Effect of Anodic Sulfur Segregation on Passive Film Stability

Comment (b)(5)

(b)(5)

By independent analyses and review of the technical literature, the staff identified anodic sulfur segregation as a potential mechanism that could compromise the long-term stability of the passive film on the WP outer barrier (NRC, 2005aa; U. S. Nuclear Waste Technical Review Board, 2001aa). Anodic sulfur segregation is a process that reduces the corrosion resistance of nickel and nickel-iron alloys by inhibiting the formation of the passive film (Marcus and Talah, 1989aa; Marcus, et al., 1988aa, 1984aa,ab, 1980aa). During anodic sulfur segregation, sulfur, which may be an impurity in Alloy 22, segregates to the metal-passive film interface because of selective dissolution of bulk metal elements such as nickel and iron. When the amount of sulfur at the metal-passive film interface reaches a critical concentration of about one atomic layer thickness, passive film breakdown has been observed (Marcus and Grimal, 1990aa). Assuming that 100 percent of the sulfur atoms in the alloy are retained at the metal-film interface, Marcus (2001aa) estimated that it would take about 900 years for the passive film of Alloy 22 to break down if the sulfur content in Alloy 22 is 5 weight parts per million (ppm) and the passive current density is 1 nA/cm^2 [6.45 nA/in^2].

In DOE Enclosure 5 (2009cl), DOE stated that the potential for anodic sulfur segregation would be mitigated by the presence of the alloying elements chromium and molybdenum in Alloy 22. In particular, molybdenum would bond with sulfur to form a molybdenum sulfide that dissolves under aqueous conditions, thus preventing a stable sulfur monolayer from forming at the alloy-passive film interface. Citing the work of NRC (Jung, et al., 2007aa), DOE also stated that chromium oxides are thermodynamically stable compared with sulfides. Thus the presence of chromium will promote passivation in spite of adsorbed sulfur.

NRC Staff's Review

The NRC staff reviewed the DOE assessment of anodic sulfur segregation of the WP outer barrier. (b)(5)

(b)(5)

(b)(5)

(b)(5)

(b)(5)

Dripping Effects on the Passive Film Stability

Comment (b)(5)
(b)(5)

DOE used corrosion data from immersion experiments to develop the model abstraction for general corrosion of the WP outer barrier (SAR Section 2.3.6.3.2). DOE identified the possibility, however, that conditions in the repository may lead to dripping seepage water contacting the WP surface (SAR Section 2.1.2.2.6). The staff determined that literature information in Ashida, et al. (2007aa, 2008aa) and Oka, et al. (2007aa), suggests that general corrosion processes may be affected if environmental conditions changed from immersion to dripping. Ashida, et al. (2008aa) observed salt deposit formation and localized corrosion (i.e., pitting and intergranular corrosion) on Alloy 22 specimens exposed to dripping of SCW for 40 days at 90 °C [194 °F]. The micropits observed were, however, not stable, and there was no evidence for propagation of these micropits. Ashida, et al. (2007aa) also reported an increase of the passive current density of Alloy 22 due to dripping induced temperature fluctuations at 90 °C [194 °F].

In DOE Enclosure 1 (2009cm), DOE assessed the corrosion behavior of Alloy 22 under dripping conditions in the repository environment. DOE stated that the Alloy 22 sample tested in Ashida, et al. (2008aa) was thermally aged, resulting in a significant second phase precipitation. This precipitate can decrease a resistance to localized corrosion. DOE stated that the Alloy 22 for the WP outer barrier will be solution annealed, eliminating the second phase precipitates. Therefore, DOE concluded the material Ashida, et al. (2008aa) evaluated was not relevant for

the WP. In the case of the change in passive current density due to temperature fluctuation as shown in the polarization test in Ashida, et al. (2007aa), DOE stated that the current TSPA model of general corrosion of Alloy 22 considers the change of general corrosion rate depending on the temperature; therefore, the increase of corrosion rate observed in Ashida, et al. (2007aa) is consistent with the TSPA general corrosion model.

NRC Staff's Review

The NRC staff reviewed the information provided in DOE Enclosure 1 (2009cm). (b)(5)

(b)(5)

(b)(5)

(b)(5)

Effect of Silica Deposits on Alloy 22 Passivity

DOE data and information in the technical literature indicates that silica deposits on Alloy 22 may affect the passive film. In BSW (pH ~12 to 13), DOE observed a thick silica deposit on Alloy 22 specimens (Orme, 2005aa), which DOE concluded arose from dissolution of test cell glassware or precipitation of silica from the test solution. DOE also noted the presence of silica in salt deposits on Alloy 22 specimens exposed to SDW, SAW, and SCW in the Long-Term Corrosion Test Facility as shown in Wong, et al., Table 4, Figures 2 and 3 (2004aa). In another experiment (Dixit, et al., 2006aa) DOE observed silica deposits on Alloy 22 specimens that experienced localized corrosion in a deaerated concentrated solution at 220 °C [428 °F]. Finally, information in Sala, et al. (1993aa, 1996aa, 1998aa, 1999aa) indicated that the presence of silica deposits can be associated with intergranular attack and SCC in nickel-based alloys in steam generator environments.

In DOE Enclosure 4 (2009cl) and DOE Enclosure 2 (2009cm), DOE stated that the presence of silicate did not significantly impact the corrosion potential and corrosion rate of Alloy 22 for tests conducted in SAW and NaCl solutions. DOE also presented experimental

Comment	(b)(5)
	(b)(5)

data (Andresen and Kim, 2007aa) for Alloy 22 tests in solutions of nitrate, chloride, and bicarbonate with 0.27 m silicate. The tests showed that the general corrosion rate of Alloy 22 was 3 to 4 nm/yr [1.18×10^{-7} to 1.57×10^{-7} in/yr] after 62 months' immersion at 95 °C [203 °F], which is close to the measured corrosion rate in solutions without silicate. Finally, DOE stated that Sala, et al. (1993aa, 1996aa, 1998aa, 1999aa) and Dixit, et al. (2006aa) considered more aggressive environmental conditions than those expected in the repository. Therefore, DOE concluded that the observations are not relevant to the WP in the repository.

NRC Staff's Review

The staff reviewed DOE's approach to assess the effects of silica deposits on the WP passive film stability. (b)(5)

(b)(5)

(b)(5)

2.2.1.3.1.3.2.1 General Corrosion of the WP Outer Barrier

In SAR Section 2.3.6.3, DOE defined general corrosion of the WP outer barrier as uniform thinning by electrochemical processes at its corrosion potential. General corrosion could lead to the release of radionuclides from the WP if the WP wall is breached. General corrosion thinning may also make the WP more susceptible to degradation processes such as SCC (SAR Section 2.3.6.5.2.3) or impacts caused by seismic ground motion (SAR Section 2.3.4.5). This section of the SER includes the NRC staff's review of the DOE model abstraction for general corrosion of the WP outer barrier.

WP General Corrosion Conceptual Model

In DOE's conceptual model for general corrosion of the WP outer barrier, general corrosion starts at the time of repository closure (SAR Section 2.3.6.2.2). DOE assumed aqueous conditions because wet conditions give higher corrosion rates than dry conditions (SAR Section 2.3.6.4). In DOE's model, the general corrosion rate is a function of the WP temperature and, at a given temperature, it is assumed to be constant over time (SAR Section 2.3.6.3.1). DOE used an Arrhenius-type equation (SAR Equation 2.3.6-3) to calculate the temperature-dependent general corrosion rate of the WP outer barrier in the temperature range of 25 to 200 °C [77 to 392 °F]. DOE also considered using a decreasing general corrosion rate over time as an alternative conceptual model (SNL, 2007a) but concluded that this would calculate a longer time to WP failure.

DOE also considered that microbial activity in the repository could affect the WP corrosion behavior—a phenomenon called microbiologically or MIC (SAR Section 2.3.6.3.3.2). DOE stated that microorganisms can change the electrochemical reactions on the material surface and change the type or degree of corrosion compared to that which would be measured in the absence of microorganisms. In the DOE conceptual model, the WP outer barrier is subject to MIC when the relative humidity is sufficiently high for microbial activities. The effect of MIC on

the general corrosion rate is quantified by a unitless scalar called the MIC enhancement factor. If the relative humidity is sufficiently high, the general corrosion rate in the absence of the microorganisms (SAR Equation 2.3.6-3) is multiplied by the MIC enhancement factor to give the enhanced general corrosion rate (SAR Equation 2.3.6-4).

NRC Staff's Review

The NRC staff reviewed the DOE conceptual model for general corrosion of the WP outer barrier. The staff reviewed the DOE model assumption that the temperature dependence of the general corrosion rate can be quantified with the Arrhenius-type equation. Corrosion involves chemical and/or electrochemical reactions and the transport of reacting species and ions on the metal surface—a process known to be thermally activated (Fontana and Greene, 1978aa).

(b)(5)

The staff also reviewed the DOE model assumption that the corrosion rate is constant over time at a given temperature. DOE provided experimental data showing that the measured general corrosion rate of Alloy 22 decreases over time at a given temperature for experiments up to 5 years in duration (SAR Figure 2.3.6-13). (b)(5)

(b)(5)

(b)(5)

The staff also reviewed the DOE's alternative conceptual model where the temperature was realistically decreased as a function of time. (b)(5)

(b)(5)

Finally, the staff reviewed the DOE model assumption that MIC will occur above a relative humidity threshold value. (b)(5)

(b)(5)

(b)(5)

General Corrosion Rate by Long-Term Weight-Loss Measurements

In SAR Equation 2.3.6.3, DOE established the general corrosion rate at the baseline temperature of 60 °C [140 °F] from 5-year weight-loss experiments (SAR Section 2.3.6.3.2.1). DOE performed corrosion tests in the Long-Term Corrosion Test Facility at 60 and 90 °C [140 and 194 °F], using Alloy 22 specimens with two different geometries: weight-loss specimens and crevice specimens. For both specimen types, tests were performed on specimens with different metallurgical conditions (i.e., mill annealed and welded) and in different corrosion test solutions, including SAW, SCW, and SDW. After 5 years of exposure to the test solutions, every specimen was covered with surface deposits. Therefore, the posttest specimens were cleaned and descaled in accordance with ASTM G 1-90 (ASTM International, 1999aa). DOE stated that the cleaning methods used to remove the scale from the tested samples did not significantly affect untested control samples. Therefore, without correction of any possible mass loss from the replicate untested control foil sample, DOE determined the general corrosion rates of Alloy 22 based upon the formula defined in ASTM G 1-90.

DOE summarized the results of its corrosion tests in SNL Section 6.4.3.2 (2007a). DOE stated that there was no appreciable difference between the general corrosion rates for mill-annealed and welded specimens, as shown in SNL Figures 6-14 and 6-19 (2007a). However, the measured corrosion rates for crevice specimens were higher than those for weight-loss specimens, as shown in SNL Figure 6-22 (2007a). For the weight-loss specimens, DOE determined that the mean general corrosion rate of weight-loss specimen was 3.15 nm/yr [1.24×10^{-7} in/yr], with the ± 1 standard deviation of 2.71 nm/yr [1.07×10^{-7} in/yr]. For the crevice specimens, DOE calculated a mean general corrosion rate of 7.36 nm/yr [2.90×10^{-7} in/yr] with ± 1 standard deviation of 4.93 nm/yr [1.94×10^{-7} in/yr]. Because the crevice specimens tend to give higher corrosion rates, DOE only used the crevice data to develop the distribution from which the 60 °C [140 °F] general corrosion rate parameter was sampled in the TSPA code.

DOE determined that uncertainty and variability in the measured corrosion rate could be attributed both to measurement uncertainty, given the very small weight loss associated with low corrosion rates, and to actual variation in the corrosion processes on the material surface, as outlined in SNL Section 6.4.3.3 (2007a). In the model abstraction, DOE accounted for this uncertainty by fitting the 5-year corrosion data to the Weibull cumulative distribution functions, which are sampled in the TSPA code, as detailed in SNL Section 6.4.3.3.2 (2007a). DOE stated that the Weibull distribution was determined to be the best fit to the experimental data as compared to other fits such as uniform distribution, normal distribution, lognormal distribution, and gamma distribution. DOE characterized the Weibull distribution with two parameters: the scale factor and the shape factor. DOE used three different scale factor/shape factor pairs, corresponding to low, medium, and high uncertainty levels, to define three different Weibull distributions for the 60 °C [140 °F] general corrosion rate parameter, as shown in SNL Table 6-7 (2007a). In the TSPA code, the low, medium, and high general corrosion rate distributions were sampled such that the low and high distributions were each used for 5 percent of the realizations and the medium distribution was used for 90 percent of the realizations. DOE used the 5–90–5 percent partitioning to ensure that there were sufficient differences in the general corrosion rates for the respective distributions, yet that each distribution was amply sampled to produce a meaningful contribution (SAR Section 2.3.6.3.3.1). The Weibull distributions from which the 60 °C [140 °F] general corrosion rate of the WP outer barrier is sampled in the TSPA code are shown in SAR Figure 2.3.6-9.

In response to the NRC staff's RAI that requested justification for the representation of uncertainties associated with cleaning the long-term corrosion specimens, DOE responded in

DOE Enclosure 3 (2009cl) that the specimens were not adequately cleaned prior to performing weight-loss measurements. In particular, DOE determined that the initial weight of the specimens was artificially high because of the failure to remove mill-annealed oxide and surface contamination. This oxide and surface contamination, however, were removed during posttest cleaning. Nevertheless, DOE assumed that the associated weight loss was attributable to the general corrosion of Alloy 22. Thus, DOE concluded that it overestimated the actual weight loss of Alloy 22 and, in turn, overestimated the general corrosion rate. DOE stated that it is in the process of recleaning and reanalyzing the specimens following the procedures in ASTM G 1-03 (ASTM International, 2003ab). DOE provided preliminary data from the reanalysis for the weight-loss specimens in DOE Enclosure 3 (2009cl) and stated that those data gave the most accurate estimate for the general corrosion rate of Alloy 22. As shown in DOE Enclosure 3, Figure 8 (2009cl), the corrosion rate from the recleaned weight-loss specimens is close to or lower than that calculated by the three Weibull distributions DOE used in the TSPA code for the Alloy 22 general corrosion rate—particularly for corrosion rates with high cumulative probabilities. DOE stated that only corrosion rates with cumulative probabilities of 0.96 and above {corrosion rate greater than ~ 15 nm/yr [5.91×10^{-7} in/yr]} are important for WP performance. Because the data from the recleaned, reanalyzed specimens provide lower corrosion rates than those calculated by the Weibull distributions at the high cumulative probabilities, DOE concluded that use of the Weibull distributions shown in SAR Figure 2.3.6-9 are acceptable because the WP failure time was not overestimated. Nevertheless, DOE stated that the final recleaning and re-analysis of the corrosion specimens will be completed and documented in a LA update.

NRC Staff's Review

The NRC staff reviewed the DOE approach to establish the WP general corrosion rate by long term tests. With regard to the material conditions for the corrosion tests, (b)(5)

(b)(5)

Comment (b)(5)

(b)(5)

(b)(5)

Temperature Dependence of the General Corrosion Rate

DOE conducted experiments to determine the temperature dependence of the general corrosion rate of the WP outer barrier by measuring the activation energy for general corrosion of Alloy 22 (SAR Section 2.3.6.3.2.2). DOE used the short-term electrochemical polarization resistance technique following the ASTM G 59-97 (ASTM International, 1998aa). Mill-annealed and welded specimens were tested in a range of solutions containing NaCl and KNO₃ at temperatures ranging from 60 to 100 °C [140 to 212 °F] (SAR Table 2.3.6-4). DOE used these solutions because they simulate the conditions of moderate relative humidity where calcium is expected to be a minor component in the aqueous environment in the repository, as outlined in SNL Section 6.4.3.4 (2007a).

From these data (SAR Figure 2.3.6-7), DOE used a linear mixed-effects statistical analysis to calculate a mean activation energy of 40.78 kJ/mol [9.74 kcal/mol], with a standard deviation 11.75 kJ/mol [2.81 kcal/mol]. DOE selected a normal distribution to represent the temperature-dependence term on the basis of statistical fitting techniques. The activation energies for the individual solutions used to determine the distribution of the activation energy are shown in SAR Table 2.3.6-5. DOE confirmed the activation energy calculated from these short-term polarization tests by comparisons to the activation energy from the long-term 5-year weight-loss data of Alloy 22 specimens immersed in SCW at 60 and 90 °C [140 and

194 °F], respectively, as described in SNL Section 6.4.3.4 (2007a). DOE calculated a mean activation energy of 40.51 kJ/mol [9.68 kca/mol] for the 5-year corrosion data, which is close to the mean calculated from the short-term polarization technique. From the 5-year corrosion data, the activation energy distribution was also obtained. This distribution was best represented by truncating the normal distribution of the short-term polarization tests at -3 and +2 standard deviations.

The deficiencies with cleaning and weighing Alloy 22 corrosion specimens discussed in DOE Enclosure 3 (2009cl), however, led DOE to reevaluate the calculation of the temperature dependence of the general corrosion rate. The deficiencies were not associated with the short-term polarization data, but rather the comparison of 5-year general corrosion rates for specimens immersed in SCW. For the latter, DOE recalculated the activation energy using the corrosion rates measured for the recleaned, reanalyzed weight-loss specimens. From these data, DOE calculated a mean activation energy of approximately 32.26 kJ/mol [7.71 kcal/mol], with minimum and maximum values of 3.37 and 60.05 kJ/mol [0.81 and 14.3 kcal/mol], respectively, as shown in DOE Enclosure 3, Figure 9 (2009cl). These values are approximately 20 percent lower than the activation energies sampled from the truncated normal distribution described in SAR Section 2.3.6.3, which was sampled in the TSPA code. Using both the updated distribution for the activation energy, as shown in DOE Enclosure 3, Figure 9 (2009cl), and the updated distribution for the 60 °C [140 °F] general corrosion rate, as shown in DOE Enclosure 3, Figure 8 (2009cl), DOE calculated the temperature-dependent general corrosion rate of Alloy 22, using SAR Equation 2.3.6-3. DOE compared the corrosion rates calculated using the updated distributions to the corrosion rates calculated using the model described in SAR Section 2.3.6.3. As shown in DOE Enclosure 3, Figures 10-12 (2009cl), for the temperature range of 25 to 200 °C [77 to 392 °F], the updated distributions derived from recleaned, reanalyzed weight-loss specimens give lower corrosion rates than obtained by the model described in SAR Section 2.3.6.3, which was implemented in the TSPA code. As such, DOE concluded that the TSPA code did not underestimate the WP general corrosion rate.

NRC Staff's Review

The NRC staff reviewed the DOE approach to calculate the temperature dependence of the WP general corrosion rate. The staff reviewed the material and environmental conditions at which DOE measured the activation energy for general corrosion of the WP outer barrier that was sampled in the TSPA code. With regard to the material conditions for the tests, (b)(5)

(b)(5)

(b)(5)

Additionally, the staff compared the activation energy for general corrosion of the WP outer barrier calculated from the recleaned, reanalyzed weight-loss specimens to the activation energy calculated by the short-term polarization test. (b)(5)

(b)(5)

(b)(5)

MIC Effects

The NRC staff reviewed DOE's approach to establish the conditions for the onset of MIC and to quantify the extent to which MIC may affect general corrosion behavior.

Comment: (b)(5)

(b)(5)

Comment: (b)(5)

(b)(5)

Threshold Relative Humidity for the Onset of MIC

As discussed in SAR Section 2.3.6.3.3.2 and DOE Enclosure 10 (2009cl), DOE concluded that the relative humidity in the repository must be greater than a threshold value for MIC to enhance the general corrosion rate of the WP outer barrier. DOE used experimental data and information from the independent studies to determine this threshold relative humidity. DOE performed experiments in which Alloy 22 specimens were embedded in crushed Yucca Mountain tuff and placed in chambers with Yucca Mountain native microorganisms at different temperature and humidity levels (Else, et al., 2003aa). DOE reported that the optimum condition for microbial growth is at a temperature of 30 °C [86 °F] and 100 percent relative humidity. Microbial growth was extremely limited at higher temperatures or lower humidity. In SNL Section 6.4 (2004ab), DOE also cited several studies which indicate that robust growth of most microorganisms requires a relative humidity of 90 percent or higher, although limited growth is seen at relative humidity as low as 75 percent (e.g., Brown, 1976aa; Pedersen and Karlsson, 1995aa). In the TSPA code, DOE accounts for uncertainty in the threshold relative humidity by sampling this threshold relative humidity from a uniform distribution between 75 and 90 percent (SAR Section 2.3.6.3.3.2).

NRC Staff's Review

The NRC staff reviewed the DOE approach to establish the threshold relative humidity for the onset of MIC. (b)(5)

(b)(5)

MIC Factor

If the relative humidity at the WP surface is greater than the threshold value, the MIC-enhanced general corrosion rate for the WP outer barrier is calculated by multiplying the general corrosion rate in the absence of the microorganisms (given by SAR Equation 2.3.6-3) by the MIC enhancement factor. DOE performed laboratory tests to determine the extent to which MIC may affect the general corrosion rate of Alloy 22 (SAR Section 2.3.6.3.2.3). DOE used the electrochemical polarization technique to measure the corrosion rate of Alloy 22 specimens in nutrient-enriched, simulated Yucca Mountain well water, with and without the presence of microbes (Lian, et al., 1999aa). Test results were shown in SNL Table 6-16 and Figure 6-54 (2007a). DOE found that the general corrosion rate for Alloy 22 in the microbial-rich solution was up to a factor of approximately two higher than the general corrosion rate in sterile solution. DOE represented epistemic uncertainty in the MIC enhancement factor to account for natural variation in the expected extent of microbial activity in repository conditions. Thus, in TSPA code, DOE samples the MIC enhancement factor from a uniform distribution between one (i.e., MIC has no effect on the general corrosion rate) and two (i.e., general corrosion rate would be double the nominal general corrosion rate).

NRC Staff's Review

The NRC staff reviewed the DOE approach to calculate the MIC enhancement factor.

(b)(5)

(b)(5)

DOE indicated that some samples from these tests contain a significant amount of microbial bacteria, even though no bacteria were deliberately introduced (Horn, et al., 2005aa).

(b)(5)

Abstraction and Integration

The model abstraction for general corrosion of the WP outer barrier is implemented in the WP and DS Degradation Submodel in the TSPA code in SNL Section 6.5.3 (2008ag). The inputs that are needed for the model abstraction are temperature of the WP and the relative humidity in the drift. These inputs come from the EBS Thermohydrologic Environment Submodel. The WP and DS Degradation Submodel includes both the CSNF configuration that uses the transportation, aging, and disposal canister configuration parameters and the CDSP configuration that uses the 5 high-level waste/1 DOE spent nuclear fuel Long configuration parameters. DOE assumed a total of 11,629 WPs divided into 5 percolation subregions, each of which is subject to different environmental conditions, as detailed in SNL Section 6.3.5.1.3 (2008ag). The WP and DS Degradation Submodel general corrosion calculations are performed for both WP configurations in each of the percolation subregions.

In the WP and DS Degradation Submodel, the WP surface is divided into subareas, referred to as patches, to account for the spatial variability of general corrosion on the WP surface, as outlined in SNL Section 6.3.5.1.2 (2008ag). Each patch may have a different general corrosion rate. The submodel uses a patch area of 231.5 cm^2 [35.88 in^2], so the CSNF and CDSP WPs have 1,430 and 1,408 patches, respectively. For each realization, each patch is assigned a different value for the 60°C [140°F] general corrosion rate, which is sampled from the Weibull distributions derived from 5-year weight-loss corrosion data from creviced Alloy 22 specimens (SAR Section 2.3.6.3.3.1). Because the size of the crevice specimens that DOE used to measure the 5-year general corrosion was about one-fourth the patch size, DOE sampled the 60°C [140°F] general corrosion rate four times for each patch and applied the highest of the four sampled rates to the patch, as described in SNL Section 6.2.5.1.2 (2008ag). The effect of rescaling the 60°C [140°F] general corrosion rate distribution, shown in SNL Figure 6.3.5-6 (2008ag), resulted in rates that are approximately twice those of the nominal distribution. To account for the temperature dependence of the general corrosion rate, a single value of the temperature-dependence parameter is sampled in each realization from the distribution derived from short-term polarization tests and applied to all WP patches. To account for potential MIC, the value of the threshold relative humidity for MIC is sampled once per realization from a uniform distribution in the range of 75 to 90 percent and applied to all WPs. If the relative humidity in the drift exceeds the threshold, the MIC enhancement factor is sampled from a uniform distribution in the range of one to two and applied to the patches.

DOE considered a WP outer barrier to be breached by general corrosion when one or more patches are penetrated. When the WP was breached, the general corrosion model was also applied to the inner surface of the WP outer barrier. The output for the general corrosion model gave the percentage of breached WPs as a function of time and the average number of patch

penetrations per breached WP as a function of time. This output was provided to the Waste Form Degradation and Mobilization Model Component and the EBS Flow and EBS Transport Submodels. SAR Figures 2.1-10(b) and 2.1-16(b) showed the fraction of CSNF WPs breached by general corrosion and the fraction of the WP surface area breached per breached WP, respectively, for the CSNF WP in the Nominal Modeling Case

A mean of less than 10 percent of CSNF WPs are breached over 1 million years, and of the breached WPs, the mean breached area is less than 0.3 percent of the total WP surface area. The results for the CDSP WP in the Nominal Modeling Case are similar [SAR Figure 2.1-17(b)]. DOE Figures 9 and 10 (2009bj) showed the fraction of CSNF and CDSP WPs, respectively, breached by general corrosion in the Seismic Ground Motion Modeling Case. For both WPs, the mean is approximately 10 percent breached in 1 million years. DOE Figures 11 and 12 of the response to RAI (DOE, 2009bj) showed the fraction of the surface area breached for the CSNF and CDSP WPs breached by general corrosion in the Seismic Ground Motion Modeling Case. For both WPs, the fraction is approximately 1 percent of the surface area.

In regard to the activation energy for general corrosion in TSPA model, the staff notes that DOE performed sensitivity analyses which show that the expected dose has a strong correlation to the activation energy for general corrosion of the WP outer barrier and tends to increase with decreasing activation energy for general corrosion (SAR Figures 2.4-151 and 2.4-155).

NRC Staff's Review

The NRC staff reviewed the implementation and integration of the model abstraction for general corrosion of the WP outer barrier in the postclosure performance assessment. (b)(5)

(b)(5)

NRC Summary of Evaluation Findings for the General Corrosion of the WP Outer Barrier

The staff reviewed the DOE model abstraction for general corrosion of the WP outer barrier that was implemented in the TSPA code. (b)(5)

(b)(5)

2.2.1.3.1.3.2.2 Localized Corrosion of the WP Outer Barrier

Comment (b)(5)
(b)(5)

Localized corrosion is a process where corrosion occurs at discrete sites, in contrast to general corrosion, which uniformly thins the entire surface of a material. Localized corrosion usually occurs in metals and alloys, such as Alloy 22, whose corrosion resistance is attributed to the presence of a passive oxide film. Localized corrosion can initiate if the passive film is removed or damaged. When localized corrosion does occur, it tends to cause degradation much faster than general corrosion. In SAR Section 2.3.6.4, DOE considered that localized corrosion could lead to the release of radionuclides from the WP if the WP wall is breached.

DOE determined that localized corrosion requires the presence of a liquid water film on the WP surface, which may come from dripping seepage water or salt deliquescence in dust particles, as outlined in SNL Section 6.3.5.2 (2008ag). DOE's evaluation of salt deliquescence indicated that brines produced from dust deposits will not lead to localized corrosion (FEP 2.1.09.28.0A; SNL, 2008ac). Consequently, DOE excluded localized corrosion caused by deliquescence from the performance assessment (SAR Table 2.2-5) and concluded that seepage water must contact the WP for localized corrosion to occur.

Comment (b)(5)
(b)(5)

In the TSPA code, DOE calculated that in-drift conditions (i.e., temperature, pH, and concentration of ionic species in seepage water) may support localized corrosion of the WP for approximately 12,000 years after repository closure, as described in DOE Enclosure 11 (2009cl). The TSPA code, however, also calculates that few drip shields fail within 12,000 years after repository closure. Therefore, the probability of WP breach by localized corrosion is low in the DOE model. Following 12,000 years after repository closure, DOE calculated that there is a low probability for conditions in the drift to support localized corrosion of the WP even if the drip shield fails and allows seepage water to contact the WP.

(b)(5)

WP Localized Corrosion Conceptual Models

DOE implemented models for both initiation and propagation of localized corrosion of the WP outer barrier in the TSPA code. The following addresses the staff's review of these models

Corrosion Initiation Models

DOE considered two potential mechanisms by which localized corrosion could be initiated on the WP outer barrier under seepage conditions. In SAR Section 2.3.6.4, DOE described the first mechanism, which is related to the WP open-circuit corrosion potential, or corrosion potential. The DOE model initiates localized corrosion if the corrosion potential for the WP is greater than or equal to a critical potential. DOE defined critical potential as the potential above which a passive film will not spontaneously reform if damaged (SAR Section 2.3.6.4.1). While localized corrosion typically encompasses both pitting and crevice corrosion, DOE treated all

WP localized corrosion as crevice corrosion because crevice corrosion initiates in less aggressive thermal and chemical conditions than pitting corrosion, as described in SNL Section 6.4.4 (2007a). As such, DOE assumed that the critical potential for localized corrosion is equivalent to the crevice repassivation potential (SAR Section 2.3.6.4.1).

The second initiation mechanism, referred to as salt separation, was described in SAR Section 2.3.5.4.2.1. During salt separation, the relative humidity at the WP surface drops below a salt precipitation threshold while seepage is occurring, causing chloride salts to precipitate out of solution. Nitrate that is still in solution moves away by advection. A chemically aggressive chloride-rich, nitrate-depleted brine forms when the relative humidity increases above this threshold value. DOE did not, however, model localized corrosion by salt separation in the TSPA code, as summarized in SAR Section 2.4. Consequently, the NRC staff submitted an RAI requesting that DOE provide technical details evaluating the significance of salt separation effects on the performance assessment of WPs in the proposed repository environment. DOE Enclosure 11 (2009c) provided additional information on this analysis and stated that the salt separation analysis will be included in a future revision of the LA.

NRC Staff's Review

The staff reviewed the DOE conceptual models for localized corrosion initiation on the WP outer barrier, as described in SAR Sections 2.3.6.4 and 2.3.5.5. (b)(5)

(b)(5)

(b)(5)

Corrosion Propagation Model

In DOE's model for localized corrosion propagation, corrosion propagates at a constant rate over time (SAR Section 2.3.6.4.3.2). DOE also considered an alternative conceptual model in which the corrosion rate decreased over time (SAR Section 2.3.6.4.3.3.2). The alternative model, based on pit growth, gives a corrosion propagation rate lower than that calculated using the primary model assumption of constant corrosion rate. Therefore, DOE implemented the model with constant corrosion rate in TSPA code because it calculated an earlier WP breach time.

NRC Staff's Review

The staff reviewed the DOE model for propagation of localized corrosion of the WP outer barrier, as described in SAR Section 2.3.6.4.3.2. (b)(5)

(b)(5)

Localized Corrosion Initiation Conditions

For localized corrosion initiation by corrosion potential and salt separation, respectively, DOE used empirical data to establish the conditions in which localized corrosion of the WP outer barrier could initiate. The staff reviewed DOE's localized corrosion initiation conditions.

Initiation by Critical Potential

In the TSPA code, DOE compared the WP outer barrier corrosion potential to the repassivation potential to determine whether electrochemical conditions on the WP would lead to passive film breakdown. DOE assumed that the corrosion potential and repassivation potential for the WP outer barrier, respectively, depended on the environmental conditions in the drift, including temperature, pH, chloride concentration, and nitrate concentration. DOE derived equations to represent the potentials as functions of these parameters by performing tests in which it measured the potentials for Alloy 22 specimens while varying the environmental parameters (SAR Section 2.3.6.4.2).

DOE established the dependence between the corrosion potential of Alloy 22 and the environmental parameters using data from 5-year tests (SAR Section 2.3.6.4.2.1). For a range of temperatures, DOE measured the corrosion potentials for Alloy 22 creviced samples with various metallurgical conditions (i.e., as welded, mill annealed, stress relieved) exposed to a range of simulated brine solutions, including SDW, SAW, and SCW, the compositions of which were given in SAR Table 2.3.6-1. The corrosion potential data used in DOE's model development were shown in SAR Table 2.3.6-6. Using regression analyses, DOE applied SAR Equation 2.3.6-7 to the data shown in SAR Table 2.3.6-6, representing the corrosion potential as a function of temperature, pH, and nitrate and chloride ion concentrations.

DOE established the dependence between the repassivation potential of Alloy 22 and the environmental parameters using data from cyclic potentiodynamic polarization tests (SAR Sections 2.3.6.4.2.2). The tests were performed using the methodology of ASTM G61-86 (ASTM International, 2003aa). In DOE Enclosure 9 (2009cl), DOE stated that while repassivation potentials can be measured by methods other than cyclic potentiodynamic polarization, the differences in measured potentials tended to be small and the cyclic potentiodynamic polarization method generally predicted greater corrosion susceptibility in aggressive brines. Similar to the tests for corrosion potential, DOE used Alloy 22 specimens with different metallurgical conditions (mill annealed and as welded) in a range of simulated brine solutions. DOE used ceramic wrapped with polytetrafluoroethylene tape to form a crevice with Alloy 22 in the cyclic potentiodynamic polarization tests. The crevice repassivation

potential data used in DOE's model development were shown in SAR Table 2.3.6-7. Sample specimens that did not show evidence of localized corrosion attack were not used to develop the model. For experiments showing localized corrosion, DOE used regression analyses to fit SAR Equation 2.3.6-6 to the data shown in SAR Table 2.3.6-7, representing the crevice repassivation potential as a function of temperature and nitrate and chloride ion concentrations. In the TSPA code, DOE accounted for fitting uncertainty in SAR Equations 2.3.6-6 and 2.3.6-7 by varying the values of the fitting parameters of the respective equations according to a Monte Carlo algorithm and by using data in the regression analysis from multiple samples for a given environmental condition, as detailed in SNL Section 6.3.5.2.2 (2008ag).

DOE compared the model calculations of corrosion potential and repassivation potential, respectively, establish the environmental conditions that would support initiating localized corrosion on the WP outer barrier (SAR Section 2.3.6.4.3.1.2). In the DOE model, the probability for initiation of localized corrosion at temperatures less than 90 °C [194 °F] generally increases with decreasing pH and decreasing nitrate-to-chloride ion ratio. DOE compared the localized corrosion initiation conditions its model calculated to experimental observations of localized corrosion initiation on Alloy 22 specimens. DOE's model calculated that localized corrosion may initiate on Alloy 22 exposed to SAW at 90 °C [194 °F], whereas in experimental tests, localized corrosion was not observed on Alloy 22 specimens exposed to this solution for 5 years (SAR Table 2.3.6-12). DOE presented a number of additional corrosion test solutions for which its model calculated that localized corrosion may initiate, yet for which localized corrosion was not observed on Alloy 22 specimens (SAR Table 2.3.6-13). DOE concluded that its model overestimates the probability of localized corrosion initiation.

NRC Staff's Review

The staff reviewed DOE's experimental methodology to measure the corrosion potential and the crevice repassivation potential of Alloy 22. (b)(5)

(b)(5)

The staff reviewed DOE's calculated values for the corrosion potential and repassivation potential, respectively, to confirm the environmental conditions (i.e., temperature, pH, concentration of ionic species in seepage water) under which the DOE model calculates that localized corrosion of the WP will initiate. The staff examined the model functional dependencies (b)(5)

(b)(5)

(b)(5)

Initiation by Salt Separation

DOE used thermodynamic analyses to calculate the threshold relative humidity below which chloride-bearing salts could precipitate out of seepage water (SNL, 2007ak). In these analyses, DOE considered that the threshold relative humidity depends upon the group water type (i.e., 1–4 as defined in SAR Section 2.3.5), quantity of alkali feldspar to be tritiated into the seepage waters [i.e., the water–rock interaction parameter (WRIP)], the partial pressure of CO₂ in the drift, and the WP temperature. In SAR Figure 2.3.5-55, the thermodynamic analyses showed that the chloride-to-nitrate ratio in a range of conditions is nearly constant until the activity of water (i.e., relative humidity) drops below a value in the range of approximately 77 to 65 percent. In the TSPA model, DOE concluded that this range represents the threshold relative humidity below which localized corrosion initiation by salt separation can occur (SAR Section 2.3.5.5).

NRC Staff's Review

The NRC staff reviewed the DOE approach for establishing the relative humidity threshold for the initiation of localized corrosion by salt separation, as DOE described in SAR Section 2.3.5.5

(b)(5)

(b)(5) The DOE model assumes that salt separation can cause the corrosion potential to exceed the repassivation potential (b)(5)

(b)(5)

Localized Corrosion Propagation Rate

In the TSPA code, DOE sampled the propagation rate for localized corrosion on the WP outer barrier using a log-uniform distribution in the range of 12.7 $\mu\text{m}/\text{yr}$ to 1,270 $\mu\text{m}/\text{yr}$ [5×10^{-4} to 5×10^{-2} in/yr] with a median value of 127 $\mu\text{m}/\text{yr}$ [5×10^{-3} in/yr] (SAR Section 2.3.6.4.3.2). This range was based on corrosion testing of Alloy 22 in aggressive environments, including 10 percent FeCl₃ (Haynes International, 1997aa) and concentrated HCl (Haynes International, 1997ab). DOE compared the corrosion rate distribution sampled in the TSPA code to independently measured corrosion rates for

similar, but less corrosion-resistant alloys, including Alloy C-276 and Alloy C-4 (SAR Section 2.3.6.4.4.2.2). DOE concluded that the measured corrosion rates fall within the bounds of the distribution sampled in TSPA code.

NRC Staff's Review

The NRC staff reviewed the DOE approach, described in SAR Section 2.3.6.4, that established the distribution sampled in the TSPA code for the propagation rate of localized corrosion on the WP outer barrier. (b)(5)

(b)(5)

Effects of Microorganisms on Localized Corrosion

Comment (b)(5)

(b)(5)

As DOE addressed in SAR Section 2.3.6.3.2.3, microorganisms in the repository may affect the corrosion processes on the WP outer barrier such that the type and extent of corrosion in the presence of the microorganisms may be different from the corrosion in the absence of the microorganisms. Though DOE incorporated MIC effects into its model abstraction for general corrosion of the WP outer barrier (SAR Section 2.3.6.3.2.3), experimental observations indicate that MIC may also affect the localized corrosion behavior. In particular, a DOE study showed that small pits, or micropores, were observed on the surface of Alloy 22 corrosion specimens exposed in a borosilicate glass vessel with unsterilized Yucca Mountain tuff rock, whereas no such micropores were observed in sterilized conditions (Martin, et al., 2004aa). In DOE Enclosure 10 (2009cl), DOE stated that the micropores Martin, et al. (2004aa) observed started to form during the first 17 months' exposure, after which the size of the micropores was less than 1 μm [0.039 mil] in diameter. DOE further stated that the same specimens were observed after an additional 40 months' exposure, after which there were more pores, but no significant increase in pore size compared to that measured after 17 months. DOE determined that, if the micropores were initiated pits, they quickly repassivated before they could propagate. Therefore, DOE concluded that it was appropriate to incorporate MIC into its model abstraction for general corrosion of the WP outer barrier, to be consistent with DOE observations in SNL Section 6.4.5 (2007al) that MIC may enhance corrosion on the entire material surface.

NRC Staff's Review

The NRC staff reviewed the information in DOE Enclosure 10 (2009cl). (b)(5)

(b)(5)

(b)(5)

Abstraction and Integration

DOE did not directly include and calculate the effects of localized corrosion of the WP outer barrier in the TSPA code. Rather, DOE performed a Localized Corrosion Initiation Uncertainty Analysis, as described in SNL Appendix O (2008ag) and DOE Enclosure 11 (2009cl), that calculated the fraction of WPs in the repository that are susceptible to localized corrosion as a function of drip shield breach time (i.e., the time at which seepage water could contact the WP). The Localized Corrosion Initiation Uncertainty Analysis implements the Localized Corrosion Initiation Submodel, as detailed in SNL Section 6.3.5.2.3 (2008ag), which determines whether the environmental conditions in the drift will initiate localized corrosion, and gives this input to the TSPA code. The Localized Corrosion Initiation Submodel is similar to the TSPA code, but incorporates only those submodels that are needed to calculate localized corrosion initiation conditions. In particular, the Localized Corrosion Initiation Submodel uses information primarily from the

- EBS Thermohydrologic Environment Submodel to determine the temperature and relative humidity history at the WP
- Drift Seepage Submodel to determine whether seepage occurs at a repository location
- EBS Chemical Environment Submodel to determine the chemical composition of seepage water
- Seismic Ground Motion Damage Submodel to determine the time of drip shield plate failure due to seismic damage
- WP and DS Degradation Submodel to account for corrosion in determining drip shield plate and WP failure times

In the Localized Corrosion Initiation Submodel, the repository was discretized into 3,264 subdomains of equal area, at the center of which were 6 CSNF and 2 CDSP WPs. The subdomains were distributed through the five percolation subregions. In the Localized Corrosion Initiation Submodel, localized corrosion could initiate because of the WP corrosion potential or by salt separation. For each subregion, at every timestep in a realization, the Localized Corrosion Initiation Submodel compares the corrosion potential, as calculated by SAR Equation 2.3.6-7, to the crevice repassivation potential, as calculated by SAR Equation 2.3.6-6. If the corrosion potential was greater than or equal to the crevice repassivation potential in seepage conditions, the Localized Corrosion Initiation Submodel assumed that localized corrosion initiated at that subregion. Similarly, if the relative humidity at the WP surface fell below the salt separation threshold humidity in seepage conditions, the Localized Corrosion Initiation Submodel assumed that localized corrosion initiated at that subregion.

The Localized Corrosion Initiation Submodel calculated that, if the drip shield were breached at the time of the repository closure (i.e., no drip shield present), there is approximately 34 percent probability that localized corrosion will initiate on a given WP surface (24 percent probability contribution by salt separation and 10 percent probability contribution by corrosion potential), as shown in DOE Enclosure 11, Figure 1 (2009cl). DOE calculated that as the time to drip shield breach increases, the probability of localized corrosion initiation decreases and is negligible if

Comment (b)(5)
(b)(5)

the drip shield fails beyond approximately 12,000 years after repository closure. In particular, DOE calculated that localized corrosion will not initiate by salt separation if drip shield breach occurs after approximately 1,000 years from the time of repository closure, because the relative humidity will remain above the threshold value. Moreover, changes in the repository environmental and chemical conditions (e.g., decreasing temperature) make initiation by corrosion potential less probable as the time to drip shield breach increases in the DOE model.

Given the results of the Localized Corrosion Initiation Uncertainty Analysis, DOE determined that localized corrosion of the WP outer barrier could only affect the timing and magnitude of the release of radionuclides from the WP if the overlying drip shield plate was breached within approximately 12,000 years after repository closure. DOE calculated that, beyond drip shield early failure, which already assumes localized corrosion for underlying WPs in seepage conditions, the probability of drip shield breach during this time period is negligible (SAR Figures 2.1-8, 2.1-11, and 2.4-24). Therefore, DOE concluded that localized corrosion of the WP outer barrier will not affect any of the TSPA modeling cases, as shown in DOE Enclosure 11, Figure 1 (2009c).

NRC Staff's Review

The NRC staff reviewed the implementation and integration of the model abstraction for localized corrosion of the WP outer barrier in the postclosure performance assessment. (b)(5)

(b)(5)

(b)(5)

NRC Summary of Evaluation Findings for Localized Corrosion of the WP Outer Barrier

The staff reviewed the DOE models for localized corrosion of the WP outer barrier that were implemented in the TSPA code. (b)(5)

(b)(5)

2.2.1.3.1.3.2.3 SCC of the WP Outer Barrier

Comment (b)(5)
(b)(5)

SCC generally refers to a process whereby cracks form in metals or alloys in a corrosive environment and under sustained tensile stresses. DOE presented data indicating that Alloy 22 is highly resistant to SCC in the environmental conditions (e.g., temperature, pH, and chemical constituents of seepage water brines) that are expected to occur in the repository, as detailed in SAR Section 2.3.6.5.2 and SNL Section 6.2 (2007bb). Because of uncertainty regarding the long-term environmental conditions in the repository, however, the DOE model in the TSPA code assumes that the repository environment supports SCC, such that sufficient residual tensile stress was the only criterion for SCC occurrence (SAR Section 2.3.6.5.1). In SAR Section 2.3.6.5, DOE evaluated SCC caused by residual stresses from WP fabrication. In SAR Section 2.3.4.5, DOE also evaluated SCC caused by the residual stresses resulting from impacts to the WP during seismic ground motions. This section of the SER includes NRC staff's review of the DOE model abstractions for SCC of the WP outer barrier.

Conceptual Models

The DOE models for SCC of the WP outer barrier treat crack initiation (i.e., the formation of cracks on the WP surface) and crack propagation (i.e., growth of cracks from the surface through the outer barrier) as distinct phenomena. In the TSPA code, DOE assumed that cracks initiated on areas of the WP surface where the magnitude of the sustained tensile stress was greater than a threshold value, which DOE referred to as the residual stress threshold (RST) (SAR Section 2.3.6.5.2.1). Cracks initiated by this sustained stress were referred to as incipient cracks. In the DOE model, the residual stresses for crack initiation could result from fabrication processes, such as welding, or from impacts to the WP during seismic ground motion. DOE stated that the concept of a threshold stress that must be exceeded for the onset of SCC is widely accepted in the technical literature (e.g., ASM International, 1987aa). In the TSPA code, DOE also assumed that WP weld flaws (e.g., voids and slag inclusions) were initiated cracks, regardless of the magnitude of the residual stress (SAR Section 2.3.6.5.3.1).

DOE used different conceptual models for the propagation of cracks initiated by fabrication stresses and weld flaws and those initiated by seismically induced stresses, respectively. With regard to cracks initiated by seismically induced stresses, DOE did not explicitly model crack propagation. Rather, DOE assumed that cracks instantaneously propagated through the wall at the time of initiation (SAR Section 2.3.4.5.1.2.1). With regard to cracks initiated by fabrication stresses and weld flaws, DOE assumed that the stress intensity factor (SIF) at the

tip of the initiated crack must be greater than a threshold value for the crack to propagate (SAR Section 2.3.6.5.3.2). DOE stated that the concept of a threshold SIF is consistent with the general understanding of crack fracture mechanics (Jones and Ricker, 1987aa; Sprowels, 1987aa).

To calculate the rate of growth for cracks with a SIF greater than the threshold value, DOE used the slip-dissolution film-rupture (SDFR) model, as discussed in SAR Section 2.3.6.5.3.2 and SNL Section 6.4.2 (2007bb). In the SDFR model, crack growth is related to the rupture and subsequent reformation of the passive metal oxide film at the crack tip. DOE stated that several studies (Ford and Andresen, 1988aa; Andresen, 1991aa; Andresen and Ford, 1994aa) used the SDFR model to accurately calculate crack growth rates in stainless steel and nickel-based alloys similar to Alloy 22 (e.g., Alloys 182 and 600). In SAR Section 2.3.6.5.3.3, DOE described an alternative conceptual model for the crack growth rate: the coupled environmental fracture model. The coupled environmental fracture model is based on conservation of electrons involved in the corrosion process (Macdonald and Urquidi-Macdonald, 1991aa; Macdonald, et al., 1994aa). It incorporates the effects of oxygen concentration, flow rate, and the conductivity of the external environment and accounts for the effect of stress on crack growth. DOE did not use the coupled environmental fracture model in the TSPA calculation because it calculated a slower crack growth rate than the SDFR model.

NRC Staff's Review

The NRC staff reviewed DOE's models for SCC initiation. (b)(5)

(b)(5)

The NRC staff also reviewed DOE's models for SCC propagation. (b)(5)

(b)(5)

Stresses for Crack Initiation and Propagation

The staff reviewed the DOE approaches to establish RST values for crack initiation and the threshold SIF for the propagation of weld flaws and cracks initiated by fabrication stresses.

RST

DOE performed laboratory tests to establish the value of the RST for Alloy 22. DOE performed constant-load crack initiation tests (SAR Section 2.3.6.5.2.1.1), slow strain rate tests (SAR Section 2.3.6.5.2.1.2), and U-bend SCC initiation tests (SAR Section 2.3.6.5.2.1.3). These tests were performed for up to 5 years for Alloy 22 specimens with metallurgical conditions representative of WP metallurgical conditions in the repository (i.e., welded, thermally aged, cold worked). The tests were performed in the temperature range of 25 to 165 °C [77 to 329 °F] in different brines, including BSW, SDW, SCW, and SAW, the compositions of which are shown in SAR Table 2.3.6-1.

For the constant-load crack initiation tests (SAR Section 2.3.6.5.2.1.1), DOE exposed Alloy 22 specimens to BSW (pH of 10.3) at 105 °C [221 °F] for up to 28,000 hours (approximately 3 years). The test specimens were subjected to tensile stress up to 2.1 times the at-temperature yield strength for as-received materials and 2.0 times the yield strength of the welded materials, which corresponds to approximately 95 percent of the ultimate tensile strength of Alloy 22 in the respective material conditions. DOE reported that no sample ruptured during the test, as shown in SAR Figure 2.3.6-28. For the slow strain rate testing (SAR Section 2.3.6.5.2.1.2), Alloy 22 specimens were exposed to SAW, BSW, SCW, and calcium-chloride-type brines over a range of temperatures, with and without applied potential (SAR Table 2.3.6-14). DOE stated that it did not observe SCC in most experimental conditions, though SCC was observed in SCW with large applied anodic potentials. DOE concluded in SNL Section 6.2.1.3 (2007bb), however, that such potentials are not representative of repository conditions. For the U-bend SCC initiation tests (SAR Section 2.3.6.5.2.1.3), Alloy 22 specimens were tested in SDW, SCW, and SAW for 5 years with no evidence of SCC initiation.

Even though SCC of Alloy 22 was not observed in the experimental testing, DOE concluded that cracks may initiate at lower stresses on the repository time scale, yet would not be observed in short-term laboratory tests, as described in SNL Section 6.2.2 (2007bb). Therefore, DOE stated that there existed some uncertainty associated with the value of the RST. Thus, to establish the RST value for the TSPA code, DOE applied a safety factor of two to the maximum stress that Alloy 22 specimens withstood with no evidence of SCC initiation. As outlined in SNL Section 6.2.2 (2007bb), DOE determined that this maximum stress was 210 percent of the Alloy 22 at-temperature yield strength, as measured during constant-load crack initiation testing in BSW. This approach established the upper bound for the RST to be 105 percent of the Alloy 22 at-temperature yield strength. DOE stated that use of a safety factor of two is consistent with general engineering practice and has been used to establish the allowable long-term fatigue stress on engineering components (American Society of Mechanical Engineers, 1969aa). To further account for uncertainty in the RST, DOE established 90 percent of the Alloy 22 at-temperature yield stress as a lower bound. Thus, in the TSPA code, DOE sampled the RST from a uniform distribution between 90 and 105 percent of the Alloy 22 at-temperature yield stress, as shown in SNL Table 6-3 (2007bb).

In response to the NRC staff's RAI for DOE to assess the observed case of SCC initiation in SCW, DOE provided new data in DOE Enclosure 1 (2009c) from U-bend testing of as-welded and mill-annealed Alloy 22 specimens at 165 °C [329 °F] in aerated SCW (Andresen and Kim,

2009aa). After 32,000 hours (approximately 3.5 years), no SCC was observed for stresses estimated to be at or slightly above the at-temperature yield strength of Alloy 22. DOE cited an additional study in which low strain rate crack initiation tests were performed on Alloy 22 specimens in SCW at 86 and 89 °C [186.8 and 192.2 °F] (Fix, et al., 2003aa). DOE reported that crack initiation did not occur until the tensile stress exceeded a value of 605 MPa [87.7 ksi], which is approximately 160 percent of the room temperature yield strength of Alloy 22. On the basis of this information, DOE concluded that the range of the RST, given in SAR Section 2.3.6.5, was acceptable.

DOE evaluated the expected fabrication-induced residual stresses during the postclosure period to determine whether such stresses could exceed the RST. DOE stated that it plans to do a stress-relief heat treatment to mitigate the stresses in the WP outer barrier after fabrication (SAR Section 1.5.2.7.1) following the standards specified in American Society of Mechanical Engineers Boiler and Pressure Vessel Code, Section III, Division 1, Subsection NC-4600 (American Society of Mechanical Engineers, 2001aa). DOE concluded that fabrication-induced residual stresses will not exceed the RST for portions of the WP that are heat treated. In the DOE fabrication process, however, the heat treatment takes place before the waste is placed in the WP and the outer lid is welded onto the shell. Welding the outer lid onto the WP shell may induce residual stresses in the region of the closure weld that the heat treatment process cannot mitigate, as described in SNL Section 6.5.3.1 (2007bb). Therefore, DOE concluded that the region of the WP closure weld is the only part of the WP outer barrier where fabrication induced stresses could cause SCC. DOE plans to implement a process called low plasticity burnishing (a process whereby the material surface is plastically deformed to create a layer with compressive residual stress) to delay the initiation of incipient SCC (SAR Section 1.5.2.7.2.2). The current WP design requires a compressive residual stress to a depth of at least 3 mm [0.12 in] below the weld surface (SAR Table 1.9-9, Design Control Parameter 03-17). DOE concluded that the initiation of SCC would be delayed by the time it would take for general corrosion to corrode through at least the 3-mm [0.12 in] burnished layer.

DOE performed finite element analyses to calculate the residual stress profile of the weld, as detailed in SAR Section 2.3.6.5.2.3 and SNL Section 6.5.3.3 (2007bb), when the closure weld was plasticity burnished resulting in compressive stresses to a depth of 3 mm [0.12 in] below the weld surface. The analysis simulated multipass welds, with the residual stress represented as a function of welding parameters, thermal transients, temperature-dependent material properties, and elastic-plastic stress reversals. The DOE analyses indicated that the residual stress decays rapidly with increasing radial distance from the weld line and is negligible at a distance from the weld line approximately equal to the thickness of the WP wall, as shown in SNL Figures 6-19 through 6-22 (2007bb). Given the rapid decay in weld-induced stress with increasing distance from the weld line, DOE assumed that initiation of SCC by fabrication-induced stress could only occur in patches representing the WP closure weld in the TSPA model. These patches represent approximately 2.67 percent and 2.95 percent of the total surface area for the CSNF and CDSP WPs, respectively, as outlined in SNL Section 6.3.5.1.2 (2008ag).

In the region of the closure weld, DOE calculated that radial stresses do not exceed the RST through the entire thickness of the weld, but that hoop stresses can exceed the RST at a depth of approximately 5 to 7.5 mm [0.20 to 0.30 in] below the weld surface, as described in SNL Section 6.5.5.2.2 (2007bb). In the TSPA code, DOE represents the hoop stress as a function of depth from the weld surface in SNL Equation 64 (2007bb). DOE also considered angular variability in the residual stress around the circumference of the WP closure weld in SNL Equation 6.3.5-6 (2008ag). On the basis of literature reports (e.g., Shack,

et al., 1980aa), DOE calculated that the residual stress may have circumferential variation up to ± 2.5 ksi [± 17.24 MPa] from the mean stress, as detailed in SNL Section 6.5.6.1 (2007bb). SAR Figure 2.3.6-30 showed the angular variability in the residual hoop stress profile in the WP closure weld. More generally, DOE identified literature reports (e.g., Mohr, 1996aa; Pasupathi, 2000aa) which indicated that welding and stress mitigation processes introduce uncertainty into the weld residual stress profile. The reports indicated that the uncertainty range for residual stress may be between 5 percent and 35 percent of the material yield strength. On the basis of the fabrication techniques and process controls planned for the WP closure weld, DOE selected a three standard deviation uncertainty range of ± 15 percent of the at-temperature yield strength of Alloy 22, as outlined in SNL Section 6.5.6.2 (2007bb). This is implemented in the TSPA model by applying a scaling factor to the residual stress. The scaling factor is sampled from a truncated (± 3 standard deviations) normal distribution where the mean is 0 and the standard deviation is 5 percent of the Alloy 22 at-temperature yield strength. SAR Figure 2.3.6-32 showed the uncertainty in the residual hoop stress profile in the WP closure weld.

DOE compared the residual stress profile calculated by the finite element analysis to the residual stress experimentally measured by Woolf (2003aa) for plasticity-burnished Alloy 22 simulated closure welds, as described in SNL Section 6.5.6.5 (2007bb). As shown in SNL Figure 6-60 (2007bb), Woolf (2003aa) measured compressive residual stress to a depth of more than 7 mm [0.28 in] from the weld surface. DOE concluded that the calculated residual stress profile implemented in the TSPA code underestimates the extent of stress mitigation by plasticity burnishing.

NRC Staff's Review

The staff reviewed the DOE approach to establish the value of the RST for the WP outer barrier.

(b)(5)

The staff reviewed DOE's use of the data from the SCC tests to establish the range for the RST.

(b)(5)

(b)(5)

The NRC staff reviewed the DOE analysis of fabrication-induced stresses in the WP outer barrier. (b)(5)

(b)(5)

The staff also reviewed DOE's calculation of the closure weld residual stress profile, as described in SAR Section 2.3.6.5.2.3. (b)(5)

(b)(5)

Threshold SIF

DOE determined the numerical value of the SIF threshold using a crack blunting criterion, as detailed in SAR Section 2.3.6.5.1 and SNL Section 6.4.5 (2007bb). According to the crack blunting criterion, crack growth will arrest if the crack tip radius decreases, because the general corrosion rate at the sides of the crack is greater than the rate at which the crack tip is advancing (Andresen and Ford, 1994aa). DOE calculated the threshold SIF as a function of the Alloy 22 general corrosion rate and the repassivation slope, a parameter related to the rate at which Alloy 22 repassivates following a passive film rupture, as shown in SNL Equation 19 (2007bb). DOE used a point value of 7.23 nm/yr [2.85×10^{-7} in] for the general corrosion rate of Alloy 22, on the basis of the 5-year corrosion data described in SAR Section 2.3.6.3. DOE determined the value of the repassivation slope by measuring the crack growth rate for fatigue precracked Alloy 22 compact tension specimens at 110 °C [230 °F] in BSW and 150 °C [302 °F] in SCW, as outlined in SAR Section 2.3.6.5.2.4 and SNL Section 6.4.4.2 (2007bb). For these conditions, the measured values of the repassivation slope are shown in SAR Table 2.3.6-17.

DOE considered epistemic uncertainty in the repassivation slope and, in turn, the threshold SIF. In the TSPA code, DOE sampled the repassivation slope from a normal distribution. The mean threshold SIF was calculated as $6.62 \text{ MPa}\cdot\text{m}^{0.5}$ [$6.02 \text{ ksi}\cdot\text{in}^{0.5}$], with lower and upper bounds of $1.96 \text{ MPa}\cdot\text{m}^{0.5}$ [$1.78 \text{ ksi}\cdot\text{in}^{0.5}$] and $15.38 \text{ MPa}\cdot\text{m}^{0.5}$ [$14.0 \text{ ksi}\cdot\text{in}^{0.5}$], respectively. DOE stated that this range corresponds to values reported in the technical literature (e.g., Jones, 1992aa) for other corrosion-resistant chromium-nickel-iron alloys.

DOE calculated the SIF profile for the WP closure weld to determine whether the SIF could exceed the threshold value to cause crack propagation during the postclosure period, as described in SAR Section 2.3.6.5.2.3 and SNL Section 6.5 (2007bb). DOE used an approach in which it calculated the SIF for a relatively simple crack geometry and given stress distribution, then modified the solution for the WP closure weld with a geometry correction factor, as detailed in SNL Section 6.5.3.3.3 (2007bb). DOE represented a radially oriented crack in the closure weld with the idealized case of a semicircular crack in an infinite plate, as outlined in SNL Section 6-17 (2007bb). The geometry correction factor was obtained by comparing the simplified solution to finite element analysis solutions for a number of crack sizes. Using this approach, DOE calculated the SIF profile for the plasticity-burnished WP closure weld, as shown in SAR Table 2.3.6-16. Because DOE's calculated SIF was a linear function of the residual stress, uncertainty and variability in the residual stress profile were also represented in the SIF profile used in the TSPA code. SAR Figure 2.3.6-30 showed the angular variability in the SIF profile for the closure weld and SAR Figure 2.3.6-32 showed the uncertainty in the SIF profile in the WP closure weld.

NRC Staff's Review

The NRC staff reviewed the approach to calculate the threshold SIF for the WP closure weld.

(b)(5)

(b)(5)

Crack Size and Density

The staff reviewed the DOE's approaches to calculate the size and density of cracks initiated by fabrication induced stresses and weld flaws, and those initiated by seismically induced stresses, respectively.

Cracks Initiated by Fabrication Induced Stresses and Weld Flaws

DOE's analytic models assumed that the cracks initiated by fabrication induced stresses exceeded the RST and have a uniform size density. DOE assumed that it is energetically favorable for the cracks to have elliptical shape, as shown in SNL Figure 6.3-3 (2007aj), with crack length (i.e., major axis of the ellipse) of 50 mm [1.97 in]. DOE selected this length because it calculated that weld-induced stresses can persist on both sides of the weld centerline up to a distance approximately equal to the nominal thickness of the WP outer barrier (i.e., 25 mm [0.98 in]). The crack opening width was calculated using a fracture mechanics equation derived from an analysis of the energy associated with crack free surfaces. In this manner, DOE calculated a crack opening width of 0.1956 mm [7.70×10^{-3} in]. Given the crack length of 50 mm [1.97 in] and width of 0.1956 mm [7.70×10^{-3} in], DOE calculated that the opening area of an individual incipient crack was 7.682 mm² [1.19×10^{-2} in²], which is assumed to be constant through the WP wall (SNL, 2007aj). DOE stated that a crack of these dimensions would permit diffusive transport, but preclude advective transport by water (FEP 2.1.03.10.0A; SNL, 2008ac). Moreover, DOE assumed that the density of through-wall cracks is constrained by stress-field interactions in the area around the crack, which limit the ability of cracks in relative proximity to propagate through the WP wall, as described in SNL Section 6.6.1 (2007bb). DOE's analysis indicated that the minimum spacing between through-wall cracks is equal to the thickness of the WP outer barrier, which is 25 mm [0.98 in] (Structural Integrity Associates, 2002aa).

DOE used a different approach to model the size and density of weld flaw cracks in the WP outer barrier closure weld. For the outer closure weld, DOE determined that the size and density of flaws would be small because of (i) highly controlled welding procedures that would limit flaw generation and (ii) extensive postweld nondestructive examination (NDE) used to identify weld flaws, as detailed in SNL Section 6.3.1 (2007aa). DOE stated in SAR Section 1.5.2.7 that weld fabrication and inspection will follow the requirements of American Society of Mechanical Engineers Boiler and Pressure Vessel Code Section III, Division 1, Subsection NC (American Society of Mechanical Engineers, 2001aa). The ASME Code specifies that flaws larger than 1.6 mm [6.30×10^{-2} in] be detected and repaired, a requirement that is incorporated as a WP Design Control Parameter [SAR Table 1.9-9, Design Control Parameter 03-17(b)]. To determine the size and density of flaws that may be expected in the WP closure welds, DOE fabricated simulated welds (Smith, 2003aa; SAR Section 2.3.6.5.2.2). DOE stated that postweld NDE detected all flaws in the simulated welds that were larger than ASME Code allowed.

DOE performed a statistical analysis using data from the simulated welds to derive probability distributions for the size and density of flaws to be sampled in the TSPA analysis, as outlined in SNL Section 6.3.1 (2007aa). DOE used a Bayesian approach, consistent with weld flaw analyses in the technical literature (e.g., American Nuclear Society/Institute of Electrical and Electronics Engineers, 1983aa). Following this approach, DOE determined that a Poisson distribution best represents the undetected weld flaw density. DOE calculated that after performing postweld NDE, the mean size of flaws that would go undetected is 1.0 mm [3.94×10^{-2} in], with 5th and 95th percentile values of 0.07 and 2.6 mm

[2.76×10^{-3} and 1.02×10^{-1} in], respectively, as described in SNL Appendix A (2007aa). DOE calculated that after the NDE, there would be a mean of approximately one weld flaw per 140 m^3 [$4.94 \times 10^3 \text{ ft}^3$] of weld volume, with 5th and 95th percentile values of approximately one weld flaw per 56 m^3 [$1.98 \times 10^3 \text{ ft}^3$] and one weld flaw per 264 m^3 [$9.32 \times 10^3 \text{ ft}^3$], respectively, as detailed in SNL Appendix A (2007aa). Given the expected closure weld volume, DOE calculated that there is about 84 percent probability that a WP will have no weld flaws, 14 percent probability that a WP has one flaw, and 2 percent probability that a WP has two or more flaws (SAR Table 2.3.6-18).

In the TSPA code, DOE calculated that only radially oriented flaws (i.e., those that make an angle of greater than 45° with respect to the weld line) are able to propagate because the primary stress component in the closure weld is the hoop stress (SAR Section 2.3.6.5.3.1). DOE determined that there is little driving force for the propagation of cracks that make an angle of less than 45° with respect to the primary stress direction, as outlined in SNL Section 6.3.4.3 (2007bb). DOE analyzed the flaws in the simulated welds to calculate a probability distribution for the orientation of flaws in the closure weld, as described in SNL Section 6.3.1.5 (2007aa). Using the Bayesian approach, DOE calculated that 0.8 percent of weld flaws will be radially oriented such that they can propagate under a hoop stress. DOE concluded that this calculation was supported by the independent analyses of Shcherbinskii and Myakishev (1970aa) who reported that most (~99 percent) weld flaws are oriented within about $\pm 13^\circ$ from the weld line.

In the TSPA code, DOE also assumed that only those weld flaws exposed to the environment by general corrosion during the postclosure period would be susceptible to propagation, as outlined in SNL Section 6.3.4.3 (2007bb). In the TSPA code, DOE calculated that 25 percent of weld flaws will be exposed and able to propagate based upon the approximate percentage of the WP weld that would be removed by general corrosion during the postclosure period (SAR Section 2.3.6.3). On the basis of the small number of embedded weld flaws capable of propagation, DOE concluded that breach of the WP outer barrier by weld flaw cracks is far less likely than breach by incipient cracks initiated where the residual stress is greater than the RST, as outlined in SNL Section 6.3.5.1.3[a] (2008ag).

NRC Staff's Review

The NRC staff reviewed the DOE approaches to calculate the size and density of cracks initiated by fabrication induced stresses and weld flaws in the WP outer barrier. (b)(5)

(b)(5)

(b)(5)

DOE

assumed a constant crack opening area through the WP wall and did not take credit for stress mitigation and crack narrowing in its model. (b)(5)

(b)(5)

The NRC staff also reviewed DOE's analysis of the size and density of flaws in the WP closure weld. (b)(5)

(b)(5)

(b)(5)

Cracks Initiated by Seismically Induced Stresses

For stress corrosion cracks caused by impacts to the WP during seismic ground motion, DOE sampled a parameter in the TSPA code called the crack area density, which is the product of the crack size and the crack density, as identified in SAR Section 2.3.4.5.1.4.1 and SNL Section 6.7.2 (2007bb). The crack area density is a unitless scalar measure that, when multiplied by the size of the damaged area on the WP surface, gives the total open area of the through-wall cracks. For seismically induced SCC, DOE assumed that through-wall cracks have the same shape characteristics as cracks in the closure welds, as in SNL Figure 6.3-3 (2007aj). In contrast to the weld cracks, however, DOE considered uncertainty in the size and density for the cracks induced by seismic ground motion. DOE evaluated the uncertainty by calculating the crack area density using two conceptual models in which the crack size and crack density values were varied, as described in SNL Section 6.7.3 (2007bb). Both conceptual models use a regular hexagonal array of cracks on the WP surface because this gives high effective crack density, as described in SNL Section 6.7.2 (2007bb). In the first conceptual model in SNL Section 6.7.3.1 (2007bb), cracks abutted tip-to-tip and the distance between parallel rows of cracks was the WP wall thickness. In the second conceptual model in SNL Section 6.7.3.2 (2007bb), cracks could overlap (crack length was two times that in the first conceptual model) and the distance between crack centers was the wall thickness (crack number density was lower than that assumed in the first conceptual model). These resulted in SNL Equations 37 and 40 (2007bb) that DOE used to calculate the lower and upper bounds, respectively, for the crack area density sampled in the TSPA code.

Using this approach, DOE calculated a lower bound for crack area density of approximately 3.27×10^{-3} (i.e., SCC breached area is 0.327 percent of the WP damaged area) and an upper bound of approximately 1.31×10^{-2} (i.e., SCC breached area is 1.31 percent of the WP damaged area) (SAR Section 2.3.4.5.1.4.1). DOE considered an alternative conceptual model in which a single crack circumscribed the damaged area, as described in SNL Section 6.7.4 (2007bb). For this conceptual model, DOE calculated a crack area density of 7.22×10^{-3} , which is within the bounds given by the hexagonal crack network models. DOE determined that the alternative conceptual model provided support for the crack area density range calculated by the primary conceptual models. Therefore, in the TSPA code, DOE samples the crack area density from a uniform distribution between the bounding values given by the hexagonal crack network models.

NRC Staff's Review

The NRC staff reviewed the DOE approach to establish the value of the crack area density for seismically induced stress corrosion cracks. (b)(5)

(b)(5)

Abstraction and Integration

For the Nominal and Seismic Ground Motion Modeling Cases in the TSPA code, the model abstraction for SCC of the WP closure weld was implemented in the WP and DS Degradation Submodel, as detailed in SNL Section 6.3.5.1 (2008ag). In the submodel, the WP closure weld area is represented by an annulus that is 1 patch wide and has the same radius as the WP, as shown in SNL Figure 6.3.5-4 (2008ag). This results in about 40 patches to model the WP closure weld. The WP general corrosion abstraction and SCC abstraction, respectively, are implemented independently on each of the patches. As each patch thinned by general corrosion, the submodel calculated the residual stress on the patch on the basis of the through-wall residual stress profile. At each realization time step, the submodel compared the residual stress on the patch to the sampled RST. If the residual stress on the patch was greater than the RST, the submodel assumed that SCC initiated. The submodel also distributed weld flaws among the patches on the basis of the probability distributions for the weld flaw size and density. To determine whether initiated cracks in the WP closure weld could propagate, the submodel calculated the SIF at the crack tip on the basis of the through-wall SIF profile, and compared it to the sampled threshold SIF. If the SIF was greater than the threshold SIF, the submodel assumed that the crack would propagate. The crack growth rate was calculated using the SDFR model. A breached patch was assumed to have cracks with a size of $7.682 \text{ mm}^2 [1.19 \times 10^{-2} \text{ in}^2]$ and spacing of 25 mm [0.98 in] (i.e., 6 cracks per patch). The output of the model was the time of WP breach and the breach area. This output was provided to the Waste Form Degradation and Mobilization Model Component and the EBS Flow and EBS Transport Submodels.

For the Nominal Modeling Case, DOE calculated that WPs were not breached by SCC in the closure weld (i.e., less than 1 in 10^{-4} probability) for approximately 150,000 years after repository closure, and within 1 million years, a mean of approximately 50 percent of WPs were breached [SAR Figure 2.1-10(a)]. Of those breached WPs, DOE calculated that the mean fraction of breached area to total WP surface area was less than 10^{-5} over 1 million years [SAR Figures 2.1-13(b) and 2.1-15(b)]. DOE calculated similar results for SCC of the closure weld in the Seismic Ground Motion Modeling Case, as shown in DOE Figures 1-4 (2009bj).

The model abstraction for SCC caused by impacts during seismic ground motion was implemented in the TSPA code in the Seismic Ground Motion Modeling Case, as outlined in SNL Section 6.6 (2008ag). In the Seismic Ground Motion Modeling Case, the RST was sampled from a uniform distribution between 90 and 105 percent of the Alloy 22 at-temperature

yield stress. Using the sampled RST, DOE calculated the size of the WP damaged area. The crack area density for the given damaged area was sampled from a uniform distribution between 3.27×10^{-3} and 1.31×10^{-2} . The product of the size of the damaged area and the crack area density gave the total open area of the SCC network. The output of the model was the time of WP breach and the breach area. This output was provided to the Waste Form Degradation and Mobilization Model Component and the EBS Flow and EBS Transport Submodels.

For SCC induced by impacts during seismic ground motion, DOE calculated that a mean of approximately 10 percent of CSNF WPs were breached within about 250,000 years of repository closure and for CDSP WPs, a mean of approximately 40 percent were breached within about 150,000 years of repository closure (DOE, 2009c). For both WP types, the fraction of the WP surface consisting of open cracks was less than 10^{-3} , as shown in DOE Figures 7 and 8 (2009c). DOE stated that the response of the respective WP types is different because CSNF WPs are generally not damaged by seismic ground motion until breached by another mechanism (e.g., SCC of the closure weld) that leads to degradation of the WP internals. Conversely, CDSP WPs are structurally weaker and can be damaged by seismic ground motion regardless of previous damage. For both WP types, the probability of seismically induced SCC plateaus within 250,000 years after repository closure because drip shields collapse and impinge the WPs.

NRC Staff's Review

The NRC staff reviewed the implementation and integration of the model abstraction for SCC of the WP outer barrier in the postclosure performance assessment. (b)(5)

(b)(5)

NRC Summary of Evaluation Findings for SCC of the WP Outer Barrier

The staff reviewed the DOE model abstraction for SCC of the WP outer barrier that was implemented in the TSPA code (b)(5)

(b)(5)

2.2.1.3.1.3.2.4 WP Early Failure

In SAR Section 2.2.2.3, DOE defined early failure to be a through-wall penetration of the WP caused by manufacturing- and handling-induced defects, at a time earlier than would be expected for a nondefective WP. DOE assumed that a WP undergoes early failure if it is emplaced in the repository with an undetected manufacturing- or handling-induced defect. On the basis of the processes associated with WP manufacturing and handling, DOE calculated

that the probability of WP early failure is best represented in the TSPA code by a lognormal distribution with a mean of 1.13×10^{-4} per WP and an error factor of 8.17, as shown in SNL Table 7-1 (2007aa). The staff reviewed the adequacy of this probability distribution in SER Section 2.2.1.2.2.3. This section addresses the staff's review of the implementation of this probability distribution in the TSPA code.

WP Early Failure Conceptual Model

The DOE's conceptual model for early WP failure is that the WP with an undetected manufacturing- or handling-induced defect completely fails (i.e., is removed as a barrier to the flow of water) at the time of repository closure (SAR Section 2.3.6.6.1). DOE selected this representation because there are uncertainties associated with the timing and extent of breach for defective WPs and a completely degraded WP will not underestimate the timing and magnitude of radionuclide releases, as described in SNL Section 6.5.2 (2007aa). DOE concluded that this is a conservative representation of the early failure because the most likely consequence of improper WP manufacturing or handling would be introduction of SCC, which tends to cause tight cracks that would limit the extent of radionuclide transport (SAR Section 2.3.6.6.4.1).

NRC Staff's Review

The NRC staff reviewed DOE's conceptual model for WP early failure. (b)(5)

(b)(5)

Abstraction and Integration

The DOE model abstraction for early failure of the WP was implemented in TSPA code in the WP Early Failure (EF) Modeling Case, as detailed in SAR Section 2.4.2.1.5.2 and SNL Section 6.4.2 (2008ag). This modeling case uses most of same modeling components and submodels as were implemented in the Nominal Modeling Case. In the Nominal Modeling Case, however, the WP and DS Degradation Submodel provides the WP and drip shield breached areas as a function of time to the EBS Flow and Transport Submodels and the Waste Form Degradation and Mobilization Model Components. In the WP EF Modeling Case, the WP and DS Degradation Submodel was replaced with the WP early failure mode, which simulated early failure by treating all patches on the failed WP as breached at the time of repository closure.

DOE considered that the dose consequence of a WP early failure would depend primarily upon the type of WP, the environmental conditions at the WP (e.g., temperature and relative humidity), and whether the WP was in seepage conditions. Therefore, the WP EF Modeling Case calculated the dose consequence of a single early failure of a CSNF and CDSP WP in each of the five percolation subregions with and without seepage conditions. The TSPA code then calculated the expected dose using the early failure probability [sampled from the distribution given in SNL Table 7-1 (2007aa)], the distribution for the WP type, and the seepage fraction for each percolation bin.

DOE calculated that there is approximately 55.8 percent probability of no WP early failures, approximately 22.4 percent probability of one early failure, approximately 9.6 percent probability of two early failures, and approximately 12.3 percent probability of three or more early failures in the repository, as outlined in SNL Table 6.4-1 (2008ag). WP early failure makes a small contribution to DOE's calculated mean annual dose within approximately 20,000 years following closure (less than 10^{-1} mrem [10^{-5} Sv]), with a declining contribution thereafter (SAR Figure 2.4-18).

NRC Staff's Review

The NRC staff reviewed the implementation of the WP early failure model in the TSPA code.

(b)(5)

NRC Summary of Evaluation Findings for WP Early Failure

The staff reviewed the DOE model abstraction for early failure of the WP outer barrier that was implemented in the TSPA code. (b)(5)

(b)(5)

2.2.1.3.1.4 Evaluation Findings

The NRC staff reviewed the applicant's SAR and other information submitted in support of the

LA and (b)(5)

(b)(5)

(b)(5)

(b)(5)

2.2.1.3.1.5 References

Ahn, T., H. Jung, X. He, and O. Pensado. 2008aa. "Understanding Long-Term Corrosion of Alloy 22 Container in the Potential Yucca Mountain Repository for High-Level Nuclear Waste Disposal." *Journal of Nuclear Materials*. Vol. 379. pp. 33–41.

American Nuclear Society/Institute of Electrical and Electronics Engineers. 1983aa. NUREG/CR-2300, "PRA Procedures Guide: A Guide to the Performance of Probabilistic Risk Assessments for Nuclear Power Plants." Vols. 1 and 2. Washington, DC: NRC.

American Society of Mechanical Engineers. 2001aa. *ASME Boiler and Pressure Vessel Code*. New York City, New York: American Society of Mechanical Engineers.

American Society of Mechanical Engineers. 1969aa. *Criteria of the ASME Boiler and Pressure Vessel Code for Design by Analysis in Sections III and VIII, Division 2*. New York City, New York: American Society of Mechanical Engineers.

Amy, P.S., C. Pantle, T.A. Else, and C. Neuwohner. 2002aa. "Humidity and Temperature Boundaries for Biofilm Formation in Yucca Mountain." TR-02-002. Rev. 0. LSN DN200000748. Las Vegas, Nevada: University of Nevada.

Anderson, T.L. 2005aa. *Fracture Mechanics*. 3rd Edition. Boca Raton, Florida: Taylor and Francis.

Andresen, P.L. 1991aa. "Fracture Mechanics Data and Modeling of Environmental Cracking of Nickel-Base Alloys in High Temperature Water." Proceedings of the CORROSION 91 Conference. Paper No. 44. Houston, Texas: NACE International.

Andresen, P.L. and F.L. Ford. 1994aa. "Fundamental Modeling of Environment Cracking for Improved Design and Lifetime Evaluation in BWRs." *International Journal of Pressure Vessels and Piping*. Vol. 59, Nos. 1-3. pp. 61-70.

Andresen, P.L. and Y.J. Kim. 2009aa. "Final Report for October 1, 2007-September 30, 2008: Stress Corrosion Crack Initiation and Growth Measurements in Environments Relevant to High-Level Nuclear Waste Packages." GE-GRC-Sandia-2008-1. DTN: MO0902SCCIGMFR.000. Niskayuna, New York: General Electric Global Research Center.

Andresen, P.L. and Y.J. Kim. 2007aa. "Stress Corrosion Crack Initiation and Growth Measurements in Environments Relevant to High-Level Nuclear Waste packages: Final Report for October 1, 2006-September 30, 2007." GE-GRC-Sandia-2007-3. Niskayuna, New York: General Electric Global Research Center.

Andresen, P.L. and Y.J. Kim. 2006aa. "Stress Corrosion Crack Initiation and Growth Measurements in Environments Relevant to High-Level Nuclear Waste packages." GE-GRC-Bechtel-2006-2. MOL.20061109.0070/MOL.20061108.0004. Niskayuna, New York: General Electric Global Research Center.

Ashida, Y., L. G. McMillion, and M. Misra. 2008aa. "Communication C: A Heated Electrode Test System for Studying Corrosion Behavior of Alloy 22." *Nuclear Waste Research: Siting, Technology and Treatment*. A.P. Lattefer, ed. Hauppauge, New York: Nova Science Publishers, Inc. pp. 25-36.

Ashida, Y., L.G. McMillion, and M.L. Taylor. 2007aa. "The Effect of Temperature Oscillation on the Passive Corrosion Properties of Alloy 22." *Electrochemistry Communications*. Vol. 9, Issue 5. pp. 1,102-1,106.

ASM International. 1993aa. "Welding, Brazing, and Soldering." Vol. 6. *Metals Handbook*. Metals Park, Ohio: ASM International.

ASM International. 1987aa. "Corrosion". Vol. 13. *Metals Handbook*. 9th Edition. Metals Park, Ohio: ASM International.

ASTM International. 2007aa. "Standard Practice for Maintaining Constant Relative Humidity by Means of Aqueous Solutions." ASTM E104-02. West Conshohocken, Pennsylvania: ASTM International.

ASTM International. 2003aa. "Standard Test Method for Conducting Cyclic Potentiodynamic Polarization Measurements for Localized Corrosion Susceptibility of Iron-, Nickel-, or Cobalt-Based Alloys." ASTM G 61-86. West Conshohocken, Pennsylvania: ASTM International.

ASTM International. 2003ab. "Standard Practice for Preparing, Cleaning, and Evaluating Corrosion Test Specimens." ASTM G 1-03. West Conshohocken, Pennsylvania: ASTM International.

ASTM International. 2000aa. "Standard Practice for Preparation and Use of Direct Tension Stress-Corrosion Test Specimens." ASTM G 49-85. West Conshohocken, Pennsylvania: ASTM International.

ASTM International. 2000ab. "Standard Practice for Slow Strain Rate Testing to Evaluate the Susceptibility of Metallic Materials to Environmentally Assisted Cracking." ASTM G 129-00. West Conshohocken, Pennsylvania: ASTM International.

ASTM International. 1999aa. "Standard Practice for Preparing, Cleaning, and Evaluating Corrosion Test Specimens." ASTM G 1-90. West Conshohocken, Pennsylvania: ASTM International.

ASTM International. 1998aa. "Standard Test Method for Conducting Potentiodynamic Polarization Resistance Measurements." ASTM G 59-97. West Conshohocken, Pennsylvania: ASTM International.

ASTM International. 1994aa. "Standard Practice for Making and Using U-Bend Stress-Corrosion Test Specimens." ASTM G 30-94. Philadelphia, Pennsylvania: ASTM International.

ASTM International. 1991aa. "Standard Test Method for Plane-Strain Fracture Toughness of Metallic Materials." ASTM E 399-90. West Conshohocken, Pennsylvania: ASTM International.

Aylor, D.M., R.A. Haysz, R.M. Kain, and R.J. Ferrara. 1999aa. "Crevice Corrosion Performance of Candidate Naval Ship Seawater Valve Materials in Quiescent and Flowing Natural Seawater." Proceedings of the CORROSION/99 Conference. Paper No. 329. Houston, Texas: NACE International.

Brossia, C.S. and G.A. Cragnolino. 2004aa. "Effect of Palladium on the Corrosion Behavior of Titanium." *Corrosion Science*. Vol. 46. pp. 1,693–1,711.

Brossia, C.S. and G.A. Cragnolino. 2001ab. "Effect of Palladium on the Localized and Passive Dissolution of Titanium." Proceedings of the Corrosion/2001 Conference. Paper No. 01127. Houston, Texas: NACE International.

Brossia, C.S. and G.A. Cragnolino. 2000aa. "Effects of Environmental, Electrochemical, and Metallurgical Variables on the Passive and Localized Dissolution of Ti Grate 7." CORROSION/2000. Paper No. 00211. Houston, Texas: NACE International.

Brossia, C.S., L. Browning, D.S. Dunn, O.C. Moghissi, O. Pensado, and L. Yang. 2001aa. "Effect of Environment on the Corrosion of Waste package and Drip Shield Materials." CNWRA 2001-003. San Antonio, Texas: CNWRA.

Brown, A.D. 1976aa. "Microbial Water Stress." *Bacteriological Reviews*. Vol. 40. pp. 803–846.

BSC. 2007as. "Local Meteorology of Yucca Mountain, Nevada, 1994–2006." TDR-MGR-MM-000002. Rev. 00. ACN 01. Las Vegas, Nevada: Bechtel SAIC Company, LLC.

BSC. 2007bu. "Yucca Mountain Project Engineering Specification Prototype Drip Shield." 000-3SS-SSE0-00100-000. Rev. 000. Las Vegas, Nevada: Bechtel SAIC Company, LLC.

BSC. 2004as. "General Corrosion and Localized Corrosion of the Drip Shield." ANL-EBS-MD-000004. Rev. 02. AD 01, ACN 01, ACN 02, ERD 01. Las Vegas, Nevada: Bechtel SAIC Company, LLC.

Chiang, K.-T., D.S. Dunn, and G.A. Cragnolino. 2006aa. "Combined Effect of Bicarbonate and Chloride Ions on Stress Corrosion Cracking Susceptibility of Alloy 22." Proceedings of the CORROSION/2006 Conference. Paper No. 06506. Houston, Texas: NACE International.

Chiang, K.-T., D.S. Dunn, and G.A. Cragnolino. 2005aa. "Effect of Groundwater Chemistry on Stress Corrosion Cracking." Proceedings of the CORROSION/2005 Conference. Paper No. 05463. Houston, Texas: NACE International.

Codell, R.B. and B.W. Leslie. 2006aa. "Drip Shield Corrosion from Fluoride in Dents." Proceedings of 11th International High-Level Radioactive Waste Management Conference, Las Vegas, American Nuclear Society.

Costa, D. and P. Marcus. 1993aa. "Modification of Passive Films Formed on Ni-Cr-Fe Alloys With Chromium Content in the Alloy and Effects of Adsorbed or Segregated Sulphur." Proceedings of the European Symposium on Modifications of Passive Film, Paris, France, February 15-17, 1993. P. Marcus, B. Barous, and M. Keddam, eds. London, England: Institute of Materials, Minerals, and Mining. pp. 17-25.

Cragnolino, G.A., D.S. Dunn, C.S. Brossia, V. Jain, and K.S. Chan. 1999aa. "Assessment of Performance Issues Related to Alternate Engineering Barrier System Materials and Design Options." CNWRA 99-003. San Antonio, Texas: Center for Nuclear Waste Regulatory Analyses.

Dixit, S., S. Roberts, K. Evans, T. Wolery, and S. Carroll. 2006aa. "General Corrosion and Passive Film Stability-FY05 Summary Report." UCRL-TR-217393. Livermore, California: Lawrence Livermore National Laboratory.

DOE. 2010ae. "Yucca Mountain—Supplemental Response to Request for Additional Information Regarding License Application (Safety Analysis Report Section 2.3.6.8), Safety Evaluation Report Vol. 3, Chapter 2.2.1.3.1, Set 2." Letter (February 22) J.R. Williams to J.H. Sulima (NRC). ML100540266. Washington, DC: DOE, Office of Technical Management.

DOE. 2009ab. "Yucca Mountain—Response to Request for Additional Information Regarding License Application (Safety Analysis Report Section 2.2, Table 2.2-5), Safety Evaluation Report Vol. 3, Chapter 2.2.1.2.1, Set 2." Letter (February 23) J.R. Williams to J.H. Sulima (NRC). ML090550101. Washington, DC: DOE, Office of Technical Management.

DOE. 2009bj. "Yucca Mountain—Response to Request for Additional Information Regarding License Application (Safety Analysis Report Section 2.4.4) Safety Evaluation Report Vol. 3, Chapters 2.2.1.4.1, 2.2.1.4.2, and 2.2.1.4.3, Set 1." Letter (July 29) J.R. Williams to J.H. Sulima (NRC). ML092110472. Washington, DC: DOE, Office of Technical Management.

DOE. 2009cj. "Yucca Mountain—Response to Request for Additional Information Regarding License Application (Safety Analysis Report Section 2.3.6.8), Safety Evaluation Report Vol. 3, Chapter 2.2.1.3.1, Set 3." Letter (May 7) J.R. Williams to J.H. Sulima (NRC). ML091280184. ML091280185. Washington, DC: DOE, Office of Technical Management.

DOE. 2009cl. "Yucca Mountain—Response to Request for Additional Information Regarding License Application (Safety Analysis Report Section 2.3.6.8), Safety Evaluation Report Vol. 3, Chapter 2.2.1.3.1, Set 2." Letter (April 13) J.R. Williams to J.H. Sulima (NRC). ML091100634. Washington, DC: DOE, Office of Technical Management.

DOE. 2009cm. "Yucca Mountain—Response to Request for Additional Information Regarding License Application (Safety Analysis Report Section 2.3.6.8), Safety Evaluation Report Vol. 3, Chapter 2.2.1.3.1, Set 4." Letter (September 10) J.R. Williams to J.H. Sulima (NRC). ML092540339. Washington, DC: DOE, Office of Technical Management.

DOE. 2009cn. "Yucca Mountain—Response to Request for Additional Information Regarding License Application (Safety Analysis Report Section 2.3.6.8), Safety Evaluation Report Vol. 3, Chapter 2.2.1.3.1, Set 1." Letter (March 25) J.R. Williams to J.H. Sulima (NRC). ML090840553. Washington, DC: DOE, Office of Technical Management.

Dunn, D.S., Y.-M. Pan, X. He, L.T. Yang, and R.T. Pabalan. 2006ab. "Evolution of Chemistry and Its Effects on the Corrosion of Engineered Barrier Materials." The 30th Symposium on the Scientific Basis for Nuclear Waste Management Materials Research Society 2006 Fall Meeting, Boston, Massachusetts, November 27–December 1, 2006. Pittsburgh, Pennsylvania: Materials Research Society.

Dunn, D.S., O. Pensado, Y.-M. Pan, R.T. Pabalan, L. Yang, X. He, and K.T. Chiang. 2005aa. "Passive and Localized Corrosion of Alloy 22—Modeling and Experiments." Rev. 01. CNWRA 2005-002. San Antonio, Texas: Center for Nuclear Waste Regulatory Analyses.

Dunn, D.S., G.A. Cragnolino, and N. Sridhar. 2000aa. "An Electrochemical Approach to Predicting Long-Term Localized Corrosion of Corrosion-Resistant High-Level Waste Container Materials." *Corrosion*. Vol. 56. pp. 90–104.

Elibiache, A. and P. Marcus. 1992aa. "The Role of Molybdenum in the Dissolution and the Passivation of Stainless Steels With Adsorbed Sulphur." *Corrosion Science*. Vol. 33, No. 2. pp. 261–269.

Else, T.A., C.R. Pantle, and P.S. Amy. 2003aa. "Boundaries for Biofilm Formation: Humidity and Temperature." *Applied and Environmental Microbiology*. Vol. 69, No. 8. pp. 5,006–5,010.

Evans, K.J., A. Yilmaz, S.D. Day, L.L. Wong, J.C. Estill, and R. Rebak. 2005aa. "Using Electrochemical Methods to Determine Alloy 22's Crevice Corrosion Repassivation Potential." *Journal of Metals*. Vol. 57, No. 1. pp. 56–61.

Evans, K.J., M.L. Stuart, R.A. Etien, G.A. Hust, J.C. Estill, and R.B. Rebek. 2005ab. "Long-Term Corrosion Potential and Corrosion Rate of Creviced Alloy 22 in Chloride Plus Nitrate Brines." UCRL–CONF–216910. Livermore, California: Lawrence Livermore National Laboratory.

Fix, D.V.; J.C. Estill; G. A. Hust, K.J. King, S.D. Day, and R.B. Rebak. 2003aa. "Influence of Environmental Variables on the Susceptibility of Alloy 22 to Environmentally Assisted Cracking." Proceedings of the CORROSION 2003/Conference. Paper No. 03542. Houston, Texas: NACE International.

Fontana, M.G. and N.D. Greene. 1978aa. *Corrosion Engineering*. 2nd Edition. New York City, New York: McGraw Hill.

Ford, F.P. and P.L. Andresen. 1988aa. "Development and Use of a Predictive Model of Crack Propagation in 304/316L, A533B/A508, and Inconel 600/182 Alloys in 288°C Water." Proceedings of the Third International Symposium on Environmental Degradation of Materials in Nuclear Power Systems—Water Reactors, Traverse City, Michigan, August 30–September 3, 1988. G.J. Theus and J.R. Weeks, eds. Warrendale, Pennsylvania: The Metallurgical Society. pp. 789–800.

Gray, J.J., J.R. Hayes, G.E. Gdowski, B.E. Viani, and C.A. Orme. 2006aa. "Inhibiting Effects of Nitrates on the Passive Film Breakdown of Alloy 22 in Chloride Environments." *Journal of the Electrochemical Society*. Vol. 153, No. 5. pp. B156–B161.

Greenspan, L. 1977aa. "Humidity Fixed Points of Binary Saturated Aqueous Solutions." *Journal of Research of the National Bureau of Standards—A: Physics and Chemistry*. Vol. 81A. pp. 89–96.

Haynes International. 1997aa. "Hastelloy Alloy C-276." Kokomo, Indiana: Haynes International.

Haynes International. 1997ab. "Hastelloy C-22 Alloy." Kokomo, Indiana: Haynes International.

He, X. and D.S. Dunn. 2005aa. "Crevice Corrosion Penetration Rates of Alloy 22 in Chloride-Containing Waters—Progress Report." CNWRA 2006-001. San Antonio, Texas: Center for Nuclear Waste Regulatory Analyses.

He, X., B. Brettmann, and H. Jung. 2009aa. "Effects of Test Methods on Crevice Corrosion Repassivation Potential Measurements of Alloy 22." *Corrosion*. Vol. 65. pp. 449–460.

He, X., J.J. Noel, and D.W. Shoesmith. 2007aa. "Temperature Effects on Oxide Film Properties of Grade-7 Titanium." *Corrosion*. Vol. 63. pp. 781–792.

He, X., D.S. Dunn, and A.A. Csontos. 2007ab. "Corrosion of Similar and Dissimilar Metal Crevices in the Engineered Barrier System of a Potential Nuclear Waste Repository." *Electrochimica Acta*. Vol. 52. pp. 7,556–7,569.

Horn, J., S. Martin, C. Carnillo, and T. Lian. 2005aa. "Microbial Effects on Nuclear Waste Packaging Materials." UCRL-TR-213915. Rev 1. Livermore, California: Lawrence Livermore National Laboratory.

Hua, F. and G. Gordon. 2004aa. "Corrosion Behavior of Alloy 22 and Ti Grade 7 in a Nuclear Waste Repository Environment." *Corrosion*. Vol. 60, No. 8. pp. 764–777.

- Hunkeler, F. and H. Boehni. 1983aa. "Pit Growth Measurements on Stainless Steels." *Passivity of Metals and Semiconductors, Proceedings of the Fifth International Symposium on Passivity, Bombannes, France, May 30–June 3, 1983*. M. Froment, ed. New York City, New York: Elsevier. pp. 655–660.
- Hur, D.H. and Y.S. Park. 2006aa. "Effect of Temperature on the Pitting Behavior and Passive Film Characteristics of Alloy 600 in Chloride Solution." *Corrosion*. Vol. 62, No. 9. pp. 745–750.
- Ishikawa, H., A. Honda, and N. Sasaki. 1994aa. "Long Life Prediction of Carbon Steel Overpacks for Geological Isolation of High-Level Radioactive Waste." *Life Prediction of Corrodible Structures*. R.N. Parkins, ed. Houston, Texas: NACE International. Vol. 1. pp. 454–483.
- Jones, D.A. 1996aa. *Principles and Prevention of Corrosion*. 2nd Edition. Upper Saddle River, New Jersey: Prentice Hall.
- Jones, R.H., ed. 1992aa. "Stress-Corrosion Cracking." Materials Park, Ohio: ASM International.
- Jones, R.H. and R.E. Ricker. 1987aa. "Stress-Corrosion Cracking." *Metals Handbook, Vol. 13: Corrosion—9th Edition*. Metals Park, Ohio: ASM International. pp. 145–163.
- Jung, H. 2010aa. "A Review for Long-Term Persistence of Passive Film of Alloy 22 Under Potential YM Repository Environments." Scientific Notebook No. 835. San Antonio, Texas: Center for Nuclear Waste Regulatory Analyses.
- Jung, H., T. Mintz, L. Yang and T. Ahn. 2008aa. "Long-Term Persistence of the Passive Film on Alloy 22 at Elevated Temperatures in the Potential Yucca Mountain Repository Environment." ML090220175 and ML090220186. Washington, DC: NRC.
- Jung, H., T. Mintz, D.S. Dunn, O. Pensado, and T. Ahn. 2007aa. "A Review of the Long-Term Persistence of the Passive Film on Alloy 22 in Potential Yucca Mountain Repository Environments." ML072880595. Washington, DC: NRC.
- Lee, S.G. and A.A. Solomon. 2006aa. "Localized Corrosion of Alloy C22 Nuclear Waste Canister Material Under Limiting Conditions." *Materials Science and Engineering*. Vol. A 434. pp. 114–123.
- Lian, T.; M.T. Whalen, and L.L. Wong. 2005aa. "Effects of Oxide Film on the Corrosion Resistance of Titanium Grade 7 in Fluoride-Containing NaCl Brines." *Proceedings of the Corrosion/2005, 60th Annual Conference and Exposition, 1945–2005, April 3–7, 2005*. Paper No. 05609. Houston, Texas: NACE International.
- Lian, T., S. Martin, D. Jones, A. Rivera, and J. Horn. 1999aa. "Corrosion of Candidate Container Materials by Yucca Mountain Bacteria." *Proceedings of the CORROSION/1999 Conference*. Paper No. 476. Houston, Texas: NACE International.
- Lin C., B. Leslie, R. Codell, H. Arlt, and T. Ahn. 2003aa. "Potential Importance of Fluoride to Performance of the Drip Shield." *Proceedings of the American Nuclear Society 10th International High-Level Radioactive Waste Management Conference, March 30–April 2, 2003*, Las Vegas, Nevada.

Lloyd, A.C., J.J. Noël, S. McIntyre, and S.W. Shoesmith. 2004aa. "Cr, Mo and W Alloying Additions In Ni and Their Effect on Passivity." *Electrochimica Acta*. Vol. 49. pp. 3,015–3,027.

Lloyd, A.C., D.W. Shoesmith, N.S. McIntyre, and J.J. Noel. 2003aa. "Effects of Temperature and Potentials on the Passive Corrosion Properties of Alloys C22 and C276." *Journal of the Electrochemical Society*. Vol. 150. pp. B120–130.

Lorenzo de Mele, M.F. and M.C. Cortizo. 2000aa. "Electrochemical Behavior of Titanium in Fluoride-Containing Saliva." *Journal of Applied Electrochemistry*. Vol. 30. pp. 95–100.

Macdonald, D.D. and M. Urquidi-Macdonald. 1991aa. "A Coupled Environment Model for Stress Corrosion Cracking in Sensitized Type 304 Stainless Steel in LWR Environments." *Corrosion Science*. Vol. B33 32, No. 1. pp. 51–81.

Macdonald, D.D., M. Urquidi-Macdonald, and P.-C. Lu. 1994aa. "The Coupled Environmental Fractal Model—A Deterministic Method for Calculating Crack Growth Rates." Proceedings of the CORROSION/1994 Conference. Paper No. 246. Houston, Texas: NACE International.

Marcus, P. 2001aa. "Long-Term Extrapolation of Passive Behavior: Proceedings From an International Workshop on Long-Term Extrapolation of Passive Behavior." Presented at the Nuclear Waste Technical Review Board Meeting, Arlington, Virginia, July 19–20, 2001. Paris, France: Université Pierre et Marie Curie. pp. 55–60.

Marcus, P. and J.M. Grimal. 1990aa. "The Antagonistic Roles of Chromium and Sulfur in the Passivation of Ni-Cr-Fe Alloys Studied by XPS and Radiochemical Techniques." *Corrosion Science*. Vol. 31. pp. 377–382.

Marcus, P. and M. Moscatelli. 1989aa. "The Role of Alloyed Molybdenum in the Dissolution and the Passivation of Nickel-Molybdenum Alloys in the Presence of Adsorbed Sulfur." *Journal of the Electrochemical Society*. Vol. 136, No. 6. pp. 1,634–1,637.

Marcus, P. and H. Talah. 1989aa. "The Sulfur Induced Breakdown of the Passive Film and Pitting Studied on Nickel and Nickel Alloys." *Corrosion Science*. Vol. 29. pp. 455–463.

Marcus, P., H. Talah, and J. Oudar. 1988aa. "Breakdown of the Passive Film on Nickel and Nickel Alloys Induced by Sulfur." *Key Engineering Materials*. Vols. 20–28, Issue 4 pp. 3,947–3,952.

Marcus, P., A. Testier, and J. Oudar. 1984aa. "The Influence of Sulphur on the Dissolution and the Passivation of a Nickel-Iron Alloy—Electrochemical and Radiotracer Measurements." *Corrosion Science*. Vol. 24, No. 4. pp. 259–268.

Marcus, P., I. Olefjord, and J. Oudar. 1984ab. "The Influence of Sulfur on the Dissolution and the Passivation of a Nickel-Iron Alloy—Sulfur Analysis by ESCA." *Corrosion Science*. Vol. 24, No. 4. pp. 269–278.

Marcus, P., J. Oudar, and I. Olefjord. 1980aa. "Studies of the Influence of Sulfur on the Passivation of Nickel by Auger Electron Spectroscopy and Electron Spectroscopy for Chemical Analysis." *Materials Science and Engineering*. Vol. 42. pp. 191–197.

Marsh, G.P.; K.J. Taylor, and A.H. Harker. 1991aa. "The Kinetics of Pitting Corrosion of Carbon Steel Applied to Evaluating Containers for Nuclear Waste Disposal." SKB TR-91-62. Stockholm, Sweden: Svensk Kärnbränsleförsörjning AB.

Martin, S., J. Horn, and C. Carrillo. 2004aa. "Micron-Scale MIC of Alloy-22 After Long-Term Incubation in Saturated Nuclear Waste Repository Microcosms." Proceedings of the CORROSION/2004 Conference. Paper No. 04596. Houston, Texas: NACE International.

Mattsson, H. and I. Olefjord. 1990aa. "Analysis of Oxide Formed on Ti During Exposure in Bentonite Clay-I. The Oxide Growth." *Werkstoffe und Corrosion*. Vol. 41, No. 7. Weinheim, Germany: VCH Verlagsgesellschaft mbH. pp. 383-390.

McMillion, L.G., A. Sun, D.D. Macdonald, and D.A. Jones. 2005aa. "General Corrosion of Alloy 22: Experimental Determination of Model Parameters From Electrochemical Impedance Spectroscopy Data." *Metallurgical and Materials Transactions A*. Vol. 36A. pp. 1,129-1,141.

Mintz, T.M. and T.M. Devine. 2004aa. "Influence of Surface Films on the Susceptibility of Inconel 600 to Stress Corrosion Cracking." *Key Engineering Materials*. Vols. 261-263. pp. 875-884.

Mintz, T. and X. He. 2009aa. "Modeling of Hydrogen Uphill Diffusion in Dissimilar Titanium Welds." Proceedings of the CORROSION/2009 Conference. Paper No. 09430. Houston, Texas: NACE International.

Miserque F., B. Huet, G. Azou, D. Bendjaballah, and V. L'Hostis. 2006aa. "X-Ray Photoelectron Spectroscopy and Electrochemical Studies of Mild Steel FeE500 Passivation in Concrete Simulated Water." *Journal de Physique IV Proceedings*. Vol. 136. pp. 89-97.

Mohr, W.C. 1996aa. "Internal Surface Residual Stresses in Girth Butt-Welded Steel Pipes." *Residual Stresses in Design, Fabrication, Assessment and Repair, PVP*. Vol. 321. New York City, New York: American Society of Mechanical Engineers. pp. 37-44.

Montemor, M.F., M.G.S. Ferreira, M. Walls, B. Rondot, and M. Cunha Belo. 2003aa. "Influence of pH on Properties of Oxide Films Formed on Type 316L Stainless Steel, Alloy 600, and Alloy 690 in High-Temperature Aqueous Environments." *Corrosion*. Vol. 59, No. 1. pp. 11-21.

Mughabghab, S.F. and T.M. Sullivan. 1989aa. "Evaluation of the Pitting Corrosion of Carbon Steels and Other Ferrous Metals in Soil Systems." *Waste Management*. Vol. 9, No. 4. Elmsford, New York: Pergamon Press. pp. 239-251.

Mulford, S.J. and D.Tromans. 1988aa. "Crevice Corrosion of Nickel-Based Alloys in Neutral Chloride and Thiosulfate Solutions." *Corrosion*. Vol. 44, No. 12. pp. 891-900.

NRC. 2009ab. "Division of High-Level Waste Repository Safety Director's Policy and Procedure Letter 14: Application of YMRP for Review Under Revised Part 63." Published March 13, 2009. ML090850014. Washington, DC: NRC.

NRC. 2006ab. NUREG-1864, "A Pilot Probabilistic Risk Assessment of a Dry Cask Storage System at a Nuclear Power Plant." Washington, DC: NRC.

NRC. 2005aa. NUREG-1762, "Integrated Issue Resolution Status Report." Rev. 1. ML051360241. Washington, DC: NRC.

NRC. 2003aa. NUREG-1804, "Yucca Mountain Review Plan—Final Report." Rev. 2. Washington, DC: NRC.

NRC. 1977aa. NUREG-0376, "Residual Stresses at Girth-Butt Welds in Pipes and Pressure Vessels." Rev. 5. Washington, DC: NRC.

Oka, Y.I., S. Mihara, and H. Miyata. 2007aa. "Effective Parameters for Erosion Caused by Water Droplet Impingement and Applications to Surface Treatment Technology." *Wear*. Vol. 263. pp. 386–394.

Orme, C.A. 2005aa. "The Passive Film on Alloy 22." UCRL-TR-215277. Livermore, California: Lawrence Livermore National Laboratory.

Pabalan, R.T. 2010aa. "Quantity and Chemistry of Water Contacting Engineered Barriers Integrated Subissue." Electronic Scientific Notebook 930E. San Antonio, Texas: Center for Nuclear Waste Regulatory Analyses.

Pasupathi, V. 2000aa. "Documentation of Literature on Residual Stress Measurements." Interoffice Correspondence (May 19) to G.M. Gordon. LV.WASTE PACKAGE.VP.05/00-070, With Enclosures. LSN DEN001312636. Las Vegas, Nevada: CRWMS M&O.

Pedersen, K. and F. Karlsson. 1995aa. "Investigation of Subterranean Microorganisms: Their Importance for performance Assessment of Radioactive Waste Disposal." SKB 95-10. Stockholm, Sweden: Swedish Nuclear Fuel and Waste Management Company.

Pensado, O.; D.S. Dunn, G.A. Cragnolino, and V. Jain. 2002aa. "Passive Dissolution of Container Materials—Modeling and Experiments." CNWRA 2003-01. San Antonio, Texas: Center for Nuclear Waste Regulatory Analyses.

Pourbaix, M. 1974aa. *Atlas of Electrochemical Equilibria in Aqueous Solutions*. Houston, Texas: NACE International.

Prevey, P.S. and J. Cammett. 2001aa. "Low Cost Corrosion Damage Mitigation and Improved Fatigue Performance of Low-Plasticity Burnished 7075-T6." *Journal of Materials Engineering and Performance*. Vol. 10. pp. 548–555.

Pulvirenti, A.L.; K.M. Needham, D.S. Wong, M.A. Adel-Hadadi, A. Barkatt, C.R. Marks, and J.A. Gorman. 2003aa. "Fluoride Corrosion of Ti-Grade 7: Effects of Other Ions." CORROSION/2003, 58th Annual Conference and Exposition, San Diego, California, March 16–20, 2003. Paper No. 03686. Houston, Texas: NACE International.

Pulvirenti, A.L.; K.M. Needham, M.A. Adel-Hadadi, A. Barkatt, C.R. Marks, and J.A. Gorman. 2002aa. "Corrosion of Titanium Grade 7 in Solutions Containing Fluoride and Chloride Salts." CORROSION/2002, 57th Annual Conference and Exposition, Denver, Colorado, April 7–11, 2002. Paper No. 02552. Houston, Texas: NACE International.

Rebak, R.B. 2005aa. "Factors Affecting the Crevice Corrosion Susceptibility of Alloy 22." Proceedings of the CORROSION/2005 Conference. Paper No. 05610. Houston, Texas: NACE International.

Rybicki, E.F. and R.B. Stonesifer. 1979aa. "Computation of Residual Stresses Due to Multipass Welds in Piping Systems." *Journal of Pressure Vessel Technology*. Vol. 101. pp. 149–154.

Sala, B., S. Chevalier, A. Gelpi, H. Takenouti, and M. Keddam. 1999aa. "Electrochemical Study of the Corrosion Processes of the Secondary Side of Steam Generators." Proceedings of the 9th International Conference on Environmental Degradation of Materials in Nuclear Power Systems—Water Reactors. S.M. Bruemmer, F.P. Ford, and G.S. Was, eds. Warrendale, Pennsylvania: Materials Research Society. pp. 587–598.

Sala, B., S. Chevalier, M. Organista, A. Gelpi, A. Stutzmann, and M. Dupin. 1998aa. "Study of the Corrosion Process of the Secondary Side of Steam Generators: An Electrochemical Study." JAIF International Conference on Water Chemistry in Nuclear Power Plants, Water Chemistry '98. Kashiwazaki City, Niigata: Japan Atomic Industrial Forum. p. 498–504.

Sala, B., P. Combrade, A. Gelpi, and M. Dupin. 1996aa. "The Use of Tube Examinations and Laboratory Simulations to Improve the Knowledge of Local Environments and Surface Reactions in TSPs." *Control of Corrosion on the Secondary Side of Steam Generators*. R.W. Staehle, J.A. Gorman, and A.R. McIlree, eds. Houston, Texas: NACE International. pp. 483–497.

Sala, B., R. Erre, and A. Gelpi. 1993aa. "Local Chemistry and Formation of Deposits on the Secondary Side of Steam Generators." Proceedings of the 6th International Conference on Environmental Degradation of Materials in Nuclear Power Systems—Water Reactors. R.E. Gold and E.P. Simonen, eds. Warrendale, Pennsylvania: Materials Research Society. pp. 215–226.

Schutz, R.W. 2005aa. "Corrosion of Titanium and Titanium Alloys." *ASM Handbook—Vol. 13B: Corrosion*. Materials. Materials Park, Ohio: ASM International.

Schutz, R.W. and J.S. Grauman. 1986aa. "Corrosion Behavior of Titanium and Other Alloys in Laboratory FGD Scrubber Environments." *Materials Performance*. Vol. 25, No. 4. Houston, Texas: NACE International. pp. 35–42.

Schutz, R.W. and D.E. Thomas. 1987aa. "Corrosion of Titanium and Titanium Alloys." *ASM Handbook—Corrosion: Vol. 13*. Materials Park, Ohio: ASM International. Pp. 669–706.

Scully, J.R., G. Ileybare, and C. Marks. 2001aa. "Passivity and Passive Corrosion of Alloys 625 and 22." SEAS Report No. UVA/527653/MSE01/103. Charlottesville, Virginia: University of Virginia, School of Engineering & Applied Science.

Shack, W.J., W.A. Ellington, and L.E. Pahis. 1980aa. "Measurement of Residual Stresses in Type 304 Stainless Steel Butt Weldments." EPRI NP–1413. Palo Alto, California: Electric Power Research Institute.

Shan, X. and J. H. Payer. 2007aa. "Comparison of Ceramic and Polymer Crevice Formers on the Crevice Corrosion Behavior of Ni-Cr-Mo Alloy C-22." Proceedings of the CORROSION/2007 Conference. Paper No. 07582. Houston, Texas: NACE International.

Sharland, S.M., C.C. Naish, K.J. Taylor, and G.P. Marsh. 1994aa. "An Experimental and Modelling Study of the Localized Corrosion of Carbon Steel Overpacks for the Geological Disposal of Radioactive Waste." *Life Prediction of Corrodible Structures*. R.N. Parkins, ed. Houston, Texas: NACE International. pp. 402–418.

Shcherbinskii, V.G. and V.M. Myakishev. 1970aa. "Statistical Distribution of Welding Defects with Respect to Azimuth." Translated from Defektoskopiya, No. 4. New York City, New York: Plenum Publishing. pp. 143–144.

Shukla, P.K., D.S. Dunn, K.-T. Chiang, and O. Pensado. 2006aa. "Stress Corrosion Cracking Model for Alloy 22 In the Potential Yucca Mountain Repository Environment." Proceedings of the CORROSION/2006 Conference. Paper No. 06502. Houston, Texas: NACE International.

Silence, W.L. and J.D. Smith. 1990aa. "High Performance Alloys for Aggressive Seawater Corrosive Services." Technical File No. 13178. Kokomo, Indiana: Haynes International.

Smailos, E. 1993aa. "Corrosion of High-Level Waste Packaging Materials in Disposal Relevant Brines." *Nuclear Technology*. Vol. 104. pp. 343–350.

Smailos, E. and R. Köster. 1987aa. "Corrosion Studies on Selected Packaging Materials for Disposal of High Level Wastes." *Materials Reliability in the Back End of the Nuclear Fuel Cycle*. Proceedings of a Technical Committee Meeting, Vienna, Austria, September 2–5, 1986. TECHDOC-421. Vienna, Austria: International Atomic Energy Agency. pp. 7–24.

Smith, D. 2003aa. "Weld Flaw Evaluation and Nondestructive Examination Process Comparison Results for High-Level Radioactive Waste Package Manufacturing Program." TDR-EBS-ND-000007. Rev. 01. ACC: ENG.20030515.0003. Las Vegas, Nevada: Bechtel SAIC Company

SNL. 2009aa. "Unexpected Test Results—Heterogeneous Alloy 22 Oxide Thickness." CR 12799. DEN001614731. Las Vegas, Nevada: Sandia National Laboratories

SNL. 2009ab. "Unexpected Test Results—Residue on Subset of Alloy 22 Coupons." CR 12868. DEN001614752. Las Vegas, Nevada: Sandia National Laboratories.

SNL. 2008ac. "Features, Events, and Processes for the Total System Performance Assessment: Methods." ANL-WIS-MD-000026. Rev. 00. Las Vegas, Nevada: Sandia National Laboratories.

SNL. 2008ag. "Total System Performance Assessment Model/Analysis for the License Application." MDL-WIS-PA-000005. Rev. 00. AD 01, ERD 01, ERD 02, ERD 03, ERD 04. Las Vegas, Nevada: Sandia National Laboratories.

SNL. 2007aa. "Analysis of Mechanisms for Early Waste package/Drip Shield Failure." ANL-EBS-MD-000076. Rev. 00. ACN 01, ERD 01, ERD 02. Las Vegas, Nevada: Sandia National Laboratories.

SNL. 2007aj. "EBS Radionuclide Transport Abstraction." ANL-WIS-PA-000001. Rev. 03. ERD 01. Las Vegas, Nevada: Sandia National Laboratories.

SNL. 2007ak. "Engineered Barrier System: Physical and Chemical Environment." ANL-EBS-MD-000033. Rev. 06. ERD 01. Las Vegas, Nevada: Sandia National Laboratories.

SNL. 2007al. "General Corrosion and Localized Corrosion of Waste package Outer Barrier." ANL-EBS-MD-000003. Rev. 03. ACN 01, ERD 01. Las Vegas, Nevada: Sandia National Laboratories.

SNL. 2007bb. "Stress Corrosion Cracking of Waste package Outer Barrier and Drip Shield Materials." ANL-EBS-MD-000005. Rev. 04. ERD 01, ERD 02. Las Vegas, Nevada: Sandia National Laboratories.

SNL. 2004ab. "Evaluation of Potential Impacts of Microbial Activity on Drift Chemistry." ANL-EBS-MD-000038. Rev. 01. ACN 02, ERD 01. Las Vegas, Nevada: Sandia National Laboratories.

Sprohls, D.O. 1987aa. "Evaluation of Stress-Corrosion Cracking." *Metals Handbook—Corrosion: Vol. 13*. 9th Edition. Metals Park, Ohio: ASM International. pp. 245–282.

Structural Integrity Associates. 2002aa. "Structural Integrity Associates Support of Waste package Design for Year 2001." LSN DEN001314737. San Jose, California: Structural Integrity Associates.

Thomas, D.E. and H.B. Bomberger. 1983aa. "The Effects of Chlorides and Fluorides on Titanium Alloys in Simulated Scrubber Environments." *Materials Performance*. Houston, Texas: NACE International. pp 29–36.

U.S. Nuclear Waste Technical Review Board. 2001aa. "Proceedings From the International Workshop on Long-Term Extrapolation of Passive Behavior Conference." Arlington, Virginia, July 19–20, 2001. A.A. Sagues and C.A. Di Bella, eds. Arlington, Virginia: U.S. Nuclear Waste Technical Review Board.

Wong, L., T. Lian, D.V. Fix, M. Sutton, and R. Rebak. 2004aa. "Surface Analysis of Alloy 22 Coupons Exposed for Five Years to Concentrated Ground Waters." Proceedings of the CORROSION 2004 Conference. Paper No. 04701. Houston, Texas: NACE International.

Woolf, R. 2003aa. "Controlled Plasticity Burnishing (CPB) for Developing a Very Deep Layer of Compressive Residual Stresses in Rectangular Specimens of Alloy 22 for Yucca Mountain Nuclear Waste package Closure Weld." SET Job No. 37 LSN DN2002365233. Cincinnati, Ohio: Surface Enhancement Technologies.

Yang, L., D. Dunn, G. Cragnolino, X. He, Y.-M. Pan, A. Csontos, and T. Ahn. 2007aa. "Corrosion Behavior of Alloy 22 in Concentrated Nitrate and Chloride Salt Environments at Elevated Temperatures." Proceedings of the CORROSION/2007 Conference. Paper No. 077580. Houston, Texas: NACE International.

Yang, L., R. Pabalan, and M. Juckett. 2006aa. "Deliquescence Relative Humidity Measurements Using an Electrical Conductivity Method." *Journal of Solution Chemistry*. Vol. 35, No. 4. pp. 583–604.

CHAPTER 5

2.2.1.3.2 Mechanical Disruption of Engineered Barriers

2.2.1.3.2.1 Introduction

This chapter of the Safety Evaluation Report (SER) evaluates the performance of the Engineered Barrier System (EBS) the U.S. Department of Energy (DOE) presented in its Safety Analysis Report (SAR) (appropriate revision of SAR cited here using author, year format). The design aspects of the EBS were described in SAR Sections 1.3.4 and 1.5.2, while the performance aspects were described in SAR Sections 2.1, 2.3.5, 2.3.6, and 2.3.7. DOE identified that the following EBS features contribute to barrier performance: emplacement drifts, drip shields, waste packages, waste forms, waste form internals, waste package pallets, and emplacement drift inverters. According to DOE, the EBS features are designed to work together with the natural barriers by preventing or substantially reducing the release rate of radionuclides from the repository to the accessible environment. A disruption of the EBS components has the potential to affect their barrier performance. Mechanical disruption of EBS components generally results from external loads generated by accumulating rock rubble. Rubble accumulation can result from processes such as (i) degrading emplacement drifts due to thermal loads, (ii) time-dependent natural weakening of rocks, and (iii) effects of seismic events (vibratory ground motion or fault displacements). This SER chapter evaluates the performance of the various components of the EBS under a reasonable range of expected loading conditions. To estimate the timing and extent of rubble accumulation, rocks in the repository block (RB) need geologic characterization. DOE characterized the repository rock mass as consisting of two major rock types: lithophysal and nonlithophysal. Lithophysal rocks (approximately 85 percent of the repository emplacement area) are characterized as relatively more deformable rocks with low compressive strength because of the voids of varying sizes contained within the rock. The nonlithophysal rocks (approximately 15 percent) are characterized as hard, strong, and jointed rocks. According to DOE, these two rock types are expected to behave differently under thermal and seismic loads and thus require different modeling approaches to account for different modes of failure (e.g., rock blocks separating from the mass and falling due to gravity, gradual unraveling or tensile failure during vibratory loads). On the basis of geologic mapping and testing, DOE categorized the lithophysal rocks into five categories based on rock mass qualities (to represent the variability in mechanical properties). DOE has conducted laboratory and in situ testing on small and large rock samples and developed a range of input parameters for the numerical models. DOE has presented several approaches to estimate the timing and extent of degradation, including numerical modeling results.

According to DOE, the functions of the drip shield are to prevent rocks from falling on the waste packages and to prevent water from contacting the waste package surface at early times when waste packages are hot, so that potential for corrosion may be minimized. The purpose of the waste package is to protect the waste form and isolate the radionuclides or slow down their rate of release to the accessible environment. To estimate the effects on timing and magnitude of radionuclide release, DOE analyses considered the loading from mechanical disruption of EBS components from seismic events. DOE considered gradual drift degradation due to thermal loads, time-dependent weakening, and seismic events as sources of generating loads from rubble accumulation on and around the drip shields. However, DOE excluded the effects of drift degradation due to thermal loads and time-dependent weakening from its Total System Performance Assessment (TSPA) code. The staff's review of DOE's technical bases for exclusion of features, events, and processes (FEP) 2.1 07.02.0A (drift collapse) is presented in

SER Section 2.2.1.2.1.3.2. The scope of this SER chapter is limited to reviewing how the applicant considered the effects of seismic disruption (i.e., vibratory ground motion, and fault displacement) and used the results in the total system performance analysis.

The staff's review followed the guidance provided in the Yucca Mountain Review Plan (YMRP) (NRC, 2003aa). YMRP Section 2.2.1 provides guidance to the staff on applying risk information throughout the review of the performance assessment. The staff used DOE's risk information derived from an initial review of DOE's treatment of multiple barriers, as appropriate. The staff's review approach is to assess the adequacy of DOE design and analyses of EBS components under anticipated demands generated by drift degradation due to seismic loads. For those cases in which there may be a reasonable doubt that the design capacities may be exceeded, staff examines the potential for continued functionality of the components under a range of expected conditions. (b)(5)

(b)(5)

2.2.1.3.2.2 Regulatory Requirements

Model abstractions used in the applicant's postclosure performance assessment must meet the regulatory requirements given in 10 CFR 63.114 (Requirements for Performance Assessment) and 63.342 (Limits on Performance Assessment), to support the predictions of compliance for 63.113 (Performance Objectives for the Geologic Repository after Permanent Closure). Specific compliance with 63.113 is reviewed in SER Section 2.2.1.4.1.

The requirements for performance assessment in 10 CFR 63.114 require the applicant to

- Include appropriate data related to the geology, hydrology, and geochemistry of the surface and subsurface from the site and the region surrounding Yucca Mountain
- Account for uncertainty and variability in the parameter values used to model mechanical disruption of engineered barriers
- Consider alternative conceptual models for mechanical disruption of engineered barriers
- Provide technical bases for the inclusion of features, events, and processes affecting mechanical disruption of engineered barriers, including effects of degradation, deterioration, or alteration processes of engineered barriers that would adversely affect performance of the natural barriers, consistent with the limits on performance assessment in 10 CFR 63.342
- Provide technical basis for the models of mechanical disruption of engineered barriers that in turn provide input or otherwise affect other models and abstractions

10 CFR 63.114(a) considers performance assessment for the initial 10,000 years following permanent closure. 10 CFR 63.114(b) and 63.342 consider the performance assessment methods for the time from 10,000 years through the period of geologic stability, defined in 10 CFR 63.302 as 1 million years following disposal. These sections require that through the period of geologic stability, with specific limitations, the applicant

- Use performance assessment methods consistent with the performance assessment methods used to demonstrate compliance for the initial 10,000 years following permanent closure
- Include in the performance assessment those FEPs used in the performance assessment for the initial 10,000 year period

For this model abstraction of mechanical disruption of engineered barriers, 10 CFR 63.342(c)(1) further provides that DOE assess the effects of seismic and igneous activity on the repository performance, subject to the probability limits in 63.342(a) and 63.342(b). Specific constraints on the analysis required for seismic and igneous activity are given in 10 CFR 63.342(c)(1)(i) and 10 CFR 63.342(c)(1)(ii), respectively.

NRC staff review of the license application follows the guidance laid out in YMRP Section 2.2.1.3.2, Mechanical Disruption of Engineered Barriers, as supplemented by additional guidance for the period beyond 10,000 years after permanent closure (NRC, 2009ab). The acceptance criteria in the YMRP generically follow 10 CFR 63.114(a). Following the guidance, the NRC staff review of the applicant's abstraction of mechanical disruption of engineered barriers considered five criteria

- System description and model integration are adequate.
- Data are sufficient for model justification.
- Data uncertainty is characterized and propagated through the abstraction.
- Model uncertainty is characterized and propagated through the abstraction.
- Model abstraction output is supported by objective comparisons

Because 10 CFR Part 63 specifies the use of a risk-informed approach for the review of a license application, the guidance provided by the YMRP, as supplemented by NRC (2009ab), is followed to the extent reasonable for aspects of mechanical disruption of engineered barriers important to repository performance. Whereas NRC staff considered all five criteria in their review of information provided by DOE, only aspects that substantively affect results of the performance assessment, as judged by NRC staff, are discussed in this chapter. NRC staff's judgment is based both on risk information provided by DOE, and staff's knowledge, experience, and independent analyses.

2.2.1.3.2.3 Seismic and Fault Displacement Inputs for Mechanical Disruption of Engineered Barriers

DOE investigated the geological, geophysical, and seismic characteristics of the Yucca Mountain region to obtain sufficient information to estimate how the site would respond to vibratory ground motions from earthquakes. In SAR Section 1.1.5.2, DOE provided its description of site seismology. DOE described its analysis of potential seismic hazards in SAR Section 1.1.5.2.4, the overall approach to developing a seismic hazard assessment for Yucca Mountain in SAR Section 2.2.2.1, and the conditioning (adaption or modification) of the ground

motion hazard at Yucca Mountain in SAR Section 1.1.5.2.5.1. Additional information was provided in DOE responses to the NRC staff's request for additional information (RAI) in DOE Enclosure 19 (2009ab) and DOE Enclosures 6, 7, and 8 (2009aq) and the references cited therein.

The DOE overall approach to developing a seismic hazard assessment for Yucca Mountain, including fault displacement hazards as described in SAR Section 2.2.2.1, involves the following three steps:

1. Conducting an expert elicitation in the late 1990s to develop a probabilistic seismic hazard assessment (PSHA) for Yucca Mountain. This assessment included a probabilistic fault displacement hazard assessment (PFDHA) (CRWMS M&O, 1998aa; BSC, 2004bp) that is discussed in SER Section 2.1.1.1.3.5.5. The PSHA was developed for a reference bedrock outcrop, specified as a free-field site condition with a mean shear wave velocity (V_s) of 1,900 m/sec [6,233 ft/sec] and located adjacent to Yucca Mountain. This value was derived from a V_s profile of Yucca Mountain with the top 300 m [984 ft] of tuff and alluvium removed, as provided in Schneider, et al., Section 5 (1996aa).
2. Conditioning PSHA ground motion results to constrain the large low-probability ground motions to ground motion levels that, according to DOE, are more consistent with observed geologic and seismic conditions at Yucca Mountain, as provided in BSC, ACN02 (2005aj).
3. Modifying the conditioned PSHA results using site-response modeling. This accounts for site-specific rock material properties of the tuff, in and beneath the emplacement drifts, and the site-specific rock and soil material properties of the strata beneath the site.

PSHA—Methodology

DOE conducted an expert elicitation on PSHA in the late 1990s (CRWMS M&O, 1998aa; BSC, 2004bp) on the basis of the methodology described in the Yucca Mountain Site Characterization Project (DOE, 1997aa). DOE stated that its PSHA methodology followed the guidance of the DOE-NRC-Electric Power Research Institute-sponsored Senior Seismic Hazard Analysis Committee (Budnitz, et al., 1997aa). In SAR Section 2.2.2.1.1.1, DOE concluded that the methodology used for the PSHA expert elicitation is consistent with NRC expert elicitation guidance, which is described in NUREG-1563 (NRC, 1996aa).

To conduct the PSHA, DOE convened two panels of experts as described in SAR Section 2.2.2.1.1.1. The first expert panel consisted of six 3-member teams of geologists and geophysicists (seismic source teams) who developed probabilistic distributions to characterize relevant potential seismic sources in the Yucca Mountain region. These distributions included location and activity rates for fault sources, spatial distributions and activity rates for background sources, distributions of moment magnitude and maximum magnitude, and site-to-source distances. The second panel consisted of seven seismology experts (ground motion experts) who developed probabilistic point estimates of ground motion for a suite of earthquake magnitudes, distances, fault geometries, and faulting styles. These point estimates incorporated random uncertainties that were specific to the regional crustal conditions of the western Basin and Range. The ground motion attenuation point estimates were then fitted to yield the ground motion attenuation equations used in the PSHA. The two expert panels were supported by technical teams from DOE, the U.S. Geological Survey, and

Risk Engineering Inc., who provided the experts with relevant data and information; facilitated the formal elicitation, including a series of workshops designed to accomplish the elicitation process; and integrated the hazard results.

According to the DOE-NRC-Electric Power Research Institute-sponsored Senior Seismic Hazard Analysis Committee (Budnitz, et al., 1997aa), the basic elements of the PSHA process are (i) identification of seismic sources such as active faults or seismic zones; (ii) characterization of each of the seismic sources in terms of their activity, recurrence rates for various earthquake magnitudes, and maximum magnitude; (iii) ground motion attenuation relationships to model the distribution of ground motions that will be experienced at the site when a given magnitude earthquake occurs at a particular source; and (iv) incorporation of the inputs into a logic tree to integrate the seismic source characterization and ground motion attenuation relationships, including associated uncertainties. According to the Budnitz, et al. (1997aa) methodology, each logic tree pathway represents one expert's weighted interpretations of the seismic hazard at the site. The computation of the hazard for all possible pathways results in a distribution of hazard curves that is representative of the seismic hazard at a site, including variability and uncertainty.

Conclusions on PSHA Methodology

The NRC staff reviewed the applicant's PSHA methodology described in SAR Sections 1.1.5.2.4 and 2.2.2.1.1 using the guidance provided in the YMRP and NUREG-1563 (NRC, 1996aa). The NRC staff also evaluated the DOE PSHA development to ensure that it included the four basic elements described in Budnitz, et al. (1997aa). In addition, the NRC staff observed all expert elicitation meetings and reviewed summary reports of those meetings as they were produced. (b)(5)

(b)(5)

PSHA—Input Data and Interpretations

During the expert elicitation, DOE's seismic source teams considered a range of information from many resources including DOE, the U.S. Geological Survey, project-specific Yucca Mountain studies, and information published in the scientific literature. This information included (i) data and models for the geologic setting as summarized in BSC (2004bp); (ii) seismic sources and seismic source characterization, including earthquake recurrence and maximum magnitude (BSC, 2004bp); (iii) historical and instrumented seismicity (CRWMS M&O, 1998ab, Appendix G); (iv) paleoseismic data (Keefer, et al., 2004aa), and (v) ground motion attenuation (Spudich, et al., 1999aa). DOE also supported the PSHA with a broad range of data, process models, empirical models, and seismological theory (CRWMS M&O, 1998ab). The expert panels built their respective inputs to the PSHA on the basis of this information and information presented to the experts during the elicitation meetings (CRWMS M&O, 1998ab). The resulting set of hazard curves was intended to provide DOE with sufficient representation of the seismic hazard for use in the TSPA.

DOE expressed the PSHA curves in increasing levels of ground motion as a function of the annual probability that the ground motion will be exceeded. These curves were developed for bedrock conditions with a mean V_s of 1,900 m/sec [6,233 ft/sec]. Such rocks are located adjacent to Yucca Mountain as described previously in the PSHA methodology subsection of this SER section. Estimates of uncertainty in the hazard curves are also included (see SAR Figure 1.1-74; e.g., hazard curves). The SAR provided PSHA results on horizontal and vertical components of peak acceleration (defined at 100 Hz), spectral accelerations (SAs) at frequencies of 0.3, 0.5, 1, 2, 5, 10, and 20 Hz; and peak ground velocity (PGV).

Conclusions on Input Data and

The NRC staff reviewed the applicant's PSHA input data and interpretations as described in SAR Sections 1.1.5.2 and 2.2.2.1.1. (b)(5)

(b)(5)

(b)(5)

Conditioning of Ground Motion Hazard

DOE provided the conditioning of ground motion hazard at the reference bedrock outcrop where the PSHA was developed in SAR Section 1.1.5.2.5.1. Since completion of the PSHA in 1998, several studies and reports, including ones from NRC staff (NRC, 1999aa), the Nuclear Waste Technical Review Board Panel on Natural System and Panel on Engineered Systems (Coraddini, 2003aa), and DOE itself (BSC, 2004bj), questioned whether the very large ground motions the PSHA predicted at low annual exceedance probabilities (below $\sim 10^{-6}$ /yr) were physically realistic. These ground motion values are well beyond the limits of existing earthquake accelerations and velocities from even the largest recorded earthquakes worldwide. They are deemed physically unrealizable because they require a combination of earthquake stress drop, rock strain, and fault rupture propagation that cannot be sustained without wholesale fracturing of the bedrock (Kana, et al., 1991aa).

(b)(5)

For Yucca Mountain, however, the seismic hazard curves were extrapolated to estimate ground motions with annual exceedance probabilities as low as 10^{-8} (SAR Section 1.1.5.2.5.1). At these low probabilities, the seismic hazard estimates are driven by the tails of the untruncated Gaussian distributions (the tail is not defined by the data, but by the assumed distribution) of the input ground motion attenuation models (Bommer, et al., 2004aa). As Anderson and Brune (1999aa) pointed out, overestimates of the hazards may also arise because of the way in which uncertainty in ground motion attenuation from empirical observations or theory is distributed between aleatory and epistemic uncertainties.

To account for these large ground motions, the applicant modified or conditioned the hazard using both a shear-strain-threshold approach and an extreme-stress-drop approach, as described in SAR Section 1.1.5.2.5.1. Rather than reconvene the PSHA expert elicitation and redo the PSHA, the applicant chose to treat the issue as part of the ground response analysis. Accordingly, the applicant's second step in developing ground motion inputs for postclosure assessment, after the development of the PSHA, is to condition the ground motion hazard. This second step in the three-step DOE process is to include information on the level of extreme ground motion that is consistent with the geological setting of Yucca Mountain. Conditioning of ground motion hazard is a unique study developed for the Yucca Mountain project.

Conclusions on Conditioning Methodology

The NRC staff reviewed the applicant's methods for conditioning its PSHA results in SAR Section 1.1.5.2.5.1 and reviewed DOE's responses to the staff's RAIs. (b)(5)

(b)(5)

DOE Results of PSHA Conditioning

The unconditioned hazard curve DOE developed, which is the annual percentage of exceedance (APE) as a function of ground motion, is convolved with the distribution of extreme ground motion for the reference bedrock outcrop to produce the conditioned ground motion hazard of the same bedrock outcrop. The shear-strain-threshold conditioning has a marginal impact as compared to the extreme-stress-drop approach. For example, for an annual probability of exceedance of 10^{-8} , the shear-strain-threshold conditioned PGV hazard is reduced from 1,200 cm/sec to about 1,100 cm/sec [472 to 433 in/sec] or about 10 percent; the Stress-drop-conditioned PGV hazard is reduced from 1,200 cm/sec to about 480 cm/sec [472 to 189 in/sec] or about 60 percent, as identified in BSC Section A4 5.1 (2008bl). The impact of conditioning at low probabilities is less significant and increases as the probability decreases (i.e., annual probabilities of exceedance of 10^{-5} , 10^{-6} , 10^{-7} , and 10^{-8}) (SAR Section 1.1.5.2.5.1). SAR Figures 1.1-79 and 1.1-80 compared the unconditioned and conditioned peak ground accelerations (PGA) and PGV mean hazard curves for the reference bedrock outcrop.

BSC Appendix A (2008bl) outlined the four workshop proceedings, which included presentations, discussions, and assessments, that were conducted to develop the expert judgment. The stress drop data from the United States and other countries were used in the expert judgment. The parameter variability involved in the empirical ground motion attenuation relationship and numerical simulations of ground motions that the experts relied on was included in the conditioning. Variability in velocity profile, stress drop, source depth, and kappa (the site- and distance-dependent parameter representing the effect of intrinsic attenuation of

the wave field as it propagates through the crust from source to the receiver) were considered in the modeling to map the stress drop into ground motion distribution.

In response to NRC RAIs (DOE, 2009bq,br,bt), the applicant provided information on applying two methods in series where the output of the extreme-stress-drop conditioning becomes the input of the shear-strain-threshold conditioning. In the RAI responses the applicant also clarified and updated the formulations for the two conditioning methods, as described in BSC Appendix A (2008bl).

Conclusions on Results of Conditioning

(b)(5)

Evaluation Summary on PSHA

The NRC staff reviewed SAR Sections 1.1.5.2 and 2.2.2.1 and DOE's responses to NRC RAIs. (b)(5)

(b)(5)

2.2.1.3.2.3.1 Seismic Site-Response Modeling

To address the effects of earthquakes during the postclosure period, the applicant performed site-response analysis, which incorporates the effects of the upper rock and soil layers on the input ground motion at the reference rock (the conditioned ground motion hazards discussed previously).

Overall Approach to Site-Response Modeling

In SAR Section 1.1.5.2.5.2 DOE discussed the ways in which the various types and thicknesses of rocks, alluvium, and soils that comprise the site would likely respond to earthquake ground motions. The results of site-response modeling include understanding and quantifying the amplification or damping factor of ground motion and how much the vertical-to-horizontal motion ratio varies from place to place. DOE used the site-specific ground motion curves that are consistent with the conditioned PSHA ground motion hazard curves.

The NRC staff reviewed the applicant's overall approach to site-response modeling using the guidance of NUREG/CR-6728 (McGuire, et al., 2001aa) and YMRP Section 2.1.1.3.3, AC 1

(b)(5)

(b)(5)

Ground Motion Inputs

DOE provided ground motion inputs developed for the RB in SAR Section 1.1.5.2.6. For the site surface, 52 combinations of site properties were evaluated in the site-response modeling (SAR Section 1.1.5.2.6.1). These combinations were from two base-case velocity profiles (south and northeast of the Exile Hill Fault splay), two base-case sets of dynamic material property curves for tuff and alluvium separately, four values of alluvium thickness northeast of the fault splay, and three values of alluvium thickness south of the fault splay. Each combination incorporated aleatory variability by averaging the amplification factors from 60 randomized velocity profiles and dynamic material property curves.

Site-Specific Hazard Curves

The seven combinations of alluvium and tuff hazard curves were combined into two sets: the northeast and south fault splay sets. The four and three combinations of hazard curves for four and three alluvium thicknesses were enveloped separately for south and northeast of the fault splay. These two sets of hazard curves were enveloped again to produce mean horizontal and vertical hazard curves (BSC, 2008bl). The final mean horizontal and vertical hazard curves for PGA; 0.05, 0.1, 0.2, 0.5, 1.0, 2.0, and 3.3 seconds SA; and PGV were provided in BSC Figures 6.5.2-34 to 6.5.2-42 (2008bl) for surface facilities area, and BSC Figures 6.5.3-9 to 6.5.3-16 (2008bl) for RB, respectively. The data for these plots are in DTN: MO0801HCUHSSFA.001, as identified in BSC Section 6.5.2.2 (2008bl).

Earthquake Time-Histories

The RB time histories for postclosure analyses were developed differently for AFEs of 10^{-5} , 10^{-6} , and 10^{-7} (SAR Section 1.1.5.2.6.2), where 17 sets of time histories were developed: one horizontal (H1) component of each seed time history was scaled according to the PGV from site-response modeling and the other two components were scaled to maintain the inter-component variability of the seed time history (SAR Section 1.1.5.2.6.2).

Conclusions on Ground Motion Inputs

(b)(5)

(b)(5)

The strain-compatible soil properties are the products of the previously described site-response analysis.

2.2.1.3.2.3.2 Fault Displacement Hazard Assessment

Fault displacement (the relative displacement between opposite sides of a fault) is a potential hazard to the underground facility because it could damage or shear drifts and/or waste packages, trigger rockfall within the drifts and shafts, degrade drift walls and ground-support systems, and degrade other components of the EBS. These hazards might affect the postclosure performance of the engineered barriers.

PFDHA—Input Data and Interpretations

The PFDHA used an integration of two data types: (i) known and/or documented faulting activity consisting of measurements of regional and local earthquakes, and measurements of fault displacements within the last ~1.8 million years (Quaternary) and (ii) inferred potential faulting activity, on the basis of analysis of mapped geological faults, overall tectonic setting, and regional estimates of ongoing crustal strain. The applicant analyzed 100 earthquakes in the Basin and Range region to determine the relationships among the amounts and patterns of both principal and distributed fault displacements, the minimum magnitude at which an earthquake may produce surface faulting, and the maximum magnitude at which an earthquake does not displace the surface.

For the largest mapped faults at Yucca Mountain, the probabilistic fault displacement hazard curves were largely based on the same detailed paleoseismic and earthquake data used to characterize these faults as potential seismic sources. The expert elicitation relied on both anecdotal evidence and expert judgment to develop conceptual models of distributed faulting and to estimate the probabilities of secondary faulting of smaller faults and fractures in the repository (Youngs, et al., 2003aa; CRWMS M&O, 1998aa).

The applicant chose the following nine sites around Yucca Mountain as demonstration sites of the application of the PFDHA, as identified in SAR Chapter 1, Table 1.1-67, p. 1.1-304: (i) Bow Ridge fault, (ii) Solitario Canyon fault, (iii) Drill Hole Wash fault, (iv) Ghost Dance fault, (v) Sundance fault, (vi) an unnamed fault west of Dune Wash, (vii) a location 100 m [328 ft] east of the Solitario Canyon fault, (viii) a location between Solitario Canyon fault and Ghost Dance fault, and (ix) a location within Midway Valley. These demonstration sites were selected to represent a range of faulting and related fault deformation conditions at the site, including large block bounding faults, such as the Solitario Canyon and Bow Ridge faults; smaller mapped faults within the repository footprint, such as the Ghost Dance fault; and unmapped minor faults near the larger faults, fractured tuff, and intact tuff.

Results of the PFDHA (CRWMS M&O, 1998aa) show that, except for the Bow Ridge and Solitario Canyon faults, mean fault displacements are less than 1 m [3.28 ft] over the next 10^7 (10 million) years (SAR Table 2.2-15). Mean displacements for the demonstration sites within the current repository footprint [demonstration sites (v), (vii), and (viii) as identified in the previous paragraph] do not exceed 0.40 m [1.3 ft] in 10 million years. For a 10,000-year period, the mean displacements are calculated to be less than 0.01 m [0.03 ft] for all 9 demonstration sites (SAR Table 1.1-67).

Individual fault displacement hazard curves were developed to characterize fault displacements at each of the nine demonstration sites. These fault displacement hazard curves are analogous to seismic hazard curves, in which increasing levels of fault displacements are computed as a function of the annual probability that those displacements will be exceeded. Example fault displacement curves for the nine demonstration sites are provided in SAR Figure 2.2-13.

The NRC staff evaluated the applicant's information regarding input to the PFDHA in the SAR and supporting documents. (b)(5)

(b)(5)

Evaluation Summary

(b)(5)

2.2.1.3.2.4 Fault Displacement Considerations in TSPA

This section reviews the information provided in SAR Section 2.3.5.3 (and selected references) to evaluate the adequacy of the conceptual model of seismic fault displacement. The applicant considered seismic fault displacement as one of the modeling cases in the TSPA. DOE assumed that fault displacement occurred concurrently with the ground motion during a low probability seismic event (SAR Section 2.3.4.5.5.1). DOE considered that only the waste packages located directly above faults were subject to damage from fault displacement. DOE expected the dose related to fault displacement to be a small fraction of the total dose for the seismic scenario class because damage from fault displacement affected a small fraction of the EBS and damage occurred only for events with very low exceedance frequencies. The applicant calculated the dose contribution from the seismic fault displacement on the basis of simplified calculations (SAR Section 2.4). The abstraction assumed waste package damage when fault displacement exceeded the available waste package clearance. To evaluate fault displacement, DOE assumed (SAR Section 2.3.4.5.5.2.1.1) (i) the faults are perpendicular to the drift axis with the displacement being vertical; (ii) the fault displacement occurs at a discrete plane, creating a sharp discontinuity; and (iii) clearances are based on emplacement drifts that are fully collapsed at the time of the seismic event.

The potentially relevant FEPs in DOE's Total System Performance Assessment-License Application (TSPA-LA) are listed in SAR Table 2.2-1. In this abstraction, DOE evaluated and included FEP 1.2.02.03.0A, Fault Displacement Damages EBS Components.

Conceptual Model

Clearance

DOE analyzed the clearances between the EBS components for intact and failed drip shield scenarios (SAR Section 2.3.4.5.5.2.1). For intact drip shield configurations, DOE defined the clearance as the interior height of the drip shield less the outside diameter of the waste package outer corrosion barrier without a pallet, to account for part of the substantial movement of the rubble (SAR Section 2.3.4.5.5.2.1.1). On the basis of this simplification, DOE used a maximum allowable displacement with drift collapse and an intact drip shield that varied from 67.3 to 96.9 cm [26.5 to 38.15 in] (SAR Table 2.3.4-52), according to the type of waste package.

The NRC staff compared the values of the applicant's clearances in SAR Table 2.3.4-52 to the EBS geometry presented in SAR Figure 2.3.4-53 that showed the distances between the top of the waste packages and bottom of the drip shields (35.6 to 68.6 cm [14 to 27 in]).

(b)(5)

For failed drip shield configurations, the applicant stated that no free space existed between the top of the waste package and bottom of the drip shield. DOE concluded that the movement of the rubble will accommodate some amount of fault displacement due to consolidation of the rubble (SAR Section 2.3.4.5.5.2.1.2). DOE stated that fault displacement had to exceed one-quarter of the outer diameter of the outer corrosion barrier to cause waste package failure (from 43.7 to 51.1 cm [17.2 to 20 in]) (SAR Tables 2.3.4-50 and 2.3.4-53) (b)(5)

(b)(5)

Expected Movements and Number of Impacted Waste Packages

The applicant identified that the probability of events exceeding 0.1 cm [0.039 in] displacement in the RB was 10^{-5} per year (SAR Section 2.3.4.5.5.1). DOE characterized the subsurface geologic repository operations area and determined that few faults were capable of producing movements greater than calculated clearances for events with a probability of exceedance of 10^{-8} per year (SAR Table 2.3.4-55). SAR Table 2.3.4-59 showed that less than 2 percent of the waste packages can potentially be impacted by a seismic faulting event with an annual exceedance frequency of 1×10^{-8} /yr to 3×10^{-8} /yr. To mitigate the potential risk of faulting that could cause mechanical damage to the waste packages, the applicant stated that waste packages would be placed 60 m [196.85 ft] from known, major faults (SAR Section 1.9, Design Control Parameter 01-05). (b)(5)

(b)(5)

(b)(5)

Damage to the EBS

The applicant sampled a uniform distribution of open areas of waste packages to model the open area of a waste package failed by fault displacement. This distribution has a lower bound of 0 m² [0 ft²] and an upper bound equal to the area of the waste package lid (SAR Section 2.3.4.5.5.4). The applicant stated that the lids for the transportation, aging, and disposal (TAD) and codisposal (CDSP) waste package groups are 2.78 and 3.28 m² [30 and 35 ft²], respectively (SAR Table 2.3.4-50). (b)(5)

(b)(5)

To determine the impact of seismic faulting on drip shield failure, the applicant assumed that the drip shield fails at the instant the underlying waste package is breached. (b)(5)

(b)(5)

Fault Displacement Evaluation Summary

(b)(5)

2.2.1.3.2.5 Seismically Induced Drift Degradation

The staff's evaluation in this SER section focuses on the applicant's assessment of potential drift degradation due to seismic ground motions and use of the information to assess potential mechanical disruption of the engineered barriers. The staff reviewed the applicant's information in SAR Section 2.3.4.4 and supporting documents (BSC, 2004a) that describe potential seismically induced degradation of emplacement drifts after permanent closure. The applicant's information included estimates of the amount of rubble accumulation in drifts, drip shield loading due to rubble, sizes of individual blocks that may strike the drip shield during a seismic event, and the associated impact velocity and location of the impact on the drip shield. The NRC

staff's evaluation focuses on the potential occurrence of rubble loading that is large enough to damage the drip shield and the time of occurrence of such rubble loading (b)(5)

(b)(5)

(b)(5)

The applicant estimated the potential for rubble accumulation in drifts through process-level analyses of the effects of seismic ground motions on drift degradation. The applicant chose the analysis approach by considering the mechanical behavior of two types of rocks (i.e., lithophysal and nonlithophysal) that constitute the repository horizon rock mass; this information is reviewed in SER Section 2.1.1.3.5.4.

DOE's Process-Level Modeling of Drift Degradation Due to Seismic Events

The staff's review of DOE's rock characterization is summarized in SER Section 2.2.1.2.1.

(b)(5)

(b)(5)

The applicant analyzed drift degradation in nonlithophysal rock by modeling motions of rock blocks on surfaces formed by existing fractures as described in SAR Section 2.3.4.4.4. The applicant used the analyses to estimate the characteristics of individual rock blocks that may strike the drip shields during a seismic event (SAR Table 2.3.4-19) and the volumes of rubble that may accumulate in the drifts (SAR Tables 2.3.4-20 and 2.3.4-24) (b)(5)

(b)(5)

(b)(5)

The applicant considered the failure mechanism by rock block impact and excluded it from TSPA (excluded FEP 1.2.03.02.0B as a result of low consequence).

For the lithophysal rock mass, the applicant indicated that mechanical deformation of the rock will consist predominantly of rock material deformations aided by lithophysae and a high density of existing small-scale fractures. As described in SAR Section 2.3.4.4.5, the applicant analyzed drift degradation in lithophysal rock by modeling potential fracturing of the rock through formation of new fractures and movement on existing fractures as dictated by the rock stress. The applicant used the analyses to estimate potential rubble accumulation for drift sections in lithophysal rock but applied it to the entire repository. The applicant stated that this approach would be bounding.

To assess potential drift degradation in lithophysal rock, the applicant used a model that focused on estimating the rock mass volume that could break up along failure surfaces determined by the effects of the prevailing stress field on a diffuse network of small "incipient" fractures. The applicant obtained the estimates by modeling the rock mass as an assemblage of polygonal blocks generated randomly using the Voronoi tessellation model, as identified in SAR Section 2.3.4.4.5.3 and BSC Sections 6.4.2.1 and 7.6.1 (2004a). The individual blocks can deform elastically or slide or separate at block contact surfaces. The blocks are initially attached together at contact surfaces and may slide or separate if the contact resistance is overcome by the prevailing stress. Thus, the contacts represent incipient fractures that could allow the blocks to detach from the assemblage if the prevailing stress permitted such detachment. Detached blocks could fall under the influence of gravity or seismically induced force. The applicant stated in BSC Section 6.4.2.1 (2004a) that the model could simulate rock deformation, stress changes, rock fracturing or breakage, and free fall of broken rock blocks. The applicant explained that mechanical behavior of the model is influenced by the block size, block elastic parameters (Young's modulus and Poisson's ratio), contact elastic parameters

(shear and normal stiffness), and contact strength parameters (tensile strength, cohesion, and friction). The applicant set the values of the model parameters by calibrating the unconfined compressive strength and elastic stiffness of the model (i.e., block assemblage) against the unconfined compressive strength and elastic stiffness of the rock mass on the basis of laboratory test data, as outlined in BSC Section 7.6.1 (2004a). The applicant implemented the model in a two-dimensional universal distinct element code UDEC, as identified in BSC Section 3.1 (2004a), and used the code to calculate changes in drift profile and amount of rubble accumulation due to seismic events, and drip shield loading due to rubble. Additional details of the rock characterization, laboratory and field testing, numerical experiments for calibration, and field validation are summarized and reviewed in SER Section 2.2.1.2.1.3.2 DOE used the same analytical and modeling approach for drift responses to seismic events. The use of this model is addressed in the following sections

Staff Evaluation of Applicant's Abstracted Model and Rubble Formation Due to Seismic Events

Consideration of the Two Rock Types in the TSPA

The applicant stated that the rockfall volume in the nonlithophysal zones is significantly less than in the lithophysal zones for the same PGV level because the nonlithophysal rock mass is significantly stronger than the lithophysal rock. (b)(5)

(b)(5)

Drift Degradation from Seismic Events

The applicant indicated that seismic ground motions could cause partial or complete collapse of drifts in lithophysal rock, resulting in various amounts of rubble accumulation for different ground motion magnitudes and mechanical categories of lithophysal rock SAR Section 2.3.4.4.5.4 (BSC, 2004a). To describe the effects of ground motion magnitude and lithophysal rock category on potential rubble accumulation, the applicant performed analyses for ground motion at PGV levels of 0.4, 1.05, and 2.44 m/s [1.31, 3.44 and 8 ft/sec], which, according to the applicant, correspond to an annual frequency of exceedance of 10^{-4} , 10^{-5} , and 10^{-6} , respectively (SNL, 2007a). The applicant performed the analyses using 15 ground motion time history cases at each annual frequency of exceedance and 5 sets of values of mechanical properties representing the 5 lithophysal rock categories the applicant defined in SAR Section 2.3.4.4.5.4 and BSC Section 6.4.2.2.2 (BSC, 2004a). The applicant concluded that (i) ground motion with an annual frequency of exceedance of 10^{-4} will have negligible effects on

drift degradation, (ii) ground motion with an annual frequency of exceedance of 10^{-6} will cause complete drift collapse, and (iii) ground motion with an annual frequency of exceedance of 10^{-5} could cause various degrees of collapse and varying amounts of rubble accumulation. The applicant selected 15 analysis cases (SAR Table 2.3.4-23) to represent potential rubble accumulation due to seismic ground motions, as described in SNL Section 6.7.1.1 (2007ay).

The applicant used the calculated rubble volumes from 11 of the 15 cases to develop relationships between rubble accumulation and the PGV of a seismic event, as described in SAR Figure 2.3.4-48 and SNL Section 6.7.1.2, Figure 6-57 (2007ay). SAR Section 2.3.4.4.8.3.1 stated that four cases calculated using rock mass Category 1 properties were eliminated because the applicant considered the rubble volumes from the four cases to be nonrepresentative. According to SAR Section 2.3.4.4.8.4, the applicant used the resulting relationship between rubble volumes and PGV to estimate the amount of rubble accumulation due to a seismic event. The applicant estimated the rubble accumulation due to multiple seismic events by adding the accumulations from the individual events, as identified in SAR Section 2.3.4.4.8.4 and SNL Section 6.7.1.4 (2007ay). The abstraction did not include weakening of the host rock due to previous events, because rapid filling of drifts in lithophysal units mitigates concerns about numerous seismic events slowly weakening the rock mass as the applicant explained in SNL Section 6.7.1.4 (2007ay). Therefore, to calculate the drift volume fraction filled with rubble in lithophysal rock areas after a sampled seismic event, the applicant accumulated rockfall volumes [using relationships based on SNL Table 6-30 and Figure 6-56 (2007ay)] and divided the accumulated volume by a number sampled from a uniform distribution between 30 and 120 m^3/m [320 ft^3/ft and 1,280 ft^3/ft]. The uniform distribution of 30–120 m^3/m [320–1,280 ft^3/ft] represents the applicant's estimate of the volume of rockfall that would fill a drift with rubble, as described in SNL Section 6.12.2 (2007ay). SAR Figure 2.1-14 summarized the applicant's estimates of potential rubble accumulation due to seismic events during a period of 1 million years. According to this figure, at 10,000 years, the volume of accumulated rubble in the drift could range up to 15 percent of the drift volume (with a mean value of approximately 4 percent). Similarly, the corresponding volume of accumulated rock rubble at 100,000 years ranged up to about 60 percent (with a mean value of about 32 percent). The volume of rubble per unit length of drift that is required to fill the drift was sampled for each epistemic realization in the TSPA, and the sampled volume ranged uniformly between 30–120 m^3/m [320–1,280 ft^3/ft].

To calculate the static load on a drip shield due to rubble, the applicant multiplied the volume fraction of drift filled with rubble (on the basis of the assessment of drifts in lithophysal rock) with the drip shield load due to a fully collapsed drift, as outlined in SNL Section 6.12.2 (2007ay). The magnitude of drip shield loading due to rubble at a given time depends on the amount of rubble accumulation, shape of the rubble pile, and the amount of rubble loading transmitted to the drip shield for a given amount and shape of the rubble pile. The applicant used the information to determine the potential occurrence of rubble loading large enough to damage the drip shield in lithophysal and nonlithophysal areas.

Staff Evaluation

The NRC staff evaluated the applicant's assessment of potential drip shield loading due to rubble accumulation in lithophysal rock sections of emplacement drifts by considering the amount of rock accumulation and the shape of rubble piles.

Amount of Rubble Accumulation

(b)(5)	
(b)(5)	In SNL Section 6.7.1.4 (2007ay), the applicant's abstraction of rubble accumulation due to seismic events did not include any effects of rock weakening, because, according to the applicant, rapid filling of drifts in lithophysal units mitigates concerns about the effects of rock weakening. (b)(5)
(b)(5)	
(b)(5)	DOE Enclosure 1, Figure 5 (DOE, 2010aa,ab) and BSC Figure 6-149 (2004al) summarized the caving potential of an excavated underground opening. Caving potential is expressed in terms of modified rock mass rating (a measure of rock quality and strength where a higher value indicates greater stability) and hydraulic radius [a dimension based on the geometry of the excavated opening; hydraulic radius is a measure of stability (i.e., a larger hydraulic radius indicates a less stable opening, and hence a higher caving potential)]. (b)(5)
(b)(5)	
(b)(5)	DOE analyses showed that the hydraulic radius of a degraded waste emplacement drift after 10,000 years of heating and time-dependent strength degradation coupled with a seismic ground motion is still far less than the hydraulic radius of a degraded opening with high caving potential. (b)(5)
(b)(5)	

Shape of Rubble Piles

The process-level model that the applicant used to analyze drift degradation in lithophysal rock appears somewhat constrained because of the upper boundary. In BSC Figure 6-116 (2004al), the tessellated domain of the model is set 10.25 m [33.6 ft] above the initial drift roof. The upper boundary of the potential degradation zone the applicant used was 1.86 drift diameters above the initial drift roof. However, contours of block displacement magnitude intersected the upper boundary of the tessellated domain. The calculated displacement contours indicate that some

additional displacement could occur outside this domain [e.g., BSC Figure 6-176 (2004a)] Also, plots of the final position of the Voronoi blocks after an analysis [e.g., BSC Figures P-17, P-18, and P-24 (2004a)] indicate blocks at the top of the model could be predicted to separate from the overlying elastic domain. Such a separation would suggest the caved zone might have extended higher if the model upper boundary had been higher.

In response to an NRC staff request, the applicant provided analyses to show that the rubble volume calculated using the applicant's model is insensitive to the size of the tessellated domain. The applicant provided results from two models with the boundary of the tessellated domain at 8.25 and 13.25 m [27 and 43.5 ft], respectively, in Enclosure 2, Section 1.3 (DOE, 2010aa,ab). The applicant used the models to estimate the extent of caving needed to fill a drift with rubble if the prevailing mechanical conditions were to cause complete drift collapse. This was accomplished by artificially degrading the rock mass strength to zero in a quasi-static analysis. The results of these studies demonstrated that the patterns of calculated displacements and stresses did not change appreciably as a result of changing the size of the tessellated domain. The quasi-static analyses showed that the caved zone extended approximately one drift diameter above the drift irrespective of the size of the tessellated domain. The applicant also provided calculations to show that potential caved zones due to seismic events will likely extend to much less than one drift diameter above the drift except for seismic events with an annual exceedance probability of 10^{-6} or smaller.

The NRC staff reviewed the applicant's analyses with the expanded boundaries. (b)(5)

(b)(5)

Rubble Loading Transmitted to the Drip Shield

The applicant used the results of the discontinuum model to estimate the potential drip shield loading due to rubble (SAR Figure 2.3.4-43). The applicant also presented alternative bounding analytical approaches for estimating the potential static loading on the drip shields (continuous curves in SAR Figure 2.3.4-46). The analytical model estimates drip shield loading due to rubble using the dead weight of rubble. However, it is well established in the field of rock mechanics that loads transmitted to a drip shield from rubble could differ because of frictional resistance among broken pieces of rock rubble, between rubble and the drift wall, or between rubble and the sides of the drip shield.

To justify using the loads from the numerical model, SAR Section 2.3.4.4.6.3.2 stated that the applicant's process-level model accounts for load transmission among rubble particles and to the drip shield. However, the applicant in BSC Section P4 (2004a) identified factors that may affect load transmission within rubble and to the drip shield, including size and shape distribution of rubble particles, rubble compaction, and deformability of the drip shield and invert. The applicant represented the rock mass in the process-level model as an assemblage of equidimensional polygonal blocks with a characteristic length of approximately 0.2 m [0.65 ft] (SAR Figure 2.3.4-40). SAR Section 2.3.4.4.5.3 and BSC Section 6.4.2.1 (2004a) stated that the model blocks are approximately the same size as potential lithophysal rock blocks.

(b)(5)

The NRC staff requested that the applicant provide an assessment of potential drip shield loading due to rubble using either a numerical model with the block size and shape distributions of lithophysal rock rubble or an alternative approach that does not bias the results toward predicting smaller drip shield loading.

In response, DOE provided additional information in DOE RAI, Enclosure 1 (2010ab) and

(b)(5)

Conclusions

The NRC staff evaluated the applicant's assessment of potential degradation of emplacement drifts due to seismic events and estimates of drip shield loading resulting from rubble accumulation. (b)(5)

(b)(5)

2.2.1.3.2.6 Drip Shield Structural/Mechanical Performance in the Context of Its Seepage Barrier Function

Comment (b)(5)

In the DOE's EBS, the drip shield is a freestanding structure that surrounds the waste package and rests on the crushed rock that forms the invert at the base of the drift. The drip shield is designed to protect the waste package from contact by seepage water and rockfall (SAR Section 2.3.4.5.1.1). The main structural elements of the drip shield are a framework consisting

of a bulkhead and support beams (legs) that will be made of Titanium Grade 29. Plates of Titanium Grade 7 are welded onto the framework to form a full composite structure in response to mechanical loading (SAR Section 2.3.4.5.1.1; SAR Figure 2.3.4-56).

Damage to the drip shield can occur from mechanical impacts of falling rocks, by loads from accumulated rock rubble that can be increased by seismic accelerations, and by corrosion processes. Through time, DOE expects that thinning of drip shield components will decrease the capacity of the drip shield to withstand loads and that the likelihood of the drip shield having experienced a potentially damaging load will increase (e.g., SAR Section 2.3.4.1). During the initial few thousand years following repository closure, temperatures within the drifts decrease from around 160 °C [320 °F] to below the boiling point. At these elevated temperatures, generalized corrosion could occur if water contacts the surface of the waste packages. Thus, if the barrier capability of the drip shield fails in the first 12,000 years following repository closure, seepage water could contact the waste package and lead to localized corrosion. DOE relied on the presence of the drip shield as a barrier to preclude significant occurrences of localized corrosion (e.g., SAR Section 2.1.2.2.6).

Consistent with the guidance in the YMRP, the staff focused its review on the risk significant aspects of the drip shield performance. On the basis of DOE's reliance on the drip shield in the demonstration of multiple barrier requirements (SAR Section 2.1.2.2.6), the staff focused on evaluating the performance of the drip shield as a barrier to seepage during the early years following drift closure.

For seepage to contact a waste package, openings must occur on the drip shield with sufficient size to permit the advective flow of water through the drip shield plates. Crack openings, such as those produced by stress corrosion cracks (SCC), are too small to allow advective flow of water through the drip shield and are excluded from the performance assessment analysis SNL FEP 2.1.03.10.0B (2008ab). Openings large enough for advective water flow could potentially occur through (i) corrosion processes, (ii) impacts of large rock blocks causing puncture of the plates, (iii) physical separation between adjacent drip shield segments due to ground motions from seismic events, (iv) fault displacements, and (v) rupture by deformations that produce effective strains greater than the failure strains in the plates (SNL, 2007ap).

The staff's evaluation of the drip shield corrosion processes is presented in SER Section 2.2.1.3.1. In that review, (b)(5)

(b)(5)

(b)(5)

DOE

excluded large-block impacts from the TSPA as part of the screening analysis for FEP 1.2.03.02.0B (SNL, 2008ab). The staff reviewed the DOE screening arguments as part of the evaluation in SER Section 2.2.1.2.1 (b)(5)

(b)(5)

Thus, the staff's detailed review focuses on DOE's representation of processes affecting drip shield separations from seismic events or fault displacements, and on the potential for plate rupture.

Separations From Seismic Shaking

Unlikely or low probability seismic events can create ground motions that may cause adjacent drip shields to separate. Consequently, DOE assessed the potential for drip shield separations during seismic events, as described in SNL Section 6.7.3 (2007ay). DOE determined that ground motions large enough to cause potential drip shield separations also cause partial to complete collapse of the repository drifts. DOE determined that rockfall associated with drift

collapse occurs during the first seconds of large seismic events. DOE modeled the effect of this rockfall on the ability of the drip shields to separate during seismic events and concluded that rockfall loads from partial drift collapse are sufficient to prevent horizontal separation of the drip shields, as outlined in SNL Section 6.7.3 (2007ay). While these models calculated that minor amounts of vertical separation might occur between the drip shield sections due to settling of the invert or framework damage, the 26-cm [10.24-in]-wide overlaps between the drip shield connectors prevent rockfall or seepage water from contacting the waste package through relatively small vertical separations. In FEP 1.2.03.02.0A (SNL, 2008ab), DOE concluded that seismically induced separations of drip shields can be excluded from the TSPA on the basis of low probability.

Staff Review of Separations From Seismic Shaking

The staff reviewed the information presented in SNL Section 6.7.3 (2007ay) and analyses in BSC Section 5.3.3.2.2 (2004bq). (b)(5)

(b)(5)

Fault Displacement

DOE concluded that fault displacement occurs concurrently with the ground motion during low probability seismic events (SAR Section 2.3.4.5.5.1) and determined that only EBS components located directly above the moving faults are subject to damage. In the analysis of the effects of fault displacements on EBS performance, DOE assumed that the drip shield fails completely if fault displacements are sufficient to breach the underlying waste package (SAR Section 2.3.4.5.5.4). DOE allows all seepage water entering the drift to pass through the failed drip shield, with no diversion of the water.

Staff Review of Fault Displacement

The staff's review of the fault displacement model, concerning waste package failure, is presented in this SER chapter. (b)(5)

(b)(5)

Plate Rupture by Deformation

(b)(5)

(b)(5)

Rupture of the

drip shield plate can occur if the magnitude of effective strain on the plate exceeds the strain threshold for the Titanium Grade 7 plates (e.g., SAR Section 2.3.4.5.1.2.2).

(b)(5)

Temperature Effects

Mechanical analyses of drip shield performance are dependent on the material properties used in the numerical models. DOE used mechanical properties for the drip shield plates and framework derived from standard handbooks and manufacturer's catalogs (SAR Section 2.3.4.5.1.3.1 and Table 2.3.4-28). DOE considered that a reference temperature of 60 °C [140 °F] for these properties was appropriate, because this temperature is representative of most of the repository closure period. Although DOE recognized that temperatures as high as 300 °C [572 °F] could potentially occur early after repository closure, DOE considered that the duration of elevated temperatures was too short to warrant consideration for drip shield performance (SAR Section 2.3.4.5.1.3.1).

DOE provided additional information to assess the potential effects of temperatures at or greater than 120 °C [248 °F] on titanium alloy material properties (DOE, 2009bp). During the first 650 years of repository closure, DOE concluded that drip shield temperatures could range from 120–300 °C [248–572 °F]. DOE expects the effect of this increase in temperature to not affect titanium alloy properties significantly, because the likelihood for potentially damaging rockfall or seismic events is sufficiently low to preclude significance in the performance assessment. For temperatures below 120 °C [248 °F], DOE compared expected changes in materials properties (e.g., yield strength, tensile strength) to assess the effects of component thinning on the likelihoods of drip shield plate or framework failure. Using small rockfall loads, DOE concluded that changes in the titanium mechanical properties between 60–120 °C [140–248 °F] are a factor of 3 to 4 less than the corresponding percentage changes in component thicknesses that have no significant effect on fragility values.

Staff's Review of Temperature Effects

The staff reviewed the mechanical properties DOE used for titanium alloys at 60 °C [140 °F].

(b)(5)

The staff evaluated the rationale DOE provided to exclude consideration of temperatures greater than 120 °C [248 °F] on titanium material properties. (b)(5)

(b)(5)

(b)(5)

Modeling Approach

To evaluate drip shield plate capacity, DOE conducted numerical modeling of the drip shield under quasi-static and dynamic loading conditions. For the quasi-static analyses, DOE calculated a rock rubble load on the drip shield and then multiplied these loads by the vertical component of peak ground acceleration and modeled the drip shield response to these loads. DOE models for quasi-static loading conditions use FLAC3D, which is a three-dimensional finite-difference computer code. DOE calculated stresses and strains on one-half of the plate on the drip shield crown, which represents one segment between two framework bulkheads.

DOE used rock rubble loads calculated from UDEC analyses of rockfall during seismic events (SAR Section 2.3.4.5.3.2). DOE evaluated two static loading configurations on the drip shield. One configuration used an average of six UDEC realizations for each modeled segment of the drip shield, which DOE used to consider spatial variability in the nonuniform load. The second configuration used a single UDEC realization, which DOE considered as representative of the highest loads on the drip shield crown (SAR Section 2.3.4.5.3.2.1).

For each loading configuration, the vertical load was applied over the entire top surface of the plate and increased incrementally until a failure mechanism developed, as described in SNL Section 6.4.3.1.2 (2007ap). For each load increment, the model compared the residual tensile stresses or accumulated plastic strain against a failure criterion of 80 percent of the yield strength for Titanium Grade 7, as outlined in SNL Section 6.4.3.1.3 (2007ap). DOE concluded that plate failure occurred at the smallest applied load that exceeded either the stress or strain criterion.

By uniformly increasing the static load in the UDEC model, DOE calculated that an intact drip shield plate has a capacity (i.e., limit load) of approximately 2,500 kPa [52,218 psf], which is approximately twice the calculated capacity of the drip shield framework (SAR Section 2.3.4.5.3.3.1). To determine the likelihood of drip shield plate failure, DOE integrated the annual likelihood of exceeding levels of ground acceleration with the likelihood of rupture for plates experiencing the loads corresponding to the level of ground acceleration. For intact drip shield plates and 100 percent rockfall load, DOE calculated that seismic events with annual probabilities of exceedance $< 5 \times 10^{-7}$ can lead to plate rupture on 1–7 percent of the drip shields (SAR Section 2.3.4.5.3.4).

As an alternative to the quasi-static analyses, DOE also conducted dynamic analyses for drip shield plate capacity using the UDEC computer code (SAR Section 2.3.4.5.3.3.3). These analyses used a two-dimensional cross section of the drip shield surrounded by rock rubble. The dynamic analyses used vertical ground accelerations from time histories that DOE views as representative of larger magnitude seismic events in the Yucca Mountain region. DOE applies these vertical accelerations to the basal boundary of the UDEC model, which allows the emplacement drift, rubble, and drip shield to interact dynamically for the modeled period of strong ground motion. DOE compared the results of the dynamic analyses with the quasi-static analyses and concluded that the quasi-static model underestimates the stability of the drip shield plates. DOE therefore concluded that the quasi-static approach is an appropriate basis to calculate the likelihoods of plate rupture, as the dynamic analysis would result in lower likelihoods of rupture (SAR Section 2.3.4.5.3.3.3).

Staff's Review of Modeling Approach

The staff reviewed the use of the FLAC3D computer code in the analyses of the drip shield plate capacity. The staff reviewed the information in SNL Section 7.3.3.1 (2007ap)(b)(5)

(b)(5)

(b)(5)

In response to staff

questions, DOE provided additional information to address the representation of nonlinear responses of materials (DOE, 2009bp). (b)(5)

(b)(5)

(b)(5)

(b)(5)

(b)(5)

Drip Shield Framework Deformation

DOE calculated the likelihood of drip shield framework failure using the same approach as implemented for the drip shield plate analyses (SAR Section 2.3.4.5.3.3.2). These analyses determined that the drip shield framework has approximately half the bearing capacity as the drip shield plates and that buckling of the drip shield legs results from exceeding the bearing capacity. DOE also determined that if the drip shield becomes tilted after the framework buckles, the drip shield connector plate and connector guide provide a physical barrier that will divert seepage from the crown to the sides of the drip shield, as outlined in SNL Section 6.7.3.2 (2007ay).

DOE postulated that if one segment of a drip shield collapsed more extensively than adjacent segments, localized stresses may lead to rupture of the drip shield plates along the crown. DOE considered the likelihood of isolated segment collapse to be low, because rubble loads are expected to be relatively uniform and the rigidity of the drip shield is expected to effectively transfer loads to the adjacent segments (DOE, 2010ac). Thus, DOE expects complete collapse of the drip shield when loads exceed the design capacity. Nevertheless, DOE analyzed stress-strain relationships for a partially collapsed drip shield and determined that plate rupture would occur if vertical displacements between adjacent segments exceeded approximately 19 cm [7.5 in] (DOE, 2010ac). DOE concluded that such displacements between adjacent segments are unlikely to occur, because the structure of the drip shield will effectively transfer stress from a deforming segment onto the adjacent segments. This stress transfer leads to a progressive collapse of adjacent drip shield segments, rather than isolated collapse and potential tearing of a single segment (DOE, 2010ac).

Staff's Review of Drip Shield Framework Deformation

(b)(5)

(b)(5)

The

staff evaluated the drip shield design DOE provided (e.g., SAR Figure 1.3.4-15); (b)(5)

(b)(5)

(b)(5)

(b)(5)

For unrestrained motion during seismic events, as would occur when the drip shield is intact, up to 4 percent of the waste package surface area can be damaged sufficiently for SCC to develop (SAR Section 2.3.4.5.2.1.4.2). In contrast, a collapsed drip shield localizes the potential damaged area on the waste package and results in an approximately order-of-magnitude decrease in the potential for SCC (SAR Section 2.3.4.5.4.3.2.1). (b)(5)

(b)(5)

(b)(5)

(b)(5)

(b)(5)

(b)(5)

(b)(5)

(b)(5)

Summary and Findings

DOE relies on the drip shields as effective barriers to advective water flow or rock rubble impacts on the waste package. The staff reviewed the information DOE presented relevant to the barrier capability of the drip shield (b)(5)

(b)(5)

(b)(5)

2.2.1.3.2.7 Waste Package Mechanical/Structural Performance

In accordance with 10 CFR 63.21(c)(9), 63.113(b)–(c), and 63.114(f), the applicant is required to provide information related to the mechanical disruption of engineered barrier abstractions and to assess the waste package performance. The applicant classified the waste package as important to waste isolation (SAR Table 2.1-1). The applicant provided information on structural response of the waste package to mechanical disruption in SAR Section 2.3.4.5. The objective of this SER section is to evaluate whether adequate technical bases have been provided for waste package abstractions used in the applicant's performance assessment.

The applicant assessed the waste package mechanical damage by performing detailed structural analyses. The results of these structural analyses were used as inputs to the Seismic Consequence Abstractions (SCA). The SCA simulates mechanical interactions among the waste packages, the drip shield, the emplacement pallet, and/or accumulated rubble as a function of PGV. The applicant calculated waste package damage as (i) SCCs that may allow diffusive radionuclide releases and (ii) rupture and puncture areas that may allow advective radionuclide releases (reviewed in SER Section 2.2.1.3.4.3.5).

The results of the SCA are used as inputs to other process-level models and direct inputs to the TSPA-LA. The waste package corrosion abstraction uses waste package breaches at the process level to initiate double-sided corrosion (reviewed in SER Section 2.2.1.3.1). Note that in this context, a breach is defined as any failure mechanism that penetrates the waste package (i.e., cracks, ruptures, and punctures). Waste package breaches also impact the chemistry inside the waste package (reviewed in SER Section 2.2.1.3.4). SCC area is used in the EBS Transport Abstraction to model a pathway for diffusive radionuclide release (reviewed in SER Section 2.2.1.3.4). Waste package rupture or puncture area is used in the flux-splitting model to calculate water flux through the waste package (reviewed in SER Section 2.2.1.3.3).

Information presented in SAR Table 2.1-3 suggests that seismic ground motion damage to the EBS components is an important mechanism that affects the EBS capability to perform its intended functions. The applicant stated that seismic-induced waste package damage is more significant in early times and that nominal failure processes are more significant at later times (DOE, 2009b). According to the applicant, seismic-induced SCC is the most probable waste package damage mechanism. The majority of commercial spent nuclear fuel (CSNF) and CDSP waste package failures due to seismic-induced SCC occur prior to drip shield plate/crown failure, DOE Figure 5 and 6 (2009b).

The applicant considered three idealized states of the EBS for analyses purposes (SAR Section 2.3.4.5):

1. Structurally stable drip shield state, when the waste packages are free to move and may be damaged due to impacts with other engineered barriers during seismic events
2. Drip shield framework failure state, when the drip shield–waste package interactions during seismic events may damage the waste package outer barrier

3. Drip shield plates failure state, when the waste package is surrounded by rubble and may be damaged due to waste package–rubble interactions during seismic events

According to the applicant, nominal SCC in a CSNF waste package would initiate between 200,000 and 300,000 years, DOE Figure 1 (2009bl), where the timeframe is dependent on the drip shield performance (reviewed in SER Section 2.2.1.3.2.3.3). This would happen after the beginning of Idealized State 2. The CSNF waste packages cannot move as freely in Idealized State 2 as in Idealized State 1, thereby reducing the potential for seismic-induced SCC.

For the three idealized states, the applicant considered two waste package failure modes.

1. The first failure mode is referred to as "the residual stress failure mode" in this SER section. The waste package damage is expressed in terms of the waste package outer corrosion barrier surface area that may be susceptible to SCC. It is defined as an area with the residual stresses exceeding one of three residual stress threshold values: 90, 100, and 105 percent of the Alloy 22 yield stress (reviewed in SER Section 2.2.1.3.1.3.3).
2. The second failure mode is referred to as "the tensile tearing failure mode" in this SER section. The applicant used Alloy 22 ultimate tensile strain as a failure criterion to evaluate the waste package outer barrier tensile tearing (rupture and/or puncture) occurrence.

For these two failure modes, the applicant developed the abstractions using a three-part approach: (i) the rupture/puncture probability was defined as a function of PGV and the effective tensile stress limits; (ii) the probability of nonzero damaged area was defined as a function of PGV and the residual stress threshold damage; and (iii) for nonzero damaged area cases, a conditional probability distribution for the magnitude of the conditional damaged area was defined as a function of PGV and the residual stress threshold.

The applicant's analyses results indicate greater mechanical damage potential to the waste package during Idealized State 1. However, the NRC staff reviewed the fundamental aspects of damages in all three idealized states and their abstractions. The review presented in this section is organized around these major topics considering the context of the applicant's performance assessment.

Idealized State 1: Waste Package Structural Response With Structurally Stable Drip Shield

Modeling Assumptions and Approach

In SAR Section 2.3.4.5.2.1, the applicant provided information on waste package structural response for the Idealized State 1 where the drip shield is structurally stable. The applicant considered that dynamic impacts of the waste package on the rest of the EBS components may lead to waste package damage and rupture of the outer corrosion barrier. The applicant evaluated the movement of and damage to waste packages resulting from seismic loads. The following three cases of impacts were considered using numerical models: (i) impacts between waste packages, (ii) impacts between the waste package and the emplacement pallet, and (iii) impacts between the waste package and the drip shield (SAR Section 2.3.4.5.2.1). The applicant analyzed the TAD and the CDSP waste packages for three waste package

conditions where the drip shield is expected to remain functional and structurally stable (SAR Section 2.3.4.5.2.1). The three conditions are (i) 23-mm [0.91-in]-thick outer corrosion barrier with intact internals; (ii) 23-mm [0.91-in]-thick outer corrosion barrier with degraded internals; and (iii) 17-mm [0.67 in]-thick outer corrosion barrier with degraded internals. (The applicant modeled a waste package with degraded internals as the waste package outer corrosion barrier only.)

The NRC staff reviewed these three waste package conditions the applicant analyzed using guidance in YMRP Section 2.2.1.3.2, Review Method 3. As mentioned earlier, the applicant considered 23- and 17-mm [0.91- and 0.67-in] waste package outer corrosion barriers. These represent corrosion thinning of 2.4 and 8.4 mm [0.09 and 0.33 in], respectively, from the initial 25.4-mm [1-in] outer corrosion barrier thickness and correspond to a timeframe of approximately 340,000 and 1.2 million years after emplacement (reviewed in SER Section 2.2.1.3.1.3.1). (b)(5)

(b)(5)

Using Review Method 1 in YMRP Section 2.2.1.3.2, the NRC staff reviewed the material properties of the EBS components the applicant incorporated into the numerical models. (b)(5)

(b)(5)

The staff notes that the applicant did not include the waste package damage potential for impact between the waste package and drip shield in the seismic damage abstractions. The applicant's decision was based on the observations of the waste package damage from the analyses of impacts between waste packages (SAR Section 2.3.4.5.2, p. 2.3.4-131). The applicant concluded that the waste package areas damaged from a side impact on a flat elastic surface were zero or very small. These damaged areas were significantly less than the damaged areas from end impacts, as described in SNL Table 6-13 (2007ay). The applicant stated that the waste package side impacts on a flat elastic surface are representative of the waste package impacts on the drip shield side wall.

(b)(5)

The applicant also stated that vertical impacts between the waste package and the drip shield would have a small contribution to the total waste package damage (SNL, 2007ay). The applicant concluded that the impact loads on the waste package would be distributed over a large contact area of the drip shield bulkheads and stiffeners. The applicant further concluded that vertical impacts between the waste package and the drip shield surrounded by rubble would be similar to impacts between waste packages, which also result in small damaged areas. Therefore, the applicant concluded that the impact damage between waste packages is

representative of the waste package damage from vertical impacts between the waste package and drip shield.

The NRC staff reviewed these assumptions and concluded that the vertical impact between the waste package and the drip shield would be similar to impacts between the waste packages and the pallets. The NRC staff also reviewed information presented on the frequency of the vertical impacts between the waste package and the drip shield in SNL Section 6.4.5 (2007ay). (b)(5)

(b)(5)

To estimate waste package damage and rupture potential, the applicant developed a two-part calculation process using numerical models developed in the computer code LS-DYNA (Livermore Software Technology Corporation, 2003aa).

First, large-scale kinematic analyses were performed to determine the impact parameters for multiple waste packages in an emplacement drift. The parameters included locations and time of impacts, relative velocity and impact angles, and forces between the impacting bodies. The applicant used 17 ground motion time histories at PGV levels of 0.4, 1.05, 2.44, and 4.07 m/sec [1.31, 3.44, 8, and 13.35 ft/sec] in these analyses. The NRC staff reviewed these values using YMRP Section 2.2.1.3.2, Review Methods 1 and 2. (b)(5)

(b)(5)

(b)(5)

The large-scale kinematic calculations presented in the SAR consider a "string" of multiple waste packages. A combination of TAD-bearing and CDSP waste packages in a section of an emplacement drift was considered. For these analyses, the applicant considered a partially or fully collapsed emplacement drift. The drip shield was considered to be in a structurally stable condition. Thus, the structurally stable drip shield provided the only restriction to the movement of the waste packages and the pallet. The applicant recorded impacts for the central waste packages (three and two central waste packages for the TAD-bearing and CDSP configurations, respectively) in the total string of waste packages (SAR Section 2.3.4.5.2.1.3.1).

Second, the applicant carried out detailed finite elements analyses for estimating damage and rupture potential. Impacts between individual waste packages and between waste package and pallet were analyzed. The applicant evaluated waste package damage over the range of impact parameters, including those determined from the large-scale kinematic analyses. Using the results of the detailed finite element analyses, the applicant estimated the waste package damage and rupture potential for the multiple impacts modeled using the large-scale kinematic analyses.

Using Review Method 1 and Acceptance Criterion 1, the NRC staff reviewed the modeling approach the applicant employed to evaluate the waste package response to vibratory ground motions while the drip shield is structurally stable. (b)(5)

(b)(5)

(b)(5)

The applicant stated that the waste package pallet eventually fails as the stainless steel connector tubes lose their structural integrity (SAR Section 2.3.4.1). For the damage analyses, however, the applicant made an assumption that the waste package pallet is intact. This assumption, according to the applicant, would lead to greater damage to the waste package outer corrosion barrier during vibratory ground motion. As the applicant explained, the reason for this conclusion is that higher magnitude stresses are generated when the waste package impacts a "relatively stiff pallet as opposed to the crushed tuff invert" (SAR Section 2.3.4.1, p. 2.3.4-10). However, the applicant initially did not consider that loss of connector integrity could result in a different range of conditions for pallet pedestal orientations, impact locations, and impact frequencies. The staff questioned whether the variability in these parameters may have exceeded the range the applicant considered. The review indicated that larger uncertainty in the pedestal orientation can potentially affect calculated results. For example, impact locations, time of impact, relative velocity of the impacting bodies, angle of impacts, and forces between the impacting bodies could be affected. Thus, DOE was requested to supplement the information presented in SAR Sections 2.3.4.5.2 and 2.3.4.5.4 to address whether such uncertainties would affect significantly the characteristics of waste package damage calculated in kinematic analyses.

In response to staff's RAI (DOE, 2009bq), the applicant provided additional information to demonstrate that the intact waste package pallet assumption did not underestimate the potential for waste package damage in the kinematic analyses. The applicant stated that at lower PGV levels, the waste package and the pallet pedestals would have limited relative motion. Therefore, if the stainless steel connector tubes were to lose structural integrity due to corrosion, the waste package damage would remain bounded by the results of the analyses with the intact waste package pallet. The applicant stated that, at higher PGV levels and degraded connector tubes, the impact between the waste package and pallet would be characterized by one of three cases: the waste package impacts both pallet pedestals (Case 1), the waste package impacts one pallet pedestal (Case 2), and the waste package impacts only the invert (Case 3).

For Case 1, the applicant stated that the angles and locations of impacts would be similar to those used in the kinematic analyses with an intact pallet. For Case 2, the applicant stated that the locations of the impacts would be toward the end of the waste packages, as the waste package would tend to slide off the remaining pedestal and onto the invert. In SNL Tables 6-49 and 6-50 (2007ap) the applicant stated that, due to higher waste package stiffness at the waste package lid, the waste package would experience less damage for impacts near the waste package lids than in the middle of the waste package. The applicant concluded that for Case 2, the waste package damage would be bounded by the results of the analyses for waste package impacts with an intact pallet. For Case 3, the applicant stated that the waste package damage would be bounded by the results of the intact pallet. This result is due to the waste package experiencing less damage from impact forces distributed over a larger waste package area. Therefore, the applicant concluded that the results of the analyses with an intact pallet would

bound the waste package damage for the case of the loss of structural integrity loss of the stainless steel connector tubes due to corrosion.

The NRC staff reviewed the applicant's responses to the staff's RAI (b)(5)

(b)(5)

The applicant considered waste package damage from angular impacts with an intact waste package pallet and concluded that the waste-package-to-pallet impacts are likely to cause more waste package damage than other types of impacts. (b)(5)

(b)(5)

Residual Stress Failure Mode

To analyze the residual stress failure mode, the applicant calculated the total damaged area of the waste package. Total damaged area is defined as the sum of the areas of all outer corrosion barrier elements in which the stress exceeds a threshold stress level at the end of a simulation. The three residual stress threshold values used are 90, 100, and 105 percent of the yield strength. (The NRC staff's evaluation of the residual stress threshold values the applicant used to estimate the waste package damaged area is presented in SER Section 2.2.1.3.1.3.2.3.)

The applicant used results from the analyses of the impacts between waste packages and between the waste package and the pallet. Inputs for the TSPA calculations were prepared in the form of lookup tables that provided damaged area as a function of the impact parameters. According to the information provided in these lookup tables (SNL, 2007ap), the amount of damage for single impacts is largest for impacts between a waste package and a pallet. The damage increases with decrease in the outer corrosion barrier thickness. Reported damage area for single impacts ranged from 0.002 percent to 14.333 percent of the total surface area for the TAD-bearing waste package, and from 0.002 percent to 20.106 percent for the CDSP waste package.

For the analyses with multiple waste packages, the amount of reported damage is largest for impacts between waste a package and a pallet. The damage increases with an increase in PGV levels and a decrease in the outer corrosion barrier thickness. The reported damage area ranged from 0.006 percent to 43.467 percent of the total surface area for the TAD-bearing waste package. The range for the CDSP waste package was from 0.006 to 19.585 percent of its surface area (SNL, 2007ap).

The NRC staff reviewed the residual stress failure mode results for these analyses and considered the applicant's response to an RAI (DOE, 2009br), addressing that the intact waste package pallet assumption would not underestimate the potential for waste package damage in the kinematic analyses. (b)(5)

(b)(5)

Tensile Tearing Failure Mode

To analyze the tensile tearing failure mode, the applicant assessed the rupture condition for a single impact. The maximum effective strain in the waste package outer corrosion barrier for the full time-history analyses was compared with the rupture tensile strain failure criterion (SAR Section 2.3.4.5.2.1.3.2). The applicant demonstrated through detailed finite element calculations that the strain for a single impact in the outer corrosion barrier was always below the ultimate tensile strain for Alloy 22 (SAR Section 2.3.4.5.2.1.3.2). For multiple impacts modeled in the large-scale kinematic analyses, the applicant stated that if an impact causes "severe" deformation, the additional large impacts to the deformed area have the potential to cause rupture. For both the TAD-bearing and the CDSP waste packages with intact internals, the applicant stated that the overall deformation of the outer corrosion barrier resulting from multiple impacts was insignificant even at the largest impact velocities. Therefore, the applicant concluded that no rupture would occur (SAR Section 2.3.4.5.2.1.3.2).

For the analyses with degraded internals, the applicant considered that the deformation from low velocity impacts (PGV levels less than 1.05 m/sec [3.44 ft/sec]) was not severe enough to lead to rupture after multiple impacts. In addition, the deformation becomes very large as the impact velocity increases. For PGV levels of 1.05 m/sec [3.44 ft/sec] and higher, a second impact of equal or greater magnitude would potentially cause a rupture of the outer corrosion barrier. Therefore, for the PGVs of 1.05 m/sec [3.44 ft/sec] and higher, which have a mean annual probability of exceedance of 10^{-5} , the waste package rupture probability exceeds zero. In some realizations of large-scale models for both the TAD-bearing and the CDSP waste package configurations with degraded internals and PGV levels of 2.44 m/sec [8 ft/sec] and higher, the applicant calculated the probability of rupture equal to one.

(b)(5)

(b)(5)

The applicant relied on engineering judgment to determine whether multiple impacts to the waste package result in tensile rupture (SAR Section 2.3.4.5.1.4.2). If the degree of deformation from a single impact was judged significant, a second impact of equal or greater magnitude was judged sufficient to cause tensile rupture. However, the applicant initially did not describe the magnitude of stress or strain on the

outer corrosion barrier, the impact velocities that caused this damage, or the threshold beyond which such damage occurs. The NRC staff determined that the SAR did not explain how variations in these or other indicators of damage were considered in the expert judgment process and therefore requested additional information.

In response to staff's RAI (DOE, 2009bq), the applicant provided information to demonstrate the acceptability of the methodology that involves engineering judgment used in the qualitative evaluation of waste package rupture probability for multiple impacts. The applicant performed a quantitative evaluation of the waste package rupture probability. The analysis is based on maximum effective strain limit and assessment of tensile strain in the waste package outer corrosion barrier. Because the quantitative approach did not predict waste package rupture, the applicant developed a qualitative approach. This approach was based on an assessment of the outer corrosion barrier deformation. The deformation results were used to estimate the waste package rupture probability for multiple impacts. In SNL Figures 6-31 through 6-36 (2007ap), the applicant examined deformation shapes of the outer corrosion barrier to determine a deformed state that could cause rupture if a second large impact occurred. For the analyses at an impact velocity of 5 m/sec [16.4 ft/sec], the applicant stated that the outer corrosion barrier developed deformations sufficient to cause rupture at a subsequent seismic event. The applicant defined this state as a lower bound such that another impact of 5 m/sec [16.5 ft/sec] or higher would cause rupture of the waste package outer corrosion barrier. The applicant used impact force values associated with impacts at 5 m/sec [16.4 ft/sec] as a threshold force to define zero probability of waste package rupture due to multiple impacts. The applicant defined the force associated with impacts at 7 m/sec [23 ft/sec] as an "upper force peg point" and used this to interpolate and extrapolate probability of waste package rupture between zero and one. The applicant concluded that this qualitative method would not underestimate waste package rupture probability, because the force threshold used as a lower bound was derived based on less severe and more frequent waste package deformations at impacts velocities of 5 m/sec [16.4 ft/sec] and higher.

(b)(5)

(b)(5) Further, for the waste-package-to-pallet impacts, the most damaging scenario is angular impacts at 6° angles into the middle of the TAD-bearing waste package with degraded internals (SNL, 2007ap). (b)(5)

(b)(5)

(b)(5) the applicant provided information on impact velocities of the drip-shield-to-waste-package impacts in SNL Tables 6-148 through 6-150 (2007ap). (b)(5)

(b)(5)

(b)(5)

The NRC staff determined that the applicant defined, in SNL Section 6.3.2.2.5 (2007ap), the maximum effective strain limit for the waste package rupture condition as 0.57 for uniaxial tension and 0.285 for biaxial tension. For realizations where the maximum effective strain was less than 0.285, the applicant considered that rupture was not credible. When the maximum effective strain exceeded 0.285, the strain limit was multiplied by the triaxiality factor, resulting in an effective strain limit between 0.285 and 0.57. Finally, the applicant evaluated the rupture condition on the basis of the newly computed strain limit. (b)(5)

(b)(5)

(b)(5) In response to staff's RAI (DOE, 2009bq), the applicant stated that for all realizations with computed effective strain in the outer corrosion barrier greater than the uniaxial tensile strain limit of 0.57, as outlined in SNL Tables 6-60, 6-90, and 6-92 (2007ap), the stress state is compressive. (b)(5)

(b)(5)

(b)(5)

Idealized State 2: Waste Package Structural Response Under Collapsed Drip Shield

Modeling Assumptions and Approach

The applicant provided information on waste package structural response for the Idealized State 2 with a collapsed drip shield framework (SAR Section 2.3.4.5.4.3.2). The applicant assessed deformations and stresses in the outer corrosion barrier of a TAD-bearing waste package loaded by a collapsed drip shield and the accumulated rubble. A 17- and a 23-mm [0.67 and 0.91-in]-thick outer corrosion barrier with intact and degraded internals were assessed. The applicant's model represented the intact internals by the inner vessel, the TAD canister, and the fuel baskets with plates inside the canister. The applicant assigned properties of Type 316 stainless steel to all internal components. The internals, which are assumed to be completely degraded, were represented by a material that can be considered to be similar to a weakly cohesive soil with no significant strength. This material fills the interior volume of the outer corrosion barrier to limit volume change to 50 percent.

The applicant performed numerical analyses to assess the waste package structural response under a collapsed drip shield using the FLAC3D finite element models (SAR Section 2.3.4.5.4.3.2). In these analyses the drip shield was not explicitly modeled and was represented by bulkhead flanges that contact the waste package after collapse of the drip shield framework. The applicant conducted these quasi-static analyses by applying vertical static loads to the drip shield bulkheads. The vertical loads were monotonically increased until

pressures ranging from 500 to 1,500 kPa [10,400 to 31,300 psf] were reached. The applicant considered that the average vertical static pressure from lithophysal rockfall for a complete drift collapse exerted onto the drip shield is 127 kPa [2,652 psf] (SAR Table 2.3.4-35). For the drip shield average vertical loading demand of 127 kPa [2,652 psf] (SAR Section 2.3.4.5.4.3.2.1), the maximum quasi-static pressures applied to the waste package are equivalent to PGAs in the range of about 3 to 9 g ("g" is acceleration due to gravity) (reviewed in SER Section 2.2.1.3.2.3.3.1). The applicant monitored the structural deformations and the residual stresses induced in the outer corrosion barrier as a function of the average vertical pressure exerted on the outer corrosion barrier by the drip shield bulkhead flanges.

The NRC staff reviewed the modeling approach for Idealized State 2 that the applicant employed to evaluate the waste package response under quasi-static loading under the collapsed drip shield using Review Method 1. (b)(5)

(b)(5)

(b)(5)

In response to staff's RAI (DOE, 2009br), the applicant provided additional information to demonstrate the adequacy of its modeling approach. The applicant provided waste package damage estimates that bounded waste package damage for angular impacts of the drip shield onto the waste package outer corrosion barrier. The applicant stated that a partially collapsed drip shield could result in angular contact between the waste package outer corrosion barrier and the drip shield bulkhead. According to the applicant, a partially collapsed drip shield does not completely lose its load-bearing capacity. The applicant stated that a modeling approach that allows the drip shield to fully collapse onto the waste package (i.e., modeling approach that produces a zero contact angle between the waste package outer corrosion barrier and the drip shield bulkheads) would overestimate the total load transferred to the waste package and, therefore, would overestimate waste package damage.

(b)(5)

(b)(5)

Residual Stress Failure Mode

For the residual stress failure mode, the applicant calculated the total damage area as the sum of areas of all outer corrosion barrier elements (including interior and exterior surfaces) in which a single residual stress threshold of 90 percent of the Alloy 22 yield stress is exceeded (SAR Section 2.3.4.5.4.3.2). The NRC staff's evaluation of the residual stress threshold values to estimate the waste package damaged area is presented in SER Section 2.2.1.3.1.3.3. For the analyses with 17- or 23-mm [0.67- or 0.91-in]-thick outer corrosion barrier with intact internals, the applicant made the following findings:

- Damaged area was less than 0.025 percent of the total outer corrosion barrier surface area for average vertical pressure up to 1,200 kPa [25,062 psf]
- Maximum damaged area was approximately 0.3 percent or less of the total outer corrosion barrier surface area for the highest evaluated vertical pressure of 1,500 kPa [31,328 psf]
- For the analyses with degraded internals, the vertical pressure of about 660 and 1,000 kPa [13,784 and 20,885 psf] may lead to a fully damaged waste package for 17- and 23-mm [0.67- and 0.91-in]-thick outer corrosion barriers, respectively
- (iv) For vertical pressure of less than or equal to 350 kPa [7,309 psf], the waste package damaged area was less than 0.1 percent of the total area (SAR Figure 2.3.4-93)

The NRC staff reviewed the residual stress failure mode results for these analyses using Review Method 2. (b)(5)

(b)(5)

Tensile Tearing Failure Mode

For the tensile tearing failure mode, the applicant provided information on the maximum stresses in the waste package outer corrosion barrier for three vertical pressure levels—486, 807, and 1,483 kPa [10,150, 16,854, and 30,972 psf]. (b)(5)

(b)(5)

(b)(5)

The NRC staff reviewed the tensile tearing failure mode results for three vertical pressure levels analyses using Review Method 2. (b)(5)

(b)(5)

For Idealized State 2, with a collapsed drip shield framework, the applicant concluded that

- State 2 bounds the case with intact waste package internals, tensile strain calculations from dynamic loads due to rock rubble after drip shield plate failure (Idealized State 3, which is reviewed in the section to follow)
- State 1 bounds State 2 for the case with degraded internals, the kinematic analyses for TAD-bearing waste packages

However, the applicant initially did not present the results of models for tensile strain of the waste package after collapse of the drip shield (SAR Section 2.3.4.5.4.4.1). In addition, the applicant initially did not discuss how free interactions between the waste package and drip shield, or dynamic interactions with rock rubble, appropriately bound localized tensile strains that could occur between a collapsed drip shield and the waste package. In response to staff's RAI (DOE, 2009bs), the applicant provided additional information to demonstrate that its results were bounding. The applicant discussed how the free interactions between the waste package and drip shield and dynamic interactions with rock rubble appropriately bound localized tensile strains that could occur between a collapsed drip shield and the waste package.

The applicant performed a quantitative comparison of the maximum effective plastic strain results of (i) the kinematic analyses for impacts between the waste package and the pallet with degraded internals and (ii) the quasi-static analyses for the waste package with degraded internals loaded by a collapsed drip shield. On the basis of this comparison, the applicant concluded that the maximum effective plastic strains from the kinematic calculations of impacts between a waste package and a pallet with degraded internals were greater. Thus, DOE concluded that the results bounded the effective plastic strains for the waste package with degraded internals loaded by a collapsed drip shield. In addition, the applicant performed a quantitative comparison of the maximum effective plastic strain results of the kinematic analyses for the waste package surrounded by rubble and the quasi-static analyses for the waste package with its intact internals loaded by a collapsed drip shield. The applicant concluded that the effective plastic strains from the calculations for the waste package surrounded by rubble were greater and, therefore, bounded the effective plastic strains for the waste package with intact internals loaded by a collapsed drip shield.

The NRC staff reviewed this information and compared quantitative results of the effective plastic strain the applicant provided. (b)(5)

(b)(5)

(b)(5)

Idealized State 3: Waste Package Structural Response in Direct Contact With Rubble Modeling Assumptions and Approach

The applicant provided information on waste package structural response for Idealized State 3 where the waste package is in direct contact with rock rubble (SAR Section 2.3.4.5.4.3.1). The applicant considered the loads produced by the weight of the rock rubble and the amplification of these loads during vibratory ground motion. These loads may lead to waste package damage through SCC, or rupture and puncture of the outer corrosion barrier. To examine the waste package damage potential, the applicant performed mechanical/structural analyses of the TAD-bearing waste package in direct contact with the rubble. Two waste package outer corrosion barrier thicknesses of 17 and 23 mm [0.67 and 0.91 in] with degraded internals were considered. The system was subjected to static loads and dynamic amplification from ground motions with PGV levels of 0.4, 1.05, 2.44, and 4.07 m/sec [1.31, 3.44, 8, and 13.35 ft/sec] (SAR Section 2.3.4.5.4.1).

The NRC staff reviewed PGVs the applicant used (b)(5)

(b)(5)

The applicant conducted two-dimensional seismic analysis of the waste package surrounded by rubble using the computer code UDEC. The UDEC model initially represented an intact emplacement drift containing a waste package and pallet resting on the invert. The drift was allowed to collapse onto the waste package. Once static equilibrium was established, the model was subjected to ground motions and equilibrium was reestablished. The applicant used a complete drift collapse simulation similar to the one used to assess potential drip shield framework buckling and drip shield plate rupture (SAR Section 2.3.4.5.3.2.1). The results included residual tensile stresses and effective tensile strains in the outer corrosion barrier. General observations on the deformed shapes of the outer corrosion barrier were also provided. The applicant did not include the inner vessel, the TAD canister, or the fuel baskets in the waste package representation and only considered the degraded state of the waste package internals. The applicant represented the degraded internals as a material similar to a weak cohesive soil with no significant strength. The applicant stated that, for the geometrical representation used, the results of the TAD-bearing waste package provided a reasonable estimate of damage for the CDSP waste package. Therefore, separate models were not developed for the TAD-bearing and CDSP waste packages.

The applicant used a two-dimensional plane strain representation of the waste package and its components for dynamic analyses under rubble loads, as outlined in SNL p. 6-216 (2007ap). This simplification assumes that the waste package extends infinitely in the direction normal to the calculation plane and that the structural response of the waste package is not affected by its boundaries (i.e., waste package lids). In SNL Appendix D (2007ap), the applicant compared results of two-dimensional and three-dimensional stress analyses, using uniform static loadings that are not representative of the dynamic loads associated with seismic events. Because of the higher rigidity of the waste package lid area, the NRC staff considered that the outer corrosion barrier area in the vicinity of the waste package lid potentially could be more susceptible to tensile tearing than an open cylinder. The NRC staff raised this as a question to the applicant.

In response to staff's RAI (DOE, 2009bt), the applicant provided additional information to demonstrate that the use of a two-dimensional waste package representation in seismic analyses of the waste package surrounded by rubble did not underestimate waste package damage. The applicant stated that the two-dimensional waste package representation had reduced stiffness because the waste package lids that provide additional structural support were not included. The two-dimensional waste package representation was chosen because it maximizes structural deformation of the outer corrosion barrier. Further, the applicant stated that three-dimensional waste package analyses were performed to investigate the potential for failure of waste package lids and connections between the waste package lids and the waste package wall. These analyses demonstrated that tensile rupture of the outer corrosion barrier would only occur when the outer corrosion barrier collapses due to the waste package wall buckling, as described in SNL Appendix D (2007ap). The applicant stated that because the two-dimensional waste package representation underestimates the loading demands needed for an outer corrosion barrier collapse, the applicant concluded that this representation would not underestimate the potential for the waste package outer corrosion barrier tensile failure.

(b)(5)

The NRC staff reviewed the kinematic analyses of the waste package surrounded by rubble analyses (b)(5)

(b)(5)

Residual Stress Failure Mode

For the residual stress failure mode, the applicant concluded that the damaged area was generally a small percentage of the total waste package surface area. For the residual stress

threshold of 90 percent of the yield stress, the damaged area resulted in 0.2 percent of the total waste package outer corrosion barrier surface area. For the residual stress threshold of 105 percent of the yield stress, the damaged area was about 3 percent of the total outer corrosion barrier surface area. The applicant stated that the increase in damaged area correlated with an increase in PGV levels and thinning of the outer corrosion barrier.

The NRC staff reviewed the results of the residual stress failure mode using Review Method 2 and Acceptance Criterion 2. The applicant's response to staff's RAI (DOE, 2009bt) demonstrated that two-dimensional waste package representation maximizes structural deformation of the outer corrosion barrier. (b)(5)

(b)(5)

Tensile Tearing Failure Mode

For the tensile tearing failure mode, the applicant concluded in SNL Section 6.5.1.4.1 (2007ap) the probability of rupture for the TAD-bearing and CDSP waste packages surrounded by rubble for the 17- and 23-mm [0.67- and 0.91-in]-thick outer corrosion barrier with degraded internals is zero. The applicant's conclusion was based on the observation that, for all simulations, the maximum effective plastic strain was below the ultimate tensile strain of Alloy 22.

For this idealized state, in addition to rupture probability, the applicant calculated puncture probability of the waste package outer corrosion barrier. The applicant considered that a severely deformed outer corrosion barrier may be punctured by the sharp edges of fractured or partially degraded internal components. The applicant calculated a potential for puncture of the outer corrosion barrier. The calculation considered the reduction in the final cross-sectional area of severely deformed outer corrosion barrier, as identified in SNL Section 6.5.1.4.1 (2007ap). The applicant assumed that the probability of outer corrosion barrier puncture is zero until deformation of the waste package outer corrosion barrier is such that the diameter is reduced by 10 cm [4 in], as outlined in SNL p. 6-234 (2007ap). According to the applicant, the puncture of the waste package outer corrosion barrier increased with increase in PGV and with decrease in the outer corrosion barrier thickness. Reported rupture probability ranged from 0.01 to 0.82 for the 23-mm [0.91-in]-thick outer corrosion barrier with degraded internals and from 0.05 to 1.00 for the 17-mm [0.67-in]-thick outer corrosion barrier.

(b)(5)

(b)(5) In SNL Section 6.5.1.2.2 (2007ap), the applicant assessed the effective plastic stresses and strains of the final waste package configuration after reestablishing equilibrium. (b)(5)

(b)(5)

In response to staff's RAI (DOE, 2009br), the applicant provided additional discussion to demonstrate that using stresses and strains computed at the end of dynamic analysis is appropriate and does not underestimate damage to the waste package. The applicant stated that, in the dynamic analyses of the waste package surrounded by rubble, the code cumulatively computes the effective plastic strain, and the plastic strains increase during the analyses' time history. In addition, the applicant stated that the effective plastic strain is larger than the effective strain for the analyses with strain reversals and loading/unloading transitions. Therefore, the applicant concluded that the use of effective plastic strain value obtained at the end of dynamic analyses is appropriate to evaluate the waste package damage. The applicant stated that this approach would not underestimate the waste package rupture probability. (b)(5)

(b)(5)

In calculating the waste package puncture probability, the applicant assumed that the probability of the waste package outer corrosion barrier puncture is zero until deformation reaches a preset value. A waste package diameter reduction of 10 cm [4 in] was selected as the preset limit, as identified in SNL p. 6-234 (2007ap). (b)(5)

(b)(5)

(b)(5) For the highest PGV level used, the applicant calculated the probability of the 17-mm [0.67-in]-thick outer corrosion barrier puncture to be 0.20. (b)(5)

(b)(5)

In SAR Section 2.3.4.5.4.3.1.2 the applicant stated that for a residual stress threshold of 90 percent of the yield stress, the damage area resulted in 0.2 percent of the total waste package outer corrosion barrier surface area. For a residual stress threshold of 105 percent of the yield stress, the damaged area was 3 percent. (b)(5)

(b)(5)

Staff Findings and Conclusions

The NRC staff reviewed the information related to the MDEB abstractions for the waste package performance assessment the applicant provided for compliance with the regulatory requirements of 10 CFR 63.21(c)(9), 63.113(b)–(c), and 63.114(f). This review was performed using guidance in YMRP Section 2.2.1.3.2, Review Methods 1–4, and in accordance with the acceptance criteria in YMRP Section 2.2.1.3.2, Acceptance Criteria 1–4, taking into account the risk significance of the waste package in the context of the repository postclosure performance. The NRC staff makes the following conclusions.

- For Idealized State 1, where the drip shield is structurally stable, the applicant concluded that (i) dynamic impacts of the waste package with the rest of the EBS may cause damage to the waste package from end-to-end impacts between waste packages and between waste package and pallet and (ii) the extent of waste package damage for TSPA abstractions is a function of the waste package type, the waste package internals state, PGV levels, and the outer corrosion barrier thickness.

(b)(5)

- For Idealized State 2, with a collapsed drip shield framework, the applicant concluded that (i) for the case with intact waste package internals, the waste package damage estimated for the Idealized State 3 is bounding and (ii) for the case with degraded internals, the waste package damage estimated for the Idealized State 1 is bounding.

(b)(5)

- For Idealized State 3, where the waste package is in direct contact with rock rubble, the applicant concluded that (i) a waste package with a 23-mm [0.91-in]-thick outer corrosion barrier and degraded internals will not be damaged under seismic events with PGVs below 2.44 m/sec [8 ft/sec] and (ii) the waste package damage depends on the waste package outer corrosion barrier thickness and the PGV levels.

(b)(5)

(b)(5)

(b)(5)

(b)(5)

(b)(5)

2.2.1.3.2.8 Evaluation Findings

The NRC staff has reviewed SAR Section 2.3.4 and associated references (b)(5)

(b)(5)

(b)(5)

2.2.1.3.2.9 References

American Society of Mechanical Engineers. 2001aa. *ASME Boiler and Pressure Vessel Code*. New York City, New York: American Society of Mechanical Engineers.

Anderson, J.G. and J.N. Brune. 1999aa. "Probabilistic Seismic Hazard Analyses Without the Ergodic Assumption." *Seismological Research Letters*. Vol. 70 pp. 19–28.

Bathe, K.-J. 1996aa. *Finite Element Procedures*. Upper Saddle River, New Jersey: Prentice-Hall, Inc.

Bommer, J.J., N.A. Abrahamson, F.O. Strasser, A. Pecker, P.-Y. Bard, H. Bungum, F. Cotton, D. Fäh, F. Sabetta, F. Scherbaum, and J. Struder. 2004aa. "The Challenge of Defining Upper Bounds on Earthquake Ground Motions." *Seismological Research Letters*. Vol. 75 pp. 82–95.

BSC. 2008bl. "Supplemental Earthquake Ground Motion Input for a Geologic Repository at Yucca Mountain, NV." MDL-MGR-MG-000007. Rev. 00. ACN 01, ACN 02. Las Vegas, Nevada: Bechtel SAIC Company, LLC.

BSC. 2005aj. "Peak Ground Velocities for Seismic Events at Yucca Mountain, Nevada." ANL-MGR-GS-000004. Rev. 00. ACN 01, ACN 02. Las Vegas, Nevada: Bechtel SAIC Company, LLC.

BSC. 2004al. "Drift Degradation Analysis." ANL-EBS-MD-000027. Rev. 03. ACN 001, ACN 002, ACN 003, ERD 01. Las Vegas, Nevada: Bechtel SAIC Company, LLC.

BSC. 2004bj. "Technical Basis Document No. 14: Low Probability Seismic Events." Rev. 1. MOL 20000510.0175. Las Vegas, Nevada: Bechtel SAIC Company, LLC.

BSC. 2004bp. "Characterize Framework for Seismicity and Structural Deformation at Yucca Mountain, Nevada." ANL-CRW-GS-000003. Rev. 00. MOL20000510.0175. DOC20040223.0007. Las Vegas Nevada: Bechtel SAIC Company, LLC.

BSC. 2004bq. "Mechanical Assessment of the Drip Shield Subject to Vibratory Motion and Dynamic and Static Rock Loading." CAL-WIS-AC-000002. Rev. 00A. Las Vegas, Nevada: Bechtel SAIC Company, LLC.

Budnitz, R.J., G. Apostolakis, D.M. Boore, L.S. Cluff, K.J. Coppersmith, C.A. Cornell, and P.A. Morris. 1997aa. NUREG/CR-6372, "Recommendations for Probabilistic Seismic Hazard Analysis: Guidance on Uncertainty and Use of Experts—Main Report." Vol. 1. Washington, DC: NRC.

Coraddini, M.L. 2003aa. "Board Comments on February 24, 2003 Panel Meeting on Seismic Issues." Letter (June 27) to Dr. Margaret S.Y. Chu, DOE, Office of Civilian Radioactive Waste Management. Washington, DC: United States Nuclear Waste Technical Review Board.

CRWMS M&O. 1998aa. "Probabilistic Seismic Hazard Analyses for Fault Displacement and Vibratory Ground Motion at Yucca Mountain, Nevada." WBS 1.2 3 2.8.3.6. Las Vegas, Nevada: CRWMS M&O.

CRWMS M&O. 1998ab. "Synthesis of Volcanism Studies for the Yucca Mountain Site Characterization Project." 3781MR1. MOL 19981207.0393. Las Vegas, Nevada: CRWMS M&O.

DOE. 2010aa. "Yucca Mountain—Response to Request for Additional information Regarding License Application (Safety Analysis Report Section 2.2.4), Safety Evaluation Report Vol. 3, Chapter 2.2.1.3.2, Set 4." Letter (January 29) J.R. Williams to J.H. Sulima (NRC). ML100290670. Washington, DC: DOE, Office of Technical Management.

DOE. 2010ab. "Yucca Mountain—Response to Request for Additional information Regarding License Application (Safety Analysis Report Section 2.2.4), Safety Evaluation Report Vol. 3, Chapter 2.2.1.3.2, Set 4." Letter (February 12) J.R. Williams to J.H. Sulima (NRC). ML100470767. Washington, DC: DOE, Office of Technical Management.

DOE. 2010ac. "Yucca Mountain—Response to Request for Additional information Regarding License Application (Safety Analysis Report Section 2.3.4), Safety Evaluation Report Vol. 3, Chapter 2.2.1.3.2, Set 3." Letter (January 28) J.R. Williams to J.H. Sulima (NRC). ML100290132. Washington, DC: DOE, Office of Technical Management.

DOE. 2009aa. "Yucca Mountain—Response to Request for Additional Information Regarding License Application (Safety Analysis Report Section 2.2.2.2), Safety Evaluation Report Vol. 3, Chapter 2.2.1.2.2, Set 2." Letter (January 27) J.R. Williams to J.H. Sulima (NRC). ML090280281. Washington, DC: DOE, Office of Technical Management.

DOE. 2009ab. "Yucca Mountain—Response to Request for Additional Information Regarding License Application (Safety Analysis Report Section 2.2, Table 2.2-5), Safety Evaluation Report Vol. 3, Chapter 2.2.1.2.1, Set 2." Letter (February 23) J.R. Williams to J.H. Sulima (NRC). ML090550099. Washington, DC: DOE, Office of Technical Management.

DOE. 2009aq. "Yucca Mountain—Response to Request for Additional Information Regarding License Application (Safety Analysis Report Sections 1.1.10, 1.2.2, 1.1.5.2, and 1.1.5.3), Safety Evaluation Report Vol. 2, Chapter 2.1.1.1, Set 1." Letter (January 12) J.R. Williams to C. Jacobs (NRC). ML090270750. Washington, DC: DOE, Office of Technical Management.

DOE. 2009bl. "Yucca Mountain—Response to Request for Additional Information Regarding License Application (Safety Analysis Report Sections 2.1, 2.3.11, 2.4.3, and 2.4.4), Safety Evaluation Report Vol. 3, Chapters 2.2.1.4.1, 2.2.1.4.2, and 2.2.1.4.3, Set 1." Letter (July 29) J.R. Williams to J.H. Sulima (NRC). ML091680648. Las Vegas, Nevada: DOE, Office of Civilian Radioactive Waste Management.

DOE. 2009bp. "Yucca Mountain—Response to Request for Additional information Regarding License Application (Safety Analysis Report Section 2.3.4.5.3.3.2), Safety Evaluation Report Vol. 3, Chapter 2.2.1.3.2, Set 1." Letter (March 6) J.R. Williams to J.H. Sulima (NRC). ML090680836. Washington, DC: DOE, Office of Technical Management.

DOE. 2009bq. "Yucca Mountain—Response to Request for Additional information Regarding License Application (Safety Analysis Report Section 2.3.4), Safety Evaluation Report Vol. 3, Chapter 2.2.1.3.2, Set 2." Letter (November 24) J.R. Williams to J.H. Sulima (NRC). ML093360253. Washington, DC: DOE, Office of Technical Management.

DOE. 2009br. "Yucca Mountain—Response to Request for Additional information Regarding License Application (Safety Analysis Report Section 2.3.4), Safety Evaluation Report Vol. 3, Chapter 2.2.1.3.2, Set 2." Letter (December 11) J.R. Williams to J.H. Sulima (NRC). ML093480212. Washington, DC: DOE, Office of Technical Management.

DOE. 2009bs. "Yucca Mountain—Response to Request for Additional information Regarding License Application (Safety Analysis Report Section 2.3.4), Safety Evaluation Report Vol. 3, Chapter 2.2.1.3.2, Set 2." Letter (December 15) J.R. Williams to J.H. Sulima (NRC). ML093500116. Washington, DC: DOE, Office of Technical Management.

DOE. 2009bt. "Yucca Mountain—Response to Request for Additional information Regarding License Application (Safety Analysis Report Section 2.3.4), Safety Evaluation Report Vol. 3, Chapter 2.2.1.3.2, Set 2." Letter (November 30) J.R. Williams to J.H. Sulima (NRC). ML093350040. Washington, DC: DOE, Office of Technical Management.

DOE. 1997aa. "Topical Report YMP/TR-002-NP: Methodology To Assess Fault Displacement and Vibratory Ground Motion Hazards at Yucca Mountain." Rev. 1. Las Vegas, Nevada: DOE, Office of Civilian Radioactive Waste Management.

Ferrill, D.A., J.A. Stamatakis, and D. Sims. 1999ab. "Normal Fault Corrugation: Implications for Growth and Seismicity of Active Normal Faults." *Journal of Structural Geology*. Vol. 21. pp. 1,027–1,038.

Ferrill, D.A., J.A. Stamatakis, S.M. Jones, B. Rahe, H.L. McKague, R. Martin, and A.P. Morris. 1996aa. "Quaternary Slip History of the Bare Mountain Fault (Nevada) From the Morphology and Distribution of Alluvial Fan Deposits." *Geology*. Vol. 24. pp. 559–562.

Gray, M.B., J.A. Stamatakis, D.A. Ferrill, and M.A. Evans. 2005aa. "Fault-Zone Deformation in Welded Tuffs at Yucca Mountain, Nevada, U.S.A." *Journal of Structural Geology*. Vol. 27. pp. 1,873–1,891.

Ibarra, L., T. Wilt, G. Ofoegbu, and A. Chowdhury. 2007aa. "Structural Performance of Drip Shield Subjected to Static and Dynamic Loading." San Antonio, Texas: CNWRA.

Ibarra, L., T. Wilt, G. Ofoegbu, R. Kazban, F. Ferrante, and A. Chowdhury. 2007ab. "Drip Shield—Waste Package Mechanical Interaction—Progress Report." San Antonio, Texas: CNWRA.

Kana, D.D., B.H.G. Brady, B.W. Vanznat, and P.K. Nair. 1991aa. NUREG/CR-5440, "Critical Assessment of Seismic and Geotechnical Literature Related to a High-Level Nuclear Waste Underground Repository." Washington DC: NRC.

Keefer, W.R., J.W. Whitney, and E.M. Taylor. 2004aa. "Quaternary Paleoseismology and Stratigraphy of the Yucca Mountain Area, Nevada." U.S. Geological Survey Professional Paper 1689. Denver, Colorado: U.S. Geological Survey.

Livermore Software Technology Corporation. 2003aa. *LS-DYNA Users Manual*. Ver. 970. Livermore, California: Livermore Software Technology Corporation.

McGuire, R.K., W.J. Silva, and C.J. Costantino. 2001aa. NUREG/CR-6728, "Technical Basis for Revision of Regulatory Guidance on Design Ground Motions Hazard- and Risk-Consistent Ground Motion Spectra Guidelines." Washington, DC: NRC.

Morris, A.P., D.A. Ferrill, D.W. Sims, N. Franklin, and D.J. Waiting. 2004aa. "Patterns of Fault Displacement and Strain at Yucca Mountain, Nevada." *Journal of Structural Geology*. Vol. 26. pp. 1,707–1,725.

Morris, A.P., D.A. Ferrill, and D.B. Henderson. 1996aa. "Slip-Tendency Analysis and Fault Reactivation." *Geology*. Vol. 24. pp. 275–278.

NRC. 2009ab. "Division of High-Level Waste Repository Safety Director's Policy and Procedure Letter 14: Application of YMRP for Review Under Revised Part 63." Published March 13, 2009. ML090850014. Washington, DC: NRC.

NRC. 2005aa. NUREG-1762, "Integrated Issue Resolution Status Report." Rev. 1. Washington, DC: NRC.

NRC. 2003aa. NUREG-1804, "Yucca Mountain Review Plan—Final Report." Rev. 2. Washington, DC: NRC.

NRC. 2003ae. Regulatory Guide 3.73, "Site Evaluations and Design Earthquake Ground Motion for Dry Cask Independent Spent Fuel Storage and Monitored Retrievable Storage Installations." Washington, DC: NRC.

NRC. 1999aa. "Issue Resolution Status Report, Key Technical Issue: Structural Deformation and Seismicity." Rev. 2. Washington, DC: NRC.

NRC. 1997ab. Regulatory Guide 1.165, "Identification and Characterization of Seismic Sources and Determination of Safe Shutdown Earthquake Ground Motion." Washington, DC: NRC.

NRC. 1996aa. NUREG-1563, "Branch Technical Position on the Use of Expert Elicitation in the High-Level Radioactive Waste Program." Washington, DC: NRC.

Ofoegbu, G., R. Fedors, C. Grossman, S. Hsiung, L. Ibarra, C. Manepally, J. Myers, M. Nataraja, O. Pensado, K. Smart, and D. Wyrick. 2007aa. "Summary of Current Understanding of Drift Degradation and Its Effects on Performance at a Potential Yucca Mountain Repository." Rev. 1. CNWRA 2006-02. ML071030115. San Antonio, Texas: CNWRA.

Pomeroy, D., L. Ibarra, K. Hricisak, T. Wilt, K.T. Chiang, R. Kazban, and A. Chowdhury. 2007aa. "Experimental Tests on Drip Shield—Waste Package Mechanical Interaction—Progress Report." San Antonio, Texas: CNWRA.

Schneider, J.F., N.A. Abrahamson, and T.C. Hanks. 1996aa. "Ground Motion Modeling of Scenario Earthquakes at Yucca Mountain: Final Report for Activity 8.3.1.17.3.3." MOL19980617.0477. Las Vegas, Nevada: Yucca Mountain Project.

SNL. 2008ab. "Features, Events, and Processes for the Total System Performance Assessment: Analyses." ANL-WIS-MD-000027. Rev. 00. ACN 01, ERD 01, ERD 02. Las Vegas, Nevada: Sandia National Laboratories.

SNL. 2008ag. "Total System Performance Assessment Model/Analysis for the License Application." MDL-WIS-PA-000005. Rev. 00. AD 01, ERD 01, ERD 02, ERD 03, ERD 04. Las Vegas, Nevada: Sandia National Laboratories.

SNL. 2007ap. "Mechanical Assessment of Degraded Waste Packages and Drip Shields Subject to Vibratory Ground Motion." MDL-WIS-AC-000001. Rev. 00. ERD 01, ERD 02. Las Vegas, Nevada: Sandia National Laboratories.

SNL. 2007ay. "Seismic Consequence Abstraction." MDL-WIS-PA-000003. Rev. 03. ERD 01. Las Vegas, Nevada: Sandia National Laboratories.

Spudich, P., W.B. Joyner, A.G. Lindh, D.M. Boore, B.M. Margaris, and J.B. Fletcher. 1999aa. "SEA99: A Revised Ground Motion Prediction Relation for Use in Extensional Tectonic Regimes." *Bulletin of the Seismological Society of America*. Vol. 89, No. 5. pp. 1,156–1,170.

Stamatakis, J.A., D. Biswas, and M. Silver. 2007aa. "Supplemental Evaluation of Geophysical Information Used To Detect and Characterize Buried Volcanic Features in the Yucca Mountain Region." San Antonio, Texas: CNWRA.

Stamatakis, J.A., D.A. Ferrill, and K.P. Spivey. 1998aa. "Paleomagnetic Constraints on the Tectonic Evolution of Bare Mountain, Nevada." *Geological Society of America Bulletin*. Vol. 100. pp. 1,530–1,546.

Stamatakis, J.A., C.B. Connor, and R.H. Martin. 1997ab. "Quaternary Basin Evolution and Basaltic Volcanism of Crater Flat, Nevada, From Detailed Ground Magnetic Surveys of the Little Cones." *Journal of Geology*. Vol. 105. pp. 318–330.

Waiting, D.J., J.A. Stamatakis, D.A. Ferrill, D.W. Sims, A.P. Morns, P.S. Justus, and K.I. Abou-Bakr. 2003aa. "Methodologies for the Evaluation of Faulting at Yucca Mountain, Nevada." *Proceedings of the 10th International High-Level Radioactive Waste Management Conference*, Las Vegas, Nevada, March 30–April 2, 2003. La Grange Park, Illinois: American Nuclear Society. pp. 377–387.

Wernicke, B., J.L. Davis, R.A. Bennett, J.E. Normandeau, A.M. Friedrich, and N.A. Niemi. 2004aa. "Tectonic Implications of a Dense Continuous GPS Velocity Field at Yucca Mountain, Nevada." *Journal of Geophysical Research*. Vol. 109, No. B12404. p. 13.

Youngs, R.R., W.J. Arabasz, R.E. Anderson, A.R. Ramelli, J.P. Ake, D.B. Slemmons, J.P. McCalpin, D.I. Doser, C.J. Friedrich, F.H. Swan III, A.M. Rogers, J.C. Yount, L.W. Anderson, K.D. Smith, R.L. Bruhn, P.L. Knuepfer, R.B. Smith, C.M. dePolo, D.W. O'Leary, K.J. Coppersmith, S.K. Pezzopane, D.P. Schwartz, J.W. Whitney, S.S. Olig, and G.R. Toro. 2003aa. "A Methodology for Probabilistic Fault Displacement Hazard Analyses (PFDHA)." *Earthquake Spectra*. Vol. 19, No. 1. pp. 191–219.

CHAPTER 6

2.2.1.3.3 Quantity and Chemistry of Water Contacting Engineered Barriers and Waste Forms

2.2.1.3.3.1 Introduction

This Safety Evaluation Report (SER) chapter addresses those features, events, and processes (FEPs) included in the U.S. Department of Energy's (DOE) abstraction¹ of the repository drift system that may alter the chemical composition and volume of water contacting the drip shield and waste package surfaces (NRC, 2005aa). DOE described this abstraction in Safety Analysis Report (SAR) Sections 2.3.5 and 2.3.7 (DOE, 2008ab). This SER chapter provides the U.S. Nuclear Regulatory Commission's (NRC) evaluation of the abstraction of key FEPs that address the following topics: (i) the chemistry of water entering the drifts, (ii) the chemistry of water in the drifts, and (iii) the quantity of water in contact with the engineered barrier system (EBS).² These three abstraction topics provide input needed to model the features and performance of the EBS (e.g., drip shield and waste package) and their contributions to barrier functions. For example, in its license application, DOE relied on corrosion tests that were conducted on waste package and drip shield materials under a range of geochemical environments. The range of aqueous testing environments was deduced from a range of potential starting water compositions (Topic i) and from knowledge of near-field and in-drift processes that alter these compositions (Topics ii and iii).

2.2.1.3.3.2 Regulatory Requirements

Model abstractions used in the applicant's postclosure performance assessment must meet the regulatory requirements given in 10 CFR 63.114 (Requirements for Performance Assessment) and 63.342 (Limits on Performance Assessment), to support the predictions of compliance for 63.113 (Performance Objectives for the Geologic Repository after Permanent Closure). Specific compliance with 63.113 is reviewed in SER Section 2.2.1.4.1.

The requirements for performance assessment in 10 CFR 63.114 require the applicant to

- Include appropriate data related to the geology, hydrology, and geochemistry of the surface and subsurface from the site and the region surrounding Yucca Mountain
- Account for uncertainty and variability in the parameter values used to model the quantity and chemistry of water contacting engineered barriers and waste forms

¹As used in the SER, the term "abstraction" refers to the representation of the essential components of a process model into a suitable form for use in a total system performance assessment. A model abstraction is intended to maximize the use of limited computational resources while allowing a sufficient range of sensitivity and uncertainty analyses. An abstracted model is a model that reproduces, or bounds, the essential elements of a more detailed process model and captures uncertainty and variability in what is often, but not always, a simplified or idealized form.

²The abstraction of key FEPs that address thermal-hydrologic processes affecting seepage rates are reviewed in SER Section 2.2.1.3.6; those that address corrosion processes affecting the drip shield and waste packages are reviewed in SER Section 2.2.1.3.1; and those that address the quantity and chemistry of water inside breached waste packages and the invert are reviewed in SER Section 2.2.1.3.4. Also, the review of the rationale for key FEPs that DOE has excluded from these abstractions is covered in SER Section 2.2.1.2.1.

- Consider alternative conceptual models for the quantity and chemistry of water contacting engineered barriers and waste forms
- Provide technical bases for the inclusion of FEPs affecting the quantity and chemistry of water contacting engineered barriers and waste forms, including effects of degradation, deterioration, or alteration processes of engineered barriers that would adversely affect performance of the natural barriers, consistent with the limits on performance assessment in 10 CFR 63.342
- Provide technical basis for the models of the quantity and chemistry of water contacting engineered barriers and waste forms that in turn provide input or otherwise affect other models and abstractions

10 CFR 63.114(a) considers performance assessment for the initial 10,000 years following permanent closure. 10 CFR 63.114(b) and 63.342 consider the performance assessment methods for the time from 10,000 years through the period of geologic stability, defined in 10 CFR 63.302 as 1 million years following disposal. These sections require that through the period of geologic stability, with specific limitations, the applicant

- Use performance assessment methods consistent with the performance assessment methods used to demonstrate compliance for the initial 10,000 years following permanent closure
- Include in the performance assessment those FEPs used in the performance assessment for the initial 10,000 year period

For this model abstraction of the quantity and chemistry of water contacting engineered barriers and waste forms, 10 CFR 63.342(c)(1) further provides that DOE assess the effects of seismic and igneous activity on the repository performance, subject to the probability limits in 63.342(a) and 63.342(b). Specific constraints on the analysis required for seismic and igneous activity are given in 10 CFR 63.342(c)(1)(i) and 10 CFR 63.342(c)(1)(ii), respectively.

In addition, for this model abstraction of the quantity and chemistry of water contacting engineered barriers and waste forms, 10 CFR 63.342(c)(2) further provides that DOE may consider climate change after 10,000 years by using a constant-in-time specification of the mean and uncertainty distribution for repository-average deep percolation rate for the period from 10,000 to 1million years. DOE elected to use this representation in its SAR. Thus, implementation of the specified representative percolation rate and its uncertainty distribution is reviewed for the post-10,000-year period.

NRC staff review of the license application follows the guidance laid out the Yucca Mountain Review Plan (YMRP), NUREG-1804, Section 2.2.1.3.3, Quantity and Chemistry of Water Contacting Engineered Barriers and Waste Forms (NRC, 2003aa), as supplemented by additional guidance for the period beyond 10,000 years after permanent closure (NRC, 2009ab). The acceptance criteria in the YMRP generically follow 10 CFR 63.114(a). Following the guidance, the NRC staff review of the applicant's abstraction of the quantity and chemistry of water contacting engineered barriers and waste forms considered five criteria:

- System description and model integration are adequate.
- Data are sufficient for model justification.

- Data uncertainty is characterized and propagated through the abstraction.
- Model uncertainty is characterized and propagated through the abstraction.
- Model abstraction output is supported by objective comparisons.

Because 10 CFR Part 63 specifies the use of a risk-informed approach for the review of a license application, the guidance provided by YMRP, as supplemented by NRC (2009ab), is followed to the extent reasonable for aspects of the quantity and chemistry of water contacting engineered barriers and waste forms important to repository performance. Whereas NRC staff considered all five criteria in their review of information provided by DOE, only aspects that substantively affect results of the performance assessment, as judged by NRC staff, are discussed in this chapter. NRC staff's judgment is based both on risk information provided by DOE, and staff's knowledge, experience, and independent analyses.

2.2.1.3.3.3 Technical Review

2.2.1.3.3.3.1 Chemistry of Water Entering Drifts

The chemistry of water entering drifts abstraction uses site-specific and literature-derived information as inputs to the applicant's Near-Field Chemistry (NFC) model, which simulates chemical interactions of minerals in the Yucca Mountain host rocks with pore waters that percolate downward toward the repository. The model calculates (i) a water-rock interaction parameter that is used to predict initial seepage water compositions important to drip shield and waste package corrosion; (ii) radionuclide solubility [key parameters are pH, ionic strength (I), and concentrations of chloride (Cl^-), nitrate (NO_3^-), and fluoride (F^-)]; and (iii) the range of in-drift carbon dioxide partial pressures ($p\text{CO}_2$). Important processes related to developing these parameters are discussed later in this chapter under the heading "Conceptual Model."

DOE used the results of its NFC model as inputs to other process-level models and direct inputs to the Total System Performance Assessment (TSPA) model. Potential seepage water compositions are used by the in-drift chemical and physical environment abstraction (reviewed in SER Section 2.2.1.3.3.3.2) and the waste package and drip shield corrosion abstraction at the process level (reviewed in SER Section 2.2.1.3.3.1). The range of in-drift $p\text{CO}_2$ values the NFC model predicts is used to generate a lookup table in the TSPA model, which is sampled to provide inputs to the waste form degradation and mobilization abstraction (reviewed in SER Section 2.2.1.3.4). SER Section 2.2.1.3.6 reviews the abstraction that addresses thermal-hydrologic processes affecting seepage rates, SER Section 2.2.1.3.1 reviews the abstraction that addresses corrosion processes affecting the drip shield and waste packages, and SER Section 2.2.1.3.4 reviews the abstraction that addresses the quantity and chemistry of water inside breached waste packages and the invert.

In SAR Table 2.1-3 and DOE (2009a), the chemistry of water flowing into drifts is recognized as important to the barrier capability of the Emplacement Drift, one component of the EBS.

(b)(5)

(b)(5)

The NRC staff review in SER Section 2.2.1.3.1 considers the conditions under which localized corrosion is not expected to occur. In DOE's system of engineered barriers, titanium drip shields prevent seepage water from contacting the waste package. DOE predicts that the drip shields will maintain their capability until

compromised by mechanical or corrosive failure. The DOE performance assessment analyses and (b)(5)

(b)(5)

(b)(5)

In the DOE model, as long as the drip shields remain intact, only slow general corrosion of waste packages occurs and only diffusional release of radionuclides is possible. (b)(5)

(b)(5)

Mechanical processes are the other means by which drip shield performance may be compromised. DOE excluded early drip shield failure due to partial or complete collapse of drifts due to thermal effects (FEP 2.1.07.02.0A) on the basis of "low consequence." The adequacy of the rationale for excluding this specific FEP is reviewed in SER Section 2.2.1.2.1.3.2. The DOE performance assessment (b)(5)

(b)(5)

(b)(5)

DOE

calculated that conditions in the drift (e.g., temperature, pH, seepage water chemistry) may support localized corrosion of the waste package if the drip shield fails and allows seepage water to contact the waste package within approximately 12,000 years after repository closure, as described in DOE Enclosure 11 (2009dg). Following 12,000 years after repository closure, DOE calculated that there is a low probability for conditions in the drift to support localized corrosion of the waste package, if the drip shield fails and allows seepage water to contact the waste package, even given a somewhat elevated temperature of the waste package. The DOE model calculated that both the pH and nitrate-to-chloride ratio of water that may contact the waste package will generally be too high to initiate localized corrosion beyond 12,000 years after repository closure.

(b)(5)

(b)(5)

This approach is consistent with YMRP guidance for conducting a risk-informed, performance-based review. (b)(5)

(b)(5)

Conceptual Model

This section addresses YMRP Section 2.2.1.3.3 Acceptance Criterion 1 and 2: "System Description and Model Integration are Adequate" (focused on system description), and "Data for Model Justification are Sufficient." The NRC staff reviewed the information provided in SAR

Section 2.3.5.3 (and relevant references) to evaluate the adequacy of the conceptual model of the chemistry of water entering the drifts.

SAR Table 2.2-1 contains the FEPs that DOE believes are potentially relevant to the chemistry of water entering drifts. DOE evaluated and included the following FEPs in this abstraction: (i) Chemical characteristics of groundwater in the unsaturated zone (FEP 2.2.08.01.0B), (ii) Chemistry of water flowing into the drift (FEP 2.2.08.12.0A), and (iii) Chemical effects of magma and magmatic volatiles (FEP 1.2.04.04.0B). DOE evaluated and excluded (on the basis of low probability or low consequence) the following FEPs from this abstraction: (i) Hydrothermal activity (FEP 1.2.06.00A), (ii) Altered soil or surface water chemistry (FEP 1.4.06.01.0B), (iii) Rind (chemically altered zone) forms in the near-field (FEP 2.1.09.12.0A), and (iv) Re-dissolution of precipitates directs more corrosive fluids to waste packages (FEP 2.2.08.04.0A). The exclusion of these FEPs from this abstraction is reviewed in SER Section 2.2.1.2.1.3.2. Furthermore, DOE's pre-10,000-year treatment of FEPs in this abstraction continues unchanged beyond the 10,000-year postdisposal period through the period of geologic stability (defined as 1 million years in 10 CFR 63.302).

The DOE conceptual model describes the chemical evolution of water as it percolates vertically toward the repository drifts. In the model, the water flows through the Topopah Spring repository host rock, a homogeneous unit that is 200 m [656.2 ft] thick, with average rock and hydrologic properties derived from measurements from equivalent units in the Yucca Mountain vicinity. Pore waters percolating through the unsaturated zone are modeled as chemically evolving by dissolution of alkali feldspar, which makes up about 60 percent of the host rock. Because of alkali feldspar's abundance, DOE assumed its dissolution represented host rock dissolution processes. The rate of feldspar dissolution increases as pore waters encounter elevated host rock temperatures that result from heat generated from radioactive waste decay.

After pore waters flow through the Topopah Spring rock to a location above the repository, the model calculates a chemical composition by combining one of four initial pore water compositions with an amount of feldspar predicted to have dissolved, and assuming chemical equilibrium with the minerals calcite and amorphous silica. Cation exchange onto clays or zeolites is not considered explicitly. Gas phase carbon dioxide (CO_2) concentrations are controlled by contributions from the CO_2 present in the local aqueous phase, CO_2 released from the evaporation of water (containing dissolved CO_2), and CO_2 ($10^{-3.5}$ atmospheres) present in the atmosphere. Calcite precipitation and feldspar dissolution influence the aqueous phase concentration of CO_2 . Temperature also has a strong effect on CO_2 because this gas partitions more strongly to the gas phase at elevated temperatures.

(b)(5)

In addition, DOE considered the seismic and igneous intrusive scenarios in the abstraction of seepage water chemistry. The conceptual model for seepage water chemistry in the seismic scenario is the same as for the nondisruptive scenario described previously. For the igneous intrusive scenario, in which basaltic magma similar in composition to dikes found in the Yucca Mountain area fills much of the drifts, DOE considered the composition of seepage waters contacting the waste to be consistent with water that has reacted with basalt [BSC

Section 6.3.1.3.5(a), (2005ad)). DOE considered three basalt water compositions from large fractured basalt reservoirs (SAR Tables 2.3.7-10 and 2.3.7-11).

On the basis of the review of this information and knowledge of likely basalt-water interactions, the NRC staff (b)(5)

(b)(5)

(b)(5)

Additional discussion of

basaltic magmas can be found in SER Section 2.2.1.3.10.1. (b)(5)

(b)(5)

Initial Range of Pore Water Chemistries

This section addresses YMRP Section 2.2.1.3.3 Acceptance Criterion 3 and 5: "Data Uncertainty is Characterized and Propagated Through the Model Abstraction," and "Model Abstraction Output is Supported by Objective Comparisons." DOE described input parameter development and parameter uncertainty in SAR Sections 2.3.5.3.2.2.1 and 2.3.5.3.2.2.2. The NRC staff reviewed the information provided in the SAR (and relevant references) to evaluate whether the model inputs for the chemistry of water entering the drift abstraction are adequate. This evaluation focused on evaluating the uncertainty in the range of initial pore water chemistry [especially pH, ionic strength (*I*), and concentrations of chloride (Cl) and nitrate (NO₃)] and carbon dioxide partial pressures (*p*CO₂). In SAR Section 2.3.5.5 DOE identified these parameters as important inputs to the abstractions that deal with drip shield and waste package corrosion.

DOE's NFC model considers four initial pore water compositions as inputs. DOE assumed these four compositions represent the range of pore water compositions expected for the entire Yucca Mountain repository. A multistep screening process, based on charge balance and partial pressure of carbon dioxide, was used to evaluate 90 pore water analyses from Yucca Mountain cores that DOE deemed to be sufficiently complete for use in the NFC model. Thirty-four pore water compositions were identified as meeting the charge balance criteria (± 10 percent) and as having been minimally affected by microbial alteration (thus suitable for further consideration). Statistical cluster analysis was performed on the 34 acceptable samples, and 4 distinct groupings, or clusters, of samples were identified. The sample with the composition closest to the centroid of each cluster was selected as representative of each cluster.³

The NRC staff evaluated the information provided in SAR Section 2.3.5.3.2.2.1 and DOE (2009ck). A large portion of the 56 pore water compositions that the DOE screening process eliminated from consideration had larger chloride-to-nitrate ratios than the 34 samples found to be acceptable. DOE attributed the high chloride-to-nitrate ratios of the screened out samples to the loss of nitrate by microbial activity during sample storage.

Comment (b)(5)

(b)(5)

(b)(5)

³Clustering analysis is a standard method for finding clusters of data that are similar in some sense to one another. The members of a cluster are more like each other than they are like members of other clusters. The centroid represents the most typical case in a cluster.

The NRC staff evaluated the support for the criteria used to screen the initial pore water compositions used as inputs to the NFC model (DOE, 2009ck). (b)(5)

(b)(5)

The Range of Seepage Water Chemistries Predicted by the NFC Model

This section addresses YMRP Section 2.2.1.3.3 Acceptance Criterion 2 and 4: "Data for Model Justification are Sufficient," and "Model Uncertainty is Characterized and Propagated Through the Model Abstraction." The NRC staff reviewed the information provided in SAR Section 2.3.5.3 (and relevant references) to evaluate whether the implementation of the conceptual model of the chemistry of water entering the drifts is adequate. (b)(5)

(b)(5)

Comment	(b)(5)
	(b)(5)

DOE used the NFC model to determine the potential chemical compositions of seepage waters entering the drifts during the thermal period and when pre-waste-emplacement conditions return. The model uses a decoupled approach where hydrological and thermal processes are calculated independently. Chemistry is loosely coupled to the thermal and hydrological processes through the dissolution of alkali feldspar. The chemical composition of potential seepage waters is calculated at a location above the repository and at the bottom of the model domain using the geochemical speciation and reaction path code EQ3/6.

The NRC staff reviewed the information provided in SAR Sections 2.3.5.3.3.3 and 2.3.5.3.3.5 (and selected documents) and DOE (2009ck) to evaluate the adequacy of model support for the range of seepage water compositions the NFC model predicted. The NRC staff reviewed the DOE's comparison of the range of pH, chloride-to-nitrate ratio, and ionic strength values the NFC model predicted with the calculated values of pH, chloride-to-nitrate ratio, and ionic strength for the 34 pore water samples included in its abstraction. (b)(5)

(b)(5)

Abstraction and Integration

This section addresses YMRP Section 2.2.1.3.3 Acceptance Criterion 1: "System Description and Model Integration are Adequate" (focused on integration). The NRC staff reviewed the information provided in SAR Section 2.3.5.3.4 (and relevant references) to evaluate whether model integration and abstraction into the TSPA model of the chemistry of water entering the drifts is adequate. None of the results from the chemistry of water entering the drifts are directly abstracted into TSPA model. The NFC model provides inputs to the EBS Physical and Chemical Environment Abstraction model. Results from the EBS Physical and Chemical Environment Abstraction model are abstracted into the TSPA model. Both the EBS Physical and Chemical Environment Abstraction model and the abstraction of results into the TSPA model are evaluated in SER Section 2.2.1.3.3.3.2.

(b)(5)

(b)(5)

The NRC staff has evaluated the information provided in SAR Section 2.3.5.3.3.2.6 and compared it with the multiscale thermal-hydrologic modeling (SAR Section 2.3.5.4.1) and the in-drift condensation modeling (SAR Section 2.3.5.4.2). (b)(5)

(b)(5)

Summary

(b)(5)

(b)(5)

The NRC staff reviewed the description of the near-field environment, the assumptions incorporated in the NFC model abstraction, the range of initial pore water compositions, the range of predicted seepage water compositions, and integration with other model abstractions. (b)(5)

(b)(5)

(b)(5)

2.2.1.3.3.2

Chemistry of Water in the Drifts

Comment (b)(5)

(b)(5)

The abstraction for the chemistry of water in the drifts receives information on input gas and water compositions from the NFC model. The main purpose of the DOE in-drift chemistry abstraction is to predict the range of chemical compositions for seepage on the waste package or in the invert for a given set of temperature, relative humidity, and $p\text{CO}_2$ conditions. This abstraction is implemented in the TSPA model in the form of lookup tables. These lookup tables enable the TSPA model to provide the parameters (and their uncertainties) needed to represent the chemical environment for the corrosion of waste package surfaces and for radionuclide transport in the invert.

The in-drift chemistry abstraction is not used to provide input to drip shield corrosion modeling. Instead, DOE modeled general corrosion of the titanium drip shield using two corrosion rate values based on weight-loss data determined from long-term corrosion tests. The NRC staff's evaluation of the DOE drip shield general corrosion model abstraction is discussed in SER Section 2.2.1.3.1.3.1.1. In addition, SER Section 2.2.1.3.6 reviews the abstraction for thermal-hydrologic processes affecting seepage rates; SER Section 2.2.1.3.1 reviews the abstraction for corrosion processes affecting the drip shield and waste packages; and SER Section 2.2.1.3.4 reviews the abstraction for the quantity and chemistry of water inside breached waste packages and the invert.

According to SAR Table 2.1-3 and DOE (2009an), the chemistry of water in the drifts is important to the capability of the EBS Barrier-Emplacement Drift. (b)(5)

(b)(5)

(b)(5)

Through its FEP screening process, DOE excluded several processes that might have been important to the chemical evolution of water in the drifts, such as deliquescence (FEPs 2.1.09.28.0A and 2.1.09.28.0B). The adequacy of the rationale for excluding specific FEPs from the in-drift water chemistry abstraction is reviewed in SER Section 2.2.1.2.1.3.2.

The NRC staff's review focuses on evaluating whether (i) the conceptual model includes important processes, (ii) data and model justification are adequate, (iii) data and model uncertainty are adequate, and (iv) model abstraction support is adequate.

Conceptual Model and Important Processes

This section addresses YMRP Section 2.2.1.3.3 Acceptance Criterion 1: "System Description and Model Integration are Adequate. The NRC staff reviewed information DOE provided in SAR Section 2.3.5.5 (and relevant references) and DOE (2009cv,cw) to evaluate whether the conceptual model used to characterize the in-drift chemical environment is adequate. (b)(5)

(b)(5)

SAR Table 2.2-1 contains the FEPs that DOE believes are potentially relevant to the chemistry of water in the drifts. DOE evaluated and included the following FEPs in the in-drift water chemistry abstraction: (i) Chemical characteristics of water in drifts (FEP 2.1.09.01.0A); (ii) Reduction-oxidation potential in drifts (FEP 2.1.09.06.0B); (iii) Reaction kinetics in drifts (FEP 2.1.09.07.0B); and (iv) Thermal effects on chemistry and microbial activity in the EBS

(FEP 2.1.11.08.0A). DOE evaluated and excluded, on the basis of low probability or low consequence, the following FEPs in this abstraction:

- Chemical effects of excavation and construction in EBS (FEP 1.1.02.00.0A)
- Undesirable materials left [in the repository] (FEP 1.1.02.03.0A)
- Seismic-induced drift collapse alters in-drift chemistry (FEP 1.2.03.02.0E)
- Chemical properties and evolution of backfill (FEP 2.1.04.02.0A)
- Erosion or dissolution of backfill (FEP 2.1.04.03.0A)
- Chemical effects of rock reinforcement and cementitious materials in EBS (FEP 2.1.06.01.0A)
- Chemical degradation of invert (FEP 2.1.06.05.0D)
- Chemical effects at EBS component interfaces (FEP 2.1.06.07.0A)
- Gas explosions in EBS (FEP 2.1.12.08.0A)
- Radiolysis (FEP 2.1.13.01.0A)
- Complexation in EBS (FEP 2.1.09.13.0A)
- Microbial activity in EBS (FEP 2.1.10.01.0A)
- Gas generation (CO₂, CH₄, H₂S) from microbial activity (FEP 2.1.12.04.0A)
- Radiological mutation of microbes (FEP 2.1.13.03.0A)
- Chemical effects of excavation and construction in the near-field (FEP 2.2.01.01.0B)

The adequacy of the rationale for excluding these specific FEPs from the in-drift water chemistry abstraction is reviewed in SER Section 2.2.1.2.1.3.2. Furthermore, DOE's pre-10,000-year treatment of FEPs in this abstraction continues unchanged beyond the 10,000-year postdisposal period through the period of geologic stability.

DOE explained its conceptual model for in-drift chemistry as follows. early in the postclosure period, drift wall temperatures higher than the boiling point of water will prevent seepage from occurring. After the drift wall temperatures fall below the boiling point of water and the rewetting process begins, seepage may occur, as local hydrologic conditions allow. Because waste package surface temperatures will still be elevated, seepage water falling on the drip shield, and on the waste package in the event of drip shield failure, will evaporate and concentrate. As waste package temperatures continue to decrease, relative humidity will increase to the point that wet conditions persist. Over time, further increases in relative humidity will suppress evaporation and result in progressively more dilute aqueous solutions on the waste package surface or in the invert.

DOE's model considers how the chemistry of seepage water will evolve after it enters the repository drifts. In its conceptual model, DOE considered the effects of seepage water evaporation, condensation, gas-water interaction, precipitation and dissolution of salts, and salt separation. (b)(5)

(b)(5)

(b)(5)

DOE's conceptual model describes in general terms how each of these processes influenced the chemistry of in-drift water. For example, seepage evaporation will cause the most soluble components to concentrate in the aqueous phase and minerals to precipitate. With precipitation, the relative concentrations of components remaining in solution will change. Salt separation may occur when seepage water flows downward over the drip shield or waste package surface while evaporation is occurring. During this process, spatial separation of chemical components could occur, transporting the more soluble aqueous components (e.g., NO_3^-) and leaving behind as precipitates the less soluble constituents (e.g., Cl^- , as NaCl precipitate). Condensation of water, which would dilute the aqueous phase concentration, could occur when the in-drift relative humidity is high enough. To model the in-drift water chemistry, DOE used the IDPS model, which is a process-level geochemical model that accounts for the effects of in-drift processes. The IDPS model was implemented using the EQ3/6 geochemical code and a Pitzer thermodynamic database that was developed for use in the IDPS model.

In natural systems, the chemical evolution of evaporating water generally is controlled by the high solubility of chloride and nitrate salt minerals relative to the moderate solubility of calcium sulfate and the low solubility of calcium carbonate minerals—a mechanism referred to as a chemical divide. Thus, evaporation of initially dilute natural waters at the Earth's surface, such as in saline lakes, typically leads to the formation of one of three brine types, depending on the initial composition of the system: calcium chloride brine, alkaline carbonate brine, or high sulfate brine. DOE concluded the same brine types could occur within the drifts because in-drift brines would be produced by processes similar to those that occur at the Earth's surface.

DOE used several assumptions in its abstraction of in-drift water chemistry. For example, all aqueous and gas constituents are assumed to achieve and maintain local equilibrium (b)(5)

(b)(5)

(b)(5)

Also, the seepage waters on the waste package surface are assumed to reach equilibrium with the relative humidity on the waste package surface. (b)(5)

(b)(5)

(b)(5)

In addition, DOE assumed that an aqueous solution is present for all temperature and relative humidity conditions once seepage onto a waste package occurs.

(b)(5)

DOE also assumed the chemical compositions of drift wall condensation and of condensation that penetrates a failed drip shield to be the same as seepage composition and to be benign.

(b)(5)

In the salt separation abstraction, DOE assumed that the solution that forms during the salt separation process is chloride rich. (b)(5)

(b)(5)

With the IDPS model, DOE conducted a series of seepage evaporation/dilution analyses at discrete temperature, relative humidity, and $p\text{CO}_2$ values. The analyses used as input the water compositions derived from the NFC model using 11 water-rock interaction parameters for each of the 4 representative pore water compositions—a total of 44 water compositions. DOE selected 3 temperatures for the analyses—30, 70, and 100 °C [86, 158, and 212 °F]—to cover the temperature range of interest while minimizing interpolation errors. At each temperature, the 44 waters were evaporated at 3 $p\text{CO}_2$ values: 10^{-2} , 10^{-3} , and 10^{-4} bar; these $p\text{CO}_2$ values were selected on the basis of the results from the NFC model. In a second set of EQ3/6 simulations, the waters were diluted by a factor of 100. The oxygen partial pressure ($p\text{O}_2$) in all the simulations was set equal to the atmospheric value to represent oxidizing conditions in the drift.

(b)(5)

The seepage evaporation/dilution analysis results formed the basis for the DOE in-drift water chemistry abstraction, which was implemented in the TSPA code in the form of 396 lookup tables (simulation results for 4 representative pore waters \times 11 water-rock interaction parameter values \times 3 temperatures \times 3 $p\text{CO}_2$ values). The lookup tables represented the range of chemical compositions that potentially could be generated by evaporation or dilution of drift wall seepage or condensation, or by waters imbibed into the invert. The lookup tables enabled the TSPA code to provide the following parameters and their uncertainties for a given set of temperature, relative humidity, and $p\text{CO}_2$ conditions: pH, ionic strength, Cl^- and NO_3^- concentrations, and the $\text{NO}_3^-/\text{Cl}^-$ ratio. These parameters are used in the TSPA model to represent the chemical environment for the corrosion of waste package surfaces and for radionuclide transport in the invert.

To determine which set of lookup tables is used for the in-drift water composition, the TSPA model used the following four inputs: the starting water identity (Groups 1, 2, 3, or 4); the water-rock interaction parameter derived from the NFC model; the $p\text{CO}_2$, which was derived from the NFC model; and the waste package surface temperature derived from the multiscale thermal-hydrologic model. The specific water composition in the table was selected on the basis of the relative humidity at the waste package surface, which in turn was derived from the multiscale thermal-hydrologic model. For water-rock interaction parameters, temperatures, and $p\text{CO}_2$ values that fell between the values listed in the lookup tables, DOE interpolated values from adjacent tables.

DOE indicated that brine compositions resulting from seepage evaporation are most sensitive to the degree of water-rock interaction and to $p\text{CO}_2$; temperature had a comparatively smaller effect. The degree of water-rock interaction—the amount of feldspar dissolved—had the greatest effect on pH. With increasing amounts of feldspar dissolved, all the waters DOE considered in the analysis evolved into carbonate-type brines because feldspar dissolution and secondary mineral precipitation consume calcium and magnesium ions and raise the pH and bicarbonate concentration. The observed relationship between degree of water-rock interaction and brine type is important because carbonate-type brines typically have chloride and nitrate

concentrations that are not conducive to localized corrosion of the Alloy 22 waste package outer barrier material. DOE concluded that corrosive calcium and magnesium-chloride brines are not expected to form in the potential repository.

The NRC staff compared DOE's conceptual model with the NRC staff's understanding of the Yucca Mountain natural system and independent analysis of in-drift processes (Browning, et al., 2003aa; 2004aa). (b)(5)

(b)(5)

The DOE model calculated that for time periods beyond 12,000 years after repository closure, there is a low probability for the repository environment (i.e., temperature, pH, and chemical composition of in-drift waters) to support localized corrosion of the waste package even if the drip shield fails and allows seepage water to contact the waste package. The DOE model calculated that the pH and nitrate-to-chloride ion ratio in in-drift water will generally be too high to initiate localized corrosion in this time period. The NRC staff conducted independent analysis of in-drift water that may contact the waste package under the temperature and relative humidity conditions that may exist in the drift at 12,000 years after repository closure or later. The NRC analysis used StreamAnalyzer 2.0 and OLIAnalyzer 3.0 (Gerbino, 2006aa) thermodynamic software to simulate the evaporative evolution of seepage waters, using as input the compositions of USGS pore water samples discussed in SER Section 2.2.1.3.3.3.1. (b)(5)

(b)(5)

Data and Model Justification

This section addresses YMRP Section 2.2.1.3.3 Acceptance Criterion 2: "Data for Model Justification are Sufficient." The NRC staff reviewed information DOE provided in SAR Section 2.3.5.5 (and relevant references) and in DOE (2009cw) to evaluate whether the data and model justification used to characterize the in-drift chemical environment are adequate.

(b)(5)

As indicated in the preceding section, the IDPS model was implemented using the EQ3/6 geochemical code and a Pitzer thermodynamic database. The parameters in the database were obtained from a variety of thermodynamic data and solubility measurements reported in the scientific literature and synthesized into an internally consistent data set. DOE evaluated the principal temperature-dependent Pitzer parameters in the synthesized data set for their ability to reproduce the original source information. (b)(5)

(b)(5)

DOE also used several chemical data sets to support its parameter values and to build confidence in the IDPS model. The data sets included (i) laboratory experiments designed to investigate the effects of evaporation on the chemical evolution of water compositions and environmental conditions relevant to the potential repository; (ii) a natural analog for evaporative concentration of seawater at the Morton Bahamas solar salt production facility on Great Inagua Island in the Bahamas; and (iii) compilations of solubility measurements in single, binary, and ternary salt systems from handbooks and published sources. DOE compared these data with results from the IDPS model in SAR Section 2.3.5.5.3.3 and referenced documents. The NRC staff evaluated these comparisons of measured data and model results.(b)(5)

(b)(5)

The NRC staff also evaluated the sufficiency of DOE's baseline data to justify the in-drift water chemistry abstraction.(b)(5)

(b)(5)

Data and Model Uncertainty

This section addresses YMRP Section 2.2.1.3.3 Acceptance Criterion 3 and 4: "Data Uncertainty is Characterized and Propagated Through the Model Abstraction" and "Model Uncertainty is Characterized and Propagated Through the Model Abstraction." The NRC staff

reviewed information DOE provided in SAR Section 2.3.5.5 (and relevant references) and in DOE (2009cw) to evaluate whether the data and model uncertainties used to characterize the in-drift chemical environment are adequate. This evaluation focused on (i) inclusion of uncertainty propagation in input data and (ii) uncertainty propagation throughout the IDPS model, because these specific topics are important to the DOE abstraction relevant to these acceptance criteria (DOE, 2008ab; NRC, 2003aa).

DOE identified that uncertainties in the IDPS result in uncertainties in the TSPA code values of pH, ionic strength, concentrations of Cl^- and NO_3^- , $\text{NO}_3^-/\text{Cl}^-$ ratio, and deliquescence relative humidity. DOE evaluated these uncertainties using model-data comparisons. Uncertainty in pH was given particular consideration due to variances in methods of measuring pH (whether true activity of the hydrogen ion is taken into account) and because there is significant experimental error when measuring the pH of concentrated brines. For solutions with water activities approximately 0.75 or higher, pH uncertainty was determined indirectly through the uncertainty in total inorganic carbon concentration, which reasonably reflects uncertainty in pH for the near-neutral range. This carbon concentration was evaluated using data from evaporation experiments and on calcite or CO_2 solubility. For more concentrated solutions with lower water activities, pH uncertainty was estimated on the basis of comparisons of calculated and measured pH in concentrated solutions. DOE evaluated the uncertainty in ionic strength by comparing values calculated using the IDPS model with those derived from evaporation experiments. Uncertainties in the Cl^- and NO_3^- concentrations and in the $\text{NO}_3^-/\text{Cl}^-$ ratio were evaluated by comparing IDPS model results with data from evaporation experiments and solubility measurements. DOE assessed the uncertainty in deliquescence relative humidity by comparing IDPS model results with deliquescence relative humidity values reported in the literature.

The NRC staff evaluated DOE's characterization and propagation of uncertainty in the in-drift water chemistry abstraction. (b)(5)

(b)(5)

Model Abstraction Support

This section addresses YMRP Section 2.2.1.3.3 Acceptance Criterion 5: "Model Abstraction Output is Supported by Objective Comparisons." The NRC staff reviewed information DOE provided in SAR Section 2.3.5.5 (and relevant references) to evaluate whether the support for the model abstraction used to characterize the in-drift chemical environment is adequate. (b)(5)

(b)(5)

In SAR Section 2.3.5.5.4.2.2, DOE described the approach it used to build confidence in the in-drift water chemistry model abstraction. For example, DOE abstracted the range of in-drift water chemistry in the form of lookup tables at discrete temperature and $p\text{CO}_2$ values. DOE supported the abstraction approach by demonstrating that the results derived by interpolation between lookup tables are within the stated model uncertainties for IDPS model simulations at the actual temperature and $p\text{CO}_2$ conditions tested. DOE provided additional support to its in-drift water chemistry model abstraction in DOE (2009cv). The NRC staff evaluated the DOE

information (b)(5)

(b)(5)

(b)(5)

Summary

The NRC staff reviewed the in-drift chemistry abstraction (including the description of the in-drift environment), the assumptions incorporated in the IDPS model abstraction, the Pitzer database for the IDPS model, supporting data and experiments, and uncertainty propagation through the IDPS model. (b)(5)

(b)(5)

(b)(5)

2.2.1.3.3.3 Quantity of Water in Contact With the EBS

The purpose of the Quantity of Water in Contact With the EBS flow abstraction is to (i) determine seepage flux⁴ rates through and around breached or intact waste packages and the drip shield and (ii) provide an estimate for partitioning of radionuclides exiting the EBS between unsaturated zone fractures and in the rock matrix. The EBS flow abstraction receives seepage flux approaching the drift wall from the drift seepage abstraction (BSC, 2004aa), condensation on the drift walls from the In-drift Natural Convection and Condensation model abstraction (BSC, 2004aw), capillary wicking (imbibition flux) into the invert from the Multiscale Thermohydrologic model abstraction (MSTHM) (BSC, 2005ah), and the size and evaluation of corrosion openings on the waste packages from the WAPDEG Corrosion model abstraction (BSC, 2004bs). Finally, SER Section 2.2.1.3.6 reviews the abstraction that addresses thermal-hydrologic processes affecting seepage, SER Section 2.2.1.3.1 reviews the abstraction that addresses corrosion processes affecting the drip shield and waste packages, and SER Section 2.2.1.3.4 reviews the abstraction that addresses the quantity and chemistry of water inside breached waste packages and the invert.

(b)(5)

The NRC staff reviewed the applicant's model for EBS Flow in SAR Section 2.3.7.12 (and relevant references). The NRC staff's review focused on evaluating whether (i) the conceptual model for flow paths and flux splitting throughout the intact and failed EBS components under both nominal and disruptive events is adequate; (ii) model integration of the EBS flow abstraction with other abstractions in the TSPA model, as well as information exchanges between the EBS flow abstraction and other abstractions, is transparent and adequately described; (iii) model parameters are adequately supported by available experimental data, and data uncertainties are adequately propagated within the EBS flow abstraction and into other abstractions in the TSPA code; and (iv) model uncertainties are adequately analyzed through alternative model abstractions.

Conceptual Model for the EBS Flow Paths and Flux Splitting

This section addresses YMRP Section 2.2.1.3.3 Acceptance Criterion 1: "System Description and Model Integration are Adequate." NRC staff reviewed the information provided in SAR Sections 2.3.7.12 and 2.2.1.2.1 (DOE, 2009av) (and relevant references) and in DOE (2009ab) to evaluate whether the conceptual model of the quantity of water in the EBS is adequate.

⁴Flux is the amount of water associated with a flow path at a given point along a pathway, at a given time. Flux rate is the amount of water per unit time.

This evaluation focused on (i) the continuity and integration of flow paths and (ii) impacts of intact and breached EBS components on the EBS flow in the nominal case and disruptive events, because these specific topics are important to the DOE abstraction relevant to this acceptance criterion (DOE, 2008ab; NRC, 2003aa).

SAR Table 2.2-1 contains the FEPs that DOE believes are potentially relevant to the quantity of water in contact with EBS. The applicant evaluated and included the following FEPs in this abstraction: (i) Capillary effects (wicking) in EBS (FEP 2.1.08.06.0A) and (ii) Unsaturated flow in the EBS (FEP 2.1.08.07.0A). The applicant evaluated and excluded, on the basis of low probability or low consequence, the following FEPs from this abstraction: (i) Advection of liquids and solids through cracks in the waste package (FEP 2.1.03.10.0A), (ii) Advection of liquids and solids through cracks in the drip shield (FEP 2.1.03.10.0B), (iii) Saturated flow in the EBS (FEP 2.1.08.09.0A), and (iv) Condensation on underside of drip shield (FEP 2.1.08.14.0A). Note that the adequacy of the rationale for excluding these specific FEPs from this abstraction is reviewed in SER Section 2.2.1.2.1.3.2. Furthermore, DOE's pre-10,000-year treatment of FEPs in this abstraction continues unchanged beyond the 10,000-year postdisposal period through the period of geologic stability.

The applicant's EBS flow abstraction is based on a mass-conserving, flux-splitting algorithm involving eight potential unsaturated flow pathways in the EBS. The flow pathways and fluxes along these pathways are labeled F1 through F8 in SAR Figure 2.3.7-8 (DOE, 2009av). The upper wall of the drift forms the top boundary (along the F1 flow path), and the bottom part of the invert forms the lower boundary (along the F8 flow path) in the EBS abstraction. The abstraction calculates time-variant flux rates along unsaturated flow pathways across the EBS for the nominal case and disruptive events.

The applicant described the flow pathways and flux rates (F1–F8) in the EBS flow abstraction as follows (Figure 6-1): the F1 flow path accounts for the total dripping flux from a drift wall. The total dripping flux is the sum of the seepage flux arriving at the drift wall from above and the condensed water on drift walls (SER Section 2.2.1.3.6.3.4); these are direct inputs to the EBS flow abstraction. The F2 flow path accounts for the flux through partially failed patches of the drip shield formed by general corrosion. Localized corrosion of the drip shield is excluded from the performance assessment (SER Section 2.2.1.2.1.3). The F3 flow path accounts for the diversion of flux around the drip shield (computed as $F3 = F1 - F2$), which will drain directly into the invert. Although the diversion of flux around the drip shield is included in the construction of the EBS flow model, the applicant did not implement the flux-splitting algorithm for drip shields in TSPA simulations, because the drip shields were modeled to be either all intact or failed, as described in SNL Section 6.1.1 (2007aj). The F4 flow path accounts for the flux through patches, formed as a result of general corrosion of the outer barrier of the waste packages. Localized corrosion of the outer barrier of waste packages is not considered important (SER Section 2.2.1.3.1.3.2.5). The F5 flow path accounts for the diversion of flux around waste packages (computed as $F5 = F3 - F4$), which will drain directly into the invert. The F6 flow path is the total flux entering the invert (computed as $F6 = F4 + F3 + F5$). The F7 flow path accounts for the imbibition flux from the host rock matrix into the invert and is a direct input to the EBS Flow abstraction. The F8 flow path is the total flux from the invert to the unsaturated zone (computed as $F8 = F6 + F7$). Thus, the magnitude of fluxes in the EBS is determined by the flux rates at the drift wall, flow exchanges between the invert and the surrounding unsaturated fractured domain, and the size of corrosion patches on the drip shield and waste packages, which are externally calculated. The rest of the fluxes in the EBS are computed on the basis of the mass-conserving, flux-splitting algorithm.

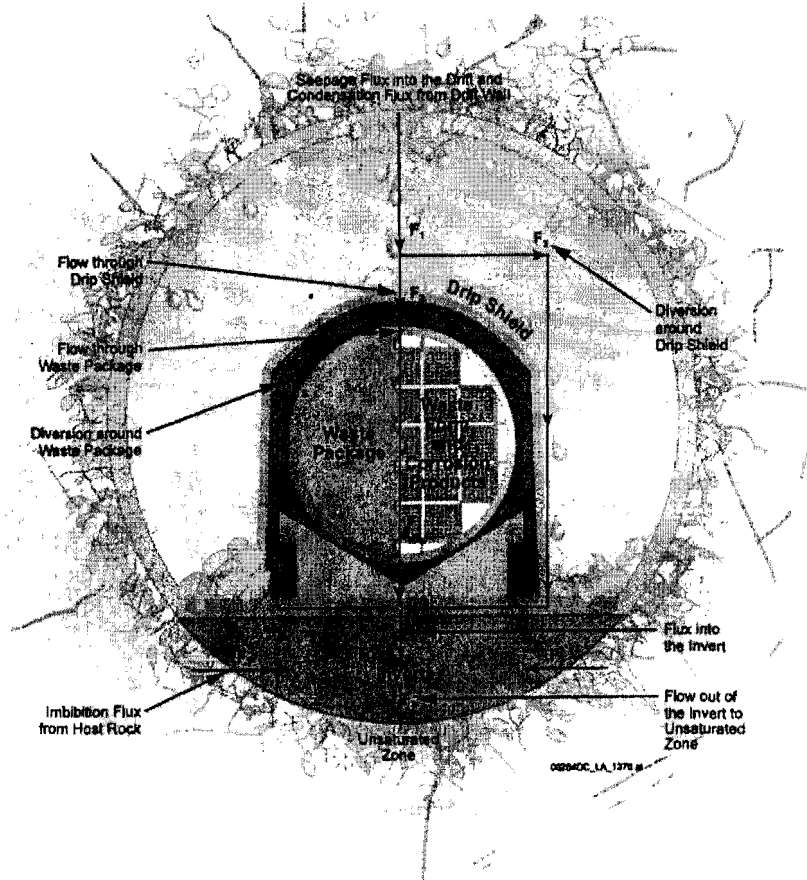


**Figure 6-1. Potential Flow Pathways in the EBS
(SAR Figure 2.3.7-8; DOE, 2008ab)**

In addition to the nominal case, the applicant addressed both the igneous intrusion and the seismic ground motion cases. (b)(5)

(b)(5)

(b)(5)

(b)(5) For the igneous intrusion scenario, the drip shield and waste packages entirely lose their integrity instantaneously at the time of the intrusive event, and all seepage water approaching the drift wall flows through the waste package, as described in SNL Section 6.1.1 (2007aj). For the seismic ground motion scenario, after the drip shield fails, the water flow rate through a damaged waste package depends on the expected fraction of the waste package surface (which increases with time) that is breached by corrosion patches, as shown in SNL Figures 8.3-11(a) and 8.3-12(a) (2008ag) and DOE (2009an).

The NRC staff reviewed the model conceptualization, mass-balance equations, and underlying assumptions of the EBS flow model abstraction and other relevant abstractions with which the EBS flow model abstraction exchanges data and information to determine whether the applicant adequately described the EBS flow model abstraction and the underlying mass-conserving flux-splitting algorithm. (b)(5)

(b)(5)

Model Integration and Information Flow

This section addresses YMRP Section 2.2.1.3.3 Acceptance Criterion 1: "System Description and Model Integration are Adequate." NRC staff reviewed the information provided in SAR Section 2.3.7.12 (and relevant references) to evaluate whether the model integration and information exchange with the other abstractions are adequate. This evaluation focused on (i) integration and continuity of flow components in the EBS flow abstraction and (ii) transparency and adequacy of information on input to and output from the EBS flow abstraction, because these specific topics are important to the DOE abstraction relevant to this acceptance criterion (DOE, 2008ab; NRC, 2003aa).

Input to the EBS Flow abstraction includes seepage flux into the drift from the drift seepage abstraction (BSC, 2004aa); condensation on the drift walls from the In-drift Natural Convection and Condensation model abstraction (BSC, 2004aw), which makes up the F1 flow path; imbibition flux into the invert; the F7 flow path from the MSTHM model abstraction (BSC, 2005aa); and patch size and its evolution from the WAPDEG corrosion model (BSC, 2004bs), which is used for calculating the F4 flow path. The F4 flow path determines the seeping or nonseeping condition in the waste package. Information on the seeping or nonseeping condition is used in the EBS radionuclides and colloid abstraction for determining the rate

constant for irreversible attachment of plutonium and americium onto mobile corrosion product colloids (DOE, 2009ay).

DOE's SAR shows the EBS-Unsaturated Zone interface model (SNL, 2007aj) uses water fluxes along the F6 and F7 flow paths to calculate advective flow rates of radionuclides and colloid suspensions to be used in the unsaturated zone transport abstraction. The F6 flow path determines the water flux rate for radionuclides and colloid suspensions from the invert into the unsaturated zone fractures in a seeping environment. In a nonseeping environment, advective flux from the invert to unsaturated zone fractures is zero unless drift wall condensation is greater than zero. The F7 flow path provides the water flux for advective transport of radionuclides and colloid suspensions from the invert into the unsaturated zone matrix. Imbibition along the F7 flow path could provide a small advective flux into the unsaturated zone matrix in both seeping and nonseeping environments (DOE, 2009am).

The NRC staff reviewed the model conceptualization, the mass-balance equations, and the underlying assumptions of the EBS flow model abstraction and other relevant abstractions with which the EBS flow model abstraction exchanges data and information to determine whether the applicant adequately described the integration of the EBS flow model abstraction and the information exchange with other abstractions in the TSPA model. (b)(5)

(b)(5)

Data Support and Uncertainties

This section addresses YMRP Section 2.2.1.3.3 Acceptance Criteria-2 and -3: "Data for Model Justification are Sufficient" and "Data Uncertainty is Characterized and Propagated through the Model Abstraction." NRC staff reviewed the information provided in SAR Section 2.3.7.12 (and relevant references) to evaluate whether the supporting data and the characterization of uncertainties for the EBS flow abstraction are adequate. (b)(5)

(b)(5)

The applicant relied on experimental data from the breached drip shield experiments, as outlined in SNL Section 6.3.2.3 (2007aj), and BSC (2003ag) to derive an equation to estimate flux through a breached drip shield (the F2 flow path). The equation is a function of the lateral spread angle of the rivulet flow on the drip shield, the number of corrosion breaches on the drip shield, the length of the breaches, and a sampled uncertainty factor. The uncertainty factor is bounded using data from the Breached Drip Shield experiment. The applicant adopted the

same equation to estimate the flux through a breached waste package (the F4 flow path). The applicant identified that the only difference in implementing the equation for the drip shield and waste forms is that (i) the radius of the curvature of the waste package is less than that of the drip shield and (ii) the nominal patch size the WAPDEG corrosion model (BSC, 2004bs) modeled is smaller for a waste package than for the drip shield. These differences affect the bounds for the uncertainty factor established for the drip shield and the waste package. The applicant supported the abstraction for the flow through a breached drip shield and waste packages on the basis of data from the Breached Drip Shield experiment. However, in the TSPA code, the data support is used only for breaches on the waste package because the drip shields are modeled to be either all intact or failed, as detailed in SNL Section 6.1.1 (2007aj).

Uncertainties associated with the seepage flow arriving at the drift wall are propagated into the EBS abstraction through the F1 flow path. Uncertainties associated with unsaturated flow in the host rock matrix are propagated into the EBS flow abstraction through the F7 flow path. The applicant bounded the uncertainty factor, as described in SNL Sections 7.1.1.1 and 7.1.1.2 (2003aj), used for the calculations of the F4 flow path on the basis of data from the breached drip shield experiments (BSC, 2003ag). The applicant assumed a uniform distribution for the uncertainty factors due to lack of supporting data for any statistical distribution.

The NRC staff reviewed the Breached Drip Shield experiments to determine whether (i) the experiments were adequately designed to support the flux-splitting model conceptualization and (ii) the experimental data were adequately used to bound uncertainties in the EBS flow processes. (b)(5)

(b)(5)

(b)(5)

Model Support and Uncertainties

This SER section addresses YMRP Section 2.2.1.3.3 Acceptance Criterion 4 and 5: "Model Uncertainty is Characterized and propagated Through the Model Abstraction," and "Model Abstraction Output Is Supported by Objective Comparisons." NRC staff reviewed the information provided in SAR Section 2.3.7.12.3.5 (and relevant references) to evaluate whether model support and uncertainties for the EBS flow abstraction are adequate. (b)(5)

(b)(5)

The applicant presented two alternative conceptualizations relevant to the EBS flow abstraction to characterize and propagate uncertainty through the model abstraction. These alternative conceptualizations included the bathtub flow model and the dual-continuum invert flow model (SAR Section 2.3.7.12.3.5).

The EBS flow abstraction is based on a flux-splitting algorithm that assumes a nonponding (no water accumulation) condition in the EBS. The applicant alternatively tested a ponding condition through a bathtub model that allows water retention and accumulation in the waste package before being released to the EBS. The applicant identified that the flow-through (nonponding) model is bounding for the bathtub (ponding) model in calculations of concentration and mass releases of radionuclides from the EBS, due to the delays in releases in the bathtub case, when (i) radionuclides are solubility rate limited or dissolution rate limited and the inflow rate is time invariant or (ii) radionuclides are dissolution rate limited and there is a step change in the inflow rate. The applicant identified that the flow-through model is not bounding for the bathtub model when the inflow rate increases, because the flow-through model (with an increased volumetric water flow rate) would result in lower mass concentrations than the bathtub model (with a fixed, completely mixed bathtub storage volume). However, the total mass releases (unlike the mass concentrations) passed from the EBS model abstraction to the unsaturated transport abstraction would be identical for the flow-through and bathtub models.

The applicant discussed another alternative conceptualization in which the flow domain in the invert is characterized as a dual-continuum model, as opposed to the single-continuum model, in the EBS flow abstraction. In this alternative model, the flow domain is divided into intergranular and intragranular flow domains. As a result, the F8 flow path is redefined as the flux from the intragranular invert continuum to the unsaturated zone. The applicant introduced an additional flow path, F9, that accounts for flux from the intergranular invert continuum to the unsaturated zone. The applicant did not include this conceptualization in the TSPA model due to insufficient experimental data to validate diffusion when, in transport simulations, the water content is very low.

The NRC staff reviewed the alternative model conceptualizations the applicant proposed to determine whether the rationale for their inclusion or exclusion in TSPA model is adequate.

(b)(5)

(b)(5)

(b)(5)

the applicant noted that when the inflow rate increases and radionuclides are solubility rate limited, the difference in the performance of the bathtub model and the flow-through model is not critical to performance.

(b)(5)

Further, the applicant demonstrated that the EBS flux-splitting algorithm tends to overestimate the fraction of drift flow that enters the breached mock-up drip shield (F2/F1) in the Breached Drip Shield experiments, as shown in SNL Table 6.5-2 and Figure D-12 (2007aj). On the basis of experimental data, the applicant estimated that the fraction of drift flow that entered the breached drip shield ranged from 0.013 to 0.275 with a median value of 0.049. The applicant also used the results from the Breached Drip Shield experiments to estimate the fraction of drift flow that enters breached waste packages. Using the flux-splitting model, the applicant calculated that when approximately 4 percent of the waste package surface area is breached by general corrosion, 10, 90, and 100 percent of the seepage flux approaching the (failed) drip shield from above enters into a breached waste package for the 5th, 50th, and 95th percentiles, respectively. In the TSPA model implementation, the average fraction of the breached waste package surface area in 1 million years is on the order of 10^{-3} for the nominal and disruptive modeling cases. The applicant estimated that 0–11 percent (with a mean/median value of 5.5 percent) of the seepage flux above the (failed) drip shield entered into a breached commercial spent nuclear fuel waste package for the nominal and seismic ground motion cases (DOE, 2009an). The NRC staff conducted similar calculations for a breached waste package for the nominal and seismic ground motion cases by using the information the applicant presented in SAR Figure 2.1-17 (DOE, 2009av).

(b)(5)

(b)(5)

Summary

The NRC staff reviewed the model conceptualization, mass-balance equations, the underlying assumptions of the EBS flow model abstraction and other relevant abstractions with which the EBS flow model abstraction exchanges data and information, the Breached Drip Shield experiments the applicant used to bound data uncertainties, and the alternative model

conceptualizations the applicant used to analyze model uncertainties. (b)(5)

(b)(5)

(b)(5)

(b)(5)

(b)(5) TSPA calculations indicated that at the end of 1 million years, on average 5.5 percent of the seepage water approaching the (failed) drift shield entered into breached commercial spent nuclear fuel waste packages under nominal and seismic scenarios. Similarly, at the end of 1 million years, on average 6 and 11 percent of the seepage water approaching the (failed) drift shield entered into a breached codisposal waste package under nominal and seismic scenarios, respectively. Thus, on average, only up to 11 percent of the seepage flux above the (failed) drip shield would be available for the advective transport of radionuclides and colloids in the waste form and corrosion products domains in the EBS radionuclide transport abstraction. In this abstraction, a zero or nonzero value of the flux through a failed waste package determines the type of the transport mechanism for the radionuclides and colloids in the waste form and corrosion products domains (diffusive transport if the flux is zero; advective transport otherwise). Because, on average, not more than 11 percent of the seepage water can enter a waste package under any circumstances (b)(5)

(b)(5)

However, as shown in Figure 6-1, this diverted flux around the failed waste package enters into the invert and is used to calculate F6, which determines the advective transport of radionuclides and colloids in the invert domain of the EBS radionuclide transport abstraction.

2.2.1.3.3.4 Evaluation Findings

The NRC staff reviewed the applicant's SAR and other information submitted in support of the license application and finds that, with respect to the requirements of 10 CFR 63.114 for consideration of the quantity and chemistry of water contacting engineered barriers and waste forms (b)(5)

(b)(5)

(b)(5)

On the basis of its review, the NRC staff (b)(5)

(b)(5)

(b)(5)

) In arriving at this conclusion, the NRC staff followed the guidance of the YMRP and the requirement of a risk-informed approach specified in the regulations.

2.2.1.3.3.5 References

Browning, L., R. Fedors, L. Yang, O. Pensado, R. Pabalan, C. Manepally, and B. Leslie. 2004aa. "Estimated Effects of Temperature-Relative Humidity Variations on the Composition of In-Drift Water in the Potential Nuclear Waste Repository at Yucca Mountain, Nevada." *Proceedings of the Materials Research Society. Symposium Proceedings 824*. J.M. Hanchar, S. Stroes-Gascoyne, and L. Browning, eds. Warrendale, Pennsylvania: Materials Research Society. pp. 417-424.

Browning, L., W. Murphy, C. Manepally, and R. Fedors. 2003aa. "Reactive Transport Model for the Ambient Unsaturated Hydrogeochemical System at Yucca Mountain, Nevada." *International Journal of Computers & Geosciences*. Vol. 29, No. 3. pp. 247-263.

BSC. 2005aa. "Analysis of Dust Deliquescence for FEP Screening." ANL-EBS-MD-000074. Rev. 01. AD 01, ACN 001, ACN 002. Las Vegas, Nevada: Bechtel SAIC Company, LLC.

BSC. 2005ad. "In-Package Chemistry Abstraction." ANL-EBS-MD-000037. Rev. 04. ACN 01, AD 01, ERD 01. Las Vegas, Nevada: Bechtel SAIC Company, LLC.

BSC. 2005ah. "Multiscale Thermohydrologic Model." ANL-EBS-MD-000049. Rev. 03. AD 01, AD 02, ERD 01, ERD 02. Las Vegas, Nevada: Bechtel SAIC Company, LLC.

BSC. 2004aa. "Abstraction of Drift Seepage." MDL-NBS-HS-000019. Rev. 01. AD 01, ERD 01. Las Vegas, Nevada: Bechtel SAIC Company, LLC.

BSC. 2004aw. "In-Drift Natural Convection and Condensation." MDL-EBS-MD-000019. Rev. 00. ACN 01, ACN 02, AD 01, ERD 01. Las Vegas, Nevada: Bechtel SAIC Company, LLC.

BSC. 2004bs. "WAPDEG Analysis of Waste Package and Drip Shield Degradation." ANL-EBS-PA-000001. Rev. 02. Las Vegas, Nevada: Bechtel SAIC Company, LLC.

BSC. 2003ag. "Atlas Breached Waste Package and Drip Shield Experiments. Breached Drip Shield Test." TDR-EBS-MD-000025. Rev. 00. Las Vegas, Nevada: Bechtel SAIC Company, LLC.

DOE. 2009ab. "Yucca Mountain—Response to Request for Additional Information Regarding License Application (Safety Analysis Report Section 2.2, Table 2.2-5), Safety Evaluation Report Vol. 3, Chapter 2.2.1.2.1, Set 2." Letter (February 23) J.R. Williams to J.H. Sulima (NRC). ML090550101. Washington, DC: DOE, Office of Technical Management.

DOE. 2009am. "Yucca Mountain—Response to Request for Additional Information Regarding License Application (Safety Analysis Report Section 2.3.8), Safety Evaluation Report Vol. 3, Chapter 2.2.1.3.7, Set 1." Letter (February 9) J.R. Williams to J.H. Sulima (NRC). ML090410352. Washington, DC: DOE, Office of Technical Management.

DOE. 2009an. "Yucca Mountain—Response to Request for Additional Information Regarding License Application (Safety Analysis Report Section 2.1), Safety Evaluation Report Vol. 3, Chapter 2.2.1.1, Set 1." Letter (February 6) J.R. Williams to J.H. Sulima (NRC). ML090400455. Washington, DC: DOE, Office of Technical Management.

DOE. 2009av. DOE/RW-0573, "Yucca Mountain Repository License Application." Rev. 1. ML090700817. Las Vegas, Nevada: DOE, Office of Civilian Radioactive Waste Management.

DOE. 2009ay. "Yucca Mountain—Response to Request for Additional Information Regarding License Application (Safety Analysis Report Section 2.3.7), Safety Evaluation Report, Vol. 3, Chapter 2.2.1.3.4, Set 2." Letter (May 12) J.R. Williams to J.H. Sulima (NRC). ML 091330282. Washington, DC: DOE, Office of Technical Management.

DOE. 2009ck. "Yucca Mountain—Response to Request for Additional Information Regarding License Application (Safety Analysis Report Section 2.3.5), Safety Evaluation Report Vol. 3, Chapter 2.2.1.3.3, Set 1." Letter (April 30) J.R. Williams to J.H. Sulima (NRC). ML091210691. Washington, DC: DOE, Office of Technical Management.

DOE. 2009cv. "Yucca Mountain—Response to Request for Additional Information Regarding License Application (Safety Analysis Report Section 2.3.5), Safety Evaluation Report Vol. 3, Chapter 2.2.1.3.3, Set 1." Letter (April 23) J.R. Williams to J.H. Sulima (NRC). ML091140343. Washington, DC: DOE, Office of Technical Management.

DOE. 2009cw. "Yucca Mountain—Response to Request for Additional Information Regarding License Application (Safety Analysis Report Section 2.3.5), Safety Evaluation Report Vol. 3, Chapter 2.2.1.3.3), Set 1." Letter (April 16) J.R. Williams to J.H. Sulima (NRC). ML091100176. Washington, DC: DOE, Office of Technical Management

DOE. 2009dg. "Yucca Mountain—Response to Request for Additional Information Regarding License Application (Safety Analysis Report Section 2.3.6.8), Safety Evaluation Report Vol. 3, Chapter 2.2.1.3.1, Set 2." Letter (April 8) J.R. Williams to J.H. Sulima (NRC). ML090980537. Washington, DC: DOE, Office of Technical Management.

DOE. 2008ab. DOE/RW-0573, "Yucca Mountain Repository License Application." Rev. 0. ML081560400. Las Vegas, Nevada: DOE, Office of Civilian Radioactive Waste Management.

Gerbino, A. 2006aa. *A Guide for Using the OLI Analyzers*. Morris Plains, New Jersey: OLI Systems, Inc.

Leslie, B., C. Grossman, and J. Durham. 2007aa. "Total-system Performance Assessment (TPA) Version 5.1 Module Descriptions and User Guide." Rev. 1. ML072710060. San Antonio, Texas: CNWRA.

Murphy, W.M. 1994aa. "Geochemical Models for Gas-Water-Rock Interactions in a Proposed Nuclear Waste Repository at Yucca Mountain, Nevada." *Proceedings of Site Characterization and Model Validation Conference (Focus '93)*, Las Vegas, Nevada, September 26–29, 1993. La Grange, Illinois: American Nuclear Society. pp. 115–121.

NRC. 2009ab. "Division of High-Level Waste Repository Safety Director's Policy and Procedure Letter 14: Application of YMRP for Review Under Revised Part 63." Published March 13, 2009. ML090850014. Washington, DC: NRC.

NRC. 2005aa. NUREG-1762, "Integrated Issue Resolution Status Report." Rev. 1. ML051360241. Washington, DC: NRC.

NRC. 2003aa. NUREG-1804, "Yucca Mountain Review Plan—Final Report." Rev. 2. Washington, DC: NRC.

Rard, J.A., K.J. Staggs, S.D. Day, and S.A. Carroll. 2006aa. "Boiling Temperature and Reversed Deliquescence Relative Humidity Measurements for Mineral Assemblages in the $\text{NaCl} + \text{NaNO}_3 + \text{KNO}_3 + \text{Ca}(\text{NO}_3)_2 + \text{H}_2\text{O}$ System." *Journal of Solution Chemistry*. Vol. 35. pp. 1,187–1,215.

SNL. 2008ag. "Total System Performance Assessment Model/Analysis for the License Application." MDL-WIS-PA-000005. Rev. 00. AD 01, ERD 01, ERD 02, ERD 03, ERD 04. Las Vegas, Nevada: Sandia National Laboratories.

SNL. 2007aj. "EBS Radionuclide Transport Abstraction." ANL-WIS-PA-000001. Rev. 03. ERD 01. Las Vegas, Nevada: Sandia National Laboratories

SNL. 2007ao. "In-Drift Precipitates/Salts Model." ANL-EBS-MD-000045. Rev. 03. ERD 01, ERD 02. Las Vegas, Nevada: Sandia National Laboratories.

Yang, L., R. Pabalan, P. Shukla, M. Juckett, X. He, K.T. Chiang, and T. Ahn. 2010aa. "Corrosion of Alloy 22 Induced by Dust Deliquescence Brines." San Antonio, Texas: CNWRA.

Yang, I.C., Z.E. Peterman, and K.M. Scofield. 2003aa. "Chemical Analyses of Pore Water From Boreholes USW SD-6 and USW WT-24, Yucca Mountain, Nevada." *Journal of Contaminant Hydrology*. Vol1, No. 878. pp. 1-20.

Yang, I.C., P. Yu, G.W. Rattray, J.S. Ferarese, and J.N. Ryan. 1998aa. "Hydrochemical Investigations in Characterizing the Unsaturated Zone at Yucca Mountain, Nevada." USGS Water Resources Investigations Report 98-4132. Denver, Colorado: U.S. Geological Survey.

Yang, I.C., G.W. Rattray, and Y. Pei. 1996aa. "Interpretation of Chemical and Isotopic Data From Boreholes in the Unsaturated Zone at Yucca Mountain, Nevada." USGS Water Resources Investigation Report 96-4058. Denver, Colorado: U.S. Geological Survey.

CHAPTER 7

2.2.1.3.4 Radionuclide Release Rates and Solubility Limits

2.2.1.3.4.1 Introduction

This chapter addresses the U.S. Nuclear Regulatory Commission (NRC) staff's evaluation of the U.S. Department of Energy's (DOE or applicant) analytic models used in its Total System Performance Assessment (TSPA) computer program to evaluate the processes that could result in water transport of radionuclides out of the engineered barrier system (EBS), including the waste package and the invert, and into the unsaturated zone (UZ) (the rock mass directly below the repository horizon and above the water table). [As used in this Safety Evaluation Report (SER), the term "abstraction" refers to the representation of site characterization data; process-level models for features, events, and processes (FEPs); uncertainty and variability; and their overall integration (in a simplified manner) in the TSPA code.] These abstractions were described in Safety Analysis Report (SAR) Section 2.3.7 (DOE, 2009av) and in supporting documents, including applicant responses to the NRC staff's requests for additional information (RAIs). The objective of this review is to evaluate whether or not DOE's models for radionuclide release rates out of the EBS are appropriate.

The EBS and the transport pathway within the drift (repository tunnel) are the initial barriers to radionuclide release. If a waste package is breached and water enters the waste package, the radionuclides contained in the package may be released from the EBS. The processes that could lead to radionuclide release are affected by the chemical characteristics of the water, which in turn are affected by the materials that interact with the water. Therefore, the performance assessment analysis includes radionuclide release rates from the EBS among those model components that significantly affect the timing and magnitude of transport for any radionuclide released from the repository, as required by 10 CFR 63.113 and 63.114.

The applicant identified five models it considered important for abstracting radionuclide releases from the EBS. The five models the applicant identified and the associated sections in this chapter that address them are

1. The in-package chemical and physical environment model (SER Section 2.2.1.3.4.3.1) used to establish the conditions under which waste forms degrade and radionuclides are mobilized
2. The waste form degradation model (SER Section 2.2.1.3.4.3.2) used to calculate the rate at which the waste form degrades and the radionuclides become available for release
3. The concentration limits model (SER Section 2.2.1.3.4.3.3) used to apply chemically based upper limits on dissolved concentrations of some radionuclides
4. The availability and effectiveness of colloids model (SER Section 2.2.1.3.4.3.4) used to calculate the stabilities and concentrations of various types of colloids (small suspended particles that may mobilize radionuclides in water)

5. The EBS radionuclide transport model (SER Section 2.2.1.3.4.3.5) used to simulate radionuclide transport from the waste form, through the waste package, and out of the EBS

The FEPs that are relevant to radionuclide release rates and solubility limits are listed in the applicant's SAR Section 2.3.7.2 and Table 2.3.7-1. NRC staff evaluates the rationales for excluding relevant FEPs from the performance assessment model in SER Section 2.2.1.2.1.3.2.

(b)(5)

(b)(5)

(b)(5)

Evaluations of those FEPs included in the performance assessment are discussed under the five topical areas in this chapter.

This chapter relies on the following information as inputs: (i) design details of the waste package, waste form, and internal components of the waste package; (ii) context for consideration of the barrier capabilities of the waste package and the drift; (iii) information on corrosion and mechanical failure of the drip shield and waste package, which may allow water into the waste package; and (iv) information on the rate of delivery of water to the waste package surface and the chemical characteristics of water that may enter the waste package.

The output from the model of radionuclide release rates and solubility limits is used as input to the model for radionuclide transport in the UZ. The information the UZ model requires for calculating the movement of the radionuclides includes the rates and magnitudes of radionuclide release from the drift, including the characteristics of dissolved and colloidal species. Information from this model is also used for evaluating the barrier capability of the waste package interior, the waste form, and the drift below the waste package (e.g., the invert) and for supporting for the scenario analysis for the EBS.

2.2.1.3.4.2 Regulatory Requirements

Model abstractions used in the applicant's postclosure performance assessment must meet the regulatory requirements given in 10 CFR 63.114 (Requirements for Performance Assessment) and 63.342 (Limits on Performance Assessment), to support the predictions of compliance for 63.113 (Performance Objectives for the Geologic Repository after Permanent Closure). Specific compliance with 63.113 is reviewed in SER Section 2.2.1.4.1.

The requirements for performance assessment in 10 CFR 63.114 require the applicant to

- Include appropriate data related to the geology, hydrology, and geochemistry of the surface and subsurface from the site and the region surrounding Yucca Mountain
- Account for uncertainty and variability in the parameter values used to model radionuclide release rates and solubility limits
- Consider alternative conceptual models for radionuclide release rates and solubility limits

- Provide technical bases for the inclusion of features, events, and processes affecting radionuclide release rates and solubility limits, including effects of degradation, deterioration, or alteration processes of engineered barriers that would adversely affect performance of the natural barriers, consistent with the limits on performance assessment in 10 CFR 63.342
- Provide technical basis for the models of radionuclide release rates and solubility limits that in turn provide input or otherwise affect other models and abstractions

10 CFR 63.114(a) considers performance assessment for the initial 10,000 years following permanent closure. 10 CFR 63.114(b) and 63.342 consider the performance assessment methods for the time from 10,000 years through the period of geologic stability, defined in 10 CFR 63.302 as 1 million years following disposal. These sections require that through the period of geologic stability, with specific limitations, the applicant:

- Use performance assessment methods consistent with the performance assessment methods used to demonstrate compliance for the initial 10,000 years following permanent closure
- Include in the performance assessment those FEPs used in the performance assessment for the initial 10,000 year period

NRC staff review of the license application follows the guidance laid out in the Yucca Mountain Review Plan (YMRP), NUREG-1804, Section 2.2.1.3.4, Radionuclide Release Rates and Solubility Limits (NRC, 2003aa), as supplemented by additional guidance for the period beyond 10,000 years after permanent closure (NRC, 2009ab). The acceptance criteria in the YMRP generically follow 10 CFR 63.114(a). Following the guidance, the NRC staff review of the applicant's abstraction of radionuclide release rates and solubility limits considered five criteria

- System description and model integration are adequate.
- Data are sufficient for model justification.
- Data uncertainty is characterized and propagated through the abstraction.
- Model uncertainty is characterized and propagated through the abstraction.
- Model abstraction output is supported by objective comparisons.

Because 10 CFR Part 63 specifies the use of a risk-informed approach for the review of a license application, the guidance provided by the YMRP, as supplemented by NRC (2009ab), is followed to the extent reasonable for aspects of radionuclide release rates and solubility limits important to repository performance. Whereas NRC staff considered all five criteria in their review of information provided by DOE, only aspects that substantively affect results of the performance assessment, as judged by NRC staff, are discussed in this chapter. NRC staff's judgment is based both on risk information provided by DOE, and staff's knowledge, experience, and independent analyses.

The regulatory requirements for evaluating radionuclide release rates out of the EBS are addressed in 10 CFR 63.114 (Performance Assessment). In conducting its review, the NRC staff followed the guidelines in the YMRP Section 2.2.1.3.4.

2.2.1.3.4.3 Technical Review

2.2.1.3.4.3.1 In-Package Chemical and Physical Environment

This section details the NRC staff's review of the applicant's abstraction and the TSPA implementation of in-package chemistry, as described in SAR Section 2.3.7.5 and references cited therein. The in-package chemistry model estimates the water chemistry inside the breached waste packages and generates abstractions for pH, ionic strength, and fluoride concentration. Water chemistry inside the waste package (especially pH and ionic strength) is important to the repository performance because it controls waste form degradation, radionuclide solubilities, and the suspension stabilities of colloids.

The NRC staff's review focused on aspects of the in-package chemistry model considered significant to risk, including conceptual design and implementation, data inputs, model limitations, sensitivity to environmental conditions, and model abstraction and support. Primary data inputs to the in-package chemistry model include (i) the compositions, surface areas, and degradation rates of waste forms and metal components in the waste package; (ii) incoming water chemistries; and (iii) the thermodynamic data used to calculate the stabilities of dissolved, aqueous, and gas phase species in the waste package. The applicant used the sensitivity of the model to variations in environmental conditions (e.g., liquid influx rate, $p\text{CO}_2$, and temperature) to determine the potential effects of disruptive events on model outputs.

Conceptual Design and Implementation

The applicant's in-package chemistry conceptual model consists of a batch reactor system composed of water, oxygen, carbon dioxide, waste forms, and metal alloys. The batch reactor system is in equilibrium with atmospheric conditions, and reactants degrade in the presence of water according to a rate determined by the physical properties and exposed surface area of each reactant. During the reactions, secondary mineral phases and metal (hydr)oxide corrosion products precipitate and water changes in composition and mass. The model simulates two water ingress conditions: (i) vapor influx, under which water vapor (simulated as pure water) is assumed to condense and react with internal waste package components, and (ii) liquid influx, under which seepage or "dripping" water (simulated as typical groundwater or drift wall condensate) enters a breached waste package, reacts with internal components, and then exits by advection. Vapor influx is included in the model because water films generated by vapor influx promote radionuclide diffusion, which is simulated in the EBS using a diffusion model (SER Section 2.2.1.3.4.3.5).

The applicant's model considers both commercial spent nuclear fuel (SNF) and codisposal waste packages. Commercial SNF waste packages contain 21 pressurized water reactor fuel assemblies (21-PWR). Codisposal waste packages contain two DOE multiccanister overpacks (MCO) and two defense high-level waste (HLW) canisters (2-MCO/2-DHLW). The applicant's model divides the waste packages into two domains: the waste form domain (Cell 1) and the corrosion products domain (Cell 2). Cell 1 of the codisposal waste packages is further divided into Cell 1a, represented by two HLW glass pour canisters (2-DHLW), and Cell 1b, represented by two MCO units containing N-Reactor fuel (2-MCO). Adsorption reactions are not simulated in the waste form cells, because the amount of iron corrosion products is low compared to Cell 2 (i.e., the corrosion products domain). Adsorption reactions within Cell 2 are simulated in the EBS flow and transport model (SER Section 2.2.1.3.4.3.5). The applicant excluded other FEPs that could potentially impact in-package chemistry, such as in-package criticality, oxide-wedging, radiolysis, and microbial activity on the basis of low probability or low

consequence (b)(5)

(b)(5)

The applicant used the geochemical reaction path equilibrium modeling code EQ6 to simulate interaction of water and materials in commercial SNF Cell 1 and codisposal Cells 1a and 1b (referred to collectively as waste form cells). For vapor influx, water is added to the waste form cells as one of the reactants at a rate corresponding to the maximum diffusion rate of vapor through openings in a breached waste package. For liquid influx, the solid-centered flow-through option of the EQ6 code is used to simulate the flow of source water into and through a constant-volume, well-mixed batch reactor. Under the flow-through option, an amount of source water is added to the reactor displacing an equal amount of water already equilibrated with the solid phases in the reactor. The water in the reactor then mixes completely, and the water, solids, and gases within the reactor reequilibrate. Kinetically controlled reactants are also added to the reactor prior to equilibrium to capture the case where the residence time within the reactor is sufficiently short that equilibrium cannot be reached with slowly degrading constituents (e.g., metal degradation). The ratio of water to reactants, which depends on liquid influx rate, is treated as a variable in the EQ6 model. At high liquid influx rates, the ratio is such that the materials of the water package are in contact with a volume of water equal to that of the void space. This case is referred to as the "bathtub" model and has the highest ratio of water to waste package materials. At low liquid influx rates, the ratio is such that the volume of water in contact with waste package materials is less than the void space. In BSC Section 6.6.1[a] (2005ad), the applicant examined the impact of varying the water-to-reactants ratio in a sensitivity analysis to evaluate the effects of differing flow conditions on in-package water chemistry. The sensitivity analysis indicated a negligible effect on pH but a distinct effect on ionic strength (i.e., as the ratio of water to reactants is decreased to simulate low flow conditions, the ionic strength of the solution increases)

NRC Staff Review

The NRC staff evaluated the modeling approach and the representation of commercial SNF and codisposal waste packages used in the in-package chemistry conceptual design (b)(5)

(b)(5)

The NRC staff evaluated the EQ6 modeling code (b)(5)

(b)(5)

(b)(5)

Waste Form and Metal Alloy Compositions, Surface Areas, and Degradation Rates

The applicant derived input data for the in-package chemistry model from existing government design documents, standard reference material specification documents, and open literature information. The sources of input data to the in-package chemistry model were justified and documented in BSC Sections 4.1 and 4.1[a], Tables 4.1 and 4.1[a] (2005ad). The input data included the compositions, surface areas, and degradation rates of waste forms (e.g., 21-PWR fuel, HLW glass, and N-Reactor fuel) and material components of the waste form cells (e.g., stainless steels and aluminum alloys).

NRC Staff Review

The NRC staff evaluated the input data the applicant used to define the surface areas and compositions of waste forms and material components in the waste form cells (b)(5)

(b)(5)

The NRC staff also reviewed the applicant's degradation rates. With the exception of the N-Reactor fuel, the applicant selected degradation rates for waste forms and material components in the waste form cells on the basis of experimental measurements (BSC, 2004ae, ah, ai, ao). (b)(5)

(b)(5)

(b)(5)

For the N-Reactor fuel, the applicant assumed that the N-Reactor fuel degraded instantaneously upon waste package breach (SAR Section 2.3.7.8). (b)(5)

(b)(5)

Incoming Water Chemistry

The applicant incorporated a range of Yucca Mountain pore water and basalt water chemistries in developing the in-package chemistry model abstractions. For seepage water input for the

nominal and seismic scenarios, the applicant selected four Yucca Mountain pore water compositions (SAR Table 2.3.7-9). The applicant also included J-13 well water chemistry as a potentially relevant seepage water because its composition is generally representative of water compositions in the saturated and UZs in the vicinity of Yucca Mountain (Harrar, et al., 1990aa). For seepage water input for the igneous intrusion case, the applicant selected three groundwaters from large, fractured basalt reservoirs (SAR Tables 2.3.7-10 and 2.3.7-11).

NRC Staff Review

The NRC staff evaluated the chemistry of incoming waters used in the in-package chemistry model to simulate seepage water input. (b)(5)

(b)(5)

Thermodynamic Database

The applicant used the thermodynamic database *data0.ymp.R5* to execute EQ6 simulations. This database allows for the calculation of mineral and gas solubilities, the chemical state of dissolved species, and the dissolution rates of solids. Uncertainty in the *data0.ymp.R5* thermodynamic database is implicit because it was constructed from the accumulation of a large number of experimental measurements or model estimations, each with its own associated uncertainty. To minimize this uncertainty, the applicant evaluated experimental data and observations from natural analogs, as identified in BSC Section 7.4.3[a] (2005ad), and the results of sensitivity analyses, as detailed in BSC Section 6.6.11 (2005ad), to select appropriate secondary phase formation for use in process-level model simulations.

NRC Staff Review

(b)(5)

Model Limitations

The applicant addressed model limitations associated with the accumulation of water inside the waste package and the evolution of material component surface area and void space due to corrosion product buildup by implementing the following assumptions in the process-level EQ6 simulations: (i) once a waste package is breached, the entire contents of the waste package are instantly exposed to oxygen, carbon dioxide, and water and (ii) secondary mineral formation and buildup inside the waste package do not reduce available void space in the waste package and do not reduce exposure of waste package internals to atmospheric gases and water (i.e., void volume and internal component surface areas are fixed and do not vary with time).

NRC Staff Review

The NRC staff evaluated the assumptions the applicant used to address model limitations. (b)(5)

(b)(5)

Environmental Conditions and Sensitivity Analyses

The applicant developed the abstractions for in-package chemistry by analyzing the results of process-level model simulations applied over the following range of environmental conditions: (i) a $p\text{CO}_2$ range of 10^{-4} to $10^{-1.5}$ bars; (ii) a liquid influx rate of 0.1 to 1,000 L/yr [0.026 to 260 gal/yr]; (iii) a temperature range of 25 to 100 °C [77 to 212 °F]; and (iv) a relative humidity range for vapor influx of 95 to 100 percent. The applicant performed sensitivity analyses to evaluate the effects of uncertain thermal-hydrologic-chemical input parameters on model outputs and approximate model uncertainty for propagation into the TSPA model. Parameters with significant effects on model outputs (e.g., $p\text{CO}_2$ for pH and liquid influx rate and relative humidity for ionic strength) were incorporated as independent variables in the model abstractions. Within the TSPA code, the values of these independent variables are provided by other TSPA submodels (e.g., the EBS thermal-hydrologic environment submodel provides relative humidity, the EBS chemical environment submodel provides $p\text{CO}_2$, and the EBS flow submodel provides liquid influx rate) (SNL, 2008ag). Parameters with smaller effects on model outputs (specifically, material degradation rates) were used to quantify model uncertainty for propagation to the TSPA model.

NRC Staff Review

The NRC staff reviewed and evaluated the range of environmental conditions that was applied to process-level model simulations to develop the abstractions for in-package chemistry. (b)(5)

(b)(5)

(b)(5)

The NRC staff reviewed the sensitivity analyses used to evaluate the effects of uncertain thermal-hydrologic-chemical input parameters on model outputs. (b)(5)

(b)(5)

Abstractions for pH

The applicant's in-package chemistry abstractions for pH provide parameter distributions in the form of lookup tables for the TSPA. Lower and upper pH limits for liquid and vapor influx in each waste form cell were quantified by simulated acid and base titrations over a range of $p\text{CO}_2$ and ionic strength (SAR Figures 2.3.7-19 to 2.3.7-21). Abstracted pH ranges were defined by secondary oxides, the presence of which limits the range of in-package pH through solubility reactions. The lower pH limit was set by dissolution of trevorite (NiFe_2O_4), which accumulates as the steel degrades. The upper pH limit was set by dissolution of schoepite, which precipitates as UO_2 fuel degrades and CO_2 reaches equilibrium conditions. To capture the uncertainty, the pH values at any given $p\text{CO}_2$ and ionic strength were assumed to be uniformly distributed between the pH limits established by the titration calculations. The applicant supported estimated ranges for pH in the waste form cells by comparing predicted secondary mineral phases and pH ranges to observations from natural soils and groundwater, natural analogs, and/or laboratory experiments.

NRC Staff Review

The NRC staff evaluated the modeling approach and information the applicant used to generate and support the in-package chemistry abstractions for pH. (b)(5)

(b)(5)

(b)(5)

(b)(5)

Abstractions for Ionic Strength

As with pH, the applicant's in-package chemistry abstractions for ionic strength provide parameter distributions in the form of lookup tables for the TSPA code. However, the manner by which ionic strength is abstracted differs under liquid and vapor influx conditions.

Under liquid influx conditions, the applicant derived abstractions for ionic strength from a series of time-dependent EQ6 simulations at different liquid influx rates. The applicant approximated uncertainty in ionic strength on the basis of variation in ionic strength observed in material degradation rate sensitivity analyses. At low liquid influx rates, the model generates high ionic strengths in the waste form cells (SAR Figures 2.3.7-22 to 2.3.7-24) because low flow rates provide sufficient residence time for the buildup in solution of waste form and metal alloy degradation products. The applicant supported high ionic strength predictions in the waste form cells by comparing predicted ionic strengths to observations from natural groundwater and laboratory experiments.

For vapor influx conditions, the applicant abstracted ionic strength as a function of relative humidity. At ionic strengths of 1 molal or less (relative humidity above ~98.5 percent), vapor influx was simulated using EQ6 and the B-dot equation to calculate activity coefficients to derive linear relationships between relative humidity and ionic strength (SAR Figure 2.3.7-25). When the ionic strength exceeded 1 molal (relative humidity at or below 98.5 percent), Pitzer calculations for simple salt solutions from the in-drift precipitates/salts model (SNL, 2007ao) were used to approximate the relationship between relative humidity and ionic strength, as described in BSC Section 6.10.2.2[a] (2005ad). Uncertainty in ionic strength was derived from ionic strength variations observed in the Pitzer calculations.

NRC Staff Review

For liquid influx, the NRC staff evaluated the modeling approach and technical support the applicant used to generate ionic strength abstractions and makes the following findings (b)(5)

(b)(5)

(b)(5)

The sensitivity analyses results of liquid influx rate and material degradation rate on in-package ionic strength in BSC Sections 6.6.4[a] and 6.6.5[a] (2005ad) were reviewed. (b)(5)

(b)(5)

For vapor influx, the NRC staff reviewed and evaluated the modeling approach used to generate the ionic strength abstractions and makes the following findings. (b)(5)

(b)(5)

The NRC staff evaluated the applicant's in-drift precipitates/salts model (SNL, 2007ao), which uses a Pitzer ion-interaction model to predict chemical conditions at high ionic strength. (b)(5)

(b)(5)

Abstraction for Fluoride Concentration

The applicant's fluoride abstraction provides maximum fluoride values for discrete ionic strength intervals for each waste form cell. Although waste glass may contain some fluoride, the major source of fluoride in breached waste packages is from liquid influx (i.e., incoming water). Under vapor influx conditions (where water vapor, simulated as pure water, is assumed to condense inside the waste package), there is no significant source of fluoride in the waste form cells and maximum fluoride concentration is set to zero. Therefore, the fluoride abstraction is only applicable under liquid influx conditions. At high ionic strengths, maximum fluoride values were selected on the basis of relationships between fluoride concentration and ionic strength observed in material degradation rate sensitivity analyses at various incoming water compositions. At low ionic strength, maximum fluoride concentration was set to the maximum concentration observed in pore waters from the Topopah Spring welded tuff: 4.8 mg/L [0.00025 molal] (SNL, 2007ak).

NRC Staff Review

The NRC staff evaluated the modeling approach and information the applicant used to generate and support the in-package chemistry abstraction for fluoride. (b)(5)

(b)(5)

Summary of Review of In-Package Chemical and Physical Environment

The applicant's in-package chemistry model estimates the water chemistry inside breached waste packages and generates abstractions for pH, ionic strength, and fluoride concentration. The in-package chemistry conceptual model consists of an equilibrium flow-through, well-mixed batch reactor composed of water, oxygen, carbon dioxide, waste forms, and metal alloys. The model simulates both vapor influx and liquid influx and considers both commercial SNF and codisposal waste packages. Inputs to the model included thermodynamic data, incoming water chemistries, and the compositions, surface areas, and degradation rates of waste forms and metal components in the waste package. The in-package chemistry abstractions are developed by analyzing the results of process-level model simulations applied over a range of $p\text{CO}_2$, liquid influx rates, temperature, and relative humidities. The applicant performed sensitivity analyses to evaluate the effects of uncertain thermal-hydrologic-chemical parameters on model output and approximate model uncertainty.

NRC Staff Review

(b)(5)

(b)(5)

2.2.1.3.4.3.2 Waste Form Degradation

This section describes the NRC staff's review of the applicant's abstraction and TSPA implementation of radionuclide mobilization from waste form degradation. This radionuclide mobilization determines the quantity of radionuclides that may be transported by water from the solid waste form and eventually to the accessible environment. The waste form types include commercial SNF, HLW glass, and DOE SNF, as described in SAR Section 1.5.1. Commercial SNF is composed of irradiated fuels from pressurized water reactors and boiling water reactors.

HLW glass is made by melting high-level radioactive materials with silica and/or other glass-forming chemicals and then solidifying them. DOE SNF (including naval SNF) comes from a range of HLW generators, from noncommercial reactors, and from the use of radioactive material that encompasses a variety of fuel types. On the basis of the significance to risk in the performance assessment calculations, the NRC staff's review focused on the inventory of radionuclides and radionuclide distribution in commercial SNF; degradation of commercial SNF; degradation of HLW glass; degradation of DOE SNF, naval SNF, and cladding; and associated model and data uncertainties, including waste form degradation under disruptive scenarios and microbial effects. Each waste form has its specific radionuclide inventory. In the nominal scenario, the waste form degrades as it dissolves after the cladding, if any, corrodes and fails in the aqueous environment. In the seismic or igneous scenarios, mechanically or thermally assisted degradation could also occur. For waste form degradation abstractions in the TSPA code, the input information includes the design description of the waste package, the waste form, the waste package internals, and in-package water chemistry and temperature. The output from this section includes waste form mobilization rates to assess EBS radionuclide transport.

SAR Sections 2.3.7.1–2.3.7.4, 2.3.7.6–2.3.7.9, 2.4, and associated references summarized the applicant's model abstractions and related FEPs related to the degradation of commercial SNF and cladding, HLW glass, and DOE SNF (including naval SNF).

Inventory of Radionuclides and Radionuclide Distribution in Commercial SNF

The NRC staff's review of the applicant's inventory data (SAR Section 1.5.1), in terms of weight, volume, and package design, for each waste form, is discussed in SER Sections 2.1.1.2.3.4.1, 2.1.1.2.3.4.2, and 2.1.1.2.3.5.1. More than 100 radionuclides may be collectively present in the

waste package at the time of repository closure. Among them, a total of 32 isotopes of 18 elements were selected as important radionuclides to potential dose for scenario classes involving groundwater transport.

NRC Staff Review

The NRC staff's evaluation of the radionuclide inventory incorporated the applicant's design features of the waste forms in the waste package (SAR Section 1.5.1). The design features include thermal loading, structural characteristics, radionuclide inventory, chemical composition, and microstructural characteristics. (b)(5)

(b)(5)

(b)(5)

Most radionuclides, and essentially all of the rare earth and actinide radionuclides (e.g., plutonium isotopes), are retained in the UO_2 matrix. Transition metals and fission products (e.g., technetium) are partly partitioned into metallic phases embedded in the matrix, SNF grain boundaries, and gap region (i.e., the interface between the pellets and the cladding).

(b)(5)

(b)(5)

Degradation of Commercial SNF

The applicant reported that if the waste package and cladding are breached, oxidation and dissolution of the commercial SNF matrix may occur. If the temperature exceeds approximately

100 °C [212 °F], solid-state oxidation or hydration will occur, depending on the relative humidity. Commercial SNF dissolves by oxidative reaction of the UO_2 matrix in humid air or in solution at temperatures less than approximately 100 °C [212 °F]. Oxidation and hydration occur faster than dissolution. Oxidation, hydration, and dissolution can be preferentially enhanced along grain boundaries. In the applicant's commercial SNF degradation evaluation (BSC, 2004ah), the high end of the dissolution rate range was obtained from tests in fast-flowing carbonate solutions. The low end of the dissolution rate range was obtained from commercial SNF rod segment tests under dripping groundwater conditions with precipitates deposited and failed cladding present. Un-irradiated UO_2 was also tested because there is no significant difference between the dissolution rates of un-irradiated UO_2 and commercial SNF under air-saturated groundwater conditions. Data from long-term immersion and dripping water tests up to 8.7 years in duration were included in the evaluation.

On the basis of these data analyses, the applicant presented quantitative models and model parameter values for (i) the instantaneous release of radionuclides from the gap and grain boundaries and (ii) matrix dissolution inducing slow long-term radionuclide releases (SAR Sections 2.3.7.7, 2.4.2.2, and 2.4.2.3). Mean fractional matrix dissolution rates were 5×10^{-4} to $6 \times 10^{-3} \text{ year}^{-1}$ at pH of 5.5–8.0 and a temperature range of 25–90 °C [77–194 °F] under wet conditions, according to DOE Enclosure 5 (2009an). Fission products and activation products were released with the matrix dissolution. Actinide releases may be controlled by solubility limits of dissolved radionuclides (SER Section 2.2.1.3.4.3.3) and also may be affected by colloids (SER Section 2.2.1.3.4.3.4). The applicant addressed uncertainties of its models and parameter values.

In the applicant's TSPA model, high-solubility fission products and activation products (e.g., I-129 and Tc-99) are released from the waste form at rates controlled by (i) the decay of radionuclide inventory of each waste package and (ii) waste package failure rate (e.g., SAR Section 2.4.2.2.3.2.1). The waste package failure rate is related in series to waste form dissolution rate and radionuclide diffusion rate. The slowest rate among the three controls the rate of release. The applicant supported its model by stating that the dissolution rates of waste forms, including commercial SNF, are sufficiently faster (e.g., hundreds to a few thousand years) than the time intervals of each waste package failure. Low-solubility radionuclides (e.g., plutonium isotopes) are released at rates controlled mainly by the concentration limits of dissolved or colloidal species.

NRC Staff Review of the Initial Condition of Spent Nuclear Fuel at Receipt

(b)(5)

(b)(5)

NRC Staff Review of Releases From the Matrix and From the Gap and Grain Boundaries

The NRC staff evaluated the applicant's processes and modeling for matrix dissolution and radionuclide release from the gap and grain boundaries. (b)(5)

(b)(5)

(b)(5)

NRC Staff Review of Environmental Conditions Inside a Waste Package

(b)(5)

(b)(5)

NRC Staff Review of Alternative Models for Matrix Dissolution

In BSC Section 6.4.2 (2004ah), the applicant presented an electrochemical model and a surface complexation model as alternative models for the dissolution of the commercial SNF. The electrochemical model describes the process of the matrix dissolution by electric current flow under oxidizing conditions, and the surface complexation model describes the dissolution process by carbonate complexation. (b)(5)

(b)(5)

Degradation of HLW Glass

The applicant conceptually modeled HLW glass as being congruently dissolved for glass constituent elements and radionuclides at relative humidity greater than or equal to 44 percent. At lower relative humidity, the glass dissolution rate is set to zero. Dissolution kinetics were considered to be chemically controlled by dissolved orthosilicic acid (H_4SiO_4). As glass reacts with solution and reaches saturation with respect to mineral phases, precipitation occurs on the glass surface. The applicant's model was supported by dissolution studies conducted with a wide range of borosilicate glass compositions under various environmental conditions. On the basis of the data available from the applicant's tests, the applicant presented a quantitative model and model parameter values for the HLW glass dissolution process.

NRC Staff Review

(b)(5)

(b)(5) The NRC staff evaluated the processes and modeling that the applicant presented for the dissolution of HLW glass. (b)(5)

(b)(5)

(b)(5)

(b)(5) The applicant considered both sodium- and calcium-based pore waters and data on the matrix dissolution under immersion, dripping groundwater, and vapor conditions. (b)(5)

(b)(5)

Comment (b)(5)
(b)(5)

(b)(5)

(b)(5)

(b)(5) The applicant quantitatively modeled the release rate of radionuclides as a function of surface area of glass contacted by water, intrinsic glass dissolution rate (i.e., release rate of boron as an indicator), pH, activation energy for temperature dependence, and the extent of orthosilicic acid saturation in solution with the glass. The dissolution rates in acidic and alkaline regimes of pH were separately modeled. At 100–250 °C [212–482 °F], a fixed pH was used. The mean fractional dissolution rates are 2×10^{-5} to $4 \times 10^{-3} \text{ year}^{-1}$ at pH of 5.5–8.0 and temperature of 25–90 °C [77–194 °F] under wet conditions, according to DOE Enclosure 5 (2009an).

(b)(5)

(b)(5) The equation used to calculate the area of glass surface contacted by water as glass dissolves accounts for (i) an increase in surface area from thermal and mechanical cracking, water access and reactivity with water and (ii) a loss in the surface area due to dissolution, as detailed in DOE Enclosure 2 (2009ax) and DOE Enclosure 2 (2009cz). The increased surface area leads to increased release of radionuclides out of the waste package to the invert from HLW glass dissolution. In the model this increasing factor of surface area is expressed as "exposure factor." (b)(5)

(b)(5)

Some literature discussion on cracking (or pitting) of various glasses in more aggressive solutions (Pulvirenti, et al., 2006aa; Morgenstein, et al., 1999aa) did not show significant increase in dissolution rates. The test solutions used were aggressive, unlike those expected in the repository, and many glasses considered were not based on borosilicates used in the repository. The applicant also assessed the volume occupied by porosity in the altered layer during the glass hydration. The porosity may increase the glass volume in a confined canister, which may create stress that further fractures the glass. The calculated porosity volume was close to the elemental mass percentage of soluble elements in the glass. Therefore, the applicant considered that isovolumetric hydration would occur. For high-solubility radionuclides in TSPA, the release rate is controlled by the radionuclide inventory of each waste package and waste package failure rate because the dissolution rate is faster, as discussed for the degradation of commercial SNF. The increased dissolution (even with further cracking by any means) associated with data or model uncertainties would not be rate controlling in the release.

Comment (b)(5)

(b)(5)

(b)(5)

As an alternative model for HLW glass dissolution, the applicant presented a dissolution model without considering the extent of orthosilicic acid saturation (i.e., affinity) (BSC, 2004ai). (b)(5)

(b)(5)

Degradation of DOE and Naval Spent Nuclear Fuel, and Cladding

DOE divided its SNF into 34 distinct forms. Except for naval SNF, these DOE SNF types were modeled as degrading instantaneously upon waste package breach. Commercial SNF waste packages were used to represent the naval SNF waste packages for all scenario classes, because radionuclide release rates from the naval SNF waste packages were predicted to be considerably lower than from commercial SNF waste packages (BSC, 2004ao). Data uncertainties were discussed with respect to the conservatisms used.

NRC Staff Review

(b)(5)

(b)(5)

(b)(5) The applicant considered colloid formation during the instantaneous degradation and subsequent alteration of the waste form. (b)(5)

(b)(5)

The applicant assumed that the zircaloy and stainless steel commercial SNF cladding failed upon emplacement. Therefore, degradation of commercial SNF cladding was not included in the TSPA analysis. The effect of the naval SNF structure on the release and transport of radionuclides was treated separately from other DOE SNF types in the assessment. DOE SNF was conservatively assumed to degrade instantaneously. The naval SNF degrades more slowly than the commercial SNF, and therefore the naval SNF can be represented by commercial SNF waste packages in the TSPA. The applicant documented the technical basis for cladding behavior in the repository briefly because the applicant conservatively assumed that the zircaloy and stainless steel commercial SNF cladding failed at time of emplacement. (b)(5)

(b)(5)

Other Model and Data Uncertainties

Waste Form Degradation Under Disruptive Scenarios

The applicant stated that under the seismic scenario class, stress corrosion cracking of the waste package would occur earlier than waste package failure in the nominal case. Seismic response (motion and rockfall) could damage the drip shield and waste package, resulting in earlier stress corrosion cracking. The waste form dissolves in the diffused-in water vapor through the stress corrosion cracks, as in the nominal case. The igneous scenario class includes eruptive and intrusive events. In the volcanic eruption case, the impacted waste form was transported to the surface; this case does not involve groundwater transport and is not discussed in this SER chapter. In the igneous intrusive case, the waste form was assumed to be rapidly altered at expected elevated temperatures and made available to groundwater.

NRC Staff Review

The NRC staff reviewed the degradation models implemented in the TSPA code abstraction to confirm that they provide consistent results with the output from the detailed process-level models and/or empirical observations on the characteristics of commercial SNF and high-level-waste glass, as described in this SER section. The applicant presented the bounding assumption regarding radionuclide release from all waste forms under igneous intrusive conditions in SAR Section 2.3.11.3.2.4. The applicant assumed that all waste forms instantaneously degrade to be mobilized for release. (b)(5)

(b)(5)

(b)(5)

For the nominal scenario case, the applicant presented concentrations of 1.2×10^{-8} to 6.2×10^{-4} g/L [1.2×10^{-5} to 6.2×10^{-1} ppm] for irreversible colloids from commercial SNF, as detailed in DOE Enclosure 16 (2009ax), and 2.7×10^{-6} to 1.4×10^{-5} g/L [2.7×10^{-3} to 1.4×10^{-2} ppm] for high-level-waste glass colloids (SAR Section 2.3.7.11.3). (b)(5)

(b)(5)

The applicant considered colloid formation during the instantaneous degradation and subsequent alteration of the waste form. (b)(5)

(b)(5)

Microbial Effects

The applicant did not specifically address the microbial effects potentially affecting the dissolution of SNF and HLW glass. However, the applicant's models may indirectly incorporate the effects to the extent that the models are consistent with natural analog and field test results. The analog data or field test results could have been affected by the potential presence of microbial effects, compared with the laboratory test results.

NRC Staff Review

The NRC staff reviewed the waste form degradation (b)(5)

(b)(5)

(b)(5) The applicant's models also include the characteristics of natural analogs of the waste form or field test results. No indication of microbe effects (e.g., lowering pH) were reported from these literature data (BSC, 2004ah, 2004ai). (b)(5)

(b)(5)

Integration in the Engineered Barrier System Radionuclide Transport Abstraction

The waste form mobilization abstraction provides radionuclide inventory, mobilized radionuclides, and waste form colloids to the EBS radionuclide transport model. (b)(5)

(b)(5)

Summary of Review of Waste Form Degradation

(b)(5)

The design features include thermal loading, structural characteristics, radionuclide inventory, chemical composition, and microstructural characteristics. The NRC staff reviewed the applicant's proposed dissolution processes of waste forms (b)(5)

(b)(5)

(b)(5)

2.2.1.3.4.3.3 Concentration Limits

This section discusses the NRC staff's review of the applicant's abstraction and TSPA implementation of dissolved radioactive element (radioelement) concentration limits, as described in SAR Section 2.3.7.10. For significant periods of time in the performance assessment model, concentration limits exert strong controls on the concentrations in water of dose-important radioelements—particularly neptunium and plutonium—and, thus, on the release rates of those elements' isotopes from the EBS. These limits are based on chemical equilibrium relationships between the dissolved element and solid substances containing the element. The abstraction calculates, on the basis of water chemistry, maximum concentrations that limit how much of the total mass of a radioelement may remain dissolved in solution in the waste form domain, the corrosion products domain, and the invert (the drift floor, consisting of crushed rock). In the waste form domain, the radionuclide concentration calculated from the waste form degradation abstraction is reduced if it, along with the concentrations of other isotopes of the same element, exceeds the calculated concentration limit. The concentration limit comparison is also implemented for the radionuclide transport abstraction in the corrosion products domain and the invert. In each case, the remaining radionuclide mass is retained in the domain as a precipitated mass that is available for re-dissolution whenever the concentration is below the concentration limit. The inputs to the concentration limits abstraction are geochemical characteristics in the domain of the water from the in-package chemistry abstraction (waste form domain; SER Section 2.2.1.3.4.3.1) or the EBS radionuclide transport abstraction (corrosion products domain and invert; SER Section 2.2.1.3.4.3.5), and gas from the EBS chemical environment abstraction (SER Section 2.2.1.3.3). The outputs from the TSPA abstraction are the concentration limits used in the EBS radionuclide transport abstraction (SER Section 2.2.1.3.4.3.5). The actual application of the concentration limits and retention of the precipitated mass is calculated in the GoldSim computer code, as outlined in GoldSim Technology Group, pp. 253–255 (2006aa). Radionuclide Solubility, Solubility Limits, and Speciation in the Waste Form and EBS is an included FEP encompassing the abstraction evaluated in this section. The related excluded FEPs are addressed in SER Section 2.2.1.2.1.3.2.

To evaluate the applicant's abstractions of radioelement concentration limits, the NRC staff reviewed SAR Section 2.3.7, the analysis model report on concentration limits (SNL, 2007ah), and the applicant's responses to the NRC staff's RAIs (DOE, 2010aj; 2009ax,ay,cz,da,db,dc). The NRC staff also relied on the technical literature on solubility limits and the application of solubility limits in performance assessments, the NRC staff's independent solubility limit evaluations (e.g., Murphy and Codell, 1999aa; Mohanty, et al., 2003aa), and the NRC staff's independent laboratory studies (e.g., Prikryl, 2008aa).

Overall Abstraction Approach

The applicant's abstraction for concentration limits calculates concentration limits for plutonium, neptunium, uranium, thorium, americium, tin, and protactinium using lookup tables that define values (in mg/L, a unit that is approximately equivalent to parts per million, or ppm) as functions of pH and $f\text{CO}_2$ (i.e., CO_2 fugacity). For radium, the value is specified as a constant that depends on the range in which the pH value falls. For technetium, carbon, iodine, cesium, strontium, selenium, and chlorine, no concentration limit is applied; this abstraction, therefore, does not affect their release rates from the EBS.

For plutonium, neptunium, uranium, thorium, americium, tin, and protactinium, the applicant determined the concentration limit value from the lookup table for each timestep in a realization. Uncertainty is incorporated into the abstraction by sampling two uncertainty terms that are then added to (or subtracted from) the value derived from the lookup table. No further uncertainty is applied to the determined radium value. Concentration limits are treated the same for nominal and disruptive events, with the exception of the uranium abstraction in the igneous intrusive case (see uranium discussion in the Concentration Limits Parameters section).

NRC Staff Review

(b)(5)

Chemical Environment for Concentration Limits

For the waste form domain, the applicant's in-package chemistry abstraction provides pH, ionic strength, and fluoride concentration to the concentration limits abstraction at each timestep, and $f\text{CO}_2$ is obtained from the EBS chemical environment abstraction. The same ionic strength and $f\text{CO}_2$ are used in the corrosion products domain, but pH is calculated from a formula that involves $f\text{CO}_2$ and the aqueous uranium concentration; this pH abstraction is based on the competitive surface complexation model discussed in SER Section 2.2.1.3.4.3.5. In the corrosion products domain, according to DOE Enclosure 3 (2009ay) and DOE Enclosure 2 (2009da), the abundant mass of products of stainless steel corrosion controls pH to a relatively narrow range of 7.0 to 8.4. For the invert, when there is no flow from the waste package, pH, ionic strength, and $f\text{CO}_2$ are obtained from the EBS chemical environment abstraction, when there is advective flow out of the waste package, according to DOE Enclosure 7 (2009ax), pH and ionic strength in the invert are the same as in the corrosion products domain.

NRC Staff Review

(b)(5)

(b)(5) Concentration limits in the waste form domain are functions of chemical parameters developed by the in-package chemistry model (SER Section 2.2.1.3.4.3.1).

(b)(5)

(b)(5)

(b)(5)

(b)(5)

Concentration Limits Parameters

The applicant calculated concentration limits for plutonium, neptunium, uranium, thorium, americium, tin, protactinium, and radium (using barium as an analog) assuming pure-phase solubility at equilibrium with solution using the geochemical modeling code EQ3NR. The solubility models were conducted at a range of pH, $f\text{CO}_2$, and fluoride values. For plutonium, neptunium, uranium, thorium, americium, tin, and protactinium, the pH and $f\text{CO}_2$ dependencies were incorporated into the lookup tables, and the fluoride sensitivity was applied through an uncertainty term. SAR Section 2.3.7.10 described the technical bases for the limiting minerals selected for the solubility models. For most of the modeled elements, equilibrium with atmospheric oxygen was assumed; this assumption was modified for plutonium in the waste package. As mentioned previously, the applicant did not apply a concentration limit for technetium, carbon, iodine, cesium, strontium, selenium, and chlorine.

NRC Staff Review

(b)(5)

(b)(5)

(b)(5)

Plutonium

On the basis of the applicant's TSPA code dose modeling results, plutonium is a risk-significant radioelement. The applicant's plutonium concentration limits abstraction is based on equilibrium geochemical modeling, but differs from other abstractions in that equilibrium with atmospheric oxygen was not assumed. Atmospheric oxygen would impose higher redox potentials that tend to lead to higher calculated dissolved plutonium concentrations. The NRC staff therefore focused on the applicant's adjusted-Eh model, which assumes lower Eh than would be imposed by atmospheric oxygen. (Eh is a measure of a solution's oxidation potential, which may be described as the tendency of the solution to convert dissolved elements to higher oxidation states.) The adopted Eh-pH relationship for plutonium solubility models is more oxidizing than the line bounding a compilation of data from waters in contact with atmosphere, as outlined in SNL (2007ah), DOE Enclosure 9 (2009ax), and DOE Enclosure 7 (2009cz). For the typical pH and CO₂ conditions in the waste package (SAR Figures 2.3.7-19 to 2.3.7-21), the sampled plutonium solubility limit in the TSPA model ranges approximately from 0.006 to 0.4 mg/L (SAR Figure 2.3.7-29); uncertainty terms extend this range as much as \pm two orders of magnitude (e.g., SAR Figure 2.3.7-38).

NRC Staff Review

(b)(5)

(b)(5)

As illustrated in

SNL (2007ah), DOE Enclosures 8 and 9 (2009ax), DOE Enclosures 5 and 6 (2009cz), and DOE (2010aj), nearly all compared plutonium experimental data lie within two standard deviations of the uncertainty in the pH-dependent solubility relationship. (b)(5)

(b)(5)

Neptunium

The applicant identified neptunium as an important risk contributor. In general, the applicant modeled neptunium solubility limits assuming equilibrium with atmospheric oxygen, but used two different solid phases depending on conditions. The controlling solid phase for the invert is the oxidized phase Np₂O₅. The choice of the neptunium-controlling mineral in the waste package (waste form and corrosion products domains)—NpO₂ or Np₂O₅—depends on the corrosion status of the steel components. The applicant argued that local reducing conditions during steel corrosion would promote precipitation of reduced NpO₂ over oxidized Np₂O₅. The applicant noted that the literature suggests that, in the presence of reducing materials, NpO₂ is an appropriate solubility-limiting solid phase under most modeled conditions. The applicant chose Np₂O₅ to limit neptunium concentration in the absence of reductants. A sodium neptunium carbonate is modeled at the high pH margin of the water chemistry range. For the typical pH and CO₂ conditions in the waste package (SAR Figures 2.3.7-19 to 2.3.7-21), the sampled neptunium solubility limit in the TSPA analysis ranges approximately from 0.02 to 11 mg/L for NpO₂ and from 0.3 to 180 mg/L for Np₂O₅ (SAR Figure 2.3.7-30); uncertainty terms extend this range to more than an order of magnitude above and below those ranges (e.g., SAR Figure 2.3.7-39).

NRC Staff Review

(b)(5)

Uranium

The applicant produced two different lookup tables for uranium, depending on the particular chemical environment. In most cases for commercial SNF packages, the hydrated uranyl oxide schoepite is the solubility-limiting solid. For the typical pH and CO₂ conditions in a commercial SNF waste package (SAR Figure 2.3.7-19), the sampled uranium solubility limit in the TSPA code ranges approximately from 1 to 100 mg/L, as described in SNL Figure 6.7-1 (2007ah). The associated uncertainty terms extend this range as much as ± an order of magnitude; for example, as detailed in SNL Figure 7-6 (2007ah). For codisposal packages in all scenarios and all packages in the igneous intrusion scenario, and for the invert in all scenarios, the uranyl silicate sodium-boltwoodite and Na₄UO₂(CO₃)₃ are included in the solubility models. For the typical pH and CO₂ conditions in a codisposal waste package (SAR Figures 2.3.7-20 and 2.3.7-21), the sampled uranium solubility limit in the TSPA code ranges approximately from 1 to more than 10,000 mg/L (SAR Figure 2.3.7-31). The associated uncertainty terms extend this range as much as ± an order of magnitude; for example, as illustrated in SNL Figure 7-6 (2007ah).

NRC Staff Review

(b)(5)

Thorium, Americium, Protactinium, Radium, and Tin

In developing lookup tables for the other modeled actinides—thorium, americium, and protactinium—the applicant chose solubility-limiting phases on the basis of available data from the literature and the Yucca Mountain program (SNL, 2007ah). For thorium, the limiting solid was $\text{ThO}_2(\text{am})$, the solubility model for which produced values more consistent with experimental measurements than models for the lower solubility, crystalline solid ThO_2 . [In mineral formulas, "(am)" indicates that this is an amorphous, rather than orderly crystalline, solid. Amorphous solids tend to have higher solubilities than the corresponding crystalline forms.] The americium model used AmOHCO_3 , which was identified as the controlling solid in Yucca Mountain program studies conducted under appropriate conditions. Protactinium was treated by analogy with neptunium and thorium; that is, the Np_2O_5 model was adopted for protactinium, with wide uncertainty terms accounting for the possibly lower concentrations if behavior was similar to thorium. The model for tin [addressed in SNL (2007ah) but not in the SAR] was also developed using available literature data and considerations of uncertainties; the controlling solid in the tin model was $\text{SnO}_2(\text{am})$, on the basis of a literature review. The applicant used barium as a radium analog for solubility calculations due to their similar chemical properties. The applicant constructed a pH-dependent, stepwise radium solubility limit on the basis of the model results.

NRC Staff Review

(b)(5)

(b)(5)

Uncertainty

In the concentration limits abstraction, the applicant addressed uncertainty in (i) thermodynamic data supporting the solubility models and (ii) the effects of fluoride ion concentration. These uncertainties are applied as additional sampled terms added or subtracted to the lookup table values, with a pH-dependent coefficient applied to the sampled fluoride uncertainty term. These thermodynamic and fluoride uncertainty terms—with normal and triangular distributions, respectively—are sampled once per realization for each element.

NRC Staff Review

(b)(5)

Integration in the Engineered Barrier System Radionuclide Transport Abstraction

The dissolved concentration limits abstraction provides maximum concentration values for each element to the EBS radionuclide transport model, with different values provided for the waste form domain, corrosion products domain, and the invert.

NRC Staff Review

(b)(5)

Summary of Review of Concentration Limits

(b)(5)

2.2.1.3.4.3.4 Availability and Effectiveness of Colloids

This section describes the NRC staff's review of the applicant's abstraction and TSPA computer code implementation of the type, stability, and mass concentration of colloid suspensions in the EBS, as described in SAR Section 2.3.7.11 and references cited therein. Colloid suspensions inside the EBS are important to repository performance, because if they are stable and exist at sufficiently high concentrations, they could enhance transport of radionuclides that are reversibly or irreversibly associated with them. (In this chapter, the term "irreversible colloids" refers to colloids with radionuclides irreversibly, or permanently, attached to them. The term "reversible colloids" refers to colloids to which radionuclides may attach and detach reversibly.)

(b)(5)

The EBS colloid model calculates the mass concentrations of reversible and irreversible colloid suspensions in the waste package, corrosion products, and invert domains of the EBS on the basis of temporal variations in aqueous chemical characteristics (pH and ionic strength), flow rates, and failure status of the EBS components under nominal and disruptive modeling cases.

Inputs to the EBS colloid mass concentration abstraction, described in SNL Section 1.1 (2008ak), include in-package ionic strength and pH from the in-package chemistry abstraction (SER Section 2.2.1.3.4.3.1) and in-drift ionic strength and pH from the EBS physical and chemical environment abstraction (SER Section 2.2.1.3.3). Mass concentrations of colloidal suspensions are used to calculate colloid-assisted radionuclide transport in the EBS radionuclide transport abstraction (SER Section 2.2.1.3.4.3.5).

Colloid Types and Radionuclides Associated With Colloids in the Engineered Barrier System

Colloids are 1 to 2- μm [4 to 8×10^{-5} -in]-sized particles; have the potential to facilitate transport of highly sorbing, low solubility radionuclides; and may allow radionuclide concentrations in water above their solubility limit. In the TSPA code, colloids in the EBS are formed by degradation of waste package internals and waste forms and also exist as groundwater colloids in seepage water. The applicant used the EBS colloid abstraction in the TSPA code to determine the stability and mass concentrations of reversible and irreversible colloid suspensions in the waste form, corrosion products, and invert domains of the EBS (SAR Section 2.3.7.11).

The EBS colloid model abstraction focuses on the following five colloid suspension types: (i) glass waste form colloids, (ii) plutonium-rich zirconium oxide commercial SNF colloids, (iii) oxidized uranium colloids derived from the SNF, (iv) iron oxide colloids, and (v) groundwater colloids. The conceptual model identifies two types of radionuclide attachment to colloids: (i) reversible (glass waste form colloids, oxidized uranium colloids, iron oxide colloids, and groundwater colloids), in which the radionuclides are reversibly (temporarily) sorbed onto colloid surfaces, and (ii) irreversible (glass waste form colloids, commercial SNF colloids, and iron oxide colloids), in which the radionuclides are permanently attached to or embedded in the colloid structure, as detailed in SNL Section 6.3.1 (2008ak) and SNL Section 6.3.4.4 (2007aj). Although glass waste form colloids, oxidized uranium colloids, iron oxide colloids, and groundwater colloids are considered in the waste form domain, iron oxide colloids are excluded from the waste form domain, as outlined in SNL Section 6.5.2.5 (2007aj) and DOE Enclosure 2 (2009ay). As shown by the data in SNL Tables 6.3.7-62, 6.3.7-63, 6.3.7-64, and 6.3.7-66 (2008ag), the sampled stable glass waste, commercial SNF, oxidized uranium, and

groundwater colloid concentration ranges are 0.0004 to 2 mg/L, 0.000015 to 0.6 mg/L, 0.001 to 200 mg/L, and 0.001 to 200 mg/L, respectively, in all the EBS domains. As shown in SNL Table 6.3.7-65 (2008ag), the sampled stable iron oxide colloid concentration range is 0.001 to 30 mg/L in the corrosion products and invert domains.

In the EBS colloid model abstraction, two radioelements (plutonium and americium) are modeled to permanently attach onto iron oxide colloids or be irreversibly embedded in glass waste form and commercial SNF colloids. As described in SNL Section 6.3.12.1 (2008ak), five radioelements (plutonium, americium, thorium, protactinium, and cesium) are modeled to reversibly sorb onto glass waste form colloids, eight radioelements (plutonium, americium, thorium, protactinium, cesium, tin, neptunium, and radium) reversibly sorb onto oxidized uranium colloids, three radioelements (plutonium, thorium, and neptunium) reversibly sorb onto iron oxide colloids, and four radioelements (uranium, neptunium, tin, and radium) reversibly sorb onto groundwater colloids. The irreversible colloids (and their associated masses of plutonium and americium) are modeled as independent species, separate from the dissolved plutonium and americium masses.

NRC Staff Review

(b)(5)

(b)(5) The applicant considered both reversible and irreversible colloids in the abstraction and noted the uncertainties associated with the mass concentrations, the stability of these colloid types, and their upscaling and applicability to the Yucca Mountain site. The applicant constructed an empirical ionic strength threshold versus pH curve on the basis of existing experimental data in the open literature to account for uncertainties in the colloid stability. If the computed ionic strength for the in-package (or in-drift) environment is below the ionic strength threshold, then the colloids are stable in the corresponding environment. (b)(5)

(b)(5)

(b)(5) The applicant addressed the uncertainty in the mass concentration of colloids by randomly sampling the mass concentration of stable colloids from the corresponding uncertainty distributions. (b)(5)

(b)(5)

Excluded Colloid Processes

In the EBS colloid model abstraction, colloidal filtration, thin-film straining (retardation of colloid transport when colloid dimensions exceed the water film thickness), gravitational settling of colloids, and sorption of colloids on stationary surfaces and onto an air-water interface were excluded due to associated uncertainties, and exclusion of these processes was considered to be conservative. The abstraction did not include biocolloids, because of low microbial activity and negligible mass concentrations of such colloids in comparison to groundwater colloids.

NRC Staff Review

(b)(5)

Risk Importance of Colloids Under Disruptive Events

The NRC staff's review in this section focused on disruptive scenarios of igneous intrusion and seismic ground motion modeling cases. The applicant demonstrated, through its analyses, that these two modeling cases contribute most to the total annual dose for 10,000 and 1 million years after repository closure (SAR Figure 2.4-18). Pu-242 is the most important contributor to the overall total mean dose at 1-million-year simulations (SAR Figure 2.4-20). Under the nominal scenario, the maximum Pu-242 activity due to irreversible colloids is about 30 percent of the total Pu-242 activity leaving the EBS; under the seismic scenario, it is only about 18 percent of the total Pu-242 activity leaving the EBS. The maximum Pu-242 release rate leaving the EBS due to irreversible colloids is 2.5 percent of the total release rate under the igneous intrusion modeling case, as described in SNL Section P18.3 (2008ag) and DOE Enclosure 5 (2009an). Hence, the applicant concluded that, in the EBS, colloid-facilitated radionuclide transport is less effective than for the dissolved phase radionuclide transport, as shown in SAR Figures 2.1-20 and 2.1-23 and SNL Table A-2 page A-130 (2008ad).

For the igneous intrusion modeling case, the drip shield and waste packages entirely fail; hence there is no distinction between seep and no-seep cases, and water chemistries and colloid stability remain nearly constant once the temperature drops below the boiling point and water flow to the waste form is established. For the igneous intrusion modeling case, smectite colloids (derived from HLW glass or from the tuff host rock) and oxidized uranium colloids (derived from SNF degradation) are stable in the EBS, but commercial SNF colloids are completely unstable in the corrosion products domain. Colloids are more stable in the codisposal waste packages than in the commercial SNF waste packages because of dissolution of the nickel molybdate corrosion products in the latter packages, leading to higher ionic strengths.

For the igneous intrusion case, unstable and settled commercial SNF colloids in the corrosion products domain are as important as the stationary corrosion products for the retention of Pu-242, as described in DOE Figure 1.1-26 (2009dc), DOE Enclosure 1 (2009dd), and DOE Enclosure 3 Figure 1 (2009ay), due to a narrow range of pH, 7 to 8.4. The narrow pH range is illustrated in DOE Enclosure 3 (2009ay) and supported in DOE Enclosure 2 (2009da). The contribution of suspended iron oxide colloids to Pu-242 mass in the corrosion products domain is about eight orders of magnitude smaller than the Pu-242 mass removed from inventory by the settled unstable commercial SNF colloids at 200,000 years for the igneous intrusion modeling case, as shown in DOE Figure 1.1-26 (2009dc). Therefore, the applicant concluded that iron oxide colloids are insignificant dose contributors. Similarly, for a particular realization in which all commercial SNF colloids are unstable in the waste form domain, but iron oxide colloids are stable in the corrosion products domain, Pu-242 mass irreversibly associated with iron oxide colloids is three orders of magnitude less than the Pu-242 mass in the dissolved phase and about seven orders of magnitude smaller than for the sorbed Pu-242 mass on stationary

corrosion products, as shown in DOE Enclosure 1 Figure 7 (2009da). This indicates insignificant effects of iron oxide colloids on Pu-242 releases.

For the seismic ground motion case, the applicant assessed that damage on waste packages is mainly due to patch failures by general corrosion. Unlike the igneous intrusion modeling case, colloid concentrations are sensitive to seep versus no-seep environments after corrosion patches develop on the waste packages, and the ionic strengths of water and pH vary in time. For the seismic ground motion case, the ionic strength of waters in the EBS depends on the relative humidity when the water flux is less than 0.1 L/yr [0.026 gal/yr] under the condition of complete filling of the drift with rubble; otherwise, ionic strength depends on the chemistry of the advective flux through corrosion patches. The ionic strengths of seep water also correlate with the rubble-filling status, as shown in DOE Enclosure 3 Figures 17, 18, 23, and 24 (2009ay).

For the seismic ground motion modeling case, the applicant noted that diffusive transport (under no-seep conditions) through the EBS and the water chemistry (pH and ionic strength) could largely limit colloid-facilitated transport, as shown in SAR Section 2.4.2.3.2.2 and DOE Enclosure 3 (2009ay).

The TSPA model results indicate that for the seismic ground motion case, initially high ionic strength leads to unstable colloid suspensions. After the waste packages are breached in both seep and no-seep conditions, the ionic strength (which depends on the relative humidity during this stage) drops to a level where smectite and oxidized uranium colloids become stable in the codisposal packages and largely stable (in more than 95 percent of realizations) in the commercial SNF waste packages. These colloids are stable for the remainder of the simulation. As was the case for the igneous intrusion modeling case, commercial SNF colloids are unstable in the corrosion products and invert domains for the seismic ground motion modeling case, as shown in DOE Enclosure 3 Figures 6, 29, and 30 (2009ay). Stability of colloid suspensions, except for the iron oxide colloids, is similar for both the seep and no-seep cases. Iron oxide colloids are stable in the corrosion products domain only when seep water enters the waste package through corrosion patches at later times, whereas they are largely unstable (in more than 95 percent of realizations) under the no-seep conditions, as shown in DOE Enclosure 3 Figures 15 and 16 (2009ay).

NRC Staff Review

(b)(5)

The NRC staff reviewed the TSPA model results for the disruptive modeling cases (highly significant to risk) to evaluate processes and features that could limit availability and transport of colloid suspensions in the waste form, corrosion products, and invert domains of the EBS, as detailed in DOE Enclosure 3 (2009ay). (b)(5)

(b)(5)

(b)(5)

(b)(5)

(b)(5)

(b)(5)

(b)(5)

Data Support and Uncertainty Propagation for Colloid Transport Abstraction for the EBS

Mass Concentration of Colloids

The applicant used experimental and scientific literature data to support its colloid mass concentrations model. Uncertainties associated with the mass concentrations and stability of glass waste form colloids in the TSPA model rely on results from drip and immersion tests for degradation of alkali borosilicate glasses, as detailed in SNL Section 6.3.2.2 (2008ak). Experimental data were used to bound plutonium mass concentrations associated with zirconium oxide colloids formed from commercial SNF, as described in SNL Section 6.3.2.4 (2008ak). Uranophane colloids are used as representative colloids for oxidized uranium colloids formed from defense and commercial SNF.

SNL Section 6.3.2.6 (2008ak) described an empirical cumulative distribution for the mass concentrations of groundwater colloids that was adopted for uranophane colloid suspensions, because both colloid suspensions display a similar stability profile. The applicant relied on bench-scale experiments using a carbon-steel miniature waste package in bathtub and flow-through configurations. These experiments used water chemically similar to well water near Yucca Mountain to induce corrosion and subsequently to determine the geometric mean concentration of iron oxide colloids. Empirical cumulative distributions of colloid mass concentrations were constructed, on the basis of laboratory-scale experimental data, to address uncertainties in colloid mass concentrations, as detailed in SNL Section 6.3 (2008ak). The applicant adopted colloid concentrations in groundwater at the Yucca Mountain site for colloid concentrations in seepage water entering breached waste packages. The applicant collected colloid data from nine different sources and fitted them to a cumulative mass distribution to address uncertainties.

NRC Staff Review

With regard to the applicant's colloidal mass concentration model, the NRC staff verified that the applicant relied on data from laboratory experiments published in peer-reviewed technical journals to determine the range for mass concentrations of reversible and irreversible colloids. The NRC staff reviewed (i) how the applicant addressed uncertainties associated with how closely geochemical and hydrogeological conditions were represented in these experiments and (ii) how the applicant upscaled laboratory findings to the field scale at the Yucca Mountain site. The applicant acknowledged uncertainties associated with the mass concentrations of colloid suspensions due to, among other things, measurements, experimental factors, and upscaling of experimental data and observations to repository scale and conditions (SAR Section 2.3.7.11.2). To be conservative, the applicant set the upper bound for mass concentrations of iron oxide colloids to be larger than natural iron oxide colloid concentrations in groundwater (SAR Section 2.3.7.11.2). (b)(5)

(b)(5)

(b)(5)

For mass concentrations of groundwater colloids, the applicant appropriately employed existing field data. (b)(5)

(b)(5)

The NRC staff's review verified that the applicant addressed uncertainties in mass concentrations by sampling them from empirically constructed cumulative mass distributions obtained from experimental data. (b)(5)

(b)(5)

(b)(5)

In-Package and In-Drift Stability of Colloids

In TSPA code calculations, in-package and in-drift stability of colloid suspensions is determined by the ionic strength of the seepage water and pH. The applicant constructed an empirical ionic strength threshold versus pH curve using experimental data specific to each colloid suspension type and using the Derjaguin-Landau-Verwey-Overbeek theory. In-package and in-drift pH and ionic strengths and dissolved radionuclide concentrations are computed outside the EBS abstraction and then fed into the empirical ionic strength threshold versus pH curve in the EBS abstraction, as outlined in SNL Section 6.5 (2008ak). For stability calculations, the applicant modeled glass waste form colloids and groundwater colloids as smectite, plutonium-rich zirconium oxide colloids as zirconium oxide, oxidized uranium oxide colloids as uranophane, and iron oxide colloids as hematite, as described in SNL Section 6.3.1 (2008ak). If the colloid suspensions are stable, their mass concentrations are sampled from empirical distribution functions specific to the colloid type (constructed from experimental data). If a colloid type is unstable, the mass concentration is set to a low nonzero value, selected such that the colloid mass is too low to have any impact on radionuclide release and transport. In the case of groundwater colloids in the waste package, the initial concentration is set to 0 mg/L until flow begins in the waste package (SNL, 2008ak).

NRC Staff Review

The NRC staff's review of the in-package and in-drift colloidal stability verified that the applicant constructed empirical relations (on the basis of experimental data in the literature) for each colloid suspension type that related the ionic strength threshold to pH to determine stability of colloidal suspension in the waste package and in the drift. These empirical relations were constructed on the basis of the Derjaguin-Landau-Verwey-Overbeek model. The applicant acknowledged that these empirical relations were purely mathematical fits and had no physical meaning, as stated in SNL Section 6.3.2.4 (2008ak), although they are driven by experimental data. The EBS model abstraction computes the ionic strength of the in-package fluid (or in-drift seepage fluid) and compares it against the ionic strength threshold read from the ionic strength threshold versus pH curve. If the in-drift (or in-package) fluid ionic strength exceeds the ionic strength threshold, then the corresponding colloidal suspensions become unstable in the abstraction, as detailed in SNL Section 6.3.2 (2008ak). (b)(5)

(b)(5)

Radionuclide Mass Sorption on Colloid Suspension

The applicant referred to previously published data to determine surface area for reversible glass waste and groundwater colloids, uranophane colloids, and iron oxide colloids in SNL Sections 6.3.2.3.1, 6.3.2.7, and 6.3.12.2 (2008ak), respectively. This information is used in calculating sorbed radionuclide mass on colloid suspensions.

NRC Staff Review

The NRC staff's review verified that the applicant determined the range of specific surface area for reversible colloid suspension based on open literature experimental data and sampled from this range to address data uncertainties. (b)(5)

(b)(5)

Kinetic Attachment Rates for Plutonium and Americium Onto Iron Oxide Colloids

In the EBS abstraction, plutonium and americium are modeled to be irreversibly attached onto iron oxide colloids. As described in SNL Section 6.3.12.2 (2008ak), the applicant constructed an uncertainty distribution function for the attachment rate constant for iron oxide colloids on the basis of data from sorption experiments. The applicant noted that the attachment rate is sampled from an experimentally supported lognormal uncertainty distribution under a no-seep condition or a condition where colloid suspensions are unstable in the corrosion products domain. Otherwise, the maximum of the sampled rate constant from a lognormal uncertainty distribution and the computed rate constant using the target flux out ratio are used, as detailed in SNL Section 6.5.2.4.6 (2007aj).

NRC Staff Review

The NRC staff reviewed the basis of the applicant's description for the attachment rate calculations and finds that the applicant used attachment rates sampled from an experimentally supported uncertainty distribution for modeling irreversible attachments of plutonium and americium onto iron oxide colloids. The model favors attachment onto iron oxide colloids by implementing the target flux out ratio if the computed attachment rate remains within the experimentally determined range for the attachment rate; otherwise, the sampled attachment rate is used and the target flux out ratio is not implemented. (b)(5)

(b)(5)

Alternative Conceptual Model Consideration

The applicant considered two alternative conceptual models: the first uses different mechanisms to generate glass colloids and the second focuses on air-water limitations on the releases of particles from weathered waste form surfaces under unsaturated conditions, as identified in SAR Section 2.3.7.11.3.2 and SNL Section 6.4 (2008ak). The applicant did not implement these alternative models in the TSPA.

NRC Staff Review

The NRC staff's review verified that the applicant used a conceptual model in the TSPA for irreversible and reversible colloidal transport on the basis of a set of mass-balance equations.

(b)(5)

(b)(5)

The applicant considered the bathtub flow model as an alternative conceptual model to the flow-through model, which is implemented in TSPA, in simulating water flow and radionuclide transport in a breached waste package. (b)(5)

(b)(5)

Summary of Review of Availability and Effectiveness of Colloids

(b)(5)

(b)(5)

2.2.1.3.4.3.5 Engineered Barrier System Radionuclide Transport

This section details the NRC staff's review of the applicant's abstraction and TSPA implementation for radionuclide transport in the EBS, as described in SAR Section 2.3.7.12.3.2 and references cited therein (particularly SNL, 2007aj). The abstraction estimates the rate of movement of radionuclides from degraded waste forms to the UZ and provides radionuclide fluxes (rates of mass transfer) versus time to the UZ transport abstraction (SER Section 2.2.1.3.7). Major inputs to the abstraction include the flow conditions inside the EBS (SER Section 2.2.1.3.3.3.3), the chemical conditions inside the EBS (SER Section 2.2.1.3.4.3.1), waste form degradation rates (SER Section 2.2.1.3.4.3.2), dissolved concentration limits (SER Section 2.2.1.3.4.3.3), and colloid parameters (SER Section 2.2.1.3.4.3.4).

(b)(5)

(b)(5)

For example, in DOE (2009dc), the applicant provided results for a representative realization of the igneous intrusion modeling case showing that approximately 8,000 kg [17,600 lb] of Pu-242 is permanently immobilized in the EBS for one percolation subregion. In the same realization and subregion, approximately 30,000 kg [66,000 lb] of Np-237 is retained on the waste package corrosion products at 100,000 years; Np-237 is released from the EBS slowly enough that more than 1,000 kg [2,200 lb] remained at 1 million years.

On the basis of the importance to the abstraction, the NRC staff's review focused on model framework and process conceptualization within the TSPA code implementation, representation of diffusion, sorption on stationary corrosion products, colloid-facilitated transport, and reasonableness and consistency of TSPA code results. The abstraction contains several included FEPs. Excluded FEPs are discussed in SER Section 2.2.1.2.1.3.2.

Model Framework and Process Conceptualization

Overall Conceptualization

The applicant based the abstraction and TSPA implementation on one-dimensional mass transport through three computational domains: (i) waste form domain, (ii) corrosion products domain, and (iii) invert domain. The waste form domain contains a single computational cell representing a porous rind of degraded waste form for the commercial SNF packages. The waste form domain for codisposal packages comprises a computational cell representing HLW glass upstream of a cell representing DOE SNF. Corrosion products formed from the degradation of steel waste packages and package internals are represented in the corrosion products domain. The invert domain is assumed to be in close contact to the waste package and composed of crushed tuff material. A fourth domain, the invert-UZ interface, facilitates transfer of the radionuclide mass from the EBS transport model to the UZ transport model.

The applicant conceptualized the transport pathway as a flow-through model in which water flows vertically through a degraded waste package. The applicant considered an alternative conceptual model in which the outlet for water is not on the underside of the waste package. In this bathtub model, water would fill the partially intact waste package until it reaches a spill point corresponding to a breach on the side of the waste package. In a variant of the bathtub model, the stored water and dissolved radionuclides would be suddenly released when a second breach develops on the underside of the waste package.

NRC Staff Review

(b)(5)

(b)(5)

(b)(5)

Transport Model Framework

In the applicant's abstraction, dissolved radionuclides and radionuclides sorbed onto the five types of mobile colloids described in SER Section 2.2.1.3.4.3.4 are transported by diffusion and, if water is flowing in the EBS, advection. Advective velocities for colloids are identical to the water velocity. Advective transport of selected dissolved radionuclides is slowed by sorption onto stationary corrosion products. Solubility limits on the dissolved radionuclide concentrations are also imposed.

NRC Staff Review

(b)(5)

Transport Under Disruptive Events

The applicant's TSPA implementation of EBS transport is similar for the disruptive and nominal modeling cases, although conditions within the EBS (input for the abstraction) may be different following disruptive events. Most importantly, the applicant assumed instant degradation of the waste forms and advective conditions within the EBS following an igneous intrusion event.

NRC Staff Review

(b)(5)

Model Abstraction and TSPA Model Results

In response to NRC staff's questions regarding consistency between the model abstraction and the TSPA code calculated results, the applicant provided additional information on the mass retained in and flux out of each computational domain for key representative radionuclides using single representative realizations of the igneous intrusion and nominal modeling cases (DOE, 2009da,dc). The NRC staff used the results for commercial SNF and the igneous intrusion modeling case to evaluate consistency between the results of the TSPA analyses and the conceptual process models the applicant described. For I-129, 99.96 percent of the initial inventory is transported out of the EBS in the first TSPA timestep following the intrusion event. Release of Np-237 is significantly delayed but not eliminated by precipitation and sorption onto

stationary corrosion products. For example, about 14 percent of the initial Np-237 inventory is released from the EBS in the first 40,500 years following the igneous intrusion event; after 1 million years the released fraction is 88 percent of the initial inventory (including ingrowth).

For Pu-242, the applicant provided information for two realizations: one with stable waste form colloids in the waste form domain, described in DOE (2009dc), and one with unstable waste form colloids in the waste form domain, described in DOE Enclosure 1 (2009da). For the realization with stable waste form colloids in the waste form domain, which according to DOE Enclosure 1 (2009dd) is representative of about 38 percent of realizations, about 11 percent of the initial inventory is released from the EBS in the first 204,000 years. Nearly all of the remaining Pu-242 mass is retained in the corrosion products domain irreversibly associated with permanently immobilized (settled) waste form colloids in this realization. In the applicant's realization results with unstable waste form colloids in the waste form domain, which is representative of 62 percent of realizations, precipitation of plutonium-bearing minerals and sorption onto stationary corrosion products delay release but do not permanently sequester Pu-242, similar to Np-237.

NRC Staff Review

(b)(5)

Summary of Diffusion Models

The various analytical models used to simulate diffusive transport in the TSPA computer code are summarized next.

The applicant calculated diffusion coefficients for dissolved radionuclides as the product of tortuosity (the effect of flow path shape in a porous medium) and species-dependent free-water diffusion coefficients. The diffusion coefficients were adjusted for temperature. The tortuosity was empirically related to porosity and liquid saturation using standard models. The applicant based diffusion coefficients for colloids on the Stokes-Einstein equation, which accounts for temperature and particle size. (b)(5)

(b)(5)

For the no-dripping situation, the applicant calculated liquid water content from relative humidity using empirical adsorption isotherms. This information is needed to establish diffusion coefficients, which are dependent on water content. The applicant developed a diffusion model for these conditions and conducted an extensive literature review on data relevant to predicting water content on the basis of relative humidity, as described in SNL Section 6.3.4.3 (2007aj).

The applicant compared the output of the abstraction for adsorbed water content versus relative humidity with literature data for adsorption on goethite, hematite, Cr_2O_3 , and NiO . (b)(5)

(b)(5)

(b)(5) The applicant also compared the model output to the results of independent modeling studies. (b)(5)

(b)(5)

The mass of steel corrosion products is needed to establish the liquid water content, which the applicant calculated as a function of time from the degradation of steel internals of the waste package. (b)(5)

(b)(5)

For the dripping situation, the applicant assumed the porous materials were saturated with liquid water. (b)(5)

(b)(5)

The applicant used data on diffusion in crushed tuff material to develop uncertainty distributions for invert diffusion coefficients. Uncertainty in the diffusion coefficients and invert porosity are explicitly represented. (b)(5)

(b)(5)

The applicant compared the output of the invert diffusion coefficient model with two sets of experimental results. The applicant's abstraction predicts larger diffusion coefficients than the experimentally determined values. (b)(5)

(b)(5)

The applicant considered two alternative conceptual models related to diffusion in the invert. One of these alternative conceptual models is based on a dual-continuum representation of diffusion. (b)(5)

(b)(5)

(b)(5) The applicant's other alternative conceptual model considers alternative relationships between diffusion coefficients and moisture content at low moisture content. (b)(5)

(b)(5)

(b)(5)

In the applicant's TSPA model, radionuclide mass enters the UZ after leaving the invert. Because the mass flux out of the invert is partly the result of diffusion, radionuclide concentrations in the UZ are needed to obtain estimates of the mass flux. The applicant modeled a portion of the UZ in the EBS/UZ interface to calculate the diffusive fluxes into the UZ transport model. The EBS/UZ interface is a network of computational cells representing a local region of the UZ just below a drift. Hydrological conditions in the EBS/UZ interface are established similarly to the UZ transport model (SER Section 2.2.1.3.7). A zero concentration boundary condition is used at the lower boundary of the interface zone. (b)(5)

(b)(5)

Sorption on Corrosion Products

In the applicant's abstraction, radionuclides enter the corrosion products domain from the waste form domain both in solution and associated with montmorillonite, plutonium, zirconium, and uranophane colloids. The transport of selected radionuclides is significantly retarded by sorption onto stationary corrosion products. The applicant treated the corrosion products domain as a single mixing cell containing a homogenous porous medium with no preferential flow paths, on the basis of a conceptualization of degraded waste form disseminated within a corrosion product mass. (b)(5)

(b)(5)

In the applicant's abstraction, corrosion product surface area is used to calculate the volume of adsorbed water and the mass of radionuclides sorbed onto corrosion products. The applicant assumed a mixture of hydrous ferric oxide and goethite for calculating corrosion product surface area without considering the aging of hydrous ferric oxide to more crystalline iron oxides with lower surface area. The applicant provided additional sensitivity information in DOE Enclosure 6 (2009ay). (b)(5)

(b)(5)

The abstraction calculates the corrosion product surface area as a function of time using an uncertainty distribution of stainless steel corrosion rates based on literature data. On the basis of additional information the applicant provided in BSC (2004ae) and DOE Enclosure 2 (2009db) and an independent literature review, (b)(5)

(b)(5)

The applicant modeled sorption on corrosion products for uranium, neptunium, thorium, americium, and plutonium using a surface complexation model to develop effective distribution coefficients (K_d s) taking into account the chemical conditions. A surface complexation model simulates equilibrium attachment of dissolved ions onto solid surfaces and incorporates the chemical complexity of the system. Other radioelements that are tracked in the UZ

transport abstraction (SER Section 2.2.1.3.7)—such as cesium, protactinium, radium, selenium, strontium, tin, technetium, iodine, chlorine, and carbon—are assumed to not sorb onto stationary corrosion products. Nickel is included in the surface complexation model to represent competition for sorption sites, but the sorbed mass of nickel is not explicitly tracked for transport purposes.

The surface complexation model is not directly incorporated in the applicant's TSPA model abstraction, but the distribution coefficients developed from the surface complexation model are directly applicable to the transport of uranium, neptunium, and thorium, which are assumed to undergo rapid and reversible sorption. Kinetic reversible sorption is modeled for americium and plutonium sorption on stationary corrosion products. The forward sorption rate constant in this case is sampled from an uncertainty distribution. The desorption rate constants are then calculated from this forward rate and the K_d s calculated using the surface complexation model.

To develop the K_d distributions used in the TSPA model abstraction, the applicant carried out the surface complexation models using the PHREEQC geochemical software the U.S. Geological Survey developed. To represent parameter uncertainty in the surface complexation model, the applicant conducted about 5,000 PHREEQC simulations, each with a unique combination of surface properties and aqueous chemistry parameters as inputs. The applicant then analyzed the PHREEQC simulation results using multiple regressions to produce functions that calculated actinide sorption as a function of key geochemical properties. These functions provide the K_d values used in the TSPA model abstraction of sorption to stationary corrosion products. (b)(5)

(b)(5)

The applicant compared the calculated surface complexation model results from almost 5,000 simulations to recent U.S. Environmental Protection Agency (EPA) compilations of soil K_d s obtained in the laboratory (SAR Section 2.3.7.12.3.4; SNL, 2007aj). The applicant compared values over a pH range from 6 to 9 (SAR Section 2.3.7.12.3.4). (b)(5)

(b)(5)

The applicant used several different approaches in developing its final TSPA abstraction for sorption to stationary corrosion products and considered and evaluated several different surface complexation model approaches before selecting the diffuse-layer model, as outlined in DOE Enclosure 3 (2009da). (b)(5)

(b)(5)

In SNL Section 6.5.2.4.2 (2007aj), the applicant stated that aqueous thermodynamic data were propagated through the surface complexation model, but did not explicitly consider uncertainty in equilibrium constants for surface complexation constants used in the surface complexation model. (b)(5)

(b)(5)

The applicant's abstraction assumes a single-rate, first-order kinetic model for plutonium and americium sorption. The forward rate constants for sorption of americium and plutonium onto corrosion products were estimated from plutonium sorption experiments in SNL (2008ak).

(b)(5)

Colloid-Facilitated Transport

In the applicant's abstraction, the transport of selected radionuclides may be enhanced by the five colloid types described in SER Section 2.2.1.3.4.3.4. (b)(5)

(b)(5)

The applicant's abstraction considers plutonium to be irreversibly associated with plutonium and zirconium colloids that originate from SNF and montmorillonite colloids originating from defense HLW glass waste. Uranium is irreversibly associated with the uranophane colloids that originate in SNF. These three colloid types and the associated radionuclides originate in the waste form.

Selected radionuclides (isotopes of americium, cesium, protactinium, plutonium, radium, tin, and thorium) are allowed to sorb reversibly and without kinetic limitations onto uranophane colloids and groundwater or waste-derived montmorillonite colloids. The empirical sorption model represents equilibrium, site-limited sorption with competition for sites. (b)(5)

(b)(5)

In the applicant's abstraction, uranium, neptunium, and thorium sorb reversibly and without kinetic limitations to corrosion product colloids. The applicant calculated equilibrium distribution coefficients (K_d s) for these elements using the same surface complexation modeling approach as for sorption on stationary corrosion products. As described in the previous subsection, the surface complexation model simulates equilibrium attachment of dissolved ions onto solid surfaces (in this case, the surfaces of mobile colloids), incorporating the chemical complexity of the system. The applicant's abstraction does not include corrosion product colloids in the waste form domain. Kinetic irreversible sorption onto corrosion product colloids is modeled for americium and plutonium in the corrosion products domain (b)(5)

(b)(5)

In the applicant's abstraction, the forward rate constants for americium and plutonium are not sampled directly. Instead, the fraction of total mobile radionuclide mass exiting the corrosion products domain that is associated with colloids (the target flux out ratio) is sampled from a uniform distribution with a range of 0.9 to 0.99. An analytical inverse solution is then used to calculate the forward rate corresponding to the sampled ratio. The computed forward rate constant and other parameters computed from the inverse solution are further compared against physically allowed ranges. If any computed value is outside its allowed range, the corresponding maximum or minimum value is used in the forward model for colloid-assisted transport in place of the sampled ratio. (b)(5)

(b)(5)

The applicant provided information suggesting that colloids will not significantly enhance transport of radionuclides in the EBS, because commercial SNF-derived colloids are expected to be unstable in the corrosion products domain and because radionuclide concentrations associated with iron oxide and glass waste form colloids are expected to be much smaller than dissolved concentrations. (b)(5)

(b)(5)

Reasonableness and Consistency of TSPA Results for Engineered Barrier System Radionuclide Releases

The NRC staff performed simplified confirmatory analyses to assess whether the applicant's TSPA results for the EBS radionuclide releases are consistent with the applicant's abstractions. As detailed in the following paragraphs, the NRC staff used hand calculations (Painter, 2010aa) to estimate peak expected total-repository EBS release rates for Tc-99, Pu-242, and Np-237 using applicant-provided information, and then compared these releases with applicant-provided values.¹ The NRC staff's confirmatory calculations focused on the igneous intrusion and seismic ground motion modeling cases because these cases result in the largest release rates from the EBS. These estimates are based on advection and diffusion of dissolved radionuclides and neglect transport of radionuclides associated with colloids. As discussed in SER Section 2.2.1.3.4.3.4, transport in the EBS is not significantly enhanced by colloids, because of low colloid concentrations in the corrosion products domain.

The applicant provided information showing that fractional EBS releases of low-solubility, sorbing radionuclides are mainly controlled by processes within the corrosion products domain because waste form dissolution and invert transport processes are fast relative to transport within the corrosion products domain. Specifically, fractional releases are controlled by advection modified by sorption and precipitation of radionuclide-bearing minerals in the igneous intrusion and seismic ground motion modeling cases, and by diffusion modified by sorption and precipitation in the nominal modeling case.

(b)(5)

(b)(5)

¹The NRC staff's calculations are estimates only, using parameters and probabilities the applicant provided in the SAR, supporting reports, and associated RAI responses. Because simplifications are involved, precise agreement between the NRC staff calculations and the applicant's results was not expected, rather, general agreement with the magnitude of the releases was evaluated.

(b)(5)

Summary of Review of Engineered Barrier System Radionuclide Transport

(b)(5)

(b)(5)

2.2.1.3.4.4 Evaluation Findings

The NRC staff reviewed the applicant's SAR and other information submitted in support of the license application and finds that, with respect to the requirements of 10 CFR 63.114 for consideration of the radionuclide release rates and solubility limits, (b)(5)

(b)(5)

(b)(5)

2.2.1.3.4.5 References

Allison, J.M. 2004aa. "Request for Referenceable Information on High-Level Waste (HLW) Radionuclide Inventories in Support of Preparation of the Yucca Mountain Project License Application, JCP-0445, 1/28/04." Memorandum (February 26, 0303040661, with attachment) to J. Authur, III, OCRWM. MOL20040317.0265. Aiken, South Carolina: DOE, Savannah River Operations Office.

Appelo, C.A.J. and Postma, D. 1994aa. *Geochemistry, Groundwater and Pollution*. Brookfield, Vermont: A.A. Balkema.

Basagaoglu, H. 2010aa. "Colloidal Transport." Electronic Scientific Notebook 844E San Antonio, Texas: CNWRA.

Beavers, J.A. and C.L. Durr. 1990aa. *Container Corrosion in High Level Nuclear Waste Repositories*. Columbus, Ohio: Cortest Columbus, Inc.

Bowman, S.M. and L.C. Leal. 2000aa. NUREG/CR-0200, "ORIGEN-ARP: Automatic Rapid Process for Spent Fuel Depletion, Decay, and Source Term Analysis." ORNL/NUREG/CSD-2/V1/R6. Oak Ridge, Tennessee: Oak Ridge National Laboratory.

Bremier, S., C.T. Walker, and R. Menzel. 2000aa. "Fission Gas Release and Fuel Swelling at Burn-Ups Higher Than 50 Mwd/kgU." Proceedings of the Fission Gas Behavior in Water Reactor Fuels. Cadarache, France, September 26–29, 2000. Paris, France: Nuclear Energy Institute. pp. 93–106.

BSC. 2005ad. "In-Package Chemistry Abstraction." ANL-EBS-MD-000037. Rev. 04 ACN 01, AD 01, ERD 01. Las Vegas, Nevada: Bechtel SAIC Company, LLC.

BSC. 2004ae. "Aqueous Corrosion Rates for Waste Package Materials." ANL-DSD-MD-000001. Rev. 01. ACN 001, ERD 01, ERD 02. Las Vegas, Nevada: Bechtel SAIC Company, LLC.

BSC. 2004ah. "CSNF Waste Form Degradation: Summary Abstraction." ANL-EBS-MD-000015. Rev. 02. ACN 02. Las Vegas, Nevada: Bechtel SAIC Company, LLC.

BSC. 2004ai. "Defense HLW Glass Degradation Model." ANL-EBS-MD-000016. Rev. 02. ACN 001, ERD 001, ERD 002. Las Vegas, Nevada: Bechtel SAIC Company, LLC.

BSC. 2004ao. "DSNF and Other Waste Form Degradation Abstraction." ANL-WIS-MD-000004. Rev. 4. Las Vegas, Nevada: Bechtel SAIC Company, LLC.

BSC. 2003af. "PWR Assembly End-Effect Reactivity Evaluation." CAL-UDC-NU-000006. Rev. 00, with 01 errata. MOL20010412.0158. DOC20031014.0007. Las Vegas, Nevada: Bechtel SAIC Company, LLC.

Corapcioglu, M.Y. and S. Jiang. 1993aa. "Colloid-Facilitated Groundwater Contaminant Transport." *Water Resources Research*. Vol. 29, No. 7. pp. 2,215–2,226.

Cvetkovic, V., S. Painter, D. Turner, D. Pickett, and P. Bertetti. 2004aa. "Parameter and Model Sensitivities for Colloid-Facilitated Transport on the Field Scale." *Water Resources Research*. Vol. 40. doi:10.1029/2004WR003048.

Da Cunha Belo, M., M. Walls, N.E. Hakiki, J. Corset, E. Picquenard, G. Sagon, and D. Noel. 1998aa. "Composition, Structure, and Properties of Oxide Films Formed on the Stainless Steel 316L in a Primary Type PWR Environment." *Corrosion Science*. Vol. 40, Nos. 2 and 3. pp. 447–463.

DOE. 2010aj. "Yucca Mountain—Supplemental Response to Request for Additional Information Regarding License Application (Safety Analysis Report Section 2.3.7), Safety Evaluation Report Vol. 3, Chapter 2.2.1.3.4, Set 1." Letter (February 24) J.R. Williams to J.H. Sulima (NRC). ML100560258. Washington, DC: DOE, Office of Technical Management.

DOE. 2009an. "Yucca Mountain—Response to Request for Additional Information Regarding License Application (Safety Analysis Report Section 2.1), Safety Evaluation Report Vol. 3, Chapter 2.2.1.1, Set 1." Letter (February 6) J.R. Williams to J.H. Sulima (NRC). ML090400455. Washington, DC: DOE, Office of Technical Management.

DOE. 2009av. DOE/RW-0573, "Yucca Mountain Repository License Application." Rev. 1. ML090700817. Las Vegas, Nevada: DOE, Office of Civilian Radioactive Waste Management.

DOE. 2009ax. "Yucca Mountain—Response to Request for Additional Information Regarding License Application (Safety Analysis Report Section 2.3.7), Safety Evaluation Report, Vol. 3, Chapter 2.2.1.3.4, Set 1." Letter (May 5) J.R. Williams to J.H. Sulima (NRC). ML091260473. Washington, DC: DOE, Office of Technical Management.

DOE. 2009ay. "Yucca Mountain—Response to Request for Additional Information Regarding License Application (Safety Analysis Report Section 2.3.7), Safety Evaluation Report, Vol. 3, Chapter 2.2.1.3.4, Set 2." Letter (May 12) J.R. Williams to J.H. Sulima (NRC). ML 091330282. Washington, DC: DOE, Office of Technical Management.

DOE. 2009cz. "Yucca Mountain—Supplemental Response to Request for Additional Information Regarding License Application (Safety Analysis Report Section 2.3.7), Safety Evaluation Report Vol. 3, Chapter 2.2.1.3.4, Set 1 and Set 2." Letter (June 26) J.R. Williams to J.H. Sulima (NRC). ML091770582. Washington, DC: DOE, Office of Technical Management.

DOE. 2009da. "Yucca Mountain—Response to Request for Additional Information Regarding License Application (Safety Analysis Report Section 2.3.7), Safety Evaluation Report Vol. 3, Chapter 2.2.1.3.4, Set 3." Letter (September 11) J.R. Williams to J.H. Sulima (NRC). ML092600883. Washington, DC: DOE, Office of Technical Management.

DOE. 2009db. "Yucca Mountain—Response to Request for Additional Information Regarding License Application (Safety Analysis Report Section 2.3.7), Safety Evaluation Report Vol. 3, Chapter 2.2.1.3.4, Set 4." Letter (October 16) J.R. Williams to J.H. Sulima (NRC). ML093200320. Washington, DC: DOE, Office of Technical Management.

DOE. 2009dc. "Yucca Mountain—Response to Request for Additional Information Regarding License Application (Safety Analysis Report Section 2.3.7), Safety Evaluation Report Vol. 3, Chapter 2.2.1.3.4, Set 2." Letter (May 28) J.R. Williams to J.H. Sulima (NRC). ML091480752. Washington, DC: DOE, Office of Technical Management.

DOE. 2009dd. "Yucca Mountain—Supplement Response to Request for Additional Information Regarding License Application (Safety Analysis Report Section 2.3.7), Safety Evaluation Report Vol. 3, Chapter 2.2.1.3.4, Set 2." Letter (September 4) J.R. Williams to J.H. Sulima (NRC). ML092470427. Washington, DC: DOE, Office of Technical Management.

DOE. 2003ad. "Review of DOE Spent Nuclear Fuel Release Rate Test Results." Rev. 0. DOE/SNF/REP-073. Idaho Falls, Idaho: Idaho National Engineering and Environmental Laboratory.

DOE. 2000aa. DOE/SNF/REP-056. "N Reactor (U-Metal) Fuel Characteristics for Disposal Criticality Analysis." Rev. 0. TIC247956. Washington, DC: DOE, Office of Environmental Management.

Finch, R.J., E.C. Buck, P.A. Finn, and J.K. Bates. 1999aa. "Oxidative Corrosion of Spent UO₂ Fuel in Vapor and Dripping Groundwater at 90 °C." 22nd Symposium on Scientific Basis for Nuclear Waste Management, 1998 Material Research Society Fall Meeting, Boston, Massachusetts, November 30–December 4, 1998. Symposium Proceedings Vol. 556. Warrendale, Pennsylvania: Materials Research Society. p. 431.

Glass, R.S., G.E. Overturf, R.E. Garrison, and R.D. McCright. 1984aa. "Electrochemical Determination of the Corrosion Behavior of Candidate Alloys Proposed for Containment of High Level Nuclear Waste in Tuff." Report UCID-20174. Livermore, California: Lawrence Livermore National Laboratory.

GoldSim Technology Group. 2006aa. *GoldSim Contaminant Transport Module User's Guide, Version 4.0*. Issaquah, Washington: GoldSim Technology Group.

Gray, W.J. 1999aa. "Inventories of Iodine-129 and Cs-137 in the Gaps and Grain Boundaries of LWR Spent Fuels." *Proceedings of the Materials Research Society. Symposium Proceedings 556*. Warrendale, Pennsylvania: Materials Research Society. pp. 487-494.

Harrar, J.E., J.F. Carley, W.F. Underwood, and E. Raber. 1990aa. "Report of the Committee to Review the Use of J-13 Well Water in Nevada Nuclear Waste Storage Investigations." UCID-21867. ACC:NNA 19910131.0274. Livermore, California: Lawrence Livermore National Laboratory.

Hem, J.D. 1995aa. *Study and Interpretation of the Chemical Characteristics of Natural Water*. 3rd Edition. Geological Survey Water-Supply Paper 2254. Washington, DC: U.S. Government Printing Office.

Jain, V., G. Cragolino, and L. Howard. 2004aa. "A Review Report on High Burnup Spent Nuclear Fuel—Disposal Issues." ML 042860337. San Antonio, Texas: CNWRA.

Jantzen, C.M., D.I. Kaplan, N.E. Bibler, D.K. Peeler, and M.J. Plodinec. 2008aa. "Performance of a Buried Radioactive High-Level Waste (HLW) Glass after 24 Years." *Journal of Nuclear Materials*. Vol. 378. pp. 244-256.

Johnson, L.H. and J.C. Tait. 1997aa. "Release of Segregated Nuclides From Spent Fuel." SKB Technical Report 97-18. Stockholm, Sweden: Swedish Nuclear Fuel and Waste Management Company.

Langmuir, D. 1997aa. *Aqueous Environmental Geochemistry*. Upper Saddle River, New Jersey: Prentice Hall.

Lassmann, K., C.T. Walker, J. van de Larr, and F. Lindstrom. 1995aa. "Modeling the High Burnup UO₂ Structure in LWR Fuel." *Journal of Nuclear Materials*. Vol. 226 pp. 1-8.

Leslie, B., C. Grossman, and J. Durham. 2007aa. "Total-system Performance Assessment (TPA) Version 5.1 Module Descriptions and User Guide." Rev. 1. ML072710060. San Antonio, Texas: CNWRA.

MacKinnon, R.J. 2008aa. "Engineered Barrier System (EBS) Transport Model Abstractions." Presentation at DOE/NRC Technical Exchange on Total System Performance Assessment (TSPA) for Yucca Mountain, Las Vegas, Nevada, April 4, 2008. LSN:DEN001594514. Washington, DC: NRC.

Manaktala, H. 1993aa. "Characteristics of Spent Nuclear Fuel and Cladding Relevant to High-Level Waste Source Term." CNWRA 93-006. ML 040200340. San Antonio, Texas: CNWRA.

McCrigh, R.D., W.G. Halsey, and R.A. Van Konynenburg. 1987aa. "Progress Report on the Results of Testing Advanced Conceptual Design Metal Barrier Materials Under Relevant Environmental Conditions for a Tuff Repository." Report No. UCID-21044. Livermore, California: Lawrence Livermore National Laboratory.

Mohanty, S., G. Adams, and R. Pabalan. 2003aa. "The Role of Solubility as a Barrier to Radionuclide Release." Proceedings of the 10th International High-Level Radioactive Waste Management Conference, Las Vegas, Nevada, March 30–April 2, 2003. La Grange Park, Illinois: American Nuclear Society. pp. 938–945.

Morgenstein, M.D., C.L. Wicket, and A. Barkatt. 1999aa. "Consideration of Hydration-rind Dating of Glass Artefacts: Alteration Morphologies and Experimental Evidence of Hydrogeochemical Soil-Zone Pore Water Control." *Journal of Archaeological Science*. Vol. 26. pp. 1,193–1,210.

Murphy, W.M. and R.C. Codell. 1999aa. "Alternate Source Term Models for Yucca Mountain Performance Assessment Based on Natural Analog Data and Secondary Mineral Solubility." Proceedings of the Materials Research Society, November 30–December 4, 1998, Boston, Massachusetts. Symposium Proceedings 556. D.J. Wronkiewicz and J.H. Lee, eds. Warrendale, Pennsylvania: Materials Research Society. pp. 551–558.

NRC. 2009ab. "Division of High-Level Waste Repository Safety Director's Policy and Procedure Letter 14: Application of YMRP for Review Under Revised Part 63." Published March 13, 2009. ML090850014. Washington, DC: NRC.

NRC. 2008aa. NUREG-1914, "Dissolution Kinetics of Commercial Spent Nuclear Fuels in the Potential Yucca Mountain Repository Environment." ML 083120074. Washington, DC: NRC.

NRC. 2003aa. NUREG-1804, "Yucca Mountain Review Plan—Final Report." Rev. 2. Washington, DC: NRC.

NRC. 1996ab. NUREG-1564, "Long-Term Kinetic Effects and Colloid Formation in the Dissolution of LWR Spent-Fuel." ML 073100056. Washington, DC: NRC.

Nuclear Energy Agency. 1997aa. "Lessons Learnt from Ten Performance Assessment Studies." Paris, France: Organisation for Economic Co-operation and Development, Nuclear Energy Agency.

Painter, S. 2010aa. "Radionuclide Transport Analysis for Yucca Mountain." Electronic Scientific Notebook 318E. San Antonio, Texas: CNWRA.

Painter, S. and V. Cvetkovic. 2006aa. "Effect of Kinetic Limitations on Colloid-Facilitated Transport at the Field Scale." 11th International High-Level Radioactive Waste Management Conference, Global Progress Toward Safe Disposal, Las Vegas, Nevada, April 30–May 4, 2006. LaGrange Park, Illinois: American Nuclear Society.

Painter, S., V. Cvetkovic, D. Turner, and D. Pickett. 2002aa. "Significance of Kinetics for Sorption on Inorganic Colloids: Modeling and Experimental Interpretation Issues." *Environmental Science and Technology*. Vol. 24. pp. 228–234.

Pearcy, E.C., J.D. Prikryl, W.M. Murphy, and B.W. Leslie. 1994aa. "Alteration of Uraninite From the Nopal I Deposit, Peña Blanca District, Chihuahua, Mexico, Compared to Degradation of Spent Nuclear Fuel in the Proposed U.S. High-Level Nuclear Waste Repository at Yucca Mountain, Nevada." *Applied Geochemistry*. Vol. 9. pp. 713–732.

Pickett, D.A. 2005aa. "Effects of Spent Nuclear Fuel Uranyl Alteration Phases on Radionuclide Dissolved Concentration Limits." San Antonio, Texas: CNWRA.

Prikryl, J.D. 2008aa. "Uranophane Dissolution and Growth in $\text{CaCl}_2\text{--SiO}_2(\text{aq})$ Test Solutions." *Geochimica et Cosmochimica Acta*. Vol. 72. pp. 4,508–4,520.

Pulvirenti, A.L., S.J. Eddy, T.M. Calabrese, M.A. Adel-Hadadi, A. Barkatt, and M.E. Morgenstein. 2006aa. "Interaction of Iron Containing Silicate Glasses with Aqueous Salt Solutions." *Physics and Chemistry of Glasses: European Journal of Glass Science and Technology Part B*. Vol. 47, No. 1. pp. 47–57.

Roxburgh, I.S. 1987aa. *Geology of High-Level Nuclear Waste Disposal: An Introduction*. New York City, New York: Chapman and Hall.

SNL. 2008ab. "Features, Events, and Processes for the Total System Performance Assessment: Analyses." ANL–WIS–MD–000027. Rev. 00. ACN 01, ERD 01, ERD 02. Las Vegas, Nevada: Sandia National Laboratories.

SNL. 2008ad. "Postclosure Nuclear Safety Design Bases." ANL–WIS–MD–000024. Rev. 01. ACN 01, ERD 01, ERD 02. Las Vegas, Nevada: Sandia National Laboratories.

SNL. 2008ag. "Total System Performance Assessment Model/Analysis for the License Application." MDL–WIS–PA–000005. Rev. 00. AD 01, ERD 01, ERD 02, ERD 03, ERD 04. Las Vegas, Nevada: Sandia National Laboratories.

SNL. 2008ak. "Waste Form and In-Drift Colloids-Associated Radionuclide Concentrations: Abstraction and Summary." MDL–EBS–PA–000004. Rev. 03. ERD 01. Las Vegas, Nevada: Sandia National Laboratories.

SNL. 2007ag. "Dike/Drift Interactions." MDL–MGR–GS–000005. Rev. 02. ERD 01, ERD 02. Las Vegas, Nevada: Sandia National Laboratories.

SNL. 2007ah. "Dissolved Concentration Limits of Elements with Radioactive Isotopes." ANL–WIS–MD–000010. Rev. 06. Las Vegas, Nevada: Sandia National Laboratories.

SNL. 2007aj. "EBS Radionuclide Transport Abstraction." ANL–WIS–PA–000001. Rev. 03. ERD 01. Las Vegas, Nevada: Sandia National Laboratories.

SNL. 2007ak. "Engineered Barrier System: Physical and Chemical Environment." ANL–EBS–MD–000033. Rev. 06. ERD 01. Las Vegas, Nevada: Sandia National Laboratories.

SNL. 2007ao. "In-Drift Precipitates/Salts Model." ANL–EBS–MD–000045. Rev. 03. ERD 01, ERD 02. Las Vegas, Nevada: Sandia National Laboratories.

SNL. 2007at. "Qualification of Thermodynamic Data for Geochemical Modeling of Mineral—Water Interactions in Dilute Systems." ANL-WIS-GS-000003. Rev. 01. Las Vegas, Nevada: Sandia National Laboratories.

SNL. 2007bm. "Total System Performance Assessment Data Input Package for Requirements Analysis for DOE SNF/HLW and Naval SNF Waste Package Overpack Physical Attributes Basis for performance Assessment." Rev. 00. TDR-TDIP-ES-000003. Las Vegas, Nevada: Sandia National Laboratories.

SNL. 2007bn. "Total System Performance Assessment Data Input Package for Requirements Analysis for TAD Canister and Related Waste Package Overpack Physical Attributes Bases for Performance Assessment." Rev. 00. TDR-TDIP-ES-000006. Las Vegas, Nevada: Sandia National Laboratories.

Spino, J., J. Cobos-Sabate, and F. Rousseau. 2003aa. "Room-Temperature Microindentation Behaviour of LWR-Fuels, Part 1: Microhardness." *Journal of Nuclear Materials*. Vol. 322. pp. 204–216.

van de Weerd, H., A. Leijnse, and W.H. van Riemsdijk. 1998aa. "Transport of Reactive Colloids and Contaminants in Groundwater: Effect of Nonlinear Kinetic Interactions." *Journal of Contaminated Hydrology*. Vol. 32. pp. 313–331.

Wang, X.Y., Y.S. Wu, L. Zhang, and Z.Y. Yu. 2001aa. "Atomic Force Microscopy and X-Ray Photoelectron Spectroscopy Study on the Passive Film for Type 316L Stainless Steel." *Corrosion Science*. Vol. 57, No. 6. pp. 540–546.

Wilson, C.N. and W.J. Gray. 1990aa. "Measurement of Soluble Nuclide Dissolution Rates From Spent Fuel." Proceedings of the Materials Research Society. Symposium Proceedings 176. V.M. Oversby and P.W. Brown, eds. Warrendale, Pennsylvania: Materials Research Society. pp. 489–498.

Wronkiewicz, D.J., K.J. Bates, S.F. Wolf, and E.C. Buck. 1996aa. "Ten-Year Results From Unsaturated Drip Tests With UO₂ at 90°C: Implications for the Corrosion of Spent Nuclear Fuel." *Journal of Nuclear Materials*. Vol. 238, No. 1. pp. 78–95.

Zhu, C. 2004aa. "Coprecipitation in the Barite Isostructural Family: 2 Numerical Simulations of Reactions and Mass Transport." *Geochimica et Cosmochimica Acta*. Vol. 68 pp. 3,339–3,349.

CHAPTER 8

2.2.1.3.5 Climate and Infiltration

2.2.1.3.5.1 Introduction

This chapter of the Safety Evaluation Report (SER) provides the U.S. Nuclear Regulatory Commission (NRC) staff's evaluation of the U.S. Department of Energy's (DOE) representation of climate and infiltration, as presented in the applicant's Safety Assessment Report (SAR) Section 2.3.1 (DOE, 2008ab), relevant references, and DOE responses to staff requests for additional information (RAIs). DOE considers the reduction of water flux from precipitation to net infiltration to be a barrier capability for the Upper Natural Barrier. Because of the generally vertical movement of percolating water through the unsaturated zone in the DOE representation of the natural system, water entering the unsaturated zone at the ground surface (infiltration) is the only source for deep percolation water in the unsaturated zone at and below the proposed repository.

DOE used the term "net infiltration" to define the volumetric flux of water passing below the active plant root zone, but often refers to net infiltration simply as "infiltration." DOE also used the term net infiltration to refer both to the output of the net infiltration model (SAR Section 2.3.1) and to the top boundary condition of the unsaturated zone model (SAR Section 2.3.2). This distinction is important because the average values from the net infiltration model differ from those used as net infiltration at the top boundary of the site-scale unsaturated zone model. NRC staff evaluates the former in the present section and the latter in SER Section 2.2.1.3.6.3.2.

Climate and infiltration are treated differently in DOE's performance assessment for the first 10,000 years following permanent closure of the repository and the period from 10,000 to 1 million years. For the first 10,000 years, DOE used paleoclimate records for the region to predict future climatic conditions and uses these predictions as input for estimating future net infiltration. In addition, DOE used the climate predictions to scale groundwater fluxes in the saturated zone portion of the performance assessment for this period. DOE described its approach for scaling the groundwater flux in SAR Section 2.3.8; NRC staff review is in SER Section 2.2.1.3.7. For the period from 10,000 years to 1 million years after permanent closure, 10 CFR 63.342(c)(2) allows the applicant to consider long-term-average deep percolation flux at the proposed repository horizon instead of explicitly predicting climate and infiltration. DOE chose to use the prescribed deep percolation flux in its performance assessment for the post-10,000-year period. In SER Section 2.2.1.3.6.3.2, NRC staff evaluates the DOE implementation of 10 CFR 63.342 with respect to average deep percolation flux at the proposed repository horizon for post-10,000-year performance assessment calculations.

This SER chapter provides the NRC staff evaluation of DOE's consideration of climate and infiltration in the first 10,000 years after closure in DOE's total system performance assessment calculations. NRC staff reviews the DOE technical bases, input data, models, and net infiltration results against the applicable regulations. The NRC staff uses its understanding of relative risk within the system to inform its review, by focusing on those aspects that are most significant for repository performance. Staff considered how the flux of water through the unsaturated zone affects seepage, release of radionuclides from the engineered barrier system, and radionuclide transport through the natural system (evaluated in SER Sections 2.2.1.3.6.3.4, 2.2.1.3.4.3.5, and 2.2.1.3.7, respectively) in determining the significant aspects of DOE's net infiltration model.

On the basis of the downstream uses of climate and infiltration calculations, staff focused its review most heavily on the DOE's estimates of the magnitude, spatial distribution, and uncertainty of net infiltration over the next 10,000 years.

2.2.1.3.5.2 Regulatory Requirements

Model abstractions used in the applicant's postclosure performance assessment must meet the regulatory requirements given in 10 CFR 63.114 (Requirements for Performance Assessment) and 63.342 (Limits on Performance Assessment), to support the predictions of compliance for 63.113 (Performance Objectives for the Geologic Repository after Permanent Closure). Specific compliance with 63.113 is reviewed in SER Section 2.2.1.4.1.

The requirements for performance assessment in 10 CFR 63.114 require DOE to

- Include appropriate data related to the geology, hydrology, and geochemistry of the surface and subsurface from the site and the region surrounding Yucca Mountain
- Account for uncertainty and variability in the parameter values used to model climate and infiltration
- Consider alternative conceptual models for climate and infiltration
- Provide technical bases for the inclusion of features, events, and processes (FEPs) affecting climate and infiltration, including effects of degradation, deterioration, or alteration processes of engineered barriers that would adversely affect performance of the natural barriers, consistent with the limits on performance assessment in 10 CFR 63.342
- Provide technical basis for the models of climate and infiltration that in turn provide input or otherwise affect other models and abstractions

10 CFR 63.114(a) considers performance assessment for the initial 10,000 years following permanent closure. 10 CFR 63.114(b) and 63.342 consider the performance assessment methods for the time from 10,000 years through the period of geologic stability, defined in 10 CFR 63.302 as 1 million years following disposal. These sections require that through the period of geologic stability, with specific limitations, the applicant

- Use performance assessment methods consistent with the performance assessment methods used to demonstrate compliance for the initial 10,000 years following permanent closure
- Include in the performance assessment those FEPs used in the performance assessment for the initial 10,000 year period

For this model abstraction of climate and infiltration, 10 CFR 63.342(c)(2) further provides that DOE may consider climate change after 10,000 years by using a constant-in-time specification of the mean and uncertainty distribution for repository-average deep percolation rate for the period from 10,000 to 1 million years. DOE elected to use this representation in its SAR. Thus, implementation of the specified representative percolation rate and its uncertainty distribution is reviewed for the post-10,000-year period.

NRC staff review of the license application follows the guidance laid out in the Yucca Mountain Review Plan (YMRP), NUREG-1804, Section 2.2.1.3.5, Climate and Infiltration (NRC, 2003aa), as supplemented by additional guidance for the period beyond 10,000 years after permanent closure (NRC, 2009ab). The acceptance criteria in the YMRP generically follow 10 CFR 63.114(a). Following the guidance, the NRC staff review of the applicant's abstraction of climate and infiltration considered five criteria

- System description and model integration are adequate.
- Data are sufficient for model justification.
- Data uncertainty is characterized and propagated through the abstraction.
- Model uncertainty is characterized and propagated through the abstraction.
- Model abstraction output is supported by objective comparisons.

Because 10 CFR Part 63 specifies the use of a risk-informed approach for the review of a license application, the guidance provided by the YMRP, as supplemented by NRC (2009ab), is followed to the extent reasonable for aspects of climate and infiltration important to repository performance. Whereas NRC staff considered all five criteria in their review of information provided by DOE, only aspects that substantively affect results of the performance assessment, as judged by NRC staff, are discussed in this chapter. NRC staff's judgment is based both on risk information provided by DOE, and staff's knowledge, experience, and independent analyses.

2.2.1.3.5.3 Technical Review

The review of the technical information DOE provided for climate and infiltration over the next 10,000 years is divided into three subsections within this SER section. The first subsection reviews the applicant's identification and description of features and processes for climate and infiltration. The second subsection focuses on the climate data, future-climate model, and climate predictions. The third subsection addresses the applicant's description of net infiltration processes, models, and estimates of net infiltration at Yucca Mountain using the future climate predictions.

2.2.1.3.5.3.1 Identification of Features and Processes

In this section, NRC staff reviews the DOE identification and description of processes important for estimating climate and net infiltration. This section addresses YMRP acceptance criteria related to system description and conceptual model justification. DOE's overall screening of FEPs is reviewed in SER Section 2.2.1.2.1.

DOE used regional and site characteristics to develop conceptual models for climate and net infiltration at Yucca Mountain. The natural features of topography and surficial soils of the Upper Natural Barrier were identified as important to waste isolation in SAR Section 2.1.2.1. On the basis of field observations, synthesis of data, and modeling over more than two decades, DOE indicated (SAR Section 2.3.1.1) that the features and processes important to the capability of the Upper Natural Barrier are (i) climate change, (ii) climate modification increases recharge, (iii) precipitation, (iv) topography and morphology, (v) rock properties of host rock and other units, (vi) surface runoff and evapotranspiration, (vii) infiltration and recharge, (viii) fractures, and (ix) fracture flow in the unsaturated zone.

The following summary is based on the information in SAR Section 2.3.1.1 and illustrates how DOE integrated these features and processes in its conceptual models of climate and infiltration. DOE described the present climate at Yucca Mountain as semi-arid, with low annual precipitation. DOE expects the climate to change over the next 10,000 years, remaining semi-arid but with changes in precipitation patterns and rates. DOE recognized that surface temperature and vegetation will also vary with changes in climate. Evapotranspiration (the combination of evaporation and plant transpiration) removes a large portion of the annual precipitation that infiltrates into the soil. In this environment, evapotranspiration is strongly influenced by temperature and low atmospheric relative humidity. DOE conceptualized that net infiltration events, where water passes into the bedrock, occur in pulses during and for a short period following some of the larger or longer duration precipitation events. Evapotranspiration continually dries the soil between precipitation events. DOE considered snow as providing a source of delayed infiltration during snowmelt events. In DOE's conceptual model, runoff and the soil's water-holding capacity limit the magnitude of net infiltration pulses, but runoff from one area may subsequently infiltrate downstream.

DOE conceived that soil, fractures, and bulk rock hydraulic properties affect the rate of water movement below the root zone, with a competition between downward flow and upward movement of water by evapotranspiration. In the DOE conceptual model, water flows quickly into the rock below shallow soil in areas where the bedrock is fractured or has a highly permeable matrix. Such rapid flow limits the effect of evapotranspiration. Surface water runoff, influenced by topography and surface morphology, spatially redistributes the flux of water. This process may reduce net infiltration in some areas (e.g., high on hillslopes) and increase net infiltration in others (e.g., washes and channels). DOE recognized that lateral movement of water below the surface, termed interflow, is known to spatially redistribute water, but the DOE conceptual model does not consider interflow to be significant at Yucca Mountain. For the semi-arid climate of Yucca Mountain, the overall water balance in DOE's model is dominated by precipitation and evapotranspiration, with infiltration and runoff representing relatively small portions of the balance.

Comment (b)(5)

Comment (b)(5)

DOE implemented its conceptualization in (i) a climate model that predicts future climatic states, (ii) climatic input data for each climate state, and (iii) an infiltration model linked to a surface-water-routing algorithm for runoff. The infiltration and routing algorithms are integrated into the Mass Accounting System for Soil Infiltration and Flow (MASSIF) model. DOE described

- A climate model for predicting climate over the next 10,000 years that uses Earth-orbital parameters and paleoclimatic data from the southwestern United States covering the past approximately 800,000 years
- Climatic input data for each climate state that uses recorded meteorological data from local, regional, and western U.S. stations
- Submodels of the infiltration model that consider precipitation, evapotranspiration, snowmelt, runoff and run on, and infiltration

DOE used site characterization data, as available, to develop inputs for the MASSIF model (SAR Section 2.3.1.3). Where sparse or no site observations are available, other information from scientific literature or other sites was used to develop inputs.

(b)(5)

(b)(5)

2.2.1.3.5.3.2 Climate

This section contains NRC staff's review of the DOE approach and results for predicting climate states for the next 10,000 years, and for predicting climatic conditions within each of the climate states. In its performance-based review, NRC staff focused most heavily on identifying whether the data, models, and results adequately represent climate and the uncertainty of climate for the intended downstream use of providing input information for estimating net infiltration for performance assessment calculations representing the first 10,000 years of repository performance. Because 10 CFR 63.342(c)(2) allows the use of a specified range and sampling distribution of average deep percolation across the repository for the period from 10,000 to 1 million years after closure, the applicant did not explicitly consider climate or meteorology during this period. NRC staff did not consider climate or meteorology for the post-10,000-year period in its evaluation. The NRC staff evaluates the DOE approach to representing deep percolation during the period from 10,000 to 1 million years after closure in SER Section 2.2.1.3.6.3.2.

The NRC staff evaluates DOE's approach to modeling climate during the first 10,000 years by separately considering the applicant's approach to estimating long-term-average climate (SER Section 2.2.1.3.5.3.2.1) and the applicant's approach to estimating daily weather parameters given a long-term-average climate state (SER Section 2.2.1.3.5.3.2.2). These two sections separate climatic considerations into long and short time scales, respectively.

2.2.1.3.5.3.2.1 Climate Change for the Next 10,000 Years

This section addresses YMRP acceptance criteria related to data for model justification, and characterization and propagation of data uncertainty, for the applicant's climate prediction for the 10,000 years following repository closure.

DOE predicted climate states covering the next 10,000 years using paleoclimate proxies from regional records and the understanding of orbital variations as the principal drivers of Earth climate over the past several million years. DOE's main paleoclimate proxies are layered mineral precipitates from Devils Hole and fossils preserved in continuously layered lake sediments from Owens Lake. Owens Lake, a present-day playa, and Devils Hole, a water-filled cave, are both within 140 km [87 mi] of Yucca Mountain. Cores from both sites record past cyclic changes in regional climate, between glacial and interglacial phases, and are generally consistent with other global climate proxy records.

From these records, the applicant derived three representative states for future climate. DOE predicted these three climates and the timing of step changes by (i) identifying the past point in time in the Devils Hole record that is equivalent to the present moment within the glacial cycle,

(ii) identifying the same equivalent point in the Owens Lake sediment sequence, (iii) identifying the sediment sequence corresponding to the 10,000 years following the equivalent point, and finally, (iv) attributing climate states to the sediment sequence (SAR Section 2.3.1.2.3.1.1).

The climate-sequence timing DOE described is based on two Earth-orbital parameters, which are accepted as climate forcing functions operating over geologic time scales: orbital eccentricity, with a period of approximately 100,000 years, and precession of the equinoxes, with a period of approximately 23,000 years (SAR Section 2.3.1.2.1.2.3). Values for these orbital parameters can be calculated to high precision from astronomical relations. DOE used oxygen isotope ratio ($\delta^{18}\text{O}$) records in Devils Hole vein calcite, dated using uranium-series methods, to relate the orbital parameters to past glacial stages. In the SAR, DOE explained that obliquity, another recognized orbital forcing with a period of approximately 41,000 years, was not used in its model, because no consistent relationship was shown between obliquity and the Devils Hole $\delta^{18}\text{O}$ record. The SAR asserted that groups of 4 eccentricity cycles, totaling approximately 400,000 years, provide analogous repetitions of glacial cycles. DOE built confidence in the selection of the first 10,000 years of the cycle as an analog for the next 10,000 years at Yucca Mountain by demonstrating that the last 400,000-year cycle was similar to the previous 400,000-year cycle (400,000 to 800,000 years ago).

DOE constructed past climates for particular glacial stages (SAR Section 2.3.1.2.1.2.4) using the Forester, et al. (1999aa) analysis of ostracode occurrences in lake sediment obtained from composite core OL-92, drilled in 1992 at Owens Lake, California, together with observed flows in Owens River for wet years. Ostracodes are microfossils, with different species having different environmental preferences for salinity and temperature. In DOE's analysis, the ostracode-based salinity of the paleo-Owens Lake serves as a proxy for annual precipitation. DOE used the abundance of five different species to infer compatible climatic parameters of temperature and seasonality and then developed future-climate parameters from meteorological stations with long records in locations where those species currently exist. DOE built confidence in the climate estimators using diatom records from the same core samples.

DOE's procedure yielded three representative climates for the first 10,000 years after closure: (i) modern (present-day) climate for the first 600 years, (ii) monsoonal climate for 1,400 years, and (iii) glacial transitional climate for the remaining 8,000 years. Relatively speaking, these three climates can be described as hot and dry, hot and wet, and cool and wet, although all are classified as arid to semi-arid climate. DOE calculated sample-average mean annual precipitation (MAP) values for the monsoon and glacial transition climates that were 1.59 and 1.63 times the sample-average MAP for the present-day climate (SAR Tables 2.3.1-2 through 2.3.1-4), and nominal mean annual temperatures (MATs) for the monsoon and glacial transition climates were 0.9 °C [1.6 °F] warmer and 5.5 °C [9.9 °F] cooler, respectively, than the nominal MAT for the present-day climate using values from SNL Tables F-22 through F-24 and Eq. F-47(a) (2007az). DOE's representation of a monsoonal climate also exhibited a shift in seasonality, with summer convection storms making up a larger fraction of its annual total precipitation than for either the present-day or glacial-transition climates.

(b)(5)

DOE considered the two primary uncertainties in the data sets used to forecast future climate at Yucca Mountain to be the standard deviation associated with the Devils Hole ages and the uncertainty of the timing of climate change implied by the Devils Hole record (SAR Section 2.3.1.2.2.1.4). DOE also considered the two primary uncertainties in model forecasts of future climates to include (i) uncertainty in the location of the past-present equivalency point in the Owens Lake record, (ii) uncertainty arising from the chaotic nature of the climate system, and (iii) uncertainty in selecting a particular past climate sequence to forecast the future (SAR Section 2.3.1.2.3.2).

(b)(5)

Uncertainty in Timing and Duration of Climate States

DOE used three climate states, each with a constant climate, to represent millennial-scale temporal variations found in the paleorecord. Uncertainty in the timing of transitions between the projected climate states could potentially impact estimates of future infiltration, which in turn, may affect unsaturated-zone flow, seepage rates, thermal histories, and radionuclide transport.

(b)(5)

(b)(5)

(b)(5)

(b)(5)

(b)(5)

The glacial-transition climate represents 8,000 years of constant climate in the DOE model. Because millennial-scale fluctuations in climate are reflected in the paleo-records, NRC staff evaluated the acceptability of using a constant climate for 8,000 years instead of an alternative representation reflecting millennial-scale variations in climate. (b)(5)

(b)(5)

Comment (b)(5)

(b)(5)

(b)(5)

Uncertainty in Climatic Conditions During the Post-Thermal-Pulse Period

The applicant used the glacial-transition climate state to represent climate during the final 80 percent of the first 10,000 years of repository performance. Of the three climate states that DOE used within the first 10,000 years of performance, (b)(5)

(b)(5)

(b)(5) During the thermal pulse, above-boiling conditions and evaporation reduce the flux of water reaching drifts (SAR Section 2.3.3.1). In evaluating the DOE approach to representing uncertainty in the glacial-transition climate state, (b)(5)

(b)(5)

DOE first considered the presence and absence of indicator species within Owens Lake to infer changes in climatic conditions relative to present-day climate, then estimated compatible climatic conditions from present-day locations where the same indicator species currently exist. DOE represented uncertainty regarding climatic conditions using upper and lower bounds for MAP and MAT for each climate state. To account for the uncertainties in translating paleoclimatic indicators into meteorological records, DOE selected several meteorological stations to represent each of the bounding climatic conditions at an elevation of 1,524 m [5,000 ft] at Yucca Mountain (SAR Section 2.3.1.2.3.1.2). The criteria for selecting present-day meteorological stations, outlined in SAR Section 2.3.1.2.3.1.2, include (i) presence of Owens Lake indicator species, (ii) MAT, (iii) rain-shadow effects, (iv) position of the polar front, and (v) length of observational record. Further, DOE selected meteorological stations such that (i) the climate states have larger MAP values for upper bounds than for lower bounds and (ii) the upper-bound MAP values are larger than the present-day observations for both the monsoonal and glacial transition climate states.

DOE concluded that MAP is one of the two parameters that control uncertainty in MASSIF estimates of net infiltration for all climate states (SAR Section 2.3.1.3.3.2.2). Further, DOE based the selection of representative meteorological stations on the station record length and on observations that are sensitive to MAT and precipitation seasonality (i.e., ostracode species) without using criteria based on specific values of MAP. Uncertainty in MAP is a dominant source of uncertainty in the DOE net infiltration estimates, and the DOE procedure for selecting representative meteorological stations yields relatively large uncertainty in MAP.

The applicant selected meteorological stations for the glacial-transition climate with average observed annual precipitation between 207 and 241 mm/yr [8.1 and 9.5 in/yr] for the lower bound and between 419 and 455 mm/yr [16.5 and 17.9 in/yr] for the upper bound (SAR Table 2.3.1-6). For comparison, meteorological stations at Yucca Mountain have observed MAP between 183 and 213 mm/yr [7.2 and 8.4 in/yr], averaging 199 mm/yr [7.8 in/yr]. Accordingly, the mean upper- and lower-bound MAP estimates for the glacial-transition climate state are approximately 2.2 and 1.2 times the average observed present-day precipitation of 199 mm/yr [7.8 in/yr] at Yucca Mountain.

DOE does not expect that a full glacial climatic state would occur within the next 30,000 years, and the SAR did not estimate climatic conditions for a full glacial climatic state. NRC staff has nonetheless reviewed published estimates for MAP during the last glacial maximum in the

Comment (b)(5)

region surrounding Yucca Mountain, as detailed in Stothoff and Walter, Section 2.2 (2007aa). These published estimates formed part of the regulatory basis used to develop the standard for constant-in-time deep percolation rate during the post-10,000-year performance period specified in 10 CFR 63.342(c)(2). Several of the published estimates listed in Stothoff and Walter (2007aa) quantitatively considered the effects of MAP on a water balance. Such quantitative estimates inferred changes in MAP and MAT by considering elevation changes for plant species that have known environmental preferences, hydrologic balances for paleolakes, extent of glacial advances, and regional groundwater balances. Among these estimates, the largest estimated value for MAP at the last glacial maximum suggests that MAP was 1.9 times larger than present-day MAP at Yucca Mountain.

(b)(5)

Uncertainty in Climatic Conditions From Anthropogenic Activities

Comment (b)(5)

DOE stated that the predicted modern climate is based on "climate records that implicitly include effects of modern society over the duration of historical record" SNL, Section 6.2, FEPs 1.4.01.00.0A and 1.4.01.02.0A (2008ab) and DOE, Enclosure 8 (2009cr). Uncertainty in the incorporation of anthropogenic effects on climate predictions used as input for net infiltration estimates is twofold. First, monsoonal and glacial-transition climate analog sites are derived from interpretation of the paleoclimatic record (e.g., Owens Lake ostracode and diatom observations). However, current levels of greenhouse gases (i.e., dominantly CO₂ but including other gases) are elevated beyond any levels indicated in paleoclimate records covering the past 800,000 years. Second, the effect of the global climatic changes on Yucca Mountain climate is uncertain. To address these uncertainties, DOE described consequences to infiltration estimates caused by reasonable projections of climate change in the desert Southwest considering anthropogenic influences.

In DOE Enclosure 8 (2009cr), DOE considered projected climate changes in the desert Southwest, described by the International Panel on Climate Change (Christensen, et al., 2007aa) to assess potential consequences of anthropogenic climate change on repository performance. Projected regional climate change estimates indicate the desert Southwest is likely to see temperature increases that are higher than average global warming and annual precipitation that is likely to decrease in the next century. DOE, Enclosure 8 (2009cr) described the projected regional climate changes as having potential consequences, including

- Improved repository performance under warmer and drier conditions, because warmer temperatures and decreased precipitation lead to decreased net infiltration
- Insignificant effects on repository performance under a warmer and wetter climate or early onset of monsoon conditions induced by anthropogenic climate change, because most of the repository would be above boiling during the first 600 years after closure [DOE considered climate changes Christensen, et al. (2007aa) projected to be

similar to but smaller than that represented by the shift from modern climate to the monsoonal state]

- Improved repository performance if anthropogenic climate change caused a delay in the onset of the glacial-transition climate because net infiltration under the cool and wet glacial-transition climate state is higher than would occur for earlier climate states.

Comment (b)(5)

(b)(5)

Summary of Conclusions Regarding Climate Change for the Next 10,000 Years

(b)(5)

2.2.1.3.5.3.2.2 Local Spatial and Temporal Variation of Meteorological Conditions

In this section, NRC staff evaluates the DOE model for climatic and meteorological conditions during each climate state (i.e., climate conditions at short time scales). This section addresses YMRP acceptance criteria related to input data characterization and uncertainty.

DOE represented meteorological conditions for each climate state using sampled 1,000-year sequences of daily estimates for total precipitation and temperature extremes, representing conditions at a reference elevation of 1,524 m [5,000 ft]. The MASSIF infiltration model subsequently estimates precipitation and temperature variability over each day using the daily values. DOE represented spatial variation by projecting the daily precipitation and temperature values to the infiltration-model cells using elevation-dependent lapse rates. DOE considered precipitation rates with up to a 1,000-year recurrence period in generating the 1,000-year sequence. The applicant selected 10 representative 1-year sequences out of each 1,000-year sequence to estimate long-term-average net infiltration. DOE used a water year representation, initiating each 1-year sequence on October 1 to capture the cycle of winter precipitation and large summer potential evapotranspiration. DOE ensured that the wettest years were sampled to capture the disproportionate influence of wet years on net infiltration and initiated each simulation with conditions representing extended summer evapotranspiration.

Comment (b)(5)

Comment (b)(5)

NRC staff reviewed the adequacy of the applicant's representation of spatial and temporal variability in meteorological parameters for estimating net infiltration in the two following sections.

Spatial Variability in Meteorological Parameters

DOE considered the effect of elevation on meteorological parameters by adjusting the estimated daily values for precipitation and temperature extremes according to regional patterns in MAP and MAT. The dependency of meteorological parameters on elevation provides the only spatial variability of those parameters across the site. (b)(5)

(b)(5)

Comment (b)(5)

(b)(5)

(b)(5)

(b)(5)

Comment (b)(5)

(b)(5)

Temporal Variability in Meteorological Parameters

DOE represented temporal variability of meteorological conditions using sampled daily values for precipitation, temperature minimum and maximum, and wind speed. On days with precipitation, the applicant subdivided the daily calculation into two parts, representing storm and nonstorm conditions, and used wet-day instead of dry-day temperature values. The applicant described the statistical parameters characterizing these meteorological components as varying sinusoidally over the year. DOE considered the representation of temporal variability adequate because measured regional and Yucca Mountain site data were used to develop precipitation and temperature sequences.

Comment (b)(5)

(b)(5)

Comment (b)(5)

(b)(5)

(b)(5)

Comment (b)(5)

(b)(5)

(b)(5)

Comment (b)(5)

2.2.1.3.5.3.3 Net Infiltration

In this section, NRC staff considers the DOE's model for net infiltration during the 10,000 years following repository closure. The NRC staff considers the downstream uses of the net infiltration results and the effect of uncertainty in net infiltration on DOE performance assessment calculations to focus the review of those aspects of DOE's net infiltration model most important for repository performance

(b)(5)

DOE also used the areal-average net infiltration results in performance assessment calculations related to the saturated zone, adjusting saturated zone groundwater fluxes for future, wetter climates using net infiltration (SAR Section 2.3.8). (b)(5)

(b)(5)

(b)(5) The following subsections give the NRC staff evaluation of the technical bases for DOE's models and inputs used to estimate areal-average net infiltration.

Submodels for Net Infiltration

This subsection addresses YMRP acceptance criteria related to model integration, justification, and uncertainty.

DOE used a water balance approach to integrate processes and features acting at and near the ground surface, to a depth at the bottom of the root zone. A water balance approach requires that the supply of water (precipitation and run on) at any location is equal to the sum of other components (e.g., evapotranspiration, change in water storage, runoff, and net infiltration). In the water balance, uncertainty in precipitation and evaporation, the largest components, can greatly affect estimation of the much smaller component of net infiltration. DOE described the development and integration of features and processes into conceptual and numerical models in SAR Sections 2.3.1.3.1 and 2.3.1.3.2 and SNL Sections 6.3 and 6.4 (2007az). DOE separates the water balance model into the key MASSIF elements of

- Climate and meteorology, using daily precipitation, temperature, and snowmelt
- Subsurface water movement and storage, using a one-dimensional vertical soil water balance
- Surface runoff and run on, using topography-based flow routing
- Evapotranspiration, using the FAO-96 approach (Allen, et al., 1998aa) modified for natural vegetation
- Reference evapotranspiration, using the FAO Penman-Monteith method (Allen, et al., 2005aa)

MASSIF comprises linked submodels for the identified processes and routines to manipulate geographically distributed input data into the formats required for the calculations. The geographically distributed input data, which are defined at each 30-m [98-ft] pixel across the Yucca Mountain area, include soil and rock hydrologic properties, topography, vegetation factors, and climate information (e.g., precipitation and temperature).

In MASSIF, net infiltration is defined as the water that moves below the active zone where evaporation and plant uptake are significant processes. DOE assumed that the active zone does not penetrate the bedrock, so that water passing into the bedrock becomes net infiltration. DOE considered this assumption to be conservative with respect to the magnitude of net infiltration, because plant roots, especially in areas with thin soil cover, develop in bedrock fractures and thus would reduce net infiltration by taking up water for transpiration.

DOE described in SNL Section 6.2.3 (2007az) six criteria used for selecting the infiltration model components: (i) the model and components should be consistent with the overall project purpose, (ii) the model component complexity should be consistent with the available input data, (iii) model components should be consistent with other model components, (iv) the model should be computationally efficient, (v) the model should be accessible and open, and (vi) the model and model components should demonstrate reasonable predictive capability. The applicant described cases in the literature where the algorithms and approaches in submodels have been utilized at other locations in semi-arid areas. DOE explained these criteria as motivated by the large spatial and temporal scales being modeled, the limited objectives of the infiltration model, and the need for numerous simulations to assess sensitivities and address multiple climate scenarios. DOE further explained that the infiltration model is not intended to describe the detailed spatial and temporal character of water movement.

(b)(5)

To build confidence in the water balance approach for one-dimensional water storage and movement, DOE compared results with both measured data and results from an alternative model solving the Richards equation for unsaturated flow (SAR Sections 2.3.1.3.4.1 and 2.3.1.3.4.2). The Richards equation includes capillary effects, unlike the water balance approach in MASSIF. The comparisons focused on the MASSIF submodels for water storage, evapotranspiration, and one-dimensional vertical movement of water. The measured lysimeter data were from two locations, the Reynolds Creek Experimental Watershed in New Mexico and the Nevada Test Site. DOE also compared MASSIF results with results from the Richards-equation-based models for one-dimensional, stylized problems with varying soil and plant root depths. (b)(5)

Comment (b)(5)

(b)(5)

Comment (b)(5)

In another comparison with measured data, DOE contrasted MASSIF results against measurements from streamflow gauges in three subwatersheds at Yucca Mountain for several storm events, as outlined in SAR Section 2.3.1.3.4.1 and SNL Section 7.1.3 (2007az). SAR Figure 2.3.1-46 illustrated that the timing and magnitude of measured and modeled runoff are reasonably well matched with a particular set of input properties that lie within the uncertainty range considered in the net infiltration model. The input properties used to match streamflow observations represent the nominal properties with soil hydraulic conductivity adjusted to increase upland runoff and enhance channel infiltration. DOE indicated that local variations within the watersheds may have also been a factor in the comparison. (b)(5)

(b)(5)

(b)(5)

(b)(5)

Input Parameters

This subsection addresses YMRP acceptance criteria related to characterization of data and propagation of data uncertainty.

(b)(5)

Available soil water storage during a precipitation event depends on soil depth, soil water-holding capacity, and the antecedent soil moisture content (i.e., how dry the soil column is prior to the event). Soil and bedrock hydraulic properties affect the rate of soil water movement toward and into the bedrock. In DOE's representation, water drains into the bedrock once the water storage capacity of the overlying soil layers is exceeded, thereby avoiding evapotranspiration. The drainage rate into the bedrock is controlled by the layer, soil or bedrock, with the smaller value bulk permeability. DOE analyses in SNL Section 7.1.4 (2007az) suggest that net infiltration estimates are not sensitive to uncertainty in bulk bedrock permeability, in part because of the limited spatial extent where bedrock controls the drainage rate. (b)(5)

(b)(5)

Areas with thin soil cover are particularly important because DOE identified infiltration as most readily occurring in shallow soil. Areas with shallow, or thin, soils comprise 70 percent of the unsaturated model domain (Soil Depth Class 4, SAR Section 2.3.1.3.2.1.3) and appear to cover an even larger fraction of the repository footprint (SAR Figure 2.3.1-19). In DOE Enclosure 5 (2009cr), DOE identified soil depth in areas with shallow soil cover as the most important hydrologic property input for the infiltration model, with model results approximately as sensitive to uncertainty effective soil depth as uncertainty in precipitation. The effective soil depth is defined as the single soil depth value that, if applied everywhere, yields the same areal-average net infiltration as the actual soil-depth distribution.

Soil Depth Class 4 represents soil depths between 0 and 0.5 m [0 and 1.6 ft] and corresponds to eolian deposits with various mixtures of entrained rock on hillslopes and ridgetops. DOE sampled a single sampled effective soil depth value to characterize Soil Depth Class 4 for each realization and assigned the value to every grid cell representing that class for the corresponding simulation. DOE used two datasets to support its effective soil depth distribution for this class: (i) 35 site observations recorded as point measurements ranging from depths of 0 to 3 m [0 to 9.8 ft], with a recommended median of 0.25 m [0.82 ft], as described in SNL Table 6.5.2.4-2(a) (2007az), and (ii) 8 site observations recorded as general site characteristics at locations such as drill pads. DOE described the measurements as approximately lognormally

distributed and, on the basis of geometric and arithmetic means of the two sets of observations, derived bounds on effective soil depth ranging from 0.1 to 0.5 m [0.33 to 1.6 ft]. DOE also analyzed 56 NRC soil depth measurements (Fedors, 2007aa) obtained from site visits focusing on the thin soils of the east-trending upper washes over the southern half of the repository footprint. DOE described the available NRC measurements as approximately following a lognormal distribution.

For performance assessment calculations, DOE described the effective soil depth in Soil Class 4 as equally likely for any value between the upper and lower bounds. In selecting the uniform statistical distribution, DOE considered the difficulty in measuring soil depth, uncertainty in the mean of the observations, and uncertainty in how soil depth affects net infiltration, as detailed in DOE, Enclosure 5 (2009cr). In the same document, DOE stated that sensitivity results in SNL Appendix H (2007az) demonstrated that calculated areal-average net infiltration is approximately linearly dependent on effective soil depth for Soil Class 4, and that shallow soil depths are not underrepresented in the effective soil depth distribution for Soil Depth Class 4. From this, DOE concluded that use of a uniform distribution for effective soil depth does not underestimate average net infiltration.

(b)(5)

NRC staff considered the effect of uncertainty in the soil depth distribution for Soil Depth Class 4 on the estimate of net infiltration. DOE used a uniform distribution, though the measured data may better fit a lognormal distribution, as described in SNL Table 6.5.2.4-2(a) and Section 7.2.4(a) (2007az) and DOE, Enclosure 5 (2009cr). (b)(5)

(b)(5)

Water-holding capacity is calculated from soil hydraulic properties; specifically, porosity and water retention characteristics and porosity. DOE utilized a pedotransfer function derived for

Comment (b)(5)

(b)(5)

Comment (b)(5)

Hanford soils to relate Yucca Mountain soil texture to hydraulic properties for each soil group in the infiltration model domain. In the MASSIF model, larger water-holding capacity values result in smaller values of net infiltration. Because the hydrologic property relationship to soil texture may be different for soils from Hanford, Washington, compared to that for soils at Yucca Mountain, DOE, Enclosure 6 (2009cr) compared water-holding capacity used in MASSIF with two estimates made for local Yucca Mountain soils. The first set covers soils in Nye County, and the second set covers soils from the Yucca Mountain area but not used in the MASSIF model. DOE, Enclosure 6 (2009cr) stated that the estimates of water-holding capacity used in MASSIF are smaller than those estimated for the other two sets of soils. (b)(5)

(b)(5)

NRC staff considered the performance consequence of the DOE assumption that all geologic and geographic parameters in the infiltration model remain the same over the transition from dryer to wetter climates during the next 10,000 years. Changes to soil depth, soil hydraulic properties, and bulk bedrock permeability under future climates may include (i) greater chemical soil profile development and enhanced weathering of bedrock at the interface with soil, (ii) relatively larger soil depths and different soil depth distributions, and (iii) relatively smaller amounts of caliche filling bedrock fractures at the soil/bedrock interface. In DOE Enclosure 2 (2009cr), DOE described the potential consequences as either inconsequential or beneficial to repository performance:

Comment (b)(5)

- Projected changes to soil depth and soil hydraulic properties would tend to reduce the estimates of net infiltration. (b)(5)
- Where bedrock permeability values are greater than soil permeability, DOE considered the effect of a change in modeled bedrock properties as either inconsequential to net infiltration (if bedrock permeability increased) or to reducing infiltration (if bedrock permeability became smaller than the soil permeability). For more than half the ambient site-scale unsaturated zone modeling domain, bedrock permeability is greater than soil permeability.
- In the remaining area, DOE considered net infiltration as having a potential to increase only in the realizations where sampled bedrock permeability is smaller than soil permeability in the present climate, and only if bedrock permeability increases under a future climate. This potential exists in less than half of the modeling domain for approximately half the realizations. (b)(5)

Comment (b)(5)
(b)(5)

(b)(5)

(b)(5)

Net Infiltration Results

This subsection addresses YMRP acceptance criteria related to propagation of uncertainty and support of model output by objective comparisons for DOE's estimates of net infiltration and changes over time for its three climate states. Effects of net infiltration model results on repository performance are considered in how the infiltration model output is used in the unsaturated flow model, including seepage and unsaturated zone transport. NRC staff reviewed the net infiltration results in the context of average ratio of infiltration to precipitation, values of areal-average net infiltration, and spatial and temporal distribution of net infiltration.

DOE represents uncertain inputs to the MASSIF model with Monte Carlo sampling, using 40 realizations of selected hydraulic properties and climate characteristics to estimate net infiltration uncertainty for a climate state (SAR Section 2.3.1.3.3). For each realization, DOE calculated a process-level map of mean annual net infiltration by (i) creating a synthetic weather history representing 1,000 years, (ii) selecting 10 water years (a water year is October 1 through September 30 of the following year) out of the 1,000-year history to represent the range of dry to wet years, (iii) calculating total net infiltration for each water year using MASSIF, and (iv) averaging the 10 water-year net infiltration maps. The applicant selected 4 of the 40 equally likely process-level mean annual net infiltration maps to represent the uncertainty in infiltration by (i) calculating areal-average net infiltration for each map, (ii) ranking the average values from low to high, and (iii) selecting the 4th, 12th, 20th, and 36th ranked map to represent the 10th, 30th, 50th, and 90th percentile ranking. The 12 maps of net infiltration are output provided to the unsaturated zone model for use as top boundary flux for the first 10,000 years. (b)(5)

(b)(5)

The applicant adjusted 4 of the 12 upper-boundary net infiltration maps developed for the first 10,000 years after closure to represent the probability distribution for deep percolation at the repository horizon for the post-10,000-year period, as specified by 10 CFR 63.342(c)(2). DOE selected the four upper-boundary net infiltration maps with the largest areal-average net infiltration within the repository footprint for the scaling procedure. The NRC staff reviews the procedure and technical basis for developing the post-10,000-year unsaturated zone model upper-boundary net infiltration maps in SER Section 2.2.1.3.6.3.2.

(b)(5)

(b)(5)

(b)(5)

Comment (b)(5)

(b)(5)

(b)(5)

Comment (b)(5)

(b)(5)

(b)(5)

(b)(5)

In support of its consideration of spatial variability in DOE's net infiltration in the vicinity of the proposed repository footprint, DOE provided an analysis in DOE Enclosure 4 (2009cr) that considers the consequences on performance from a variant property set that favors focused (channel) infiltration instead of distributed infiltration. The variant property set was based on

simulations of observations in Pagany Wash. DOE considered the consequences of both spatial and temporal aspects of the variant property set with the infiltration model from two washes, stating that the consequences of a focused infiltration pattern are insignificant to repository performance calculations. The basecase and variant simulations yield similar calculated values of areal-average net infiltration, with somewhat less net infiltration within the repository footprint for maps with larger total net infiltration, as described in SNL, Table 7.1.3.2-1(a) (2007az). DOE explained that the similarity in areal-average net infiltration arises from conservation of mass, in that the water infiltrating into channels in the variant case would have otherwise infiltrated into hillslopes without the enhanced runoff. In other words, redistributing water through overland flow does not appreciably increase areal-average net infiltration in DOE's model. (b)(5)

(b)(5)

(b)(5)

(b)(5)

Comment (b)(5)
(b)(5)

(b)(5)

Comment (b)(5)
(b)(5)

2.2.1.3.5.4 Evaluation Findings

(b)(5)

(b)(5)

(b)(5)

(b)(5)

The NRC staff reviewed the applicant's SAR and other information submitted in support of the license application and finds that, with respect to the requirements of 10 CFR 63.114 for consideration of climate and infiltration, (b)(5)

(b)(5)

(b)(5)

2.2.1.3.5.5 References

Allen, R.G., I.A. Walter, R.L. Elliott, T. Howell, D. Itenfisu, and M. Jensen. 2005aa. *The ASCE Standardized Reference Evapotranspiration Equation*. Reston, Virginia: American Society of Civil Engineers.

Allen, R.G., L.S. Pereira, D. Raes, and M. Smith. 1998aa. "Crop Evapotranspiration. Guidelines for Computing Crop Water Requirements." FAO Irrigation and Drainage Paper 56. Rome, Italy: Food and Agriculture Organization of the United Nations.

Bull, W.B. 1991aa. *Geomorphic Responses to Climate Change*. New York City, New York: Oxford University Press.

Christensen, J.H., B. Hewitson, A. Busuioac, A. Chen, X. Gao, I. Held, R. Jones, R.K. Kolli, W.-T. Kwon, R. Laprise, V. Magana Rueda, L. Mearns, C.G. Menendez, J. Raisanen, A. Rinke, A. Sarr, and P. Whetton. 2007aa. *In Climate Change 2007: The Physical Science Basis*. Contribution of Working Group I to the 4th Assessment Report of the Intergovernmental Panel on Climate Change. S. Solomon, D. Quin, M. Manning, Z. Chen, M. Marquis, K.B. Averyt, M. Tignor, and H.L. Miller, eds. Cambridge, United Kingdom and New York City, New York: Cambridge University Press.

DOE. 2010ai. "Yucca Mountain—Supplemental Response to Request for Additional Information Regarding License Application (Safety Analysis Report Section 2.3.1), Safety Evaluation Report Vol. 3, Chapter 2.2.1.3.5, Set 1 and (Safety Analysis Report Sections 2.3.2 and 2.3.3), Safety Evaluation Report Vol. 3, Chapter 2.2.1.3.6, Set 1." Letter (February 2) J.R. Williams to J.H. Sulima (NRC). ML100340034. Washington, DC: DOE, Office of Technical Management.

DOE. 2009bo. "Yucca Mountain—Response to Request for Additional Information Regarding License Application (Safety Analysis Report Sections 2.3.2 and 2.3.3), Safety Evaluation Report Vol. 3, Chapter 2.2.1.3.6, Set 1." Letter (June 1) J.R. Williams to J.H. Sulima (NRC). ML091530403. Washington, DC: DOE, Office of Technical Management.

DOE. 2009cr. "Yucca Mountain—Response to Request for Additional Information Regarding License Application (Safety Analysis Report Section 2.3.1), Safety Evaluation Report Vol. 3, Chapter 2.2.1.3.5, Set 1." Letter (June 24) J.R. Williams to J.H. Sulima (NRC). ML0918308480 and ML0918300710. Washington, DC: DOE, office of Technical Management.

DOE. 2008ab. DOE/RW-0573, "Yucca Mountain Repository License Application." Rev. 0. ML081560400. Las Vegas, Nevada: DOE, Office of Civilian Radioactive Waste Management

Fedors, R. 2007aa. "Soil Depths Measured at Yucca Mountain During Site Visits in 1998." Note (January 9) R. Fedors to J. Guttman (NRC). ML063600082. Washington, DC: NRC.

Forester, R.M., J.P. Bradbury, C. Carter, A.B. Elvidge-Tuma, M.L. Hemphill, S.C. Lundstrom, S.A. Mahan, B.D. Marshall, L.A. Neymark, J.B. Paces, S.E. Sharpe, J.F. Whelan, J.F. Wigand, and P.E. Wigand. 1999aa. "The Climatic and Hydrologic History of Southern Nevada During the Late Quaternary." USGS Open-File Report 98-635. Denver, Colorado: U.S. Geological Survey.

Groeneveld, D.P., S.A. Stothoff, and R. Fedors. 1999aa. "Weedy Brome Grasses and Their Potential Effect on the Infiltration and Recharge Rates in the Vicinity of Yucca Mountain, Nevada." San Antonio, Texas: CNWRA.

NRC. 2009ab. "Division of High-Level Waste Repository Safety Director's Policy and Procedure Letter 14: Application of YMRP for Review Under Revised Part 63." Published March 13, 2009. ML090850014. Washington, DC: NRC.

NRC. 2005aa. NUREG-1762, "Integrated Issue Resolution Status Report." Rev. 1. Washington, DC: NRC.

NRC. 2003aa. NUREG-1804, "Yucca Mountain Review Plan—Final Report." Rev. 2. Washington, DC: NRC.

SNL. 2008ab. "Features, Events, and Processes for the Total System Performance Assessment: Analyses." ANL-WIS-MD-000027. Rev. 00. ACN 01. ERD 01, ERD 02. Las Vegas, Nevada: Sandia National Laboratories.

SNL. 2007az. "Simulation of Net Infiltration for Present-Day and Potential Future Climates." MDL-NBS-HS-000023. Rev. 01. AD 01, ERD 01, ERD 02. Las Vegas, Nevada: Sandia National Laboratories.

SNL. 2006aa. "Data Analysis for Infiltration Modeling: Extracted Weather Station Data Used To Represent Present-Day and Potential Future Climate Conditions in the Vicinity of Yucca Mountain." ANL-MGR-MD-000015. Rev. 00. ACN 01. Las Vegas, Nevada: Sandia National Laboratories.

Stothoff, S.A. 2010aa. "Infiltration and Unsaturated Zone Confirmatory Analyses." Electronic Scientific Notebook 1005E. San Antonio, Texas: CNWRA.

Stothoff, S.A. 2009aa. "Subsurface Observations Related to Infiltration at Yucca Mountain." ML093160095. San Antonio, Texas: CNWRA.

Stothoff, S.A. 2008aa. "Infiltration Tabulator for Yucca Mountain: Bases and Confirmation." CNWRA Report 2008-001. ML082350701. San Antonio, Texas: CNWRA.

Stothoff, S.A. 2008ab. "Compilation of Prelicensing Field Observations Related to Infiltration at Yucca Mountain and Future-Climate Analogs." ML082000174. San Antonio, Texas: CNWRA.

Stothoff, S.A. 1999aa. "Infiltration Abstractions for Shallow Soil Over Fractured Bedrock in a Semiarid Climate." ML061370364. San Antonio, Texas: CNWRA.

Stothoff, S.A. 1997aa. "Sensitivity of Long-Term Bare Soil Infiltration Simulations to Hydraulic Properties in an Arid Environment." *Water Resources Research*. Vol. 22, No. 4. pp. 547–558.

Stothoff, S.A. 1995aa. NUREG/CR-6333, "BREATH Version 1.1—Coupled Flow and Energy Transport in Porous Media: Simulator Description and User Guide." Washington, DC: NRC.

Stothoff S. and M. Musgrove. 2006aa. "Literature Review and Analysis: Climate and Infiltration." CNWRA Report 2007-002. ML063190115. San Antonio, Texas: CNWRA.

Stothoff, S. and G. Walter. 2007aa. "Long-Term-Average Infiltration at Yucca Mountain, Nevada: Million-Year Estimates." CNWRA Report 2007-003. ML072760607. San Antonio, Texas: CNWRA.

Stothoff, S.A., D. Or, D.P. Groeneveld, and S.B. Jones. 1999aa. "The Effect of Vegetation on Infiltration in Shallow Soils Underlain by Fissured Bedrock." *Journal of Hydrology*. Vol. 218. pp. 169–190.

Winograd, I.J., A.C. Riggs, and T.B. Coplen. 1998aa. "The Relative Contributions of Summer and Cool-Season Precipitation to Groundwater Recharge, Spring Mountains, Nevada, USA." *Hydrogeologic Journal*. Vol. 6, No. 1. pp. 77–93.

Woolhiser, D. R.W. Fedors, R.E. Smith, and S.A. Stothoff. 2006aa. "Estimating Infiltration in the Upper Split Wash Watershed, Yucca Mountain, Nevada." *Journal of Hydrologic Engineering*. Vol. 11, No. 2. pp. 123–133.

Woolhiser, D.A., S.A. Stothoff, and G.W. Wittmeyer. 2000aa. "Estimating Channel Infiltration From Surface Runoff in the Solitario Canyon Watershed, Yucca Mountain, Nevada." *Journal of Hydrologic Engineering*. Vol. 5, No. 3. pp. 240–249.

CHAPTER 9

2.2.1.3.6 Unsaturated Zone Flow

2.2.1.3.6.1 Introduction

This chapter of the Safety Evaluation Report (SER) addresses the U.S. Department of Energy's (DOE's) abstraction of groundwater flow in that portion of the repository system above the water table. DOE presented this information in its Safety Analysis Report (SAR) of June 3, 2008 (DOE, 2008ab) and subsequent update of February 19, 2009 (DOE, 2009av). Although information from other sections of the SAR is cited in the review of the unsaturated zone flow abstractions, the primary SAR Sections are 2.3.2 (Unsaturated Zone Flow), 2.3.3 (Water Seeping into Drifts), and 2.3.5.4 (In-Drift Thermohydrological Environment).

The proposed Yucca Mountain repository site has up to 400 m [1,300 ft] of variably saturated rock between the ground surface and the repository, and at least 200 m [650 ft] between the repository and the underlying water table (SAR Sections 2.1.1.1 and 2.1.1.3). Water percolating through the unsaturated zone may enter the drifts, thereby providing the means to interact with and potentially corrode the waste packages. Water percolating through the unsaturated zone below the repository also provides flow pathways for transporting radionuclides downward to the water table. Once radionuclides pass below the water table, they may move laterally within the saturated zone to the accessible environment. In this chapter, the term "unsaturated zone flow" includes not only flow processes in the host rock under ambient and thermally perturbed conditions, but also in-drift hydrological processes related to flow through natural rubble and in-drift convection and condensation. Unsaturated flow both above and below the repository horizon is addressed in this chapter.

The unsaturated zone plays a role in two of the DOE-defined barriers: the Upper Natural Barrier and the Lower Natural Barrier (SAR Section 2.3.2). These barriers are reviewed in SER Sections 2.2.1.1.3.2. Together with Climate and Infiltration (reviewed in SER Section 2.2.1.3.5), processes in the unsaturated zone above the repository comprise the Upper Natural Barrier. They influence system performance through the amount of water reaching the engineered barrier system (EBS) and their control on hydrological conditions in the drift. In DOE's model of the nominal scenario, the Quantity and Chemistry of Water Contacting Engineered Barriers and Waste Forms (reviewed in SER Section 2.2.1.3.3), Degradation of Engineered Barriers (reviewed in SER Section 2.2.1.3.1), and Radionuclide Release Rates and Solubility Limits (reviewed in SER Section 2.2.1.3.4) abstractions use in-drift liquid water, relative humidity, and temperature to assess the potential for corrosion of waste packages, release of waste, and transport to the natural system. In the disruptive scenarios of seismic and igneous intrusion (reviewed in SER Sections 2.2.1.3.2 and 2.2.1.3.10), DOE's model uses the flux of water to assess the movement of radionuclides to the natural system below the repository. The portion of the unsaturated zone below the repository is part of the Lower Natural Barrier. The magnitude and distribution of flux in the unsaturated zone below the repository are used to determine the flow pathways for Radionuclide Transport in the Unsaturated Zone (reviewed in SER Section 2.2.1.3.7). The unsaturated zone below the repository links the repository EBS to the Saturated Zone Flow and Transport System (reviewed in SER Sections 2.2.1.3.8 and 2.2.1.3.9) and ultimately to the biosphere in the accessible environment (reviewed in SER Sections 2.2.1.3.12 to 2.2.1.3.14).

The purpose of this chapter is to evaluate repository performance with respect DOE estimates of the

- Magnitude and distribution of the mass flux of water (percolation) moving through the unsaturated zone and reaching the drift
- Amount and distribution of liquid water seeping into the drift, contacting the engineered barriers (i.e., drip shield), and becoming available to carry radionuclides out of the drift and into the natural environment
- Environmental conditions inside the drift (i.e., temperature, relative humidity, and moisture redistribution and condensation)
- Magnitude and distribution of flux in the unsaturated zone below the repository as is important for transport of radionuclides

2.2.1.3.6.2 Regulatory Requirements

Model abstractions used in the applicant's postclosure performance assessment must meet the regulatory requirements given in 10 CFR 63.114 (Requirements for Performance Assessment) and 63.342 (Limits on Performance Assessment), to support the predictions of compliance for 63.113 (Performance Objectives for the Geologic Repository after Permanent Closure). Specific compliance with 63.113 is reviewed in SER Section 2.2.1.4.1.

The requirements for performance assessment in 10 CFR 63.114 require the applicant to

- Include appropriate data related to the geology, hydrology, and geochemistry of the surface and subsurface from the site and the region surrounding Yucca Mountain
- Account for uncertainty and variability in the parameter values used to model unsaturated zone flow
- Consider alternative conceptual models for unsaturated zone flow
- Provide technical bases for the inclusion of features, events, and processes (FEPs) affecting unsaturated zone flow, including effects of degradation, deterioration, or alteration processes of engineered barriers that would adversely affect performance of the natural barriers, consistent with the limits on performance assessment in 10 CFR 63.342
- Provide technical basis for the models of unsaturated zone flow that in turn provide input or otherwise affect other models and abstractions

10 CFR 63.114(a) considers performance assessment for the initial 10,000 years following permanent closure. 10 CFR 63.114(b) and 63.342 consider the performance assessment methods for the time from 10,000 years through the period of geologic stability, defined in 10 CFR 63.302 as 1 million years following disposal. These sections require that through the period of geologic stability, with specific limitations, the applicant

- Use performance assessment methods consistent with the performance assessment methods used to demonstrate compliance for the initial 10,000 years following permanent closure
- Include in the performance assessment those FEPs used in the performance assessment for the initial 10,000-year period

For this model abstraction of unsaturated zone flow, 10 CFR 63.342(c)(1) further provides that DOE assess the effects of seismic and igneous activity on the repository performance, subject to the probability limits in 63.342(a) and 63.342(b). Specific constraints on the analysis required for seismic and igneous activity are given in 10 CFR 63.342(c)(1)(i) and 10 CFR 63.342(c)(1)(ii), respectively.

In addition, for this model abstraction of unsaturated zone flow, 10 CFR 63.342(c)(2) further provides that DOE may consider climate change after 10,000 years by using a constant-in-time specification of the mean and uncertainty distribution for repository-average deep percolation rate for the period from 10,000 to 1 million years. DOE elected to use this representation in its SAR. Thus, implementation of the specified representative percolation rate and its uncertainty distribution is reviewed for the post-10,000-year period.

The U.S. Nuclear Regulatory Commission (NRC) staff review of the license application follows the guidance laid out in the Yucca Mountain Review Plan (YMRP), NUREG-1804, Section 2.2.1.3.6, Flow Paths in the Unsaturated Zone (NRC, 2003aa), as supplemented by additional guidance for the period beyond 10,000 years after permanent closure (NRC, 2009ab). The acceptance criteria in the YMRP generically follow 10 CFR 63.114(a). Following the guidance, the NRC staff review of the applicant's abstraction of unsaturated zone flow considered five criteria

- System description and model integration are adequate.
- Data are sufficient for model justification.
- Data uncertainty is characterized and propagated through the abstraction.
- Model uncertainty is characterized and propagated through the abstraction.
- Model abstraction output is supported by objective comparisons.

Because 10 CFR Part 63 specifies the use of a risk-informed approach for the review of a license application, the guidance provided by the YMRP, as supplemented by NRC (2009ab), is followed to the extent reasonable for aspects of unsaturated zone flow important to repository performance. Whereas NRC staff considered all five criteria in their review of information provided by DOE, only aspects that substantively affect results of the performance assessment, as judged by NRC staff, are discussed in this chapter. NRC staff's judgment is based both on risk information provided by DOE, and staff's knowledge, experience, and independent analyses.

2.2.1.3.6.3 Technical Review

The review of the technical information DOE provided for unsaturated zone, seepage, and in-drift hydrological conditions in this section is divided into six subsections. The first subsection is an overview of the DOE description of processes and models, and a summary of results for the entire unsaturated zone flow area of review. The overview (SER Section 2.2.1.3.6.3.1) provides context for and reviews the integration between models and results separately

evaluated in the remaining five subsections (SER Sections 2.2.1.3.6.3.2–2.2.1.3.6.6) within the unsaturated zone. The remaining five subsections follow a natural flow through the unsaturated zone system: (i) ambient flow above the repository, (ii) thermohydrology, (iii) ambient and thermal seepage, (iv) in-drift hydrologic conditions, and (v) ambient flow below the repository.

2.2.1.3.6.3.1 Integration Within the Unsaturated Zone

In this section, the NRC staff's review covers a range of processes and features occurring at widely disparate spatial and temporal scales within the Upper and Lower Natural Barriers and, to a lesser extent, within the EBS. Within this area of review, the NRC staff evaluates aspects of repository performance pertaining to

- Unsaturated zone flow fields (SAR Section 2.3.2) above and below the repository
- Seepage into drifts (SAR Section 2.3.3)
- Hydrological aspects of the in-drift environment (SAR Section 2.3.5); in particular, the Multiscale Thermohydrologic Model (MSTHM) (SAR Section 2.3.5.4.1), the In-Drift Condensation Model (SAR Section 2.3.5.4.2), and the thermohydrologic response to the range of design thermal loadings (SAR Section 2.3.5.4.3)

The NRC staff evaluates the DOE treatment of interactions between liquid fluxes and engineered barriers inside drifts (i.e., drip shields, waste packages, and inverters) in SER Sections 2.2.1.3.3 and 2.2.1.3.4.

DOE's unsaturated zone flow models receive input from and provide output to several areas of review. SAR Section 2.3.1 provided spatially distributed net infiltration rates for the different predicted future climates for use as the top boundary flux of models in the unsaturated zone. For outputs, in-drift liquid-phase water, relative humidity, and temperature were used for abstractions of chemistry for the in-drift environment (SAR Sections 2.3.5.3, 2.3.5.5), corrosion of engineered components (SAR Section 2.3.6), waste form degradation and in-drift transport (SAR Section 2.3.7) in the Total System Performance Assessment (TSPA). In SAR Section 2.3.5, feedback from thermal-hydrological-chemical models in the host rock during the thermal period provided information on the perturbation of hydrological properties caused by emplaced waste. Output flow fields from the ambient unsaturated zone mountain-scale model (SAR Section 2.3.2), along with radionuclide flux from the EBS (SAR Section 2.3.7), were then used by Radionuclide Transport in the Unsaturated Zone abstraction (SAR Section 2.3.8).

This SER section focuses on higher level issues common to each of the unsaturated zone flow models, including (i) integration among those models, (ii) representative flow reduction through the mountain, and (iii) propagation of uncertainty in performance assessment calculations

Integration of Unsaturated Zone Flow Models

DOE represented water and heat transfer in the unsaturated zone using a variety of process-level models covering features and processes at a range of scales from millimeters to kilometers [fraction of inches to miles]. In addition to models that provide direct input, DOE used additional models to support aspects of conceptual model assumptions and parameter input. The models require different computational grids, different data needs, and different model support. Therefore, NRC considered integration among the models; specifically, spatial

continuity of percolation flux (consistent propagation of high and low flux patterns) and quantification of barrier capability through the mountain.

The following list of models, inputs, and outputs used in performance assessment calculations provides context to the parts of SER Section 2.2.1.3.6.3. NRC staff evaluation in the remainder of SER Section 2.2.1.3.6.3 parallels this list, which follows the flow of water through the mountain.

Ambient Site-Scale Unsaturated Flow Model (SAR Section 2.3.2)

- Receives top flux boundary condition from net infiltration model
- Creates set of flow fields for TSPA
 - Above-repository flux distribution to MSTHM
 - Below-repository flow field for unsaturated zone transport (see last item in this list)
- Reviewed by NRC staff in SER Sections 2.2.1.3.6.3.2 (Above Repository Only)

MSTHM (SAR Section 2.3.5.4)

- Composed of a set of five linked process-level thermal and thermohydrology models
- Creates a set of thermal response abstractions that provides
 - In-drift temperature and relative humidity for chemistry of seepage and corrosion of engineered barriers abstractions
 - Deep percolation field for seepage and chemistry models
 - Flux from host rock into invert for EBS transport
- Reviewed by NRC staff in SER Section 2.2.1.3.6.3.3

Ambient and Thermal Seepage Models (SAR Section 2.3.3)

- Process-level models used to create seepage abstractions for TSPA that provide
 - Seepage fraction (number of waste packages getting wet) to EBS transport
 - Seepage flux to EBS transport
 - Temperature threshold at drift wall, above which no seepage occurs
- Reviewed by NRC staff in SER Section 2.2.1.3.6.3.4

In-Drift Convection and Condensation Models (SAR Section 2.3.5.4)

- Convection model provides dispersion coefficients to condensation model
- Condensation model provides flux rate and distribution to EBS transport

- Reviewed by NRC staff in SER Section 2.2.1.3.6.3.5

Site-Scale Unsaturated Flow Below the Repository (see first item in this list)

- Provides flow field to unsaturated zone transport model
- Reviewed by NRC staff in SER Section 2.2.1.3.6.3.6

The NRC staff reviews repository performance with respect to water and heat transfer within the unsaturated zone by separately evaluating the individual process models and their abstractions (SER Sections 2.2.1.3.6.3.2 through 2.2.1.3.6.3.6) and the overall integration among models (the present section). (b)(5)

(b)(5)

NRC staff reviewed the information passed between the unsaturated zone models. (b)(5)

(b)(5)

(b)(5) DOE used five percolation bins to maintain continuity of flow above, through, and below drifts for both ambient and thermal periods. (b)(5)

(b)(5)

(b)(5) Also, NRC staff evaluations of the adequacy of spatial variability, upscaling, downscaling, and other linkages between models, as appropriate, are included in SER Sections 2.2.1.3.6.3.2 through 2.2.1.3.6.3.4. (b)(5)

(b)(5)

Barrier Capabilities Focusing on Flow Through the Mountain

NRC staff review also considered the DOE implementation of barrier capabilities, represented by changes to percolation flux rates as water moves through the mountain from the ground surface into the drifts and onto the water table. Table 9-1 illustrates the quantitative reduction in flux from the ground surface to water entering the drift using flux averages over the repository footprint. Flux values in the table are from DOE Enclosure 1, Tables 1, 5, and 8 (2010ai), and seepage fraction values are from SAR Tables 2.1-6 to 2.1-9. The table also provides the component of the Upper Natural Barrier, primary features or processes, and the relevant SAR section for each step of the flux reduction.

DOE presented seepage flux values as volumetric flux over the area of a waste package, calculated by multiplying seepage flux values determined in units of volumetric flux per unit area

Table 9-1. Quantitative Reduction in Flux From the Ground Surface to Water Entering the Drift Using Flux Averages Over the Repository Footprint

	Precipitation mm/yr*	Net Infiltration mm/yr*	Unsaturated Zone Site-Scale Top Boundary Net Infiltration mm/yr*	Deep Percolation mm/yr*	Seepage Repository Footprint	
					Flux mm/yr*	Fraction of Area
Component of Upper Natural Barrier	—	Topography and Soils	—	Unsaturated Zone	Unsaturated Zone	
Primary Feature or Processes	Semiarid Climate	Evapo- transpiration, Runoff, Sublimation	Uncertainty in Net Infiltration	—	Capillary Diversion and Vapor Barrier	
Section of SAR	2.3.1	2.3.1	2.3.2	2.3.2	2.3.3	
Thermal Period†	—	—	—	—	0	0
At 10,000 years,‡ Nominal	296.7	38.88	21.37	21.74	2.0 {6.4}§	0.31
At 10,000 years,‡ Seismic					2.3 {7.4}§	0.31
Post-10,000 years, Nominal	—	—	—	31.83	3.4 {8.5}§	0.40
Post-10,000 years, Seismic					15 {22}§	0.69

* Units: 25.4 mm/yr = 1 in/yr
† Thermal period defined by drift wall temperature > 100 °C [212 °F] (SAR Section 2.3.3.3.4).
‡ Values of precipitation and percolation for initial 10,000 years are for glacial transition climate
§ Average flux for seeping environment is in brackets

by a waste package footprint that is 5.1 m [17 ft] long and 5.5 m [18 ft] wide (i.e., drift width). To maintain consistent units of flux for this table, the NRC staff divided the DOE-provided seepage flux values by the same scaling factor. DOE Enclosure 1, Tables 5 and 8 (2010ai) used million-year simulation results to provide the seepage flux and fraction values for the 10,000-year period, the latter of which may differ slightly from the simulation results used in TSPA calculations for 10,000-year dose estimates. Flux values of net infiltration through deep percolation retain the significant figures DOE presented. In Table 9-1, seepage fraction is that portion of the drifts where dripping is predicted to occur (also called the seeping environment).

The table includes DOE values for its nominal case (no disruptive events) and seismic ground motion scenario. In its igneous intrusion scenario (not included in the table), DOE

(b)(5) assumed that seepage processes at the drift wall do not act as a barrier.

Condensation rates are similarly not included in Table 9-1, because these fluxes are short lived.

(b)(5)

(b)(5)

Representative thermal effects (peak waste package temperature, drift wall temperature, duration of drift wall temperatures at or above boiling) caused by waste package emplacement were summarized in SAR Tables 2.3.5-7 and 2.3.5-8 and are not reflected in Table 9-1.

(b)(5)

For the first 10,000 years of performance

- DOE calculated net infiltration for the first 10,000 years that is a small portion (approximately 13 percent) of precipitation. (b)(5)

(b)(5)

- DOE compared subsurface observations with simulations based on the site-scale ambient unsaturated flow model to calibrate the uncertainty in net infiltration, leading to a further reduction of 45 percent in the percolation flux. (b)(5)

(b)(5)

- DOE calculated an average seepage flux that is approximately 10 percent of average percolation and calculated that 31 percent of waste package locations become wet.

(b)(5)

For the post-10,000-year period, NRC staff's review includes the seismic ground motion and igneous intrusion modeling scenarios. (b)(5)

(b)(5)

(b)(5)

(b)(5)

(b)(5)

(b)(5)

Detailed NRC staff review of repository performance with respect to DOE results for net infiltration, percolation, seepage, and condensation is given in SER Sections 2.2.1.3.5.3 and 2.2.1.3.6.3.2 through 2.2.1.3.6.3.6.

Propagation of Uncertainty in Performance Assessment

NRC staff evaluates propagation of uncertainty in DOE performance assessment calculations by examining (i) the technical basis for selecting parameters and uncertainties for sensitivity analyses and (ii) the DOE sensitivity analysis for the selected parameters with respect to TSPA intermediate results and calculated doses.

DOE conducted a series of analyses to determine the sensitivity of model outputs to input parameter uncertainties in its performance assessment calculations (SAR Section 2.4.2.3.3.3). The applicant treated a subset of parameters in the unsaturated zone and EBS as uncertain in the analyses. These parameters relate to infiltration (linked to percolation), seepage into the drift, host rock thermal and hydrogeologic parameters, and in-drift thermal processes that affect the release of radionuclides. In SER Sections 2.2.1.3.5.3.3 and 2.2.1.3.6.3.2–2.2.1.3.6.3.6, the NRC staff evaluated (i) the analyses used to identify uncertain parameters carried into performance assessment calculations and (ii) the technical basis for describing uncertain parameters when evaluating individual models and abstractions. (b)(5)

(b)(5)

(b)(5)

(b)(5)

DOE evaluated the sensitivity of intermediate results and expected mean annual dose as calculated by TSPA with respect to the selected parameters. In general, the DOE analyses identified key uncertain inputs associated with waste package failure as the dominant

factors affecting performance (SAR Table 2.4-12); saturated zone transport and net infiltration were also identified as key uncertain inputs under some scenarios.

The DOE analyses consistently identified uncertainty in net infiltration, which is closely related to percolation fluxes within the unsaturated zone, as significantly affecting uncertainty in intermediate results (e.g., drift seepage, drift wall temperatures, radionuclide releases from the EBS, unsaturated zone radionuclide transport rates) and expected mean annual doses (SNL, 2008ag). The DOE analyses also identified (i) relatively smaller contributions to uncertainty in seepage into drifts arising from uncertainty in host rock permeability and capillary strength and (ii) contributions to uncertainty in in-drift temperature and relative humidity from host rock thermal conductivity, as outlined in SNL Section K4 (2008ag).

The NRC staff examined the DOE sensitivity analyses with respect to intermediate results and expected mean annual dose by comparing the sensitivity results with the DOE description of the physical processes governing barrier function as represented in the models used for performance assessment. (b)(5)

(b)(5)

(b)(5)

(b)(5)

2.2.1.3.6.3.2 Ambient Mountain-Scale Flow Above the Repository

DOE represented the unsaturated zone and EBS using a hierarchy of far-field, near-field, and within-drift models. DOE used its site-scale unsaturated zone flow model to represent far-field ambient mountain-scale flow from the ground surface to the water table (i.e., above, within, and below the proposed repository). In DOE documentation, site-scale and mountain-scale flow are interchangeable terms referring to the large scale of the computational grid, and ambient flow is the percolation flux that occurs without the flow-diverting effects of drifts and waste-produced thermal boiling fronts. DOE used output from the site-scale unsaturated zone flow model to account for far-field effects. This SER section evaluates repository performance with respect to ambient water flow within the upper unsaturated zone between the ground surface and the proposed repository horizon, focusing on the site-scale unsaturated zone flow model and an

intermediate-scale model that links mountain-scale flow to seepage models. The NRC staff evaluates repository performance related to the effects of drift openings and thermal perturbation on flow patterns within and below the proposed repository horizon in SER Sections 2.2.1.3.6.3.3 through 2.2.1.3.6.3.6.

In its review, NRC staff considered the site-scale unsaturated-zone flow model from two perspectives: (i) in the context of flow within the unsaturated zone as a whole and (ii) in the context of the applicant-defined upper and lower natural barriers. The NRC staff evaluation in this SER section focuses on aspects of repository performance primarily related to the upper natural barrier, in particular aspects of flow that affect seepage. The evaluation presented in SER Section 2.2.1.3.6.3.6 addresses aspects of repository performance primarily related to the lower natural barrier, in particular, aspects of flow that affect transport. However, to minimize repetitive discussion, the present section also considers some aspects of repository performance that apply to the entire unsaturated zone, such as model parameterization. This SER section also describes the NRC staff evaluation of aspects of the repository performance specifically related to DOE's implementation of 10 CFR 63.342(c)(2), regarding percolation during the period from 10,000 to 1 million years after permanent closure.

Conceptual Model

The DOE conceptual model for flow in the unsaturated zone is based on the primary hydrogeologic units within a column (SAR Section 2.3.2.2.1). The uppermost, the Tiva Canyon welded unit, features vertical episodic and fracture-dominated flow strongly influenced by episodic infiltration pulses. The underlying Paintbrush Tuff nonwelded (PTn) unit exhibits essentially vertical matrix-dominated flow with a strong potential for dampening and smoothing flows, thereby buffering lower units from episodic and localized infiltration pulses. The repository host horizon is within the Topopah Spring welded (TSw) unit, which features essentially vertical fracture-dominated flows in equilibrium with decadal-average net infiltration. In the TSw, mountain-scale flow patterns are controlled by mountain-scale infiltration patterns and fine-scale flow patterns are controlled by the TSw rock properties. The DOE conceptual model for the units underlying the repository host horizon, Calico Hills nonwelded (CHn) and Crater Flat undifferentiated (CFu) units are discussed and evaluated in detail in SER Section 2.2.1.3.6.3.6.

(b)(5)

Implementation of the Conceptual Model

DOE used several models to represent various aspects of flow within the upper unsaturated zone, each considering different processes and scales. Because several DOE abstractions consider flows in the upper unsaturated zone, and multiple downstream models depend on the calculated flows, the NRC staff considered how the flow abstractions interact with the other

calculations affecting repository performance by (i) separately evaluating individual flow abstractions, (ii) evaluating downstream uses of the flow abstractions for consistency between abstractions, and (iii) evaluating the effects of the abstractions on performance assessment calculations as a whole. In this SER section, the NRC staff evaluates the ambient mountain-scale flow model, focusing on the linkages between the model and both upstream models (i.e., the infiltration model) and downstream models (e.g., the MSTHM and seepage models).

In performing a risk-informed, performance-based review of the DOE's representation of ambient flow in the upper unsaturated zone, the NRC staff considered the DOE-defined function of the Upper Natural Barrier to prevent or substantially reduce water seeping into emplacement drifts. (b)(5)

(b)(5)

(b)(5)

The following sections describe the NRC staff evaluation of these aspects of repository performance with respect to ambient flow in the upper unsaturated zone.

Integration of Flow Models

Comment (b)(5)

The NRC staff considered the DOE approach to integrating the site-scale unsaturated zone flow model representation of ambient flow above the repository with (i) the MASSIF infiltration model (SAR Section 2.3.1), (ii) the MSTHM (SAR Section 2.3.5.4), (iii) seepage models, and (iv) ambient flow below the repository. The NRC staff identified the integration of ambient flow above the repository with seepage models as the most risk significant among these for the following reasons:

- The MASSIF net infiltration model, site-scale unsaturated zone flow model, and MSTHM are decoupled models that are linked in only one direction (see SER Section 2.2.1.3.6.3.1); the site-scale unsaturated zone flow model seamlessly considers ambient flow above and below the repository, and the linkages locally conserve mass.

- Performance assessment calculations are sensitive to seepage, which is in turn sensitive to the representation of fluxes near emplacement drifts at scales smaller than represented by the site-scale unsaturated zone flow model.

(b)(5)

(b)(5)

The NRC staff evaluates DOE's integration between flow at the mountain and seepage scales, also considering integration between infiltration and seepage, in the remainder of this subsection. The NRC staff evaluates the DOE approach to modeling seepage in SER Section 2.2.1.3.6.3.4.

DOE used a hierarchical approach to link percolation fluxes within the repository horizon at the mountain scale to seepage, progressing from mountain-scale flow to the smaller scales of intermediate- or drift-scale flow and fine-scale flow (SAR Section 2.3.3.2). The site-scale unsaturated zone flow model, which calculates mountain-scale flow, represents flow averaged over an area approximately corresponding to the combined area of a drift and the pillar between drifts. Intermediate-scale flow represents average flow over an area approximately corresponding to the width of a drift. Fine-scale flow represents flow at scales smaller than a drift wall. DOE considered all three scales in calculating average seepage into drifts.

DOE represented both intermediate-scale and fine-scale flow statistically, as described in SAR Section 2.3.3.2.3 and DOE Enclosure 4 (2009b). DOE derived an abstraction for the statistical distribution of intermediate-scale fluxes from numerical model calculations considering hydraulic-property heterogeneity in the densely welded TSW unit above the proposed repository using model parameters based on field observations. DOE provided simulation results demonstrating that the statistical patterns of predominantly vertical unsaturated zone flow at the intermediate scale stabilize within a short vertical distance from the top boundary and geological unit changes, using several representations of the top boundary flux (SAR Section 2.3.3.2.3.5). DOE also performed sensitivity studies considering alternative statistical representations of intermediate-scale variability. (b)(5)

(b)(5)

(b)(5)

(b)(5)

Mountain-Scale/Site-Scale Flow Patterns

The site-scale unsaturated zone flow model represents mountain-scale flow as steady state in equilibrium with climatic conditions, with water flowing from the upper boundary to the water table without lateral inflow or outflow. (b)(5)

(b)(5)

(b)(5)

The

NRC staff evaluates the site-scale model separately for the Upper Natural Barrier portion of the unsaturated zone, above the proposed repository (this section), and the Lower Natural Barrier portion of the unsaturated zone, below the repository (SER Section 2.2.3.6.3.6). The NRC staff evaluates the DOE representation for the spatial patterns of percolation flux in this section and evaluates the DOE representation for the magnitude of areal-average percolation flux through the repository footprint, which is determined by net infiltration, in a subsequent subsection (Infiltration Uncertainty).

DOE represents spatial variability in percolation fluxes as dominated by intermediate- and fine-scale variability in the seepage calculations for performance assessment. In the preceding section of this chapter (Integration of Flow Models), (b)(5)

(b)(5)

DOE demonstrated that the site-scale unsaturated zone flow model calculates mountain-scale spatial patterns of percolation fluxes, combining matrix and fracture flows, that are essentially vertical from the ground surface through the repository horizon within the repository footprint, in accordance with the DOE conceptual model, as shown in SNL Figures 6.1-2 through 6.1-5 and 6.6-1 through 6.6-4 (2007bf). DOE numerical analyses indicate that substantial lateral diversion (associated with the PTn unit) away from the repository footprint may occur, which would reduce the amount of water passing through the footprint at the repository horizon (SAR Section 2.3.2.2.1.1).

(b)(5)

Site-Scale Unsaturated Zone Model Parameters

The NRC staff's risk-informed, performance-based review of the site-scale unsaturated zone model parameters includes consideration of (i) the technical bases for the parameters and (ii) the use of the parameters in the site-scale unsaturated zone model and downstream models used for performance assessment calculations. DOE does not base input parameters for the downstream seepage models on site-scale unsaturated zone model parameters; the NRC staff evaluates the seepage model input in SER Section 2.2.1.3.6.3.4.

DOE's site-scale unsaturated zone flow model represents the stratigraphy at Yucca Mountain using 32 homogeneous material property layers, with the same set of material properties assigned to every grid cell in a property layer (SAR Section 2.3.2.4.1.2.2). The material property layers were developed from geologic layers described in the Geologic Framework Model. DOE justified the use of layerwise homogeneous material properties on numerical simulations by comparing outputs from simulations with different levels of heterogeneity, concluding that similarities in fracture flux patterns and tracer transport times demonstrate that heterogeneities within units have only a minor effect on site-scale flow processes (SAR Section 2.3.2.4.1.1.4). DOE developed some model parameters directly from site observations (e.g., porosity) and some from model calibration to field measurements of saturation, potential, pneumatic pressure, and perched water elevations. DOE used a set of *in-situ* observations not used for model calibration (e.g., calcite, Carbon-14, and strontium) to build confidence in the flow model (SAR Section 2.3.2.5.1). DOE further used a set of *in-situ* observations not used for either model calibration or for building confidence in the flow model (i.e., chloride and temperature observations) to calibrate the uncertainty in infiltration (SAR Section 2.3.2.4.1.2.4.5).

Comment (b)(5)

(b)(5)

The DOE performance assessment explicitly considered uncertainty in model parameters arising from uncertainty in infiltration flux, using a separate set of calibrated properties for the 10th, 30th, 50th, and 90th percentiles of the infiltration map uncertainty distribution. DOE ensured that the flow fields resulting from each set of calibrated properties featured predominantly vertical flow from the ground surface through the repository horizon within the repository footprint, in accordance with the DOE conceptual model. DOE did not propagate the full range of parameter uncertainties into the TSPA on the basis that sensitivity analyses demonstrating that the model results, including performance-affecting results such as flow pathways, are insensitive to the parameter values in the range that the applicant considered (SAR Section 2.3.2.4.2.2).

(b)(5)

Infiltration Uncertainty

Comment (b)(5)
(b)(5)

The NRC staff evaluates infiltration uncertainty by considering (i) the technical bases for the DOE approach and (ii) consequences of the approach in performance assessment calculations. Whereas DOE addressed uncertainty in infiltration estimates derived from the net infiltration model using input parameter uncertainty, DOE derived infiltration uncertainty evaluated in this section from deep subsurface observations. DOE also referred to the results from incorporating this uncertainty as the unsaturated zone top (upper) boundary net infiltration to distinguish it from results derived from the net infiltration model.

For each climate state in the first 10,000 years after repository closure, DOE selected four infiltration maps calculated by the MASSIF infiltration model, out of the 40 equally likely realizations for the climate state (SNL, 2007az), to represent the uncertainty in infiltration. Initial probabilities of 0.2, 0.2, 0.3, and 0.3 were assigned to the four selected maps under each climate state, on the basis of the percentile rankings for the infiltration maps. Because the site-scale unsaturated zone model uses larger grid cells than the MASSIF model, DOE created upper boundary net infiltration maps for the site-scale unsaturated zone model grid. DOE transferred the infiltration values for each site-scale unsaturated zone model grid cell by accumulating infiltration fluxes from nearby MASSIF grid cells. For the post-10,000 year climate state, the applicant assigned weights to the upper boundary net infiltration maps to be consistent with the draft standard describing deep percolation in the post-10,000 year period. The NRC staff evaluates DOE's treatment of net infiltration during the post-10,000-year period in a subsequent subsection (Post-10,000-Year Approach).

DOE found that model predictions for temperature and chloride distributions in the unsaturated zone, using models based on the site-scale unsaturated flow model, did not reflect average measured quantities in the unsaturated zone. The applicant used a version of the Generalized Likelihood Uncertainty Estimation (GLUE) methodology (Beven and Binley, 1992aa) to update the initial probability weights assigned to each flow field (SAR Section 2.3.2.4.1.2.4.5). The GLUE methodology revises initial probability weights on the basis of differences between field observations and numerical model predictions. DOE updated the probability weights using temperature observations from 5 boreholes and chloride observations from 12 boreholes, the Exploratory Studies Facility, and the Enhanced Characterization for the Repository Block Cross Drift. DOE used four different likelihood functions to compare the model predictions with observations.

SAR Section 2.3.2.4.1.2.4.5.5 reported estimated final weighting factors of 0.619, 0.157, 0.165, and 0.0596 for the 10th, 30th, 50th, and 90th percentile upper boundary net infiltration maps, respectively, by combining the analyses considering temperature and chloride data. These final weights, when applied to the average infiltration rates over the upper boundary condition infiltration maps (SAR Table 2.3.2-14), result in weighted-average infiltration over the ambient flow model domain of 6.7, 13.1, and 17.1 mm/yr [0.26, 0.52, and 0.67 in/yr] under present-day, monsoon, and glacial transition climate states. (b)(5)

(b)(5)

(b)(5)

DOE identified several uncertainties in interpreting field observations using the temperature and chloride models (SAR Section 2.3.2.4.1.2.4.5.2). These uncertainties may affect the calculated weights for the assigned flow fields. DOE also demonstrated that there is uncertainty associated with the likelihood functions used to determine the weights, with the calculated weights differing between likelihood functions (SAR Tables 2.3.2-25 through 2.3.2-27).

DOE considered expected doses in the first 10,000 years of performance for the seismic ground motion and igneous intrusion scenarios, which collectively account for approximately 97 percent of the calculated peak expected mean annual dose, as described in DOE Enclosure 5 (2009bo). DOE compared the performance assessment dose calculations of expected doses with and without the GLUE weighting, finding that the original weighting scheme (without the GLUE procedure) results in a 29 percent greater peak expected dose than the GLUE weights. DOE concluded that, because the calculated doses are so similar, adjusting the infiltration uncertainty with the GLUE procedure is inconsequential to the compliance determination.

(b)(5)

(b)(5)

Temporal and Spatial Variability in the Upper Unsaturated Zone

DOE described a primary role for the upper unsaturated zone (i.e., above the proposed repository) as strongly dampening and smoothing episodic infiltration pulses, to the extent that flows below the PTn within the proposed repository footprint are essentially steady, in equilibrium with the long-term climate. This is a screening argument for FEP 2.2.07.05.0A, Flow in the UZ (Unsaturated Zone) from Episodic Infiltration (SNL, 2008ab). DOE identified the consequence of this dampening effect as reducing time-averaged seepage rates into intact or degraded drifts, with the reduction effect becoming less significant as the drift degrades in DOE Enclosure 2 (2009an).

Comment (b)(5)

(b)(5)

Comment (b)(5)

(b)(5)

(b)(5)

(b)(5)

(b)(5)

(b)(5)

DOE considers decadal to

centennial variability in percolation likely to occur below the PTn because the PTn has a finite storage capacity, but expects that the increase in calculated average seepage would be small if decadal to centennial variability was explicitly included. DOE demonstrated that fluctuations in percolation flux of 20 and 50 percent about the mean (i.e., coefficients of variation of 0.2 and 0.5) yielded a systematic increase in GLUE-weighted seepage of approximately 2.7 and 17 percent, respectively, under glacial transition conditions, as outlined in DOE Enclosure 1 (2009cc). Using an analysis demonstrating that a systematic increase in GLUE-weighted seepage by a factor of approximately 2.5 has a negligible effect on the expected dose, as described in DOE Enclosure 5 (2009bo), DOE concluded by analogy that the smaller systematic increases in seepage induced by decadal to centennial climatic fluctuations also have a

negligible effect on the demonstration of compliance. (b)(5)

(b)(5)

(b)(5)

(b)(5)

(b)(5)

DOE relied on numerical simulations to justify the representation of spatial variability in performance assessment calculations and to demonstrate that episodic flow is expected to be rare below the PTn. DOE described several mechanisms to explain why some field evidence, such as modern tritium observations below the PTn, may not completely support the DOE assumptions related to drift-scale variability and episodic flow. These mechanisms include transport through faults, episodic flow, spatially variable infiltration patterns, and heterogeneous hydrologic properties, as outlined in DOE Enclosure 1 (2009cc). (b)(5)

(b)(5)

(b)(5)

DOE considered the effect on seepage for several alternative statistical relationships for the effect of rock heterogeneity on flow focusing, as shown in SNL Section 6.8.2, Case 6 (2007bf), ranging from no intermediate-scale focusing (Case 6a) to flow focusing that is more extreme than used for performance assessment calculations (Case 6c). DOE characterized the Case 6c distribution, which has a maximum flow-focusing factor more than six times larger than the distribution used in performance assessment calculations, as unrealistically extreme to represent rock heterogeneity, as described in DOE Enclosure 4 (2009bo). (b)(5)

(b)(5)

DOE demonstrated that incorporation of the Case 6c distribution yields a minor increase in expected dose for the million-year seismic ground motion modeling case, as shown in DOE Enclosure 1 (2009cx). DOE described the seismic ground motion modeling case as the dominant contributor to calculated expected dose. (b)(5)

(b)(5)

(b)(5)

(b)(5)

DOE represented the PTn unit as a barrier with a strong potential to dampen episodic pulses below the PTn. This conceptual model was supported by numerical modeling results interpreting chloride, temperature, and radioisotope data obtained from within and below the PTn. DOE estimated that approximately 1 percent of the repository is affected by fast pathways, predominantly in faults (SAR Section 2.3.2.2.1.1), and argued that these fast pathways are not necessarily a consequence of episodic flow, but instead would represent spatial variability. (b)(5)

(b)(5)

(b)(5)

(b)(5)

(b)(5)

(b)(5)

Post-10,000-Year Approach

Consistent with the regulatory direction provided in 10 CFR 63.342(c)(2), the applicant chose not to model climate or infiltration for the post-10,000-year period. Instead, DOE (i) selected four of the upper boundary condition net infiltration maps used to represent specific climate states in the first 10,000 years of performance; (ii) modified these maps into four new maps to achieve areal-average deep percolation flux target values within the repository footprint, consistent with the probability distribution the draft revision to 10 CFR 63.342 specified, at the infiltration-map probability values used in the first 10,000 years after closure; and (iii) created four site-scale unsaturated zone model flow fields on the basis of these boundary conditions (SAR Section 2.3.2.4.1.2.4.2).

DOE used the percolation distribution from the draft rule (SAR Section 2.3.2.4.1.2.4.2) because the final rule was not promulgated until a few months before DOE submitted the license application. Reflecting the difference between the draft and final percolation distributions, the mean percolation in the final rule (10 CFR 63.342(c)(2)) is 16 percent larger than that in the

draft rule. In DOE Enclosure 6 (2009cb), DOE performed sensitivity analyses that showed no significant affect on repository performance when using the distribution from the draft rule instead of that from the final rule.

(b)(5)

(b)(5)

Summary

The NRC staff reviewed the model conceptualization, the underlying assumptions of the ambient site-scale unsaturated zone flow model and other relevant abstractions with which the ambient site-scale unsaturated zone flow model exchanges data and information, and the alternative model conceptualizations the applicant used to analyze model uncertainties. (b)(5)

(b)(5)

(b)(5)

2.2.1.3.6.3.3 Thermohydrologic Effects of Waste Emplacement

DOE represented the unsaturated zone and EBS using a hierarchy of far-field, near-field, and within-drift models to account for thermal effects due to emplacement. DOE used a conceptual and numerical model, the MSTHM, to represent near-field and in-drift thermohydrologic conditions. DOE used input from the site-scale unsaturated zone flow model to account for far-field effects and output from MSTHM in downstream models that estimate the effects of in-drift thermohydrologic conditions on thermal seepage, quantity and chemistry of water contacting engineered barriers and waste forms, degradation of engineered barriers, and radionuclide release rates and solubility limits. This SER section describes the NRC staff evaluation of the effects of waste emplacement on near-field and in-drift thermohydrologic conditions. The NRC staff evaluated repository performance related to the effects of thermal load on (i) seepage, (ii) quantity and chemistry of water contacting engineered barriers and waste forms, (iii) degradation of engineered barriers and radionuclide release rates, and (iv) solubility limits in SER Sections 2.2.1.3.6.3.4, 2.2.1.3.3, 2.2.1.3.1, and 2.2.1.3.4, respectively.

DOE passed MSTHM output to several downstream models in its performance assessment calculations. DOE used drift-wall temperature to switch between two limiting conditions for seepage, assuming that (i) no seepage occurs where drift-wall temperature is greater than 100 °C [212 °F] (the boiling temperature of water at the repository elevation is approximately 96 °C [205 °F]) and (ii) seepage occurs at the ambient rate for lower drift-wall temperatures. DOE modeled waste-package corrosion rates as depending on waste-package temperature and relative humidity, and temperature-dependent chemistry of seeping water. DOE modeled a diffusive-release pathway forming within failed waste packages once a continuous liquid film forms at elevated waste-package relative humidity levels. DOE used invert saturation, invert temperature, and imbibition fluxes into the invert to estimate properties and fluxes affecting released radionuclide transport from the waste package to the host rock.

The DOE repository design basis places limits on the (i) peak waste package temperature {300 °C [572 °F] for 500 years, followed by 200 °C [392 °F] for 9,500 years} to reduce the potential for degradation of Alloy 22 waste packages; (ii) peak post-closure drift wall temperature {200 °C [392 °F]} to reduce thermal effects on drift stability; and (iii) peak mid-pillar temperature {96 °C [205 °F]} to facilitate drainage of percolation water between emplacement

drifts (SAR Section 2.3.5.4.3; SAR Table 1.3.1-2). DOE's design accomplished these peak temperature limits through prescribed thermal loading criteria for waste packages (SAR Section 1.3.1.2.5). DOE used MSTHM to demonstrate that these design basis temperature limits can be achieved using (i) a stylized postclosure reference case based on expected waste package receipts over the emplacement period and (ii) two estimated limiting waste streams developed with different management options (SAR Section 1.3.1.2.5).

In evaluating repository performance with respect to near-field and in-drift thermohydrologic conditions, the NRC staff reviewed (i) the DOE conceptual model, (ii) the process-level implementation of the DOE conceptual model, (iii) data support and propagation of uncertainty, (iv) abstraction of the process-level model into performance assessment calculations, and (v) use of the model outputs in downstream models. The NRC staff's review of these topics focuses on aspects of repository performance that affect (i) duration of above-boiling temperatures at the drift wall, (ii) waste-package temperatures, (iii) in-drift humidity after onset of seepage, and (iv) seepage fluxes into inverts. These aspects of the MSTHM model are outputs that are used as input for downstream models that calculate seepage, corrosion of waste packages, and release pathways within the EBS. The NRC staff review also focused on the DOE representation of collapsed drifts, because burial of waste packages by an insulating rubble layer could result in elevated waste-package temperatures.

Conceptual and Implemented Numerical Models

(b)(5)

DOE implemented the conceptual model into the four submodels of the MSTHM. The submodels were linked through the mathematical principle of superposition, representing different aspects of coupled thermohydrologic processes at different spatial scales (SAR Section 2.3.5.4.1.3.1). These submodels consider (i) three-dimensional mountain-scale conduction, (ii) two-dimensional drift-scale thermal-hydrology in cross-sections ("chimneys") perpendicular to the drift axis, (iii) links between the mountain-scale and chimney submodels, and (iv) effects of discrete waste packages. (b)(5)

(b)(5)

(b)(5)

DOE used its Drift Scale Test to validate the conceptual model underlying the drift-scale thermal-hydrologic submodel, as described in SAR Section 2.3.5.4.1.3.3 and SNL Section 7.4 (2008aj), and used its Large Block Test, shown in SNL Section 7.3 (2008aj), to build confidence in the ability of the MSTHM to predict thermal-hydrologic processes in the host rock. DOE (i) simulated the thermohydrologic behavior observed in the Drift Scale Test and Large Block Test using the same modeling techniques included in the thermohydrologic submodel of MSTHM; (ii) compared modeled and observed temperature, relative humidity, and liquid-phase saturation values; and (iii) concluded that the differences were within the parametric uncertainty of MSTHM results. (b)(5)

(b)(5)

DOE identified several assumptions and limitations associated with linking the submodels (SAR Section 2.3.5.4.1.3.1), including restrictions related to mountain-scale and along-drift convection. DOE considered alternative conceptual models by comparing MSTHM results with those of (i) an east-west cross section from a smeared-heat-source mountain-scale model; (ii) a three-dimensional, mountain-scale, nested-grid thermal-hydrologic model for a three-drift test case; and (iii) a three-dimensional, pillar-scale model with different axial in-drift vapor transport assumptions (SAR Section 2.3.5.4.1.3.3). (b)(5)

(b)(5)

(b)(5)

DOE assumed that mobilized water predominantly moves perpendicular to the axis of the emplacement drifts within the host rock. (b)(5)

(b)(5)

(b)(5)

Abstraction of MSTHM for TSPA

The MSTHM calculates time-dependent thermal-hydrologic variables for each of the 8 waste packages simulated for the 3,264 subdomains, each representing a 20-m [66-ft] segment of an emplacement drift. DOE referred to this as the comprehensive set of MSTHM outputs. DOE performed the calculations for 7 parameter uncertainty cases, representing 12 combinations of infiltration uncertainty and thermal conductivity uncertainty, as described in the next subsection. DOE mapped each of the 3,264 subdomains to one of the five percolation bins abstracting the effects of seepage.

DOE provided the comprehensive set of MSTHM outputs for waste package temperature and relative humidity for different waste package types and drift-wall temperature, for all MSTHM subdomains in each percolation bin, as input to the Waste Package Degradation Model Component, the Drift Seepage Submodel, and the Drift Wall Condensation Submodel within the TSPA model, as shown in SNL Section 6.3.2.2 (2008ag). These downstream models use the MSTHM outputs to calculate waste package failure rates. (b)(5)

(b)(5)

DOE also abstracted the MSTHM results by selecting a single representative codisposal waste package and commercial spent nuclear fuel waste package for each percolation bin. DOE used the codisposal and commercial spent nuclear fuel waste packages with peak waste package temperature and drift-wall boiling duration closest to the median values to represent thermohydrologic conditions for all waste packages in the percolation bin. DOE provided the time-dependent output values of waste package surface temperature and relative humidity, drift wall temperature, invert temperature, invert saturation, and flux into the invert for the selected representative waste packages to the Waste Form Degradation and Mobilization Model Component, the EBS Flow and Transport Model Component, the EBS Chemical Environment Submodel, and the Drift Wall Condensation Submodel within the TSPA model, as outlined in SNL Section 6.3.2.2 (2008ag). These downstream models use the MSTHM outputs to calculate radionuclide release rates from failed waste packages and radionuclide transport within the EBS. DOE provided analyses in SNL Section 7.3.4.3.1 (2008ag) comparing estimates of cumulative radionuclide releases from a single failed waste package using the representative location with estimates calculated using the comprehensive set of MSTHM output. These analyses demonstrated essentially identical cumulative release of representative radionuclides from the EBS after both 10,000 and 1 million years. (b)(5)

(b)(5)

(b)(5)

Data Support and Uncertainty Propagation in the MSTHM

NRC staff reviewed the information provided in SAR Section 2.3.5.4.1.2 and selected references to evaluate the DOE supporting data and characterization of uncertainties in the MSTHM. Because of the importance in performance assessment calculations, the NRC staff

focuses its review on (i) input parameters that significantly affect MSTHM results, (ii) data support for uncertainty bounds in input parameters, and (iii) uncertainty propagation in the MSTHM.

MSTHM simulations require input to describe the EBS and natural barriers (SAR Section 2.3.5.4.1.2.2). DOE identified the design control parameters and associated design constraints in SAR Table 2.2-3. DOE derived EBS parameters from the design information. DOE based natural barrier parameters on the site-scale unsaturated zone flow model (evaluated in SER Section 2.2.1.3.6.3.3), including hydrologic properties of the unsaturated zone, natural system geometry, and percolation fluxes below the PTn.

DOE explicitly represented the drift, drip shield, and invert components of the EBS (SNL, 2008aj, Section 4[a]). DOE screened out representing the thermohydrologic behavior of other engineered components potentially affecting performance (e.g., rock bolts and associated boreholes used for ground support) on the basis of low consequence for performance assessment calculations. (b)(5)

Comment	(b)(5)
	(b)(5)

(b)(5)

(b)(5)

DOE described the design information representing engineered features in MSTHM as consistent with the design of subsurface structures, systems, and components (SAR Section 2.3.5.4.1.2.1). In SNL Section 4.1 (2008aj), DOE described repository subsurface and waste package design information as obtained from controlled sources and based on the current repository design.

(b)(5)

DOE identified host rock thermal conductivity and percolation flux as the dominant parameters responsible for variability and uncertainty in simulated thermal-hydrologic conditions (SAR Section 2.3.5.4.1.3.2). NRC staff evaluated the adequacy of percolation flux in SER Section 2.2.1.3.6.3.2; incorporation of uncertainty in percolation is described in the paragraphs that follow. DOE considered the uncertainty in thermal conductivity of the host rock using a geostatistical model supported by laboratory measurements and core samples to constrain and condition the geostatistical model (BSC, 2004bf). DOE extracted host rock thermal conductivity values from the geostatistical model, evaluated the influence of thermal conductivity on peak waste package temperatures and duration above boiling, and assigned weights for implementation in TSPA, as outlined in SNL Section 6.2.13.3[a] (2008aj). DOE averaged the thermal properties of nonrepository units to facilitate computational efficiency, using a sensitivity analysis to demonstrate that the averaging does not affect the MSTHM results, as shown in SNL Section 6.2.13.4[a] (2008aj). The percolation flux applied at the top boundary in the thermohydrologic submodel is the percolation flux at the base of the PTn unit calculated in the site-scale unsaturated zone flow model for the nominal 10th, 30th, 50th, and 90th percentile scenarios. The uncertainty in percolation flux in the site-scale unsaturated zone flow model at the mountain scale is propagated consistently in the MSTHM. (b)(5)

(b)(5)

(b)(5)

DOE propagated uncertainty in host rock thermal conductivity and percolation flux into simulations using 7 of the 12 combinations of 10th, 30th, 50th, and 90th percentile flux scenarios with low, mean, and high thermal conductivities as input (SAR Section 2.3.5.4.1.3.2). For each of the remaining five combinations, DOE used the results from one of the seven simulations as a surrogate based on similarity in boiling duration, as described in SAR Section 2.3.5.4.1.3.2 and SNL Section 6.2.12.3[a] (2008aj). DOE propagated the full set of 12 combinations into performance assessment calculations. (b)(5)

(b)(5)

(b)(5)

Use of MSTHM Results in Downstream Models

NRC staff evaluated predictions of thermohydrologic conditions in part by considering how DOE used MSTHM results in downstream models. The downstream models using MSTHM results include (i) thermal seepage, (ii) quantity and chemistry of water contacting engineered barriers and waste forms, (iii) degradation of engineered barriers, and (iv) radionuclide release rates and solubility limits. The NRC staff evaluates these downstream models in SER Sections 2.2.1.3.6.3.4, 2.2.1.3.3, 2.2.1.3.1, and 2.2.1.3.4, respectively.

(b)(5)

Uncertainty in Thermal Loading

DOE described the loading strategy implemented in the MSTHM as a stylized postclosure reference case based on expected waste package receipts over the emplacement period (SAR Section 1.3.1.2.5). DOE considered the actual future waste stream to be uncertain and considered flexibility in emplacement strategies necessary to manage acceptance of a wide spectrum of waste streams (SAR Section 1.3.1.2.5). For example, the design heat load DOE described in SNL (2008ai) updated the heat load used for MSTHM calculations (SAR Section 2.3.5.4.1). In SAR Section 2.3.5.4.3, DOE described how temperature estimates

using the design heat load compared with the temperature estimates from the MSTHM results. DOE committed to develop an emplacement drift plan (SAR Section 1.3.1.2.5; Enclosure 1 of DOE, 2009ct) for each drift, or set of drifts, that will (i) provide specific information, such as waste characteristics, waste package emplacement locations, and ventilation duration, and (ii) describe how preclosure and postclosure performance requirements will be met using the selected emplacement strategy

DOE demonstrated that management approaches using temperature index functions representing three- and seven-package segments are capable of achieving performance targets for mid-pillar, drift-wall, and waste-package peak temperatures (SAR Section 2.3.5.4.3) for the two estimated limiting waste streams. The management approaches utilize extended duration of ventilation beyond 50 years or different surface handling facilities and aging capacities. DOE concluded that (i) only minor modifications to the TSPA model inputs are needed to represent the anticipated range of thermal loading; (ii) the geomechanical, hydrogeologic, and geochemical system responses for the two estimated limiting waste streams are each within the range of applicability for the respective models, as shown in SNL Section 6.4 (2008ai); and (iii) the changes in system responses arising from future waste streams different than the reference case do not significantly affect the screening justifications for excluded FEPs or the modeling basis for included FEPs, as outlined in SNL Section 6.5 (2008ai). (b)(5)

(b)(5)

DOE expects that, under bounding assumptions, peak waste package temperatures for some waste packages may exceed the design basis temperature by nearly 100 °C [180 °F] if drifts were to collapse within the first 90 years after closure (SAR Section 2.3.5.4.3, SAR Figure 2.3.5-37). DOE considered several mechanisms for drift collapse, including seismic-induced ground motion, thermally induced stresses, and gravitational stresses. DOE screened out all mechanisms for drift collapse other than seismic-induced ground motion (FEP 2.1.07.02.0A, Drift Collapse) on the basis of low consequence (SNL, 2008ab). (b)(5)

(b)(5)

(b)(5)

DOE screened in mechanisms of drift degradation from seismic-induced ground motion, including in-drift temperature and relative humidity consequences from seismic-induced drift collapse. DOE performed a bounding probabilistic risk analysis considering uncertainty in seismic events and the key thermohydrologic parameter (thermal conductivity). This risk analysis used methods and assumptions consistent with DOE's performance assessment calculations to calculate a probability of approximately 1 in 10,000 that the hottest waste package in the stylized postclosure reference case exceeded the 300 °C [572 °F] waste package temperature design basis because of drift collapse during the first 10,000 years after closure, as described in SAR Section 2.3.5.4.3, SNL Section 6.3.17[a] (2008aj), and SNL Section 6.4.2.5 (2008ai). DOE screened out consideration of peak waste package temperatures exceeding the established temperature limits in performance assessment calculations on the basis of the probabilistic calculation and additional information describing the nature of the bounding assumptions (SAR Section 2.3.5.4.3). (b)(5)

(b)(5)

The NRC staff recognizes that actual waste sent to Yucca Mountain, flexible emplacement strategies, and natural system and modeling factors may increase or decrease estimated peak temperatures relative to the stylized reference case [e.g., SNL Figure 6.4.2-28 (2008ai)], which may result in locally different thermal regimes compared to the performance assessment and screening calculations. DOE committed to developing an emplacement drift plan prior to waste emplacement that specified for each drift, or set of drifts, the (i) waste characteristics, (ii) waste package emplacement locations, (iii) ventilation duration, and (iv) how preclosure and postclosure performance requirements will be met using the selected emplacement strategy, as described in SAR Section 1.3.1.2.5 and DOE Enclosure 1 (2009ct). (b)(5)

(b)(5)

Summary

(b)(5)

2.2.1.3.6.3.4 Ambient and Thermal Seepage Models

This section contains the NRC staff review of DOE's model and results for water seeping into drifts. Seepage into drifts encompasses a subset of processes in the unsaturated flow system that occurs in the vicinity of the drift wall. DOE described seepage as a component of the second feature, the unsaturated zone above the repository, within the Upper Natural Barrier (SAR Section 2.1.2.1). DOE considered seepage (SAR Section 2.3.3) separately from unsaturated zone flow (SAR Section 2.3.2) because of the smaller scale of analysis needed for the processes important for seepage and, consequently, the need for a different set of data and models to produce results for use in the performance assessment.

DOE strictly defined seepage as liquid water that drips from the drift ceiling and thus could potentially contact engineered barrier components. Two primary processes provide barrier capability in DOE's seepage model: capillary diversion of liquid water around large openings (drifts in this case) and vaporization in the host rock that creates a dry zone around the drifts (SAR Section 2.1.2.1). Capillary forces may make drifts barriers to flow by inducing water to laterally flow (divert) around the large opening. During the thermal period, the vaporization barrier refers to the boiling of water in the host rock and migration of the resultant vapor to locations away from the heat source. In the DOE abstraction, the resultant creation of a dryout zone surrounding a drift leads to liquid flux elimination at the drift wall.

Three inputs are provided to the seepage abstraction from other areas of the natural systems. First, MSTHM passes the distribution of percolation rates across the repository to the seepage abstraction (SAR Section 2.3.5.4.1). The values used are consistent with those from the ambient, site-scale unsaturated zone model (SAR Section 2.3.2). Second, MSTHM passes the temperature history for the drift wall to the seepage abstraction (SAR Section 2.3.5.4.1). Third, the thermal-mechanical model abstraction (SAR Section 2.3.4) passes the accumulated amount of rubble to the seepage abstraction, which uses it to reflect the degradation state of drift openings for seepage calculations.

The DOE seepage abstraction passes two outputs to the EBS models: the seepage rate and the fraction of drift segments where liquid water seeps into drifts. Drift segments can be thought of as waste package locations. The total dripping flux (SAR Section 2.3.3), which is the sum of the seepage and condensation flux (SAR Section 2.3.5.4.2), is the flux of liquid water leaving the drift wall and contacting engineered components. NRC staff reviews DOE estimates of condensation flux in SER Section 2.2.1.3.6.3.5.

In its review of the DOE seepage estimates, NRC staff considered how and to what extent seepage affects performance. The fraction of waste package locations getting wet and seepage flux in those wet areas are both passed directly from the DOE seepage abstraction model to the EBS models. (b)(5)

(b)(5) When intact, drip shields prevent liquid water from contacting the waste package. In this case, seepage has no influence on the release of radionuclides, and transport rates out of failed waste packages are constrained to the slower diffusive rate of radionuclide movement rather than the faster advective rate. When degraded, drip shields do not divert all water away from waste packages. In this case, the EBS models use seepage estimates, which may influence the (i) corrosion of engineered components; (ii) number of waste packages contacted by water; and (iii) dissolution, mobilization, and transport of radionuclides to the unsaturated zone below the drifts. NRC staff reviews these three areas, which include processes and features from the drip shield to the invert/host rock interface, in SER Sections 2.2.1.3.1, 2.2.1.3.3, and 2.2.1.3.4.

Following the risk-informed approach in 10 CFR Part 63 and related guidance (NRC, 2003aa), the remainder of this seepage section focuses on review of the information and bases DOE provided for the (i) development of the ambient seepage abstraction; (ii) capillary diversion for intact drifts; (iii) capillary diversion for degraded drifts; (iv) seepage fraction, which is the fraction of repository that is in the seeping environment; (v) spatial variability of flow; and (vi) thermal seepage.

Development of Ambient Seepage

This section reviews DOE's description of seepage processes, field tests, and measured data and how they are incorporated into the seepage abstraction.

DOE stated that capillary diversion of liquid water around large openings is the dominant seepage process providing barrier capability during the ambient period (SAR Section 2.1.2.1). In the context of seepage, DOE defined the thermal period as the time when the drift wall temperature exceeds 100 °C [212 °F]. Thus, DOE used the ambient seepage model to estimate water flux entering the drift from approximately the first few thousand years through a million years (SAR Section 2.3.3.1).

For ambient seepage, DOE described (i) the theoretical treatment of seepage into circular openings in porous media; (ii) its choice of a fracture-only, stochastic, porous-media continuum seepage model; and (iii) field tests at Yucca Mountain used to calibrate seepage models (SAR Section 2.3.3.1). Because drifts are approximately circular in cross section, DOE drew on the theoretical treatment derived from an analysis in Philip, et al. (1989aa) of water diversion around large circular openings in homogeneous porous media. Because water is more likely to drip from fractures than from matrix, and to simplify the numerical models, DOE developed seepage models that include only the fracture network as the porous media. DOE described field tests at Yucca Mountain and observations from analog sites that illustrated the capability to divert water.

DOE implemented a seepage approach predicated on continuum models based on the Richards equation for granular porous media and the representative element volume assumption. (b)(5)

(b)(5)

(b)(5)

DOE models solve the Richards equation (Richards, 1931aa) for saturated-unsaturated flow through porous materials, with the van Genuchten-Mualem relations describing the capillary pressure and relative liquid permeability in the fracture continuum as a function of liquid saturation (van Genuchten, 1980aa). (b)(5)

(b)(5)

DOE used two separate numerical seepage models: one for calibration to field tests and the other to generate ambient seepage abstraction lookup tables for the performance assessment model. Injection tests at Yucca Mountain, as described in BSC Section 6.2 (2004av), form the basis of the DOE calibrated seepage model that was designed specifically for the injection test domains (SAR Section 2.3.3.2.3.3). The key parameter for estimating seepage is the unsaturated zone property of capillary strength. It is the inverse of the van Genuchten α term (van Genuchten, 1980aa) and reflects the ability of the fracture continuum to offset gravity for water dripping into drifts. DOE conceptually separated percolating water reaching the drift ceiling into (i) water diverted by capillarity, which remains in the host rock, (ii) water dripping from ceiling, which is defined as the seepage flux; and (iii) water entering the drift but not dripping, which includes along-wall flow and evaporation. Because the capillary strength parameter is calibrated from the injection tests, it implicitly includes the effects of evaporation, along-wall flow, and capillary diversion.

The seepage abstraction was developed using the second seepage model that kept the same grid characteristics as the seepage calibration model, but was designed for the geometry of emplacement drifts (SAR Section 2.3.3.2.3.4). DOE used the second seepage model to generate two tables: one for intact drifts and one for collapsed drifts for the seismic modeling cases. These tables covered a wide range of percolation rates, and permeability and capillary strength parameter values. To estimate seepage at any location using the abstraction, DOE sampled capillary strength and permeability from uncertainty distributions (SAR Section 2.3.3.2.4.1) and used a spatially dependent local percolation rate.

Comment (b)(5)

(b)(5)

Comment (b)(5)

Comment (b)(5)

(b)(5)

The local percolation flux input for the seepage lookup table is the product of a sampled flow-focusing factor and the spatially corresponding percolation flux at the base of the PTn in the MSTHM (SAR Section 2.3.5.4.1). DOE used the spatially variable flow-focusing factor to incorporate intermediate-scale heterogeneity (e.g., nonvertical small faults) that might lead to convergence or divergence of flow in the rock layers immediately above drifts. Spatially variable net infiltration and other large-scale heterogeneities from the ambient site-scale unsaturated flow model were propagated to the MSTHM and thus were automatically brought into the seepage abstraction. DOE described intermediate scale as falling between the grid scale of the ambient site-scale unsaturated flow model (approximately on the order of 100 m [330 ft]) and several drift diameters. Spatial variability driven by heterogeneity below the scale of several drift diameters was inherently incorporated into the seepage numerical models used to generate the seepage lookup tables. Flow-focusing factors increased local percolation in some areas and decreased it in other areas, but the flow-focusing factor did not modify the total flux over the entire area.

For the seismic ground motion, seismic fault displacement, and igneous intrusion modeling cases, DOE predicted changes to the drift opening that might lead to changes in seepage rate and distribution. To account for changes in the drift wall caused by seismic events that lead to changes in dripping, DOE utilized the second seepage table for collapsed drifts. The degree of drift degradation controls the switch from the intact to the collapsed seepage table. For lithophysal rocks only, values from both tables are obtained and some intermediate value is calculated on the basis of scaling to the volume of rubble detached from the drift ceiling. For nonlithophysal rocks, accumulated rockfall above a specified threshold causes the seepage to be set equal to the percolation rate. The two seismic modeling cases are treated slightly differently. For the seismic ground motion modeling case, all drifts are shifted to a degraded state. For the seismic fault displacement, only a small number of drifts and waste package sections are affected by the seismic event. As with the seismic scenario for nonlithophysal rocks, the DOE seepage abstraction for the igneous scenario is simplified by neglecting the effect of capillary diversion.

(b)(5)

Capillary Diversion around Intact Drifts

DOE described the effectiveness of the unsaturated zone in the Upper Natural Barrier in terms of two metrics: seepage flux and seepage fraction (SAR Section 2.1.2.1.6). This subsection focuses on the seepage flux, which is calculated as the amount of water percolating through the host rock above the drift that the capillary diversion process does not divert around the drift by capillary diversion process. Capillary strength is the key parameter in the DOE seepage model for estimating the amount of water diverted around drifts, both because of the sensitivity of seepage estimates to this input parameter and because of the uncertainty in estimating representative values of this parameter. Percolating water (i) drips from the drift ceiling (seepage); (ii) flows laterally around the drift in the host rock; (iii) enters the drift, but flows along

Comment (b)(5)
(b)(5)

the drift wall; or (iv) enters the drift in the gas phase (vapor flux). DOE defined seepage as only the water dripping from the drift ceiling.

NRC staff reviewed the information provided in the SAR to evaluate the adequacy of DOE's estimate of seepage during the ambient period considering data and model support. (b)(5)

(b)(5)

To evaluate seepage rates for performance assessment, NRC staff notes that the 10,000-year and million-year periods may be considered separately. NRC staff evaluates seepage rates for the million-year period in its review of the seepage for degraded drifts in the next subsection.

(b)(5)

(b)(5)

Capillary Diversion for Degraded Drifts

NRC staff reviewed the DOE approach and estimate of seepage flux that account for the disruptive modeling cases of seismic ground motion, seismic fault displacement, and igneous intrusion. In the DOE model, capillary diversion remains the predominant barrier for seismically degraded drifts. This evaluation focuses on seepage in lithophysal units reflecting seismically degraded drifts.

To address drift collapse, DOE developed a collapsed drift seepage table similar to the intact drift seepage lookup table. The table was developed using an enlarged drift opening, with an 11-m [36-ft] instead of 5.5-m [18-ft] diameter. DOE selected a perfectly circular 11-m [36-ft]-diameter drift opening, as outlined in BSC Section 6.6.3 (2004be), based on inspection of simulation results from rock mechanics modeling, as described in BSC Appendix R (2004al).

(b)(5)

A tiered abstraction was used to account for the degree of drift degradation (SAR Section 2.3.3.4.1.1). For nonlithophysal rock, seepage estimates from the intact seepage table were used with estimated accumulated rubble less than 0.5 m^3 per meter of drift length [5.4 ft^3 per foot of drift length]. Otherwise, seepage was set to the percolation rate, including adjustments from the sampled focusing factor. For lithophysal rock, the intact seepage table was used for accumulated rubble less than 5 m^3 per meter of drift length [54 ft^3 per foot of drift length]. For accumulated rubble greater than 60 m^3 per meter of drift length [650 ft^3 per foot of drift length], the collapsed drift seepage table was used. Seepage was interpolated from the entries in both the intact and collapsed drift seepage tables for intermediate values of rubble accumulation (between 5 and 60 m^3 per meter of drift length [54 and 650 ft^3 per foot of drift length]) in lithophysal rock.

(b)(5)

For the million-year period, DOE's model determined disruption by seismic ground motion to be the most important contributor to dose estimates. To evaluate DOE's estimates of seepage rate for the million-year period, NRC staff considered the following:

(b)(5)

(b)(5)

Seepage Fraction

DOE described the effectiveness of the unsaturated zone in the Upper Natural Barrier in terms of two metrics: seepage flux and seepage fraction (SAR Section 2.1.2.1.6). This subsection

focuses on the latter. DOE defined seepage fraction as the number of drift segments where seepage occurs, divided by the total number of drift segments (SAR Section 2.3.3.1). In this context, drift segments can be thought of as waste package locations. (b)(5)

(b)(5)

Conceptually, DOE defined seepage fraction as the area portion of the repository where dripping is expected to occur, using the footprint of a waste package (drift diameter and waste package length) to define a seepage area. Thus, seepage fraction is linked to the number of waste packages that would get wet if no drip shields were present, divided by the total number of waste packages. The remainder of the repository is thus the nonseeping environment, where the flux of liquid water potentially dripping in a waste package location is set to zero in the DOE abstraction.

In the DOE abstraction, seepage fraction is important because releases of radionuclides in the seeping environment are transported by advection. In that portion of the repository where the liquid flux is zero, any released radionuclides are transported by diffusive processes out of the waste package, which are slow compared to advective transport rates. Releases in the nonseeping environment rely on transport by diffusion along stagnant water films. Therefore, determination of the threshold at which seepage occurs can impact radionuclide transport.

DOE used the seepage model to predict seepage at all locations. At locations where calculated seepage was less than some small rate, DOE set the value to zero in the performance assessment. Because the seepage fraction is sensitive to the selection of a value for the seepage threshold, DOE Enclosure 5 (2009ct) described sensitivity analyses showing that reducing the seepage threshold value to zero led to a negligible change in performance.

In the abstraction, seepage fraction is fixed at a constant value for any particular TSPA realization. To determine the constant value, DOE selected the highest calculated seepage fraction that would occur at any time during the simulation period. This value of seepage fraction was then applied throughout the simulation. Separate TSPA realizations were run for the 10,000-year (using a 20,000-year simulation period) and million-year calculations. DOE provided average values for TSPA realizations in SAR Tables 2.1-6 through 2.1-9. DOE estimated an average seepage fraction of 0.10 for the first 10,000 years when seismic and igneous scenarios do not influence seepage. Similarly, DOE estimated an average seepage fraction of 0.69 for the million-year period when the seismic ground modeling case is the dominant dose contributor. Igneous intrusion and seismic fault displacement scenarios do not influence the seepage fraction used in the million-year calculation, because (i) the abstraction for igneous intrusion sets seepage fraction to one, but probability is low for any particular realization and (ii) seismic fault displacement only affects a small number of drifts.

(b)(5)

(b)(5)

(b)(5)

Comment (b)(5)

(b)(5)

Comment (b)(5)

(b)(5)

Representation of Spatial Variability

NRC reviewed the representation and propagation of spatial variability across the repository to determine whether DOE's model underestimated seepage. DOE incorporated spatial variability at several levels in developing its seepage results for performance assessment, including (i) integration of variability from upstream model results, (ii) variability of permeability and capillary strength in the seepage model, (iii) incorporation of a flow-focusing factor, and (iv) abstraction of spatial variability for performance assessment. The key aspect for NRC staff's evaluation of adequacy of spatial variability reflected in the performance assessment is the upscaling of results to five percolation bins for the entire repository

DOE incorporated spatial variability in the seepage by

- Integrating aspects of spatial variability related to net infiltration and large-scale heterogeneities from the ambient site-scale unsaturated-flow model (and propagated to the MSTHM) directly into the seepage model through the input of percolation distribution across the repository. This aspect of variability is evaluated in SER Section 2.2.1.3.6.3.2.

- Incorporating spatial variability and uncertainty in permeability and capillary strength directly into the seepage model used to create the seepage lookup tables. This incorporated variability at the scale of several drift diameters. Permeability was stochastically varied across the seepage model grid. Capillary strength was treated as an upscaled parameter for the model domain.
- Incorporating a flow-focusing factor in the seepage abstraction that addressed the possibility of convergence or divergence of flow in the rock layers above drifts. The flow-focusing factor represents intermediate-scale heterogeneity, which DOE described as falling between the grid scale of the ambient site-scale unsaturated flow model (approximately on the order of 100 m [330 ft]) and several drift diameters (seepage model grid). Flow-focusing factors increased local percolation in some areas and decreased it in other areas, but the total flux over the entire area remained constant in the DOE performance assessment. The resulting values of flow-focusing factors reflect spatial variability and range from 0.116 to 5.016, as outlined in SNL Section 6.6.5.2.3 (2007bk). To provide confidence in estimates of the distribution of flow-focusing factors, DOE performed additional modeling exercises using different assumptions for calculating the focusing factor (SAR Section 2.3.3.2.3.7.6). Results of alternative flow-focusing distributions led DOE to use a narrower range for the distribution of flow-focusing factors.
- Using five percolation bins, and thus five seepage histories, to address spatial variability in the performance assessment. The use of average seepage histories for a percolation bin represents an upscaling of spatial variability.

(b)(5)

(b)(5) DOE used five percolation bins to separate the repository into areas of similar percolation rates. The areas of any one bin are not necessarily contiguous. The binning of percolation rates roughly ensured spatial continuity of flow zones above and below the repository (i.e., high percolation and thus high seepage zones correspond with high flow zones for transport below the repository). DOE Enclosure 2 (2009bo) compared calculated release results using the five percolation flux bins with results using the 3,264 locations. The analysis demonstrated that the two approaches have similar time histories of radionuclide release, but the bin approach tended to estimate larger repository-wide cumulative release of radionuclide mass to the lower unsaturated zone by the end of regulatory periods of interest (i.e., 10,000 and 1 million years). (b)(5)

(b)(5)

Thermal Seepage

DOE described two important features created by the thermal pulse that affect seepage into drifts: the dryout zone around a drift and a reflux zone at the outer edge of the dryout zone. DOE's abstraction for thermal seepage sets seepage to zero for drift wall temperatures exceeding 100 °C [212 °F]. This temperature threshold for seepage is the focus of NRC staff's evaluation of thermal seepage in the following paragraphs. NRC staff reviewed the description of features and processes incorporated into the conceptual and numerical models that DOE used to develop the seepage threshold of thermal seepage. Considering uncertainty derived from observations used to develop the thermal seepage abstraction, staff focused its evaluation on the impact to performance.

DOE described the predominant seepage barrier capability for the thermal period as the elimination of liquid flux at the drift wall due to the dryout zone. The applicant referred to this as the vaporization barrier (SAR Section 2.1.2.1.6.2). Flow diversion due to capillary forces (capillary diversion) remains a relevant process at all temperatures. DOE indicated that this vapor barrier would eliminate liquid water reaching the drift wall at temperatures exceeding 100 °C [212 °F] (SAR Section 2.3.3.4). In the DOE thermohydrological characterization, two-phase flow (liquid and vapor) in the host rock occurs at the outer edge of the dryout zone. Referred to as the reflux zone or heat pipe, because of increased heat transfer, evaporated liquid water rises and condenses in a continuous cycle. This zone of elevated liquid saturation above the dryout zone can serve as a supply of water added to the local percolation that potentially may breach the dryout zone as focused flow in large fractures, possibly reaching the drift wall and dripping into the drift.

DOE separated the thermal evolution into three regimes: dryout, transition, and low temperature (SAR Section 2.3.5.4.1.1.3). DOE asserted that no water enters the drift during the dryout period, and seepage may occur during the transition period and continue into the lower temperature period transitioning to ambient temperature conditions. The applicant defined the dryout period as the time when drift wall temperatures are estimated to exceed 100 °C [212 °F]. Whereas DOE eliminated seepage into drifts at a threshold value of 100 °C [212 °F] for intact and partially degraded drifts, no threshold was implemented for fully collapsed drifts in the seismic scenario. Drift wall temperature is provided to the thermal seepage abstraction from the MSTHM, which incorporates host rock heat transport, dryout, and rewetting (presented in SAR Section 2.3.5.4; reviewed by NRC staff in SER Section 2.2.1.3.6.3.3).

DOE derived the seepage threshold value of 100 °C [212 °F] from process-level thermohydrological modeling exercises to evaluate the possibility of preferential flow breaching the dryout zone under different realistic and bounding flow conditions. DOE described the thermal seepage model as a dual-continuum (matrix and fracture) representation with coupled heat and mass transport. The model necessarily uses a different property set than that used for the fracture-only continuum models for ambient seepage. DOE assumed that hydrologic properties need not incorporate the effect of thermal-mechanical and thermal-chemical processes. This assumption is based on results of DOE's thermal-mechanical and thermal-hydrological-chemical modeling of the heated field tests, which suggest that changes to the flow patterns are smaller than the variability and uncertainty already considered for seepage. In addition, DOE indicated these changes may be transient and likely would disappear with the decay of the thermal pulse. Generally, the modeling exercises included pulses of water applied to a single fracture and assessment of whether the pulse would evaporate before reaching the drift ceiling. Thermal aspects of the numerical model were supported by field and laboratory

Comment (b)(5)

(b)(5)

observations from thermal tests DOE performed. (b)(5)

(b)(5)

(b)(5)

DOE stated that the value of 100 °C [212 °F] for the thermal seepage threshold temperature at the drift wall, being several degrees above the ambient boiling point (96.3 °C [205 °F]), accounts for modeling uncertainties and the possibility of a heat pipe occurring near the drift wall (SAR Section 2.3.3.3.4). (b)(5)

(b)(5)

(b)(5)

(b)(5)

DOE Enclosure 7

(2009bo) provided information on drip shield integrity during the thermal period and noted that intact drip shields will divert any dripping water away from waste packages. (b)(5)

(b)(5)

Summary

(b)(5)

(b)(5)

2.2.1.3.6.3.5 In-Drift Convection and Moisture Redistribution

This section contains NRC staff evaluation of DOE models, data, and results representing in-drift convection and moisture redistribution. Condensation flux, which results from moisture redistribution via vapor movement, is added to the seepage flux to obtain the total flux of water that may reach the engineered barrier components.

In SAR Section 2.3.5.4.2.1 and SNL Section 6.1 (2007b), DOE described in-drift convection and moisture redistribution as driven by temperature differences between the waste package, drift wall, and other engineered components. In the DOE conceptual model, decay heat from emplaced waste will create large temperature differences, both radially and axially within a drift. The temperature differences will produce buoyancy-driven natural convective flow of air inside the drift opening that will increase heat transfer and redistribute moisture. Convective air flow will cause water evaporation at warmer locations in the host rock and subsequent transport by in-drift convection to cooler locations where it may condense on cooler surfaces. DOE described the ensemble of evaporation, convective moisture redistribution, and condensation on cooler surfaces inside the drift as the cold trap phenomenon.

The in-drift convection and condensation models provide two outputs. First, the convection model provides support for the effective thermal conductivity used in the thermohydrological model, reviewed in SER Section 2.2.1.3.6.3.3. Second, the condensation model, using dispersion coefficients calculated from the convection model, provides probability and flux of condensation to performance assessment. Condensation is added to the dripping flux to obtain a total seepage flux entering drifts. Condensation is linked to DOE's abstraction for chemistry of liquid water contacting engineered barrier components (reviewed in SER Section 2.2.1.3.3) and to flux of water in the invert, which influences radionuclide transport (reviewed in SER Section 2.2.1.3.4).

The NRC staff evaluation of the convection and condensation models and results are divided into two parts. The following two subsections contain NRC staff's evaluation of (i) in-drift heat transfer and convection and (ii) moisture redistribution and condensation.

2.2.1.3.6.3.5.1 In-Drift Heat Transfer and Convection

NRC staff reviews the DOE conceptual model for in-drift heat transfer and implementation of the numerical model in this section. The review considers the adequacy of the heat transfer model to estimate representative dispersion coefficients and effective thermal conductivity.

In-drift heat exchange processes involve conduction, convection, radiation, and phase-change (latent) heat transfer (SAR Section 2.3.5.4.2.3.1). Heat transfer processes reduce temperature differences created by emplacing heated waste packages in a drift (SAR Section 2.3.5.4.2.3). Though the heat transfer model generally will be referred to here as the convection model,

radiative and conductive heat transfer processes are also included in the applicant's model and analyses.

DOE implemented the convection model using the commercial computational fluid dynamics solver FLUENT®. (b)(5) DOE set up FLUENT® to solve the steady-state form of the Navier-Stokes equation over a highly discretized grid for selected times during the thermal pulse. DOE models incorporate, as appropriate, the complex arrangement of engineered components and take advantage of vertical axial symmetry to reduce computational effort. Radiation and conduction are included, but latent heat transfer is excluded because DOE demonstrated in SNL Sections 6.3.7.2.4 and 6.3.5.1.2 (2007b1) it does not significantly affect overall heat transfer and convection. (b)(5)

(b)(5)

(b)(5)

(b)(5) DOE Sections 6.1 and 6.2 (2007b1) used numerical models at local and drift scales to represent heat transfer at scales ranging from large-scale heat transfer along drifts (center to repository edge) to small-scale heat transfer across boundary layers at solid-air interfaces. The DOE local-scale model emphasizes cross-sectional patterns in its simulations of temperature gradients between the waste package, drip shield, and drift wall. The DOE drift scale models address temperature gradients between the hot repository center and cooler edges. Model support was provided by DOE laboratory convection experiments and other experiments in the general literature using similar geometries (Kuehn and Goldstein, 1978aa).

(b)(5)

In its two- and three-dimensional convection models, DOE used dimensions and physical properties of waste packages, drip shield, invert, and heat loads consistent with upstream models, as shown in SAR Sections 2.3.5.4.2.2 and 1.3.2 and SNL Section 4.1 (2007b1), and used values for physical properties of fluids and solids derived from standard thermal textbooks (i.e., Incropera and DeWitt, 1996aa; Kreith and Bohn, 2001aa). DOE assumed that convection is based on pure air (i.e., without water vapor) and demonstrated that this assumption would slightly underestimate in-drift vapor transport, as outlined in SNL Section 6.1.3.2.1 (2007b1).

(b)(5)

(b)(5) On the basis of this assumption, DOE used a neutrally buoyant tracer gas in the simulations and calculated the dispersion coefficients using the resulting concentration gradients. (b)(5)

(b)(5)

(b)(5)

NRC staff considered DOE's use of the convection model results to estimate dispersion coefficients for the condensation model. DOE stated that dispersion coefficients are dependent on a number of factors, including axial drift wall temperature variation, convective flow pattern, presence of drip shields, and time, as outlined in SNL Section 6.2.7 (2007bl). DOE calculated dispersion coefficients at two locations in the simulated drift and at discrete timesteps during the thermal pulse. DOE addressed uncertainty in the dispersion coefficient using parametric studies and bounding analyses, as described in SNL Sections 6.1.7 and 6.2.7 (2007bl). (b)(5)

(b)(5)

(b)(5)

(b)(5)

DOE computed an effective thermal conductivity from output of the convection model between (i) drip shield and drift wall and (ii) drip shield and waste package, as shown in SNL Table 6.4.7-3 (2007bl). The calculated values supported the Francis, et al. (2003aa) correlations used in the MSTHM submodels, as described in SNL Appendix I[a] (2007aj). (b)(5)

(b)(5)

(b)(5)

2.2.1.3.6.3.5.2 Moisture Redistribution and Condensation

NRC staff reviewed the information DOE presented to support estimates of condensation flux in drifts. DOE described the conceptual, numerical, and abstraction models for moisture transport and condensation in SAR Section 2.3.5.4.2. Treatment of data and model uncertainty was

described in SAR Sections 2.3.5.4.2.2 and 2.3.5.4.2.3.3. Considering the support DOE provided for models and results, NRC focused its evaluation on the consequence of condensation flux on repository performance.

Condensation Approach

This section reviews the DOE description of the conceptual, numerical, and abstracted models used to estimate condensate rate for the performance assessment model.

Moisture redistribution and condensation inside the drift is also referred to as the cold trap process. The process involves water evaporation from hotter locations, convection to cooler locations, and the condensation of vapor on cooler surfaces. DOE considered surface condensation, which requires direct contact of the convecting gas-phase with a cooler surface, but did not provide information on the potential effects of dust or volumetric condensation (Cussler, 1995aa) in its conceptualization. DOE predicted that condensation will only occur on the drift wall because the drift wall will be cooler than the drip shield, waste package, or invert at each axial position along any drift. DOE added condensation flux to the dripping rate to obtain a total seepage rate contacting engineered barrier components and reaching the invert and, thus, affecting advective radionuclide transport rates to the natural system.

Comment (b)(5)

DOE described the evolution of moisture transport and condensate formation using three stages controlled by drift wall temperature (SAR Section 2.3.5.4.2.1). In Stage 1, the initial cooling stage, the drift wall temperature exceeds boiling along the entire length of the emplacement drift. DOE stated that no condensate formation takes place during the initial stage. In Stage 2, the intermediate cooling stage, the drift wall temperature exceeds boiling in most of the drift, but the end of the drift (repository edge) is below the boiling temperature. For the intermediate stage, DOE performed a bounding analysis to calculate condensation flux occurring on codisposal waste packages at cooler locations. In Stage 3, the final cooling stage, the drift wall temperature is below boiling along the entire length of the drift. In the DOE abstraction, condensation occurs at both codisposal and spent nuclear fuel waste package locations, but all condensation ceases at 2,000 years. Results for process-level models for the intermediate and final cooling stages provide the basis for the abstraction model used in the performance assessment.

For the intermediate cooling stage, DOE estimated condensation using a three-dimensional, pillar-scale thermal-hydrological model (SAR Section 2.3.5.4.2.4). This is an alternative conceptual model supporting the thermohydrological results the MSTHM calculated (SAR Section 2.3.5.4.1.3.3; reviewed in SER Section 2.2.1.3.6.3.3). Described as a bounding approach, DOE used a range of dispersion coefficients and percolation values in the three-dimensional, pillar-scale model to determine that condensation occurs on codisposal waste packages, but not on spent nuclear fuel waste packages.

For the final cooling stage, DOE used a one-dimensional analytical moisture transfer model to estimate condensation occurrence and flux when drift wall temperatures along the entire length of the drift are below boiling. The DOE network model calculates quantity of condensate at a given location along the drift (SAR Section 2.3.5.4.2.3.1) for specified percolation rates and thermal input. The one-dimensional model is based on a diffusion-type equation and uses values of dispersion coefficients calculated by the convection model as an effective diffusion-type parameter. Conductive heat transfer in host rock is based on an analytical mountain-scale conduction model, as outlined in SNL Section 6.3.5.1.1 (2007b), and in-drift heat transfer between components is calculated based on correlations derived from simple systems and

reported in open literature (Raithby and Hollands, 1985aa; Kuehn and Goldstein, 1976aa; Burmeister, 1993aa). DOE considered the supply of water for evaporation at drift walls to be bounded by the sum of capillary-pumping flow and local percolation flux intercepted by the emplacement drift footprint. An important design feature integrated into the condensation model is the control parameter that commits DOE to an unheated open length at the ends of drifts, which allows axial convection to convey a portion of the moisture beyond the last waste package before condensation would occur (SAR Section 1.9, Control Parameter Number 01-18, Table 1.9-9).

DOE implements the abstraction of condensation in the performance assessment using a three-step process (SAR Section 2.3.5.4.2.4). First, DOE used the process-level condensation models to generate a set of results for different parametric variations that account for dispersion coefficient, percolation rates, invert assumptions, and temporal variation of heat load. Second, DOE developed a set of regression curves that establishes a functional relationship between percolation flux, probability of condensation, and condensate mass. Third, DOE used the regression curves for each percolation subregion to determine the occurrence (fraction of area) and magnitude of condensation. DOE added condensate flux directly to dripping flux to obtain a total flux of water entering drifts.

In DOE's model, condensation within emplacement drifts would be altered if a disruptive event occurs during the thermal period. The DOE abstraction sets condensation to zero once an igneous intrusion or drift collapse event occurs (SAR Section 2.4.2.3.2.1.12.3), because these processes would fill drifts with rock and substantially reduce air gaps. However, such events have low probability and DOE expects drifts to remain intact throughout the first 2,000 years, as described in DOE Enclosure 7 (2009ct).

(b)(5)

Condensation Results

The DOE condensation model results can be summarized as follows:

- During the intermediate cooling period, all codisposal waste package locations receive condensation dripping from the drift ceiling at rates 8 to 35 times greater than the mean seepage rate [calculated from SAR Table 2.1-11 and DOE Table 7 (2010ai)]. Whereas DOE conservatively applied condensation to all codisposal waste package locations, no spent fuel waste package locations receive any condensation.
- During the final cooling stage (after approximately 1,500 years), mean condensation rates are less than 1 percent of mean seepage rate, and condensation only occurs at a small fraction of locations for both codisposal and spent fuel waste packages, as shown in SAR Tables 2.1-10 and 2.1-11 and DOE Tables 6 and 7 (2010ai).

The average condensation rate in a percolation bin is calculated by multiplying the fraction of waste package locations receiving condensation times the condensation flux rate, which is then added to the seepage rate (SAR Section 2.3.3) rate to obtain a total dripping rate. The presence of intact drip shields keeps water from contacting waste packages.

NRC staff considered two types of information DOE provided to gain confidence in the condensation model and results used in the performance assessment. One, in developing the conceptual model, DOE stated that observations of vapor movement and condensation in response to small thermal gradients in the East-West Cross-Drift infer the importance of the cold trap process in the repository (SAR Section 2.3.5.4.2). (b)(5)

(b)(5)

(b)(5)

(b)(5)

During the first 2,000 years after permanent closure, the presence of the intact drip shield ensures that the condensate will not directly contact waste packages. During this period, DOE asserts that drip shields will be sufficiently warm that any condensation will occur on drift walls, above or away from drip shields. (b)(5)

(b)(5)

(b)(5)

(b)(5)

- Beyond 255,000 years, DOE predicts that drifts will be collapsed (SAR Section 2.1.2.2.6) and axial convection along drifts will no longer occur. (b)(5)

(b)(5)

Summary

(b)(5)	
(b)(5)	Drip
shield performance is evaluated in SER Sections 2.2.1.3.1 and 2.2.1.3.2. (b)(5)	
(b)(5)	

2.2.1.3.6.3.6 Ambient Mountain-Scale Flow—Below the Repository

NRC staff's evaluation of the flow field in the unsaturated zone below the repository considers how the flow magnitudes and patterns affect radionuclide transport. Flow above the repository is evaluated in SER Section 2.2.1.3.6.3.2, and flow below the repository is evaluated in this section. The site-scale unsaturated flow model provides flow fields both above and below the repository for different climates (SAR Section 2.3.2.3). In SER Section 2.2.1.3.6.3.2, NRC staff evaluates the use of site characterization data, development of a conceptual model, calibration procedure, and confidence building exercise and validation for this model. The following factors influence aspects of the ambient site-scale flow fields that are relevant to the flow fields below the repository: (i) the CHn influences flow in the southern and northern portions of the repository footprint, (ii) the active fracture model (AFM) influences the fracture-to-matrix flux, and (iii) the uncertainty of flow fields influences transport. Output of the ambient site-scale flow model (i.e., flow patterns, water saturations, and flow rates) is direct input to the radionuclide transport abstraction, which NRC staff reviews in SER Section 2.2.1.3.7.

Evaluation of the adequacy of flow fields below the repository is separated into three parts: (i) NRC staff reviews the DOE description of the conceptual model for flow below the repository, (ii) NRC staff evaluates information and observations supporting flow features in the southern vitric CHn zone and in the northern zeolitic CHn zone, and (iii) NRC staff evaluates how uncertainty in flow fields can affect repository performance regarding radionuclide transport.

2.2.1.3.6.3.6.1 Flow Model Conceptualization

DOE described aspects of the flow below the repository in SAR Section 2.3.2.2.1.4 and how these aspects are related to the hydrogeologic units (SAR Table 2.3.2-2) below the repository. The hydrogeologic units include

- TSw; welded tuff, dominantly fracture flow
- CHn
 - Calico Hills Formation; nonwelded vitric and zeolitic zones
 - Prow Pass Tuff and top of Bullfrog Tuff, devitrified and zeolitic horizons
- CFu; varied degree of welding
- Fault zones crossing all hydrologic units

DOE described flow in the first layer underlying the repository, the TSw, as occurring dominantly through fractures (SAR Section 2.3.2.2.1.3). DOE assumed steady-state flow was based on dampening of episodic infiltration pulses by the overlying PTn unit (SAR Section 2.3.2.2.1.2; reviewed by NRC staff in SER Section 2.2.1.3.6.3.2). Percolating water moves approximately vertically from the ground surface through the proposed repository to the base of the TSw. Below the TSw, DOE described flow patterns in the CHn that differ markedly between the northern and southern portions of the repository footprint (SAR Section 2.3.2.2.1.4). The CHn is the only unit where lateral variation has been incorporated into the ambient site-scale unsaturated flow model. DOE described portions of the originally vitric CHn layer as altered to zeolites, which strongly modifies hydraulic properties. The distribution of alteration is described as increasing with depth and increasing to the north and east across the repository footprint (SAR Section 2.3.2.2.1.4). Below the southern portion, DOE expects flow in the vitric CHn to be dominated by matrix flow, because matrix permeability is higher than percolation rates. DOE expects little fracture flow where the CHn is unaltered. Below the northern portion, where most of the CHn has been altered to zeolites, perched water occurs in overlying units due to low permeability of the zeolitic tuff. DOE described that perched water affected performance by causing lateral flow to faults and fast vertical flow and transport down to the groundwater table (saturated zone). Because flow through the matrix of vitric CHn units is much slower than flow through fractures and faults, DOE predicted travel times in the southern portion to be much longer than in the northern portion of the repository (SAR Section 2.3.8.1).

(b)(5)

(b)(5)

DOE described these units as layers of devitrified, zeolitic, welded, and nonwelded tuff (SAR Table 2.3.2-2). In SAR Section 2.3.2.2.1.4, DOE noted that these units comprise a small volume of rock above the water table.

(b)(5)

2.2.1.3.6.3.6.2 Flow Features Below Southern and Northern Portions of Repository

NRC staff reviewed the support DOE provided for flow features below the repository that may affect performance. Flow patterns below the repository can be described in terms of water velocity, which together with water saturation is directly tied to transport travel times. Flow patterns can be separated into three horizons starting at the repository and proceeding downward: (i) fracture flow in welded tuffs of the TSw, (ii) influence of nonwelded tuffs of the CHn, and (iii) flow in the variably welded tuffs below the CHn. DOE described flow through the TSw as primarily vertical and rapid because of the pervasive fracture network, but described rock alteration in the underlying CHn as causing different flow patterns in the southern and northern portions of the repository footprint (SAR Section 2.3.2.2.1.4 and supporting documents). In the southern portion, travel times are slow and sorption potential is high due to flow predominantly through the matrix of the unaltered, vitric CHn. This is contrasted with fast travel times for transport in the northern portion of the repository where fracture and fault flows dominate, because the low permeability of the altered, zeolitic CHn led to the formation of perched water. Below the CHn, alternating layers of tuff with differing degrees of welding are host to the present-day and expected future water table.

(b)(5)

Flow in Welded Topopah Spring Tuff

NRC staff reviewed the basis provided for flow patterns through the fracture network of the welded tuffs of the TSW immediately below the repository. The review here focuses on support for the hydrologic properties of the fracture network, including support for the conceptualization and parameterization of the AFM.

DOE utilized air permeability and fracture data (SAR Section 2.3.2.3.3.2) as prior information for calibration of fracture hydrological properties. DOE assumed that fractures follow the van Genuchten–Mualem constitutive relations for saturation, water potential, and relative permeability, adjusted by the AFM. Support for the AFM parameter values is discussed later in this chapter. DOE based fault hydrological properties on air permeability measurements (SAR Section 2.3.2.3.3.3) and integrated these properties into the transition of one-dimensional calibration values to three-dimensional values across the site. DOE did not include sorption on fracture surfaces (SAR Section 2.3.8.1) and represented flow through welded-tuff fractures and faults as fast (e.g., tens to hundreds of years; SAR Figure 2.3.8-49 and DOE Enclosure 6, 2009an). (b)(5)

(b)(5)

Parameterization of the AFM may affect performance because the AFM controls the flux of water from fractures into the surrounding matrix. Increasing the flux of water moving from fractures to matrix increases the movement of radionuclides into the matrix, where slower travel times and increased sorption occurs relative to the fracture continuum. Therefore, NRC staff reviewed the basis and uncertainty of parameter values used for the AFM.

DOE described and implemented the AFM of Liu, et al. (1998aa) in the site-scale unsaturated flow model to capture the effects of gravity-driven fingering flow through a limited number of water-conducting or active fractures. In the site-scale unsaturated zone flow model, the applicant kept layerwise AFM parameters constant in TSPA realizations, but varied the values with infiltration uncertainty scenario, as shown in SAR Tables 2.3.2-8 through 2.3.2-11 and SNL Section 6.5.6 (2008an). DOE estimated the AFM parameters for the three-dimensional model by calibrating one-dimensional flow simulations with field data (SAR Section 2.3.2.4.1.2.3.2). The applicant adjusted the calibrated AFM parameter values to induce perching for model layers with observed perched water, thereby forming a fast pathway for water to flow into faults and bypass the underlying low-permeability and high-sorption units. (b)(5)

(b)(5)

(b)(5)

NRC evaluated the support DOE provided for representative estimates of the AFM parameter values used in performance assessment calculations. (b)(5)

(b)(5)

(b)(5)

(b)(5) DOE used different values and uncertainty distributions for the AFM parameter values for flow and transport simulations. DOE used fixed values of the gamma parameter in the AFM in flow simulations (SAR Tables 2.3.2-8 to 2.3.2-11, 2.3.2-13, and 2.3.2-21 to 2.3.2-24). The applicant, however, treated the same parameter as uncertain in transport simulations by probabilistically sampling from a distribution of values (SAR Section 2.3.8.4.5.2) (b)(5)

(b)(5)

(b)(5) The effect of transport in small-scale fractures of a network is not explicitly addressed in the DOE algorithm, as specifically shown in SNL Equation C-40 (2008a), but the effect is incorporated in the sampling of gamma for transport calculations. NRC staff reviews the distribution of gamma parameter values for transport in SER Section 2.2.1.3.7.3.2.3. (b)(5)

(b)(5)

Influence of CHn in Southern Portion of Repository

DOE described the CHn in the southern portion of the repository as unaltered, though some zeolitic alteration is present and increases with depth. DOE identified the unaltered, or vitric, zones of the CHn as an important component of the Lower Natural Barrier in terms of water travel times and the unit's capability for delaying radionuclide movement (SAR Section 2.1.2.3.1). Because the travel times through the matrix of the vitric CHn are longer than in other units above and below the CHn where fast fracture flow may dominate, transport through the vitric CHn dominates the travel times of the entire sequence of hydrogeologic units below the southern portion of the repository to the water table. Therefore, NRC staff included the uncertainty of the hydrologic properties and the spatial distribution of the vitric CHn in its review.

The applicant characterized flow in the vitric CHn unit as matrix flow dominant (i.e., little or no fracture flow) due to the unit's relatively high matrix permeability and porosity (SAR Section 2.3.2.2.1.4) (b)(5)

(b)(5) NRC staff reviewed observations, measurements, and model-calibrated values for hydrologic properties of the vitric CHn. DOE provided information from boreholes near the repository and from the Busted Butte analog

site. The latter was an experiment DOE performed to support the importance of capillarity and matrix-dominated flow in the CHn vitric tuff using several injection tracer tests (SAR Section 2.3.2.3.2.4). Noting that the CHn at Busted Butte is a distal portion of the CHn found at Yucca Mountain, as described in BSC Appendix H (2004av), DOE provided a lithologic and mineralogic comparison of the CHn near the repository with the units at Busted Butte, but did not provide a hydrologic comparison. Additionally, DOE suggested that the test bed units at Busted Butte may be affected by surficial processes because of their close proximity to the ground surface. (b)(5)

(b)(5)

(b)(5) Calibrated matrix permeability values at Busted Butte vary from one to four orders of magnitude lower, as shown in SNL Tables 7-8, 7-9, 7-13, and 7-14 (2007bj), than those calibrated for the site-scale unsaturated flow model for the vitric CHn unit (SAR Table 2.3.2-3). Because the models for the field experiments are on a smaller scale than the unsaturated zone flow model scale, the difference in calibrated values may be related to scale effects. (b)(5)

Measured values of hydraulic conductivity from Busted Butte, as shown in BSC Table H-3 (2004av), are one to two orders of magnitude larger than the geometric mean of measured hydrologic conductivities values from cores at Yucca Mountain, as shown in Flint Table 7 (1998aa). (b)(5)

(b)(5)

(b)(5)

(b)(5)

DOE indicated there are few available data to constrain the spatial distribution of vitric and zeolitic zones below the repository. As a result, uncertainty about spatial variability of the CHn units (i.e., vitric versus zeolitic) may increase with depth and distance from the repository footprint (SAR Section 2.3.2.3.5.3). In its analysis, DOE incorporated data from surface mapping and 23 boreholes spread in and around Yucca Mountain, as described in BSC Section 6.2.3 (2004bt). Six of these boreholes lie within or near the edge of the repository footprint. (b)(5)

(b)(5)

(b)(5)

(b)(5)

Influence of CHn in Northern Portion of Repository

DOE described released radionuclides in the northern portion of the repository as starting out in the welded units of the TSw; proceeding vertically, predominantly in the fracture system to perched water above the zeolitic zones of the CHn, predominantly bypassing the low-permeability, high-sorptivity zeolitic zones by rapidly moving laterally to faults in the perched water body; and finally rapidly moving vertically within faults to the water table (SAR Section 2.3.2.2.1.4). DOE did not include sorption on fracture surfaces (SAR Section 2.3.8.1) and represented flow through welded-tuff fractures and faults as fast (e.g., tens to hundreds of years; SAR Figure 2.3.8-49 and DOE Enclosure 6, 2009a). NRC reviewed the DOE treatment of model uncertainty for (i) perching of water and (ii) extent of the zeolitic unit that causes the perching to ensure that the DOE representations did not lead to underestimates of dose.

DOE implemented a permeability-barrier conceptual model for perched water (SAR Section 2.3.2.4.1.2.4.4) in which sufficient local percolation flux, poorly interconnected and conductive fractures, and locally low vertical and horizontal permeabilities contribute to the occurrence of perched water. DOE incorporated the conceptual model for flow in the perched water by adjusting the calibrated model parameters for the layers where perched water has been observed in the field. (b)(5)

(b)(5)

DOE constrained the spatial extent zeolitic CHn, and thus perched water, in the site-scale unsaturated zone model using borehole data. Through hydraulic testing and interpretation of borehole observations, DOE suggested that the volume and extent of the perched-water bodies at Yucca Mountain may vary greatly (SAR Section 2.3.2.2.2.4). The extent of perched water is inversely related to the extent of vitric CHn, which NRC staff reviews in the previous subsection on the southern portion of the repository. (b)(5)

(b)(5)

(b)(5)

Flow Patterns Below the CHn

DOE provided sparse observations related to hydrologic properties and flow patterns below the CHn in the northern and southern repository areas traversing the Prow Pass, Bullfrog, and CFu Tufts. In its review of flow patterns below the CHn unit, NRC staff considered uncertainty caused by the sparseness of observations and data.

NRC staff reviewed the hydrologic characterization of layers below the CHn. To estimate the hydrologic properties of the lowermost layers to calibrate the site-scale unsaturated flow model, DOE supplemented the available information and observations with analog data from the PTn and TSw (SAR Section 2.3.2.3.5.3). (b)(5)

(b)(5)

NRC staff considered model support for the spatial distribution of zones of focused flow potentially provided by the pattern of water table temperatures. (b)(5)

(b)(5)

(b)(5) Alternative interpolations of water table temperature were presented in the SAR Figure 2.3.2-37, SNL Figure 6.3.1-7 (2008ag), and Sass, et al. (1988aa). Because the distribution of water table temperatures in any of the interpolations was not consistent with the large-scale spatial distribution of percolation in the DOE site-scale unsaturated zone flow model, DOE suggested that water table temperature was not a sensitive indicator to percolation rate, as outlined in DOE Enclosure 1 (2009cy). DOE suggested that multiple factors make it difficult to interpret potential relationships between temperature and percolation, including (i) uncertainty in ground surface temperature, (ii) thickness of the unsaturated zone, (iii) uncertainty in thermal conductivity of unsaturated zone units, (iv) influence of vertical groundwater flow in the saturated zone, and (v) uncertainty in the deep subsurface heat flux.

(b)(5)

(b)(5) DOE demonstrated with sensitivity analyses that the exact locations of radionuclide release from the unsaturated zone to the saturated zone are not important (SAR Section 2.3.2.3.5.4). (b)(5)

(b)(5)

NRC staff reviewed water table position because of its effect on unsaturated zone transport length. Future, wetter climates affect flow below the repository in two ways: increased flow rates and water table rise. The increased percolation rates during future climates are evaluated as part of the site-scale unsaturated flow model in SER Section 2.2.1.3.6.3.2. The present-day

water table is located in the dipping layers of the Prow Pass, Bullfrog, and Crater Flat Tuffs. Mineralogical and geochemical evidence suggests the water table occurred at higher elevations in the past. DOE found no evidence supporting higher perched water elevations underneath the repository. (b)(5)

DOE accounted for water table rise under future, wetter climate conditions by raising the location to a uniform 850-m [2,790-ft] elevation, which is approximately 120 m [394 ft] higher than the present-day estimate for the water table position. DOE stated (SAR Section 2.3.2.5.2) this rise in the water table is significantly greater than indicated by geologic evidence, which includes mineralogic alteration and isotopic ratios in secondary minerals, and flow modeling exercises with increased precipitation and recharge. (b)(5)

(b)(5)

2.2.1.3.6.3.6.3 Adequacy of Flow Fields for Transport

NRC staff reviewed the effect of uncertainty of flow fields on transport through the unsaturated zone. DOE passed the flow fields below the repository to the Unsaturated Zone Transport (SAR Section 2.3.8.5) portion of the DOE performance assessment. Overall, DOE considered advection to be the most important transport process in the unsaturated zone because the rate of water movement in the unsaturated zone largely controls radionuclide travel times, as outlined in SNL Section 6.1.2.1 (2007b) and DOE Enclosure 6 (2009a). DOE also identified matrix diffusion and sorption as highly important for moderately to strongly sorbing radionuclides, particularly radionuclides with a short half-life that pass through a matrix unit, as described in DOE Enclosure 6 (2009a). DOE identified matrix diffusion and sorption as more important in the southern half of the repository because of the control from matrix transport in the CHn vitric facies, and more important for the 10,000-year period than the million-year period, as outlined in DOE Enclosure 6 (2009a). On the basis of these DOE assessments, the NRC staff focuses its review on the flow fields with respect to transport for nonsorbing and moderately to strongly sorbing dissolved radionuclides. NRC staff evaluates the repository performance with respect to unsaturated zone transport, including colloidal transport, in SER Section 2.2.1.3.7.3.2.4.

Flow path differences between the northern and southern portions of the repository influence the travel times of nonsorbing and sorbing radionuclides. DOE provided model results (SAR Figures 2.3.8-36 and 2.3.8-49) that exhibited the presence of three predominant types of transport pathways. (b)(5)

(b)(5)

(b)(5) The DOE ambient site-scale unsaturated zone model includes perching below the repository horizon in the northern half of the repository. In the DOE implementation, perching diverts fracture waters into faults and thereby creates a large difference in travel times for the northern and southern halves of the repository.

NRC staff first considered nonsorbing radionuclides. In DOE Enclosure 1 (2009a), several single-realization simulations with 30th and 50th percentile infiltration maps demonstrated transport properties for the unsaturated zone. Using DOE Enclosure 1, Table 4 (2009a), DOE calculated that total activity released from the unsaturated zone in the first 10,000 years after

Comment (b)(5)

(b)(5)

closure is 73 percent of total activity released from the EBS for Tc-99 (a nonsorbing radionuclide) in the northern half of the proposed repository and 78 percent in the southern half under the seismic ground motion scenario. DOE calculated that total Tc-99 activity released from the unsaturated zone in the first million years after closure is at least 98 percent of that released from the EBS for the igneous intrusion and seismic ground motion scenarios, regardless of release location.

(b)(5)

The NRC staff next evaluates the extent to which the unsaturated zone flow fields affect the applicant's performance assessment with respect to moderately to strongly sorbing radionuclides. DOE classified the porous matrix as either zeolitic, devitrified, or vitric and assigned all three classifications with sorptive capability. DOE explained that sorbing radionuclides are preferentially released to the fracture system as a result of sorption within the invert, as outlined in DOE Enclosure 1, Section 1 (2009am). As a result of the DOE release and flow models, which route fracture waters through the perched zone and into faults draining to the water table in the northern half of the repository, sorbing radionuclides predominantly bypass the matrix in the north. In the DOE flow model, both matrix and fracture waters pass into the matrix of the permeable and sorbing CHn unit in the south.

(b)(5)

2.2.1.3.6.3.6.4

Summary

(b)(5)

2.2.1.3.6.4

Evaluation Findings

(b)(5)

(b)(5)

(b)(5)

(b)(5)

2.2.1.3.6.5 References

Basagaoglu H., S. Succi, C. Manepally, R. Fedors, and D. Wyrick. 2009aa. "Sensitivity of the Active Fracture Model Parameter to Fracture Network Orientation and Injection Scenarios." *Hydrogeology Journal*. Vol. 17. pp. 1,347–1,358.

Basagaoglu, H., K. Das, R. Fedors, R. Green, C. Manepally, S. Painter, O. Pensado, S. Stothoff, J. Winterle, and D. Wyrick. 2007aa. "Seepage Workshop Report." ML072980846, ML172980851, and ML072980850. San Antonio, Texas: CNWRA.

Beven, K. and A. Binley. 1992aa. "The Future of Distributed Models: Model Calibration and Uncertainty Prediction." *Hydrological Processes*. Vol. 6, No. 3. pp. 279–298.

BSC. 2004al. "Drift Degradation Analysis." ANL-EBS-MD-000027. Rev. 03. ACN 001, ACN 002, ACN 003, ERD 01. Las Vegas, Nevada: Bechtel SAIC Company, LLC.

BSC. 2004av. "In-Situ Field Testing of Processes." ANL-NBS-HS-000005. Rev. 03. ACN 01, ACN 02, ERD 01. Las Vegas, Nevada: Bechtel SAIC Company, LLC.

BSC. 2004be. "Seepage Model for PA Including Drift Collapse." MDL-NBS-HS-000002. Rev. 3. ACN 001. Las Vegas, Nevada: Bechtel SAIC Company, LLC.

BSC. 2004bf. "Thermal Conductivity of the Potential Repository Horizon." MDL-NBS-GS-000005. Rev. 01. Las Vegas, Nevada: Bechtel SAIC Company, LLC.

BSC. 2004bt. "Mineralogic Model (MM3.0) Report." MDL-NBS-GS-000003. Rev. 01. Las Vegas, Nevada: Bechtel SAIC Company, LLC.

Burmeister, L.C. 1993aa. *Convective Heat Transfer*. 2nd Edition. New York City, New York: John Wiley & Sons, Inc.

Cussler, E.L. 1995aa. *Diffusion Mass Transfer in Fluid Systems*. 2nd Edition. New York City, New York: Cambridge University Press.

Das, K., S. Green, and C. Manepally. 2007aa. "FLOW-3D YMUZ2 Version 1.0 Users Manual." ML073030286. San Antonio, Texas: CNWRA.

DOE. 2010ai. "Yucca Mountain—Supplemental Response to Request for Additional Information Regarding License Application (Safety Analysis Report Section 2.3.1), Safety Evaluation Report Vol. 3, Chapter 2.2.1.3.5, Set 1 and (Safety Analysis Report Sections 2.3.2 and 2.3.3), Safety Evaluation Report Vol. 3, Chapter 2.2.1.3.6, Set 1." Letter (February 2) J.R. Williams to J.H. Sulima (NRC). ML100340034. Washington, DC: DOE, Office of Technical Management.

DOE. 2009am. "Yucca Mountain—Response to Request for Additional Information Regarding License Application (Safety Analysis Report Section 2.3.8), Safety Evaluation Report Vol. 3, Chapter 2.2.1.3.7, Set 1." Letter (February 9) J.R. Williams to J.H. Sulima (NRC). ML090410352. Washington, DC: DOE, Office of Technical Management.

DOE. 2009an. "Yucca Mountain—Response to Request for Additional Information Regarding License Application (Safety Analysis Report Section 2.1), Safety Evaluation Report Vol. 3, Chapter 2.2.1.1, Set 1." Letter (February 6) J.R. Williams to J.H. Sulima (NRC). ML090400455. Washington, DC: DOE, Office of Technical Management.

DOE. 2009av. DOE/RW-0573, "Yucca Mountain Repository License Application." Rev. 1. ML090700817. Las Vegas, Nevada: DOE, Office of Civilian Radioactive Waste Management.

DOE. 2009bo. "Yucca Mountain—Response to Request for Additional Information Regarding License Application (Safety Analysis Report Sections 2.3.2 and 2.3.3), Safety Evaluation Report Vol. 3, Chapter 2.2.1.3.6, Set 1." Letter (June 1) J.R. Williams to J.H. Sulima (NRC). ML091530403. Washington, DC: DOE, Office of Technical Management.

DOE. 2009cb. "Yucca Mountain—Response to Request for Additional Information Regarding License Application (Safety Analysis Report Section 2.2, Table 2.2-5), Safety Evaluation Report Vol. 3, Chapter 2.2.1.2.1, Set 5." Letter (June 5) J.R. Williams to J.H. Sulima (NRC). ML091590581. Washington, DC: DOE, Office of Technical Management.

DOE. 2009cc. "Yucca Mountain—Supplemental Response to Request for Additional Information Regarding License Application (Safety Analysis Report Section 2.2, Table 2.2-5), Safety Evaluation Report Vol. 3, Chapter 2.2.1.2.1, Set 5." Letter (August 12) J.R. Williams to J.H. Sulima (NRC). ML092250006. Washington, DC: DOE, Office of Technical Management.

DOE. 2009ct. "Yucca Mountain—Response to Request for Additional Information Regarding License Application (Safety Analysis Report Sections 2.3.2, 2.3.3, and 2.3.5), Safety Evaluation Report Vol. 3, Chapter 2.2.1.3.6, Set 2." Letter (July 20) J.R. Williams to J.H. Sulima (NRC). ML0920204130 and ML0920204141. Washington, DC: DOE, Office of Technical Management.

DOE. 2009cx. "Yucca Mountain—Supplemental Response to Request for Additional Information Regarding License Application (Safety Analysis Report Sections 2.3.2 and 2.3.3), Safety Evaluation Report Vol. 3, Chapter 2.2.1.3.6, Set 1." Letter (December 14) J.R. Williams to J.H. Sulima (NRC). ML093490398. Washington, DC: DOE, Office of Technical Management.

DOE. 2009cy. "Yucca Mountain—Response to Request for Additional Information Regarding License Application (Safety Analysis Report Sections 2.3.2, 2.3.3, and 2.3.5), Safety Evaluation Report Vol. 3, Chapter 2.2.1.3.6, Set 2." Letter (August 3) J.R. Williams to J.H. Sulima (NRC). ML092160370 and ML092160371. Washington, DC: DOE, Office of Technical Management.

DOE. 2008ab. DOE/RW-0573, "Yucca Mountain Repository License Application." Rev. 0. ML081560400. Las Vegas, Nevada: DOE, Office of Civilian Radioactive Waste Management.

Fedors, R., S. Green, D. Walters, G. Adams, D. Farrell, and S. Svedeman. 2004aa. "Temperature and Relative Humidity Along Heated Drifts With and Without Drift Degradation." ML042160472. San Antonio, Texas: CNWRA.

Flint, L.E. 1998aa. "Characterization of Hydrogeologic Units Using Matrix Properties, Yucca Mountain, Nevada." Water-Resources Investigation Report 97-4243. Denver, Colorado: U.S. Geological Survey.

Francis, N.D., Jr., S.W. Webb, M.T. Itamura, and D.L. James. 2003aa. "CFD Modeling of Natural Convection Heat Transfer and Fluid Flow in Yucca Mountain Project (YMP)." SAND 2002-4179. ACC:MOL20030906.0165. Albuquerque, New Mexico: Sandia National Laboratories.

Ghezzehei, T.A. 2004aa. "Constraints for Flow Regimes on Smooth Fracture Surfaces." doi:10.1029/2004WR003164. *Water Resources Research*. Vol. 40. p. W11503.

Green, S. and C. Manepally. 2006aa. "Software Validation Report for FLOW3D® Version 9.0." ML063050289. San Antonio, Texas: CNWRA.

Green, R.T., C. Manepally, R.W. Fedors, and M.M. Roberts. 2008aa. "Examination of Thermal Refluxing in *In-Situ* Heater Tests." ML083030097. San Antonio, Texas: CNWRA.

Incropera, F.P. and D.P. DeWitt. 2002aa. *Fundamentals of Heat and Mass Transfer*. 5th Edition. New York City, New York: John Wiley & Sons, Inc.

Incropera, F.P. and D.P. DeWitt. 1996aa. *Fundamentals of Heat and Mass Transfer*. 4th Edition. New York City, New York: John Wiley & Sons, Inc.

Kreith, F. and M.S. Bohn. 2001aa. *Principles of Heat Transfer*. 6th Edition. Pacific Grove, California: Brooks/Cole.

Kuehn, T.H. and R.J. Goldstein. 1978aa. "An Experimental Study of Natural Convection Heat Transfer in Concentric and Eccentric Horizontal Cylindrical Annuli." *Journal of Heat Transfer*. Vol. 100. pp. 635–640.

Kuehn, T.H. and R.J. Goldstein. 1976aa. "An Experimental Study and Theoretical Study of Natural Convection in the Annulus Between Horizontal Concentric Cylinders." *Journal of Fluid Mechanics*. Vol. 74, Part 4. pp. 695–719.

Leslie, B., C. Grossman, and J. Durham. 2007aa. "Total-system Performance Assessment (TPA) Version 5.1 Module Descriptions and User Guide." Rev. 1. ML072710060. San Antonio, Texas: CNWRA.

Liu, H.H., C. Doughty, and G.S. Bodvarsson. 1998aa. "An Active Fracture Model for Unsaturated Flow and Transport in Fractured Rocks." *Water Resources Research*. Vol. 34. pp. 2,633–2,646.

Manepally, C., S. Green, F. Viana, and R. Fedors. 2007ab. "Evaluation of In-Drift Heat Transfer Processes." ML071070508. San Antonio, Texas: CNWRA.

Manepally, C., A. Sun, R. Fedors, and D. Farrell. 2004aa. "Drift-Scale Thermohydrological Process Modeling—In-Drift Heat Transfer and Drift Degradation." CNWRA 2004-05. ML042160447. San Antonio, Texas: CNWRA.

NRC. 2009ab. "Division of High-Level Waste Repository Safety Director's Policy and Procedure Letter 14: Application of YMRP for Review Under Revised Part 63." Published March 13, 2009. ML090850014. Washington, DC: NRC.

NRC. 2005aa. NUREG-1762, "Integrated Issue Resolution Status Report." Rev. 1. ML051360241. Washington, DC: NRC.

NRC. 2003aa. NUREG-1804, "Yucca Mountain Review Plan—Final Report." Rev. 2. Washington, DC: NRC.

Or, D., M. Tuller, and R. Fedors. 2005aa. "Seepage Into Drifts and Tunnels in Unsaturated Fractured Rock." doi:10.1029/2004WR003689 *Water Resources Research*. Vol. 41. p. WR05022.

Painter, S., C. Manepally, and D.L. Hughson. 2001aa. "Evaluation of U.S. Department of Energy Thermohydrologic Data and Modeling Status Report." ML043080474. San Antonio, Texas: CNWRA.

Philip, J.R., J.H. Knight, and R.T. Waechter. 1989aa. "Unsaturated Seepage and Subterranean Holes: Conspectus and Exclusion Problem for Circular Cylindrical Cavities." *Water Resources Research*. Vol. 25, No. 1. pp. 16–28.

Raithby, G.D. and K.G.T. Hollands. 1985aa. "Natural Convection." *Handbook of Heat Transfer Fundamentals*. 2nd Edition. W.M. Rohsenow, J.P. Hartnett, and E.N. Ganic, eds. New York City, New York: McGraw-Hill.

Richards, L.A. 1931aa. "Capillary Conduction of Liquids Through Porous Mediums." *Physics*. Vol. 1. pp. 318–333.

Salve, R. and T.J. Kneafsey. 2005aa. "Vapor-Phase Transport in the Near-Drift Environmental at Yucca Mountain." *Water Resources Research*. Vol. 41. p. W01012.

Sass, J.H., A.H. Lachenbruch, W.W. Dudley, Jr., S.S. Priest, and R.J. Munroe. 1988aa. "Temperature, Thermal Conductivity, and Heat Flow Near Yucca Mountain, Nevada: Some Tectonic and Hydrologic Implications." USGS Open-File Report 87-649. Denver, Colorado: U.S. Geological Survey.

SNL. 2008ab. "Features, Events, and Processes for the Total System Performance Assessment: Analyses." ANL-WIS-MD-000027. Rev. 00. ACN 01, ERD 01, ERD 02. Las Vegas, Nevada: Sandia National Laboratories.

SNL. 2008ag. "Total System Performance Assessment Model/Analysis for the License Application." MDL-WIS-PA-000005. Rev. 00. AD 01, ERD 01, ERD 02, ERD 03, ERD 04. Las Vegas, Nevada: Sandia National Laboratories.

SNL. 2008ai. "Postclosure Analysis of the Range of Design Thermal Loadings." ANL-NBS-HS-000057. Rev. 00. ERD 01, ERD 02. Las Vegas, Nevada: Sandia National Laboratories.

SNL. 2008aj. "Multiscale Thermohydrologic Model." ANL-EBS-MD-000049. Rev. 03. ADD 02. Las Vegas, Nevada: Sandia National Laboratories.

SNL. 2008an. "Particle Tracking Model and Abstraction of Transport Processes." MDL-NBS-HS-000020. Rev. 02. ADD 02. Las Vegas Nevada. Sandia National Laboratories.

SNL. 2007az. "Simulation of Net Infiltration for Present-Day and Potential Future Climates." MDL-NBS-HS-000023. Rev. 01. AD 01, ERD 01, ERD 02. Las Vegas, Nevada: Sandia National Laboratories.

SNL. 2007bf. "UZ Flow Models and Submodels." MDL-NBS-HS-000006. Rev. 03. ACN 01, ERD 01, ERD 02, ERD 03. Las Vegas, Nevada: Sandia National Laboratories

SNL. 2007bj. "Radionuclide Transport Models Under Ambient Conditions (U0060)." MDL-NBS-HS-000008. Rev. 02. CAN 002, AD 01. Las Vegas, Nevada: Sandia National Laboratories.

SNL. 2007bk. "Abstraction of Drift Seepage." MDL-NBS-HS-000019. Rev. 01. Las Vegas, Nevada: Sandia National Laboratories.

SNL. 2007bl. "In-Drift Natural Convection and Condensation." MDL-EBS-MD-000001. Rev. 00. ADD 01. Las Vegas, Nevada: Sandia National Laboratories

Stothoff, S.A. 2010aa. "Infiltration and Unsaturated Zone Confirmatory Analyses." Electronic Scientific Notebook 1005E. ML101620418. San Antonio, Texas: CNWRA.

Stothoff, S. and G. Walter. 2007aa. "Long-Term-Average Infiltration at Yucca Mountain, Nevada: Million-Year Estimates." CNWRA Report 09-003. ML072760607. San Antonio, Texas: CNWRA.

van Genuchten, M.Th. 1980aa. "A Closed-Form Equation for Predicting the Hydraulic Conductivity of Unsaturated Soils." *Soil Science Society of America Journal*. Vol. 44. pp. 892-898.

Zhou, Q., H.H. Liu, F.J. Molz, Y. Zhang, and G.S. Bodvarsson. 2007aa. "Field-Scale Effective Matrix Diffusion Coefficient for Fractured Rock: Results From Literature Survey." *Journal of Contaminant Hydrology*. Vol. 93, Nos. 1-4. pp. 161-187.

CHAPTER 10

2.2.1.3.7 Radionuclide Transport in the Unsaturated Zone

2.2.1.3.7.1 Introduction

This chapter provides the U.S. Nuclear Regulatory Commission (NRC) staff's evaluation of the U.S. Department of Energy's (DOE's) representation of radionuclide transport in the unsaturated zone (UZ). This is a key component in DOE's performance assessment for the proposed geologic repository at Yucca Mountain, Nevada, as identified in its Safety Analysis Report (SAR) Figure 2.3-2 (DOE, 2008ab). DOE's performance assessment analysis included the flow of water from precipitation falling on Yucca Mountain, its migration as groundwater through the UZ above and below the repository, and the flow of groundwater in the saturated zone to the accessible environment. Exposure to radionuclides in groundwater extracted by pumping is one of the principal pathways for radiological exposures to the reasonably maximally exposed individual and for releases of radionuclides into the accessible environment. Therefore, the performance assessment analysis included radionuclide transport in the UZ among those model components that significantly affect the timing and magnitude of transport for any radionuclides released from the repository, as required by 10 CFR 63.113 and 63.114(a)(5). In SAR Section 2.3.8, DOE (i) described the features, events, and processes (FEPs) that DOE included to model the transport of radionuclides in groundwater in the UZ below the repository and (ii) provided the technical basis for DOE's implementation (or abstraction)¹ of the UZ transport model in the Total System Performance Assessment (TSPA) model. The NRC staff's evaluation focuses on the following processes, detailed in subsequent sections of this chapter, that DOE included in its SAR Section 2.3.8 as important for radionuclide transport in the UZ: (i) advection, because most of the radionuclide mass is carried through the UZ by water flowing downwards to the water table; (ii) sorption, because sorption in porous media in the southern half of the repository area has the largest overall effect on slowing radionuclide transport in the UZ; (iii) matrix diffusion in fractured rock, because matrix diffusion coupled with sorption slows radionuclide transport in the northern half of the repository area; (iv) colloid-associated transport, because radionuclides attached to colloids may travel relatively unimpeded through the UZ; and (v) radioactive decay and ingrowth, because these processes affect the quantities of radionuclides released from the UZ over time. The NRC staff's review of DOE's technical basis for excluding other FEPs is addressed in the Safety Evaluation Report (SER) Section 2.2.1.2.1 (Scenario Analysis).

DOE's radionuclide transport abstraction for the UZ receives information on the magnitude and patterns of groundwater flow in the UZ and the flux of radionuclides released from the waste forms and engineered barrier systems (EBS). In turn, the UZ radionuclide transport abstraction provides information about the mass flux of radionuclides released to the saturated zone.

2.2.1.3.7.2 Regulatory Requirements

Model abstractions used in the applicant's postclosure performance assessment must meet the regulatory requirements given in 10 CFR 63.114 (Requirements for Performance Assessment) and 63.342 (Limits on Performance Assessment), to support the predictions of compliance for

¹The term "abstraction" is defined as a representation of the essential components of a process model into a suitable form for use in a total system performance assessment. Model abstraction is intended to maximize the use of limited computational resources while allowing a sufficient range of sensitivity and uncertainty analyses.

63.113 (Performance Objectives for the Geologic Repository after Permanent Closure). Specific compliance with 63.113 is reviewed in SER Section 2.2.1.4.1.

The requirements for performance assessment in 10 CFR 63.114 require the applicant to

- Include appropriate data related to the geology, hydrology, and geochemistry of the surface and subsurface from the site and the region surrounding Yucca Mountain
- Account for uncertainty and variability in the parameter values used to model radionuclide transport in the UZ
- Consider alternative conceptual models for radionuclide transport in the UZ
- Provide technical bases for the inclusion of FEPs affecting radionuclide transport in the UZ, including effects of degradation, deterioration, or alteration processes of engineered barriers that would adversely affect performance of the natural barriers, consistent with the limits on performance assessment in 10 CFR 63.342
- Provide technical basis for the models of radionuclide transport in the UZ that in turn provide input or otherwise affect other models and abstractions

10 CFR 63.114(a) considers performance assessment for the initial 10,000 years following permanent closure. 10 CFR 63.114(b) and 63.342 consider the performance assessment methods for the time from 10,000 years through the period of geologic stability, defined in 10 CFR 63.302 as 1 million years following disposal. These sections require that through the period of geologic stability, with specific limitations, the applicant

- Use performance assessment methods consistent with the performance assessment methods used to demonstrate compliance for the initial 10,000 years following permanent closure
- Include in the performance assessment those FEPs used in the performance assessment for the initial 10,000 year period

NRC staff review of the license application follows the guidance laid out in the Yucca Mountain Review Plan (YMRP), NUREG-1804, Section 2.2.1.3.7, Radionuclide Transport in the Unsaturated Zone (NRC, 2003aa), as supplemented by additional guidance for the period beyond 10,000 years after permanent closure (NRC, 2009ab). The acceptance criteria in the Yucca Mountain Review Plan generically follow 10 CFR 63.114(a). Following the guidance, the NRC staff review of the applicant's abstraction of radionuclide transport in the UZ considered five criteria

- System description and model integration are adequate.
- Data are sufficient for model justification.
- Data uncertainty is characterized and propagated through the abstraction.
- Model uncertainty is characterized and propagated through the abstraction.
- Model abstraction output is supported by objective comparisons.

Because 10 CFR Part 63 specifies the use of a risk-informed approach for the review of a license application, the guidance provided by the YMRP, as supplemented by NRC (2009ab) is

followed to the extent reasonable for aspects of radionuclide transport in the UZ important to repository performance. Whereas NRC staff considered all five criteria in their review of information provided by DOE, only aspects that substantively affect results of the performance assessment, as judged by NRC staff, are discussed in this chapter. NRC staff's judgment is based both on risk information provided by DOE, and staff's knowledge, experience, and independent analyses.

2.2.1.3.7.3 Technical Review

The NRC staff reviewed information in SAR Section 2.3.8 and references therein that described how DOE predicted the transport of radionuclides in the UZ below the repository. The NRC staff's technical review focused on how DOE (i) represented transport-related geological, hydrological, and geochemical features of Yucca Mountain in the UZ transport abstraction, (ii) integrated the transport abstraction with other TSPA model components, and (iii) established the technical basis for modeling the major, risk-significant transport processes in DOE's process-level models and in the UZ radionuclide transport abstraction.

2.2.1.3.7.3.1 System Description and Model Framework

DOE used the Yucca Mountain site data in analyzing the downward flow of water in the UZ, through fractures, major faults, and rock matrix from the repository drifts to the water table. DOE used the same analytical framework for its modeling of UZ transport of radionuclides as for its site-scale UZ flow model (SAR Section 2.3.2): a three-dimensional representation of layered volcanic tuff units with specified geological and hydrological properties, in which water and radionuclides move through fractures in the rock, through the rock matrix, and between fractures and matrix. Major faults, which DOE assumed to provide fast transport pathways through the UZ, are represented in the model framework separately by a model with limited fracture-matrix interaction, as documented in Section P21 of SNL (2008ag).

DOE simulated the transport of radionuclides as (1) dissolved species and as (2) attached to mobile, colloid-sized particles. These two modes of transport are subject to various physical and chemical processes that affect radionuclide transport rates. DOE's conceptual model addresses how each of the transport-affecting processes influences the rate at which radionuclides travel through the UZ relative to the rate that water travels (SAR Section 2.3.8.2).

NRC Staff's Review

(b)(5)

(b)(5)

2.2.1.3.7.3.1.1 Model Integration for the TSPA Code

DOE represented UZ transport as a model abstraction that simulates the transport of dissolved radionuclides and colloid-associated radionuclides through the UZ beneath the repository. This model generates breakthrough curves at the water table for the 27 aqueous species and 12 colloidal species that DOE determined were the most representative and risk significant (SAR Sections 2.3.8.6, 2.3.7.4.1.2, and 2.3.8.5.4). DOE simulated radionuclide transport in the abstraction with a residence-time particle-tracking technique in an external process model, FEHM, as identified in Section 3.6 of SNL (2008ag). The particle-tracking technique determines the amount of time that a particle spends in each cell of the model and determines, on the basis of flow field information, which cell (fracture or matrix) the particle travels to next.

DOE integrated the UZ radionuclide transport abstraction with three other TSPA model components (SAR Figure 2.3.8-2): the EBS radionuclide transport abstraction (SAR Section 2.3.7.12), the site-scale UZ flow model (SAR Section 2.3.2.4.1), and the saturated zone radionuclide transport abstraction (SAR Section 2.3.9.3). Using flow conditions and concentration gradients at the boundary between the EBS and the unsaturated rock beneath the repository, the EBS transport abstraction calculates the radionuclide mass flux that enters the UZ fractures and rock matrix (SAR Section 2.3.7.12.3.2). Because the radionuclides travel more slowly in the rock matrix than in fractures (SAR Figure 2.3.8-49), DOE identified release of radionuclides from the EBS into the rock matrix as being a significant barrier mechanism (SAR Section 2.3.8.5.4). Accordingly, the NRC staff has evaluated DOE's technical basis for the flux-splitting submodel that calculates the release of radionuclides from the EBS into the rock matrix and into the fractures (SER Section 2.2.1.3.7.3.1.2).

DOE's site-scale UZ flow model passes flow field information to the UZ transport abstraction, such that radionuclide transport through the fractures and rock matrix in the model grid depends on the percolation (downward flow) fluxes provided by the flow fields. In particular, the flow fields generated by the site-scale UZ flow model provide the transport abstraction with spatial distributions of fracture-to-fracture, matrix-to-matrix, fracture-to-matrix, and matrix-to-fracture flow rates and moisture contents in the three-dimensional model framework, as detailed in Section 6.3.9.2 of SNL (2008ag). During a calculated TSPA realization, the UZ transport abstraction receives flow field information from a sequence of up to four steady-state flow fields associated with different climate states (i.e., present-day, monsoon, glacial-transition, and post-10,000-year period) to account for future changes in percolation flux at specified points in time (SAR Section 2.3.8.5.3). In DOE's UZ transport abstraction model, the elevation of the water table beneath Yucca Mountain increases at the transition from the present-day climate state to a future, wetter climate state. The water table remains at the higher elevation for the remainder of the realization, effectively shortening the modeled thickness of the UZ transport path (Section 6.4.8, SNL, 2008an; Section 6.3.9.3, SNL, 2008ag). All other features of the UZ transport model grid and the sampled values of model parameters for the UZ transport abstraction remain constant throughout a TSPA realization.

The output of the UZ transport abstraction calculation provides time-dependent radionuclide mass flux as input to the saturated zone transport abstraction water table. The UZ transport abstraction groups the radionuclide mass fluxes into four collection regions and transfers the grouped mass fluxes to the saturated zone transport abstraction, which then initiates radionuclide transport in the saturated zone at an arbitrarily selected location for each of the four regions (SAR Section 2.3.8.5).

NRC Staff's Review

The NRC staff evaluated the information DOE provided in SAR Section 2.3.8 and in Sections 6.3, 6.4, and 6.5 of SNL (2008a) and references therein about the development of the UZ transport abstraction and its integration with related model abstractions in TSPA calculations.

(b)(5)

The NRC staff compared DOE's integration of the UZ transport abstraction (SAR Section 2.3.8.5 and references therein) and the site-scale UZ flow model (SAR Section 2.3.2.4.1 and references therein). (b)(5)

(b)(5)

The NRC staff evaluated DOE's integration of the UZ transport abstraction (SAR Section 2.3.8.5 and references therein) and the saturated zone transport abstraction (SAR Section 2.3.9.3 and references therein). (b)(5)

(b)(5)

2.2.1.3.7.3.1.2 EBS—UZ Boundary Condition

DOE's EBS transport abstraction provides the UZ transport abstraction with the time-dependent radionuclide mass flux out of the EBS. In DOE's model for the EBS, radionuclides are transported out of breached waste packages by advection (flow) or by diffusion, travel through the crushed tuff invert, and exit into the unsaturated rock at the base of the repository drift (SAR Section 2.3.7.12.3.2). At the model exit boundary, the EBS transport abstraction uses a submodel, which DOE termed the EBS—UZ interface submodel (Section 6.5.2.6, SNL (2007a)), to distribute the radionuclides between the fractures and the rock matrix, according to modeled flow conditions and concentration gradients at the boundary. As stated in DOE Enclosure 6 (2009a), the overall result of the flux-splitting calculations in the EBS—UZ interface submodel is that most radionuclides released from waste packages in seeping drifts are transferred by

advection into fractures, and most radionuclides released from nonseeping drifts are transferred by diffusion into the rock matrix.

In SAR Section 2.3.8.5.4 and DOE Enclosure 9 (2009am), DOE identified the initiation of transport in the low permeability rock matrix beneath the drifts as a mechanism that significantly delays the transport of radionuclides in the UZ. Accordingly, the NRC staff reviewed the technical basis for the flux-splitting submodel that DOE used to integrate the EBS transport abstraction and the UZ radionuclide transport abstraction in TSPA calculations. DOE provided information about the flux-splitting model in SAR Section 2.3.7.12.3.2; Sections 6.5.2.5 and 6.5.2.6 of SNL (2007aj); Sections 6.3.8 and 7.7.1[a] of SNL (2008ag); and DOE Enclosures 1, 9, 11, and 12 (2009am). The NRC staff has separately reviewed the technical basis and model properties for DOE's EBS transport abstraction and model properties in SER Section 2.2.1.3.4.3.5.

NRC Staff's Review

In the EBS–UZ interface submodel, DOE represents the near-field UZ as a localized, two-dimensional vertical array of overlapping fractures and rock matrix beneath the repository drift. (b)(5)

(b)(5)

2.2.1.3.7.3.2 UZ Radionuclide Transport Processes

In DOE's UZ transport abstraction, the migration of radionuclides through the UZ is influenced by the transport-affecting processes of advection and dispersion, sorption, matrix diffusion, and colloid-associated radionuclide transport, as well as radioactive decay and ingrowth (SAR Section 2.3.8.1). Four of these processes—advection, dispersion, matrix diffusion, and colloidal transport—are transport mechanisms that move radionuclides from one location to another. In contrast, sorption may delay the transport of a radionuclide by attachment to stationary surfaces such as the rock matrix. Radioactive decay removes a radionuclide permanently from the system. Ingrowth is the replacement of a decayed radionuclide with a newly formed (daughter) nuclide, which may have different radioactivity and transport properties than the parent.

2.2.1.3.7.3.2.1 Advection and Dispersion

In DOE's UZ transport model and abstraction, advection refers to the transport of radionuclides, as either dissolved or colloid-associated phases, by the bulk movement of water. Overall, DOE considered advection to be the most important transport process in the UZ because, as DOE stated in Section 6.1.2.1 of SNL (2007bj), the rate of water movement largely controls radionuclide travel times in the UZ. DOE coupled the advective transport of radionuclides with the bulk movement of water in fractures, in the rock matrix, and between fractures and matrix, using the groundwater flow rates and flow paths supplied by the site-scale UZ flow model, as detailed in SAR Section 2.3.8.5.2.1 and Section 6.3.9.2 of SNL (2008ag). Because the UZ flow model predicts that water flows through the UZ at different rates in different rock units, the advective radionuclide transport rates vary correspondingly at different locations in the UZ. For example, in the fracture-dominated northern part of the repository area, DOE's UZ transport model predicts generally fast advective transport of radionuclides due to high modeled flow rates in fractures and faults. In the southern part of the repository area, advective transport of radionuclides in the UZ is slower due to low flow rates in the matrix-dominated flow system of the Calico Hills vitric tuff units (SAR Section 2.3.8.5.4).

DOE described dispersion as a spreading plume of dissolved radionuclides caused by localized differences in flow conditions, as identified in SAR Section 2.3.8.2.2.1 and Section 6.3.9.1 of SNL (2008ag). As stated in Section 4.1.6, AD01 of SNL (2008an), DOE did not identify dispersion as an important transport-affecting process at the scale of the UZ transport model, but DOE chose to include a simple fixed-value longitudinal dispersion term in the transport model to support numerical analyses of breakthrough curves at the water table (SAR Section 2.3.8.5.2.2). To estimate a value for the dispersion term, DOE used results from saturated zone flow and transport tests at Yucca Mountain that were comparable in scale to site-scale UZ flow and transport paths (SAR Section 2.3.8.5.2.2).

The NRC staff reviewed information DOE provided about advection in SAR Section 2.3.8 and references therein. (b)(5)

(b)(5)

The NRC staff reviewed the information DOE provided about dispersion in SAR Section 2.3.8 and references therein. (b)(5)

(b)(5)

2.2.1.3.7.3.2.2 Sorption

Sorption is a general term for chemical and physical processes that transfer a fraction of dissolved species to the surface of a solid phase. Depending on specific properties of the dissolved species, solid, and liquid, some dissolved species will sorb more readily onto solids than others will, and some will not sorb at all. DOE modeled sorption of dissolved radionuclide species in the UZ rock matrix but assumed that there was no sorption on fracture surfaces, except for those portions of the model framework that are designated as fault zones, as identified in SAR Section 2.3.8.5.2.3 and DOE Enclosure 2 (2009am). DOE also included sorption in modeling colloid-associated radionuclide transport, as discussed separately (SER Section 2.2.1.3.7.3.2.4).

In DOE's UZ transport model, sorption of radionuclides onto immobile rock surfaces slows the transport rate of radionuclides through the rock relative to the flow rate of water, a delaying effect that is called retardation (SAR Section 2.3.8.2.2.2). Sorption potentially can retard the transport of moderately or strongly sorbing radionuclides in the UZ for thousands of years or longer, contributing more significantly to UZ barrier capability than any other retardation process, as identified in DOE Enclosure 6 (2009an). In contrast, sorption of radionuclides onto mobile colloids, instead of onto immobile rock surfaces, may decrease the overall retardation effect.

DOE represented sorption in the UZ rock matrix with a sorption coefficient (K_d), an empirically determined or modeled value that represents the ratio of the sorbed-phase radionuclide concentration to the dissolved-phase radionuclide concentration. Low or zero values of K_d indicate that little or no sorption occurs; higher values indicate moderate or strong sorption, and therefore retardation. Factors that influence K_d values include the radionuclide chemistry and dissolved-phase concentration; the solution pH and major ion water chemistry; the temperature of the system; and the physical and chemical properties of the solid phase, including its surface area. Retardation by sorption is expressed in transport calculations by a retardation factor that depends on the value of the sorption coefficient and the physical properties (porosity and density) of the solid medium through which the radionuclide is transported. Retardation calculations assume that K_d does not vary with changes in radionuclide concentration, sorption and desorption reactions are fast relative to the flow rate, and bulk chemical composition of the water is constant (Davis and Curtis, 2003aa; Langmuir, 1997aa; Davis and Kent, 1990aa). In the UZ transport model and abstraction, DOE assumed that four radioelements are nonsorbing (carbon, chlorine, iodine, and technetium) and assigned a fixed value of $K_d = 0$ for each. For the remaining 11 radioelements modeled in UZ transport calculations (americium, cesium, neptunium, plutonium, protactinium, radium, selenium, strontium, thorium, tin, and uranium), DOE developed ranges and statistical distributions of K_d values for each radioelement and for each modeled rock unit from a combination of empirical data, process modeling, and professional judgment, as summarized in SAR Table 2.3.8-2. DOE detailed the K_d selection process in SNL Appendices A, B, I, and J and Addendum 1 (2007bj) and in DOE Enclosure 3 (2009am).

In terms of the barrier capability of the lower UZ (SAR Section 2.1.2.3), DOE attributed a higher overall importance to sorption than to any other transport process, as identified in DOE Enclosure 6 (2009an). Accordingly, the NRC staff has conducted a detailed review of the information DOE provided about sorption in SAR Section 2.3.8 and references therein, with a particular focus on (i) how DOE obtained data for the sorption model, (ii) how DOE addressed data and model uncertainty, and (iii) how DOE supported the sorption model as implemented in performance assessment calculations.

To obtain estimates of K_d values for sorption modeling, DOE grouped the various rock units below the repository into three rock types that have different sorption characteristics—zeolitized tuff, devitrified tuff, and vitric tuff (SAR Section 2.3.8.3.1). DOE measured sorption data from batch experiments that used site-specific crushed tuff samples and saturated zone water samples from two wells (J-13 and UE-25 p#1). DOE chose these water chemistries to bracket the major ion chemistry observed in pore waters and perched zone waters in the UZ, as provided in SAR Section 2.3.8.3.1 and Section A4 of SNL (2007bj). DOE provided summaries of major ion chemistry (e.g., calcium, sodium, bicarbonate) for UZ pore waters and perched waters and compared the reported ranges with the two waters used in the sorption experiments, as identified in Section A4 of SNL (2007bj). (b)(5)

(b)(5)

(b)(5)

For the long-lived actinides (americium, neptunium, plutonium, and uranium), DOE further characterized the effects of variability in geochemistry and mineral surface area using a non-electrostatic surface complexation modeling approach described in Davis, et al. (1998aa) and SNL Addendum 1 and Appendix A, Sections A7 and A8 (2007bj). (b)(5)

(b)(5)

(b)(5)

In some cases, DOE supplemented the experimental and modeling sorption data with data from peer-reviewed scientific literature and reports prepared by other agencies (e.g., Section A1[a] of SNL (2007bj)). In the TSPA model, DOE sampled K_d values from the specified ranges to account for experimental uncertainty and variability in geologic conditions, including water chemistry and rock type, as detailed in SAR Table 2.3.8-2, SNL Appendices A, B, I, and J and Addendum 1 (2007bj) and DOE Enclosure 3 (2009am).

DOE identified mineral surface area and particle size as potential sources of data uncertainty related to the use of crushed tuff in experiments. The general DOE approach to addressing this uncertainty was to use batch experiments for a range of particle sizes and to bias the minimum and maximum limits for the K_d distributions toward lower (weaker sorption) values, as documented in DOE Enclosure 3, Table 1.1.2-1 (2009am). DOE referenced studies both from within and outside the DOE program in Section 6.1.3.1 of SNL (2007bj). These studies indicated the effects of particle size on sorption are typically small except for the very fine (e.g., clay-sized) fraction. (b)(5)

(b)(5)

DOE addressed data uncertainty by obtaining empirical sorption data that assessed K_d variability as a function of time, radioelement concentration, atmospheric composition, water composition, particle size, and temperature. Although most of the data were gathered from batch sorption experiments, DOE also performed a limited number of confirmatory column tests on selected radionuclides that DOE had identified as important contributors to mean annual dose in previous performance assessment calculations. This is addressed in SAR Section 2.3.8.3.1 and SNL Table 4-1 (2007ba). In some cases, DOE indirectly addressed uncertainty related to radionuclide solubility by assigning low (conservative) K_d values. In selecting experimental data to inform the TSPA K_d distributions (b)(5)

(b)(5)

Comment (b)(5)

(b)(5)

Comment (b)(5)

(b)(5) DOE outlined this approach in SAR Section 2.3.8.3.1, SNL Appendix A (2007b)), and SNL (2007ah).

(b)(5)

(b)(5)

(b)(5) DOE addressed model uncertainty in its TSPA calculations by sampling K_d values stochastically from uncertainty distributions in which the distribution ranges were developed from expected system conditions. Rather than sample the K_d distribution independently for each radionuclide, DOE developed a correlation matrix for the 11 sorbing radioelements on the basis of their ranked sensitivities to six variables (pH, Eh, water chemistry, rock composition, rock surface area, and radionuclide concentration). DOE used this approach to approximate similarities in sorption behavior among radioelements and to ensure that transport behaviors were represented consistently within a single realization of the model, as detailed in [SNL Appendix B, Section B1 (2007b)]. In addressing model uncertainty, DOE did not take credit for sorption (i.e., $K_d = 0$) in fractures (fast flow paths), except for fault zones, and DOE implemented K_d uncertainty distributions for matrix sorption that in most cases predicted less sorption compared to measured distributions. (b)(5)

(b)(5)

DOE developed information from natural analogs to provide qualitative comparisons for sorption model confidence building at the field scale (SAR Section 2.3.8.4.4). DOE did not apply the UZ transport abstraction to sorption modeling for these analog sites, and DOE did not use results from natural analog studies to inform the K_d distributions. Instead, DOE used general observations of sorption-related transport behavior to support the conceptual models (e.g., SAR Section 2.3.8.4.4.6). DOE also used observations from field sites at Busted Butte south of Yucca Mountain and alcove tracer tests with nonradioactive chemical homologues in the Exploratory Studies Facility to provide limited quantitative evaluations of sorption in the radionuclide transport model abstraction (SAR Section 2.3.8.3.3).

(b)(5)

(b)(5)

2.2.1.3.7.3.2.3 Matrix Diffusion

Diffusion is a physical process in which dissolved species or suspended particles move from a region of high concentration to a region of low concentration in accordance with the concentration gradient. DOE described matrix diffusion as a fracture–matrix interaction that uses diffusion to transfer radionuclides between fractures and the rock matrix. In DOE Enclosure 6 (2009a), DOE identified matrix diffusion as an important transport mechanism in the UZ transport abstraction, especially for strongly sorbing radionuclides, because it is the main process by which radionuclides can move from a fracture-dominated flow path into the matrix.

As DOE described in Section 6.1.2.4 of SNL (2007b), radionuclide transport by matrix diffusion in the unsaturated zone depends on (i) the matrix diffusion rate (i.e., the rate that a radionuclide can diffuse from water in a fracture into water in the pore spaces of the rock matrix) and (ii) the effective fracture–matrix interface, which is the area across which diffusion can occur. In turn, the matrix diffusion rate depends on (i) the radionuclide concentration gradient between fracture and matrix; (ii) the calculated water saturation of the rock; and (iii) the value of the effective matrix diffusion coefficient, which is a measure of how readily a particular radioelement diffuses through a tortuous pathway of interconnected pores in the rock matrix. To calculate the effective matrix diffusion coefficient, DOE estimated tortuosities from empirical data obtained from representative Yucca Mountain tuff samples and developed standard normal cumulative probability distributions that were sampled stochastically in the TSPA analysis for each radioelement with respect to the individual model units (SAR Section 2.3.8.3.2; Reimus, et al., 2007aa).

DOE stated that not all connected fractures in unsaturated rocks actively conduct water (SAR Section 2.3.2.2.1), and, instead of uniform flow, individual fractures may have gravity-driven fingering flow that wets only a portion of a fracture surface (SAR Section 2.3.8.2.2.1). To adjust the size of the effective fracture–matrix interface area to account for the general observations of flow in the unsaturated fractures, DOE adopted the active fracture model (Liu, et al., 1998aa) for fracture–matrix interactions (SAR Section 2.3.2.2.1). In particular, DOE used an active fracture model parameter, *gamma*, and the modeled effective water saturation (i.e., the average water saturation of the connected fractures, adjusted by the UZ flow model for residual fracture saturation) to increase the modeled distance between flowing fractures. This reduced the size

of the effective (i.e., wetted) fracture–matrix interface area for the UZ fracture–matrix interactions, thereby decreasing the amount of matrix diffusion and its capacity to retard radionuclide transport through the fractured rock.

In applying the active fracture model for flow field calculations in the site-scale UZ flow model (SAR Section 2.3.2.2.2.1), DOE used fixed values of the *gamma* parameter for individual model layers, estimated by flow model calibration, as detailed in Section 6.3.2 of SNL (2007ad). In contrast, sensitivity analyses in Section 6.6.4 of SNL (2008an) indicated that the radionuclide transport model calculations were more sensitive to gamma uncertainty values than the fluid flow model calculations. DOE reasoned that it would be inappropriate in the radionuclide transport calculations to assume that the *gamma* parameter was tightly constrained by the calibrated values from the fluid flow model. For radionuclide transport calculations, DOE instead sampled *gamma* values independently from an uncertainty distribution that was not limited to the calibrated fluid flow model values (SAR Section 2.3.8.5.2.4).

DOE's conceptual model of matrix diffusion in Section C5 of SNL (2008an) assumes that matrix diffusion should be less effective in the unsaturated rocks than in the saturated rocks due to the reduced size of the wetted fracture–matrix interface area in unsaturated fractures. DOE cited field observations and numerical simulations of tracer migration in several large-scale transport experiments in the Exploratory Studies Facility to support its conceptual model of matrix diffusion in fractured, unsaturated rocks and use of the active fracture model for matrix diffusion calculations in the TSPA model (SAR Sections 2.3.8.3.3.2.1 and 2.3.8.3.3.3). DOE provided empirical observations and sensitivity analyses from field-scale experiments and process-level model analyses to address matrix diffusion model uncertainty. These were addressed in Section 6.3.2 of SNL (2007ad); Sections 7.4.1 and 7.4.2 of BSC (2004ag); Section 6.12.2.4 of BSC (2004av); Section 7.5 of SNL (2007bf); and Liu, et al. (2003aa).

In developing and supporting the matrix diffusion model, DOE acknowledged the impracticality of conducting large-scale transport tests to observe and measure the effects of fracture–matrix interactions in unsaturated rocks under natural conditions (SAR Section 2.3.8.3), and DOE cited uncertainties about the potential significance of scale-dependent transport processes in fractured rocks (Section 6.4.1 of BSC, 2006aa; Liu, et al., 2004aa). Section 6.6.4 of SNL (2008an) identified that the size of the effective fracture–matrix interface area was the most uncertain term affecting radionuclide diffusion rates in the matrix diffusion model. To address model uncertainties about quantifying the effective fracture–matrix interface area for UZ transport calculations, DOE sampled the value of the active fracture model *gamma* parameter from a broad, uniform distribution that covered an intermediate range of 40 percent of all possible *gamma* values. The wide range of sampled *gamma* values produced a correspondingly wide range of results for radionuclide transport by matrix diffusion, as described in Section 6.6.4 of SNL (2008an).

(b)(5)

(b)(5)

(b)(5)

(b)(5)

DOE addressed the uncertainty of the effects of fracture coatings on matrix diffusion by conducting diffusion experiments with paired core samples (i.e., samples with fracture coatings and without). In the tested sample pairs, mineral coatings on fracture surfaces did not impede diffusion rates (Reimus, et al., 2007aa). In addition, in Section 5.2.1.1 of BSC (2004bi), DOE identified site characterization studies that showed secondary mineral coatings (e.g., calcite, oxides, clay minerals) are not abundant on fracture surfaces in Yucca Mountain tuffs, limiting their potential effects on matrix diffusion.

(b)(5)

(b)(5)

DOE conducted no UZ field experiments for model support specifically to evaluate DOE's matrix diffusion model under expected repository conditions, but DOE observed in several large-scale experiments in the Exploratory Studies Facility that tracer transport in fractured rocks took significantly longer than predicted by matrix diffusion in DOE's process-level models (SAR Sections 2.3.8.3.3.2.1, 2.3.8.3.3.2.2, and 2.3.8.3.3.3). DOE's numerical simulations of these tracer tests included numerical analyses based on the same model assumptions and the same broad range of *gamma* parameter values as DOE used for matrix diffusion in the unsaturated transport abstraction (SAR Section 2.3.8.4.4.4.3). (b)(5)

(b)(5)

(b)(5)

DOE also provided the Total System Performance Assessment–License Application performance assessment results in SAR Section 2.4.2; Section 7.7.1[a] of SNL (2008ag); and DOE Enclosure 6 (2009an) (b)(5)

(b)(5)

(b)(5)

(b)(5)

Comment (b)(5)

2.2.1.3.7.3.2.4 Colloid-Associated Transport

Colloids are minute solid particles of any origin or composition that are suspended in a liquid. Colloids can form by many processes in natural or engineered systems—for example, by physical or chemical degradation of preexisting solid materials or by precipitation from a solution—or they can be of biological or geological origin (e.g., microbes, clay minerals). Colloids influence radionuclide transport in the UZ because the transport path and transport rate of radionuclides associated with a colloid (e.g., radionuclides attached by sorption to the colloid surface) are determined by the transport behavior of the colloid instead of by processes that might otherwise affect the transport rate of the radionuclide as a dissolved species (e.g., matrix diffusion, or sorption in the rock matrix). Compared to dissolved radionuclides, colloids migrate preferentially in fractures, where travel times tend to be fast, because the small size of matrix pore openings inhibits the transfer of colloidal particles from fractures to matrix.

DOE's conceptual model in Section 6.3.9.1 of SNL (2008ag) defined two modes of colloid-associated radionuclide transport: reversible colloids, in which radionuclides are temporarily (reversibly) attached to colloids by sorption, and irreversible colloids, in which radionuclides are assumed to be permanently attached to or embedded in the colloid. According to Section 6.5.3 of SNL (2007bi), the effectiveness of radionuclide transport by colloids depends on the transport characteristics of the colloids themselves; the concentration of colloids; and radionuclide sorption coefficients onto colloids and onto the immobile rock matrix; but the overall effect of colloid-associated transport of reversible colloids is to facilitate the transport of radionuclides through the system.

DOE represented reversible colloid transport by modeling reversible sorption of dissolved radionuclides onto naturally occurring colloids in groundwater, using the same empirical K_d modeling approach that DOE used for reversible sorption in the rock matrix. DOE then applied an empirically determined colloid retardation factor, described in Section 6.4.3 of BSC (2004bc), to account for colloid attachment and detachment processes in fractures that can hinder colloid movement in fractures. For simplicity, DOE assumed that all reversible colloids in the UZ are represented by the smectite clay mineral montmorillonite, a colloid-forming mineral in Yucca Mountain tuffs that has a high sorption capacity. DOE, in Section 6.5.3 of SNL (2007bi), described how it modeled colloid-associated reversible sorption for six radioelements (americium, cesium, plutonium, protactinium, thorium, and tin) on the basis of their strong affinity for sorption onto montmorillonite under expected conditions in the UZ. DOE estimated the concentration of colloids in groundwater from data collected in saturated zone field studies.

from the Yucca Mountain area and from tabulated data for groundwater analyses elsewhere, as provided in SNL Table 6-21 (2008an). To address data uncertainty, DOE used the same estimated range of variability for groundwater colloid concentrations in the EBS, the UZ, and the saturated zone, but each transport abstraction sampled the range of values independently from the others in TSPA code simulations to account for the potential variability in groundwater colloid concentrations among the different environments, as identified in Section 6.5.12 of SNL (2008an). DOE further addressed data uncertainty for reversible colloids by selecting ranges of montmorillonite sorption coefficients that emphasized large K_d values (i.e., strong sorption onto colloids), so as not to underestimate the effectiveness of radionuclide attachment to colloid surfaces, as described in DOE Enclosure 14 (2009am).

For irreversible colloids, DOE's colloid-associated transport model assumes that all irreversible colloids are generated within the EBS by the degradation of metals or wasteform materials, and the only radionuclides associated with irreversible colloids are isotopes of plutonium and americium (SAR Section 2.3.7.12.3.2). On the basis of field evidence for fast colloid transport in groundwater (e.g., Kersting, et al., 1999aa), DOE designated a small fraction (less than 0.2 percent) of the irreversible colloid flux as a "fast fraction" that is transported from the EBS to the accessible environment without any retardation. The rest of the irreversible colloid flux is subject to several potential retardation processes, including (i) fracture-related colloid attachment and detachment processes, as DOE detailed in Section 6.5.13 of SNL (2008an), (ii) the direct release of irreversible colloids from the EBS into the low permeability rock matrix beneath the repository drifts, as described in DOE Enclosure 9 (2009am); and (iii) the advective transfer of irreversible colloids laterally from fracture flow paths into the rock matrix, subject to flow field conditions (i.e., matrix permeability large enough to accommodate the advective flux) and subject to colloid size exclusions at the fracture-matrix interface, as described in SAR Section 2.3.8.4.5.4 and Sections 6.3.9.1 and 6.3.9.2 of SNL (2008ag). In Section 6.3.9.1 of SNL (2008ag), and in Section 6.5.9 of SNL (2008an), DOE also described a fourth retardation process, the matrix filtration (straining) of irreversible colloids at the interface between the matrix of one rock unit and the matrix of the underlying rock unit, resulting in the permanent immobilization of colloids in the UZ. DOE compared UZ breakthrough curves for irreversible colloids with and without matrix filtration in SNL, ERD 02, Section III (2008an) and observed that including matrix filtration as a retardation process diminished the flux of irreversible colloids out of the UZ by as much as 80 percent in the southern half of the repository area, as illustrated in SNL, ERD 02, Figure 6.6.2-6[c] (2008an). However, DOE's final TSPA model conservatively did not implement matrix filtration in the TSPA simulations that DOE used to support compliance with 10 CFR 63.113, as explained in DOE Enclosure 11 (2009am).

The NRC staff reviewed DOE's technical basis for the colloid-associated transport model in the context of the NRC staff's independent understanding of colloid-associated transport modeling, colloid stability, and colloid transport properties in natural and engineered systems. As DOE noted in SAR Section 2.3.8.3, colloid transport mechanisms in unsaturated, fractured rocks are not well characterized by field studies. Accordingly, the NRC staff's review of DOE's technical basis for colloid-associated transport of radionuclides in the UZ focuses on how DOE addressed data and model uncertainty in developing parameter values and modeling colloid-associated transport processes. The NRC staff evaluated information DOE provided in SAR Section 2.3.8 and references therein, particularly Section 7.7.1[a] of SNL (2008ag) and SNL (2008an). The NRC staff also considered additional information that DOE provided to clarify details of the colloid-associated transport model in DOE Enclosures 9 through 14 (2009am).

(b)(5)

(b)(5)

(b)(5)

DOE addressed model uncertainty for colloid-associated transport in the UZ by applying a number of simplifying assumptions about colloid-associated transport processes. (b)(5)

(b)(5)

(b)(5)

(b)(5)

(b)(5)

2.2.1.3.7.3.2.5 Radionuclide Decay and Ingrowth

Radioactive decay is a general term for the processes by which unstable radionuclides spontaneously disintegrate to form a different nuclide that may or may not also be radioactive. DOE's particle tracking model in the UZ transport abstraction includes the loss of radionuclides over time due to radioactive decay and, where applicable, the model calculates the corresponding increase (ingrowth) of daughter radionuclides in decay chains, as described in Section 6.4.4 of SNL (2008a). DOE assumed that upon radioactive decay of plutonium and americium in irreversible colloids, the decay chain daughters (e.g., uranium, neptunium) would be released from the irreversible colloid to migrate as dissolved species, with the exception of plutonium-239 produced by radioactive decay of americium-243, which DOE assumed would remain irreversibly attached to the colloid (SAR Section 2.3.8.2.2.3).

(b)(5)

2.2.1.3.7.4 Evaluation Findings

The NRC staff reviewed the applicant's SAR and other information submitted in support of the license application and finds that, with respect to the requirements of 10 CFR 63.114 for consideration of radionuclide transport in the UZ, (b)(5)

(b)(5)

(b)(5)

2.2.1.3.7.5 References

BSC. 2006aa. "Analysis of Alcove 8/Niche 3 Flow and Transport Tests." ANL-NBS-HS-000056. Rev. 00. ACN 01. Las Vegas, Nevada: Bechtel SAIC Company, LLC.

BSC. 2004ag. "Conceptual Model and Numerical Approaches for Unsaturated Zone Flow and Transport." MDL-NBS-HS-000005. Rev. 01. ACN 01. Las Vegas, Nevada: Bechtel SAIC Company, LLC.

BSC. 2004av. "In-Situ Field Testing of Processes." ANL-NBS-HS-000005. Rev. 03. ACN 01, ACN 02, ERD 01. Las Vegas, Nevada: Bechtel SAIC Company, LLC.

BSC. 2004bc. "Saturated Zone Colloid Transport." ANL-NBS-HS-000031. Rev. 02. ACN 01, ERD 01. Las Vegas, Nevada: Bechtel SAIC Company, LLC.

BSC. 2004bi. "Yucca Mountain Site Description, Volume I: Sections 1-5." TDR-CRW-GS-000001. Rev. 02 ICN 01. ERD 01, ERD 02. Las Vegas, Nevada: Bechtel SAIC Company, LLC.

Dahan, O., R. Nativ, E.M. Adar, B. Berkowitz, and Z. Ronen. 1999aa. "Field Observation of Flow in a Fracture Intersecting Unsaturated Chalk." *Water Resources Research*. Vol. 35. pp. 3,315–3,326.

Davidson, G.R., R.L. Bassett, E.L. Hardin, and D.L. Thompson. 1998aa. "Geochemical Evidence of Preferential Flow of Water Through Fractures in Unsaturated Tuff, Apache Leap, Arizona." *Applied Geochemistry*. Vol. 13. pp. 185–195.

Davis, J.A. and G.P. Curtis. 2003aa. NUREG/CR-6820, "Application of Surface Complexation Modeling To Describe Uranium (VI) Adsorption and Retardation at the Uranium Mill Tailings Site at Natunta, Colorado." Washington, DC: NRC.

Davis, J.A. and D.B. Kent. 1990aa. "Surface Complexation Modeling in Aqueous Geochemistry. Mineral-Water Interface Geochemistry." M.F. Hochella, Jr. and A.F. White, eds. *Mineralogy*. Vol. 23. pp. 177–260.

Davis, J.A., J.A. Coston, D.B. Kent, and C.C. Fuller. 1998aa. "Application of the Surface Complexation Concept to Complex Mineral Assemblages." *Environmental Science & Technology*. Vol. 32. pp. 2,820–2,828.

DOE. 2009am. "Yucca Mountain—Response to Request for Additional Information Regarding License Application (Safety Analysis Report Section 2.3.8), Safety Evaluation Report Vol. 3, Chapter 2.2.1.3.7, Set 1." Letter (February 9) J.R. Williams to J.H. Sulima (NRC). ML090410352. Enclosures (14). Las Vegas, Nevada: DOE, Office of Civilian Radioactive Waste Management.

DOE. 2009an. "Yucca Mountain—Response to Request for Additional Information Regarding License Application (Safety Analysis Report Section 2.1), Safety Evaluation Report Vol. 3, Chapter 2.2.1.1, Set 1." Letter (February 6) J.R. Williams to J.H. Sulima (NRC). ML090400455. Enclosures (7). Las Vegas, Nevada: DOE, Office of Civilian Radioactive Waste Management.

DOE. 2008ab. DOE/RW-0573, "Safety Analysis Report Yucca Mountain Repository License Application." Rev. 00. Las Vegas, Nevada: DOE, Office of Civilian Radioactive Waste Management.

Doughty, C. 1999aa. "Investigation of Conceptual and Numerical Approaches for Evaluating Moisture, Gas, Chemical, and Heat Transport in Fractured Unsaturated Rock." *Journal of Contaminant Hydrology*. Vol. 38, No. 1–3. pp. 69–106.

Freeze, R.A. and J.A. Cherry. 1979aa. *Groundwater*. Englewood Cliffs, New Jersey. Prentice-Hall, Inc.

Hu, Q., R. Salve, W.T. Stringfellow, and J.S.Y. Wang. 2001aa. "Field Tracer-Transport Tests in Unsaturated Fractured Tuff." *Journal of Contaminant Hydrology*. Vol. 51. pp. 1–12.

International Union of Pure and Applied Chemistry. 1997aa. *Compendium of Chemical Terminology*. 2nd Edition. A.D. McNaught and A. Wilkinson, eds. Oxford, United Kingdom: Blackwell Science.

- Kersting, A.B., D.W. Efur, D.L. Finnegan, D.J. Rokop, D.K. Smith, and J.L. Thompson. 1999aa. "Migration of Plutonium in Ground Water at the Nevada Test Site." *Nature*. Vol. 397, No. 6714. pp. 56–59.
- Langmuir, D. 1997aa. *Aqueous Environmental Geochemistry*. Upper Saddle River, New Jersey: Prentice Hall.
- Leslie, B., C. Grossman, and J. Durham. 2007aa. "Total-system Performance Assessment (TPA) Version 5.1 Module Descriptions and User Guide." Rev. 1. ML072710060. San Antonio, Texas: CNWRA.
- Liu, H.H., G.S. Bodvarsson, and G. Zhang. 2004aa. "Scale Dependency of the Effective Matrix Diffusion Coefficient." *Vadose Zone Journal*. Vol. 3. pp. 312–315. Madison, Wisconsin: Soil Science Society of America.
- Liu, H.H., R. Salve, J.S. Wang, G.S. Bodvarsson, and D. Hudson. 2004ab. "Field Investigation Into Unsaturated Flow and Transport in a Fault: Model Analyses." *Journal of Contaminant Hydrology*. Vol. 74. pp. 39–59. New York City, New York: Elsevier.
- Liu, H.H., C.B. Haukwa, C.F. Ahlers, G.S. Bodvarsson, A.L. Flint, and W.B. Guertal. 2003aa. "Modeling Flow and Transport in Unsaturated Fractured Rock: An Evaluation of the Continuum Approach." *Journal of Contaminant Hydrology*. Vol. 62–63. pp. 173–178.
- Liu, H.H., C. Doughty, and G.S. Bodvarsson. 1998aa. "An Active Fracture Model for Unsaturated Flow and Transport in Fractured Rocks." *Water Resources Research*. Vol. 34. pp. 2,633–2,646.
- McMurry, J. 2007aa. "Overview of Field and Laboratory Studies of Unsaturated Zone Matrix Diffusion and Related Fracture–Matrix Interactions." ML072630430. San Antonio, Texas: CNWRA.
- NRC. 2009ab. "Division of High-Level Waste Repository Safety Director's Policy and Procedure Letter 14: Application of YMRP for Review Under Revised Part 63." Published March 13, 2009. ML090850014. Washington, DC: NRC.
- NRC. 2005aa. NUREG–1762, "Integrated Issue Resolution Status Report." Rev. 1. Washington, DC: NRC.
- NRC. 2003aa. NUREG–1804, "Yucca Mountain Review Plan—Final Report." Rev. 2. Washington, DC: NRC.
- Pearcy, E.C., J.D. Prikryl, and B.W. Leslie. 1995aa. "Uranium Transport Through Fractured Cilicic Tuff and Relative Retention in Areas With Distinct Fracture Characteristics." *Applied Geochemistry*. Vol. 10. pp. 685–704.
- Reimus, P.W., T.J. Callahan, S.D. Ware, M.J. Haga, and D.A. Counce. 2007aa. "Matrix Diffusion Coefficients in Volcanic Rocks at the Nevada Test Site: Influence of Matrix Porosity, Matrix Permeability, and Fracture Coating Minerals." *Journal of Contaminant Hydrology*. Vol. 93. pp. 85–95.

Robinson, B.A., C. Li, and C.K. Ho. 2003aa. "Performance Assessment Model Development and Analysis of Radionuclide Transport in the Unsaturated Zone, Yucca Mountain, Nevada." *Journal of Contaminant Hydrology*. Vol. 62–63. pp. 249–268

Salve, R., J.S.Y. Wang, and C. Doughty. 2002aa. "Liquid-Release Tests in Unsaturated Fractured Welded Tuffs: I. Field Investigations." *Journal of Hydrology*. Vol. 256. pp. 60–79

Sheppard, M.I. and D.H. Thibault. 1990aa. "Default Soil Solid/Liquid Partition Coefficients, K_d s, Four Major Soil Types: A Compendium." *Health Physics*. Vol. 59. pp. 471–482.

SNL. 2008ag. "Total System Performance Assessment Model/Analysis for the License Application." MDL-WIS-PA-000005. Rev. 00. AD 01, ERD 01, ERD 02, ERD 03, ERD 04. Las Vegas, Nevada: Sandia National Laboratories.

SNL. 2008ak. "Waste Form and In-Drift Colloids-Associated Radionuclide Concentrations: Abstraction and Summary." MDL-EBS-PA-000004. Rev. 03. ERD 01. Las Vegas, Nevada: Sandia National Laboratories.

SNL. 2008an. "Particle Tracking Model and Abstraction of Transport Processes." MDL-NBS-HS-000020. Rev. 02. ADD 02. Las Vegas Nevada: Sandia National Laboratories.

SNL. 2007ad. "Calibrated Unsaturated Zone Properties." ANL-NBS-HS-000058. Rev. 00. ACN 01, ERD 01, ERD 02. Las Vegas, Nevada: Sandia National Laboratories.

SNL. 2007ah. "Dissolved Concentration Limits of Elements with Radioactive Isotopes." ANL-WIS-MD-000010. Rev. 06. Las Vegas, Nevada: Sandia National Laboratories.

SNL. 2007aj. "EBS Radionuclide Transport Abstraction." ANL-WIS-PA-000001. Rev. 03. ERD 01. Las Vegas, Nevada: Sandia National Laboratories.

SNL. 2007an. "Hydrogeologic Framework Model for the Saturated Zone Site-Scale Flow and Transport Model." MDL-NBS-HS-000024. Rev. 01. ERD 01. Las Vegas, Nevada: Sandia National Laboratories.

SNL. 2007au. "Radionuclide Screening." ANL-WIS-MD-000006. Rev. 02. ACN 01, ERD 01, ERD 02. Las Vegas, Nevada: Sandia National Laboratories.

SNL. 2007ba. "Site-Scale Saturated Zone Transport." MDL-NBS-HS-000010. Rev. 03. ACN 01, AD 001. Las Vegas, Nevada: Sandia National Laboratories.

SNL. 2007bf. "UZ Flow Models and Submodels." MDL-NBS-HS-000006. Rev. 03. ACN 01, ERD 01, ERD 02, ERD 03. Las Vegas, Nevada: Sandia National Laboratories.

SNL. 2007bi. "Waste Form and In-Drift Colloids-Associated Radionuclide Concentrations: Abstraction and Summary." MDL-EBS-PA-000004. Rev. 03. ERD 01. Las Vegas, Nevada: Sandia National Laboratories.

SNL. 2007bj. "Radionuclide Transport Models Under Ambient Conditions." (U0060) MDL-NBS-HS-000008. Rev. 02. CAN 002, AD 01. Las Vegas, Nevada: Sandia National Laboratories.

Sudicky, E.A. and E.O. Frind. 1982aa. "Contaminant Transport in Fractured Porous Media: Analytical Solutions for a System of Parallel Fractures." *Water Resources Research*. Vol. 18. pp. 1,634–1,642.

Till, J.E. and H.R. Meyer. 1983aa. NUREG/CR-3332, "Radiological Assessment: A Textbook on Environmental Dose Analysis." Washington, DC: NRC.

Turner, D.R., F.P. Bertetti, and R.T. Pabalan. 2002aa. "The Role of Radionuclide Sorption in High-Level Waste Performance Assessment: Approaches for the Abstraction of Detailed Models." *Geochemistry of Soil Radionuclides*. P.-C. Zhang and P.V. Brady, eds. Special Publication 59. Madison, Wisconsin: American Society of Agronomy. pp. 211–252.

Winterle, J.R. and W.H. Murphy. 1999aa. "Time Scales for Dissolution of Calcite Fracture Fillings and Implications for Saturated Zone Radionuclide Transport at Yucca Mountain, Nevada." Scientific Basis for Nuclear Waste Management. Boston, Massachusetts, November 30–December 4, 1998. Materials Research Society Symposium Proceedings 556. Warrendale, Pennsylvania: Materials Research Society. pp. 713–720.

Zhou, Q., H.H. Liu, F.J. Molz, Y. Zhang, and G.S. Bodvarsson. 2007aa. "Field-Scale Effective Matrix Diffusion Coefficient for Fractured Rock: Results From Literature Survey." *Journal of Contaminant Hydrology*. Vol. 93, Nos. 1–4. pp. 161–187.

CHAPTER 11

2.2.1.3.8 Flow Paths in the Saturated Zone

2.2.1.3.8.1 Introduction

This section of the Safety Evaluation Report (SER) provides the U.S. Nuclear Regulatory Commission (NRC) staff's review of the applicant's representation of flow paths in the saturated zone within the context of the applicant's performance assessment evaluation. The NRC based its review on information provided in the U.S. Department of Energy's (DOE) Safety Analysis Report (SAR) included with the license application submitted on June 3, 2008 (DOE, 2008ab).

Groundwater flow in the saturated zone is a key process in the applicant's performance assessment evaluation for the proposed geologic repository at Yucca Mountain, Nevada. The performance assessment analysis summarized in the SAR includes the flow of water from precipitation falling on Yucca Mountain, its migration as groundwater through the unsaturated zone above and below the repository, and the flow of groundwater in the saturated zone through the controlled environment to the accessible environment. This groundwater is the principal means by which radionuclides released from the repository could be transported to the accessible environment. Exposure to extracted groundwater is one of the risk-significant pathways to the reasonably maximally exposed individual (RMEI); therefore, the performance assessment must include those components that significantly affect the timing and magnitude of transport for any radionuclides released from the repository.

The applicant identified the saturated zone as a feature important to the capability of the lower natural barrier (SAR Section 2.1.1.3). Specifically, the applicant indicated in Table 2.1-1 Expanded (DOE, 2009a) that the function of the saturated zone is to substantially reduce the rate of movement of radionuclides to the RMEI location by a combination of slow advective flow, long transport distance, and geochemical retardation of radionuclides. Hence, groundwater flow in the saturated zone is both the principal means for radionuclides to be transported to the location of the RMEI as well as an important function of the lower natural barrier to delay the movement of radionuclides along the path of travel to the location of the RMEI. Saturated zone groundwater flow, as described in SAR Section 2.3.9, includes the features, events, and processes (FEPs) that affect the movement of groundwater in the saturated zone to the accessible environment and their implementation (or abstraction)¹ in the Total System Performance Assessment (TSPA).

The saturated zone groundwater flow abstraction receives information about the magnitude and patterns of groundwater flow downward through the unsaturated zone. In turn, the saturated zone flow abstraction provides information about the direction, distance (flow paths), and amount (specific discharge) of groundwater flow to the saturated zone transport abstraction.

SER Section 2.2.1.1 provides the NRC staff's evaluation of the applicant's identification and description of barriers and their capabilities as well as the consistency of these descriptions with the specific representations of these barriers in the TSPA and process-level models. The NRC staff's evaluation of those processes and characteristics most specific to radionuclide transport in the saturated zone is provided in SER Section 2.2.1.3.9. The applicant's analysis of the

¹As used in the SER, the term "abstraction" refers to the representation of site characterization data, process-level models for FEPs, uncertainty and variability, and their overall integration in a (simplified) manner in the TSPA evaluation.

effect of future climate change on water flow in the saturated zone is evaluated in this section while the NRC staff's evaluation of the nature of future climate change is presented in SER Section 2.2.1.3.5.

The other feature of the lower natural barrier the applicant identified is the unsaturated zone below the proposed repository horizon (SAR Section 2.1.1.3). The NRC staff evaluates those features and processes related to the unsaturated zone below the proposed repository horizon in SER Sections 2.2.1.3.6 and 2.2.1.3.7.

2.2.1.3.8.2 Regulatory Requirements

Model abstractions used in the applicant's postclosure performance assessment must meet the regulatory requirements given in 10 CFR 63.114 (Requirements for Performance Assessment) and 63.342 (Limits on Performance Assessment), to support the predictions of compliance for 63.113 (Performance Objectives for the Geologic Repository after Permanent Closure). Specific compliance with 63.113 is reviewed in SER Section 2.2.1.4.1.

The requirements for performance assessment in 10 CFR 63.114 require the applicant to

- Include appropriate data related to the geology, hydrology, and geochemistry of the surface and subsurface from the site and the region surrounding Yucca Mountain
- Account for uncertainty and variability in the parameter values used to model flow paths in the saturated zone
- Consider alternative conceptual models for flow paths in the saturated zone
- Provide technical bases for the inclusion of FEPs affecting flow paths in the saturated zone, including effects of degradation, deterioration, or alteration processes of engineered barriers that would adversely affect performance of the natural barriers, consistent with the limits on performance assessment in 10 CFR 63.342
- Provide technical basis for the models of flow paths in the saturated zone that in turn provide input or otherwise affect other models and abstractions

10 CFR 63.114(a) considers performance assessment for the initial 10,000 years following permanent closure. 10 CFR 63.114(b) and 63.342 consider the performance assessment methods for the time from 10,000 years through the period of geologic stability, defined in 10 CFR 63.302 as 1 million years following disposal. These sections require that through the period of geologic stability, with specific limitations, the applicant

- Use performance assessment methods consistent with the performance assessment methods used to demonstrate compliance for the initial 10,000 years following permanent closure
- Include in the performance assessment those FEPs used in the performance assessment for the initial 10,000 year period

NRC staff review of the license application follows the guidance laid out in the Yucca Mountain Review Plan (YMRP), NUREG-1804, Section 2.2.1.3.8, Flow Paths in the Saturated Zone

(NRC, 2003aa), as supplemented by additional guidance for the period beyond 10,000 years after permanent closure (NRC, 2009ab). The acceptance criteria in the YMRP generically follow 10 CFR 63.114(a). Following the guidance, the NRC staff review of the applicant's abstraction of flow paths in the saturated zone considered five criteria

- System description and model integration are adequate.
- Data are sufficient for model justification.
- Data uncertainty is characterized and propagated through the abstraction.
- Model uncertainty is characterized and propagated through the abstraction.
- Model abstraction output is supported by objective comparisons.

Because 10 CFR Part 63 specifies the use of a risk-informed approach for the review of a license application, the guidance provided by the YMRP as supplemented by NRC (2009ab) is followed to the extent reasonable for aspects of flow paths in the saturated zone important to repository performance. Whereas NRC staff considered all five criteria in their review of information provided by DOE, only aspects that substantively affect results of the performance assessment, as judged by NRC staff, are discussed in this chapter. NRC staff's judgment is based both on risk information provided by DOE, and staff's knowledge, experience, and independent analyses.

2.2.1.3.8.3 Technical Review

The applicant analyzed the groundwater flow system in the vicinity of the proposed repository at Yucca Mountain to establish the direction and magnitude of water movement. The applicant delineated the direction of water flow (flow paths) and computationally estimated the magnitude (specific discharge) of water flow using multiple groundwater flow models at different scales and degree of simplification. Specific discharge, in turn, is used to determine the timing of radionuclide transport.

The objective of the NRC staff's technical evaluation in this section is to determine the acceptability of the applicant's delineated flow paths and estimates of specific discharge (for both present and future conditions). The documents evaluated in this section come from SAR Section 2.3.9 and relevant supporting documents as cited in this section of the SER.

SER Section 2.2.1.3.8.4 discusses the staff's conclusion as to whether the requirements of 10 CFR 63.114 are met with respect to flow paths in the saturated zone.

2.2.1.3.8.3.1 System Description and Integration of Models Relevant to Flow Paths in the Saturated Zone

The applicant used multiple models at different scales to describe and quantify portions of the saturated zone groundwater flow system in the vicinity of the Yucca Mountain site. The NRC staff evaluates the roles of these models and their interdependencies in this section. The site of the proposed repository at Yucca Mountain is within the Death Valley regional groundwater flow system located in the southern part of the Great Basin, which in turn constitutes a subprovince of the larger Basin and Range physiographic province. At the regional scale, the Death Valley groundwater system reflects the arid climatic conditions and the complex geology of Basin and Range flow systems (SAR Section 2.3.9.2.1).

Groundwater in the regional system generally flows from recharge areas at high altitudes to the regional hydrologic sink in the bottom of Death Valley (SAR Section 2.3.9.2.1). The regional groundwater flow pattern is also conceptualized as a series of shallow and localized flow paths superposed on deeper regional flow paths (SAR Section 2.3.9.2.1).

In the Yucca Mountain region, groundwater flows from generally north to south, following these regional flow patterns. A relatively small amount of recharge occurs in the immediate vicinity of Yucca Mountain migrating downward through the unsaturated zone to the saturated zone. Once in the saturated zone, groundwater flows through a volcanic rock aquifer in the northern portions of the general flow system, transitioning into an alluvial aquifer system in the southern portions of the Yucca Mountain region. Beneath both the volcanic and alluvial aquifers is a carbonate rock aquifer (SAR Section 2.3.9.2.1).

The applicant indicated that at the regional scale, a significant amount of groundwater flows through the relatively permeable, laterally continuous, and thick carbonate aquifer, below volcanic and alluvial aquifers. On the basis of the regional geological framework and observations obtained from several drilled boreholes, the applicant concluded that an upward hydraulic head gradient generally exists between the carbonate aquifer and the overlying volcanic and alluvial aquifers (SAR Section 2.3.9.2.2.4), which indicates that vertical groundwater movement, to the extent it occurs, is upward rather than downward.

The applicant conceptualizes that the upward hydraulic gradient restricts groundwater flow paths originating from the proposed repository location to the shallower volcanic and alluvial aquifers, precluding radionuclides from entering the regional carbonate aquifer. The applicant also believes the upward gradient will be sustained during future climates and water uses (SAR Section 2.3.9.2.2.4).

At the site scale, the applicant stated that groundwater flow occurs from the recharge areas in the north, through the Tertiary volcanic aquifers into the valley-fill aquifer, and continues south toward the compliance boundary. The applicant used various site-scale saturated zone flow and transport models to predict groundwater flow paths and calculate the transport of radionuclides from their introduction at the water table below the proposed repository to the accessible environment. The applicant summarized the interdependencies and information exchanges among these models (SAR Figure 2.3.9-1). The nominal case site-scale saturated zone flow model is conceptualized, and input parameters determined, on the basis of information derived from *in-situ* field tests, the U.S. Geological Survey Death Valley Regional Groundwater Flow System Model (DVRGFSM; which provides recharge and boundary conditions), the applicant's site-scale hydrogeologic framework model, the applicant's site-scale unsaturated zone flow model, and expert elicitation (SAR Section 2.3.9.1).

The applicant's site-scale hydrogeologic framework model is a three-dimensional conceptual model of the spatial distribution of hydrogeologic units in the Yucca Mountain area. It covers an area of 1,350 km² [521 mi²] and a thickness of about 6 km [3.7 mi] (SNL, 2007a). Direct input to the site-scale hydrogeologic framework model consists of hydrogeologic information from the DVRGFSM; the applicant's site-scale geologic framework model, which was generated from the applicant's investigations; and lithostratigraphic interpretations and coordinates from the Nye County Early Warning Drilling Program (NC-EWDP)² boreholes (SNL, 2007a). Within the

²The Nye County Early Warning Drilling Program is a DOE-funded, Nye County-directed and -implemented hydrogeologic investigation program. The applicant used information from this program to supplement its own investigations.

site-scale hydrogeologic framework model, the applicant divided the Yucca Mountain geologic units into five basic saturated zone hydrogeologic units on the basis of similar hydrogeologic properties: upper volcanic aquifer, upper volcanic confining unit, lower volcanic aquifer, lower volcanic confining unit, and lower carbonate aquifer (SNL, 2007an). The applicant stated that certain characteristics affecting flow, primarily the porosity and permeability³ of the hydrogeologic units, are highly variable. To represent discrete features and regions having distinct hydrological properties within the model domain, the applicant identified and incorporated 10 hydrogeologic features into the flow model to represent such features as fault zones, hydrologic flow barriers, and zones of enhanced permeability (SNL, 2007ax).

The applicant's site-scale saturated zone flow model is a three-dimensional finite-element numerical model that simulates groundwater flow in the area defined by the site-scale hydrogeologic framework model (i.e., $30 \times 45 \times 6$ km [$18.6 \times 28.0 \times 3.7$ mi]). The applicant stated the flow model domain is sufficiently large to (i) assess groundwater flow and contaminant transport to the accessible environment, (ii) minimize boundary effects on flow magnitude and direction at Yucca Mountain, and (iii) include wells in the Amargosa Desert at the southern end of the modeled area (SAR Section 2.3.9.2.3.1). The site-scale saturated zone numerical flow model requires hydrogeologic information about the saturated zone flow system to predict flow magnitude and direction. The applicant also provided this information, which includes groundwater flux from the system boundaries and physical attributes of the geologic media, in SAR Section 2.3.9.

The applicant stated that the sources of surface recharge in the immediate vicinity of Yucca Mountain are precipitation and flood flows from Fortymile Wash and its tributaries (SAR Section 2.3.9.2.1). The site-scale saturated zone flow model obtains surface recharge information from the applicant's site-scale unsaturated zone flow model over the area that lies directly below the site-scale unsaturated zone flow model domain. The applicant used the 2004 version of the site-scale unsaturated zone flow model. However, the applicant stated that an updated site-scale unsaturated zone flow model has been developed and is used in other parts of the TSPA (SAR Section 2.3.9.2.2.3). The NRC staff evaluates the impact of using an older version of the site-scale unsaturated zone flow model to estimate surface recharge over the area directly below the site-scale unsaturated zone flow model domain in SER Section 2.2.1.3.8.3.2.

The applicant's three-dimensional site-scale saturated zone flow and transport abstraction model receives flow field information from the site-scale saturated zone flow model to generate 200 stochastic realizations of the flow field that reflect uncertainty in key parameters. The applicant prepared the input for each flow realization by scaling all permeability values in the site-scale saturated zone flow model using a scaling factor sampled stochastically from the probability distribution of a groundwater-specific discharge (GWSPD) multiplier. For permeability values within the volcanic aquifer hydrogeologic units, the applicant also sampled stochastically the horizontal anisotropy ratio (the ratio in the permeability in one horizontal principal direction relative to the permeability in a different principal direction, usually vertical). The steady-state groundwater flow solution for each realization was established by running the site-scale saturated zone flow model (SAR Section 2.3.9.3.4.1). After completing the 200 realizations using the site-scale saturated zone flow model, the resulting 200 flow fields were input to the site-scale saturated zone flow and transport abstraction model. These flow fields provided the TSPA model with 200 radionuclide unit mass breakthrough curves at the

³Permeability is one of the most important characteristics of geologic media that affects the rate at which fluids can move through the medium.

compliance boundary for 4 source subregions and 12 radionuclide groups, resulting in 9,600 breakthrough curves (SAR Figure 2.3.9-16). These breakthrough curves are evaluated in SER Section 2.2.1.3.9.

The one-dimensional saturated zone transport abstraction model, which provides the transport simulation capability for radionuclide daughter products resulting from decay and ingrowth, uses a simplistic one-dimensional representation of the three-dimensional saturated zone flows. The one-dimensional saturated zone transport abstraction model consists of three pipe segments. The first pipe segment is 5 km [3.1 mi] long. The lengths of the second and third pipe segments are estimated from particle tracking results of the three-dimensional saturated zone flow and transport abstraction model. The variable lengths account for uncertainty in the location of the volcanic/alluvial aquifer contact. Average, homogeneous material properties and specific discharges are specified within each pipe. The average specific discharge along each pipe segment is calculated by dividing the flow path length by the 50th percentile of particle travel times in Section 6.5.1 (BSC, 2005ak).

The NRC staff has evaluated the applicant's description of the saturated zone groundwater flow system in the vicinity of the proposed repository and the applicant's approach to integrate the multiple models used to quantify groundwater flow paths from the location of the proposed repository to the compliance boundary (b)(5)

(b)(5)

(b)(5)

The NRC staff's evaluation of the approach the applicant used to calibrate the site-scale saturated zone flow model is documented in SER Section 2.2.1.3.8.3.2.

The NRC staff evaluated the applicant's descriptions of relevant included FEPs and the manner in which they are included in the saturated zone flow models presented in SAR Section 2.3.9. The capability of the saturated zone to function as a barrier to delay radionuclide migration by slow advective flow and/or long transport distance depends on a number of processes and characteristics. The applicant identified a number of general characteristics and processes important to the function of the saturated zone barrier including stratigraphy, water-conducting features, faults, fractures, properties of host rock and other (alluvial) units, groundwater flow in

the geosphere (magnitude and direction of groundwater flow), advection and dispersion, climate change, matrix diffusion, and sorption (SAR Sections 2.1.1.3 and 2.3.9.1). Additionally, the applicant stated these types of characteristics and processes of the saturated zone have been included in saturated zone flow and transport models presented in SAR Section 2.3.9 (Saturated Zone Flow and Transport).

2.2.1.3.8.3.2 Sufficiency of Baseline Data to Justify Models of Flow Paths in the Saturated Zone

The applicant used site-specific data to develop and corroborate the conceptual model of groundwater flow in the saturated zone and to calibrate the site-scale saturated zone flow model. The site-specific data used include water-level measurements, *in-situ* hydrologic and tracer testing conducted in the vicinity of Yucca Mountain, regional hydrogeologic model predictions, and parameters from expert elicitation. The NRC staff evaluated the sufficiency of the applicant's baseline data used to develop predictions of flow paths and groundwater flow rates in the saturated zone in this section.

The NRC staff evaluated the sufficiency of geological data that were relevant to the hydrogeologic framework used in the site-scale saturated flow model. The applicant updated its site-scale hydrogeologic framework model to include stratigraphic information inferred from recently drilled Nye County wells (b)(5)

(b)(5)

(b)(5)

In the performance assessment model, the applicant stochastically varied the lateral extent of an alluvium uncertainty zone to propagate uncertainty associated with the tuff and alluvium contact. The NRC staff evaluates the applicant's approach to treat uncertainty associated with the tuff/alluvium contact in SER Section 2.2.1.3.8.3.3.

The NRC staff reviewed the test methods and results of the hydraulic and tracer tests the applicant conducted to corroborate its conceptualization of groundwater flow in the volcanic aquifers. These tests included several hydraulic and tracer tests (cross-hole tests) at the C-Wells Complex, consisting of boreholes UE-25 c#1, UE-25 c#2, and UE-25 c#3 (SAR Figure 2.3.9-7). The applicant concluded that flow in the volcanic rock units mainly occurs through a well-connected fracture network and that large-scale horizontal anisotropy of aquifer permeability exists in the saturated zone, which is preferentially oriented in a north-northeast direction. The open-hole surveys done at the C-Wells Complex also yielded information on stratigraphy, lithology, matrix porosity, fracture density, and the major flowing intervals.

(b)(5)

(b)(5)

The NRC staff reviewed the results of the hydraulic and tracer tests the applicant conducted to corroborate its conceptualization of groundwater flow in the alluvium. These tests included the hydraulic and tracer tests conducted at the Alluvial Testing Complex (centered at Nye County well NC-EWDP-19D), which is located along the simulated flow paths (SAR Section 2.3.9.2.4.2). The applicant indicated that the saturated alluvium significantly reduces the movement of radionuclides to the accessible environment. The alluvial aquifer is generally conceptualized as a homogeneous hydrogeologic unit in the site-scale saturated zone flow model, except near the Fortymile Wash area. Testing results described in SNL Section 7.2.2.3 (2007ax) from the Alluvial Testing Complex and Nye County well 22S indicated that alluvium permeabilities vary over two orders of magnitude. The applicant added a high-permeability zone—the Lower Fortymile Wash alluvial zone—to take into account “possible channelization” within the alluvium, as identified in SNL Section 6.4.3.7 (2007ba) and SAR Table 2.3.9-8. Similarly, the applicant accounted for the effect of alluvium spatial heterogeneity on radionuclide transport by varying the effective porosity parameter in its performance assessment code (b)(5)

(b)(5)

The NRC staff evaluated the sufficiency of water-level data the applicant used to calibrate its site-scale saturated zone flow model. The applicant used 161 time-averaged water-level measurements from 132 wells (multilevel measurements were obtained from some wells) within the model domain to (i) provide calibration targets for the site-scale saturated zone flow model, (ii) truncate the top of the flow model grid, and (iii) provide the boundary conditions around the perimeter of the model. The applicant stated that water-level calibration targets represent steady-state values and reflect current water uses wherever pumping takes place (SNL, 2007ax) (b)(5)

(b)(5)

Water Flow Between the Lower and Upper Aquifers

The applicant used water-level data from 17 wells to determine whether an upward gradient exists from the lower volcanic aquifer to the upper volcanic aquifer within the modeled domain (SAR Table 2.3.9-6). The applicant concluded that (i) a notable upward vertical gradient appears to exist between the lower and upper volcanic aquifer at locations nearest Yucca Mountain and (ii) the direction of the vertical hydraulic gradient varies from location to location away from Yucca Mountain (SNL, 2007ax).

The NRC staff evaluated the methodology and the sufficiency of data the applicant used to establish the boundary conditions of the site-scale saturated zone flow model. The applicant derived constant-head boundary conditions from water-level data. In Section 6.3.1.5 (SNL,

2007ax), the applicant stated that coverage of water-level measurements was insufficient to specify depth-dependent head boundaries. In SAR Section 2.3.9.2.3.1, the applicant indicated that vertical gradients develop internally in the model domain in response to geohydrologic conditions and the calibrated model is capable of representing the upward vertical gradients observed between the deeper regional carbonate aquifer and overlying volcanic aquifers. The applicant supplemented the SAR with a contour map of vertical hydraulic gradient distributions simulated by the site-scale saturated zone flow model, as shown in Figure 1.1 (DOE, 2009bc).

(b)(5)

Recharge Data

The NRC staff reviewed the sufficiency of recharge data used in the applicant's site-scale saturated zone flow model. The applicant used recharge derived from a now-obsolete version of the site-scale unsaturated zone flow model. (b)(5)

(b)(5)

(b)(5)

Surface recharge for other portions of the upper boundary within the domain of the site-scale saturated zone flow model was derived from the DVRGFSM model and measured stream losses along Fortymile Wash. (b)(5)

(b)(5)

Vertical Anisotropy of Permeability

Vertical anisotropy of permeability is fixed at a ratio of 10:1 on the basis of information the expert elicitation panel provided (CRWMS M&O, 1998ac). In an alternative conceptual model, the applicant considered the effect of vertical anisotropy on simulated flow paths. (b)(5)

(b)(5)

Site-Scale Model Calibration

The applicant calibrated the site-scale saturated zone flow model using an industry-standard parameter estimation program (PEST) followed by manual adjustments. (b)(5)

(b)(5)

After calibrating the site-scale model using the PEST program, manual adjustments were made to several zones to improve model match. The calibrated site-scale saturated zone flow model has a weighted root-mean-square (RMS) residual of 0.82 m [2.7 ft] (calculated using differences

between observed and simulated heads). SAR Figure 2.3.9-13 shows locations of all water-level measurements and calibration residuals (i.e., differences between simulated and observed water levels at the calibration target locations). (b)(5)

(b)(5)

The NRC staff notes that the purpose of model calibration is to provide parameter estimates for a given conceptual model and is not intended to resolve uncertainties in model conceptualization (e.g., uncertainty in stratigraphy). Thus, the applicant considered different alternative conceptual models to address model uncertainties. The staff evaluates the applicant's treatment of model uncertainty and alternative conceptual models in SER Sections 2.2.1.3.8.3.4 and 2.2.1.3.8.3.5.

The NRC staff has evaluated the data the applicant used to develop and corroborate the conceptual model of groundwater flow in the saturated zone and to calibrate and validate the site-scale saturated zone flow model. (b)(5)

(b)(5)

2.2.1.3.8.3.3 Uncertainty in Data Used in Models of Flow Paths in the Saturated Zone

Uncertainties in model input parameters may directly affect the advective flow rate of groundwater and lengths of groundwater flow paths predicted by the applicant's nominal case site-scale saturated zone flow model. In the performance assessment evaluation, the applicant incorporated the uncertainty in model parameter inputs by stochastically sampling values from probability distributions of the GWSPD multiplier, horizontal anisotropy in permeability, flowing interval spacing and fracture porosity in the volcanic units, effective porosity in the alluvium, and longitudinal dispersivity, as identified in Section 6.3 (SNL, 2007ax). This SER section focuses on reviewing the applicant's methodologies for developing probability distributions of the specific discharge multiplier and horizontal anisotropy in permeability. The NRC staff evaluates the other uncertain model parameter inputs relevant to radionuclide transport calculations in SER Section 2.2.1.3.9.

Specific Discharge Values and Multiplier

To incorporate uncertainty in specific discharge in model abstractions, the applicant generated multiple realizations of the three-dimensional saturated zone flow field (refer to SER Section 2.2.1.3.8.3.1 for additional discussion on the interdependencies of the different saturated zone abstraction models). For each realization, the applicant scaled (i) the values of recharge and all values of permeability simultaneously using a stochastically sampled specific discharge multiplier and (ii) the values of north-south and east-west permeability within the zone of volcanic rocks using a stochastically sampled horizontal anisotropy ratio.

The applicant established a probability distribution for the GWSPD multiplier, whose function is to capture the range in variability and uncertainty in the parameters that generate the specific discharge calculations. In turn the specific discharge calculations provide the basis from which groundwater travel times and radionuclide mass breakthrough curves are generated (SAR Section 2.3.9.2.3.3).

The uncertainty range and probability distribution for the GWSPD multiplier was originally obtained through an expert elicitation process (CRWMS M&O, 1998ac). The expert elicitation panel suggested a truncated log-normal distribution ranging from 0.01 to 10. The median specific discharge derived from the expert elicitation process is 0.6 m/yr [2 ft/yr], as defined in Section 3.2 (CRWMS M&O, 1998ac). On the basis of recent tracer tests performed at the Alluvial Testing Complex and Nye County well cluster 22S, the applicant reduced the range of uncertainty of the specific discharge multiplier using a Bayesian update procedure, where the range the expert elicitation panel supplied was assumed as a prior probability distribution and the estimated specific discharges from the Alluvial Testing Complex were used to estimate a log-normal likelihood function.

The NRC staff reviewed the Bayesian update procedure the applicant used and (b)(5)

(b)(5)

(b)(5)

In

Figure 1-1 (DOE, 2009bc), the applicant provided additional information explaining the rationale for using the Bayesian statistical procedure, stating that (i) each combination of interpretation method and effective porosity value provides an independent and equally likely outcome and (ii) the 12 data values follow approximately a log-normal distribution. (b)(5)

(b)(5)

The applicant used specific discharge estimates derived from alluvium testing to update the specific discharge multiplier that is subsequently applied to the entire flow model. The applicant conceptualized fluid flow in volcanic tuff aquifers differently from the alluvium. The former is dominated by flow in well-connected fractures, while the latter is a porous medium. The Bayesian prior distribution the expert elicitation panel provided was based on tests performed at the C-Wells Complex, which were conducted in volcanic aquifers. (b)(5)

(b)(5)

As a final result, the applicant obtained a truncated log-normal distribution for the specific discharge multiplier that ranges from 1/8.93 to 8.93 (BSC, 2005ak). (b)(5)

(b)(5)

(b)(5) In response to a request for additional information (RAI), the applicant (DOE, 2009bc) stated that (i) variations in mean specific discharge along the flow paths have been captured in the baseline, three-dimensional site-scale flow model and (ii) it is inappropriate to directly use specific discharge data from alluvial testing to update the expert elicitation estimates; instead, the update should be performed after normalization (i.e., the specific discharge multiplier). (b)(5)

(b)(5)

Horizontal Anisotropy

The NRC staff reviewed the probability distribution the applicant established for the horizontal anisotropy of permeability. The applicant stated in Section 6.2.6 (SNL, 2007aw) that hydraulic testing at the C-Wells Complex indicated significant flow anisotropy at larger scales in the fractured volcanic tuffs. In SAR Section 2.3.9.2.2.1, the applicant indicated the horizontal anisotropy ratio is estimated using different methods and the ratio ranges from 3.3 to 17, with directionality orienting flow paths more north-south than east-west. The cumulative distribution function for the horizontal anisotropy ratio, which has lower and upper bounds of 0.05 and 20, respectively, is specified through a tabulated form in the performance assessment model.

(b)(5)

(b)(5)

Potentially Undetected Fast Flow Paths

The NRC staff reviewed the applicant's conceptualization of the alluvial aquifers as homogeneous hydrogeologic units. (b)(5)

(b)(5)

(b)(5)

The applicant stated that the suite of performance assessment transport simulations encompasses the range of behavior that would be obtained with a fault-based flow and transport model and other alternative conceptual models that explicitly model fast-flow paths (e.g., channeling in the alluvium) (SAR Section 2.3.9.2.3.5). The applicant stated that the potential impacts of undetected features on groundwater flow are incorporated in the site-scale saturated zone flow and transport abstraction model through parameter distributions, which ultimately propagate to the TSPA model through variation in radionuclide breakthrough curves (BSC, 2005ak). The key parameters the applicant used to assess the effect of undetected features on radionuclide transport are (i) specific discharge, (ii) porosity, (iii) flowing interval spacing in the volcanic rocks, (iv) longitudinal dispersion, (v) horizontal anisotropy of permeability, (vi) alluvial bulk density, and (vii) sorption coefficients for the nine classes of radionuclides modeled in both the alluvium and volcanic units (BSC, 2005ak). (b)(5)

(b)(5)

Volcanic and Alluvial Aquifer Contact Zone

The applicant introduces an alluvium uncertainty zone in TSPA model to treated uncertainty associated with the contact location between volcanic aquifer and the alluvium. On the basis of drilling records, the applicant conceptualizes the uncertainty zone as a quadrilateral area in which the boundary between volcanic units and alluvium is randomly varied among realizations. The boundaries of the alluvium uncertainty zone are determined for a particular realization by the parameters FPLAW (western boundary) and FPLAN (northern boundary) in the applicant's one-dimensional saturated zone transport abstraction model. These parameters have uniform distributions from 0.0 to 1.0, where a value of 0.0 corresponds to the minimum extent of the uncertainty zone and 1.0 corresponds to the maximum extent of the uncertainty zone in a westerly direction and northerly direction, respectively (SNL, 2007ax). Thus, in the one-dimensional transport abstraction model, the flow path length of each pipe segment varies as a function of the horizontal anisotropy, the western boundary of the alluvial uncertainty zone, and the region from which the radionuclide source originates beneath the repository.

(b)(5)

(b)(5)

An expert elicitation process was used to obtain a probability distribution for the specific discharge multiplier (now considered prior distribution) and vertical anisotropy ratio. The NRC staff reviewed the information the expert elicitation panel provided. (b)(5)

(b)(5)

The NRC staff evaluates the applicant's consideration of model uncertainty and model support in SER Sections 2.2.1.3.8.3.4 and 2.2.1.3.8.3.5.

(b)(5)

2.2.1.3.8.3.4 Uncertainty in Flow Paths in the Saturated Zone Models

In this section, the NRC staff evaluates the alternative conceptual models the applicant used to assess model uncertainties for the saturated zone flow paths, as presented in SAR Section 2.3.9.2.3.4. The applicant used five alternative conceptual models to assess the significance of model uncertainties of certain features and processes in the abstraction, including: (i) vertical anisotropy, (ii) horizontal anisotropy, (iii) permeability in the northern high-gradient region of Yucca Mountain, (iv) increased vertical permeability of the Solitario Canyon Fault, and (v) climate-induced water table rise.

The site-scale saturated zone flow model that the applicant used to develop the performance assessment abstraction uses a 10:1 anisotropy ratio for horizontal-to-vertical permeability in volcanic and valley-fill alluvium units. This vertical anisotropy ratio was originally suggested from an expert elicitation panel (CRWMS M&O, 1998ac) because reduced vertical permeability is inherent in any layered groundwater flow system. To test whether this assumption leads to any systematic bias, the applicant considered an alternative model with vertical permeability equal to the horizontal permeability. This alternative model resulted in a 28 percent increase in calculated specific discharge at a location 5 km [3.1 mi] downgradient from the proposed repository boundary and also resulted in a near doubling of the weighted RMS calibration error.

(b)(5)

The NRC staff reviewed the alternative model the applicant used to demonstrate the sensitivity of the nominal case site-scale saturated zone model to horizontal anisotropy. The applicant's analysis demonstrated that removal of horizontal anisotropy (i.e., assuming isotropic horizontal permeability) results in a 31 percent decrease in modeled specific discharge rates across the 5-km [3.1-mi] boundary and shifts the flow paths eastward. (b)(5)

(b)(5)

(b)(5) On the basis of this analysis, the applicant included a range of horizontal anisotropy ratios for saturated zone flow and transport model abstraction. (b)(5)

(b)(5)

The NRC staff reviewed another alternative modeling analysis by the applicant in which the applicant removes the large hydraulic gradient north of the proposed repository area by increasing permeability in this region. This alternative model results in a 15-fold increase in calculated specific discharge 5-km [3.1-mi] downgradient from the proposed repository and an eightfold increase in RMS calibration error. On the basis of this result, the applicant concluded that, although the cause of the high gradient is not entirely certain, it is nevertheless important to represent this feature in the model. (b)(5)

(b)(5)

The NRC staff evaluated the applicant's alternative model used to examine the potential effects of vertical anisotropy in the permeability of the Solitario Canyon fault. Such anisotropy could support along-fault flow or upward flow at the fault while acting as a barrier to cross-fault flow.

(b)(5)

The site-scale saturated zone flow model the applicant used to develop the abstracted flow paths for the performance assessment does not consider explicitly the effect of an elevated water table under future, wetter climate conditions. Instead, the applicant incorporates the effect of long-term climate change by applying a scaling factor to instantly increase the volumetric flow rate or specific discharge. The scaling factors for monsoonal and glacial-transition climatic conditions are 1.9 and 3.9, respectively. To demonstrate that this simplified approach for including effect of climate change does not bias results, the applicant provided an alternative evaluation of the potential effects of water table rise on abstracted flow paths. On the basis of an estimated increase in specific discharge by a factor of 3.9 for the glacial-transition climate state, the applicant estimated the increased hydraulic gradient necessary to drive this increased groundwater flow would result in a water table rise of

approximately 20 m [66 ft] at the southern end of the model area that gradually increases to about 50 m [160 ft] in the area below the proposed repository location and as much as 100 m [328 ft] in areas north of the repository. Projecting this linear increase in water table elevation onto the hydrogeologic framework model indicates that elevated flow paths could travel a greater proportion of distance through the lower permeability Calico Hills formation in the volcanic tuffs, which could result in longer travel times. The applicant, therefore, concluded that using present-day water table elevations combined with a scaling factor approach to increase specific discharge estimates for future climates sufficiently approximates the performance-affecting aspects of future, wetter climate conditions. (b)(5)

(b)(5)

In SAR Section 2.3.9.2.3.5, the applicant provided qualitative consideration of several additional model uncertainties that could affect estimates of specific discharge. These considerations and the NRC staff's review are summarized in the following paragraphs.

The NRC staff evaluated the applicant's treatment of uncertainty in the hydrogeologic contact surfaces (as in the hydrogeologic framework model) represented in the model. The applicant explained that horizontal contact-surface uncertainty would have a lesser effect on specific discharge compared to uncertainty of contact surfaces in the vertical direction. The applicant concluded that the potential effect of this model uncertainty is within the bounds of uncertainty considered for the specific discharge uncertainty multiplier parameter used in the performance assessment. (b)(5)

(b)(5)

The NRC staff evaluated the applicant's consideration of model uncertainty related to the potential for a fault-dominated flow system with specific discharge focused in flow paths along major fault systems. (b)(5)

(b)(5)

(b)(5)

Numerous realizations in the performance assessment produce transport times for nonsorbing solutes on the order of 10–100 years for the glacial-transition climate state (SAR Section 2.3.9.3.4.1 and Figure 2.3.9-16). (b)(5)

(b)(5)

(b)(5)

(b)(5)

2.2.1.3.8.3.5

Model Support Based on Comparison With Alternative Models or Other Information

In SAR Section 2.3.9.2.4, the applicant presented its use of objective comparisons to build confidence in the saturated zone flow model abstraction. In this section, the NRC staff review focuses on support for the range of flow paths and specific discharge estimates considered for the saturated zone flow and transport model abstraction on the basis of relative importance to overall system performance.

The NRC staff reviewed information the applicant used to support model-simulated groundwater flow paths. This information includes a comparison of simulated water-level elevations to those observed in wells not used in the model calibration (e.g., NC-EWDP Phase V data) (SAR Table 2.3.9-9). This comparison shows the largest differences between simulated and observed water levels generally occur in areas of steep hydraulic gradients near geologic features, such as the U.S. Highway 95 fault and the Solitario Canyon fault. Residual errors between observed and simulated water levels are generally smaller in the areas of simulated flow paths from the repository to the compliance boundary. The highest residual errors are generally in areas where water levels change by tens of meters (1 m = {3.28 ft}) over short distances, and the overall range of residual errors is shown to be similar to the range of errors obtained during the site-scale saturated zone model calibration (SAR Figure 2.3.9-13). SNL (2007ax) described the calibration and confidence-building process.

(b)(5)

The applicant discussed analyses by Freifeld, et al. (2006aa) of testing done in Nye County well 24PB that provides a range of estimates for specific discharge at the top of the Crater Flat

tuff unit in the transition area from the volcanic aquifer to the valley-fill alluvial aquifer. On the basis of fluid electrical conductivity logging and distributed thermal perturbation sensor measurements, and assuming a porosity of 0.01, the estimated specific discharge in the flowing intervals ranged from 5–310 m/yr [16–1,018 ft/yr], as identified in Section 3.3.3 and Table 4 (Freifeld, et al., 2006aa). The upper end of this range is significantly greater than the specific discharge rates considered in the performance assessment. The applicant stated the high flow rate was observed in a relatively narrow interval of the borehole and that upscaling this estimate using an assumed median flow interval spacing of 25.8 m [84.6 ft] (from the parameter uncertainty distribution) reduces the estimated specific discharge to a range of 0.07–4.1 m/yr [0.2–13.5 ft/yr].

(b)(5)

The applicant also provided model support for estimates of potential future water table rise during future climates. This support included observations of mineralogical alteration and analysis of the strontium isotope ratio in calcite veins in the saturated and unsaturated rocks beneath the proposed repository footprint. This information is interpreted to indicate a past water table rise of approximately 85 m [278 ft] above present-day conditions beneath the proposed repository. Modeling studies using different assumptions about future recharge (Czarnecki, 1985aa; D'Agnese, et al., 1999aa) produce water-table-rise estimates from 130 to 150 m [427 to 492 ft] above present conditions beneath the repository. On the basis of this supporting information, the applicant's performance assessment included a 120-m [394-ft] water table rise for the unsaturated zone flow and transport model abstraction. In the saturated zone flow and transport model abstraction, however, future water table water rise is not explicitly considered. Rather, the applicant used an assumed rise of 85 m [278 ft] beneath the repository in an alternative conceptual model analysis to demonstrate the effect on saturated zone groundwater flow paths is not significant (see SER Section 2.2.1.3.8.3.4 for NRC staff review of this model uncertainty). South of the proposed repository near the compliance boundary, the maximum extent of water table rise is constrained to approximately 30 m [98 ft] by the ground surface elevation and observed evaporite deposits at locations where springs flowed during past occurrences of elevated water table (SAR Section 2.3.9.2).

Observations from well UE-25p#1 the applicant cited as model support show the hydraulic head is 21 m [69 ft] higher in the carbonate aquifer system compared to the overlying volcanic aquifer

system. The two aquifer systems are separated by a thick low-permeability aquitard. The calibrated site-scale saturated zone flow model reproduces this upward hydraulic gradient at well UE-25p#1, but with a lesser magnitude of a 6-m [20-ft] head difference across the aquitard unit. The NRC staff notes that, in addition to well UE-25p#1, the presence of this upward gradient along the area of model-simulated groundwater flow paths is also supported by observations in well NC-EWDP-2DB. The applicant stated that these wells, which show an upward vertical gradient, are assigned a weight factor of 10 during model calibration to ensure the model will match the upward gradient. However, this statement appeared to be inconsistent with other information in the SAR where the applicant apparently assigned a weight factor of 20 to UE-25 p#1 and a weight factor of 1 to Nye County well 2DB. In response to the staff's RAI, the applicant confirmed the actual weight factors used in the model calibration were 10 for both well locations. The applicant agreed to make changes in SAR Section 2.3.9.2.3.2 and the related supporting report (SNL, 2007ax) to reflect the actual values used.

The NRC staff has evaluated the approaches the applicant used to compare performance assessment output to process-level model outputs and/or empirical studies (b)(5)

(b)(5)

(b)(5)

2.2.1.3.8.4 Evaluation Findings

The NRC staff reviewed the applicant's SAR and other information submitted in support of the license application and finds that, with respect to the requirements of 10 CFR 63.114 for consideration of flow paths in the saturated zone (b)(5)

(b)(5)

(b)(5)

2.2.1.3.8.5 References

BSC. 2005ak. "Saturated Zone Flow and Transport Model Abstraction." MDL-NBS-HS-000021. Rev. 03. AD 01, AD 02, ERD 01. Las Vegas, Nevada: Bechtel SAIC Company, LLC.

CRWMS M&O. 1998ac. "Saturated Zone Flow and Transport Expert Elicitation Project." SL5X4AM3. Las Vegas, Nevada: CRWMS M&O.

Czarniecki, J.B. 1985aa. "Simulated Effects of Increased Recharge on the Groundwater Flow System of Yucca Mountain and Vicinity, Nevada-California." U.S. Geological Survey Water Resources Investigations Report 84-4344.

D'Agnese, F.A., G.M. O'Brien, C.C. Faunt, and C.A. San Juan. 1999aa. "Simulated Effects of Climate Change on the Death Valley Regional Ground-Water Flow System, Nevada and California." U.S. Geological Survey Water-Resources Investigations Report 98-4041.

DOE. 2009an. "Yucca Mountain—Response to Request for Additional Information Regarding License Application (Safety Analysis Report Section 2.1), Safety Evaluation Report Vol. 3, Chapter 2.2.1.1, Set 1." Letter (February 6) J.R. Williams to J.H. Sulima (NRC). ML090400455. Enclosures (7). Las Vegas, Nevada: DOE, Office of Civilian Radioactive Waste Management.

DOE. 2009bc. "Yucca Mountain—Response to Request for Additional Information Regarding License Application (Safety Analysis Report Section 2.3.9.2.2 and 2.3.9.2.3), Safety Evaluation Report Volume 3, Chapter 2.2.1.3.8, Set 1." Letter (January 30) J.R. Williams to J.H. Sulima (NRC). Enclosures (3): Numbers 1, 2, and 3. Las Vegas, Nevada: DOE, Office of Civilian Radioactive Waste Management.

DOE. 2008ab. DOE/RW-0573, "Safety Analysis Report Yucca Mountain Repository License Application." Rev. 00. Las Vegas, Nevada: DOE, Office of Civilian Radioactive Waste Management.

Ferrill, D.A., J. Winterle, G. Wittmeyer, D. Sims, S. Colton, A. Armstrong, and A.P. Morns. 1999aa. "Stressed Rock Strains Groundwater at Yucca Mountain, Nevada." *GSA Today*. Vol. 9, No. 5. pp. 1–8.

Freifeld, B., C. Doughty, and S. Finsterle. 2006aa. "Preliminary Estimates of Specific Discharge and Transport Velocities Near Borehole NC-EWDP-24PB." LBNL-60740. Berkeley, California: Lawrence Berkeley National Laboratory.

NRC. 2009ab. "Division of High-Level Waste Repository Safety Director's Policy and Procedure Letter 14: Application of YMRP for Review Under Revised Part 63." Published March 13, 2009. ML090850014. Washington, DC: NRC.

NRC. 2003aa. NUREG-1804, "Yucca Mountain Review Plan—Final Report." Rev. 2. Washington, DC: NRC.

SNL. 2008ab. "Features, Events, and Processes for the Total System Performance Assessment: Analyses." ANL-WIS-MD-000027. Rev. 00. ACN 01, ERD 01, ERD 02. Las Vegas, Nevada: Sandia National Laboratories.

SNL. 2007an. "Hydrogeologic Framework Model for the Saturated Zone Site-Scale Flow and Transport Model." MDL-NBS-HS-000024. Rev. 01. ERD 01. Las Vegas, Nevada: Sandia National Laboratories.

SNL. 2007aw. "Saturated Zone *In-Situ* Testing." ANL-NBS-HS-000039. Rev. 02. ACN 01, ACN 02, ERD 01. Las Vegas, Nevada: Sandia National Laboratories.

SNL. 2007ax. "Saturated Zone Site-Scale Flow Model." MDL-NBS-HS-000011. Rev. 03. ACN 01, ERD 01, ERD 02. ERD 03. Las Vegas, Nevada: Sandia National Laboratories.

SNL. 2007ba. "Site-Scale Saturated Zone Transport." MDL-NBS-HS-000010. Rev. 03. ACN 01, AD 001. Las Vegas, Nevada: Sandia National Laboratories.

Spitz, K. and J. Moreno. 1996aa. "A Practical Guide to Groundwater and Solute Transport Modeling." New York City, New York: John Wiley & Sons.

Sun, A., R. Ritzi, and D. Sims. 2008aa. "Characterization and Modeling of Spatial Variability in a Complex Alluvial Aquifer: Implication on Solute Transport." *Water Resources Research*. Vol. 44, W04402, doi:10.1029/2007WR006119.

Winterle, J.R. 2005aa. "Simulation of Spring Flows South of Yucca Mountain, Nevada, Following a Potential Future Water Table Rise." ML052630242 San Antonio, Texas: CNWRA.

Winterle, J.R. and D.A. Farrell. 2002aa. "Hydrogeologic Properties of the Alluvial Basin Beneath Fortymile Wash and Amargosa Valley, Southern Nevada." San Antonio, Texas: CNWRA.

Winterle, J.R., A. Claisse, and H.D. Arlt. 2003aa. "An Independent Site-Scale Groundwater Flow Model for Yucca Mountain." Proceedings of the 10th International High-Level Radioactive Waste Management Conference (IHLRWM), Las Vegas, Nevada, March 30–April 2, 2003. La Grange Park, Illinois: American Nuclear Society. pp. 151–158.

CHAPTER 12

2.2.1.3.9 Radionuclide Transport in the Saturated Zone

2.2.1.3.9.1 Introduction

This Safety Evaluation Report (SER) chapter addresses the U.S. Department of Energy's (DOE's) model abstraction¹ for transport of radionuclides in the saturated zone (SZ). DOE presented its description of this abstraction in Safety Analysis Report (SAR) Section 2.3.9 of its license application (DOE, 2008ab). Radionuclide transport in the SZ is a key process in the performance assessment for the proposed geologic repository at Yucca Mountain, Nevada. The performance assessment includes the flow of water from precipitation falling on Yucca Mountain, its migration as groundwater through the unsaturated zone (UZ) above and below the repository, and the flow of groundwater in the SZ through the controlled environment to the accessible environment. This groundwater flow is the principal means by which radionuclides released from the repository are transported to the accessible environment. Because exposure to groundwater contaminated with radionuclides from the repository is one of the principal contributors to dose to the reasonably maximally exposed individual (RMEI), the performance assessment must include those components that affect significantly the timing and magnitude of transport for any radionuclides released from the repository. Radionuclide transport in the SZ, as described in SAR Section 2.3.9, includes the features, events, and processes (FEPs) that affect the movement of radionuclides from where they enter the SZ below the repository to the accessible environment boundary, approximately 18 km [11.18 mi] south of the repository, and their implementation (or abstraction) in the Total System Performance Assessment (TSPA).

The SZ radionuclide transport abstraction receives information about the time-dependent flux of radionuclides released from the UZ to the water table below the repository. In turn, the SZ radionuclide transport abstraction provides information about the mass flux and arrival or transport times of radionuclides moving through the SZ to the representative volume in the accessible environment.

This chapter provides the U.S. Nuclear Regulatory Commission's (NRC's) evaluation of DOE's representation of radionuclide transport in the SZ as part of its performance assessment. Because DOE represented the barriers to radionuclide migration in the SZ in terms of radionuclide transport processes and how the processes were influenced by the natural features of the SZ, this chapter is organized by the major, risk-significant processes affecting transport.

2.2.1.3.9.2 Regulatory Requirements

Model abstractions used in the applicant's postclosure performance assessment must meet the regulatory requirements given in 10 CFR 63.114 (Requirements for Performance Assessment) and 63.342 (Limits on Performance Assessment), to support the predictions of compliance for 63.113 (Performance Objectives for the Geologic Repository after Permanent Closure). Specific compliance with 63.113 is reviewed in SER Section 2.2.1.4.1.

¹The term "abstraction" is defined as a representation of the essential components of a process model into a suitable form for use in a total system performance assessment. Model abstraction is intended to maximize the use of limited computational resources while allowing a sufficient range of sensitivity and uncertainty analyses.

The requirements for performance assessment in 10 CFR 63.114 require the applicant to

- Include appropriate data related to the geology, hydrology, and geochemistry of the surface and subsurface from the site and the region surrounding Yucca Mountain
- Account for uncertainty and variability in the parameter values used to model radionuclide transport in the SZ
- Consider alternative conceptual models for radionuclide transport in the SZ
- Provide technical bases for the inclusion of FEPs affecting radionuclide transport in the SZ, including effects of degradation, deterioration, or alteration processes of engineered barriers that would adversely affect performance of the natural barriers, consistent with the limits on performance assessment in 10 CFR 63.342
- Provide technical basis for the models of radionuclide transport in the SZ that in turn provide input or otherwise affect other models and abstractions

10 CFR 63.114(a) considers performance assessment for the initial 10,000 years following permanent closure. 10 CFR 63.114(b) and 63.342 consider the performance assessment methods for the time from 10,000 years through the period of geologic stability, defined in 10 CFR 63.302 as 1 million years following disposal. These sections require that through the period of geologic stability, with specific limitations, the applicant:

- Use performance assessment methods consistent with the performance assessment methods used to demonstrate compliance for the initial 10,000 years following permanent closure
- Include in the performance assessment those FEPs used in the performance assessment for the initial 10,000 year period

NRC staff review of the license application follows the guidance laid out in the Yucca Mountain Review Plan (YMRP), NUREG-1804, Section 2.2.1.3.9, Radionuclide Transport in the Saturated Zone (NRC, 2003aa), as supplemented by additional guidance for the period beyond 10,000 years after permanent closure (NRC, 2009ab). The acceptance criteria in the YMRP generically follow 10 CFR 63.114(a). Following the guidance, the NRC staff review of the applicant's abstraction of radionuclide transport in the SZ considered five criteria

- System description and model integration are adequate.
- Data are sufficient for model justification.
- Data uncertainty is characterized and propagated through the abstraction
- Model uncertainty is characterized and propagated through the abstraction
- Model abstraction output is supported by objective comparisons.

Because 10 CFR Part 63 specifies the use of a risk-informed approach for the review of a license application, the guidance provided by YMRP, as supplemented by NRC (2009ab), is followed to the extent reasonable for aspects of radionuclide transport in the SZ important to repository performance. Whereas NRC staff considered all five criteria in their review of information provided by DOE, only aspects that substantively affect results of the performance assessment, as judged by NRC staff, are discussed in this chapter. NRC staff's judgment is

based both on risk information provided by DOE, and staff's knowledge, experience, and independent analyses.

2.2.1.3.9.3 Technical Review

DOE provided information in SAR Section 2.3.9, relevant references, and responses to NRC staff requests for additional information, that it uses to predict the transport of radionuclides in the SZ, from below the repository to the accessible environment. The NRC staff's technical review focuses on (i) how DOE represented the geological, hydrological, and geochemical features of the SZ in a framework for modeling the transport processes; (ii) how DOE integrated the SZ transport abstraction with other Total System Performance Assessment (TSPA) abstractions for performance assessment calculations, and (iii) how DOE included and supported important transport processes in process-level transport models and in the SZ radionuclide transport abstraction.

2.2.1.3.9.3.1 Conceptual Model and Model Framework

DOE related Yucca Mountain site characteristics to a conceptual model of the SZ from beneath the repository to the accessible environment boundary in which the flow of water would transport released radionuclides through fractures, major faults, and porous alluvium. DOE used the same three-dimensional model grid for SZ transport modeling as for the site-scale SZ flow model (SAR Section 2.3.9.2, SER Section 2.2.1.3.8). There are two primary geological units through which water flows in the SZ: fractured volcanic tuff and alluvium. Unlike the UZ, where flow in the volcanic tuff occurs in fractures, faults, and matrix, the applicant models flow in volcanic tuff of the SZ to occur only through fractures and faults. Water in the volcanic tuff matrix is connected to water in the fractures but is considered stagnant (flow velocities in the matrix are extremely low relative to the fast-flowing fractures)

DOE simulated the transport of radionuclides as dissolved species and as species sorbed to mobile, colloid-sized particles. These two modes of transport are subject to various physical and chemical processes that affect their transport in groundwater. DOE identified advection, dispersion, sorption and matrix diffusion, colloidal transport, and radionuclide decay and ingrowth as important transport-affecting processes, and incorporated these processes in the numerical models of radionuclide transport (SAR Table 2.3.9-1). DOE's conceptual model described how each of the transport-affecting processes influences the rate at which radionuclides travel through the SZ model relative to the rate that water travels (SAR Section 2.3.9.2). DOE used sensitivity analyses and single-realization analyses of TSPA simulations to demonstrate how the SZ transport abstraction integrated specific processes with the natural features of the SZ to slow the migration of radionuclides through the SZ, as detailed in SAR Section 2.1.2.3.6 and Section 6.3.10 of SNL (2008ag)

(b)(5)

(b)(5)

On the basis of field and modeling evidence, DOE determined groundwater flow and migration of radionuclides in the SZ would begin in fractured volcanic rock beneath the repository and travel southeasterly toward Fortymile Wash before turning in a southerly direction beneath the wash to the accessible environment, approximately 18 km [11.18 mi] south of the repository. About 10 km [6.21 mi] south of the repository along this path, the water and radionuclides are expected to flow from the volcanic rock and enter the alluvium. The location of the transition from volcanic rock to alluvium is a key geologic data uncertainty in DOE's transport abstraction (BSC, 2005ak). This uncertainty was incorporated in DOE's model as an alluvium uncertainty zone, which was constrained by geologic data from Nye County Early Warning Drilling Program (EWDP) wells. The length of travel of radionuclides in the volcanic rock or alluvium is dependent on the source zone (location of release from the repository), the value of horizontal anisotropy in permeability, and the size of the alluvium uncertainty zone.

In DOE's model, the two geologic media encountered in the SZ, fractured volcanic rock and alluvium, are expected to have very different effects on water flow and radionuclide transport. The fractured volcanic rock has low porosity (void space) and sparsely distributed fractures that control flow and transport. Consequently, the water and radionuclides move relatively quickly through fractures in the volcanic rock. The sparse distribution of fractures limits interactions between the radionuclides and the rock that could slow radionuclide transport. In contrast, the alluvium behaves and was modeled as a porous medium, with significantly higher porosity than the volcanic rock. Consequently, water moves more slowly through the alluvium. Because of the way in which the alluvium was deposited, some preferential flow paths could exist in buried gravel deposits. DOE accounted for these potential higher velocity flow paths by including effective porosity as an uncertain parameter, with a range of values to accommodate these features in the model abstraction (BSC, 2005ak). Consistent with results from field-based transport testing (SNL, 2007aw), DOE did not take credit for one of the retardation processes, matrix diffusion, that might result from the dual porosity aspect of the alluvial system.

DOE modeled radionuclide release from the UZ into the SZ as occurring at one to four point sources near the water table. The point source locations were randomly sampled from within each of the four corresponding UZ source regions that generally represented preferential flow pathways in the UZ flow model.

In the applicant's TSPA model, two model abstractions of SZ flow and transport were implemented. The primary model of radionuclide transport in the SZ was a site-scale, three-dimensional, single (effective)-continuum, dual-porosity, particle-tracking transport model. The dual-porosity aspect allowed for consideration of matrix diffusion in fractured volcanic tuff. The two porosities refer to those of the fractures and of the matrix, while the effective continuum aspect of the approach allowed the applicant to assign average values to flow and transport parameters applied to cells of the numerical model representing the system. Radionuclides were subdivided into 12 groups on the basis of their similar transport characteristics. The three-dimensional model abstraction used flow fields and other hydrologic characteristics defined by the three-dimensional SZ flow model and calculated unit breakthrough curves for each of the 12 radionuclide groups transported in the SZ. The three-dimensional model was

run, and the unit breakthrough curves were developed and stored external to the TSPA model, as outlined in Section 6.3.10 of SNL (2008ag).

The second SZ model abstraction was a one-dimensional transport model. The main purpose of the one-dimensional model was to calculate the radioactive decay, ingrowth, and transport for second-generation radionuclide daughters for four decay chains—the actinium, uranium, thorium, and neptunium series. The one-dimensional transport model was implemented as four groups of GoldSim (GoldSim Technology Group, 2006aa) pipe elements. One group was used for each of the four repository source regions. Each group of pipe elements consisted of three segments, representing the volcanic tuffs (the first two segments) and the alluvium (the last segment). The lengths of the last two segments were considered uncertain and were derived from particle-tracking results of the three-dimensional SZ model. Groundwater-specific discharge values in each pipe segment were also estimated from the three-dimensional model (SNL, 2008ag, Section 6.3.10). Where possible, the one-dimensional model used the same transport parameters, such as sorption coefficients, as the three-dimensional model. DOE adjusted other features of the one-dimensional model, such as dispersivity and flow tube diameters, to improve consistency between the breakthrough curve results from the two abstractions. (b)(5)

(b)(5)

The SZ radionuclide transport abstraction was coupled to input from the UZ and output to the biosphere using the convolution integral method. In this method, a unit saturated-zone radionuclide mass breakthrough curve was computed (by the three-dimensional model) for a step-function mass flux source; this breakthrough curve was then combined with the radionuclide mass flux history from the UZ to produce a radionuclide mass flux history that was output to the biosphere. Within TSPA, the convolution integral technique was implemented by a module called *SZ_Convolute*. *SZ_Convolute* was also used to apply changes in specific discharge due to climate change and to correct radionuclide releases from the three-dimensional model for the effects of radioactive decay. The convolution integral method rests on the key assumptions of linear behavior and steady-state SZ flow conditions. The SZ output mass that crosses the accessible boundary in a year was assumed dissolved in 3700467 m³ [3,000 acre-ft] of water.

DOE considered three climate states in modeling the initial 10,000-year performance period: (i) current, (ii) monsoonal, and (iii) glacial transition conditions. For evaluating repository performance after 10,000 years following repository closure, the applicant used “constant-in-time” climate with a prescribed deep percolation rate, as allowed in 10 CFR 63.342(c)(2). The SZ transport model abstraction assumed steady-state flow conditions under each specified climate state and assumed the steady-state conditions were achieved instantaneously for each climate transition. Although potential water table elevation changes and flow path changes could occur for different climate conditions, DOE did not implement these changes explicitly in the SZ transport abstraction. Instead, DOE used specific discharge multipliers to increase flux for the wetter future climates. Also, the potential change in water table elevation near the repository was simulated by shortening the flow path length through the UZ during wetter climates, and releasing instantaneously to the SZ any radionuclides that are present in the portion of the UZ that is inundated at the time of climate change. NRC evaluates the use of specific discharge multipliers in SER Section 2.2.1.3.8.3.3.

The specific discharge multipliers affect radionuclide transport. Doubling the specific discharge doubles the radionuclide flux across the accessible environment boundary. (b)(5)

(b)(5)

(b)(5)

DOE evaluated the effects of changes in water table elevations and flow due to climate change by using the three-dimensional site-scale transport model to generate particle tracks, as described in SNL Appendix E (2007ba). DOE stated that the simulation results showed that the path lengths and travel times for radionuclides increased relative to the model formulation used in performance assessment, and thus, exclusion of these changes in the SZ abstraction model did not result in an underestimation of dose, as outlined in SNL Appendix E (2007ba). In its response to an NRC staff request for additional information concerning geochemical assumptions of the SZ transport models under different climatic conditions (DOE, 2009df), DOE described how elevated water-table flow paths would pass through rocks containing higher percentages of zeolites. In general, water movement and transport of certain radionuclides is slower through rocks containing zeolites compared to non-zeolitic rocks. Instead of explicitly considering these different pathways, DOE chose to simplify its climate change model by employing only the specific discharge multipliers (see SER Section 2.2.1.3.8.3.3). (b)(5)

(b)(5)

(b)(5)

2.2.1.3.9.3.1.1 Model Integration for TSPA

DOE's SZ transport abstraction simulated the transport of dissolved radionuclides and colloid-associated radionuclides through the SZ from beneath the repository, generating breakthrough curves at the accessible environment boundary for 27 radionuclides that DOE determined were risk significant. For TSPA calculations, DOE integrated the SZ radionuclide transport abstraction with three other model components: the UZ transport abstraction model (SAR Section 2.3.8), the site-scale SZ flow model (SAR Section 2.3.9), and the biosphere model (SAR Section 2.3.10).

2.2.1.3.9.3.1.2 UZ/SZ Boundary Condition

In the UZ transport abstraction (SAR Section 2.3.8), radionuclides released from waste packages migrated through the fractures and rock matrix at rates affected by flow fields

generated from the site-scale UZ flow model. The boundary through which radionuclides from the UZ passed to the SZ was divided into four regions (or subareas). Releases of radionuclides that occurred within any portion of each of the subareas were collected for release into the SZ at one point (also within the same subarea). Each point source mass of radionuclides was transferred to the three-dimensional (via *SZ_Convolute*) and the one-dimensional SZ transport model abstractions. The three-dimensional model breakthrough curves were generated by randomly sampling different locations within each of the four subareas to create a starting point for the SZ flow path(s). In contrast, the one-dimensional model uses a fixed, centroid location within each subarea as a starting point for each of its four flow tubes. As a result of the different starting points for the three-dimensional and one-dimensional simulations, the path lengths were not necessarily the same for both methods. DOE described the comparison of the three-dimensional and one-dimensional simulations as not consistently overestimating or underestimating the travel time to the accessible environment. (b)(5)

(b)(5)

DOE sensitivity analyses of the effects of releasing radionuclide mass from the UZ as point sources indicated that the point source releases generally produced faster breakthroughs, as described in Section 6.8.4 of SNL (2007ba). DOE also noted that the release of radionuclides as a point source generally produced a plume with less dispersion.

(b)(5)

SZ—Accessible Environment Boundary Condition

The SZ transport model passes the time-varying mass of radionuclides that cross the compliance boundary to the biosphere model. The SZ transport model explicitly simulates the transport of 27 radionuclides. These radionuclides are carried in the groundwater in the dissolved state and as temporarily and/or permanently associated with colloids. Parameters affecting the transport in the SZ (see SER Sections 2.2.1.3.9.3.2.2 and 2.2.1.3.9.3.2.4) were assigned to the 27 radionuclides. In the TSPA model four additional radionuclides—Ac-227, Ra-228, Th-228, and Pb-210—were assumed to be in secular equilibrium and were released to the biosphere at the same activity concentration as their longer lived parents, Pa-231, Th-232, U-232, and Ra-226, respectively. In response to a request for additional information that asked for justification for setting the released activity concentration of daughters equal to that of their released parents, DOE (2009de) acknowledged that the activities of these daughters are affected by differences in the sorption characteristics of the parents and daughters. DOE (2009de) analyses indicated that mean activities for the daughters of Th-232/Ra-228, Pa-231/Ac-227, Ra-226/Rn-222, and Ra-226/Pb-210 parent-daughter pairs could range from 1 (e.g., Ra-226/Pb-210) to more than 1,400 (e.g., Ra-226/Rn-222) times greater than the respective activities of the parents. DOE defined the sorption enhancement factor (SEF) as the ratio of the daughter activity relative to

its parent in groundwater, resulting from the differences in sorption coefficients of the parent and daughter. DOE concluded that explicitly including the increased daughter activities in the dose calculation of the four parent/daughter pairs would increase the calculated maximum total mean annual dose from 2.0 to 2.4 mrem [0.02 to 0.024 mSv], which would be a small change relative to the 100 mrem [1mSv] individual protection standard for the 10,000- to 1-million-year postclosure performance period. (b)(5)

(b)(5)

The 27 radionuclides that are explicitly transported through the SZ plus the 4 that are assumed to be in secular equilibrium with their transported parents comprise the 31 radionuclides that DOE's biosphere model terms the primary radionuclides. The outputs of the biosphere model include the biosphere dose conversion factors for the groundwater exposure scenario, equivalent to the annual dose from all potential exposure pathways that the RMEI would experience as a result of the release of a unit concentration 1 Bq/m³ [0.227 dpm/gal] of the primary radionuclide in groundwater at the accessible environment boundary. The biosphere model considers 75 radionuclides composed of the 31 primary radionuclides and their relatively short-lived daughters, which are assumed to be in secular equilibrium (i.e., have the same activity concentrations as those of their parents). Of the 75 radionuclides, 20 do not contribute to dose via ingestion and inhalation, leaving 55 that do. For the exposure to contaminated soil, 66 of the 75 radionuclides contribute to dose.

(b)(5)

2.2.1.3.9.3.2 SZ Transport Processes

In DOE's SZ transport abstraction, the migration of radionuclides through the SZ is influenced by the transport-affecting processes of advection and dispersion, sorption, matrix diffusion, and colloid-facilitated transport, as well as radioactive decay and ingrowth (SAR Section 2.3.9.1). NRC staff review of these processes focuses on the YMRP acceptance criteria of system description and integration, data support, data uncertainty, and model uncertainty and support.

2.2.1.3.9.3.2.1 Advection and Dispersion

Advection is the process by which radionuclides, both dissolved and associated with colloids, are carried in flowing water. Overall, DOE considered advection to be the most important transport process in the SZ because, as DOE stated, advection is the primary mechanism driving the migration of radionuclides in the SZ, as outlined in Section 6.3.1 of BSC (2005ak)

(b)(5)

Unlike DOE's model framework for UZ radionuclide transport, which allows radionuclides to travel advectively in both fractures and the matrix, in the SZ, radionuclides in the fractured volcanic tuff move advectively only in the fractures and fault zones. Radionuclides can, however, move into and out of the matrix by diffusion, driven by concentration gradients (see SER Section 2.2.1.3.9.3.2.3). Hydrologic testing in boreholes in the volcanic aquifer revealed that flow through fractures was generally spaced at intervals significantly greater than the spacing of the fractures themselves as determined in drill core logging. This site characteristic was included in the model abstraction as the uncertain parameter *flowing interval spacing in volcanic units*. Along with this parameter, the applicant coupled an uncertain parameter, termed *Fracture porosity in volcanic units* (SAR p. 2.3.9-132), or *flowing interval porosity in the fractured tuffs* (SAR Section 2.3.9.3.2.1). Values for this parameter were estimated using various conservative tracers and reactive tracers in C-Wells Complex testing (SNL, 2007aw). DOE used a combination of the spacing and the porosity parameters to describe the characteristic of preferential pathways through the fracture volcanic aquifer.

(b)(5)

(b)(5)

Advection in alluvium, like advection in the volcanic aquifer, involves preferential pathways. In the alluvium, DOE used an effective porosity parameter to compensate for the potentially reduced volume of the alluvium through which flow might occur. A smaller effective porosity results in higher average linear velocity (i.e., the distance water moves through porous material per unit time). The applicant modeled the alluvium as a single-continuum medium.

(b)(5)

The applicant provided supporting information about advective transport processes from SZ tracer experiments in densely welded, fractured tuffs (fracture-flow dominated systems) at the C-Wells Complex and in the porous alluvium (SAR Section 2.3.9.3.2.1; SNL, 2007aw).

(b)(5)

Dispersion describes the transverse spreading, perpendicular to flow, both horizontal and vertical, and longitudinal spreading, parallel to flow, of dissolved radionuclides in response to localized differences in flow conditions. At the large scale of the SZ transport model grid framework, DOE considered the effect of dispersion to be minimal (SAR Section 2.3.9.3.2.1). However, to allow transport calculations to provide an analysis of radionuclide travel time distributions, DOE included a longitudinal dispersion term in the transport model to capture the arrival of a dispersed solute front at the accessible environment boundary (SAR Section 2.3.9.3.2.1). Inclusion of longitudinal dispersion is supported by the field evidence of preferential pathways in the SZ in the vicinity of Yucca Mountain. (b)(5)

(b)(5)

2.2.1.3.9.3.2.2 Sorption

As discussed previously in SER Section 2.2.1.3.7.3.2.2, sorption is a general term for chemical and physical processes that transfer a fraction of dissolved species to the surface of a solid phase. Depending on specific properties of the dissolved species, the solid, and the liquid, some radionuclides will sorb to the solid, some will sorb more onto solids than others, and some will not sorb at all. Specific sorption processes DOE considered include ion exchange reactions, in which ions of one element replace ions of another element within a mineral structure, and surface complexation, which involves reactions that form bound species at the mineral-water interface. As modeled in the DOE TSPA, sorption of radionuclides onto the fractured volcanic tuff matrix or alluvium results in retardation, or slowing, of transport relative to rates of water flow through the SZ. In contrast, radionuclide sorption onto mobile colloids may enhance the transport rate relative to radionuclides that attach onto a stationary solid (see SER Section 2.2.1.3.9.3.2.4). Sorption is an important process contributing to the barrier capability of the SZ (SAR Section 2.3.9). In particular, sorption within the alluvium effectively delays the transport of moderately and strongly sorbing radionuclides for thousands of years or longer (SAR Sections 2.3.9 and 2.1.2.3.6). Sorption of dissolved thorium, americium, and protactinium is so effective at slowing their movement, that on entering the SZ, these radionuclides cannot reach the accessible environment within the regulatory period of 1 million years. To be present at the accessible environment boundary, these radionuclides either are transported through the SZ as colloids or are ingrown as decay products of mobile parents. DOE noted that the primary controls on sorption are (i) characteristics of the minerals surfaces onto which sorption occurs, (ii) chemistry of groundwater in the SZ, and (iii) sorption characteristics of each element (SAR Section 2.3.9.3.2.2).

DOE represented sorption in the SZ with a sorption coefficient (K_d), an empirically determined or modeled value that represents the ratio of the sorbed-phase radionuclide concentration to the

dissolved-phase radionuclide concentration. Low values of K_d indicate that little or no sorption (i.e., $K_d = 0$) occurs; higher values indicate moderate or strong sorption, and therefore retardation. Retardation by sorption is expressed in transport calculations by a retardation factor (R_f) that depends on the K_d value and the physical properties (porosity and density) of the solid medium through which the radionuclide is transported. Thus, a retardation factor (R_f) equal to one indicates the solute is transported at the velocity of groundwater, while an $R_f > 1$ indicates the solute transport is delayed relative to groundwater. (b)(5)

(b)(5)

(b)(5)

For example, DOE varied the concentration of radionuclides in sorption experiments to determine the effect on K_d . DOE varied the duration of sorption/desorption experiments to determine the rate of these reactions. By using groundwaters of different compositions, DOE demonstrated the effect of bulk chemistry on K_d s.

DOE assumed that sorption of dissolved radionuclides would occur only in the matrix of the volcanic tuff or in the alluvium; dissolved radionuclides transported in fractures do not sorb to fracture surfaces in the DOE model (SAR Section 2.3.9.3.2.2). DOE excluded sorption onto fracture surfaces because of high uncertainties in the nature of fracture coatings (BSC, 2005ak). However, solutes transported through designated fault or fracture zones could undergo sorption depending on the characteristics of the fault or fracture zone (BSC, 2005ak). In fracture zones, a small portion of the rock matrix within the fracture zone was conceptualized as having rapid diffusion and a retardation factor was calculated accordingly (BSC, 2005ak). In contrast to dissolved radionuclides, mobile colloids were retarded within fractures of the volcanic tuff (SAR Section 2.3.9.3.3). (b)(5)

(b)(5)

In the SZ transport model and abstraction, DOE assumed that four radioelements (carbon, chlorine, iodine, and technetium) were nonsorbing and assigned a fixed value of $K_d = 0$ (corresponding to $R_f = 1$) for each. While results of field-based testing in the alluvium indicated that the transport of the important radioelements, technetium and iodine, may be retarded, laboratory-based sorption tests indicated a $K_d = 0$ was warranted, as described in SNL Appendix G (2007ba). For the remaining radioelements modeled in SZ transport calculations (americium, cesium, neptunium, plutonium, protactinium, radium, selenium, strontium, thorium, tin, and uranium), DOE developed ranges and statistical distributions of K_d values for each radioelement and for each modeled rock unit from a combination of empirical data, process modeling, statistical analyses, and expert judgment, as shown in SAR Table 2.3.9-4 and SNL Appendices A, C, G, and J (2007ba). (b)(5)

(b)(5)

For sorption modeling, DOE grouped the various stratigraphic units in the SZ into two geologic media that have different sorption characteristics: fractured volcanic tuff and alluvium (SAR Section 2.3.9.3.2.2). DOE measured sorption data from batch and column experiments that used site-specific crushed tuff samples and alluvium and used SZ water samples from wells in the saturated volcanic tuff (UE-25 J-13), carbonate aquifer (UE-25 p#1), and alluvium (various EWDP wells). Water from wells UE-25 J-13 and UE-25 p#1 were used for batch experiments with volcanic tuff samples, while experiments with alluvium utilized water from the alluvial aquifer, as described in SNL Appendix G (2007ba). DOE argued that these water chemistries

bracket the major ion chemistry observed in the SZ, as outlined in BSC Appendix A (2005ak). For the long-lived actinides (americium, neptunium, plutonium, and uranium), DOE further characterized the effects of variability in geochemistry and mineral surface area using a non-electrostatic surface complexation modeling approach, supported by Davis, et al. (1998aa) and BSC Appendix A (2005ak). In some cases, DOE supplemented the experimental and modeling sorption data with data from the open literature (BSC, 2005ak). In TSPA, DOE sampled K_d values from the specified ranges to account for experimental uncertainty and variability in geologic conditions, including water chemistry and rock type, as shown in SAR Table 2.3.9-4, BSC Appendices A, C, G, and J (2005ak); and DOE Enclosure 3 (2009am).

(b)(5)

Comment (b)(5)

DOE identified mineral surface area and particle size as potential sources of data uncertainty related to the use of crushed tuff and alluvium in experiments. DOE referenced studies both from within and outside the DOE program that indicate the effects of particle size on sorption are typically small except for the very fine (e.g., clay-sized) fraction (BSC, 2005ak). The smallest particle size results in higher K_d s. The general DOE approach to addressing this uncertainty was to use batch experiments for a range of particle sizes and to bias the minimum and maximum limits for the K_d distributions toward lower (weaker sorption) values, as shown in DOE Table 1.1.2-1 (2009am).

(b)(5)

(b)(5)

SNL Appendix A (2007ba) gave the range of K_d s used in the TSPA. In SNL Appendix J (2007ba), however, DOE described how batch sorption experiments may underestimate the K_d that should be applied to transport in the field. The experiments described in SNL Appendix J (2007ba) involved sorption/desorption of uranium and neptunium. The effective K_d s for these radionuclides were up to two orders of magnitude greater than those used in the TSPA. DOE stated that the higher K_d s are likely due to multiple sorption sites of different strengths. There are strongly sorbing sites and weakly sorbing sites on the solids in the SZ. Batch sorption experiments are of short duration and preferentially measure the weak sites. Desorption experiments of longer duration measure the reactions with the stronger sites. DOE chose not to use the effective K_d s from SNL Appendix J (2007ba) for uranium and neptunium, because they would be inconsistent with the K_d s of the other radionuclides determined by the batch sorption method.

In selecting experimental data to inform the TSPA K_d distributions, DOE excluded data from experiments where the final radionuclide concentration indicates that the solubility limit of the radionuclide may have been exceeded, as described in SAR Section 2.3.9.3.2. BSC Appendix A

Comment (b)(5)

(2005ak). and SNL (2007ah) (b)(5)

(b)(5)

(b)(5)

DOE also addressed data uncertainty by obtaining sorption data that assessed K_d variability as a function of time, radioelement concentration, atmospheric composition, water composition, particle size, and temperature. Although most of the data were gathered from batch sorption experiments, DOE also performed a limited number of confirmatory column tests on selected radionuclides that DOE had identified as important contributors to mean annual dose in previous performance assessments, as outlined in SAR Section 2.3.9.3.2.2 and SNL Table 4-1 (2007ba).

(b)(5)

(b)(5)

This aspect of biasing K_d distributions is described and evaluated later in this section when radioactive decay of parents and ingrowth of daughters is considered.

(b)(5)

(b)(5)

DOE addressed model uncertainty in TSPA calculations by sampling K_d values stochastically from uncertainty distributions in which the distribution ranges were developed from expected system conditions and conducted additional analyses to evaluate the effects of model scale and heterogeneity, as outlined in SNL Appendices C and D (2007ba). Rather than sample the K_d distribution independently for each radionuclide, DOE developed a correlation matrix for the 11 sorbing radioelements on the basis of their ranked sensitivities to six variables (pH, Eh, water chemistry, rock composition, rock surface area, and radionuclide concentration). DOE used this

approach to approximate similarities in sorption behavior among radioelements and to ensure that transport behaviors were represented consistently within a single realization of the model, as outlined in SNL Appendix A (2007ba). In addressing model uncertainty, DOE neglected sorption (i.e., $K_d = 0$) in fractures (fast flow paths), except for fault zones, and implemented K_d uncertainty distributions for matrix sorption. (b)(5)

(b)(5)

DOE developed information from natural analogs and field testing to provide qualitative comparisons for sorption model confidence building at the field scale (SAR Section 2.3.9.3.4.1.3). DOE did not apply the SZ transport abstraction to sorption modeling for the analog sites, nor did DOE use results from natural analog studies to inform the K_d distributions. However, DOE used general observations of sorption-related transport behavior to support the conceptual models (e.g., SAR Section 2.3.9.3.4.1.4). DOE also used observations from field tests at Busted Butte south of Yucca Mountain, from the C-Wells location, and from two alluvium tracer tests to provide qualitative and limited quantitative evaluations of sorption in the radionuclide transport model abstraction.

(b)(5)

(b)(5)

(b)(5)

DOE (2009de) acknowledged that K_d s affect radionuclide concentrations. DOE (2009de), however, used the distributions of K_d s from the TSPA, as described in BSC Appendix A (2005ak). (b)(5)

(b)(5)

(b)(5)

The NRC staff noted that the pipe elements representing the alluvium were between 6.5 and 8.5 km [4.04 and 5.28 mi, respectively] long. For each realization, a single K_d for each radionuclide is assigned to the full extent of the alluvium. This is compared to the three-dimensional model, which contains cells 500 m [546 yd] on a side. (b)(5)

(b)(5)

(b)(5)

(b)(5)

2.2.1.3.9.3.2.3 Matrix Diffusion

Diffusion is a physical process in which dissolved radionuclides move from a region of high concentration to a region of low concentration without advective flow. DOE described matrix diffusion as a fracture-matrix interaction that uses diffusion to transfer radionuclides between the water in fractures and the water in the rock matrix. DOE identified matrix diffusion as a moderately important transport mechanism in the SZ transport abstraction, especially for strongly sorbing radionuclides, because it is the main process by which radionuclides can move from a fracture-dominated flow path into the matrix. The modeled effectiveness of matrix diffusion depends on (i) the matrix diffusion rate (i.e., the rate that a radionuclide can diffuse from the water in a fracture into water in the pore spaces of the rock matrix) and (ii) the area of

Comment (b)(5)

the fracture–matrix interface across which diffusion occurs, as outlined in Section 6 1.2.4 of SNL (2007b)). In turn, the matrix diffusion rate depends on the concentration gradient of the radionuclide between fracture and matrix, and the value of the effective matrix diffusion coefficient, which is a measure of how readily a particular radioelement diffuses through a tortuous pathway of interconnected pores in the rock matrix. DOE estimated tortuosities from empirical data for representative Yucca Mountain tuff samples and developed standard normal cumulative probability distributions for effective matrix diffusion coefficients that were sampled stochastically in TSPA for each radioelement with respect to the individual model units (SAR Section 2.3.9.3.2; Reimus, et al., 2007aa).

In contrast to fractures in the UZ, where not all connected fractures in unsaturated rocks are water-bearing at the same time, all fractures in the SZ are, by definition, water bearing. However, as described in SER Section 2.2.1.3.9.3.2.1, not all fractures of the SZ aquifer participate in the flowing system. The flowing interval spacing reduces the number of fractures contributing to flow. This is a site characteristic measured in the field. Drill core logging yields spacing between fractures. Downhole spinner tests at packed locations yield spacing of flowing intervals. In the Yucca Mountain vicinity, the flowing interval spacing is greater than that of the fractures.

The NRC staff's evaluation of the information DOE provided about matrix diffusion in SAR Section 2.3.9.3.2.1 and relevant references considers staff's independent understanding of matrix diffusion models, the hydrogeologic characteristics of the SZ at the Yucca Mountain site, and field and laboratory studies of fracture–matrix interactions in saturated fractured rocks at Yucca Mountain and elsewhere. (b)(5)

(b)(5)

DOE accounted for SZ transport-related model uncertainties by sampling values for the flowing interval spacing, the fracture porosity, and the effective diffusion coefficient in volcanic units. DOE's field experiments at the C-Wells Complex included cross hole tests where tracers with distinct diffusion coefficients were simultaneously injected into one well and the breakthrough curves of the different tracers were measured in a pumped well 30 m [32.8 yd] from the first. The differences in the breakthrough curves for the various tracers were used to demonstrate matrix diffusion was affecting tracer migration. (b)(5)

(b)(5)

(b)(5)

(b)(5)

2.2.1.3.9.3.2.4 Colloid-Associated Transport

As described in SER Section 2.2.1.3.7.3.2.4, colloids are minute solid particles of any origin or composition that become suspended in a liquid. Because colloids are mobile in water, a radionuclide that is attached to a colloid (e.g., by sorption to the colloid surface) will be transported by the processes that move the colloid instead of by processes that would otherwise delay transport of the radionuclide as a dissolved species. Moreover, radionuclides attached to colloids tend to be transported preferentially in fast flow zones such as fractures or large pore throats because the size of colloids, compared to dissolved species, inhibits the transfer of colloids into fine-grained matrix, as described in Section 6.8.2 of SNL (2008an).

(b)(5)

(b)(5)

Colloids

with irreversibly attached radionuclides were modeled as separate transported entities, with a retardation factor applied specifically to the fractured volcanic tuff and alluvial aquifers to simulate the effects of nonpermanent filtration (BSC, 2005ak); DOE assumed that the size of irreversible colloids could exceed that of the pores of the volcanic matrix. Consequently, matrix diffusion of irreversible colloids in the SZ was neglected in the transport abstraction (BSC, 2005ak). (b)(5)

(b)(5)

(b)(5)

Reversible colloidal transport was modeled using the K_c factor, which represented equilibrium sorption of aqueous radionuclides onto natural system colloids (BSC, 2005ak). Radionuclides associated with reversible colloid transport comprised 4 of the 12 radionuclide groups modeled in the SZ flow and transport abstraction (BSC, 2005ak). These four groups included (i) plutonium, (ii) cesium, (iii) tin, and (iv) americium, protactinium, and thorium (BSC, 2005ak). Application of the K_c factor and inclusion of reversible sorption to colloids lowered the effective diffusion coefficient and the sorption coefficient, K_d , for the radionuclides (BSC, 2005ak), enhancing advective transport.

(b)(5)

DOE included colloid-associated transport in both the three-dimensional SZ flow and transport abstraction and the one-dimensional SZ transport model (BSC, 2005ak). (b)(5)

(b)(5)

In the TSPA model abstraction, radionuclide mass exiting the UZ was partitioned into solution and onto colloids for transport in the SZ, as outlined in Section 6.1.4.9 of SNL (2008ag). Irreversible colloids leaving the UZ were passed to the SZ transport abstraction as a single, irreversible colloid flux. For SZ transport calculations, the irreversible colloid flux was divided into a "slow" irreversible colloid fraction that is subject to modeled retardation processes during transport and a much smaller "fast" irreversible colloid fraction that was assumed to travel unretarded throughout the SZ. Colloid-associated transport of radionuclides is affected by filtration, the rate of desorption from the colloid, and the colloid concentrations

in the groundwater (SAR Section 2.3.9.3). Each of these factors was included in the SZ colloid-associated transport model.

The DOE colloid-associated transport model treats radioactive decay in irreversible colloids by assuming that if a decay product was also one of the two radioelements associated with an irreversible colloid in the model (i.e., isotopes of plutonium and americium), then the decay product remained irreversibly associated with the colloid (SAR Section 2.3.9.3.2.3). Otherwise, the decay product enters the aqueous phase as a dissolved species (SAR Section 2.3.9.3.2.3). In the model abstraction there was no permanent filtration of irreversible colloids due to size exclusion in the tuff matrix, at the transition from tuff to alluvium, or in the alluvium, so no colloid size parameter was required in the SZ transport models (SAR Section 2.3.9.3.2.3). The nonpermanent filtration of irreversible colloids was implicitly included as part of the basis and development of the irreversible colloid retardation factor for both the tuff and the alluvium (SAR Section 2.3.9.3.2.3; BSC, 2005ak, 2004bc). (b)(5)

(b)(5)

DOE's conceptual model assumed that reversible colloids could be represented by particles with the composition and characteristics of the clay mineral montmorillonite. (b)(5)

(b)(5)

DOE developed the uncertainty distributions for the concentration of groundwater colloids from data collected in SZ field studies from the Yucca Mountain region and from groundwater analyses elsewhere (BSC, 2005ak; SNL, 2007aw,bi). (b)(5)

(b)(5)

(b)(5)

Colloids were assumed to be stable for all water chemistry conditions in the SZ.

(b)(5)

The only radioelements irreversibly associated with colloids in DOE's model are plutonium and americium. After the general corrosion failure of waste containers in TSPA simulations, up to 30 percent of the Pu-242 flux transported to the accessible environment is by irreversible colloids (e.g., SAR Section 2.4.2.2.3.2.2 and Figure 2.4-108). On the basis of evidence from field experiments that some colloids travel with little or no retardation (Kersting, et al., 1999aa; SNL, 2007aw), DOE designated a small fraction (less than 0.2 percent) of the irreversible colloid flux as a completely unretarded "fast fraction."

On the basis of the NRC staff's independent experience with colloid-associated transport processes and models, the NRC staff is familiar with the uncertainties involved in characterizing colloidal transport processes in heterogeneous natural systems such as the SZ at Yucca

Mountain. In reviewing DOE's technical basis for colloid-associated transport in the SZ, the NRC staff evaluated information DOE provided in SAR Section 2.3.9 and references therein (BSC, 2004bc; SNL, 2008ag,an, 2007bi). The NRC staff also considered additional information in DOE Enclosures 9-14 (2009am).

(b)(5)

(b)(5)

(b)(5)

2.2.1.3.9.3.2.5 Radionuclide Decay and Ingrowth

Radioactive decay is a general term for the processes by which unstable radionuclides spontaneously disintegrate to form a different nuclide that may or may not be radioactive. Loss of radionuclides over time due to radioactive decay and, where applicable, the potential ingrowth (increase) of radionuclide daughters were included in the DOE SZ transport abstraction. Several heavy radionuclides are parents to decay chains of multiple radioactive daughters. In the absence of chemical fractionation, the radionuclides in the chain reach secular equilibrium, where parents and daughters have equal activity. Disequilibrium of naturally occurring decay chains is observed in many groundwater systems, due to geochemical processes in the aquifers (e.g., Faure, 1986aa).

Unlike its UZ transport abstraction, DOE did not directly calculate radioactive decay and ingrowth processes in its three-dimensional site-scale SZ transport model. Instead, decay was included in the convolution integral model during the calculation of mass breakthrough. Moreover, the three-dimensional SZ transport model as formulated did not explicitly include the ingrowth of decay progeny. The mass releases of the radionuclides C-14, Cs-135, Cs-137, I-129, Sr-90, Tc-99, Am-243, Pu-239, Am-241, Pu-240, Pu-242, Pu-238, Cl-36, Se-79, Sn-126, Np-237, U-234, U-232, U-236, and U-238 were determined from the

results of the three-dimensional transport model. DOE used two mechanisms to account for daughter ingrowth.

First, at the transition from the UZ to the SZ, the masses of first-generation daughters, Np-237, U-234, U-236, U-238, and Pu-239, were boosted by the amount their parents were expected to decay during the remainder of the simulated performance time period, as outlined in Section 6.3.10.3 of SNL (2008ag). The parent and boosted daughter pairs are Am-241/Np-237, U-238/U-234, Pu-238/U-234, Am-243/Pu-239, Pu-240/U-236, and Pu-242/U-238.

(b)(5)

DOE used its one-dimensional SZ transport model to calculate the ingrowth of second-generation daughter radionuclides in selected decay chains (SAR Section 2.3.9.3.4.2; BSC, 2005ak). The mass of secondary daughters the one-dimensional model transported through the SZ was added to the mass of radionuclides the three-dimensional model transported to determine the total mass of radionuclides transported through the SZ. The mass releases of the radionuclides U-235, U-233, Th-230, Pa-231, Th-229, Th-232, and Ra-226 were determined from the results of the one-dimensional transport model. The DOE model assumed that Ac-227, Ra-228, and Pb-210 were in secular equilibrium with their parents. Secular equilibrium occurs when the activity of a short-lived daughter is equal to that of a longer lived parent due to radioactive ingrowth. (b)(5)

(b)(5)

The applicant further analyzed this effect in DOE (2009de). DOE's analysis showed that the K_d of the parent divided by the K_d of the daughter times the activity of the parent in groundwater can be used to determine the activity of the daughter in groundwater. In DOE (2009de), DOE calculated that the activity of Ra-228 in groundwater is on average 14 times greater than that of its parent Th-232, and the activity of Ac-227 in groundwater is on average 6.8 times greater than that of its parent Pa-231. The activity of Pb-210 in groundwater is approximately the same as its distant parent, Ra-226, due to their comparable K_d distributions. An extreme example showing the effect of K_d s on activities of parent and daughter is the Ra-226/Rn-222 pair. Radon, an inert gas, is assumed not to sorb, whereas radium strongly sorbs, as indicated by a uniform K_d distribution from 100 to 1,000 mL/g [1533 to 15338 lb/fl oz]. DOE calculated the activity of Rn-222 to be, on average, 1,400 times that of Ra-226 in groundwater. DOE (2009de) showed that these corrections to activity concentrations of these daughters were not enough to significantly increase dose (an increase from 2.0 to 2.4 mrem [0.02 to 0.024 mSv] for the

maximum total mean annual dose} relative to the regulatory limits. (b)(5)

(b)(5)

The groundwater exposure scenario in the biosphere model assumes that short-lived daughters (half-life less than 180 days) are in secular equilibrium with their parent primary radionuclide. The biosphere model calculates biosphere dose conversion factors when the receptor uses water containing a nominal specific activity of the primary radionuclide. That water also is assumed to contain the same specific activity of each of the short-lived daughters. (b)(5)

(b)(5)

Evaluations of biosphere pathways are described in SER Section 2.2.1.3.14.

An important aspect of the contribution of short-lived daughters to dose is that generally the calculated dose for a given activity decreases down the decay chain. Consequently, increasing activities of daughters when considering the SEF are often compensated for by the decreased dose coefficient. Evaluations of biosphere dose coefficients are described in SER Section 2.2.1.3.14. (b)(5)

(b)(5)

Radioactive decay and ingrowth processes were modeled for dissolved, reversible colloids and irreversible colloid radionuclide species all of the types included in the SZ transport abstraction. (b)(5)

(b)(5)

2.2.1.3.9.4 Evaluation Findings

The NRC staff reviewed the applicant's SAR and other information submitted in support of the license application and finds that, with respect to the requirements of 10 CFR 63.114 for consideration of radionuclide transport in the SZ, (b)(5)

(b)(5)

2.2.1.3.9.5 References

BSC. 2005ak. "Saturated Zone Flow and Transport Model Abstraction."
MDL-NBS-HS-000021. Rev. 03. AD 01, AD 02, ERD 01. Las Vegas, Nevada: Bechtel SAIC Company, LLC.

BSC. 2004bc. "Saturated Zone Colloid Transport." ANL-NBS-HS-000031. Rev. 02.
ACN 01, ERD 01. Las Vegas, Nevada: Bechtel SAIC Company, LLC.

Davis, J.A. and G.P. Curtis. 2003aa. NUREG/CR-6820. "Application of Surface Complexation Modeling To Describe Uranium (VI) Adsorption and Retardation at the Uranium Mill Tailings Site at Naturita, Colorado." Washington, DC: NRC.

Davis, J.A. and D.B. Kent. 1990aa. "Surface Complexation Modeling in Aqueous Geochemistry." *Mineral-Water Interface Geochemistry*. M.F. Hochella, Jr. and A.F. White, eds. *Mineralogy*. Vol. 23. pp. 177–260.

Davis, J.A., J.A. Coston, D.B. Kent, and C.C. Fuller. 1998aa. "Application of the Surface Complexation Concept to Complex Mineral Assemblages." *Environmental Science & Technology*. Vol. 32. pp. 2,820–2,828.

DOE. 2009am. "Yucca Mountain—Response to Request for Additional Information Regarding License Application (Safety Analysis Report Section 2.3.8), Safety Evaluation Report Vol. 3, Chapter 2.2.1.3.7, Set 1." Letter (February 9) J.R. Williams to J.H. Sulima (NRC). ML090410352. Washington, DC: DOE, Office of Technical Management.

DOE. 2009de. "Yucca Mountain—Response to Request for Additional Information Regarding License Application (Safety Analysis Report Section 2.3.9), Safety Evaluation Report Vol. 3, Chapter 2.2.1.3.9, Set 1." Letter (November 16) J.R. Williams to J.H. Sulima (NRC). ML092820675. Washington, DC: DOE, Office of Technical Management.

DOE. 2009df. "Yucca Mountain—Response to Request for Additional Information Regarding License Application (Safety Analysis Report Section 2.3.9), Safety Evaluation Report Vol. 3, Chapter 2.2.1.3.9, Set 1." Letter (October 9) J.R. Williams to J.H. Sulima (NRC). ML093210213. Washington, DC: DOE, Office of Technical Management.

DOE. 2008ab. DOE/RW-0573, "Yucca Mountain Repository License Application." Rev. 0. ML081560400. Las Vegas, Nevada: DOE, Office of Civilian Radioactive Waste Management.

Faure, G. 1986aa. *Principles of Isotope Geology, 2nd Edition*. New York City, New York: John C. Wiley & Sons, Inc.

Freeze, R.A. and J.A. Cherry. 1979aa. *Groundwater*. Englewood Cliffs, New Jersey: Prentice-Hall, Inc.

GoldSim Technology Group. 2006aa. *GoldSim Contaminant Transport Module User's Guide*. Version 4.0. Issaquah, Washington: GoldSim Technology Group.

Kersting, A.B., D.W. Efrud, D.L. Finnegan, D.J. Rokop, D.K. Smith, and J.L. Thompson. 1999aa. "Migration of Plutonium in Ground Water at the Nevada Test Site." *Nature*. Vol. 397, No. 6714. pp. 56–59.

Langmuir, D. 1997aa. *Aqueous Environmental Geochemistry*. Upper Saddle River, New Jersey: Prentice-Hall, Inc.

NRC. 2009ab. "Division of High-Level Waste Repository Safety Director's Policy and Procedure Letter 14: Application of YMRP for Review Under Revised Part 63." Published March 13, 2009. ML090850014. Washington, DC: NRC.

NRC. 2003aa. NUREG-1804, "Yucca Mountain Review Plan—Final Report." Rev. 2. Washington, DC: NRC

Reimus, P.W., T.J. Callahan, S.D. Ware, M.J. Haga, and D.A. Counce. 2007aa. "Matrix Diffusion Coefficients in Volcanic Rocks at the Nevada Test Site: Influence of Matrix Porosity, Matrix Permeability, and Fracture Coating Minerals." *Journal of Contaminant Hydrology* Vol. 93. pp. 85–95.

Sheppard, M.I. and D.H. Thibault. 1990aa. "Default Soil Solid/Liquid Partition Coefficients, K_d s, Four Major Soil Types: A Compendium." *Health Physics*. Vol. 59. pp. 471–482

SNL. 2008ag. "Total System Performance Assessment Model/Analysis for the License Application." MDL-WIS-PA-000005. Rev. 00. AD 01, ERD 01, ERD 02, ERD 03, ERD 04 Las Vegas, Nevada: Sandia National Laboratories.

SNL. 2008an. "Particle Tracking Model and Abstraction of Transport Processes." MDL-NBS-HS-000020. Rev. 02. ADD 02. Las Vegas Nevada: Sandia National Laboratories.

SNL. 2007ah. "Dissolved Concentration Limits of Elements with Radioactive Isotopes." ANL-WIS-MD-000010. Rev. 06. Las Vegas, Nevada: Sandia National Laboratories

SNL. 2007aw. "Saturated Zone *In-Situ* Testing." ANL-NBS-HS-000039. Rev. 02. ACN 01, ACN 02, ERD 01. Las Vegas, Nevada: Sandia National Laboratories.

SNL. 2007ba. "Site-Scale Saturated Zone Transport." MDL-NBS-HS-000010. Rev. 03. ACN 01, AD 001. Las Vegas, Nevada: Sandia National Laboratories

SNL. 2007bi. "Waste Form and In-Drift Colloids-Associated Radionuclide Concentrations: Abstraction and Summary." MDL-EBS-PA-000004. Rev. 03. ERD 01. Las Vegas, Nevada: Sandia National Laboratories.

SNL. 2007bj. "Radionuclide Transport Models Under Ambient Conditions (U0060)." MDL-NBS-HS-000008. Rev. 02. CAN 002, AD 01. Las Vegas, Nevada: Sandia National Laboratories.

Sudicky, E.A. and E.O. Frind. 1982aa. "Contaminant Transport in Fractured Porous Media: Analytical Solutions for a System of Parallel Fractures." *Water Resources Research*. Vol. 18. pp. 1,634–1,642.

Till, J.E. and H.R. Meyer, eds. 1983aa. NUREG/CR-3332, "Radiological Assessment: A Textbook on Environmental Dose Analysis." Washington, DC: NRC.

Turner, D.R. and R.T. Pabalan. 1999aa. "Abstraction of Mechanistic Sorption Model Results for Performance Assessment Calculations at Yucca Mountain, Nevada." *Waste Management*. Vol. 19. pp. 375–388.

Turner, D.R., F.P. Bertetti, and R.T. Pabalan. 2002aa. "The Role of Radionuclide Sorption in High-Level Waste Performance Assessment: Approaches for the Abstraction of Detailed Models." *Geochemistry of Soil Radionuclides*. P.-C. Zhang and P.V. Brady, eds. Special Publication 59. Madison, Wisconsin: American Society of Agronomy. pp. 211–252.

CHAPTER 13

2.2.1.3.10 Igneous Disruption of Waste Packages

2.2.1.3.10.1 Introduction

This Safety Evaluation Report (SER) chapter evaluates the U.S. Department of Energy's (DOE) models for the potential consequences of disruptive igneous activity at Yucca Mountain if basaltic magma rising through the Earth's crust intersects and enters a repository drift or drifts [DOE's igneous intrusion modeling case, Safety Analysis Report (SAR) Section 2.3.11.3 (DOE 2009av)] or enters a drift and later erupts to the surface through one or more conduits (DOE's volcanic eruption modeling case, SAR Section 2.3.11.4). The proposed Yucca Mountain repository site lies in a region that has experienced sporadic volcanic events in the past few million years, such that the applicant previously determined the probability of future igneous activity at the site to exceed 1×10^{-8} per year (SAR Section 2.2.1.2.2; CRWMS M&O, 1996aa). DOE therefore included igneous activity as one of three scenario classes in its performance assessment. Because basalt is the only type of magma that has been erupted in the past 8 million years in the Yucca Mountain region, the applicant's performance assessment considers only basaltic igneous activity. As discussed in SER Section 2.2.2.1, the probability of more silicic (explosive) igneous activity, of the type that produced extensive pyroclastic deposits in the area more than 10 million years ago, is well below 1 in 10,000 over 10,000 years; DOE screened this out as a potential disruptive event.

This chapter evaluates the subsurface igneous processes DOE described (i.e., intrusion of magma into repository drifts, damage to waste packages and other engineered barriers, and formation of conduits to the surface, which involves entrainment of waste into the conduit and toward the surface). The applicant's models for volcanic ejection and dispersal of waste material into the surface environment are reviewed in SER Section 2.2.1.3.13. Together, SER Sections 2.2.1.3.10 and 2.2.1.3.13 evaluate DOE information and output that is used in the Total System Performance Assessment (TSPA) under the Igneous Scenario Class (see SER Sections 2.2.1.2.1, 2.2.1.2.2, and 2.2.1.4.1).

The applicant examined the consequences of igneous disruption of the repository (Igneous Scenario Class) using the results of TSPA calculations through the two linked modeling cases, igneous intrusion and volcanic eruption (intrusion always precedes eruption). DOE's igneous intrusion modeling case provides TSPA parameter values for the number of waste packages failed (mass of waste) during an intrusive event, the temperature in the invaded drifts in the period after intrusion, and chemical changes to groundwater that may react with the basalt filling the drifts. The igneous disruption of waste packages abstraction integrates with other TSPA model components, such as the unsaturated zone radionuclide transport abstraction, and provides information about the flux of radionuclides released from the waste form into water entering the unsaturated zone after an intrusive event (SER Section 2.2.1.3.7). Exposure to radionuclides in groundwater extracted by pumping is one of the principal pathways for radiological exposure to the reasonably maximally exposed individual (RMEI).

In the DOE volcanic eruption modeling case, a key parameter affecting the overall dose calculation is the number of directly affected waste packages and thus the amount of waste entrained in a volcanic eruption. DOE's model of the airborne transport and redistribution of radionuclides into soil includes the amount of waste erupted into the atmosphere, the amount deposited on the ground, and the redistribution of the waste-contaminated volcanic ash. This

airborne transport and redistribution model is evaluated in SER Section 2.2.1.3.13 and provides information for the Volcanic Ash Exposure Scenario described in DOE's Biosphere Model (SAR Section 2.3.10). DOE's estimate of the annual probability of igneous events intersecting the repository (1.7×10^{-8} per year; SAR Table 2.3.11-4) is reviewed in SER Section 2.2.1.2.2 and briefly discussed later in this chapter. For these abstractions and the TSPA, the applicant calculates probability-weighted results for both an intrusive-only dose and a total dose (intrusive plus volcanic) to the RMEI, which are detailed in SER Section 2.2.1.4.1 and outlined in the Risk Perspectives subsection in SER Section 2.2.1.3.10.3.1.

Igneous disruption models evaluated in this chapter are the first in a sequence of models that track radionuclides released from the repository to the RMEI as a result of possible future igneous activity. Accordingly, the model abstractions evaluated in this SER chapter serve as input to those reviewed in other chapters, including those that examine the effects of potential igneous disruption of natural and engineered barriers in the subsurface repository (SER Section 2.2.1.3.2). DOE recognized that igneous events potentially have large consequences but a low likelihood (probability) of occurring in the future (SAR Section 2.3.11.1). Thus, DOE provided only a qualitative description of igneous effects on engineered system barrier capabilities in its demonstration of multiple barriers (SAR Section 2.1.1). Because DOE did not rely on an evaluation of igneous events in its demonstration of multiple barriers, staff did not include a discussion of igneous events in SER Section 2.2.1.1. Nevertheless, basaltic igneous activity represents a disruptive event that significantly degrades most of the capabilities of the engineered barrier system (EBS) (SAR Section 2.1.2.2.5)(b)(5)

(b)(5)

(b)(5) To represent igneous events in the performance assessment, DOE removes the barrier capabilities of the waste package and drip shield and degrades the waste form, consistent with information provided in SAR Section 2.3.11. DOE further concluded in SAR Section 2.1.1 that igneous events will have negligible effects on the upper and lower natural barrier systems because the possible igneous intrusive rock bodies have very small dimensions compared with the large volume of rock through which groundwater is flowing and the zone of influence around the intrusions is limited (SAR Section 2.1.2.3.5)(b)(5)

(b)(5)

2.2.1.3.10.2 Regulatory Requirements

Model abstractions used in the applicant's postclosure performance assessment must meet the regulatory requirements given in 10 CFR 63.114 (Requirements for Performance Assessment) and 63.342 (Limits on Performance Assessment), to support the predictions of compliance for 63.113 (Performance Objectives for the Geologic Repository after Permanent Closure). Specific compliance with 63.113 is reviewed in SER Section 2.2.1.4.1.

The requirements for performance assessment in 10 CFR 63.114 require the applicant to

- Include appropriate data related to the geology, hydrology, and geochemistry of the surface and subsurface from the site and the region surrounding Yucca Mountain
- Account for uncertainty and variability in the parameter values used to model igneous disruption of waste packages

- Consider alternative conceptual models for igneous disruption of waste packages
- Provide technical bases for the inclusion of features, events, and processes (FEPs) affecting igneous disruption of waste packages, including effects of degradation, deterioration, or alteration processes of engineered barriers that would adversely affect performance of the natural barriers, consistent with the limits on performance assessment in 10 CFR 63.342
- Provide technical basis for the models of igneous disruption of waste packages that in turn provide input or otherwise affect other models and abstractions

10 CFR 63.114(a) considers performance assessment for the initial 10,000 years following permanent closure. 10 CFR 63.114(b) and 63.342 consider the performance assessment methods for the time from 10,000 years through the period of geologic stability, defined in 10 CFR 63.302 as 1 million years following disposal. These sections require that through the period of geologic stability, with specific limitations, the applicant

- Use performance assessment methods consistent with the performance assessment methods used to demonstrate compliance for the initial 10,000 years following permanent closure
- Include in the performance assessment those FEPs used in the performance assessment for the initial 10,000 year period

For this model abstraction of igneous disruption of waste packages, 10 CFR 63.342(c)(1) further provides that DOE assess the effects of seismic and igneous activity on the repository performance, subject to the probability limits in 63.342(a) and 63.342(b). Specific constraints on the analysis required for seismic and igneous activity are given in 10 CFR 63.342(c)(1)(i) and 10 CFR 63.342(c)(1)(ii), respectively.

NRC staff review of the license application follows the guidance laid out in the Yucca Mountain Review Plan (YMRP), NUREG-1804, Section 2.2.1.3.10, Volcanic Disruption of Waste Packages, (NRC, 2003aa), as supplemented by additional guidance for the period beyond 10,000 years after permanent closure (NRC, 2009ab). The acceptance criteria in the YMRP generically follow 10 CFR 63.114(a). Following the guidance, the NRC staff review of the applicant's abstraction of igneous disruption of waste packages considered five criteria

- System description and model integration are adequate.
- Data are sufficient for model justification.
- Data uncertainty is characterized and propagated through the abstraction.
- Model uncertainty is characterized and propagated through the abstraction
- Model abstraction output is supported by objective comparisons.

Because 10 CFR Part 63 specifies the use of a risk-informed approach for the review of a license application, the guidance provided by the YMRP, as supplemented by NRC (2009ab), is followed to the extent reasonable for aspects of igneous disruption of waste packages important to repository performance. Whereas NRC staff considered all five criteria in their review of information provided by DOE, only aspects that substantively affect results of the performance assessment, as judged by NRC staff, are discussed in this chapter. NRC staff's judgment is

based both on risk information provided by DOE, and staff's knowledge, experience, and independent analyses.

2.2.1.3.10.3 Technical Review

The applicant's analysis of potentially disruptive FEPs considered ways that igneous activity could affect the proposed repository site. NRC staff evaluation of the applicant's FEP screening is given in SER Section 2.2.1.2.1. The applicant included the following FEPs and defined the igneous scenarios for the performance assessment (SAR Table 2.3.11-1): 1.2.04.03.0A, Igneous Intrusion into Repository; 1.2.04.04.0A, Igneous Intrusion Interacts with EBS Components; 1.2.04.06.0A, Eruptive Conduit to Surface Intersects Repository; and 1.2.04.04.0B, Chemical Effects of Magma and Magmatic Volatiles (SAR Table 2.2-5). This chapter evaluates repository performance as affected by these FEPs. Other included FEPs related to potential igneous activity are reviewed in SER Sections 2.2.1.3.2 and 2.2.1.3.13.

This review is based on information presented in SAR Section 2.3.11 and relevant analysis and model reports (AMRs), on material in other publicly available DOE and NRC reports, and on relevant information published in peer-reviewed literature. The applicant also described and evaluated background information used to assess the likelihood and style of future igneous activity in the Yucca Mountain region in SAR Volume 1, General Information, and Volume 2, Section 1.1.2. That material is reviewed in SER Section 2.1.1.1.3.6 as part of NRC's evaluation of site characterization.

2.2.1.3.10.3.1 General Approach by DOE

Igneous activity can be solely intrusive (i.e., magma intruded into rocks below the Earth's surface) or extrusive (i.e., volcanic, in which, following intrusion, magma breaks through to the surface and an eruption ensues). NRC staff notes that the terms "volcanic" and "intrusive" have sometimes been used interchangeably in the DOE license application and supporting documents. To avoid confusion, staff will refer to igneous activity that occurs beneath the Earth's surface as "intrusive" and activity above surface as "extrusive" or "volcanic." All subsurface igneous processes beneath a possible future active volcano that could disrupt the repository are considered intrusive and are reviewed in this chapter, whereas the above-surface volcanic processes are discussed and reviewed in SER Section 2.2.1.3.13.

To evaluate the potential effect of future igneous activity on dose to the RMEI, DOE adopted a conceptual model in which rising basalt magma entering a repository drift (or drifts) could cause release of radionuclides via two pathways (SAR Section 2.3.11.1). During intrusive igneous events, magma rising toward the surface as a dike, or set of dikes, enters drifts but stays beneath the surface. [DOE also considers the other type of small igneous intrusion, sills, but due to their rarity in the Yucca Mountain region, does not include them in the igneous disruption scenario for the repository (see discussion in SER Section 2.2.1.2.2)]. In the igneous intrusive scenario, DOE assumes that all drifts in the repository are intersected by the dike(s), magma fills all drifts, and all waste packages in the repository are damaged but remain in the drifts. No waste is released directly into the accessible environment in an intrusive igneous event, but radionuclides are released to the accessible environment through subsequent groundwater transport. DOE models this transport to occur through the same pathways represented in the nominal, seismic and early failure scenario classes, which are evaluated in SER chapters on unsaturated zone flow and transport (Sections 2.2.1.3.6, 2.2.1.3.7, 2.2.1.3.8, and 2.2.1.3.9). During an extrusive, or volcanic, igneous event, DOE considered that magma continues to rise to the surface as a dike after possibly intersecting repository drifts and, on the basis of the

behavior of basaltic eruptions in general, that surface activity along the resulting initial fissure would rapidly localize, or focus, to a single, or few, points of effusion (SNL, 2007ae; SAR Section 2.3.11.4.1). A wider volcanic conduit would be expected to develop at that focus somewhere along the dike by excavation from the surface vent downwards. This conduit can potentially intersect a drift(s) or develop in the area between the drifts. Magma flow up a drift-intersecting conduit entrains waste from disrupted packages, thereby providing a direct pathway for waste material to be released to the accessible surface environment during a volcanic eruption.

DOE explained that the volcanic (extrusive) part of the igneous scenario is an extension of the intrusive part (SAR Section 2.3.11.1) and concluded that every intrusive event that might intersect the repository is likely to have a conduit develop somewhere along one of the dikes, as described in SAR Section 2.3.11.2.1.2 and SNL Table 7-1 (2007ae). The conduit (or conduits) may, however, form outside the repository footprint or may not intersect a drift, and in that case, no waste material would be entrained into the magma that rises to feed the eruption. In effect, this would be equivalent to the intrusive-only case. In addition, DOE determined that conduits that might feed surface volcanoes may only develop along specific parts of dikes (SAR Section 2.3.11.4.2.1) and thus concluded that the probability of a volcanic event occurring at the repository is expected to be lower than the probability of an intrusive event. DOE also concluded that if an eruption that entrained waste material and transported it into the surface environment did occur at the repository, the potential doses to the RMEI location from radionuclides released through the intrusive and extrusive pathways would be additive. Further details of conduit development are evaluated in the review of the volcanic eruption modeling case (SER Section 2.2.1.3.10.3.3).

Risk Perspective

Staff has assessed the risks caused by an igneous event at the proposed repository on the basis of the applicant's information. As stated previously, while the probability of an igneous event is low, the consequences could be potentially high. The igneous intrusion modeling case would constitute most of the calculated dose for the first 1,000 years following permanent closure, as shown in SAR Figure 2.4-18(a), and is approximately half the calculated dose for the seismic ground motion modeling case in the ensuing 9,000 years. However, for the first 10,000 years, SAR Figure 2.4-18(a) indicates that the mean annual dose from igneous intrusion is at least approximately 100 times lower than the dose limit. Moreover, DOE indicated that for the post-10,000-year period, the igneous intrusion modeling case and seismic ground motion modeling case provide approximately equal contributions to the total mean annual dose to the RMEI for the last 300,000 years of the time period, and that each modeling case is about 100 times lower than the dose limit. SAR Figure 2.4-18(b) results supported this statement (in SAR Section 2.1).

In SAR Section 2.4.2.2.1.2.3, DOE provided the probability-weighted consequences of igneous activity (intrusive and extrusive) using the probability distribution from its expert elicitation for a Probabilistic Volcanic Hazard Assessment (PVHA). DOE identified that the probability-weighted igneous intrusive dose is estimated to be less than 0.1 mrem for the 10,000-year period and less than 0.5 mrem for the post-10,000-year time period (SAR Section 2.4.2.2.1.2.3.1). The DOE estimates for the probability-weighted igneous extrusive (volcanic eruptive) dose alone are about 10^{-4} mrem for the 10,000-year period and less than 6×10^{-5} mrem for the post-10,000-year time period (SAR Section 2.4.2.2.1.2.3.2).

(b)(5)

(b)(5)

2.2.1.3.10.3.2 NRC Review of DOE Igneous Intrusion Modeling Case

The DOE model for igneous intrusion and its effect on repository performance rely on four key conclusions:

- Magma rising as a dike beneath repository drifts will intersect and flow into the drifts
- Any dike intersection into the repository footprint floods all drifts with magma, causing engineered barrier system (EBS) components, including all waste packages and drip shields, to fail while magma and waste remain in the drift
- Igneous intrusion does not alter the ambient hydrologic flow and transport regime significantly (i.e., the natural barriers above and below the drifts are not affected)
- Subsurface conduits that develop beneath volcanoes can be represented by cylinders and only entrain waste within the part of the cylinder that intersects the drift

Conclusions 1–3 solely concern the intrusive model case, while Conclusion 4 is also applicable to the volcanic model case. Staff's review focuses on the risk-significant aspects of these conclusions, which are evaluated under the following subsections

Effects of Igneous Intrusion on Performance of Natural Barriers

DOE screened out of its performance assessment the effect of igneous dikes and sills on groundwater flow and transport pathways surrounding drifts in the upper and lower natural barriers, as described in SNL (2008ac) (FEP 1.2.04.02.0A). At the drift wall, however, DOE included the effect of igneous intrusions, by assuming the drifts become degraded and the seepage barrier is eliminated. For this case in the performance assessment, seepage is set equal to percolation. Igneous activity near repository drifts may alter hydrologic properties of the host rock or cause perching of water in the unsaturated zone. DOE's sensitivity analyses indicate that these effects on unsaturated zone flow in repository performance are small (FEP 1.2.04.02.0A; SNL, 2008ac). In particular, the potential effect of increased fracturing in and around a dike providing preferred water pathways has relatively little impact, given the predominance of fracture flow in the existing, undisturbed unsaturated zone beneath much of the repository footprint (see NRC staff review of unsaturated zone flow in SER Section 2.2.1.3.6). Farther into the far field, igneous dikes and sills may modify saturated zone flow and plume pathways, but again, DOE suggested these effects to be minor for performance (FEP 1.2.04.02.0A; SNL, 2008ac).

(b)(5)

(b)(5)

Behavior of Intruding Magma in Drifts and Effects on EBS

In developing the model for subsurface igneous processes, DOE concluded that basaltic magmas in the Yucca Mountain region would contain appreciable amounts of dissolved volatiles, primarily water. This dissolved water would form a gas phase as pressure on the magma becomes lower due either to normal ascent toward the surface or by intersection with a repository drift (SAR Section 2.3.11.2.1.2). Significant amounts of gas expansion in the upper 300 m of rise [above ~1,000-ft depth] would cause magma in potential igneous events to flow more rapidly, and perhaps more extensively, than would be expected for magmas with little gas-driven expansion. In part because of the relatively high dissolved water contents expected for Yucca Mountain basaltic magmas, DOE concluded that all repository drifts would be rapidly filled by magma flow if a future intrusive igneous event occurred within the repository footprint (SAR Section 2.3.11.2.1.2).

Staff reviewed the information DOE presented to support the conclusion that basaltic magmas are expected to have relatively high dissolved water contents. (b)(5)

(b)(5)

In the DOE intrusive igneous case, the applicant assumes that if a single rising dike intersects any part of the repository footprint where drifts containing waste packages are located, then all drifts in the repository are rapidly filled with magma. DOE developed this approach to account for the uncertainties in determining the physical characteristics of dikes at repository depths and for uncertainties in magma flow processes in drifts intersected by dikes (SAR Section 2.3.11.3.1). For the ascending magma entering the drifts, the applicant recognized that there are two end member possibilities for flow behavior, considering how rapidly and violently magma could enter a drift. The less rapid end-member is termed effusive, as in a lava-like flow, while the other is more explosive, resulting in a fragmental, or pyroclastic, flow (SAR Section 2.3.11.2.1.2; SNL, 2007a; Woods, et al., 2002a; Dartevelle and Valentine, 2005aa, 2009aa) (b)(5)

(b)(5)

(b)(5)

According to calculations the applicant reported, after intersection and intrusion by magma drift temperatures are modeled at or near magmatic temperatures of 1,046–1,169 °C [1,915–2,136 °F], at which point plastic deformation of the waste packages begins. Additional DOE analysis showed waste packages could also be damaged by magmatic pressures as low as 4 MPa [580 lb in⁻²]. DOE concluded waste package failure could result in waste forms that are exposed to high temperatures and that undergo chemical reactions with magma and its constituents. The applicant assumed that the packages would encounter additional mechanical loads from the cooling and solidification of enveloping magma. Already weakened by the thermal effects of the magma, the mechanical loads associated with the magma would result in deformation of the waste package. DOE proposed that similar effects would occur for drip shields exposed to magmatic conditions. Thus DOE concluded that uncertainties associated with the potential effects of magma on waste package and drip shield performance are sufficient to warrant the assumption that all waste package and drip shield barrier capabilities are removed in models for igneous intrusive events (SAR Section 2.3.11.3.2.4). DOE also concluded that exposure to magmatic conditions will result in unprotected waste forms that are, effectively, instantaneously degraded, such that radionuclides are assumed to be immediately available for hydrologic transport, as soon as the intrusion is cool enough to allow water to contact waste (SAR Section 2.3.11.3.2.4). As discussed in the next section, the cooling time of the intrusion is not long relative to the time scale of groundwater percolation and flow and relative to the regulatory period for postclosure repository performance. DOE further concluded that although the waste package no longer serves as a barrier to water flow after an igneous event, corrosion products from degradation of waste package materials will be present and will strongly retard release of certain radionuclides into the unsaturated zone, in the same manner as in the nominal scenario. NRC staff evaluates the role of corrosion products in radionuclide release in SER Section 2.2.1.3.4.

Staff reviewed the information DOE provided in SAR Section 2.3.11.3.2 to support the representation of engineered barrier and waste form responses to potential igneous intrusive events (b)(5)

(b)(5)

(b)(5)

(b)(5)

Magma Cooling and Heat Flow to Host Rock

The temperature in the drifts after magma intrusion is an output parameter to TSPA (SAR Section 2.3.11.6.7). This subsection evaluates the DOE estimates of centerline and wall temperature in the invaded drifts in the period after intrusion and the timing of the intrusive event with respect to the repository life cycle, reflecting the temperature of the host rocks during the period of heating by radionuclide decay. The applicant included these for consideration of the postintrusion environment in the damaged drifts and the period of time after which groundwater seepage through the drifts could return.

The temperature in the drifts after magma intrusion provides an estimate of the cooling time of the basalt inside the drift. The cooling of the basalt inside the drift and the drift centerline temperature, as well as drift-wall temperature, also influence the spent fuel dissolution model and the calculation of diffusion coefficients. Diffusion coefficients are used to calculate near-field contaminant transport in the unsaturated zone rock.

DOE concluded that a short-lived (hours to days) intrusive event, as in SNL Figure F-1 (2007ab), would fill every drift in the proposed repository with basaltic magma at a temperature of approximately 1,100 °C [2,012 °F]. Following the intrusive event, the magma in the drifts begins to cool. DOE performed numerical simulations to model the magma cooling and heat flow in the rock between drifts, via non-steady-state heat conduction, with radial flow of heat from the magma-filled drifts into the host rock. DOE's model considers a single basalt-filled drift, recognizing that the heat from one 5-m [16-ft]-diameter magma-filled drift will not influence the next drift approximately 80 m [262 ft] away (SNL, 2007ag). The calculated temperature decreases with time and distance from the centerline of the drift. The thermal diffusivity of the rock is calculated using the rock volumetric heat capacity and the thermal conductivity of the welded tuff at the repository horizon. The host rock in the heat-flow calculation is assumed to be either completely dry or completely wet. Thermal diffusivity of the welded tuff and the basaltic magma are assumed to be the same. The drift wall temperature prior to magma intrusion in the DOE model runs was between 25 and 200 °C [77 and 392 °F]. DOE concluded that this range suitably represents temperatures at different times for the intrusive event (reflecting elevated repository temperatures for several thousand years after closure; e.g., see SAR Figure 2.3.5-33 for calculated repository drift-temperature decay curves). These temperature distributions provided the DOE estimate of the cooling rate and thermal history of the repository and the drifts following an intrusive event.

The applicant identified that the model does not include the effects of latent heat of magma crystallization or the property contrasts between the magma and the tuff. Without latent heat effects, the one-dimensional model results underestimated peak temperatures and time needed for cooling. Therefore, the applicant considered alternative models, including an analytical solution that approximated the effects of latent heat and numerical solutions in two dimensions that included both latent and radioactive heat. Noting that latent heat would be liberated during magma crystallization and that its effects would be most pronounced at very early times while the magma is still partially liquid, the applicant accounted for the effect of latent heat by increasing the initial temperature of the magma.

DOE considered the main uncertainty when modeling magma cooling and solidification to be the initial magma temperature. (b)(5)

(b)(5)

(b)(5)

Other uncertainties the applicant considered included thermal conductivity, grain density, specific heat capacity, matrix porosity, saturation, and the lithophysal porosity of the host tuff. Heat loss was modeled as purely conductive, as the applicant did not expect convection to occur in stagnant magma within drifts. For an igneous intrusion event occurring after about 1,000 years into the preclosure period, DOE concluded that the repository drift walls would attain a temperature of 100 °C [212 °F] about 100 years after the intrusive event occurs, as in SNL Figure 2.3.5-33 (2008ag).

(b)(5)

(b)(5)

DOE used the final temperature of the drift and the cooled basalt temperature as an input to calculate the spent fuel dissolution model and diffusion coefficients. (b)(5)

(b)(5)

Percolation Flux Through Cooled Basalt

Chemical changes, expressed as the pH and ionic strength, to groundwater that may react with the new basalt rock filling repository drifts after a future intrusive magmatic event is an output parameter to TSPA (SAR Section 2.3.11.6.7; SNL, 2005ae). This subsection evaluates DOE estimates of possible chemical changes that might occur to groundwater as it begins to seep through and possibly react with cooling, and cooled, basaltic material filling the drifts (SER Section 2.2.1.3.3).

In considering percolation of groundwater through the drift after an igneous intrusion into the repository, the applicant assumed that solidified basalt rock in the drift has the same fracture, porosity, and permeability characteristics as the surrounding tuff. DOE also concluded that the newly introduced basalt rock could affect the chemistry of water that seeps into the drift, in particular, pH and ionic strength. To examine possible changes in these two chemical parameters of the seepage water, DOE selected for numerical analysis three groundwater samples from large, fractured basalt-hosted reservoirs and conducted an extensive literature

review of the chemistry of basalt-hosted waters to provide a range of pH and ionic strength values, as described in SAR Sections 2.3.7.5.3.1 and 2.3.11.3.2 and SNL Section 4.1.2 (2007ae). Temperature can affect the pH of incoming fluids, so to avoid underestimating radionuclide solubilities, DOE calculated the parameter values at 25 °C [77 °F], rather than at higher temperatures that would have resulted in lower solubility limits (radionuclides of concern show retrograde solubility in this pH range) and therefore smaller mass releases.

As discussed in the previous subsection, for an igneous intrusion event occurring approximately 1,000 years into the postclosure period, water seepage and flow through the host rock mass is estimated to resume about 100 years after an intrusion occurs: the time when the basalt in the drifts would reach ~100 °C [212 °F] along the drift centerline (SAR Section 2.3.11.3.3.8; SNL, 2008ag). This time also corresponds to when the repository drifts walls are assumed to cool below the local boiling temperature, as shown in SNL Figure 2.3.5-33 (2008ag). DOE modeled reestablishment of groundwater percolation through the invaded repository drifts and failed engineered barriers. DOE did not model release of radionuclides in gaseous form from the waste packages, because DOE's analyses indicate that this does not influence the final dose at the receptor (SNL, 2008ag). Hence, groundwater percolation was the only pathway the applicant considered for release of radionuclides. (b)(5)

(b)(5)

(b)(5)

(b)(5)

(b)(5)

The NRC staff review of release and transport of radionuclides following a possible igneous intrusion is further detailed in SER Section 2.2.1.3.4 (specifically, Sections 2.2.1.3.4.3.2 on waste form degradation and 2.2.1.3.4.3.4 on colloid formation and stability).

Summary and Findings on Igneous Intrusion Modeling Case

(b)(5)

2.2.1.3.10.3.3 NRC Review of DOE Volcanic Eruption Modeling Scenario

DOE concluded that in all potential igneous intrusive events that intersect the repository footprint, a rising dike would reach the surface and develop a conduit at some location along the intrusion and magma would be extruded. If a conduit is located wholly or partially in a repository drift, waste from disrupted waste packages could be entrained by magma flow up the conduit and erupted from a volcano at the surface. Compared with the intrusion scenario, in which the contents of all waste packages in the repository are made available for hydrologic transport, DOE concluded that, for the volcanic scenario, only a limited amount of high-level waste could be entrained directly into a conduit or conduits (SAR Section 2.3.11.4).

In the type of basaltic volcanic activity the applicant predicted for the case of a future eruption through the repository, a dike reaches the surface and activity begins along a fissure (an elongated system of vents, which is the surface expression of the dike; see SAR Sections 2.3.11.2.1 and 2.3.11.4.1.1 and SAR Figure 2.3.11.5). In DOE's model, magma flow to the surface in the dike usually localizes to a single, or a few, points over a period of hours to a few days, as observed at past basaltic eruptions and previously discussed in SER Section 2.2.1.3.10.3.2. Such behavior was seen in analog historic events [e.g., the 1943–1952 eruption of Parícutín, Mexico; the 1973 Heimaey eruption in Iceland; and the 1975 Tolbachik eruption in Kamchatka (Thorarinsson, et al., 1973aa; Doubik and Hill, 1999aa; Pioli, et al., 2008aa)]. DOE studies of igneous products exposed in the rock record also inferred a similar style for some prehistoric basaltic eruptions (e.g., SAR Section 2.3.11.4; SNL 2007ae; Valentine, et al., 2006aa; Keating, et al., 2008aa). At this point in the modeled eruption, a conduit is considered to develop below the point of localization, with the main vent at the surface. This conduit feeds an explosive and lava-flow-forming Strombolian-style eruption. DOE adopted a violent Strombolian style for the entire model eruption considered, on the basis of the characteristics of the young Lathrop Wells scoria cone near Yucca Mountain (see SER Section 2.2.1.2.2). The applicant recognized that conduits grow (widen) downwards from the

surface in the plane of the dike, as detailed in SAR Section 2.3.11.4.2.1.2 and SNL p. 6-46 (2007ae), and thus, in DOE's repository-disruption scenario, intersect a drift through the roof.

DOE characterized subsurface volcanic conduits as flaring inward down from the top of the surface vent, such that conduit diameters at repository depths will be smaller than those observed near the surface. DOE characterized the size and shape of conduits using studies at exposed analog volcanoes (e.g., SAR Section 2.3.11.4 and Figure 2.3.11-6; SNL, 2007ae; Valentine, et al., 2006aa; Keating, et al., 2008aa) and theoretical considerations and model studies (e.g., Wilson and Head, 1981aa; Valentine, et al., 2007aa). In the performance assessment, DOE represents subvolcanic conduits as simple cylinders (SAR Section 2.3.11.4.1). DOE used the area of the conduit that intersects a drift to calculate the mass of waste the conduit entrains. DOE concluded that entrained waste is mixed uniformly in the volume of magma that is subsequently erupted at the surface.

From a risk-perspective, the DOE performance assessment calculates that the expected annual dose from the igneous volcanic modeling case alone is approximately 0.1 percent of the dose calculated for the intrusive scenario (SNL, 2007ag). This difference between the volcanic and intrusive scenarios arises, in part, because DOE concluded that the volcanic scenario entrains and erupts approximately 0.1 percent of the amount of high-level waste that is disrupted during the intrusive case. Thus, staff's review of the subsurface processes associated with the volcanic case focuses on the DOE basis for concluding that a volcanic conduit, or conduits, would entrain a limited amount of waste.

Development of Conduits and Likelihood of Ejecting Waste in a Volcanic Eruption

In the DOE-developed model, one to three eruptive conduits may occur along the thickest dike. DOE treats the predicted location of a single conduit along a dike, the most likely occurrence, as random (SAR Section 2.3.11.4.2.1). In SAR Section 2.3.11.2.2, DOE developed a basis to determine the likelihood that at least one conduit will form through the repository footprint and, more specifically for risk significance, through an emplacement drift containing waste packages if a dike intersected the repository. The DOE model for conduit formation is based on observations at basaltic volcanoes and supported by calculations constrained by information obtained from studies of analog eroded volcanoes (SNL, 2007ae).

On the basis of observations of Quaternary volcanoes in the Yucca Mountain region, where mostly only one volcano develops along a dike (Keating, et al., 2008aa), DOE heavily weighted the distribution of the likely number of conduits that might develop along a dike toward one conduit per eruption (SAR Section 2.3.11.2.1.2; SNL, 2007ae), and in this way treated uncertainty. DOE determined that the presence of repository drifts would not affect the rise of a dike, nor subsequent eruptive processes, because the drifts would be negligible in volume compared to the volume of rock the dike transects. (b)(5)

(b)(5)

(b)(5)

DOE

determined that 85 percent of past eruptive events have formed a single conduit, 10 percent formed 2 conduits, and 5 percent formed 3 conduits. (b)(5)

(b)(5)

DOE also

considered five alternative conceptual models to represent the location of a conduit along a dike. On the basis of field analogs, models, and studies presented in SNL (2007ae, 2007ag), DOE concluded that a model for random location of a conduit along an existing dike is the only supportable approach.

To calculate the likelihood that at least one volcanic conduit will form through an emplacement drift and entrain waste, DOE used numerical models to simulate the number of dikes that could penetrate the repository footprint, using dike characteristics from CRWMS M&O (1996aa). For each simulation, DOE calculated the length of the dike, or dikes, located inside and outside the repository footprint and found there was a 60 percent chance that more than one dike would form in an event. For the widest dike in each simulation, DOE constrained its model to form one to three conduits at random locations along that dike and determined whether this location coincided with the repository footprint (SER Section 2.3.11.4.2.1.3; SNL, 2007ar). Using this approach, DOE estimated that there was a 20 to 35 percent chance, with a mean of 28 percent, that at least one conduit would form within the repository footprint. This value reflects the relatively small size of the repository footprint in comparison with the total area that dikes could impact (SAR Section 2.3.11.2.2). On the basis of alternative volcanic event characteristics and behavior, the applicant acknowledged that the conditional likelihood of at least one eruptive center (conduit) within the repository footprint might range from 43 to 78 percent (SAR Section 2.3.11.2.2.6). However, the applicant concluded that, on the basis of features of Yucca Mountain repository volcanoes, a mean conditional eruption probability of 0.28 (28 percent) times the probability of dike intersection with the repository footprint was most consistent with basaltic volcanic events that are expected to include multiple dikes and in which conduit(s) form on the widest dike. On this basis, the mean conditional probability of a conduit forming within the repository, using the mean intrusive probability from the PVHA expert elicitation of 1.7×10^{-6} per year (SAR Section 2.3.11.4.2.1; SER Section 2.2.1.1.3), is 4.8×10^{-6} per year.

The 28 percent conditional factor DOE provided is for a conduit that develops within the repository footprint, but which may not necessarily eject waste. DOE then developed a second conditional probability, given as 0.296 (NRC staff rounded this to 0.3, or 30 percent), to represent the fraction of conduits within the repository footprint that may actually intersect a drift containing waste packages and eject the waste contents through a volcanic vent (SAR Section 2.3.11.4.2.1). This factor accounts for the spatial distribution of waste emplacement drifts within the repository footprint area and the likely orientation of dikes.

Staff reviewed DOE information regarding the likelihood for conduit development at repository drifts. (b)(5)

(b)(5)

(b)(5)

Staff reviewed the DOE methodology that developed the 28 percent factor for conduit development in the repository and the 30 percent factor for conduit intersection with a drift. (b)(5)

(b)(5)

Eruptive Conduit Growth and Size, and Impact on Waste Packages and Waste

According to the applicant's scenario presented in SAR Section 2.3.11.4.2.1, one or more conduits may intersect repository drifts, all the waste packages within the area of the conduits are assumed to be destroyed, and all the waste is assumed to be incorporated into the erupting magma (SNL, 2007ag). The waste is assumed to mix with magma and be carried up the conduit toward the surface, where the magma-waste mixture would be explosively ejected into the atmosphere or flow as lava along the ground.

The applicant considered the failed waste packages directly intersected by a conduit to provide no protection against waste release, so in the DOE model, the conduit size at repository depth directly determines the number of waste packages disrupted. More specifically, DOE calculated the number of waste packages intersected by conduits as a cumulative distribution function that is based on a distribution for the number of conduits, a distribution for conduit diameters, and the likelihood factors for location of the conduits on the dikes, which includes the design configuration of the subsurface repository. Accordingly, DOE considered additional parameters including waste package size and spacing, drift location and dimensions, and distributions for dike length, orientation, thickness, and number of dikes in an intrusive event. The applicant concluded that rising magma in a dike that enters a drift will slow relative to that in solid rock pillars between drifts; thus the dike segment above drifts will lag slightly in breaching the surface. From that conclusion, DOE proposed that vents and conduits are more likely to form between drifts than above them. In most realizations the applicant tested, this led to a condition where the volcanic conduit forms along the dike in the rock pillars between drifts and not the drift itself; thus the most likely value for the number of disrupted waste packages in the model is zero. From zero to seven waste packages were modeled in the TSPA as intersected by a conduit during an eruption.

In DOE's model, uncertainty in conduit size is bounded by a size distribution based on observed host-rock fragments in violent-Strombolian deposits at Lathrop Wells volcano (Doubik and Hill, 1999aa) and in SNL Section 6.4 and Appendix C (2007ae) and on field studies at analog sites, which DOE interpreted as suggesting that the diameter is largest at the surface and decreases with depth. The applicant gave a distribution for conduit diameters from approximately 4 m [13 ft] (bounded by dike width) to a mean value of 15 m [50 ft] and a 95th percentile value of 21 m [69 ft] for an expected conduit diameter at repository depth (SAR Section 2.3.11.4.2.1.1), with DOE's volcanic scenario analysis conduits developed only where the trend of a dike intersected a drift (SAR Section 2.3.11.4.1.1.1). The applicant concluded that it is highly unlikely that a secondary conduit will form at some point along the drift away from the dike intersection. This conclusion was based on DOE's view that magma will solidify quickly and pressures will be insufficient to allow the formation (or maintain the opening) of a secondary dike, fed from the magma in the drift. In the analysis involving pyroclastic flow of magma inside a drift (an alternative conceptual model mentioned previously with respect to the intrusive case), DOE assessed one situation where it assumed that a secondary fracture had already formed and a secondary opening was created on the drift-top wall (BSC, 2005af). DOE applied a multiphase fluid dynamics analysis to this scenario. Simulated results exhibited intermediate behavior with a down-drift multiphase flow on the roof and a return flow on the floor. The whole system with these two openings formed a clearly defined recirculation pattern in the drift with some materials leaving the system and some materials recycling back into the drift along the roof. Simulations also showed that this scenario leads to relatively high dynamic pressures compared with a single-conduit situation. Other simulations indicated that blockage of the volcanic conduit might also create secondary breakouts at a point away from the location of initial dike intersection (SAR Section 2.3.11.3.2.2). Although DOE acknowledged that the

chance of these scenarios occurring was unlikely, it concluded that such scenarios could lead to a one to two order-of-magnitude increase in the amount of waste released during a volcanic igneous event (essentially equivalent to the waste content of a single drift, ~70–100 waste packages), which would cause no more than a one to two order-of-magnitude increase in expected annual dose (SAR Section 2.3.11.3.2.2).

(b)(5)

Evaluation of Magma–Waste Interaction and Mixing in a Drift and Conduit

In DOE's TSPA, the amount of waste incorporated into a volcanic conduit is determined by the area of a drift intersected by a stylized cylindrical conduit. This model assumes that waste from disrupted packages located outside the boundary of the conduit will not be entrained into the upward-flowing magma in the conduit. Additional DOE analyses (SAR Section 2.3.11.3.4.4) described how circulation of magma and gas might occur between a conduit and other parts of the intersected drift. (b)(5)

(b)(5)

(b)(5)

(b)(5)

Further, staff reviewed the information DOE provided in SAR Section 2.3.11.3.2.2 to evaluate the potential effects of secondary conduits developing away from the location of dike intersection with the drift. (b)(5)

(b)(5)

In the DOE volcanic eruption modeling scenario, the number of waste packages intersected becomes input in TSPA for calculating the amount of waste erupted, along with the probability that a conduit will develop in a drift containing waste packages. DOE used a Monte Carlo technique to account for parameter uncertainties such as the future time at which an eruption might occur and the possibility that more than one eruption could happen in the future of the repository. DOE calculates a magma partitioning factor (SAR Section 2.3.11.4.2.2.2; SNL, 2007ab) to determine the amount of the waste partitioned into a potential volcanic tephra fall deposit, the only volcanic product that is significant to dose (SER Section 2.2.1.3.13.3.1). The applicant determined that 10 to 50 percent of the total amount of waste entrained in an eruption will be in the resulting tephra fall deposit. The magma partitioning factor and the expected style of eruption (violent Strombolian) from the volcanic conduit(s) is evaluated as part of the abstraction for airborne volcanic transport in SER Section 2.2.1.3.13.

DOE proposed that the amount of waste particles incorporated into the erupting magma would only constitute a minor amount (trace phase) in the magma in all the applicant's scenarios and that its presence would not be expected to influence the eruptive behavior of the magma (SNL, 2007ab). (b)(5)

(b)(5)

Summary and Findings on the Volcanic Eruption Modeling Case

(b)(5)

(b)(5)

2.2.1.3.10.4 Evaluation Findings

The NRC staff reviewed the applicant's SAR and other information submitted in support of the license application and finds that, with respect to the requirements of 10 CFR 63.114 for consideration of igneous disruption of waste packages, (b)(5)

(b)(5)

(b)(5)

2.2.1.3.10.5 References

BSC. 2005af. "Magma Dynamics at Yucca Mountain, Nevada." ANL-MGR-GS-000005. Rev. 00. Las Vegas, Nevada: Bechtel SAIC Company, LLC

BSC. 2003ab. "Technical Basis Document No. 13: Volcanic Events." Rev. 02. Las Vegas, Nevada: Bechtel SAIC Company, LLC.

CRWMS M&O 1996aa. "Probabilistic Volcanic Hazard Analysis for Yucca Mountain, Nevada." BA0000000-01717-2200-00082. Rev. 0. Las Vegas, Nevada: CRWMS M&O.

Dartevelle, S. and G.A. Valentine. 2009aa. "Multiphase Magmatic Flows at Yucca Mountain, Nevada." *Journal of Geophysical Research, Solid Earth* Vol. 113 pp. B12209. doi:10.1029/2007JB005367.

Dartevelle, S. and G.A. Valentine. 2005aa. "Early Time Multiphase Interactions Between Basaltic Magma and Underground Repository Openings at the Proposed Yucca Mountain Radioactive Waste Repository." *Geophysical Research Letters*. Vol. 32. pp. L22311. doi:1029/2005GL024172.

Delaney, P.T. and A.E. Gartner. 1997aa. "Physical Processes of Shallow Mafic Dike Emplacement Near the San Rafael Swell, Utah." *Geological Society of America Bulletin*. Vol. 109, No. 9. pp. 1,177–1,192.

Detournay, E., L.G. Mastin, J.R.A. Pearson, A.M. Rubin, and F.J. Spera. 2003aa. "Final Report of the Igneous Consequences Peer Review Panel." DN2000219072. MOL20031014:0097. Las Vegas, Nevada: Bechtel SAIC Company, LLC.

DOE. 2009av. DOE/RW-0573, "Safety Analysis Report Yucca Mountain Repository License Application." Rev. 01. Las Vegas, Nevada: DOE, Office of Civilian Radioactive Waste Management.

Doubik, P. and B.E. Hill. 1999aa. "Magmatic and Hydromagmatic Conduit Development During the 1975 Tolbachik Eruption, Kamchatka, With Implications for Hazards Assessment at Yucca Mountain, NV." *Journal of Volcanology and Geothermal Research*. Vol. 91. pp. 43–64.

Hill, B.E. and C.B. Connor. 2000aa. "Technical Basis for Resolution of the Igneous Activity Key Technical Issue." ML011930254. San Antonio, Texas: CNWRA.

Keating, D.N., G.A. Valentine, D.J. Krier, and F.V. Perry. 2008aa. "Shallow Plumbing Systems for Small-Volume Basaltic Volcanoes." *Bulletin of Volcanology*. Vol. 70. pp. 563–582.

Lejeune, A., B.E. Hill, A.W. Woods, R.S.J. Sparks, and C.B. Connor. 2009aa. "Intrusion Dynamics for Volatile-Poor Basaltic Magma Into Subsurface Nuclear Installations." *Volcanic and Tectonic Hazard Assessment for Nuclear Facilities*. C.B. Connor, N.A. Chapman, and L.J. Connor, eds. Cambridge, United Kingdom: Cambridge University Press.

Menand, T., J.C. Phillips, and R.S.J. Sparks. 2008aa. "Circulation of Bubbly Magma and Gas Segregation Within Tunnels of the Potential Yucca Mountain Repository." *Bulletin of Volcanology*. Vol. 70. pp. 947–960.

Nicholis, M.G. and M.J. Rutherford. 2004aa. "Experimental Constraints on Magma Ascent Rate for the Crater Flat Volcanic Zone Hawaiiite." *Geology*. Vol. 32. pp. 489–492.

NRC. 2009ab. "Division of High-Level Waste Repository Safety Director's Policy and Procedure Letter 14: Application of YMRP for Review Under Revised Part 63." Published March 13, 2009. ML090850014. Washington, DC: NRC.

NRC. 2003aa. NUREG-1804, "Yucca Mountain Review Plan—Final Report." Rev. 2. Washington, DC: NRC.

Pioli, L., E. Erlund, E. Johnson, K. Cashman, P. Wallace, M. Rosi, and H. Delgado Granados. 2008aa. "Explosive Dynamics of Violent Strombolian Eruptions: The Eruption of Parícutin Volcano 1943–1952 (Mexico)." *Earth and Planetary Science Letters*. Vol. 271. pp. 359–368.

SNL. 2008ac. "Features, Events, and Processes for the Total System Performance Assessment: Methods." ANL-WIS-MD-000026. Rev. 00. Las Vegas, Nevada: Sandia National Laboratories.

SNL. 2008ag. "Total System Performance Assessment Model/Analysis for the License Application." MDL-WIS-PA-000005. Rev. 00. AD 01, ERD 01, ERD 02, ERD 03, ERD 04. Las Vegas, Nevada: Sandia National Laboratories.

SNL. 2007ab. "Atmospheric Dispersal and Deposition of Tephra From a Potential Volcanic Eruption at Yucca Mountain, Nevada." MDL-MGR-GS-000002. Rev. 03. ERD 01. Las Vegas, Nevada: Sandia National Laboratories.

SNL. 2007ae. "Characterize Eruptive Processes at Yucca Mountain, Nevada." ANL-MGR-GS-000002. Rev. 03. ERD 01, ERD 02. Las Vegas, Nevada: Sandia National Laboratories.

SNL. 2007ag. "Dike/Drift Interactions." MDL-MGR-GS-000005. Rev. 02. ERD 01, ERD 02. Las Vegas, Nevada: Sandia National Laboratories.

SNL. 2007ar. "Number of Waste Packages Hit by Igneous Events." ANL-MGR-GS-000003. Rev. 03. ERD 01. Las Vegas, Nevada: Sandia National Laboratories.

SNL. 2005ae. "In-Package Chemistry Abstraction." ANL-EBS-MD-000037. Rev. 04. ADD 01. Las Vegas, Nevada: Sandia National Laboratories.

Thorarinsson, S., S. Steinthorsson, T. Einarsson, K. Kristmannsdottir, and N. Oskarsson. 1973aa. "The Eruption on Heimaey, Iceland." *Nature*. Vol. 241. pp. 372-375.

Valentine, G.A. and K.R. Groves. 1996aa. "Entrainment of Country Rock During Basaltic Eruptions of the Lucero Volcanic Field, New Mexico." *Journal of Volcanology and Geothermal Research*. Vol. 161, No. 1-2. pp. 57-80.

Valentine, G.A. and F.V. Perry. 2007aa. "Tectonically Controlled, Time-Predictable Basaltic Volcanism From a Lithospheric Mantle Source (Central Basin and Range Province, USA)." *Earth and Planetary Science Letters*. Vol. 261, No. 3. pp. 201-216.

Valentine, G.A., F.V. Perry, D.J. Krier, D.N. Keating, R.E. Kelley, and A.H. Cogbill. 2006aa. "Small-Volume Basaltic Volcanoes: Eruption Products and Processes, and Post-eruptive Geomorphic Evolution in Crater Flat (Pleistocene), Southern Nevada." *Geological Society of America Bulletin*. Vol. 118, No. 5. pp. 1,313-1,330.

Wilson L. and J.W. Head, III. 1981aa. "Ascent and Eruption of Basaltic Magma on the Earth and Moon." *Journal of Geophysical Research*. Vol. 86, No. B4. pp. 2,971-3,001.

Woods, A.W., S. Sparks, O. Bokhove, A. LeJune, C.B. Connor, and B.E. Hill. 2002aa. "Modeling Magma-Drift Interaction at the Proposed High-Level Radioactive Waste Repository at Yucca Mountain, Nevada, USA." *Geophysical Research Letters*. Vol. 29, No. 13. p. 1,641.

CHAPTER 14

2.2.1.3.12 Concentration of Radionuclides in Groundwater

2.2.1.3.12.1 Introduction

This section of the Safety Evaluation Report (SER) provides the U.S. Nuclear Regulatory Commission (NRC) staff's review of information the applicant provided in the Safety Analysis Report (SAR) (DOE, 2008ab) on the concentration of radionuclides in groundwater extracted by pumping and used in the annual water demand. The NRC staff (staff) considered the methods and assumptions the applicant used to estimate groundwater radionuclide concentrations. The staff's review focused on SAR Sections 2.3.9 and 2.4.4.

2.2.1.3.12.2 Regulatory Requirements

10 CFR 63.312(c) states that the reasonably maximally exposed individual (RMEI) uses well water with average concentrations of radionuclides, that is based on an annual water demand of 3,000 acre-ft [3.7×10^9 L]. In performing its review, the staff followed the guidance provided in the Yucca Mountain Review Plan (YMRP), Section 2.2.1.3.12 (NRC, 2003aa). Consistent with the YMRP, the staff considered risk information to determine how to evaluate the concentration of radionuclides.

2.2.1.3.12.3 Assessment of Well Water Concentration Estimates

(b)(5)

(b)(5)

2.2.1.3.12.4 Evaluation Findings

(b)(5)

2.2.1.3.12.5 References

DOE. 2009de. "Yucca Mountain—Response to Request for Additional Information Regarding License Application (Safety Analysis Report Section 2.3.9), Safety Evaluation Report Vol. 3, Chapter 2.2.1.3.9, Set 1." Letter (November 16) J.R. Williams to J.H. Sulima (NRC). ML092820675. Washington, DC: DOE, Office of Technical Management.

DOE. 2008ab. DOE/RW-0573, "Safety Analysis Report Yucca Mountain Repository License Application." Rev. 0. Las Vegas, Nevada: DOE, Office of Civilian Radioactive Waste Management.

NRC. 2003aa. NUREG-1804, "Yucca Mountain Review Plan—Final Report." Rev. 2. Washington, DC: NRC.

CHAPTER 15

2.2.1.3.13 Airborne Transport and Redistribution of Radionuclides

2.2.1.3.13.1 Introduction

This chapter evaluates the U.S. Department of Energy's (DOE) information on airborne transport and deposition of radionuclides expelled by a potential future volcanic eruption following igneous disruption of waste packages. It also evaluates DOE information on the redistribution of those radionuclides in soil. This evaluation of DOE's performance assessment for the volcanic eruption modeling case is a sequel to the evaluation of possible igneous disruption of the proposed repository [DOE's igneous intrusion modeling case; see Safety Evaluation Report (SER) Section 2.2.1.3.10]. This chapter also evaluates redistribution of radionuclides in soil in the accessible environment, which in DOE's model arrives in the accessible environment via groundwater transport. The U.S. Nuclear Regulatory Commission (NRC) staff's evaluation is based on information in the DOE Safety Analysis Report (SAR) (DOE, 2009av), as supplemented by DOE's responses (DOE, 2009bk–bm) to the staff's requests for additional information (RAIs).

This chapter addresses 2 of the 14 model abstraction sections indicated in the Yucca Mountain Review Plan (YMRP) (NRC, 2003aa), namely airborne transport of radionuclides (YMRP Section 2.2.1.3.11) and redistribution of radionuclides in soil (Section 2.2.1.3.13). The NRC staff's assessment of information in DOE's SAR for these two abstraction sections used the guidance in the YMRP to conduct a risk-informed review. Together, airborne transport of radionuclides during a potential future explosive volcanic eruption that generates tephra (ash) and redistribution of radionuclides deposited on the landscape by that eruption constitute DOE's volcanic ash exposure scenario in its biosphere model for the Total System Performance Assessment (TSPA) (SAR Section 2.3.10.2.6). As part of the review of redistribution of radionuclides, the staff evaluated DOE's performance assessment for the exposure scenario where radionuclide-contaminated groundwater may cause the reasonably maximally exposed individual (RMEI) to be exposed to a dose (SAR Section 2.3.10.2.3). SAR Figure 2.3.10-1 displayed a separate flow of information for the volcanic ash exposure scenario compared to the groundwater exposure scenarios in the DOE performance assessment. This chapter reflects this separation of information and presents the staff's review and evaluation, first for the volcanic ash exposure scenario and second for the groundwater exposure scenario.

For the volcanic ash exposure scenario, the staff evaluated the following three abstracted models addressed in DOE's SAR:

- Airborne transport, dispersion, and deposition of tephra and high-level waste
- Redistribution by fluvial (running water or stream) transport of contaminated tephra within the Fortymile Wash catchment basin, mixing and dilution with noncontaminated sediment, and deposition of the tephra-sediment mixture on the Fortymile Wash alluvial fan at the RMEI location
- The downward migration of radionuclides in the soil at the alluvial fan in the accessible environment

The latter two abstracted models comprise DOE's performance assessment appropriate for redistribution of radionuclides in soil (YMRP Section 2.2.1.3.13), while the first abstracted model constitutes DOE's performance assessment for airborne transport of radionuclides (YMRP Section 2.2.1.3.11).

For the groundwater exposure scenario, this chapter presents the staff's evaluation of DOE's surface soil submodel, which is also part of the performance assessment for redistribution of radionuclides in soil. For both exposure scenarios, the final outputs of the abstractions evaluated in this chapter are radionuclide concentrations in soil, which are direct inputs to the DOE biosphere model for calculating annual doses to the RMEI (reviewed by the staff in SER Section 2.2.1.3.14). Associated with this, SER Section 2.2.1.3.4 presents the staff's evaluation of the radionuclide inventory, which is an input to the volcanic ash exposure scenario (SAR Figure 2.3.10.3). Last, to complete the staff's evaluation of the performance of DOE's volcanic eruption modeling case, SER Section 2.2.1.4 assesses the demonstration of compliance with the postclosure public health and environmental standards.

2.2.1.3.13.2 Regulatory Requirements

Model abstractions used in the applicant's postclosure performance assessment must meet the regulatory requirements given in 10 CFR 63.114 (Requirements for Performance Assessment) and 63.342 (Limits on Performance Assessment), to support the predictions of compliance for 63.113 (Performance Objectives for the Geologic Repository after Permanent Closure). Specific compliance with 63.113 is reviewed in SER Section 2.2.1.4.1.

The requirements for performance assessment in 10 CFR 63.114 require the applicant to

- Include appropriate data related to the geology, hydrology, and geochemistry of the surface and subsurface from the site and the region surrounding Yucca Mountain
- Account for uncertainty and variability in the parameter values used to model airborne transport and redistribution of radionuclides
- Consider alternative conceptual models for airborne transport and redistribution of radionuclides
- Provide technical bases for the inclusion of features, events, and processes (FEPs) affecting airborne transport and redistribution of radionuclides, including effects of degradation, deterioration, or alteration processes of engineered barriers that would adversely affect performance of the natural barriers, consistent with the limits on performance assessment in 10 CFR 63.342
- Provide technical basis for the models of airborne transport and redistribution of radionuclides that in turn provide input or otherwise affect other models and abstractions

10 CFR 63.114(a) considers performance assessment for the initial 10,000 years following permanent closure. 10 CFR 63.114(b) and 63.342 consider the performance assessment methods for the time from 10,000 years through the period of geologic stability, defined in 10 CFR 63.302 as 1 million years following disposal. These sections require that through the period of geologic stability, with specific limitations, the applicant

- Use performance assessment methods consistent with the performance assessment methods used to demonstrate compliance for the initial 10,000 years following permanent closure
- Include in the performance assessment those FEPs used in the performance assessment for the initial 10,000 year period

For this model abstraction of airborne transport and redistribution of radionuclides, 10 CFR 63.342(c)(1) further provides that DOE assess the effects of seismic and igneous activity on the repository performance, subject to the probability limits in 63.342(a) and 63.342(b). Specific constraints on the analysis required for seismic and igneous activity are given in 10 CFR 63.342(c)(1)(i) and 10 CFR 63.342(c)(1)(ii), respectively

In addition, 10 CFR 63.305 provides the following requirements for characteristics of the reference biosphere, as used in this abstraction for redistribution of radionuclides in soil

- FEPs that describe the reference biosphere must be consistent with present knowledge of the conditions in the region surrounding the Yucca Mountain site.
- DOE should not project changes in society, the biosphere (other than climate), or human biology or increases or decreases of human knowledge and technology; in all analyses done to demonstrate compliance with this part, DOE must assume that all of those factors are constant as they are at the time of submission of the license application.
- DOE must vary factors related to the geology, hydrology, and climate based upon cautious but reasonable assumptions of the changes in these factors that could affect the Yucca Mountain disposal system during the period of geologic stability, consistent with the requirements for performance assessments specified at 10 CFR 63.342.
- Biosphere pathways must be consistent with arid or semi-arid conditions

NRC staff review of the license application follows the guidance laid out in the YMRP Sections 2.2.1.3.11, Airborne Transport of Radionuclides, and 2.2.1.3.13, Redistribution of Radionuclides in Soil, as supplemented by additional guidance for the period beyond 10,000 years after permanent closure (NRC, 2009ab). The acceptance criteria in the YMRP generically follow 10 CFR 63.114(a). Following the guidance, the NRC staff review of the applicant's abstraction of airborne transport and redistribution of radionuclides considered five criteria

- System description and model integration are adequate.
- Data are sufficient for model justification.
- Data uncertainty is characterized and propagated through the abstraction.
- Model uncertainty is characterized and propagated through the abstraction.
- Model abstraction output is supported by objective comparisons.

Because 10 CFR Part 63 specifies the use of a risk-informed approach for the review of a license application, the guidance provided by the YMRP, as supplemented by NRC (2009ab), is followed to the extent reasonable for aspects of airborne transport and redistribution of radionuclides important to repository performance. Whereas NRC staff considered all five criteria in their review of information provided by DOE, only aspects that substantively affect

results of the performance assessment, as judged by NRC staff, are discussed in this chapter. NRC staff's judgment is based both on risk information provided by DOE, and staff's knowledge, experience, and independent analyses.

2.2.1.3.13.3 Technical Review

In SAR Figure 2.3.11-1, DOE presented the information flow for the volcanic eruption modeling case. As stated previously, DOE's abstracted model on atmospheric dispersal and deposition of tephra constitutes its performance assessment of airborne transport of radionuclides. DOE's abstracted models for tephra redistribution and vertical radionuclide migration in soil together comprise the performance assessment of redistribution of radionuclides in soil.

Airborne transport of radionuclides pertains to the volcanic ash exposure scenario, which involves a possible disruption of the Yucca Mountain repository by a future volcanic eruption. In this scenario, high-level radioactive waste is mixed with magma and ejected into the atmosphere incorporated within the volcanic tephra (fragments of cooled magma that are transported through the air, including ash particles that have diameters less than 2 mm [0.08 in]). The airborne transport abstracted model accepts the number of waste packages intersected by volcanic conduits, provided in SAR Section 2.3.11.4.2.1 and evaluated in SER Section 2.2.1.3.10, and estimates the concentration and thickness of radionuclide-contaminated tephra that could be deposited on the ground surface of the Yucca Mountain region (SAR Figure 2.3.11-1). As depicted in SAR Figure 2.3.11-1, DOE then uses this information as input to the volcanic ash exposure scenario (SAR Section 2.3.10) for estimating the dose to the RMEI via surface redistribution of contaminated tephra and by migration of radionuclides from tephra particles into the soil, as described next.

Redistribution abstracted models together calculate the time-dependent profile of radionuclide concentration in the contaminated soil horizon at the RMEI location. The airborne transport abstracted model (described previously) provides input on the tephra deposit for the tephra redistribution calculations of waste concentrations in redistributed tephra. Another redistribution-related abstracted model uses this information to estimate the downward migration of radionuclides from tephra into soil at the alluvial fan of Fortymile Wash and calculate the concentration of waste in redistributed tephra at the RMEI location (SAR Figure 2.3.11-1). Waste concentration information from redistribution models is coupled with information on the radionuclide inventory (radionuclide activities per unit mass of waste) to yield radionuclide concentration profiles in soil. The fraction of tephra that can be resuspended and inhaled by the RMEI during activities such as tillage is also important, this is the dominant exposure pathway for the first 10,000 years after repository closure.

In this section, the staff also evaluates the DOE surface soil submodel for the groundwater exposure scenario, described in SAR Section 2.3.10. In this model, radionuclides are considered to be added to the surface soil from irrigation with contaminated groundwater. The surface soil submodel accepts the concentration of radionuclides in groundwater in the accessible environment (as provided in SAR Section 2.4.4 and reviewed in SER Section 2.2.1.3.12) and calculates loss of radionuclides from the surface soil via mechanisms such as radioactive decay, leaching into deeper zones, erosion of soil particles, and gaseous releases to the atmosphere. As depicted in SAR Figures 2.3.10-1 and 2.3.10-10, the output from the surface soil model is used by the rest of biosphere model, which is reviewed in SER Section 2.2.1.3.14.

Risk Perspective

The volcanic ash exposure scenario and groundwater exposure scenario provide different contributions to repository performance. The volcanic ash exposure scenario (volcanic eruption modeling case) does not significantly influence repository performance, because its mean dose contribution is more than a factor of 1,000 smaller than the overall peak dose within 10,000 years and more than a factor of 10,000 smaller than the overall peak dose after 10,000 years (SAR Figure 2.4-18). The remaining modeling cases depicted in SAR Figure 2.4-18 constitute the groundwater exposure scenario. The groundwater exposure scenario dominates the overall peak dose within 10,000 years and after 10,000 years (SAR Figure 2.4-18). Although this risk information suggests that the staff should focus more attention on the surface soil submodel in the groundwater exposure scenario and only conduct a simplified review of the volcanic ash exposure focusing on the bounding assumptions, the staff also used DOE's multiple barrier information, consistent with YMRP Section 2.2.1.3, to inform its review.

SER Section 2.2.1.1 describes the staff's evaluation of multiple barriers. (b)(5)

(b)(5)

(b)(5) DOE did identify that a volcanic event could adversely affect the engineered barrier system's ability to prevent the release or reduce the release rate of radionuclides from the waste, and to prevent or reduce the movement of radionuclides away from the repository (SAR Section 2.3.11.1) by destroying the waste packages and releasing the contained radionuclides in the erupting material (SAR Section 2.1.2.2.5). (b)(5)

(b)(5)

Finally, in determining the scope of its risk-informed review for both the volcanic ash exposure scenario and groundwater exposure scenario, the staff considered those results from the abstracted models reviewed in this chapter that factor into the staff's evaluation of DOE's performance assessment used to determine compliance with the requirements of the postclosure individual protection standard. The staff's individual protection evaluation is presented in SER Section 2.2.1.4.1. One part of the individual protection evaluation focuses on whether the TSPA code provides a credible representation of repository performance.

For the volcanic ash exposure scenario, the staff's evaluation of DOE's performance assessment is presented in SER Section 2.2.1.4.1.3.2. The four input quantities identified for that evaluation (fraction entrained in ash, tephra volume, tephra density, and ash areal concentration) directly relate to the airborne transport abstracted model reviewed in this chapter.

(b)(5)

(b)(5)

(b)(5)

SAR Figure 2.4-32 identified the contribution of radionuclides to mean annual dose for the volcanic eruption modeling case.

SAR Table 2.3.10-15 identified the average percentage exposure pathway contributions to the annual dose for the volcanic ash exposure scenario. On the basis of this information, at early times (i.e., before 500 years), the overall dose is dominated by six radionuclides: Sr-90, Cs-137, Pu-238, Pu-239, Pu-240, and Am-241. At longer times (i.e., after 5,000 years), the dose is dominated by Pu-239 and Pu-240, and at very long times (i.e., after 100,000 years), the dose is dominated by Ra-226 (SAR Figure 2.4-32). On the basis of the identification of the dominant dose contributors and information in SAR Table 2.3.10-15, inhalation of particulates from the resuspension of contaminated tephra deposits is the dominant dose pathway for 10,000 years. After about 100,000 years, for Ra-226, the dominant exposure pathway is external exposure (SAR Table 2.3.10-15). (b)(5)

(b)(5)

For the groundwater exposure scenario, the surface soil submodel reviewed in this chapter is one component of the abstracted model for the biosphere that calculates biosphere dose conversion factors. For the radionuclides Tc-99, I-129, Np-237, and Pu-242 discussed in SER Section 2.2.1.4.1.3 in the table on groundwater biosphere dose conversion factors and SER Section 2.2.1.4.1.3.3, the pathways linked to the surface soil submodel account for up to 50 percent of the radionuclide biosphere dose conversion factor, as identified in SNL Tables 6.13-1 and 6.13-2 (2007ac).

On the basis of these risk considerations, the staff conducted a risk-informed review of airborne transport of radionuclides and redistribution of radionuclides in the soil by evaluating the DOE information relative to the acceptance criteria in YMRP Sections 2.2.1.3.11.3 and 2.2.1.3.13.3. The staff focused on those aspects of these model abstractions that impact individual protection compliance. To assess the effect that the combined uncertainties could have on calculated dose, the staff also focused on those aspects that could cause at least a factor of two effect on intermediate model outputs over the range of an individual parameter value.

As identified previously, SAR Figure 2.3.10-1 displayed a separate flow of information for the volcanic ash exposure scenario compared to the groundwater exposure scenarios in the DOE performance assessment. The staff's evaluations of the DOE information on the volcanic ash exposure scenario and the surface soil submodel for the groundwater exposure scenario are documented in SER Sections 2.2.1.3.13.3.1 and 2.2.1.3.13.3.2, respectively.

2.2.1.3.13.3.1 Assessment and Review of the Volcanic Ash Exposure Scenario

The NRC staff's evaluations of DOE's abstracted models on (i) airborne transport, dispersion, and deposition of tephra and high-level waste, (ii) redistribution of tephra, and (iii) the vertical movement of radionuclides in the soil at the alluvial fan in the accessible environment are presented separately in three subsections. Each subsection first identifies those important aspects of DOE's abstracted model that were the focus of the staff's review. The staff then summarizes the DOE license application for the abstracted model, followed by its review and evaluation. After the staff's evaluation of vertical movement of radionuclides in the soil, a final subsection presents the overall evaluation findings for the volcanic ash exposure scenario.

In addition to reviewing the individual abstracted models, the NRC staff also reviewed how DOE implemented these models into the Total System Performance Assessment-License Application (TSPA-LA). Because the acceptability of DOE's implementation of the abstracted models in the TSPA-LA is dependent on the staff's findings for the individual model abstractions, the staff's evaluation of DOE's implementation of the abstracted models in the TSPA-LA is presented in the overall evaluation findings for the volcanic ash exposure scenario. To place the individual model abstractions into the framework of the TSPA-LA, the staff summarizes DOE's implementation of the volcanic eruption modeling case next.

The applicant integrated abstracted models of TSPA-LA for the volcanic eruption modeling case (volcanic interaction with the repository, atmospheric transport, tephra redistribution, volcanic ash exposure) in a GoldSim modeling environment. The applicant used the initial radionuclide inventory from a "blended" waste package to calculate radionuclide transport, as described in the review of the previously mentioned submodels. A blended waste package inventory was calculated by using a weighted average of commercial spent nuclear fuel and codisposal waste packages and inventories. Following a conditional future eruptive event, tephra transport and redistribution are abstracted to occur instantaneously (i.e., radionuclide waste transport to the RMEI is instantaneous) (SAR Section 2.3.11.4.2.3.1). The time dependence of radionuclide diffusion (downward migration) into the soil at the RMEI location was accounted for in the tephra redistribution model. The radionuclide concentration in the soil at the RMEI location, in g/cm², was modified by a "decay factor" to account for radionuclide decay and ingrowth. The resultant source term was provided to the volcanic ash exposure submodel to calculate dose.

2.2.1.3.13.3.1.1 Airborne Transport Modeling

The NRC staff conducted a risk-informed review of airborne transport of radionuclides, concentrating on aspects important to the volcanic ash exposure scenario in the DOE performance assessment.

Important Aspects of Airborne Transport

The abstracted model for atmospheric transport of radionuclides determines the characteristics of contaminated tephra deposited on the surrounding landscape. The applicant's analysis results indicated that the following parameters for airborne transport were influential to the volcanic ash exposure scenario: magma partitioning factor, tephra volume, eruptive power and duration, and mean ash particle diameter, wind direction, and wind speed. The magma partitioning factor is a fraction between zero and one and acts as a direct multiplier on the eruption source term and eruptive dose, similar to the number of waste packages entrained into the erupting magma that pertains to the review in SER Section 2.2.1.3.10. DOE's analysis results [e.g., SNL Figures C-1 and C-2 (2007ab)] showed that waste concentration in tephra is sensitive to tephra volume, eruptive power, and mean ash particle diameter. DOE's sensitivity analyses concluded that the initial tephra thickness at the RMEI location (near the Fortymile Wash alluvial fan apex) is strongly dependent on wind direction, wind speed, and mean ash particle diameter, and moderately dependent on eruptive power and eruptive duration, as identified in SNL Appendix C (2007ab). Other parameters of the airborne transport abstracted model applicant investigated were less influential on tephra thickness.

Summary of Information in DOE License Application on Airborne Transport

The volcanic eruption modeling case was described in SAR Section 2.3.11.4. In SAR Table 2.3.11-1, DOE identified the FEPs included in the TSPA.

For a repository-drift-penetrating basaltic eruption, DOE modeled the contamination of tephra with waste and the amount of radionuclides contained within the tephra-fall deposit. On the basis of studies of analog volcanoes, DOE apportioned contaminated magma into three volcanic products; namely, lava, scoria cone-forming deposits (selectively composed of the largest tephra fragments), and more widespread tephra-fall deposits. To account for waste that is incorporated in volcanic ejecta that form scoria cones and lava flows, the applicant applied a magma partitioning factor for the fraction of waste incorporated with tephra to the total waste erupted. In the DOE model for the extrusive event, only waste incorporated with tephra contributes radiological dose to the RMEI; waste apportioned into lava flows and scoria cones does not contribute to dose. The amount of waste incorporated in tephra scales with the magma partitioning factor.

In its igneous eruption modeling, the applicant identified that all the explosive phases of the most likely future eruption, on the basis of the interpreted behavior of the youngest volcano near the repository site (Lathrop Wells), are considered to be violent Strombolian (SAR Section 2.3.11.4.1). The eruption would produce plumes of tephra in the atmosphere that could transport particulates, including high-level radioactive waste, downwind from the vent. This process could deposit radionuclides at the RMEI location, either from direct sedimentation of contaminated ash particles from the volcanic plume or from the remobilization by wind or surface water of the radionuclide-contaminated volcanic ash after initial deposition. DOE's approach to determining waste concentration in the tephra is sensitive to the tephra volume. For example, smaller tephra volumes result in higher waste concentration in tephra (i.e., waste mass per unit mass of tephra) for the same number of waste packages entrained. In SNL (2008ag), DOE evaluated exposure to airborne concentrations of radionuclides that are captured in the tephra during the eruption (direct tephra-fall exposure) and found that it did not increase expected annual dose significantly due to the extremely short exposure duration. In the following review, "tephra" refers to airborne magmatic fragments of all sizes, whereas "ash" refers specifically to particles less than 2 mm [0.08 in] in diameter.

A violent Strombolian-type eruption is characterized by the development of a sustained, buoyant plume of hot air and volcanic tephra that commonly rises several kilometers [a few miles] above the volcano. DOE modeled the dispersal processes as turbulent advection diffusion using the Suzuki (1983aa) model. The Ashplume conceptual model and the ASHPPLUME code (Jarzemba, et al., 1997aa), as used by the applicant, implement the Suzuki approach to model the dispersal of tephra on the basis of the diffusion of particles from an eruption column, horizontal diffusion of particles by atmospheric turbulence, horizontal advection by atmospheric circulation, and settling of particles by gravity. ASHPPLUME accounts for incorporation and entrainment of waste particles into magma during a potential volcanic eruption through the repository and estimates the concentration (expressed as g/cm²) and thickness of radionuclide-contaminated tephra deposited on the ground surface. Following a conditional eruptive event, tephra transport is abstracted to occur instantaneously (i.e., radionuclide waste transport to the RMEI is instantaneous).

In DOE's approach, wind direction significantly affects tephra dispersal and deposit location. Tephra deposits that might fall at the RMEI location are strongly dependent on the presence of northerly winds that would transport the tephra plume to the south from a volcanic vent within

the repository area (SAR Figure 2.3.11-13). The tephra deposit at the RMEI location becomes negligible for winds without a strong northerly component (north, north-northwest, or north-northeast), as identified in SNL Figure C-7 and Table D-5 (2007ab). The majority of the wind vectors at the site result in tephra being deposited to the east of Yucca Mountain (SAR Figure 2.3.11-15). According to SNL Appendix K (2007ab), this wind direction provides a source of material for remobilization within the Fortymile Wash catchment basin. Applicant-performed sensitivity analyses indicated that wind direction produced a greater contribution to dose than plume spread and divergence, as outlined in SNL Figure K-4c (2007ab). These sensitivity analyses also demonstrated that increasing the wind speed causes the tephra deposit center mass to shift downwind.

Staff's Evaluation of Airborne Transport

The staff reviewed SAR Section 2.3.11 on the volcanic eruption modeling case, additional information provided in response to the staff's RAIs (DOE, 2009bk-bm), the supporting DOE information on atmospheric transport of contaminated tephra presented in SNL (2007ab), and information published in peer-reviewed literature (e.g., Suzuki, 1983aa; Hurst and Turner, 1999aa; Andronico, et al., 2008aa).

Model Integration

Potentially relevant FEPs in DOE's TSPA-LA were listed in SAR Table 2.2-1. Model abstractions comprise FEPs that have been screened in from the applicant-conducted scenario analysis. SER Section 2.2.1.2.1 documents the staff's evaluation of the DOE scenario analysis and FEPs screening. As part of the review of the volcanic modeling case, the staff examined DOE's information on igneous-related FEPs. In SER Section 2.2.1.2.1.3.1, the staff determines that DOE identified a complete list of FEPs for the volcanic exposure scenario, including airborne transport (b)(5)

(b)(5)

DOE

excluded a related FEP from consideration due to low consequence (FEP 1.2.04.07.0B). That FEP is concerned with leaching of radionuclides from tephra on the surface into the subsurface and into groundwater, whereby radionuclides could be dispersed via the groundwater transport pathway. (b)(5)

(b)(5)

(b)(5)

The staff's review of the airborne transport abstracted model evaluates the applicant's implementation of the only included FEP (FEP 1.2.04.07.0A) associated with airborne transport modeling.

FEP 1.2.04.07.0A describes finely divided waste particles that may be erupted from a volcanic vent and deposited on the land surface from a waste-particle-contaminated ash (tephra) cloud or plume. This FEP is included in the performance assessment through the modeling of an eruption that includes airborne transport and tephra deposition (SNL, 2008ab).

The NRC staff evaluated modeling assumptions and integration in the DOE airborne transport abstracted model. DOE assumed that the tephra in a future eruption would be dispersed by a violent Strombolian eruption column, characterized by heating of entrained air. (b)(5)

(b)(5)

(b)(5)

In its tephra-fall modeling, DOE assumed violent Strombolian activity for the entire duration of the tephra-forming activity. (b)(5)

(b)(5)

DOE calculated tephra and waste deposited at the RMEI location for a point located 18 km [11 mi] south of the volcanic vent, as outlined in SNL Section 6.5.2.1.17 and Table 8-2 (2007ab). (b)(5)

(b)(5)

(b)(5)

Data Sufficiency and Data Uncertainty

(b)(5)

(b)(5)

(b)(5) The staff reviewed the range of important parameters DOE derived from analog volcanoes (SNL, 2007ab,ae). (b)(5)

(b)(5)

Magma Partitioning Factor

The applicant accounted for a proportion of disrupted and erupted waste that is partitioned into erosion-resistant products (scoria cone and lava flows) by using a magma partitioning factor with a uniform distribution from 0.1 to 0.5 (also discussed in SER Section 2.2.1.3.10). This range is based on volumetric proportions of cones and lava flows to total erupted volume estimated from field measurements at analog volcanoes, as identified in SNL Section 6.5.2.22 (2007ab). DOE identified in SAR Section 2.3.11.4.1.1.3 that very little erosional modification of lava fields of ~350,000-year-old volcanoes (Little Black Peak and Hidden Cone) has occurred. The applicant also indicated that little if any cone scoria has yet been remobilized to the base of the cone where it would be available for fluvial transport for the 80,000-year-old Lathrop Wells (SAR Section 2.3.11.4.1.1.3). (b)(5)

(b)(5)

(b)(5) DOE used data from eight analog volcanic eruptions to determine a range of 0.1 to 0.5 for the magma partitioning factor (BSC, 2003ad, SNL, 2007ab). (b)(5)

(b)(5)

(b)(5) The applicant used analog data to support the parameter range for the magma partitioning factor, including the lower part of the range with values less than 0.3, as discussed in DOE Enclosure 8, Table 1 (2009bk). DOE Enclosure 8 (2009bk) stated the tephra component is small in many of these basaltic analog eruptions. (b)(5)

(b)(5)

Magma Volume

The NRC staff reviewed the data synthesis and documentation on likely magma volumes for future eruptions the applicant provided in SNL (2007ab) and SNL Section 6.3.4.4 (2007ae). (b)(5)

(b)(5)

(b)(5)

(b)(5)

In the Ashplume model, DOE used the relationship among eruption power, eruption volume (rather than tephra volume), and eruption duration to constrain the range of total mass of tephra. As discussed in SNL Section 6.5.2.1 (2007ab), DOE constrained eruptive power on the basis of a few observed violent Strombolian eruptions. DOE showed that the tephra-fall volume in the DOE TSPA ranged from 0.004 to 0.14 km³ [0.001 to 0.03 mi³] with a mean value of 0.038 km³ [0.01 mi³], as identified in DOE Enclosure 3, Figure 1 (2009bl).

(b)(5)

Ash Particle Diameter

(b)(5)

Eruptive Power and Duration

The applicant analyzed the eruptive parameters of analog volcanoes to develop the range and parameter distribution for eruptive power. (b)(5)

(b)(5)

The upper part of the applicant's eruptive power range for possible future basaltic eruptions at Yucca Mountain leads to modeled eruption column heights of up to 8.2 km [5.0 mi] (SNL, 2007ab). (b)(5)

(b)(5)

(b)(5)

To build confidence in the ASHPLUME model, the applicant exercised this extended upper range for column height to model tephra dispersal for a volcano in New Zealand with a different eruption type, as identified in SNL Appendix J, p. J-23 (2007ab) and compare it with published results on tephra dispersal for that volcano. (b)(5)

(b)(5)

(b)(5)

The applicant clarified that column heights in the ASHPLUME realizations ranged from lower values of about 2 km [1.2 mi] up to a maximum value of 8.2 km [5.0 mi] in the DOE TSPA, as identified in DOE

Enclosure 1 (2009bk). (b)(5)

(b)(5)

Wind Direction and Speed

The applicant developed distribution functions for wind speed and wind direction from data provided in National Oceanic and Atmospheric Administration (NOAA) (2004aa). The full range of wind speeds from near zero to the maximum winds observed at the higher altitudes was represented in the wind-speed distribution used in TSPA analyses (SNL, 2007ab). The applicant accounted for uncertainty by stochastically sampling wind speed and direction for each eruption realization. DOE Enclosure 1 (2009bk) provided a technical basis by demonstrating that wind speed and wind direction are not correlated at different altitudes in the Ashplume model. DOE assigned the same wind speed for the top and lower heights within the column. (b)(5)

(b)(5)

Eruption Column Parameter

Although the column diffusion constant (β) was not determined to be an influential parameter, the NRC staff reviewed the DOE application of this parameter in the Ashplume model, which determines the vertical distribution of the mass of tephra particles within the eruption column and helps determine the height at which particles exit the column and enter downwind atmospheric transport. The parameter range for β DOE used is 0.01 to 0.5, and values at the lower end of the distribution lead to more of the tephra mass diffusing (falling) from the eruption column at relatively low altitudes in the modeled eruption (SNL, 2007ab). The applicant modeled (DOE, 2009bk) small tephra particle diameters (e.g., 0.005 cm [0.002 in]), relatively high initial rise velocities (e.g., 9,000 cm/s [3,543 in/s]), and column diffusion coefficient values (β) less than 0.3 to support upward-concentration particle distributions at realistic heights for violent Strombolian eruption columns. (b)(5)

(b)(5)

(b)(5) DOE (2009bk) estimated that varying β from 0.01 to 0.5 reduces the estimated waste concentration by less than 30 percent. (b)(5)

(b)(5)

Model Output: Waste Concentration in Tephra

NRC evaluated the outputs from the DOE abstracted model, described in SNL p. 6-10 (2007ab), on airborne transport for the waste concentration in tephra and its spatial variation with distance and direction from the vent. (b)(5)

(b)(5)

(b)(5) In DOE Enclosure 2 (2009bk) and DOE Enclosures 2 and 3 (2009bm), the applicant provided information on the spatial variation of waste concentration in tephra, which demonstrates how much calculated concentrations varied within the same realization (e.g., how the concentration at downwind distances differed from waste concentrations in tephra closer to the vent). On a per-mass basis, waste constitutes a very small fraction of the mass in tephra deposits. Specifically, the applicant showed the mass of waste per unit mass of tephra was between 10^{-5} and 10^{-6} in deposits for two representative realizations in DOE Enclosure 2, Figure 1 (2009bk) and DOE Enclosure 3, Supplemental Figure 1 (2009bm). In DOE Enclosures 2 and 3 (2009bm), the applicant clarified that these values correspond to a single waste package and do not account for the partitioning of waste into scoria cone and lava flows. (b)(5)

(b)(5)

Model Uncertainty

The NRC staff evaluated model uncertainty in the DOE abstracted model for airborne transport. DOE addressed model uncertainty by considering alternative models such as a Gaussian plume model, PUFF; a gas-thrust code, ASHFALL; and TEPHRA in SNL (2007ab). The applicant also evaluated the alternative igneous source term model the NRC staff developed (Codell, 2003aa) to investigate the processes of waste fragmentation and incorporation into the tephra and concluded that this alternative model was not significantly different from Ashplume (SNL, 2007ab). (b)(5) The applicant specifically chose the Ashplume model because it incorporates both tephra dispersal and waste incorporation required for performance assessment analyses. (b)(5)

(b)(5)

Model Support

The applicant supported its model results with (i) an independent technical review, SNL Appendix E (2007ab); (ii) a comparison to field observations from an analog eruption; and (iii) a comparison to another airborne transport code. With regard to the latter, the ASHFALL code (Hurst and Turner, 1999aa) represents sophisticated models incorporating the physics of tephra transport and deposition but does not include radionuclide transport. ASHFALL uses the same advective-diffusive relationships as Ashplume, but employs time- and altitude-dependent wind conditions for tephra dispersal and more explicitly treats tephra particle settling velocities. The ASHPLUME code was used in two sets of model runs to reproduce published output from the ASHFALL code for constant wind conditions and a variable wind field. SNL Appendix J (2007ab), the applicant's comparison of ASHPLUME and ASHFALL model computations, indicated that ASHPLUME calculates tephra thicknesses that are within a factor of two of ASHFALL results. The applicant also supported its abstracted model with a comparison to field measurements of tephra thickness for the 1995 eruption at Cerro Negro, Nicaragua, outlined in SNL Appendix L (2007ab). (b)(5)

(b)(5)

Evaluation Findings for Airborne Transport

(b)(5)

In SER Section 2.2.1.4.1.3.2, the staff evaluates the applicant's demonstration of compliance with the postclosure public health and environmental standards for the volcanic ash exposure scenario. In that evaluation, four input quantities (fraction entrained in ash, tephra volume, tephra density, and ash areal concentration) relate to the representation of the performance assessment for atmospheric transport and are evaluated next.

In the DOE model for an extrusive volcanic event, the amount of waste incorporated in tephra scales with the magma partitioning factor (SNL, 2007ab). On the basis of the relative proportions of eruptive products at analog volcanoes, the applicant selected a range between 0.1 and 0.5 for this parameter, which acts as a direct multiplier on the eruption source term and

eruptive dose (b)(5)
(b)(5)

The applicant analyzed tephra-fall volumes for Quaternary Period (approximately last 2 million years) volcanoes in the Yucca Mountain region by comparison with fall cone and cone: lava volume ratios for well-preserved young basaltic volcanoes. (b)(5)

(b)(5)

(b)(5) For Lathrop Wells volcano, an appropriate example of the type of eruptive event that could disrupt the potential repository at Yucca Mountain, the estimated tephra volume is 0.07 km³ [0.017 mi³] (SNL, 2007ae). (b)(5)

(b)(5)

Bulk *in-situ* density of tephra-fall deposits typically ranges from 0.3 to 1.5 g/cm³ [0.01 to 0.5 lbs/in³] (Sparks, et al., 1997aa). (b)(5) Blong (1984aa) measured a range of tephra deposits that have a density of approximately 1.0 g/cm³ [0.4 lbs/in³]. DOE (SNL, 2007ae) used 1.0 g/cm³ [0.4 lbs/in³] for TSPA calculations on the basis of both this value from Blong (1984aa) and a normal distribution of deposit densities ranging from 0.3 to 1.5 g/cm³ [0.01 to 0.5 lbs/in³] with a mean of 1.0 g/cm³ [0.4 lbs/in³]. (b)(5)

(b)(5)

The ash areal concentration was derived from an assumed 1-cm [0.54-in] thickness of deposited tephra. In SNL Appendix G (2007ac), DOE calculated an arithmetic mean of 0.97 cm [0.54 in] for tephra thickness at the RMEI location for a wind direction fixed to the south. (b)(5)

(b)(5)

2.2.1.3.13.3.1.2 Tephra Redistribution in Fortymile Wash

The NRC staff conducted a risk-informed review of tephra redistribution, concentrating on those aspects important to the volcanic ash exposure scenario in the DOE performance assessment, as given next.

Important Aspects of Tephra Redistribution

DOE modeling of redistribution of tephra includes fluvial (running water or stream) transport of contaminated tephra within the Fortymile Wash catchment basin, mixing and dilution with noncontaminated sediment, and deposition of the tephra-sediment mixture on the Fortymile Wash alluvial fan at the RMEI location. These processes are modeled to occur instantaneously, thus not allowing for any radioactive decay of contaminated tephra before its deposition at the RMEI. In DOE's model, on the alluvial fan, tephra is deposited in distributary channels by redistribution processes and on interchannel divides from airborne transport.

DOE performance assessment results for the volcanic ash exposure scenario are influenced by radionuclide concentrations in soil from both distributary channels and interchannel divides, as described in DOE Enclosure 5, Figure 1 (2009bk). Radionuclides in distributary channels contribute dose to the volcanic ash exposure scenario from the large number of realizations that result in an initial tephra deposit in the Fortymile Wash catchment basin. Fluvial sediment in

distributary channels contributes more (two thirds, on average, in the DOE model) to the airborne particle concentration at the RMEI location than soils on interchannel divides (one third).

The NRC staff reviewed auxiliary Monte Carlo simulations by Pelletier, et al. (2008aa) that indicated the fluvial transport abstracted model reduced the concentration of tephra in sediment deposited in distributary channels by a factor of about 100 (arithmetic mean of 20 simulations), compared to the tephra concentration in the original tephra deposit. DOE expects any waste attached to tephra particles to remain attached during fluvial transport. Thus, any reduction in tephra concentration from fluvial transport should reduce waste concentration by the same amount, as outlined in SNL Section 5.2.5 (2007av). On the basis of sensitivity analyses the applicant performed, identified in SNL Section 6.6.1, Figures 6.6.1-1 to 6.6.1-3 (2007av), realizations with the largest waste concentrations were most sensitive to critical slope and scour depth, in that order, and slightly sensitive to drainage density. Because DOE took credit for waste dilution during fluvial transport in the FAR model, the NRC staff also focused its review on modeling assumptions and model support.

Summary of Information in DOE License Application on Tephra Redistribution

The applicant's model of radionuclide redistribution in Fortymile Wash for the volcanic ash exposure scenario was described in SAR Section 2.3.11. In SAR Table 2.3.11-1, DOE identified the FEPs included in the TSPA.

Following deposition of contaminated tephra (SER Section 2.2.1.3.13.2) from a potential eruption where a volcanic conduit intersects waste packages, the tephra redistribution model accounts for the mobilization of contaminated tephra in the Fortymile Wash catchment basin, dilution of contaminated tephra with noncontaminated sediments in fluvial (stream) channels, and fluvial deposition at the location of the RMEI. Fortymile Wash lies east of the repository, which DOE showed to be the most likely direction for tephra dispersal at typical heights for violent Strombolian eruption columns (SAR Figure 2.3.11-15). DOE developed the FAR Version 1.2 code, referred to hereafter as the FAR model, and incorporated this code into its TSPA as a dynamically linked library. The tephra redistribution is abstracted to occur instantaneously (i.e., radionuclide waste transport to the RMEI is instantaneous) (SAR Section 2.3.11.4.2.3.1). Eolian (wind-induced) processes are not included in the tephra redistribution model.

In the DOE model described in SNL (2007av), tephra is mobilized and transported downstream if it is initially deposited either on slopes steeper than a critical slope angle or in active channels with stream power exceeding a threshold value. Critical slope parameter values were determined from field measurements at analog sites. DOE determined active channel networks from digital elevation model data and drainage density estimates, on the basis of calibrations to field observations. Channel geomorphology in the Fortymile Wash catchment basin was based on recent observations and is modeled as time invariant. Effects on surface slope, elevation, stream power, and drainage density due to the presence of an initial tephra deposit and its weathering over time were not modeled. DOE considered these effects within the context of existing parametric values and propagated uncertainty, and exclusion of these effects from the model was not expected to significantly change the model results, as described in DOE Enclosure 10, Section 1 (2009bk).

DOE used scour depth estimates to determine the mixing and dilution of tephra with noncontaminated channel sediments. After the 1995 flood event, DOE measured scour depth

in Fortymile Wash and estimated a total scour depth to account for the cumulative effect of flood events over time in the DOE TSPA. Nevertheless, sediment transport time is not explicitly accounted for in the model for fluvial remobilization and tephra dilution. Instead, a simplification is made that remobilized tephra is instantaneously diluted in fluvial sediments and directly deposited at the alluvial fan (i.e., fluvial remobilization, dilution, and deposition occur at the same simulation timestep as initial tephra-fall deposition).

The Fortymile Wash alluvial fan is located at the southern end of the drainage system; DOE modeled it as active (distributary) stream channels and areas between channels (interchannel divides). In the DOE tephra redistribution model, the whole alluvial fan is assumed to be an RMEI-occupied area (SAR Figure 2.3.11-13). Parameter values for the area of the Fortymile Wash alluvial fan and the fraction of that area associated with channels were determined from field measurements and soil geomorphic mapping. In the event of a future model volcanic eruption, initial radionuclide concentrations on interchannel divides arise from original tephra-fall deposits across the fan. Redistributed tephra mixed with ambient sediment from the Fortymile Wash drainage system is deposited in distributary channels and not on interchannel divides. Radionuclide concentrations in distributary channels therefore include a mixture of redistributed tephra from the Fortymile Wash drainage system and any original tephra-fall deposits. DOE assumed redistributed tephra is transported as bedload material, which neglects the potential for silt-sized material to be transported in the suspended (streamflow-borne) load past the RMEI location and into the Amargosa River Valley. DOE considered alternative modeling approaches during the development and validation of the scour-dilution-mixing approach in its tephra redistribution abstracted model (SNL, 2007av). DOE also referred to model-confidence building, supporting comparisons, and sensitivity analyses documented in SNL (2007av) and a published application of the scour-dilution-mixing model to the area around the Lathrop Wells Volcano (Pelletier, et al., 2008aa).

Time-dependent radionuclide concentrations with soil depth in stream channels and on channel divide surfaces are the ultimate outputs of the tephra redistribution model. SER Section 2.2.1.3.13.3.1.3 evaluates the time-dependent vertical migration of radionuclides in soil for the volcanic ash exposure scenario. In the biosphere model, reviewed in SER Section 2.2.1.3.14.3, the FAR model outputs are combined with biosphere dose conversion factors in the DOE TSPA to estimate annual doses to the RMEI (SAR Figure 2.3.10-10).

Staff's Evaluation of Tephra Redistribution

The staff reviewed SAR Section 2.3.11 on the volcanic eruption modeling case, additional information provided in response to the staff's RAIs (DOE, 2009bk-bm), the supporting DOE information on tephra redistribution presented in SNL (2007av), and information published in peer-reviewed literature (e.g., Pelletier et al., 2008aa).

Model Integration

Model abstractions comprise FEPs that have been screened in from the scenario analysis the applicant conducted. (b)(5)

(b)(5)

(b)(5)

DOE did not exclude any FEPs associated with this abstracted model. The staff's review of the tephra redistribution abstracted model evaluates the applicant's implementation of the included FEP 1.2.04 07.0C.

FEP 1.2.04.07.0C accounts for the surface transport processes that redistribute radionuclides following the initial tephra-fall deposition. (b)(5)

(b)(5)

The following addresses the staff's evaluation of DOE's modeling assumptions used for the fluvial transport in the FAR model.

The applicant determined that wetter future climates would increase vegetation on hill slopes and reduce the amount of remobilized tephra from hill slopes into channels. (b)(5)

(b)(5)

(b)(5)

(b)(5)

The NRC staff evaluated the implementation of the channel area fraction in the FAR model, which also considered its coupling with the biosphere model in the DOE TSPA. The applicant assessed (i) the relative susceptibility of the two surfaces, interchannel divides and active fluvial channels, to airborne resuspension and (ii) the assumption that dose contributions from these two surfaces are proportional to their respective fractions of the total area of the alluvial fan. DOE concluded that differences in these two surfaces were accounted for in the DOE TSPA estimates for airborne particle concentration. The applicant also showed in DOE Enclosure 5, Figure 1 (2009bk) that dose contributions for the volcanic ash exposure scenario were much greater from interchannel divides than channels for thousands of years after repository closure. (b)(5)

(b)(5)

Although the applicant acknowledged that a future eruption could alter the channel geomorphology to some degree by deposition of fresh tephra, it assumed that eruption-induced changes would have little effect on the overall geomorphology of the Fortymile Wash catchment basin, as described in SNL Section 5.1.4 (2007av). (b)(5)

(b)(5)

(b)(5)

Rather than accounting for significant rainfall and flooding events individually and tracking the movement of redistributed tephra from each event over time, the FAR model applies a representative deposit for long-term redistribution and dilution of tephra in the same simulation time step. Because FAR model results are integrated with biosphere modeling in the DOE TSPA, the NRC staff considered the coupling of the FAR and biosphere models in the evaluation of FAR model assumptions concerning time dependency. The applicant assessed the replenishment of contaminated fluvial deposits over time with respect to time-dependent estimates of resuspended airborne particle concentrations in the DOE TSPA, according to DOE Enclosure 4 (2009bk). DOE clarified that the active outdoor category for RMEI activities includes time spent walking outdoors on uncompacted soil or tephra. The applicant also acknowledged that airborne particle concentrations would be higher in the DOE TSPA for walking on uncompacted tephra deposits following an eruption than during preeruption conditions. (b)(5)

(b)(5)

In SNL Section 1.2 (2007av), the applicant acknowledged that eolian (wind) sediment transport is a significant geomorphic process in the Yucca Mountain region. (b)(5)

(b)(5)

The applicant clarified in DOE Enclosure 12, Section 1.1 (2009bk) that airborne resuspension of tephra deposits at the RMEI location is included in the DOE TSPA, as a local-scale eolian redistribution process. In SNL Section 5.2.2 (2007av), the applicant also accounted for potential local-scale eolian transport of contamination in channel sediments onto interchannel divide surfaces by increasing the range for the channel fraction of land area in the Fortymile Wash alluvial fan. As described in SNL Section 5.2.2 (2007av), direct tephra-fall deposition and fluvial processes dominate radionuclide concentrations in the soil and air at the RMEI location. DOE considered the long-range eolian transport of freshly deposited tephra south to the RMEI location from the Fortymile Wash catchment basin to be negligible on the basis of the applicant's characterization of the prevailing direction for strong southerly winds, as identified in SNL Appendix D (2007ab) and Pelletier and Cook (2005aa). The applicant also considered relevant wind data in CRWMS M&O Site 9 (1997aa) and determined that southerly winds exhibited higher wind speeds compared to northeasterly winds, described in DOE Enclosure 12, Section 1.2 (2009bk). Because higher speeds for south-to-north winds would tend to drive the

net transport of contaminated tephra toward the north and away from the RMEI location, as DOE Enclosure 12, Section 1.2 (2009bk) identified, the applicant concluded that eolian transport of radionuclides deposited in the Fortymile Wash catchment basin to the RMEI would be negligible, as stated in SNL Section 5.2.2 (2007av), and not modeling these eolian effects would tend to overestimate tephra and waste concentration at the RMEI location. (b)(5)

(b)(5)

Fluvial transport of sediment and tephra in Fortymile Wash is modeled as bedload transport.

(b)(5)

(b)(5)

Using grain-size data from analog volcanic eruptions, the applicant expects a range of tephra particle sizes with an approximate median value of 0.01–1.0 mm [0.0004–0.04 in], as identified in SNL Section 5.2.3 (2007av). With diameters between 0.002–0.05 mm [0.00008–0.002 in], as described in BSC Section 6.5.3.2 (2006ah), silt-sized particles represent a small portion of this range. The applicant considered that silt-sized material could be transported past the RMEI location in the suspended load (rather than in the bedload) and concluded that not modeling suspended load transport and deposition is conservative, as stated in SNL Section 5.2.3 (2007av). (b)(5)

(b)(5)

(b)(5)

(b)(5)

To enhance confidence in its system description and model integration, the applicant had critical reviews performed on an earlier version of the technical basis document and included the review and resolution of comments in SNL Appendix C, Section 7.3.2 (2007av). (b)(5)

(b)(5)

Data Sufficiency and Data Uncertainty

The NRC staff reviewed the data sufficiency and propagation of uncertainty the applicant presented for the FAR model parameters of critical slope, scour depth, and drainage density.

(b)(5)

Critical Slope

The applicant collected field data from several analog volcanic sites near Flagstaff, Arizona (i.e., Rattlesnake Crater, Cochrane Hill, Moon Crater, and Cinder Cone), to determine the critical slope parameter range and represent the steepest slope for stable tephra deposits on hill slopes, as outlined in SNL Section 6.5.2 (2007av). The applicant assessed the measurement scale of the field observations for critical slope and representativeness of the 30 by 30-m [97 by 97-ft]-grid cell size for the digital elevation map of the Fortymile Wash drainage system. Slopes were measured at a scale of tens of meters [tens to hundreds of feet] in the field, and DOE concluded that the slope angles are representative of hill slopes in DOE Enclosure 6.

Section 1.1 (2009bk). (b)(5)

(b)(5)

(b)(5) DOE clarified that the representation of topography in the FAR model does not smooth steeper slopes and assessed the appropriateness of field data from analog volcanic sites to estimate fluvial erosion of tephra deposits in the Yucca Mountain region. (b)(5)

(b)(5)

Scour Depth

SNL Section 6.5.6 (2007av) described the site-specific field data DOE used to establish the parameter distribution for scour depth: the depth to which water flow will erode (pick up) and move sediment in a stream channel. Parameter values for scour depth were inferred from scour chains, which the U.S. Geological Survey (USGS) installed at the Narrows section of Fortymile Wash and was subsequently buried about 10 years later by flood sediment in 1995, as shown in SNL Table 6.5.6-1 (2007av). In DOE Enclosure 10, Section 1 (2009bk), the applicant explained that another station does not represent tributary conditions of the upper drainage basin:

(b)(5)

(b)(5)

The average measured value from the scour chain data, 73 cm [2.4 ft], was chosen as the lower bound (SNL, 2007av). (b)(5)

(b)(5)

The applicant based its determination of the parameter range for scour depth on site-specific field measurements at Fortymile Wash for current conditions without a surplus of tephra. The applicant assessed the potential effect of fresh tephra in Fortymile Wash on scour depth in channels and concluded that scour depth would not be affected by the proportion of tephra in channel sediments. According to DOE Enclosure 10, Section 1 (2009bk), the expected grain

sizes of tephra are similar to the observed grain sizes for channel bed material; therefore, different hydraulic conditions were not expected for a fluvial deposit mixing sediment and tephra, as outlined in SNL Section 5.2.3 (2007av) and Pelletier, et al., p. 236 (2008aa). (b)(5)

(b)(5)

The NRC staff reviewed the applicant's scaling approach outlined in SNL Section 6.3.3, Step 3 (2007av) for computing scour depth at different locations in the Fortymile Wash drainage basin. DOE sampled values for the maximum scour depth within the drainage system and computed scour depth at other locations in SNL Equation 6.3-14 (2007av). SNL Figure 6.3.3-6 (2007av) illustrated the variability of scour depth within the drainage basin. (b)(5)

(b)(5)

Drainage Density

(b)(5)

(b)(5)

The drainage density is the ratio of the total length of streams to the area of the drainage system (length per unit area). DOE estimated drainage density from simulations of 34 channel heads on the eastern slope of Yucca Mountain. In SNL Equation 6.3-7 and p. 6-16 (2007av), the applicant used the reciprocal of the drainage density as a stream power threshold for determining active channels within the Fortymile Wash catchment basin; in SNL Section 6.5.6 and Figure 6.5.6-3 (2007av), the applicant compared modeled channel head locations to actual locations and selected the drainage density that yielded the smallest average distance difference. (b)(5)

(b)(5)

(b)(5)

Model Uncertainty

The NRC staff reviewed the DOE consideration of alternative models in Pelletier, et al. (2008aa) and SNL Sections 6.2.2, 6.3.3, and 7.2.4 (2007av). (b)(5)

(b)(5)

(b)(5)

In DOE Enclosure 7, Section 1 (2009bk), the applicant considered the classic dilution-mixing model as appropriate only for tributary systems but not well suited for Fortymile Wash, because it is a tributary-distributary drainage system. The applicant also identified other shortcomings with classic dilution-mixing models, such as their inability to model the vertical distribution of contamination and dilution of contaminated with uncontaminated sediments. Because the applicant considered scour-dilution mixing as the predominant mode of dilution, it concluded in DOE Enclosure 7, Section 1.1 (2009bk) that the scour-dilution-mixing model more accurately represented the processes at Fortymile Wash and in DOE Enclosure 7, Section 1.2 (2009bk) that dilution-mixing models were not directly applicable. (b)(5)

(b)(5)

Model Support

The NRC staff evaluated the applicant's model support for the FAR model. The applicant supported its model results with (i) independent technical reviews, as outlined in SNL Appendix C (2007av), and (ii) a peer-reviewed journal article (Pelletier, et al., 2008aa) that included a site-specific comparison for fluvial redistribution and dilution of tephra from the Lathrop Wells volcano. (b)(5)

(b)(5)

(b)(5) In SNL Section 7.3.1.2 (2007av), the applicant also pointed to the 77,000-year-old analog volcano at Lathrop Wells for observations of long-term storage of tephra below the scour depth. (b)(5)

(b)(5)

(b)(5)

Evaluation Findings for the Tephra Redistribution

(b)(5)

2.2.1.3.13.3.1.3 Downward Migration of Radionuclides in Soil

The NRC staff conducted a risk-informed review of the model of downward migration of radionuclides in soil, concentrating on those aspects important to the volcanic ash exposure scenario in the DOE performance assessment, as given next.

Important Aspects of Downward Migration of Radionuclides in Soil

In the DOE TSPA, both long- and short-term inhalation significantly contribute to the total dose for the volcanic ash exposure scenario for 100,000 years. Because the short-term inhalation contribution is dominated by a much faster rate of reduction in airborne mass loading, the vertical migration of radionuclides has greater potential influence on long-term inhalation dose. As previously discussed, contributions to total dose from the inhalation of particulates diminish after 100,000 years.

The DOE results indicated that processes contained in this abstracted model for the volcanic ash exposure scenario result in a small reduction in radionuclide concentrations over time. The NRC staff obtained quantitative insights by investigating intermediate output files from the DOE TSPA. For unplowed soil, the reduction of radionuclide concentration due to vertical migration out of the resuspendable layer is gradual and slows with increasing time following initial deposition. On average, the radionuclide concentration in the resuspendable layer required approximately 20, 150, 700, and 4,000 years to decrease by a factor of 2, 4, 8, and 16, respectively, from its initial value in the DOE TSPA. For plowed soil, radionuclides are uniformly

mixed within the tillage depth, and the time-dependent reduction in radionuclide concentration due to vertical migration is small (reduction by a factor of about 2 in 10,000 years). For fluvial channels, radionuclides are assumed to be well mixed within the fluvial sediment deposit, and the time-dependent reduction in concentration due to vertical migration of radionuclides out of either the resuspendable layer or tillage depth is minimal (leading to a reduction of less than a factor of 2 in 10,000 years). Sensitivity analyses the applicant performed indicated that radionuclide concentration is most sensitive to the diffusivity rate in soil on interchannel divides, followed by a lesser sensitivity to the diffusivity rate in fluvial channels. There was a negligible sensitivity to different values of permeable depth on the interchannel divides, as described in SNL Section 6.6 (2007av).

Summary of DOE License Application on Downward Migration of Radionuclides in Soil

Modeling of radionuclide concentration migration into soil for the volcanic ash exposure scenario was described in SAR Sections 2.3.10, Biosphere Transport and Exposure, and 2.3.11, Igneous Activity. In SAR Tables 2.3.10-1 and 2.3.11-1, DOE identified the FEPs included in the TSPA.

Calculation of radionuclide concentrations with soil depth at the RMEI location is one of the main elements of the DOE FAR model for tephra redistribution. The applicant developed this part of the FAR model specifically for the Fortymile Wash alluvial fan, consisting of active channels and interchannel divide surfaces. The exposure of the RMEI to radionuclides in soil was modeled for two layers: (i) a thin upper surface layer from which particles can be suspended into the atmosphere by disturbances and (ii) a thicker, lower surface layer that may undergo mixing by agricultural practices such as tillage (SAR Section 2.3.10.2.6).

The FAR model includes the downward migration of radionuclides into soil for the volcanic ash exposure scenario. Incorporated into the DOE TSPA as a dynamically linked library, the FAR model is connected to the surface soil submodel of the DOE biosphere model, Environmental Radiation Model for Yucca Mountain Nevada (ERMYN), which calculates biosphere dose conversion factors for the volcanic ash exposure scenario on the basis of unit concentrations of radionuclides in volcanic ash deposited on the ground. The surface soil submodel is included in the biosphere analysis of all exposure pathways for the volcanic ash exposure scenario (refer to SAR Figures 2.3.10-8 and 2.3.10-10). Biosphere dose conversion factors are combined with time-dependent radionuclide concentrations in soil from the FAR model to estimate annual doses for the volcanic ash exposure scenario.

The applicant modeled time-dependent vertical migration of radionuclides in soil within the FAR tephra redistribution model as a diffusive process in one dimension. Values for radionuclide diffusivity and permeable depth differed between those areas on interchannel divides and those in fluvial channels. Field data on Cs-137 concentration profiles from the upper Fortymile Wash alluvial fan were used to determine radionuclide diffusivities and the associated uncertainties.

Permeable depths in soils were determined from field measurements in pits dug on interchannel divides of the Fortymile Wash alluvial fan and from USGS data on scour depth in fluvial channels. Although advection is not explicitly modeled, the applicant identified that diffusivity data accounted for all transport mechanisms, including advection and bioturbation. The applicant does not include effects of future climate change on the modeled processes and parameters in the tephra redistribution model, because DOE concluded that processes associated with future climate change would only decrease radionuclide concentrations in soils (SAR Section 2.3.11.4.4.3). In the FAR model, radionuclides are restricted from migrating into a deeper horizon by use of a reduced permeability. The reduced permeability was assumed to be

caused by a greater carbonate or clay content than the minor content in surface and near-surface soils. The applicant's approach limited possible reduction of radionuclide concentrations in the surface layer due to vertical migration over long time periods.

For the volcanic ash exposure scenario, the surface soil submodel calculates radionuclide mass concentrations in the tilled surface soil layer and in the thin resuspendable layer for noncultivated soil. In the DOE TSPA, radionuclide concentrations in the resuspendable layer and tilled soil are applied to different environmental exposure pathways. Weighting factors for land usage (e.g., fractions of land that are tilled and not tilled) are not included in the dose calculations. Igneous eruption dose calculations include weighting factors for the fraction of land area apportioned into active fluvial channels and interchannel divides. Volcanic material (basaltic tephra) is assumed to be mixed uniformly in tilled surface soil. Concentrations of radionuclides in tilled surface soil are factored into the pathway analysis for ingestion of contaminated crops and animal products. Inhalation and external exposure pathway calculations are dependent on radionuclide concentrations in the resuspendable layer. Because erosion and other surficial processes are accounted for in the tephra redistribution model, DOE's surface soil submodel does not include these processes for the volcanic ash exposure scenario.

Staff's Evaluation of Downward Radionuclide Migration in Soil

The staff reviewed SAR Sections 2.3.10 and 2.3.11 on the volcanic eruption modeling case, additional information provided in response to the staff's RAIs (DOE, 2009bk), and the supporting DOE information on tephra redistribution presented in SNL (2007av).

Model Integration

Model abstractions comprise FEPs that have been screened in from the scenario analysis the applicant conducted. (b)(5)

(b)(5)

(b)(5)

DOE did not exclude any FEPs associated with this abstracted model. The staff's review of the abstracted model for downward migration in soil evaluates the applicant's implementation of the included FEPs: (i) FEP 1.2.04.07.0C, (ii) FEP 2.3.02.01.0A, (iii) FEP 2.3.02.02.0A, and (iv) FEP 2.3.02.03.0A.

(b)(5)

(b)(5)

SER Section 2.2.1.3.13.1.2 evaluates the treatment of climate in the DOE FAR model. The technical basis for this abstracted model was described in SNL (2007av); modeling assumptions were described in SNL Section 5 (2007av). (b)(5)

(b)(5)

The NRC staff evaluated critical modeling assumptions for this abstracted model. The applicant assumed that all radionuclides migrate into the soil at the same rate, because in temperate

climates, weathering of radionuclides from the soil surfaces into deeper soil layers is mainly a physical, rather than a chemical, process. (b)(5)

(b)(5)

(b)(5)

Data Sufficiency

The NRC staff evaluated data sufficiency in the DOE abstracted model for the downward migration of radionuclides in soil. This abstracted model consists of parameters for permeable depth in fluvial channels and on interchannel divides, soil diffusivity of radionuclides in channels and on interchannel divides, and land fraction of the Fortymile Wash alluvial fan attributed to channels. Parameter values for permeable depth in channels were inferred from USGS data on scour depth in channels and the previously mentioned site-specific field data from soil pits, as described in SNL Section 6.5.5.2 (2007av). Diffusivity rates for radionuclide migration in soils on interchannel divides and in fluvial channels were determined from site-specific field data of Cs-137 profiles. These profiles resulted from contaminated fallout deposited approximately 50 years earlier from atmospheric nuclear weapons testing. The applicant performed soil-geomorphic mapping of the Fortymile Wash alluvial fan to determine the fraction of the fan area that has been subjected to fluvial erosion and deposition within the past 10,000 years, as identified in SNL Appendix A (2007av). Diffusivity rates for fluvial channels were determined from measurements from surfaces the applicant characterized as active channels. Measured data from older terraces were used to calculate the diffusivity rate for interchannel divides. On the basis of these two field data sets, the applicant specified separate diffusivity parameters for older surfaces of the interchannel divides and younger surfaces in fluvial channels. (b)(5)

(b)(5)

Data Uncertainty

In the DOE abstracted model for the vertical migration of radionuclides in soil, parameter distributions are applied to account for data uncertainty. (b)(5)

(b)(5)

(b)(5) A permeable depth in fluvial channels of 200 cm [79 in] was derived from field measurements and is used as a constant value, as outlined in SNL Section 7.1.3 and Table 4.1-4 (2007av). The applicant supported this constant value with an argument that the permeable depth in fluvial channels could be much deeper. (b)(5)

(b)(5)

Model Uncertainty

The NRC staff evaluated model uncertainty for the downward migration of radionuclides in soil following an eruption. For conditions after a potential future volcanic eruption that intersects the repository and entrains waste, radionuclides on the ground surface would originate as radionuclide contamination in basaltic tephra deposits, as discussed previously. The applicant used site-specific data from the deposition and migration of fine radionuclide particulates into current surface soils of the Fortymile Wash alluvial fan, which are not rich in basaltic material, to support its model for the downward migration of radionuclides following deposition in the volcanic ash exposure scenario (SAR Section 2.3.11.4.2.3; SNL, 2007av). The applicant provided a technical basis for neglecting the effects of fresh basaltic tephra on radionuclide diffusion in soil. The technical basis for radionuclide migration was provided in two parts: one for channel sediments and the other for soils on interchannel divides. For channel sediments, the applicant used field observations at Lathrop Wells, described in SNL Section 7.3.1.1 (2007av), to show that basaltic and nonbasaltic sediments in the drainages exhibited similar grain sizes and transport rates. The applicant also found basaltic and nonbasaltic sediments to be well mixed. The applicant reported a significant amount of dilution of fresh basaltic tephra with nonbasaltic sediments during fluvial transport in the Fortymile Wash drainage basin. In particular, tephra concentrations in channel sediments were less than 20 percent at the RMEI location in the DOE TSPA. For these reasons, the applicant concluded that determining separate diffusion rates of radionuclides in basaltic tephra was not necessary for estimating the downward migration of radionuclides in mixed channel sediments.

(b)(5)

(b)(5)

For soils on interchannel divides, the applicant concluded in DOE Enclosure 3 (2009bk) that differences in diffusivity for a basaltic tephra deposit on ambient soils would be negligible because tephra thicknesses at the RMEI location would be thin (less than 0.33 cm [0.85 in] for about 90 percent of TSPA simulations with a primary tephra-fall deposit near the RMEI location) and grain-size ranges for tephra and ambient soils on interchannel divides are similar. (b)(5)

(b)(5)

Model Support

The NRC staff evaluated model support for the downward migration of radionuclides in soil. DOE used a one-dimensional diffusion model for the downward migration of radionuclides in soil with measurements of Cs-137 radioactivity profiles in soils at Fortymile Wash. (b)(5)

(b)(5)

(b)(5)

DOE did not

identify any alternative conceptual models that would likely affect the timing or magnitude of dose. (b)(5)

(b)(5)

Evaluation Findings of Downward Radionuclide Migration in Soil

(b)(5)

Summary Evaluation Findings on Volcanic Ash Exposure Scenario

(b)(5)

(b)(5)

2.2.1.3.13.3.2 Assessment and Review of Groundwater Exposure Scenarios

For the groundwater exposure scenario, the surface soil submodel addresses the vertical movement of radionuclides in the soil that follows from irrigation with contaminated groundwater (SAR Figure 2.3.10-1) and calculates a time-dependent profile of radionuclide concentration in the contaminated soil horizon at the RMEI location. Radionuclide contamination in groundwater can result from waste package failure due to corrosion, mechanical disruption, or potential disruption by intruding magma. Radionuclide contamination in groundwater serves as input to the surface soil submodel. SER Section 2.2.1.3.12 documents the staff's review of the DOE approach to estimating radionuclide contamination in groundwater. This section addresses the vertical movement of radionuclides in the soil from contaminated groundwater irrigation together with background precipitation. As described next, the applicant's results indicated the influence of the surface soil submodel on the DOE calculated repository performance.

The NRC staff conducted a risk-informed review of DOE's surface soil submodel using YMRP Section 2.2.1.3.13. The staff reviewed the important aspects of the groundwater exposure scenario in the DOE performance assessment.

Important Aspects of the DOE Surface Soil Submodel

The staff reviewed the SAR and assessed the extent to which the DOE surface soil submodel influences the DOE calculation of repository performance. The surface soil submodel is used to estimate radionuclide doses for the groundwater exposure scenarios, including the seismic ground motion and igneous intrusion scenarios. SAR Figure 2.4-18(a and b) showed that the seismic ground motion and igneous intrusion scenarios dominate the estimated total mean annual dose for 10,000 and 1 million years after repository closure. Total doses from the groundwater exposure scenarios are controlled by multiple radionuclides and dose pathways. Because the surface soil submodel is a component of the DOE biosphere model ERMYN (SAR Figure 2.3.10-9; BSC, 2006a; SNL, 2007a), its importance within the DOE TSPA depends on specific exposure pathways and radionuclides.

(b)(5)

(b)(5)

Summary of DOE License Application on Surface Soil Submodel

The surface soil submodel is one component of the DOE biosphere model, which is described in SAR Section 2.3.10, Biosphere Transport and Exposure. In SAR Table 2.3.10-1, DOE identified the FEPs included in the TPSA.

The surface soil submodel calculates the radionuclide concentrations in both cultivated field and garden surface soils following radionuclide release in the groundwater pathway. The output from the surface soil submodel serves as input for various biosphere submodels (animal, ingestion, external, plant, and air). The outputs of the biosphere model are biosphere dose conversion factors, which are factors that provide the dose per unit concentration in a medium such as water, for groundwater exposure (SAR Figure 2.3.10-9). Biosphere dose conversion factors are combined with the time-dependent radionuclide concentrations in groundwater from the saturated zone transport models to calculate annual dose to the RMEI from groundwater exposure (SAR Figure 2.3.10-9). The applicant's calculation used the groundwater exposure and volcanic ash exposure doses to demonstrate compliance with the individual protection standards at 10 CFR 63.311 and 10 CFR 63.321 (SAR Section 2.3.10.1). Results from the surface soil model are used to determine potential doses from inhalation of suspended soil particles, consumption of radionuclide-containing crops, soil ingestion by humans and animals, exposure to radioactive gases from the surface soil, and external exposure to radionuclide-containing soils. SER Section 2.2.1.3.14 addresses the NRC staff's evaluation of biosphere dose conversion factors and biosphere submodels other than the surface soil submodel.

In the surface soil submodel, radionuclides are considered to be added to the soil from irrigation using contaminated groundwater. They may decrease through the mechanisms of radioactive decay, leaching into deeper zones, erosion of soil particles, and gaseous release to the atmosphere (i.e., radon and carbon dioxide). Two soil layers are considered: a thin upper surface layer from which particles can be suspended into the atmosphere by disturbances and a thicker lower surface layer that may undergo mixing by agricultural practices such as tilling the land.

Staff's Evaluation of Surface Soil Submodel

The staff reviewed SAR Sections 2.3.10 on the surface soil submodel and the supporting DOE information on the surface soil submodel presented in SNL (2007ac) and BSC (2006ah).

Model Integration

Model abstractions comprise FEPs that have been screened in from the scenario analysis the applicant conducted (b)(5)

(b)(5) DOE screened out the transport of radionuclides past these soil layers to greater depths in its analysis of FEPs (b)(5)

(b)(5)

The staff's review of the downward migration modeling in soil evaluates the applicant's implementation of the included FEPs: (i) FEP 2.3.02.01.0A, (ii) FEP 2.3.02.02.0A, and (iii) FEP 2.3.02.03.0A.

DOE considered two soil layers in the surface soil submodel: (i) a thin surface layer that is susceptible to particles being suspended in the atmosphere from disturbances such as agricultural activities and wind and (ii) a lower, thicker layer that is approximately the thickness of the plow or till zone. Radionuclide concentrations for primary radionuclides and two long-lived decay products are calculated for varying climate conditions. Radionuclide concentrations are assumed to be uniform in the thin resuspendable layer and uniform in the thicker surface layer, if tilling is practiced.

The NRC staff evaluated the modeling assumptions and integration for the surface soil submodel. Radionuclides in the surface soil submodel originate from contaminated groundwater used for irrigation. The applicant used a unit concentration for each radionuclide of 1 Bq/m³ in the irrigation water to determine normalized biosphere dose conversion factors. TSPA computes the radionuclide doses by multiplying these normalized factors by the radionuclide concentrations in the groundwater. To not underestimate the potential dose to the RMEI at earlier times, DOE determined radionuclide concentrations in soil by assuming irrigation with contaminated well water for periods up to 1,000 years before estimating the potential dose to the RMEI. This assumption allowed the radionuclide concentration absorbed on soils to build up toward equilibrium conditions before estimating the potential dose to the RMEI. Once equilibrium conditions are obtained, longer irrigation periods would not affect radionuclide concentrations in soil. (b)(5)

(b)(5)

The mathematical model DOE used, outlined in SNL Equation 6.4.1-1, p. 6-73 (2007ac), to represent addition and removal of radionuclides in the surface soil is a differential equation that considers the dominant governing processes. The differential equation relates the rate of radionuclide accumulation to the difference between the rate of radionuclide addition and the rate of radionuclide loss in a volume of soil. (b)(5)

(b)(5)

(b)(5) Inherent in the equation is mass balance that accounts for the difference between radionuclide addition and removal per unit time. The differential equation accounts for changes in storage or radionuclide concentration in the soil's surface. (b)(5)

(b)(5)

(b)(5)

(b)(5)

Short-lived radioactive decay products

(i.e., having half-lives shorter than 180 days) are assumed to be in equilibrium with the long-lived primary radionuclides. (b)(5)

(b)(5)

Data Sufficiency and Data Uncertainty

The NRC staff evaluated data sufficiency and uncertainty for the irrigation rate source term. The irrigation rates were determined separately for field and garden crops. Irrigation rates directly affect radionuclide concentrations in the soil, because more radionuclide mass is added to the soil when the irrigation rate is higher. An average irrigation rate was calculated from irrigation rates from several crops on the basis of current practices at Amargosa Valley, Nevada. Vegetables and fruit were assumed to be grown in gardens, whereas grains and forage were assumed to be grown in fields. An average irrigation rate was used due to crop rotation in fields and gardens in Amargosa Valley. DOE accounted for crop overwatering to prevent the buildup of soluble salts in the rooting zone. (b)(5)

(b)(5)

The NRC staff evaluated data sufficiency and uncertainty for surface soil submodel parameters. DOE developed parameters for the surface soil submodel from surveys of land use in Amargosa Valley (e.g., type of crops grown, crop rotation, and crop acreage). The applicant applied documented physical and chemical properties (e.g., soil properties, radionuclide properties/characteristics). (b)(5)

(b)(5)

(b)(5) Documented physical and chemical parameters were obtained from measurements and analyses by independent groups, such as the U.S. Department of Agriculture's soil surveys and established literature sources. (b)(5)

(b)(5)

(b)(5)

The applicant used parameter distributions to account for parameter uncertainty. (b)(5)

(b)(5)

Model Uncertainty and Model Support

The NRC staff evaluated the model support and applicant's treatment of model uncertainty for the surface soil submodel. In SNL Section 6.3.3 (2007ac), DOE concluded that there are no alternative conceptual models for the biosphere evaluation. (b)(5)

(b)(5)

(b)(5) The applicant compared ERMYN with two other established models that assess radionuclide concentrations in soil, GENII (Napier, et al., 2006aa) and BIOMASS ERB2A (International Atomic Energy Agency, 2003aa), to evaluate the technique used to solve the mathematical model. The mathematical development all these models used, including the surface soil submodel used in ERMYN, is similar after the terms are combined or redefined, as identified in SNL Section 7.3.1.1 (2007ac). The applicant explained differences in the models and concluded that the calculations were equivalent. (b)(5)

(b)(5)

Evaluation Findings for Groundwater Exposure Scenario

(b)(5)

(b)(5)

2.2.1.3.13.4 Evaluation Findings

The NRC staff reviewed the applicant's SAR and other information submitted in support of the license application and finds that, with respect to the requirements of 10 CFR 63.114 for consideration of the airborne transport and redistribution of radionuclides (b)(5)

(b)(5)

(b)(5)

2.2.1.3.13.5 References

- Andronico, D., S. Scollo, S. Caruso, and A. Cristaldi. 2008aa. "The 2002–03 Etna Explosive Activity: Tephra Dispersal and Features of the Deposits." *Journal of Geophysical Research*. Vol. 113, No. B04209. doi:10.1029/2007JB005126.
- Anspaugh, L.R., S.L. Simon, K.I. Gordeev, I.A. Likhtarev, R.M. Maxwell, and S.M. Shinkarev. 2002aa. "Movement of Radionuclides in Terrestrial Ecosystems by Physical Processes." *Health Physics*. Vol. 82, No. 5. pp. 669–679.
- Benke, R.R., D.M. Hooper, J.S. Durham, D.R. Bannon, K.L. Compton, M. Necsoiu, and R.N. McGinnis, Jr. 2009aa. "Measurement of Airborne Particle Concentrations Near the Sunset Crater Volcano, Arizona." *Health Physics*. Vol. 96, No. 2. pp. 97–117.
- Bird, R.B., W.E. Stewart, and E.N. Lightfoot. 1960aa. *Transport Phenomena*. New York City, New York: John Wiley & Sons. pp. 74–76.
- Blong, R.J. 1984aa. *Volcanic Hazards—A Sourcebook on the Effects of Eruptions*. Orlando, Florida: Academic Press. P. 427.
- BSC. 2006ah. "Soil-Related Input Parameters for the Biosphere Model." ANL–NBS–MD–000009. Rev. 03. AD 01. Las Vegas, Nevada: Bechtel SAIC Company, LLC.
- BSC. 2003ad. "Characterize Eruptive Processes at Yucca Mountain, Nevada." ANL–MGR–GS–000002. Rev. 01. Las Vegas, Nevada: Bechtel SAIC Company, LLC.
- CNWR. 2007aa. "Software Validation Report for Total-System Performance Assessment (TPA) Code Version 5.1." ML072840502. San Antonio, Texas: CNWR.
- CRWMS M&O. 1997aa. "Regional and Local Wind Patterns Near Yucca Mountain." B00000000–01717–5705–00081. Rev. 00. MOL.19980204.0319. Las Vegas, Nevada: CRWMS M&O.
- Codell, R.B. 2004aa. "Alternate Igneous Source Term Model for Tephra Dispersal at the Yucca Mountain Repository." *Nuclear Technology*. Vol. 148. pp. 205–212.
- Codell, R.B. 2003aa. "Alternative Igneous Source Term Model for the Yucca Mountain Repository." Proceedings of the 10th International High-Level Radioactive Waste Management Conference (IHLRWM), Las Vegas, Nevada, March 30–April 2, 2003. LaGrange Park, Illinois: American Nuclear Society.
- DOE. 2009ab. "Yucca Mountain—Response to Request for Additional Information Regarding License Application (Safety Analysis Report Sections 2.2, Table 2.2-5), Safety Evaluation Report Vol. 3, Chapter 2.2.1.2.1, Set 2." Letter (February 23) J.R. Williams to J.H. Sulima (NRC). ML090550101. Las Vegas, Nevada: DOE, Office of Civilian Radioactive Waste Management.

DOE. 2009av. DOE/RW-0573, "Safety Analysis Report Yucca Mountain Repository License Application." Rev. 01. Las Vegas, Nevada: DOE, Office of Civilian Radioactive Waste Management.

DOE. 2009bk. "Yucca Mountain—Response to Request for Additional Information Regarding License Application (Safety Analysis Report Sections 2.3.10 and 2.3.11), Safety Evaluation Report Vol. 3, Chapter 2.2.1.13, Set 1." Letter (July 27) J.R. Williams to J.H. Sulima (NRC). ML092090273. Las Vegas, Nevada: DOE, Office of Civilian Radioactive Waste Management.

DOE. 2009bl. "Yucca Mountain—Response to Request for Additional Information Regarding License Application (Safety Analysis Report Sections 2.1, 2.3.11, 2.4.3, and 2.4.4), Safety Evaluation Report Vol. 3, Chapters 2.2.1.4.1, 2.2.1.4.2, and 2.2.1.4.3, Set 1." Letter (July 29) J.R. Williams to J.H. Sulima (NRC). ML092110472. Las Vegas, Nevada: DOE, Office of Civilian Radioactive Waste Management.

DOE. 2009bm. "Yucca Mountain—Response to Request for Additional Information Regarding License Application (Safety Analysis Report Sections 2.3.10 and 2.3.11), Safety Evaluation Report Vol. 3, Chapter 2.2.1.13, Set 1." Letter (September 17) J.R. Williams to J.H. Sulima (NRC). ML092610250. Las Vegas Nevada: DOE, Office of Civilian Radioactive Waste Management.

Hawkes, H.E. 1976aa. "The Downstream Dilution of Stream Sediment Anomalies." *Journal of Geochemical Exploration*. Vol. 6. pp. 345–358.

Heffter, J.L. and B.J.B. Stunder. 1993aa. "Volcanic Ash Forecast Transport and Dispersion (VAFTAD) Model." *Weather and Forecasting*. Vol. 8. pp. 533–541.

Hill, B.E. and C.B. Connor. 2000aa. "Technical Basis for Resolution of the Igneous Activity Key Technical Issue." ML011930254. San Antonio, Texas: CNWRA.

Hill, B.E., C.B. Connor, J. Weldy, and N. Franklin. 2000ab. "Methods for Quantifying Hazards From Basaltic Tephra-Fall Eruptions." Proceedings of the Cities on Volcanoes 2 Conference, Auckland, New Zealand, February 12–14, 2001. C. Stewart, ed. Lower Hutt, New Zealand: Institute of Geological and Nuclear Sciences Limited. Institute of Geological and Nuclear Sciences Information Series. Vol. 49. p. 158.

Hill, B.E., C.B. Connor, M.S. Jarzempa, P.C. La Femina, M. Navarro, and W. Strauch. 1998aa. "1995 Eruptions of Cerro Negro Volcano, Nicaragua and Risk Assessment for Future Eruptions." *Geological Society of America Bulletin*. Vol. 110, No. 10. pp. 1,231–1,241.

Hurst, A.W. and R. Turner. 1999aa. "Performance of the Program ASHFALL for Forecasting Ashfall During the 1995 and 1996 Eruptions of Ruapehu Volcano." *New Zealand Journal of Geology and Geophysics*. Vol. 42. pp. 615–622.

Inbar, M., J. Lugo, and L. Villers. 1994aa. "The Geomorphological Evolution of the Paricutin Cone and Lava Flows, Mexico, 1943–1990." *Geomorphology*. Vol. 9. pp. 57–76.

International Atomic Energy Agency. 2003aa. "Reference Biospheres" for Solid Radioactive Waste Disposal, Report of BIOMASS Theme 1 of the BIOSphere Modelling and ASSESSment (BIOMASS) Programme, Part of the IAEA Co-ordinated Research Project on Biosphere

Modelling and Assessment (BIOMASS).” IAEA–BIOMASS–6. Vienna, Austria: International Atomic Energy Agency, Waste Safety Section.

Janetzke, R., R. Benke, and D. Hooper. 2008aa. “Software Validation Test Plan and Report for the Volcanic Ash Dispersal and Deposition Code TEPHRA, Version 1.0.” ML081210677 San Antonio, Texas: CNWRA.

Jarzemba, M.S. 1997aa. “Stochastic Radionuclide Distributions After a Basaltic Eruption for Performance Assessments at Yucca Mountain.” *Nuclear Technology*. Vol. 118. pp. 132–141.

Jarzemba, M.S., P.A. LaPlante, and K.J. Poor. 1997aa. “ASHPLUME Version 1.0—A Code for Contaminated Ash Dispersal and Deposition.” CNWRA 97-004. San Antonio, Texas: CNWRA.

Leopold, L.B., W.W. Emmett, and R.M. Myrick. 1966aa. “Channel and Hillslope Processes in a Semiarid Area, New Mexico.” U.S. Geological Survey Professional Paper 352–G. pp. 193–253.

Leopold, L.B., M.G. Wolman, and J.P. Miller. 1964aa. “Fluvial Processes in Geomorphology.” San Francisco, California: W.H. Freeman and Co. 1964. Reprinted in 1995. New York City, New York: Dover Publications.

Leslie, B., C. Grossman, and J. Durham. 2007aa. “Total-System Performance Assessment (TPA) Version 5.1 Module Descriptions and User Guide.” Rev. 1. ML080510329. San Antonio, Texas: CNWRA.

Marcus, W.A. 1987aa. “Copper Dispersion in Ephemeral Stream Sediments.” *Earth Surface Processes and Landforms*. Vol. 12. pp. 217–228.

Napier, B.A., D.L. Streng, J.V. Ramsdell, Jr., P.W. Eslinger, and C. Fosmire. 2006aa. “GENII Version 2 Software Design Document.” PNNL–14584. Rev. 1. Richland, Washington: Pacific Northwest National Laboratory.

NOAA. 2004aa. “Upper Air Data for Desert Rock, Nevada, Years 1978–2003.” National Climatic Data Center Digital Upper Air Files TD 6201 and 6301. Asheville, North Carolina: National Oceanic and Atmospheric Administration.

NRC. 2009ab. “Division of High-Level Waste Repository Safety Director’s Policy and Procedure Letter 14: Application of YMRP for Review Under Revised Part 63.” Published March 13, 2009. ML090850014. Washington, DC: NRC.

NRC. 2005aa. NUREG–1762, “Integrated Issue Resolution Status Report.” Rev. 1. Washington, DC: NRC.

NRC. 2003aa. NUREG–1804, “Yucca Mountain Review Plan—Final Report.” Rev. 2. Washington, DC: NRC.

Pelletier, J.D. and J.P. Cook. 2005aa. “Deposition of Playa Windblown Dust Over Geologic Time Scales.” *Geology*. Vol. 33, No. 11. pp. 909–912.

Pelletier, J.D., S.B. DeLong, M.L. Cline, C.D. Harrington, and G.N. Keating. 2008aa. “Dispersion of Channel-Sediment Contaminants in Distributary Fluvial Systems: Application to Fluvial Tephra and Radionuclide Redistribution Following a Potential Volcanic Eruption at Yucca Mountain.” *Geomorphology*. Vol. 94. pp. 226–246.

Pelletier, J.D., C.D. Harrington, J.W. Whitney, M. Cline, S.B. DeLong, G. Keating, and K.T. Ebert. 2005aa. "Geomorphic Control of Radionuclide Diffusion in Desert Soils." *Geophysical Research Letters*. Vol. 32. p. L23401.

Pioli, L., E. Erlund, E. Johnson, K. Cashman, P. Wallace, M. Rosi, and H. Delgado Granados. 2008aa. "Explosive Dynamics of Violent Strombolian Eruptions: The Eruption of Parícutin Volcano 1943–1952 (Mexico)." *Earth and Planetary Science Letters*. Vol. 271. pp. 359–368.

Segerstrom, K. 1966aa. "Parícutin, 1965—Aftermath of Eruption." U.S. Geological Survey Professional Paper 550–C. pp. C93–C101.

Segerstrom, K. 1950aa. "Erosion Studies at Parícutin, State of Michoacán, Mexico." U.S. Geological Survey Bulletin 965–A. pp. 1–164.

SNL. 2008ab. "Features, Events, and Processes for the Total System Performance Assessment: Analyses." ANL–WIS–MD–000027. Rev. 00. ACN 01, ERD 01. Las Vegas, Nevada: Sandia National Laboratories.

SNL. 2008ag. "Total System Performance Assessment Model/Analysis for the License Application." MDL–WIS–PA–000005. Rev. 00. AD 01, ERD 01, ERD 02, ERD 03, ERD 04. Las Vegas, Nevada: Sandia National Laboratories.

SNL. 2007ab. "Atmospheric Dispersal and Deposition of Tephra From a Potential Volcanic Eruption at Yucca Mountain, Nevada." MDL–MGR–GS–000002. Rev. 03. ERD 01. Las Vegas, Nevada: Sandia National Laboratories.

SNL. 2007ac. "Biosphere Model Report." MDL–MGR–MD–000001. Rev. 02. ERD 01. Las Vegas, Nevada: Sandia National Laboratories.

SNL. 2007ae. "Characterize Eruptive Processes at Yucca Mountain, Nevada." ANL–MGR–GS–000002. Rev. 03. ERD 01. Las Vegas, Nevada: Sandia National Laboratories.

SNL. 2007av. "Redistribution of Tephra and Waste by Geomorphic Processes Following a Potential Volcanic Eruption at Yucca Mountain, Nevada." MDL–MGR–GS–000006. Rev. 00. ERD 01. Las Vegas, Nevada: Sandia National Laboratories.

Sparks, R.S.J., M.I. Bursik, S.N. Carey, J.S. Gilbert, L.S. Glaze, H. Sigurdsson, and A.W. Woods. 1997aa. *Volcanic Plumes*. New York City, New York: John Wiley & Sons. p. 574.

Suzuki, T. 1983aa. "A Theoretical Model for the Dispersion of Tephra." *Arc Volcanism: Physics and Tectonics*. D. Shimozuru and I. Yokiyama, eds. Tokyo, Japan: Terra Scientific Publishing Company. pp. 95–113.

Till, J.E. and R.E. Moore. 1988aa. "A Pathway Analysis Approach for Determining Acceptable Levels of Contamination of Radionuclides in Soil." *Health Physics*. Vol. 55, No. 3. pp. 541–548.

Winfrey, B. 2005aa. "Software Validation Test Plan and Report, TEPHRA, Version 1.0."
ML063050217 San Antonio, Texas: CNWRA.

CHAPTER 16

2.2.1.3.14 Biosphere Characteristics

2.2.1.3.14.1 Introduction

This chapter evaluates the U.S. Department of Energy's (DOE) postclosure performance assessment model used to calculate biosphere transport and the annual dose to the reasonably maximally exposed individual (RMEI). The sources of radionuclides used in the applicant's biosphere model calculations are calculated by other models in its performance assessment analysis. Those models calculate repository releases from postclosure engineered-barrier-system failures and then model the transport of the released radionuclides from the repository location to the biosphere. Results from these other transport models provide the sources of radionuclides from two primary biosphere media: groundwater and soil contaminated with tephra deposits. In the model, tephra (hereafter, volcanic ash) is deposited on the ground from postulated volcanic events. The applicant's biosphere model then calculates the subsequent transport of these radionuclides within the biosphere through a variety of exposure pathways (e.g., soil, food, water, air) and applies dosimetry modeling to convert the RMEI exposures into annual dose.

10 CFR 63.2 defines the reference biosphere as "the description of the environment inhabited by the [RMEI]." The RMEI is defined by regulation (10 CFR 63.312). It is a hypothetical adult who (i) lives in the accessible environment above the highest concentration of radionuclides in the plume of contamination; (ii) has a diet and living style representative of current Amargosa Valley, Nevada, residents; (iii) uses well water with average concentrations of radionuclides based on an annual water demand of 3,000 acre-feet (3.7×10^9 L); (iv) drinks 2 L [0.528 gal] of water per day from groundwater extracted from wells drilled at the location specified in (i) of this paragraph; and (v) is an adult with metabolic and physiological considerations consistent with present knowledge of adults.

DOE estimated the dose to the RMEI on the basis of the concentrations of radionuclides in groundwater and in contaminated ash. These concentrations were calculated by DOE's model abstractions for saturated zone transport [Safety Analysis Report (SAR) Revision 1 Section 2.3.9], extrusive (volcanic eruption) atmospheric dispersal (SAR Section 2.3.11.4.5.2), and volcanic ash redistribution (SAR Section 2.3.11.4.5.3). These model abstractions, which provide inputs for the biosphere calculations within the Total System Performance Assessment (TSPA) model, are reviewed in Safety Evaluation Report (SER) Sections 2.2.1.3.9 and 2.2.1.3.13, respectively. This chapter of the SER focuses on the U.S. Nuclear Regulatory Commission (NRC) staff's (staff) review of the performance assessment calculations of biosphere transport and dose to the RMEI described in SAR Section 2.3.10. The staff's evaluation of biosphere modeling of radionuclide concentrations in soil can be found in SER Section 2.2.1.3.13.

In SAR Section 2.3.10, DOE analyzed the characteristics of the Yucca Mountain region and Amargosa Valley, Nevada, for its biosphere transport and RMEI dose calculations. The applicant identified features, events, and processes (FEPs) and developed biosphere conceptual and mathematical models for use in its TSPA computer model. The applicant described environmental conditions, resident lifestyle, exposure media, environmental transport pathways, and human exposure pathways it used for evaluating the impacts of repository performance on dose to the RMEI.

Exposure pathways in the DOE biosphere model are based on assumptions about residential and agricultural uses of the water and indoor and outdoor activities. These pathways include ingestion, inhalation, and direct exposure to radionuclides deposited to soil from irrigation (SAR Section 2.3.10.1). Ingestion pathways include drinking contaminated water, eating crops irrigated with contaminated water, eating food products produced from livestock raised on contaminated feed and water, eating farmed fish raised in contaminated water, and inadvertently ingesting soil. Inhalation pathways include breathing resuspended soil, aerosols from evaporative coolers, and radon gas and its decay products.

DOE's approach to biosphere modeling was twofold. The applicant used a standalone computer code entitled Environmental Radiation Model for Yucca Mountain Nevada (ERMYN) to calculate biosphere dose conversion factors, which were used as inputs in DOE's TSPA code. The TSPA multiplied the appropriate biosphere dose conversion factor by either a soil concentration or a water concentration to obtain the dose to the RMEI for each exposure scenario (i.e., volcanic ash, groundwater). The substance of DOE's biosphere modeling approach is contained primarily in the ERMYN code.

This chapter evaluates the technical bases for the applicant's conceptual and mathematical biosphere models, input parameter selections, parameter uncertainty propagation, model support, and model implementation and integration within the applicant's performance assessment evaluation. These evaluations are organized by subsections that address specific components of the applicant's biosphere model (or model development process), including system description and model integration, biosphere transport pathways, human exposure, dosimetry, and integrated biosphere modeling results. The staff's review evaluates both the biosphere modeling in the ERMYN code and how the applicant used the ERMYN output (the biosphere dose conversion factors) to calculate RMEI dose in the TSPA model.

2.2.1.3.14.2 Regulatory Requirements

Model abstractions used in the applicant's postclosure performance assessment must meet the regulatory requirements given in 10 CFR 63.114 (Requirements for Performance Assessment) and 63.342 (Limits on Performance Assessment), to support the predictions of compliance for 63.113 (Performance Objectives for the Geologic Repository after Permanent Closure). Specific compliance with 63.113 is reviewed in SER Section 2.2.1.4.1.

The requirements for performance assessment in 10 CFR 63.114, subject to the constraints for this model abstraction given 10 CFR 63.102(o), 63.305, and 63.312, require the applicant to

- Include appropriate data related to the geology, hydrology, and geochemistry of the surface and subsurface from the site and the region surrounding Yucca Mountain
- Account for uncertainty and variability in the parameter values used to model biosphere characteristics
- Consider alternative conceptual models for biosphere characteristics
- Provide technical bases for the inclusion of features, events, and processes affecting biosphere characteristics, including effects of degradation, deterioration, or alteration processes of engineered barriers that would adversely affect performance of the natural barriers, consistent with the limits on performance assessment in 10 CFR 63.342

- Provide technical basis for the models of biosphere characteristics that in turn provide input or otherwise affect other models and abstractions

10 CFR 63.114(a) considers performance assessment for the initial 10,000 years following permanent closure. 10 CFR 63.114(b) and 63.342 consider the performance assessment methods for the time from 10,000 years through the period of geologic stability, defined in 10 CFR 63.302 as 1 million years following disposal. These sections require that through the period of geologic stability, with specific limitations, the applicant

- Use performance assessment methods consistent with the performance assessment methods used to demonstrate compliance for the initial 10,000 years following permanent closure
- Include in the performance assessment those FEPs used in the performance assessment for the initial 10,000 year period

The applicant's model abstraction for biosphere characteristics is subject to the specific constraints given in

- 10 CFR 63.102(o), specifying the implementation of total effective dose equivalent (TEDE)
- 10 CFR 63.305, specifying the required characteristics of the reference biosphere
- 10 CFR 63.311(b), requiring inclusion of all potential pathways of radionuclide transport and exposure
- 10 CFR 63.312, specifying the required characteristics of the reasonably maximally exposed individual

NRC staff review of the license application follows the guidance laid out in the Yucca Mountain Review Plan, NUREG-1804, Section 2.2.1.3.14, Biosphere Characteristics (NRC, 2003aa), as supplemented by additional guidance for the period beyond 10,000 years after permanent closure (NRC, 2009ab). The acceptance criteria in the Yucca Mountain Review Plan generically follow 10 CFR 63.114(a). Following the guidance, the NRC staff review of the applicant's abstraction of biosphere characteristics considered five criteria

- System description and model integration are adequate.
- Data are sufficient for model justification.
- Data uncertainty is characterized and propagated through the abstraction.
- Model uncertainty is characterized and propagated through the abstraction.
- Model abstraction output is supported by objective comparisons.

Because 10 CFR Part 63 specifies the use of a risk-informed approach for the review of a license application, the guidance provided by the YMRP, as supplemented by NRC (2009ab), is followed to the extent reasonable for aspects of biosphere characteristics important to repository performance, given the specific constraints in the regulation. Whereas NRC staff considered all five criteria in their review of information provided by DOE, only aspects that substantively affect results of the performance assessment, as judged by NRC staff, are discussed in this chapter.

NRC staff's judgment is based both on risk information provided by DOE, and staff's knowledge, experience, and independent analyses.

2.2.1.3.14.3 Technical Review

The staff's technical review of DOE's biosphere characteristics model abstraction evaluated both the biosphere model and the model development process. The review focused on five topics: (i) system description and model integration, (ii) biosphere transport pathways, (iii) human exposure, (iv) dosimetry, and (v) the integrated biosphere modeling results. These reviews are documented in subsections of this SER chapter. The system description and model integration review evaluated the applicant's overall conceptualization of the biosphere including FEPs that were selected and included in the applicant's biosphere conceptual models.

The staff's detailed review focused on the most risk-significant parts of the applicant's biosphere model. Risk insights that apply to both the applicant's TSPA results and to the applicant's detailed abstraction modeling of the biosphere (i.e., using the ERMYN code to generate the biosphere dose conversion factors) informed the staff's review. These risk insights focused the staff's detailed review on those aspects of the applicant's biosphere modeling that contributed most to the calculated RMEI dose results in the TSPA.

The staff analyzed the risk-significance aspects of the TSPA biosphere model abstraction in the TSPA code by evaluating the applicant's sensitivity analysis results using the TSPA code. (b)(5)

(b)(5)

(b)(5)

Table 16-1. Exposure Pathways and Radionuclides Found To Be the Most Risk Significant in the DOE Performance Assessment for the 10,000-Year Simulation Period

(b)(5)

**Table 16-2. Exposure Pathways and Radionuclides Found To Be
the Most Risk Significant in the DOE Performance Assessment for
the 1-Million-Year Simulation Period**

(b)(5)

(b)(5)

(b)(5)

(b)(5)
(b)(5)
(b)(5)

2.2.1.3.14.3.1 System Description and Model Integration

In SAR Section 2.3.10.2 and in supporting references, the applicant described the biosphere characteristics of the Yucca Mountain region; of Amargosa Valley, Nevada, that impact its residents; of included FEPs; and of the biosphere conceptual models in the ERMYN code that were used to calculate biosphere dose conversion factors. This section documents the staff's review of these applicant's descriptions. As discussed next, this review evaluated whether the applicant's included FEPs and conceptual models satisfy applicable regulatory requirements found at 10 CFR 63.114(a)(5); 10 CFR 63.305(a); 10 CFR 63.305(b); 10 CFR 63.311(b); 10 CFR 63.312(a), (b), (d), and (e); and 10 CFR 63.305(c) and (d). An additional part of the staff's review evaluated integration (i.e., couplings, consistency, and assumptions) of the TSPA biosphere model abstraction with other TSPA model abstractions.

Features, Events, and Processes

The applicant described the Yucca Mountain region characteristics in SAR Section 2.3.10.2.1. This information addressed topics including climate, topography and soils, native flora and fauna (i.e., plants and animals), local communities, infrastructure (including water source), and agricultural conditions. Information on the characteristics of Amargosa Valley, Nevada, residents (summarized in SAR Section 2.3.10.2.2) originated predominantly from local and national surveys. The SAR addressed topics such as diet and lifestyle factors, including the use of evaporative coolers, gardening, employment, commuting, housing, and metabolic considerations. The applicant documented the screening approach for the FEPs in SAR

Comment	(b)(5)
---------	--------

Section 2.2.1.2 and listed all the FEPs that were evaluated for the TSPA model in SAR Table 2.2-1. FEPs that were included in the biosphere model were tabulated in SAR Table 2.3.10-1 and are reviewed in this SER section. The staff's review of excluded FEPs is documented in SER Section 2.2.1.2.1.3.2.

The staff's review evaluated the technical bases the applicant used to support its disposition of included FEPs in the performance assessment with respect to the following: (i) the applicant provided satisfactory technical bases for including biosphere FEPs in compliance with 10 CFR 63.114(a)(5); (ii) the included FEPs were consistent with present knowledge of the conditions in the region surrounding the Yucca Mountain site and in compliance with 10 CFR 63.305(a); and (iii) the applicant included all biosphere-related FEPs that could significantly change the magnitude or timing of the radiological exposures to the RMEI in its performance assessment in compliance with 10 CFR 63.114(a)(5)

The staff evaluated the applicant's technical bases for included FEPs and reviewed the applicant's descriptions of how each included biosphere FEP was incorporated into the performance assessment calculation. In this review, the staff verified that the FEPs which could significantly contribute to the RMEI dose were included in the performance assessment calculation and that information supporting the FEPs was based on present knowledge of the Yucca Mountain region conditions. (b)(5)

(b)(5)

(b)(5)

Conceptual Models

In SAR Section 2.3.10.2.3, the applicant considered included FEPs and NRC regulatory requirements for the reference biosphere model and dose calculation of the RMEI in identifying applicable exposure pathways and developing exposure scenarios for modeling dose to the RMEI. An exposure scenario, in general, describes a set of facts, assumptions, and inferences

about how exposure occurs. In the applicant's Yucca Mountain biosphere model, an exposure scenario is a conceptual model that describes the biosphere characteristics which lead to the RMEI's exposure to radionuclides that enter the biosphere from different transport routes (i.e., groundwater or volcanic ash). DOE's conceptual representations of the exposure pathways for groundwater and volcanic ash exposure scenarios were provided in SAR Figures 2.3.10-6 and 2.3.10-8. DOE incorporated these conceptual representations into mathematical submodels in the ERMYN code. The mathematical submodels in the ERMYN code were depicted in SAR Figures 2.3.10-9 and 2.3.10-10 and described in SAR Sections 2.3.10.2.5 and 2.3.10.2.6.

The staff evaluated the applicant's conceptual representations (i.e., conceptual models) and associated mathematical submodels in the ERMYN code for consistency with the applicable NRC regulations for the biosphere model and the performance assessment analysis: 10 CFR 63.305(b) and (d); 10 CFR 63.311(b); and 10 CFR 63.312(a), (b), (d), and (e). The staff reviewed both the applicant's groundwater exposure scenario (the modeling of biosphere characteristics that lead to the RMEI exposure to radionuclides from contaminated groundwater) and the volcanic ash exposure scenario. These reviews, documented in the subsections that follow, evaluated whether DOE's conceptual representations of the biosphere model included all potential pathways of radionuclide transport and exposure to comply with 10 CFR 63.311(b) requirements. These reviews also evaluated whether the applicant has complied with requirements for the biosphere and RMEI in 10 CFR 63.305 and 10 CFR 63.312, respectively, that apply to the conceptual model level of analysis of the biosphere. Compliance with the portions of the biosphere and RMEI requirements that are applicable to the input parameters and data level of analysis is discussed in SER Sections 2.2.1.3.14.3.2, 2.2.1.3.14.3.3, and 2.2.1.3.14.3.4.

Groundwater Exposure Scenario Conceptual Model

The staff's review of the applicant's conceptual model of the groundwater exposure scenario included biosphere FEPs, their functional relationships, and the resulting exposure pathways for modeling biosphere transport and dose to the RMEI. The staff's evaluation of functional relationships among FEPs considered how the applicant accounted for interactions among related FEPs in the biosphere conceptual model so that all potential pathways could be identified. For example, farming practices, such as soil irrigation, can lead to soil accumulation of radionuclides, which can contribute to plant uptake of radionuclides from that soil.

The applicant's groundwater exposure scenario includes an RMEI to an adult who lives in the accessible environment above the highest concentration of radionuclides in the plume of contamination, in compliance with 10 CFR 63.312(a) and (e). The RMEI is assumed to use wells to draw groundwater from the plume of contamination and water for domestic and agricultural purposes (b)(5)

(b)(5)

The applicant's conceptualization of dose to the RMEI involves three routes of exposure: external exposure, inhalation, and ingestion. The inhalation dose portion of the applicant's conceptual model includes RMEI inhalation of radionuclides in (i) resuspended soil particles, (ii) gaseous emissions from the soil and their radioactive decay products, and (iii) aerosols generated by evaporative coolers. The ingestion dose portion of the applicant's conceptual

model includes (i) drinking water; (ii) crops, including leafy vegetables, other vegetables, fruits, and grains; (iii) animal products, including meat, poultry, milk, and eggs; (iv) freshwater fish; and (v) soil. The meat category is a combination of all edible portions of beef, pork, and wild game (BSC, 2005ab)

Comment (b)(5)

(b)(5)

(b)(5)

(b)(5)

Volcanic Ash Exposure Scenario Conceptual Model

The NRC staff's review of the volcanic ash exposure scenario conceptual model evaluated the included biosphere system FEPs, their functional relationships, and the included exposure pathways for modeling biosphere transport and dose to the RMEI. (b)(5)

(b)(5)

Other models in the applicant's performance assessment address the transport of contaminated volcanic ash to the ground in the biosphere. Those models are reviewed in SER Section 2.2.1.3.13. (b)(5)

(b)(5)

(b)(5)

The applicant's conceptualization of inhalation dose in the volcanic ash exposure scenario includes resuspension of radionuclides in soil particles and release of Rn-222 (radon) gas. (b)(5)

(b)(5)

(b)(5) The applicant's inclusion of resuspension in its conceptual approach also addressed a variety of dust-generating activities and RMEI exposure environments (SAR Sections 2.3.10.2.6 and 2.3.10.3.2.2). (b)(5)

(b)(5)

The applicant considered that groundwater pathways which did not include a soil component (e.g., evaporative coolers, ingestion of groundwater, and ingestion of fish) did not apply to the volcanic ash exposure scenario, based upon the applicant's exclusion of FEP 1.2.04.07.0B for ash in groundwater (SNL, 2008ab). The staff's review of the applicant's exclusion of this FEP is documented in SER Section 2.2.1.2.1.3.2.

(b)(5)

Integration of Biosphere Model in the TSPA

The staff reviewed the integration between the biosphere model abstraction and other TSPA abstractions for couplings among models that share or utilize similar information and consistency of assumptions among models. (b)(5)

(b)(5)

The staff's evaluation of direct couplings between the TSPA biosphere abstraction and other TSPA model abstractions considered the flow of information from other abstractions to the biosphere abstraction within selected TSPA model files. (b)(5)

(b)(5)

(b)(5) The applicant's model file for the volcanic eruption modeling case passes the ash redistribution model results (radionuclide and pathway-specific soil concentrations) for multiplication by the volcanic ash exposure scenario radionuclide and pathway-specific biosphere dose conversion factors. (b)(5)

(b)(5)

(b)(5)

(b)(5)

The applicant quantitatively evaluated the effects of climate change as follows. The applicant's analysis: (i) evaluated biosphere model parameters on the basis of the expected parameters impacted by climate change, (ii) derived values for these parameters on the basis of its analysis of potential future climate states, and (iii) executed biosphere calculations for three separate climate states (present-day interglacial, monsoon, glacial transition). The results showed that future climate evolution in the biosphere lowers dose to the RMEI (SAR Section 2.3.10.5.1.1)

(b)(5)

(b)(5)

2.2.1.3.14.3.2 Assessment of Biosphere Transport Pathways

A series of integrated submodels in the DOE ERMYN biosphere model calculates radionuclide transport through pathways within the biosphere. Five transport submodels (surface soil, plant uptake, animal uptake, fish uptake, and air) calculate environmental media concentrations used in the ERMYN calculations of biosphere dose conversion factor input parameters for the TSPA model. The staff's review of the surface soil submodel is documented in SER Section 2.2.1.3.13.3.2. This section documents the staff's review of the applicant's technical bases for input parameters, treatment of parameter uncertainty, and, as appropriate, evaluation of alternative conceptual models applicable to the biosphere transport submodels in ERMYN. The staff's risk-informed review focused on transport submodels and applicable input parameters for exposure pathways that contribute most to the TSPA results, as discussed in SER Section 2.2.1.3.14.3.

These submodels address plant uptake, animal uptake, fish uptake, and air transport. Air transport includes localized resuspension of particulates from soil or ash, generation of indoor evaporative cooler aerosols, and the release of radon gas from soil or ash. (b)(5)

(b)(5)

(b)(5)

The applicant further documented that RMEI inhalation of resuspended particulates was the predominant pathway for the volcanic ash exposure scenario biosphere dose conversion factors for Pu-239 and Pu-240 (SAR Table 2.3.10-15). (b)(5)

(b)(5)

Plant Uptake Submodel

The applicant's plant uptake submodel in the ERMYN code (SAR Section 2.3.10.3.1.3) calculates plant radionuclide concentrations on the basis of direct deposition of irrigation water and dust on plant surfaces and root uptake from estimated soil radionuclide concentrations computed by the surface soil model (or provided as direct model input for volcanic ash biosphere dose conversion factor calculations as discussed in SAR Section 2.3.10.3.2.1). For root uptake processes, soil-to-plant transfer factors are used as input parameters to calculate plant radionuclide concentration from the radionuclide concentration in the soil.

DOE selected soil-to-plant transfer factors from laboratory and field study results obtained from available literature using the methods discussed in BSC (2004ap).

DOE evaluated soil-to-plant transfer factors from data obtained through a variety of references, including original data from literature reviews and biosphere analyses that selected and reported values from available sources. For its analysis, the applicant identified five unique crop groups: leafy vegetables, other vegetables, fruit, grain, and forage. For each crop group and radionuclide, DOE selected soil-to-plant transfer factor values that it considered most applicable to the Yucca Mountain biosphere conditions, based upon area soil characteristics and crop types (SAR Section 2.3.10.3.1.3). The applicant then calculated geometric means and standard deviations from the values selected from each reference. The applicant assumed that soil-to-plant transfer factors followed truncated lognormal distributions with a 99 percent confidence interval around the geometric mean of the selected point values (BSC, 2004ap).

(b)(5)

Comment (b)(5)

(b)(5)

(b)(5)

The applicant averaged applicable point estimates from a combination of original data sources and other documented analyses; this approach results in selecting geometric mean values that are representative of values presented in the source documents. For example, as shown in BSC Table 6-2 (2004ap), the applicant evaluated the data for soil-to-plant transfer of technetium in leafy vegetables. This data included 8 point values ranging from 9.5 to 180. The DOE-derived truncated lognormal distribution ranged from 3.8 to 550 with a geometric mean of 46.

(b)(5)

(b)(5)

(b)(5)

(b)(5)

For direct deposition of radionuclides on plant surfaces, the plant uptake model in the ERMYN code calculates the radionuclide concentrations in crops from leaf uptake and retention of intercepted irrigation water and dust (SAR Section 2.3.10.3.1.3). These calculations are based on the irrigation deposition rate or dust deposition rate, the fraction of irrigation that originated from above-plant spraying, the crop interception fraction, the translocation factor (fraction of deposited radionuclides that are absorbed and move to other parts of the plant), the weathering half-life (removal rate of contaminants from leaves), the crop growing time, and the crop yield, as identified in SAR Section 2.3.10.3.1.3 and SNL Sections 6.4.3.2 and 6.4.3.3 (2007ac).

(b)(5)

(b)(5)

Animal Uptake Submodel

SAR Section 2.3.10.3.1.4 described the applicant's ERMYN code animal uptake submodel. This submodel calculates radionuclide concentrations in human food products that are derived from livestock that ingest contaminated food and water. For the purpose of modeling, the applicant identified four distinct animal product groups: meat, milk, eggs, and poultry. The animal product radionuclide concentrations were calculated on the basis of estimated animal intakes of radionuclides from contaminated feed, water, and soil, as applicable to the groundwater or volcanic eruption modeling cases. Animal feed radionuclide concentrations are computed by the plant uptake submodel (e.g., the applicant assumes cows eat locally grown forage and chickens eat local grain). As discussed in BSC (2004ap), the applicant used animal product transfer coefficients as input parameters for the fraction of an animal's daily intake of a radionuclide that is transferred to a unit mass or volume of produced food product. The applicant's animal product transfer coefficients were selected using the same methods (BSC, 2004ap) described in the previous subsection for soil-to-plant transfer factors.

The staff evaluated the sufficiency of the applicant's technical bases and supporting data for the selected values and uncertainty ranges for the animal product transfer coefficients used in ERMYN code to calculate biosphere dose conversion factor input parameters for the TSPA model. (b)(5)

Comment (b)(5)

(b)(5)

(b)(5)

(b)(5)

(b)(5)

(b)(5)

(b)(5)

DOE assumed a truncated lognormal distribution using the geometric standard deviation computed from the source data and applied a 99 percent confidence interval approach similar to that used for deriving parameter distributions for soil-to-plant transfer factors. (b)(5)

(b)(5)

(b)(5)

Fish Uptake Submodel

The ERMYN code fish uptake submodel (SAR Section 2.3.10.3.1.5) calculates radionuclide concentrations in fish raised in local fish farms that are assumed to use contaminated groundwater. The input parameter that most influences the results of this model is the bioaccumulation factor. This element-specific factor relates the concentration of radionuclides in the edible portion of the fish to the concentration of radionuclides in the contaminated water in which the fish is submerged. DOE selected bioaccumulation factors on the basis of a review of the applicable literature. The applicant's review included fish in all portions of the food chain as well as bottom-feeding fish. DOE assumed a lognormal distribution. For the fish farms noted in Amargosa Valley during the applicant's consumption survey, the fish were fed commercial feed that is not locally derived. Feed that is not locally derived would therefore not be expected to become contaminated with radionuclides from a Yucca Mountain release scenario. Therefore, the applicant applied a bioaccumulation factor (that accounts for fish ingesting contaminated food and water) to a Yucca Mountain biosphere calculation. Actual conditions suggest that only the water would be contaminated and the analysis will overestimate the fish intake and thereby overestimate the radionuclide concentration in fish. The resulting dose to the RMEI from fish consumption is therefore expected to be overestimated.

The staff evaluated the sufficiency of the applicant's technical bases and supporting data for the selected point values and uncertainty ranges for the bioaccumulation factors used in the fish uptake submodel. (b)(5)

(b)(5)

(b)(5)

(b)(5)

The staff's review of the fish bioaccumulation factors identified an apparent transcription error in the DOE report (BSC, 2004ap). The geometric mean of the fish bioaccumulation factor for carbon was reported differently in two separate tables that should have contained the same values. Specifically, BSC Table 6-64 (2004ap), which is the table that initially

derives the value from source data, showed a geometric mean fish bioaccumulation factor for carbon of 1.6×10^4 L/kg [1.9×10^3 gal/lb]. BSC Table 6-65 (2004ap) listed a different value of 4.6×10^3 L/kg [5.5×10^2 gal/lb] for this same parameter (a factor of 3.5 lower than the original value computed in Table 6-64). The applicant used the lower value reported in Table 6-65 in the ERMYN calculations, as indicated by SAR Table 2.3.10-10. To evaluate the significance of this discrepancy, staff considered whether using the lower value would significantly affect the applicant's dose results. This evaluation considered that the applicant's fish consumption dose scales linearly with the bioaccumulation factor. The staff also evaluated the TSPA results for the 10,000-year simulation period in SAR Figure 2.4-20, which shows that the carbon dose contributes approximately 20 percent of the peak mean total dose. SAR Table 2.3.10-11 indicated that the fish pathway contributed 59 percent to the carbon dose

(b)(5)

Air Submodel

The ERMYN air submodel (SAR Sections 2.3.10.3.1.2 and 2.3.10.3.2.2) models radionuclide concentrations in air from (i) resuspension of contaminated soil or ash, (ii) evaporative cooler aerosols from the use of contaminated groundwater, and (iii) radon gas emanation from contaminated soil or ash. Inhalation of resuspended particulates is the predominant exposure pathway for Pu-239, Pu-240, and Pu-242 in the applicant's performance assessment. Resuspended particulate exposure is modeled in both the groundwater and volcanic ash exposure scenarios. Particulate inhalation also contributes approximately 21 percent to the groundwater dose from Np-237 in the DOE model (SAR Table 2.3.10-11).

(b)(5)

An important input parameter in the DOE calculation of air concentration of particulates is the mass loading factor (g/m^3 [lb/ft^3]) based on the DOE biosphere dose conversion factor sensitivity analysis results documented in SNL, p. 6-150 (2007ac) and SAR Table 2.3.10-17.

(b)(5)

(b)(5)

The mass

loading factor computes the concentration of radionuclides in air {Bq/m³ [Ci/m³]} from the estimated concentration of radionuclides deposited on the soil surface {Bq/g [Ci/g]}.

In SAR Sections 2.3.10.3.1.2 and 2.3.10.3.2.2 and supporting references, DOE described its derivation of separate mass loading factors for each exposure scenario (i.e., irrigated soil, volcanic ash) on the basis of available literature. DOE derived individual mass loading input parameters for RMEI activity level (active and inactive) and environment (outdoor, indoor, or away from potentially contaminated areas) in its inhalation exposure model.

The staff evaluated the adequacy of the applicant's technical bases and supporting data for the mass loading input parameters used in biosphere exposure scenarios involving groundwater and volcanic ash. The applicant detailed these in BSC (2006ad).

In reviewing the applicant's technical bases for groundwater exposure scenario mass loading input parameter values, the staff evaluated the adequacy of the supporting data the applicant used to derive mass loading input parameters against independent NRC estimates derived from available technical information. (b)(5)

(b)(5)

As part of the NRC staff's review of the applicant's groundwater exposure scenario mass loading values, the staff evaluated the magnitude of the applicant's selected values. (b)(5)

(b)(5)

(b)(5)

For the volcanic ash scenario, the staff recognizes that limited data are applicable to mass loading for a volcanic eruption in the Yucca Mountain region or for analogous conditions elsewhere. DOE reviewed literature that included measured dust levels of volcanic ash resuspended in air for ambient and surface-disturbing conditions at various sites where volcanoes had recently erupted (within 5 years) and also compared the relevance of each analog site (including the Soufrière Hills Volcano in Montserrat, British West Indies, and the Mt. Spurr Volcano in Alaska) to expected conditions in the Yucca Mountain region.

The NRC staff's review of the applicant's technical bases for volcanic ash exposure scenario mass loading input parameter values evaluated the adequacy of the supporting data the applicant used and the methodology used to derive mass loading input parameters. (b)(5)

(b)(5)

(b)(5)

Comment (b)(5)

(b)(5)

The staff reviewed the applicant's treatment of uncertainty and variability in mass loading values for both exposure scenarios and concludes that the applicant has accounted for uncertainty and

variability in parameter values and has provided the technical bases for parameter ranges and probability distributions used in the air submodel. (b)(5)

(b)(5)

(b)(5)

The applicant then addressed uncertainty and variability in the mass loading parameters [provided in BSC Sections 6.2 and 6.3 (2006ad)] by deriving triangular parameter distributions. These distributions were based on its assessment of the range of applicable literature values and the central tendencies in the data that support selection of a value for the mode of each distribution. The applicant conducted similar literature-based evaluation and selection of mass loading ranges and modes to characterize triangular input distributions for each activity environment and for groundwater and ash exposure scenarios. The resulting input distributions were provided in BSC Table 7-1 (2006ad).

The applicant evaluated personal exposure measurements of total suspended particulates collected during farming activities at 10 farms near Davis and Sacramento, California, that supported a range of 0.30 to 7.93 mg/m³ [8.1×10^{-6} to 2.1×10^{-4} oz/yd³]. After evaluating additional data from 7 other studies involving mostly farming activities and 22 sets of measurements taken in Amargosa Valley for various types of activities, a range of 1 to 10 mg/m³ [2.7×10^{-5} to 2.736×10^{-4} oz/yd³] (with a mode of 3 mg/m³ [8.1×10^{-5} oz/yd³]) was derived for the ERMYN input for the TSPA analyses for mass loading in the active outdoor environment for groundwater-based biosphere dose calculations. The mode of 3 mg/m³ [8.1×10^{-5} oz/yd³] was the mean of the maximum mass loading values measured for 22 surface-disturbing activities in Amargosa Valley, as identified in BSC Section 6.2.1.3 (2006ad).

(b)(5)

As discussed in SAR Section 2.3.10.3.1.2, the air submodel in the ERMYN code also calculates indoor air radionuclide concentrations from aerosols released from evaporative coolers. This calculation is based on the concentration of radionuclides in groundwater, the rate of water evaporation from coolers, the indoor air exchange rate, and the fraction of radionuclides in water that transfer to air (the water-to-air transfer fraction). DOE identified the water-to-air transfer

¹A mode is a statistic of central tendency for a set of values that represents the value that occurs most frequently in that set

fraction in the evaporative cooler model as an important input parameter in the evaporative cooler calculation. (b)(5)

(b)(5)

(b)(5) The applicant assumed a uniform concentration ratio distribution from 0 to 1 for dissolved solids and 1 for gases on the basis of a lack of available studies on contaminant aerosols from evaporative coolers. (b)(5)

(b)(5)

Airborne concentrations of radon gas released from soils irrigated with contaminated water or from contaminated volcanic ash were also calculated in the air submodel (SAR Sections 2.3.10.3.1.2 and 2.3.10.3.2.2; SNL, 2007ac; BSC, 2004ap). Both exposure scenarios consider indoor and outdoor radon concentrations. In the volcanic ash scenario, the outdoor air concentration is also used for the indoor air concentration because the applicant expected the outdoor concentration to be higher than the indoor concentration as a result of the small radon contribution from ash below the RMEI's house. The applicant's groundwater scenario calculates separate radon concentrations for indoor and outdoor environments. The applicant's indoor radon concentration calculations evaluated radon released from soil beneath a hypothetical house built on land that was previously irrigated by contaminated water. In this model, the rate of radon released into the house is a proportion of the outdoor radon flux that accounts for diffusion of radon from underlying soil through the foundation. Indoor radon concentrations in the model were calculated based on (i) the radon flux into the house from soil beneath the house and from outdoors, (ii) the interior air exchange rate, and (iii) the interior volume of the house. The interior air exchange rates account for periods of evaporative cooler use and nonuse based on increased ventilation during cooler operation, which decreases radon concentration in air. The indoor radon diffusion methods are consistent with those used in the RESRAD dose assessment code (Yu, et al., 2001aa) that the U.S. Environmental Protection Agency (EPA) developed. Outdoor radon concentrations are based on factors that relate the airborne concentration of Rn-222 to either (i) the Ra-226 concentration in the soil for the groundwater scenario or (ii) the Rn-222 flux density for the volcanic ash scenario.

The staff evaluated the applicant's technical bases and supporting data for input parameters used in the indoor and outdoor radon concentration modeling in the ERMYN code. (b)(5)

(b)(5)

(b)(5)

DOE chose the concentration fraction of the radon flux from soil underneath the house that would diffuse into the house to be uniformly distributed from 0.1 to 0.25 on the basis of measurements in homes with concrete foundations (SAR Section 2.3.10.3.1.2). The home ventilation rates (for evaporative cooler nonuse periods) were based on minimum ventilation recommendations for manufactured homes, data from a survey of approximately 3,000 U.S. homes, and information from a trade organization representing home ventilation equipment manufacturers (BSC, 2004ap). The home ventilation rates for evaporative cooler use were estimated on the basis of cooler flow rates and the average home interior volume. Uncertainty and variability in the ventilation rates were propagated by deriving a truncated lognormal distribution on the basis of the survey data (for no cooler use) and a

uniform distribution for cooler use ventilation rates that spans the estimated range (BSC, 2004a). (b)(5)

(b)(5)

(b)(5)

(b)(5)

The radon concentrations are used for calculating biosphere dose conversion factor input parameters for the TSPA code.

(b)(5)

2.2.1.3.14.3.3 Assessment of Human Exposure

DOE calculated human exposures from estimated concentrations of radionuclides in groundwater and soil in three exposure submodels of the ERMYN code (SNL, 2007a). These submodels are the primary exposure pathways addressed in the DOE exposure scenarios and include the external exposure submodel, the inhalation exposure submodel, and the ingestion exposure submodel (SAR Sections 2.3.10.3.1.7, 2.3.10.3.1.8, and 2.3.10.3.1.9 for the groundwater exposure scenario and SAR Sections 2.3.10.3.2.5, 2.3.10.3.2.6, and 2.3.10.3.2.7 for the volcanic ash exposure scenario). Considering the biosphere pathways that are the primary contributors to dose to the RMEI (SER Tables 2.2.1.3.14-1 and 2.2.1.3.14-2), the staff's risk-informed review focused on the inhalation and ingestion exposure submodels. These exposure submodels compute the RMEI's annual intake of radionuclides (e.g., Bq/yr [Ci/yr]) on the basis of the environmental media concentrations (e.g., air, water, livestock products, fish) calculated by the biosphere environmental transport submodels that are depicted in SAR Figures 2.3.10-9 and 2.3.10-10, described in SAR Section 2.3.10.3, and evaluated in SER Sections 2.2.1.3.14.3.2 and 2.2.1.3.12.3. The applicant's exposure models also convert the calculated RMEI radionuclide intakes to dose. The staff's review of the applicant's conversion of intakes into dose is evaluated in SER Section 2.2.1.3.14.3.4.

Inhalation Exposure Model

The applicant's ERMYN inhalation exposure submodel calculates RMEI radionuclide intakes by modeling the inhalation of contaminated air. In the model, airborne contaminants include resuspended soil or ash particulates, aerosols from evaporative coolers, or radon gas emanating from contaminants in soil or ash. DOE calculations showed that the inhalation exposure pathways that are the most risk significant contributors to the applicant's performance

assessment results (SER Tables 2.2.1.3.14-1 and 2.2.1.3.14-2) are resuspended particulates from soil and aerosols from evaporative coolers. Inhalation of gaseous emissions of radon from contaminants in soil also contributes to DOE's long-term dose calculation results, but that contribution is less than the contributions from particulates and aerosols.

The applicant's exposure calculations for these three inhalation exposure pathways involve exposure time and breathing rate input parameters (b)(5)

(b)(5)

DOE's exposure time input parameters in the ERMYN inhalation exposure submodel apportion the amount of time the RMEI spends in various environments where exposure could occur into three categories: outdoor, indoor, and away from areas potentially contaminated by Yucca Mountain activities. The DOE inhalation exposure submodel also apportions the amount of time spent conducting surface-disturbing activities, which DOE identified as active, to account for increased exposure to radionuclides resuspended from the ground surface by the activity. The applicant identified the amount of time that the RMEI was not conducting surface-disturbing activities as inactive. The applicant grouped the Amargosa Valley population into four population categories: nonworkers, commuters, local outdoor workers, and local indoor workers. The applicant apportioned time spent into five activity-environment categories (by combining the three environment categories with the two activity-level categories): active outdoors, inactive outdoors, active indoors, inactive indoors (sleep), and away from areas potentially contaminated by Yucca Mountain activities. Exposure times were derived from census information on age distribution; employment, commuting characteristics of Amargosa Valley, Nevada, residents; and national survey data on activity times (BSC, 2005ab).

The staff evaluated the applicant's technical bases and supporting data for the exposure times that were used to derive activity-environment categories (BSC, 2005ab). The applicant provided a derivation of exposure times on the basis of data from surveys of the Amargosa Valley and national populations. Year 2000 census data from the Amargosa Valley census county division (Bureau of the Census, 2002aa) provided the population distribution by age, work status and hours worked, commute time, and industry of employment. DOE also used detailed national survey data on activity time budgets from Klepeis, et al. (1996aa) and EPA (1997aa) to assign the fraction of time spent inside a residence; outdoors; in a vehicle; and at stores, restaurants, and other indoor locations.

(b)(5)

(b)(5)

The applicant's data synthesis approach used percentages of time spent conducting activities at various locations by age group with Amargosa Valley population information to generate percentages applicable to the Amargosa Valley population. DOE then used additional national survey results (EPA, 1997aa) on time spent outdoors to derive active and inactive outdoor exposure times and apportioned the resulting times spent at various locations to derive its exposure time input parameter values. The applicant's estimates for the fraction of outdoor

activity that includes surface-disturbing activities (20 percent of public outdoor time and 50 percent of construction worker outdoor time) were based on EPA survey data and information on local practices. (b)(5)

(b)(5)

(b)(5) DOE lognormal distributions of exposure time estimates to propagate variation in ERMYN code were based on the standard errors provided with the survey data and the application of standard lognormal distribution statistical methods. For some parameters, the applicant intentionally assigned standard errors that were larger than those associated with the national survey data to account for uncertainties in applying national data to local conditions. These uncertainties result from potential differences in local human activity practices compared to national patterns and the effect of differences in survey sample sizes on standard errors. (b)(5)

(b)(5)

The applicant derived breathing rates for each population group and for each level of activity within the four potentially contaminated exposure environments (active outdoors, inactive outdoors, active indoors, and inactive indoors). DOE combined breathing rate information for adults by gender and level of physical activity from International Commission on Radiological Protection (1994aa) with census demographic information for Amargosa Valley to derive population gender-weighted breathing rates. DOE then used information from International Commission on Radiological Protection (1994aa) on the fraction of daily time devoted to different levels of activity to derive breathing rates for each exposure environment category. In this manner, the exposure environment categories applied to all population groups considered in the model and were derived, in part, on the basis of surveys of Amargosa Valley, Nevada, residents.

The staff evaluated the applicant's technical bases and supporting data for the breathing rates detailed in BSC (2005ab). The gender-weighted breathing rate values DOE calculated from International Commission on Radiological Protection breathing rates and census data for Amargosa Valley were 0.39, 0.47, 1.38, and 2.86 m³/hr [0.51, 0.61, 1.81, and 3.74 yd³/hr] for sleep, sitting, light exercise, and heavy exercise, respectively. (b)(5)

(b)(5)

The NRC staff also reviewed DOE's methods for deriving the final set of breathing rates for each of the four exposure environments. (b)(5)

(b)(5)

(b)(5)

The applicant used these breathing rates in ERMYN calculations as individual fixed input parameters for each exposure environment, and the model propagates breathing rate input parameter uncertainty or variability due to differences in activity level by using different exposure environments. (b)(5)

(b)(5)

(b)(5)

Ingestion Exposure Model

The applicant's ingestion exposure submodel in ERMYN calculates RMEI radionuclide intakes by modeling RMEI consumption of contaminated water, crops, animal products (milk, meat, poultry, eggs, fish), and soil. Ingestion pathways have a more pronounced effect on the applicant's performance assessment results during the 10,000-year compliance period than on the results for the 1-million-year period because of the radionuclides that dominate the dose calculations. Exposure pathways that contribute most to the applicant's performance assessment results (SER Section 2.2.1.3.14.3) include drinking water, fish consumption, and animal product consumption (milk, meat, eggs). The exposure calculations for these ingestion exposure pathways involve consumption rate input parameters for modeled food products the RMEI consumes (i.e., water, fish, and animal food products including milk, meat, and eggs).

DOE derived food consumption rates used in the ERMYN ingestion exposure submodel from a DOE-sponsored survey of Amargosa Valley residents (DOE, 1997ab). The exception is DOE's modeling of drinking water consumption, which the applicant stated was based on the requirements in 10 CFR 63.312(d). The Amargosa Valley survey measured how often residents consumed various locally produced food products. The calculated arithmetic mean [the method specified in 10 CFR 63.312(b)] annual consumption rates for various food types and corresponding standard deviations were then used as input parameters for sampling parameter values in ERMYN assuming a lognormal distribution, as detailed in BSC Section 6.4.2, Table 6-21 (2005ab).

The staff evaluated the adequacy of the applicant's technical bases and supporting data for the food and water consumption rates as detailed in BSC (2005ab). The requirements of 10 CFR 63.312(b) direct DOE to use projections based upon surveys of Amargosa Valley residents. (b)(5)

(b)(5)

(b)(5)

(b)(5)

Comment (b)(5)

(b)(5)

2.2.1.3.14.3.4 Assessment of Dosimetry

The DOE biosphere model uses dose coefficients from the Federal Guidance Report 13 (EPA, 1999aa), which uses tissue-weighting factors recommended in International Commission on Radiological Protection, Publication 60 (1991aa) to calculate effective dose from both internal and external radiation sources. In its TSPA modeling, DOE identified 28 primary radionuclides that were the primary contributors to dose to the RMEI using a radionuclide screening analysis (SNL, 2007ac; SAR Section 2.3.7.4.1.2). DOE then converted radionuclide intake or external exposure to dose using the dose coefficients for the 28 primary radionuclides. DOE used dose coefficients for external exposure that are defined as the effective dose rate per unit radionuclide concentration in the soil. DOE also used dose coefficients for inhalation and ingestion as the committed effective dose per unit radionuclide intake by inhalation or ingestion.

DOE chose dose coefficients for intake of radionuclides used in the biosphere model for adults and a TEDE commitment period of 50 years. The biokinetic and dosimetric models

used to develop these dose coefficients are based on a hypothetical average adult person with the anatomical and physiological characteristics the International Commission on Radiological Protection (1975aa) defined with further modifications as described in Federal Guidance Report 13 (EPA, 1999aa). DOE used breathing rates in its biosphere model that are based on the more recent biometric results for adults from the respiratory tract model the International Commission on Radiological Protection (1994aa) developed, as discussed in SER Section 2.2.1.3.14.3.3. (b)(5)

(b)(5)

(b)(5)

DOE calculated the TEDE to the RMEI as the sum of the effective dose equivalent from external sources plus the committed dose equivalent from internal sources (i.e., sources either inhaled or ingested). (b)(5)

(b)(5)

(b)(5)

(b)(5)

2.2.1.3.14.3.5 Assessment of Integrated Biosphere Modeling Results

DOE biosphere modeling results were provided in SAR Section 2.3.10 and analyzed in greater detail in the Biosphere Model Report (SNL, 2007ac). The exposure pathways found to be the most risk significant in the DOE performance assessment varied depending on the particular radionuclide. The radionuclides and pathways that were most risk significant in the DOE TSPA calculations are summarized in SER Table 2.2.1.3.14-1 for the 10,000-year simulation period and SER Table 2.2.1.3.14-2 for the 1-million-year simulation period.

To validate the integrated biosphere model, DOE compared the calculation results for each environmental transport and exposure submodel of the ERMYN code with comparable calculation results from five other biosphere transport and exposure process-level models (SAR Section 2.3.10.6). DOE concluded that the results of the process-level calculations used in those other models were the same, or similar, to the results obtained using the biosphere model (SNL, 2007ac). To verify implementation, DOE compared the results of the biosphere model for representative radionuclides (Pu-239, Ra-226, Th-232, and C-14) with the results of spreadsheet calculations—on the basis of equations used in the biosphere mathematical model—and the results were identical (SNL, 2007ac). (b)(5)

(b)(5)

(b)(5)

(b)(5)

2.2.1.3.14.4 Evaluation Findings

(b)(5)

(b)(5)

(b)(5)

(b)(5)

2.2.1.3.14.5 References

BSC. 2006ad. "Inhalation Exposure Input Parameters for the Biosphere Model." ANL-MGR-MD-000001. Rev. 04. ACN 01. Las Vegas, Nevada: Bechtel SAIC Company, LLC.

BSC. 2005ab. "Characteristics of the Receptor for the Biosphere Model." ANL-MGR-MD-000005. Rev. 04. Las Vegas, Nevada: Bechtel SAIC Company, LLC.

BSC. 2004ap. "Environmental Transport Input Parameters for the Biosphere Model." ANL-MGR-MD-000007. Rev. 02. ERD 01. Las Vegas, Nevada: Bechtel SAIC Company, LLC.

Bureau of the Census. 2002aa. "2000 Summary File 3 (SF 3) Sample Data, Amargosa Valley CCD, Nye County, Nevada." ANL-MGR-MD-000005, Rev. 4, DIRS 159728. Washington, DC: U.S. Department of Commerce, Bureau of the Census.

DOE. 1997ab. "The 1997 Biosphere Food Consumption Survey Summary Findings and Technical Documentation." ANL-MGR-MD-000005. Rev. 4. DIRS 100332. Las Vegas, Nevada: DOE, Office of Civilian Radioactive Waste Management.

EPA. 1999aa. "Federal Guidance Report 13, Cancer Risk Coefficients for Environmental Exposure to Radionuclides." EPA 402-R-99-001. Washington, DC: U.S. Environmental Protection Agency.

EPA. 1997aa. "Exposure Factors Handbook, Volume III, Activity Factors." EPA/600/P-95/002Fc. Washington, DC: U.S. Environmental Protection Agency.

International Atomic Energy Agency. 1994aa. "Handbook of Parameter Values for the Prediction of Coefficients: Workers and Members Radionuclide Transfer in Temperate Environments." Technical Report Series No. 364. Vienna, Austria: International Atomic Energy Agency.

International Commission on Radiological Protection. 1994aa. "Human Respiratory Tract Model for Radiological Protection." ANL-MGR-MD-000005. Rev. 4. DIRS 153705. *Annals of the ICRP*. Publication 66. Vol. 24, No. 1-3. New York City, New York: Pergamon Press.

International Commission on Radiological Protection. 1991aa. "1990 Recommendations of the International Radiological of Commission Protection." ANL-MGR-MD-000005. Rev. 4. DIRS 153705. *Annals of the ICRP*. Publication 60. Vol. 21, No. 1-3. New York City, New York: Pergamon Press.

International Commission of Radiological Protection. 1975aa. "Report of the Task Group on Reference Man." *Annals of the ICRP*. Publication 23. Vol. 23. New York City, New York: Pergamon Press.

Klepeis, N.E., A.M. Tsang, and J.V. Behar. 1996aa. "Analysis of the National Human Activity Pattern Survey (NHAPS) Respondents From a Standpoint of Exposure Assessment, Percentage of Time Spent, Duration, and Frequency of Occurrence for Selected Microenvironments by Gender, Age, Time-of-Day, Day-of-Week, Season, and U.S. Census Region—Final Report." EPA/600/R-96/074. ANL-MGR-MD-000005. Rev. 4. DIRS 159299. Washington, DC: U.S. Environmental Protection Agency, Office of Research and Development.

LaPlante, P.A. and K. Poor. 1997aa. "Information and Analyses to Support Selection of Critical Groups and Reference Biospheres for Yucca Mountain Exposure Scenarios." CNWRA 97-009. San Antonio, Texas: CNWRA.

Leslie, B., C. Grossman, and J. Durham. 2007aa. "Total-system Performance Assessment (TPA) Version 5.1 Module Descriptions and User Guide." Rev. 1. ML072710060. San Antonio, Texas: CNWRA.

NRC. 2009ab. "Division of High-Level Waste Repository Safety Director's Policy and Procedure Letter 14: Application of YMRP for Review Under Revised Part 63." Published March 13, 2009. ML090850014. Washington, DC: NRC.

NRC. 2005aa. NUREG-1762, "Integrated Issue Resolution Status Report." Rev. 1. Washington, DC: NRC.

NRC. 2003aa. NUREG-1804, "Yucca Mountain Review Plan—Final Report." Rev. 2. Washington, DC: NRC.

NRC. 1992ae. NUREG-5512, "Residual Radioactive Contamination From Decommissioning: Technical Basis for Translating Contamination Levels To Annual Total Effective Dose Equivalent—Final Report." Vol. 1. Washington, DC: NRC.

SNL. 2008ab. "Features, Events, and Processes for the Total System Performance Assessment: Analyses." ANL-WIS-MD-000027. Rev. 00. ACN 01, ERD 01, ERD 02. Las Vegas, Nevada: Sandia National Laboratories.

SNL. 2008ag. "Total System Performance Assessment Model/Analysis for the License Application." MDL-WIS-PA-000005. Rev. 00. AD 01, ERD 01, ERD 02, ERD 03, ERD 04. Las Vegas, Nevada: Sandia National Laboratories.

SNL. 2007ac. "Biosphere Model Report." MDL-MGR-MD-000001. Rev. 02. ERD 01. Las Vegas, Nevada: Sandia National Laboratories.

Yu, C., A.J. Zielen, J.-J. Cheng, D.J. LePoire, E. Gnanapragasam, S. Kamboj, J. Arnish, A. Wallo, W.A. Williams, and H. Peterson. 2001aa. "User's Manual for RESRAD Version 6." ANL/EAD-4. Argonne, Illinois: Argonne National Laboratory.

CHAPTER 17

2.2.1.4.1 Demonstration of Compliance With the Postclosure Public Health and Environmental Standards (Individual Protection)

2.2.1.4.1.1 Introduction

By letter dated June 3, 2008, as supplemented on February 19, 2009, the U.S. Department of Energy (DOE) provided in its license application [Safety Analysis Report (SAR) Section 2.4.2 (DOE, 2008ab)] its basis for demonstrating compliance with the individual protection standards for the initial 10,000 years after closure and the period after 10,000 years up to 1 million years.

DOE has conducted an analysis, through its Total System Performance Assessment (TSPA) computer model, that evaluates the behavior of the high-level waste repository in terms of an annual dose due to potential releases from the repository. The performance assessment provides a method to evaluate the range of features (e.g., geologic rock types, waste package materials), events (e.g., earthquakes, igneous activity), and processes (e.g., corrosion of metal waste packages, sorption of radionuclides onto rock surfaces) that are relevant to the behavior of a repository at Yucca Mountain. This chapter of the Safety Evaluation Report (SER) provides the U.S. Nuclear Regulatory Commission (NRC) staff's review of the performance assessment used to demonstrate compliance with the individual protection standards. In particular the NRC staff's review evaluates whether (i) the performance assessment includes the appropriate scenario classes [a set or combination of features, events, and processes (FEPs) that the performance assessment uses to represent a class or type of scenario such as seismic activity], (ii) the representation of the scenario classes within the performance assessment is credible (e.g., the performance assessment results are consistent with the models, parameters, and assumptions that make up the performance assessment), and (iii) the annual dose the performance assessment estimates is less than the dose limits set by the regulations for the reasonably maximally exposed individual (RMEI).

2.2.1.4.1.2 Regulatory Requirements

10 CFR 63.311 requires that the average annual dose must be no greater than 0.15 mSv/yr [15 mrem/yr] during the initial 10,000 years after closure of the repository and no greater than 1.0 mSv/yr [100 mrem/yr] after 10,000 years up to 1 million years. The regulations specify that a performance assessment must be used to demonstrate compliance with the individual protection dose limit and set forth requirements for the performance assessment. According to 10 CFR 63.2, *performance assessment* is defined as an analysis that

- (1) Identifies the FEPs (except human intrusion), and sequences of events and processes (except human intrusion) that might affect the Yucca Mountain disposal system and their probabilities of occurring during 10,000 years after disposal
- (2) Examines the effects of those FEPs and sequences of events and processes upon the performance of the Yucca Mountain disposal system
- (3) Estimates the dose incurred by the RMEI, including the associated uncertainties, as a result of releases caused by all significant FEPs, and sequences of events and processes, weighted by their probability of occurrence

The requirements for developing performance assessment analyses (e.g., consideration of FEPs included in the performance assessment, determination of event probabilities, consideration of uncertainties) are relevant to previous SER chapters (Sections 2.2.1.2 and 2.2.1.3). These previous chapters evaluate DOE's development of the performance assessment. The requirements also specify how the performance assessment is used to estimate the annual dose to the RMEI. In general, DOE is required to use the performance assessment to

- Estimate the annual dose as a result of releases caused by all significant FEPs weighted by their probability of occurrence (10 CFR 63.2 and 63.302)
- Demonstrate that the arithmetic mean (i.e., average) of the annual dose over the initial 10,000 years is no greater than 0.15 mSv [15 mrem] per 10 CFR 63.303 and 63.311(a)(1)
- Demonstrate that the arithmetic mean (i.e., average) of the annual dose after 10,000 years up to 1 million years is no greater than 1.0 mSv [100 mrem] per 10 CFR 63.303 and 63.311(a)(2)

Consistent with the review guidance identified in the Yucca Mountain Review Plan (YMRP) (NRC, 2003aa), the NRC staff assessed whether the average annual dose

Reflects the scenario classes included in the performance assessment
Provides a credible representation of repository behavior
Is below the dose limits and is computationally stable

2.2.1.4.1.3 Technical Review

2.2.1.4.1.3.1 Introduction

The regulations require DOE to use a performance assessment to demonstrate compliance with the dose limits for individual protection. DOE's performance assessment is implemented through its TSPA code. The TSPA code is used to represent the range of behavior of a Yucca Mountain repository, accounting for uncertainty in the FEPs that could affect the repository evolution over the compliance period. DOE developed its analysis of repository performance using distinct groupings of FEPs—referred to as "scenario" or "event" classes. In very general terms, there are two broad categories of scenario classes: nominal and disruptive. The nominal scenario class comprises those FEPs that are present under "normal" conditions (e.g., infiltration of water, corrosion of the waste package, release of radionuclides, transport of radionuclides in groundwater). The disruptive scenario class includes additional FEPs that account for the effects of specific events (i.e., seismic events, volcanic activity, fault movement) that disrupt or alter the repository performance differently from what the nominal scenario class portrays. In DOE's TSPA the nominal scenario class is considered part of the seismic ground motion modeling case so that the combined effects of waste package corrosion, which degrades the mechanical strength of the waste package, and mechanical damage of the waste package due to seismic ground motion are appropriately considered in the post-10,000-year period (SAR p. 2.4-36). (Note: for the initial 10,000 years the nominal scenario class does not result in any dose, as detailed in SAR p. 2.4-62 and Figure 2.4-22a.) A key aspect of the disruptive scenario classes is the consideration of the probability or likelihood that the disruptive event will occur. By regulation, the annual dose is weighted by the probability of its occurrence.

The NRC staff reviewed SAR Sections 2.4.1 and 2.4.2, Total System Performance Assessment-License Application (TSPA-LA) Analysis Model Report, and the TSPA model files including intermediate results provided as part of the license application. Additionally, the NRC staff's review in this chapter incorporates and integrates the NRC staff's reviews on multiple barriers, scenarios, event probabilities, and model abstraction (SER Sections 2.2.1.1–2.2.1.3.14).

The NRC staff's review entails

- Determining that the probabilities and consequences of each of the scenario classes are appropriately included in the average annual dose (SER Section 2.2.1.4.1.3.2)
- Determining that the results of the performance assessment provide a credible representation of repository performance [e.g., the intermediate results, such as waste package failure, and release rates from the engineered barrier system (EBS), unsaturated, and saturated zones, are consistent with the model abstractions and the average annual dose; confirmatory calculations are consistent with the performance assessment results] (SER Section 2.2.1.4.1.3.3)
- Determining that the average annual dose meets the regulatory limits and is statistically stable [e.g., increasing the number of simulations (statistical sample size) performed with DOE's TSPA is not expected to significantly change the average annual dose] (SER Section 2.2.1.4.1.3.4)

2.2.1.4.1.3.2 Probabilities and Consequences of Scenario Classes

2.2.1.4.1.3.2.1 Summary of DOE Approach

DOE has identified three scenario classes (sometimes referred as event classes) that are included in its TSPA to demonstrate compliance with the individual protection standard: (i) early failures, (ii) seismic events, and (iii) igneous events. DOE has used two modeling cases within each scenario class to represent specific aspects of the scenario. The early failure scenario class is composed of an early waste package failure modeling case and an early drip shield failure modeling case. The seismic scenario class is composed of a seismic ground motion modeling case and a seismic fault displacement modeling case. The igneous scenario class is composed of an igneous intrusion modeling case and a volcanic eruption modeling case.

DOE's average annual dose curve for individual protection (SAR Figure 2-4-18) is determined by summing the effects of all the scenario classes (i.e., early failure, seismic, and igneous). The annual doses attributed to each of the scenario classes are a direct result of the FEPs used to represent the scenario class and its probability of occurrence.

FEPs included in the scenario classes are reviewed in the NRC staff's model abstraction review (SER Sections 2.2.1.3.1–2.2.1.3.14). The NRC staff has also reviewed and evaluated the FEPs that DOE considered and excluded from the performance assessment (see SER Section 2.2.1.2.1)(b)(5)

(b)(5)

Scenario Class Probabilities

The DOE's TSPA assessment incorporates the following three scenario classes: (i) the igneous activity scenario class, which has a very low annual probability [on the order of a 1 in 100 million chance of occurring per year, as outlined in CRWMS M&O (1996aa)]; (ii) the seismic scenario class, which typically results in numerous events occurring over 1 million years (according to SAR Section 2.4.2.1.6, p. 2.4-50, seismic events are expected to occur frequently; however, it is important to evaluate the timing and magnitude of seismic events); and (iii) the early failure scenario class, for which there is a low probability of occurrence for an individual waste package (SAR Section 2.4.2.1.6, p. 2.4-49). These three scenario classes are not independent (SER Section 2.2.1.2.1.3.4; SAR Section 2.4.2.1.6, p. 2.4-51);(b)(5)

(b)(5)

Igneous Scenario Class

Probability

The igneous scenario class is composed of an igneous intrusion modeling case and a volcanic eruption modeling case. The probability for the igneous intrusion modeling case is described in the DOE model as a Poisson process, and intrusive events are distributed in time with a mean recurrence frequency of 1.7×10^{-8} per year, with a 5th and 95th percentile uncertainty spanning nearly two orders of magnitude, 7.4×10^{-10} to 5.5×10^{-8} per year. DOE describes the probability of the volcanic eruption modeling case as a subset of the probability used for the igneous intrusion modeling case by using a conditional probability that an igneous intrusive event will also have an eruptive component that ejects waste into the atmosphere. The conditional probability is composed of (i) a conditional probability of 0.28 that an igneous intrusive event could have an eruptive component and (ii) a conditional probability of 0.2968 that the eruptive component of an igneous intrusive event could intersect the waste packages. The combination of these two probabilities results in a net conditional probability of 0.083 that an igneous intrusive event would also manifest a volcanic eruption that intersects waste packages in the repository footprint. Thus, the mean recurrence frequency for the volcanic eruption modeling case is 1.4×10^{-9} per year based on the mean recurrence frequency provided previously for the igneous intrusion modeling case (i.e., 1.7×10^{-8} per year).

Igneous Event Contribution to Average Annual Dose Curve

DOE evaluated the igneous intrusion modeling case and the volcanic eruption modeling case separately assuming the entire intact or degraded repository inventory is available for release for each modeling case. A decrease in the repository inventory due to the occurrence of other scenarios is not considered.(b)(5)

(b)(5)

The average annual dose from the igneous scenario class is the sum of the contributions from the igneous intrusion modeling case and the volcanic eruption modeling case. The average annual dose from the igneous intrusion modeling case is more than 99 percent of the average annual dose from the igneous scenario class (intrusion plus volcanic eruption) (SAR Figure 2.4-18).

The igneous intrusion modeling case is the second largest contributor to the overall average annual dose (i.e., summation of average annual dose from all scenario classes) in the 10,000-year period and the largest contributor to the overall average annual dose after 10,000 years (SAR Figure 2.4-18). In the 10,000-year period, Tc-99, Pu-239, Pu-240, and I-129 radioactive elements or radionuclides are the dominant contributors to the average annual dose. After 10,000 years, the dominant radionuclide contributors to the average annual dose are Pu-239, Pu-242, Np-237, and Ra-226 (SAR Figure 2.4-30).

Early Failure Scenario Class

Probability

The early failure scenario class includes two modeling cases: early drip shield failure and early waste package failure. Early failure of either the drip shield or waste package is associated with undetected defects accounting for manufacturing processes such as improper heat treatment, base metal selection flaws, improper weld filler material, and emplacement errors. DOE assumed that all of the waste packages under early failed drip shields would also be considered failed if contacted by seepage water, as described in SNL Section 6.4.1, p. 6.4-4 (2008ag). The probability of having a large number of drip shields and waste packages fail early due to undetected defects is very small. On average, the number of waste packages affected by early failure of drip shields and waste packages is less than 0.02 percent of the total number of waste packages (SAR Section 2.4.2.1.7.2, p. 2.4-52).

Early Failure Contribution to Average Annual Dose Curve

The early failure scenario class contributes on the order of 1 percent or less to the overall average annual dose curve (SAR Figure 2.4-18). In particular, the average annual dose for the early drip shield failure modeling case, which includes contributions from waste packages under drip conditions and unprotected by the drip shields against contact with seepage water, is below 1×10^{-5} mSv [0.001 mrem] for all times. The average annual dose for the early waste package failure modeling case is generally 10 times or more greater than the average annual dose for the early drip shield failure modeling case but still on the order of 100 times less than the overall average annual dose curve (SAR Figure 2.4-18).

Seismic Scenario Class

Probability

The seismic scenario class is composed of a seismic ground motion modeling case and a seismic fault displacement modeling case. The DOE model describes seismic ground motion events as a Poisson process, with events distributed in time with a maximum mean recurrence frequency of 4.287×10^{-4} per year (corresponding to the frequency of events with a peak ground velocity exceeding 0.219 m/s [0.72 ft/s] (SAR Section 2.4.2.1.6, p. 2.4-50)). This is the maximum recurrence frequency of seismic ground motion events that could result in repository damage. Given a recurrence frequency of 4.287×10^{-4} per year, it is expected that seismic ground motion events of that magnitude could occur, on average, every 2,200 years. Thus, because it is expected that multiple seismic events will occur during the compliance period, DOE considered cumulative effects of seismic ground motion from multiple events.

The DOE model describes seismic fault displacement events as a Poisson process with events distributed in time, with a maximum mean recurrence frequency of 2×10^{-7} per year. Because

multiple seismic fault displacement events that could affect the repository are expected to be sufficiently rare and therefore inconsequential to repository performance, DOE evaluated only the effects of single seismic fault displacements.

In both modeling cases for the seismic scenario class, the consequence of events that have a recurrence frequency between the maximum mean recurrence frequency (i.e., those which could cause repository damage) down to the compliance limit of 1×10^{-6} per year are evaluated. The magnitude of an individual seismic event is determined through the use of a probabilistic seismic hazard analysis (PSHA) curve. The PSHA was developed primarily through the use of an expert elicitation process and is documented in CRWMS M&O (1998aa) (see also SER Sections 2.2.1.2.2.3.2 and 2.2.1.3.2 for further details on the NRC staff's evaluation).

Seismic Event Contribution to Average Annual Dose Curve

The average annual dose from the seismic scenario class is the sum of the contributions from the two seismic modeling cases: (i) the seismic ground motion modeling case, which addresses the potential for seismic events to damage waste packages and drip shields due to vibratory ground motion and (ii) the seismic fault displacement modeling case, which addresses the effects of fault displacement on waste packages and drip shields.

Nominal corrosion processes have the potential to alter the engineered barriers' susceptibility to damage during seismic ground motion events as the corrosion processes gradually weaken the mechanical strength of the waste package. Therefore, the seismic ground motion modeling case also includes both waste package degradation from the nominal processes (e.g., general corrosion) and seismic ground motion.

The average annual dose from the seismic ground motion modeling case is at least 10 times larger than the average annual dose from the seismic fault displacement modeling case over the entire 1-million-year compliance period (see SAR Figure 2.4-18). Although the average annual dose curve from the seismic ground motion modeling case also includes the effects from the nominal scenario class, the nominal scenario class contributes no more than 50 percent to the seismic ground motion modeling case average annual dose curve (compare SAR Figures 2.4-18 and 2.4-22).

The seismic ground motion modeling case is second only to the igneous intrusion modeling case in overall significance to the overall average annual dose curve. The seismic ground motion modeling case is the largest contributor to the overall average annual dose curve for the period after 1,500 years through 20,000 years. The overall average annual dose curve in either the initial 10,000 years or after 10,000 years is dominated by contributions from the seismic ground motion modeling case and the igneous intrusion modeling case.

2.2.1.4.1.3.2.2 NRC Staff Evaluation

(b)(5)

(b)(5)

2.2.1.4.1.3.3 Credible Representation of Repository Performance

DOE has used two modeling cases for each of the three scenario classes [for igneous (intrusive and eruption), for seismic (ground motion and fault displacement), and for early failure (drip shield and waste package)] to estimate overall performance of the Yucca Mountain repository (see Table 17-1). Only one modeling case (volcanic eruptive) releases radionuclides directly to the atmosphere via volcanic ash. The other five modeling cases (seismic ground motion, seismic fault displacement, igneous intrusion, early waste package failure, and early drip shield failure) release radionuclides through groundwater movement. The NRC staff reviewed the TSPA documentation in SAR Volume 2 and in the TSPA GoldSim computer model and associated computer files (including intermediate results saved in the GoldSim output files). The NRC staff's review of the TSPA analyses considered how the collection of FEPs that are included in the TSPA represents a credible characterization of the repository. The NRC staff's review approach entails a quantitative evaluation of the attributes of DOE's TSPA calculation that most significantly impact estimating the annual dose to the reasonably maximally exposed individual. Identification of the important attributes for performance are based on

Table 17-1. Scenario Classes and Modeling Cases Included in the DOE's TSPA		
Scenario Class	Modeling Case	Transport Pathway*
Early failure	Drip shield	Groundwater
	Waste package	Groundwater
Seismic	Ground motion	Groundwater
	Fault displacement	Groundwater
Igneous	Intrusive	Groundwater
	Eruption	Atmospheric (volcanic ash)
*Transport pathway indicates the primary pathway for radionuclides to be transported away from the repository to the compliance location specified in 10 CFR 63.312		

the NRC staff's review of the capabilities of the barriers important to waste isolation (SER Section 2.2.1.1) and the model abstractions in the TSPA (SER Sections 2.2.1.3.1–2.2.1.3.14), and the NRC staff's independent analysis with its performance assessment model, as outlined in Center for Nuclear Waste Regulatory Analyses (CNWRA and NRC, 2008aa) and NRC Appendix D (2005aa).

2.2.1.4.1.3.3.1 DOE's TSPA Calculation Related to Groundwater Releases

2.2.1.4.1.3.3.1.1 Summary of DOE Approach

The modeling cases associated with groundwater releases are described by tracking the water through the system. For example, water could infiltrate the top of the mountain and move downward to the repository; after waste packages are breached and radionuclide releases occur, water could transport radionuclides through the unsaturated zone then through the saturated zone to the location of the RMEI. In general, the description of the groundwater releases is based on the following repository performance characteristics:

- Seepage of water entering the drifts (tunnels containing the waste packages)
- Damage to engineered barriers (drip shield and waste package)
- Seepage of water into the waste packages
- Release of radionuclides from the waste package
- Transport of radionuclides in the unsaturated zone
- Transport of radionuclides in the saturated zone
- Annual dose to the RMEI

The volcanic eruption modeling case evaluates the release of radionuclides via volcanic ash deposited on the ground. The volcanic eruption modeling case is evaluated separately (see "Description and Understanding of TSPA Calculation Related to Releases from a Volcanic Eruption Event" later in this chapter) from the modeling cases that involve radionuclide release through the groundwater pathway.

2.2.1.4.1.3.3.1.1.1 Seepage of Water Into Drifts

The flux of water reaching the drifts (i.e., drift seepage) is originally derived from rainfall over the mountain. Two important metrics for performance for the upper natural barrier are seepage flux (the amount of liquid water entering repository drifts) and seepage fraction (number of waste package locations with dripping water). The latter is the fraction of the repository area where seepage occurs (the seeping environment); the remainder of the area would not receive

seepage. Seepage, or dripping water, has the potential to fall onto drip shields and later contact waste packages after drip shields degrade sufficiently to allow water to pass through the drip shield.

Precipitation to Deep Percolation

DOE divided the first 10,000 years into three periods: present day (0–600 years), monsoonal (600–2,000 years), and glacial transition (2,000–10,000 years) climates (SAR Tables 2.3-1–2.3-4; DOE, 2008ab). The glacial transition climate spans 80 percent of the first 10,000 years and has the most significant impact on the performance of the repository over this initial period. For the glacial period, the applicant calculated an average precipitation of 296.7 mm/yr [11.7 in/yr] in the repository footprint, as described in DOE Enclosure 5, Table 1 (2010ai). Processes including runoff of water from hillsides, evaporation, and lateral diversion of water caused by the Paintbrush Tuff nonwelded rock layer alter the amount of rainfall that eventually ends up as deep percolation (the amount of water reaching the repository level). DOE estimated an average deep percolation of 21.74 mm/yr [0.86 in/yr] at the repository horizon, as detailed in DOE Enclosure 5, Table 1 (2010ai) at the repository footprint for the initial 10,000 years. Thus, approximately 7 percent of the rainfall ends up as deep percolation at the repository footprint. (SER Sections 2.2.1.3.5 and 2.2.1.3.6 provide further details on climate and infiltration.)

For the post-10,000-year period, DOE used the 10 CFR Part 63 time-independent flux for deep percolation, representing average climate conditions over the long term. The final regulation [10 CFR 63.342(c)(2)] specifies a range of 10 to 100 mm/yr [3.9 to 39 in/yr] using a lognormal distribution (with an arithmetic mean of 41 mm/yr [1.6 in/yr] and a standard deviation of 33 mm/yr [1.3 in/yr]). In the license application, DOE used a log-uniform distribution with an arithmetic mean of 32 mm/yr [1.3 in/yr] and a range between 13 and 64 mm/yr [0.51 and 2.5 in/yr] (SAR Section 2.3.2.3.5.1), as specified in the draft regulation (70 FR 53319). The final regulation specifies a 16 percent higher average deep percolation. Using this higher deep percolation for a bounding calculation, the applicant estimated a corresponding increase in the 1-million-year RMEI average annual dose from 2.00 mrem/yr to 2.32 mrem/yr [0.02 mSv/yr to 0.023 mSv/yr], which remains below the regulatory limit of 100 mrem/yr [1 mSv/yr], as detailed in DOE Enclosure 1 (2009cb).

Deep Percolation to Seepage

The TSPA includes a number of factors such as focusing or diverging of flow at the repository footprint, vapor barrier surrounding a drift when the drift temperature is above the boiling point of water, different waste package types, capillary diversion, drift degradation (prevalent in the seismic cases) in estimating seepage fraction, and drift seepage. Seepage is set to zero if the drift wall temperature exceeds 100 °C [212 °F] (SAR Section 2.3.3.4.1.1). The period of time when drift wall temperatures exceed 100 °C [212 °F] is generally limited to the first 2,000 years, as the heat generated by radionuclide decay decreases.

(b)(5)

(b)(5)

The uncertainties of the effects on the longevity of the drip shield and waste package are evaluated in SER Sections 2.2.1.3.1 and 2.2.1.3.2.

Over the repository footprint, seepage flux is approximately 10 percent of the deep percolation for intact drifts and can increase up to 49 percent for degraded drifts as the applicant predicted

through the seismic ground motion modeling case, outlined in DOE Enclosure 5 (2010ai). For the igneous intrusive scenario, all of the percolating flux enters the drift at all locations, as described in DOE Enclosure 10 (2009ct). Table 17-2 provides the DOE values for the seepage fraction and the average seepage rate over the repository footprint (i.e., averaged over both seeping and nonseeping environments). As the seepage rate increases, the number of locations where dripping occurs (seepage fraction) also increases.

2.2.1.4.1.3.3.1.1.2 Damage to Engineered Barriers (Drip Shield and Waste Package)

The drip shield and the waste package are two important components of the engineered barrier system (SER Sections 2.2.1.3.1 and 2.2.1.3.2 evaluate behavior of the drip shield and waste package). The drip shield degrades gradually over time (from general corrosion) or at specific times from large seismic events or igneous events. From the distributions considered in the TSPA to represent corrosion rates of Titanium Grade 7, time to failure by general corrosion of the drip shield was computed to range from 260,000 to 340,000 years (SAR Figures 2.1-8 and 2.4-24). Seismic ground motion can collapse the drip shield by mechanical failure due to static and dynamic loads caused by rockfall and ground motion. As illustrated in SAR Figure 2.1-11, drip shield collapse due to seismic ground motion occurs primarily between 25,000 and 350,000 years with the vast majority of the failures occurring between 200,000 and 300,000 years (see SAR Figure 2.4-24). Drip shields are assumed to fail whenever an intrusive igneous event occurs, when a fault displacement event breaches the waste package, or when significant general corrosion occurs. Once the drip shield is failed, seepage water that enters the drifts can contact the surface of the waste package.

The damage mechanisms leading to waste package failure are "crack" and "patch" (holes) failure. Within the DOE's TSPA, crack and patch failures of the waste package are treated separately because of differences in how water may enter a breached waste package. DOE assumed that seepage water cannot freely flow through cracks on the waste package because of the small size of the cracks. Because of processes such as general corrosion, or ruptures and punctures of the waste package, patch failures represent significantly larger openings and seepage water is assumed to enter the waste package through these holes or openings. The waste packages with large or patch openings could allow release of radionuclides carried by flowing water (i.e., advective release), while those with crack openings could only allow release by diffusion.

The five modeling cases associated with groundwater releases have very distinct characteristics for the timing and extent of waste package failure. Assumed to occur at the time of closure, the early failure scenario class consists of two modeling cases: drip shield early failure and waste package early failure. The early failure scenario has, in probabilistic terms, on average, fewer than one waste package and one drip shield failing (see SER Section 2.2.1.3.1.3.2.4 for early waste package failure and SER Section 2.2.1.3.1.3.1.2 for drip shield failure). The igneous intrusion modeling

Table 17-2. DOE's Mean Values for the Seepage Rate Into Drifts*

Time Period	Nominal/Early Failure	Seismic Ground Motion	Igneous Intrusive
Seepage from 2,000 to 10,000 years	2.0 (mm/yr)	2.3 (mm/yr)	21.7 (mm/yr)
Seepage fraction from 2,000 to 10,000 years	31%	31%	100%
Seepage after 10,000 years	3.4 (mm/yr)	15.3 (mm/yr)	31.8 (mm/yr)
Seepage fraction after 10,000 years	40%	69%	100%

*See SER Section 2.2.1.3.6 for further information

case assumes all waste packages fail at the time of the event and lead to release to the water pathway (see SER Section 2.2.1.3.10 for further details). The seismic scenario class consists of a ground motion modeling case, where the waste packages are damaged by seismic ground motion, and a fault displacement modeling case, where displacement along a fault may damage the waste packages that lie along the fault. The seismic fault displacement modeling case has, on average, tens of waste packages failing (see SER Section 2.2.1.3.2 for further details). The seismic ground motion modeling case contains a range of waste package failures—typically initial damage is primarily due to cracks in the waste package from ground motion, and, later in time (e.g., after 100,000 years), general corrosion, ruptures and punctures, and further cracking damages the waste packages.

Table 17-3 provides the percentage of waste package failures accounted for in the seismic ground motion modeling case for selected times (i.e., 10,000; 100,000; 400,000; and 800,000 years) to provide some perspective on the time-dependent nature of waste package failure. In the first 10,000 years, a small fraction of waste packages fails in the seismic ground motion modeling case due to rare but potentially damaging earthquakes. The majority of the failed waste packages are codisposal packages (CDSP). These packages are not equivalent to the more robustly designed transportation, aging, and disposal canisters that contain the commercial spent nuclear fuel (CSNF) waste packages. Most of the initial damage is attributed to cracks that are small enough to prevent seepage water from entering the waste package. At approximately 100,000 years, the mean fraction of failed CDSP packages due to cracks is 40 percent and the mean fraction of failed CSNF packages is below 1 percent. At 1 million years, approximately 50 percent of the CSNF and CDSP waste packages fail due to cracks. Some of these cracks are from seismically induced stress corrosion cracks on the waste package surface. Others are due to stress corrosion cracks in the closure welds—considered a general corrosion process. Waste packages start to fail by general corrosion patches at around 500,000 years, and approximately 10 percent of the waste packages have at least one failed patch due to general corrosion by 1 million years, as described in DOE Enclosure 1, Response Number 1, Figures 9 and 10 (2009b). Waste package failure due to ruptures and punctures is limited: approximately 1 percent of the packages failed after 700,000 years and on the order of

Table 17-3. Percentage of CSNF* and CDSP† Waste Packages Breached for the Seismic Ground Motion Modeling Case in DOE's TSPA‡				
Process	10,000 Years	100,000 Years	400,000 Years	800,000 Years
Stress corrosion cracks in closure welds	Little to no failures	CSNF 0.0003% CDSP 0.0003%	CSNF 8% CDSP 8%	CSNF 40% CDSP 40%
Stress corrosion cracks	CSNF 0.01% CDSP 1%	CSNF 0.4% CDSP 30%	CSNF 10% CDSP 40%	CSNF 10% CDSP 40%
Ruptures and punctures (patches)	Little to no failures	CSNF 0% CDSP 0.02%	CSNF 0.3% CDSP 0.4%	CSNF 1% CDSP 1%
General corrosion (patches)	Little to no failures	Little to no failures	CSNF 0.004% CDSP 0.1%	CSNF 4% CDSP 7%
*Repository contains 8,213 commercial spent nuclear fuel (CSNF) waste packages. †Repository contains 3,416 codisposal (CDSP) waste packages. ‡Values were approximated from DOE Figures 1–14 [DOE, 2009. "Yucca Mountain—Response to Request for Additional Information Regarding License Application (Safety Analysis Report Section 2.4.4) Safety Evaluation Report Vol. 3, Chapters 2.2.1.4.1, 2.2.1.4.2, and 2.2.1.4.3, Set 1." Letter (July 29) J.R. Williams to J.H. Sulima (NRC). ML092110472. Washington, DC: DOE, Office of Technical Management.]				

2–3 percent after 1 million years, as shown in DOE Enclosure 1, Response Number 1, Figures 13 and 14 (2009bj).

The majority of the waste package failures are associated with the seismic ground motion modeling case, which includes the nominal processes such as general corrosion, and the igneous intrusion modeling case. In DOE's TSPA model, the seismic ground motion and igneous intrusion modeling cases contribute most to the overall average annual dose curve and are generally more than a factor of 10 greater than the other modeling cases (SAR p. 2.4-18).

(b)(5)

2.2.1.4.1.3.3.1.1.3 Seepage of Water into Waste Packages

In TSPA model, two conditions are required for seepage water to enter a waste package:

(i) drip shield failure must occur to allow water to contact the waste package outer barrier and
(ii) the waste package outer barrier must be breached by patches (it is assumed that seepage or dripping water cannot flow into waste package cracks due to the small opening of cracks; therefore, seepage water enters the waste package only through patch failures). When these required conditions are met, water flow through the waste package is modeled as quasi-steady state, where water flux into the waste package is equal to water flux out.

The waste package surface is divided into a large number of patches with each patch having distinct properties that can affect the corrosion rate of the patch. The extent of waste package degradation (i.e., number of patch failures on the waste package) determines the quantity of water entering the waste package. The waste package outer barrier is considered unable to divert water when a mean value of approximately 62 patches fail (62 patches comprises approximately 4 percent of the total surface area of the waste package), at which point water flow through the waste package equals the incoming seepage rate. When fewer than 62 patches fail, water flux through the waste package is linearly related to the number of patches that fail. Generally, a single patch failure allows 1/62 of the seepage flux to pass through the waste package. Because of uncertainty incorporated into the submodel, this value can range from 0 to 2.4 times the 1/62 value.

The waste package patch failures in the seismic ground motion modeling case are limited (see Table 17-3). Approximately 1 percent of the waste package surface area is breached by general corrosion after 1 million years, as described in DOE Enclosure 1, Response Number 1, Figures 11 and 12 (2009bj). Patch failure by ruptures and punctures compromises approximately 0.2 percent of the waste package surface by 1 million years, as outlined in DOE Enclosure 1, Response Number 1, Figures 15 and 16 (2009bj). Thus, the compromised area remains limited for the 1-million-year period after patch failure occurs due to general corrosion, ruptures, or punctures. Additionally, the number of waste package patch failures is limited over the 1-million-year time period: 10 percent of waste package failures are from general corrosion and approximately 3 percent of waste package failures from ruptures and punctures. These failures occur primarily at long times [e.g., after 400,000 years, as shown in DOE Enclosure 1, Response Number 1, Figures 9, 10, 13, and 14 (2009bj)].

For the igneous intrusion modeling case, the drip shield and waste package are assumed to be ineffective barriers against seepage in the TSPA model (i.e., no credit to decrease seepage is given to the drip shield or waste package after the time at which the event occurs). Thus, all

drip shields and waste packages are assumed failed and the entire surface area of the waste package is assumed failed.

2.2.1.4.1.3.3.1.1.4 Release of Radionuclides From the Waste Package

Waste form degradation and subsequent radionuclide release cannot occur prior to waste package breach and/or failure. Assuming waste package failure, radionuclide release may be advective if seepage water enters the waste package; otherwise, the release will be a diffusive release.

Because seepage water does not flow through crack failures, the radionuclide release from cracks in the waste package is controlled by radionuclide diffusion in an assumed continuum of aqueous pathways through the cracks. DOE described patch failure as a more extensive damage mechanism of the waste package surface from general corrosion, or waste package ruptures and punctures driven by seismic events and mechanical interactions with drip shields or other waste packages. Radionuclide release through damaged patches is assumed to be diffusive if seepage does not contact the waste package, which could occur in the DOE model if the drip shield is not breached, or if the waste package is under nondrip conditions. If, on the other hand, the waste package is under drip conditions, the drip shield is failed, the waste package is breached by patches (by corrosion or processes driven by seismic events), and radionuclides are released from the waste package by flowing water (i.e., advective release) and diffusion. Advective release is effective also in the igneous intrusion case, in which all waste packages fail completely and seepage is assumed to contact all waste packages.

In general, diffusive and advective release of radionuclides from a waste package will be affected by the size of the openings, degradation rate of the waste, solubility limits, sorption onto corrosion products, and the presence of colloids. The significance of these features and processes can vary for specific radionuclides, as described next.

Size of the Openings

The overall surface area of the crack and patch openings directly affects radionuclide diffusion out of the waste package (more surface area results in more release). Additionally, the overall surface area of the patch openings can affect the amount of water entering the waste package and thus the amount of dissolved radionuclides released from the waste package in the advective or flowing water. (Note: once an average of 4 percent of the waste package surface is failed, due to patches, DOE assumes that the waste packages no longer divert drift seepage water.)

Degradation Rate of Waste

Radionuclides cannot leave the waste package faster than the waste degrades. Generally, the degradation rates used in TSPA for CSNF result in somewhat short times (e.g., hundreds to thousands of years) for the waste form to significantly degrade, as outlined in DOE Enclosure 5, Table 1.1-1 (2009an); therefore, the degradation rate only affects those radionuclides that are not limited by other release constraints inside the waste package (e.g., Tc-99 and I-129 are not solubility limited and are not sorbed or attached onto corrosion products). For CDSP waste packages glass waste form can degrade much slower than CSNF (e.g., thousands to millions of years for the glass waste form to significantly degrade versus hundreds to thousands of years for CSNF); however, the defense spent nuclear fuel waste form is assumed to instantly degrade, as described in DOE Enclosure 5, p. 6 (2009an).

Solubility Limit

Some radionuclides have a solubility limit—a function of the properties of the radionuclide and the water chemistry inside the waste package—that controls the amount that can be dissolved in water. Radionuclides such as plutonium (e.g., Pu-242) and neptunium (e.g., Np-237) have the potential for low release rates due to solubility limits (see SER Section 2.2.1.3.4).

Corrosion Products

The TSPA includes a process by which certain radionuclides attach onto corrosion products within the waste package, and thus release from the waste package is delayed. This is especially effective for a radionuclide such as Np-237 that is somewhat soluble and attaches onto corrosion products, as described in DOE Enclosure 5, p. 22 (2009a).

Colloids

Colloids can facilitate release of radionuclides out of the waste package; radionuclides sorbed or attached onto irreversible colloids are not affected by solubility limits and stationary corrosion products. Colloids can also sequester radionuclides by becoming unstable (see SER Section 2.2.1.3.4). DOE stated that the contribution to annual dose from irreversible colloids is small [i.e., contribution from irreversible colloids never exceeds 30 percent, as shown in DOE Enclosure 5, pp. 24–25 (2009a)]. The contribution to annual dose from a radionuclide such as Pu-242 will be mainly from aqueous releases, which are composed of both dissolved radionuclides and reversible colloids (e.g., SAR p. 2.4-93 and SAR Figure 2.4-73).

Release rates of radionuclides from an individual waste package are dependent on the type of radionuclide. High mobility characterizes the soluble, nonsorbing radionuclides (e.g., Tc-99, I-129, Cl-36, Se-79), which may result in nearly complete release of the inventory of the high-mobility radionuclides from the EBS over the 1-million-year compliance period (SAR Figure 2.1-24). Much lower mobility characterizes the relatively insoluble, sorbing nuclides (e.g., Np-237, Pu-242). For the concentration-limited radionuclides (e.g., Pu-242 and Np-237), DOE explained that releases will be significantly lower than the release rates for soluble radionuclides (e.g., Tc-99) and will increase as water flow into the waste packages increases. For example, as corrosion patch area increases in size over time, more water may enter the waste package (SAR p. 2.4-63). At the end of the 1-million-year compliance period, approximately 0.1 percent of the Np-237 inventory has been released from the EBS with the majority of the release occurring over the later portion of the compliance period (SAR Figure 2.1-25).

2.2.1.4.1.3.3.1.1.5 Transport of Radionuclides in the Unsaturated and Saturated Zones

Transport of radionuclides through the unsaturated zone is affected by the following processes: (i) relatively fast fracture flow versus slow flow in the porous rock matrix, (ii) radionuclides that sorb onto mineral surfaces, and (iii) colloid-facilitated transport of radionuclides.

Transport of radionuclides can depend significantly on whether water flow occurs principally in fractures or in porous media. Flow in fractures is conceptualized as being relatively fast because the effective porosity is relatively small [average estimated value of 0.001 (SAR Table 2.3.9-4)]. Conversely, flow in porous media is conceptualized as relatively slow because the effective flow porosity is relatively high [average estimated value of 0.18 (SAR

Table 2.3.9-4)]. Additionally, given the limited surface area for fracture surfaces as compared to rock pores, radionuclides can be significantly delayed by sorption to mineral surfaces.

Colloids are tiny particles that remain suspended in water and are thus able to move with the water and facilitate the transport of certain radionuclides. Transport times of strongly sorbing radionuclides, such as plutonium and americium, can decrease (e.g., increase transport velocity) by permanently attaching onto colloids. This colloid attachment can also occur reversibly when radionuclides temporarily attach to or detach from colloids as they move through the system. Generally, most of the release of Pu-242 from the unsaturated and saturated zone is via dissolved plutonium and plutonium reversibly associated with colloids (referred to as "aqueous" release in SAR Figure 2.4-108). Limited release of Pu-242 is associated with irreversible colloids, whereby Pu-242 permanently attaches onto the colloid.

Transport of Radionuclides in the Unsaturated Zone

Transport of radionuclides in the unsaturated zone depends to some extent on the location from which they are released. In the northern area of the repository, water is expected to move principally within fractures. Average travel times for nonsorbing solutes from the repository to the saturated zone from the northern area of the repository are on the order of 5 to 100 years for an infiltration rate of 12 mm/yr [0.47 in/yr] (SAR Figure 2.3.8-36). Conversely, in the southern repository area, the Calico Hills nonwelded tuff unit has higher matrix permeability that can accommodate flow almost entirely within the rock matrix (porous flow). Average travel times from the southern repository area to the saturated zone are on the order of 500 to 5,000 years for an average infiltration rate of 12 mm/yr [0.47 in/yr] (SAR Figure 2.3.8-36).

For sorbing radionuclides, travel times depend on the radionuclide-specific sorption coefficient. More strongly sorbing aqueous species, such as Pu-242, have transport times on the order of hundreds of years in the northern area and several hundred thousand years in the southern area. Radionuclide species with half-lives that are short relative to their unsaturated zone transport times can be significantly or completely decayed before reaching the water table (e.g., Cs-137, Sr-90, Ra-226, Th-229, Th-230, Th-232, Pu-238, Am-241, Am-243).

Table 17-4 shows how the combined processes affect flow of different radionuclides through the unsaturated zone by providing representative transport times for nonsorbing Tc-99, moderately sorbing Np-237, strongly sorbing Pu-242, and Pu-242 attached to colloids.

Table 17-4. Radionuclide Transport Times in the Unsaturated Zone for the Northern and Southern Repository Areas From DOE Breakthrough Curves		
	Transport Time* for Release in Northern Repository Area	Transport Time* for Release in Southern Repository Area
Tc-99	10 years	1,000 years
Np-237	10 years	10,000 years
Pu-242	30 years	>1 million years
Pu-242 irreversible colloids	100 years	1,000 years
*Transport times reflect approximate arrival for 50 percent of peak concentration for a model case with point releases at representative locations in northern and southern model areas, representative parameter values, and Glacial Transition 10 th percentile infiltration map. See SAR Figures 2.3.8-43 for Tc-99, 2.3.8-44(b) for Np-237, 2.3.8-47(a) for Pu-242, and 2.3.8-48 for Pu-242 irreversible colloids for complete breakthrough curves for all radionuclides.		

Transport of Radionuclides in the Saturated Zone

Radionuclides released from a Yucca Mountain repository would eventually enter the saturated zone within the fractured volcanic tuffs of the Crater Flat group. Transport away from the repository area would occur through permeable flowing fracture networks in the volcanic aquifer system for more than 10 km [6.2 mi] and transition to a valley fill alluvial flow system for the last few kilometers before reaching the regulatory compliance boundary approximately 18 km [11.2 mi] from the southern boundary of the repository footprint. The exact location of the volcanic rock–alluvium contact is uncertain and is treated stochastically in the saturated zone transport abstraction model using an alluvium uncertainty zone. The fracture flow path for the volcanic tuff is conceptualized as being relatively fast because the effective porosity is relatively small [average estimated value of 0.001 (SAR Table 2.3.9-4)]. Flow in the alluvial portion of the flow system is conceptualized as relatively slow because the effective flow porosity is relatively high [average estimated value of 0.18 (SAR Table 2.3.9-4)]. Overall, the transport time for nonsorbing radionuclides ranges from about 10 years to several thousand years (SAR p. 2.3.9-9). Sorbing radionuclides can be significantly delayed by sorption to alluvium mineral grains in which case transport times for strongly sorbing radionuclides generally exceed 10,000 years (SAR p. 2.3.9-9). Table 17-5 provides transport times for select radionuclides representing a range of sorption behavior.

2.2.1.4.1.3.3.1.1.6 Annual Dose to the RMEI

Following postclosure EBS release and groundwater radionuclide transport, the DOE TSPA model executes the biosphere model abstraction to calculate biosphere radionuclide transport and the annual dose to the RMEI. The exposure scenarios implemented in the DOE TSPA model (i.e., groundwater, volcanic ash) calculate annual dose to an individual adult member of a hypothetical farming community located 18 km [11.2 mi] south of the potential repository along the path of groundwater flow. Exposure pathways in the DOE biosphere model are based on assumptions about residential and agricultural uses of the water and indoor and outdoor activities. These pathways include ingestion, inhalation, and direct exposure to radionuclides deposited to soil from irrigation (SAR Section 2.3.10.1). Ingestion pathways include drinking contaminated water, eating crops irrigated with contaminated water, eating food products produced from livestock raised on contaminated feed and water, eating farmed fish raised in contaminated water, and inadvertently ingesting soil. Inhalation pathways include breathing resuspended soil, aerosols from evaporative coolers, and radon gas and its decay products.

Table 17-5. Summary of DOE Simulated Transport Times in the Saturated Zone Under Glacial-Transition Climate State*

Species	Range of Median Transport Times (years)	Median Transport Time Among All Realizations
C-14, Tc-99, I-129 (aqueous, nonsorbing)	10 to 22,190	230
Reversible colloids: americium, thorium	1,000 to >1 million	>1 million
Reversible colloids: plutonium	3,000 to >1 million	95,000
Neptunium	100 to 455,300	3,700
Irreversible colloids: plutonium, americium	100 to 501,900	4,500
*SNL. 2008. "Saturated Zone Flow and Transport Model Abstraction." Rev. 03. ADD 02. Table 6-16[a]. MDL-NBS-HS-000021. Las Vegas, Nevada: Sandia National Laboratory.		

(SAR Section 2.3.10.1). The NRC staff's review of the applicant's biosphere model abstraction is documented in SER Section 2.2.1.3.14.

DOE biosphere model results are quantified by the Biosphere Dose Conversion Factors (BDCFs). A BDCF is the calculated annual dose to the RMEI from all potential exposure pathways as a result of a unit concentration of a radionuclide in groundwater or surface soil mixed with volcanic ash (SAR Section 2.3.10.1). Mean groundwater exposure scenario BDCFs and primary exposure pathways (from SAR Tables 2.3.10-11 and 2.3.10-12) for radionuclides that are important contributors to DOE's TSPA annual dose results (SAR Figure 2.4-26 a and b) are provided in Table 17-6. (Note: the volcanic ash exposure scenario for the igneous eruptive modeling case is discussed in the next section.)

The average annual doses are largest for the seismic ground motion and igneous intrusive modeling cases (generally a factor of 10 or more larger than the other modeling cases; see SAR Figure 2.4-18). Tc-99 (a nonsorbing radionuclide) is the largest contributor to the average annual dose in the initial 10,000 years. Tc-99 accounts for approximately 0.001 mSv/yr [0.1 mrem/yr] of the peak of the overall average annual dose of approximately 0.003 mSv/yr [0.3 mrem/yr] (SAR Figure 2.4-20a). After 10,000 years and up to 1 million years, the peak of the overall average annual dose occurs at 1 million years, with Pu-242 and Np-237 being the largest contributors to the peak of the overall average annual dose. Pu-242 and Np-237 account for approximately 0.01 mSv/yr [1.0 mrem/yr] of the peak of the overall average annual dose of approximately 0.02 mSv/yr [2.0 mrem/yr] (SAR Figure 2.4-20b).

2.2.1.4.1.3.3.1.2 NRC Staff Evaluation

The NRC staff conducted confirmatory calculations to assist its review of DOE's TSPA. The confirmatory calculations provide both a quantitative understanding of the attributes of the performance assessment and an understanding of whether there is a general consistency between submodels of the performance assessment and the overall results, including uncertainty (e.g., whether the timing and extent of breaching of the waste package are consistent with the timing and magnitude of the average annual dose). The confirmatory calculations were performed for selected time periods (i.e., 10,000; 100,000; 400,000, and 800,000 years) to provide some perspective on the time-dependent nature of waste package failure, associated radioactive decay and release of specific radionuclides.

Table 17-6. DOE Groundwater BDCFs*		
Radionuclide	Mean BDCF Sv/yr per Bq/m ³ [mrem/yr per pCi/L]	Primary Pathways
Tc-99	1.1×10^{-6} [4.1×10^{-3}]	42% drinking water 37% animal product 17% crop
Np-237	2.7×10^{-7} [1.0]	56% inhalation 29% drinking water
Pu-242	9.1×10^{-7} [3.4]	75% inhalation 19% drinking water
*Biosphere dose conversion factors		

(b)(5)

Amount of Water Entering Failed Waste Packages

(b)(5)

(b)(5)

Release of Radionuclides From Waste Packages

(b)(5)

(b)(5)

**Table 17-8. NRC Staff's Confirmatory Calculation Results for the
Average Release Rates for Tc-99 (Seismic Ground Motion Modeling Case)
for CSNF* and CDSP† Waste Packages**

(b)(5)

(b)(5)

Transport of Radionuclides through the Unsaturated and Saturated Zones

(b)(5)

**Table 17-9. NRC Staff's Confirmatory Calculation Results for the
Average Release Rates for Np-237 and Pu-242 in the Seismic Ground Motion
Modeling Case for CSNF* and CDSP+ Waste Packages**

(b)(5)

Table 17-10. NRC Staff's Confirmatory Calculation Results for the Average Release Rates for Tc-99 in the Igneous Intrusive Modeling Case for CSNF* and CDSP† Waste Packages

(b)(5)

Table 17-11. NRC Staff's Confirmatory Calculation Results for the Average Release Rates for Np-237 and Pu-242 in the Igneous Intrusive Ground Motion Case for CSNF* and CDSP† Waste Packages

(b)(5)

**Table 17-12. NRC Staff's Confirmatory Calculation Values for the Effectiveness
(Expressed as a Percentage Reduction in Release) of the Unsaturated and Saturated
Zones for Reducing Release Rates for Specific Radionuclides***

(b)(5)

**Table 17-13. NRC Staff's Confirmatory Calculation Results for the
Average Dose Estimates for Tc-99 for the Seismic Ground Motion Modeling
Case and Igneous Intrusive Modeling Case**

(b)(5)

Table 17-14. NRC Staff's Confirmatory Calculation Results for the Annual Dose for Np-237 for the Seismic Ground Motion Modeling Case and Igneous Intrusive Modeling Case

(b)(5)

Table 17-15. NRC Staff's Confirmatory Calculation Results for the Annual Dose for Pu-242 for the Seismic Ground Motion Modeling Case and Igneous Intrusive Modeling Case

(b)(5)

(b)(5)

Comment (b)(5)

(b)(5)

2.2.1.4.1.3.3.2 Description and Understanding of TSPA Calculation for the Volcanic Eruption Modeling Case

2.2.1.4.1.3.3.2.1 Summary of DOE Approach

An eruptive volcanic event at the repository involves the intersection of ascending magma and a drift and eruption at the surface (see SER Section 2.2.1.3.10). Radioactive material entrained in tephra can be transported downwind and deposited on the ground surface where potential exposures can occur from (i) inhalation of radionuclides due to high level waste entrained in ash particles, which are suspended in the air, including the breathing of radon gas and its daughter products from high level waste entrained in the ash deposited on the ground surface and (ii) ingestion of radionuclides from locally produced crops and animal products that are assumed to be contaminated from direct (e.g., crops grown in soil containing contaminated tephra) and indirect (e.g., animals raised on feed that has been grown in soil containing contaminated tephra) contact with contaminated tephra. Estimating the consequences of such an event is dependent on the concentration of radionuclides in tephra and the amount of ash persisting at the RMEI location (from both the direct deposition of tephra during the event and redistribution of tephra after the event due to water and wind action over time).

On average, the volcanic eruption modeling case impacts four (a range of one to seven) waste packages and entrains all of the waste into magma. Of this magma and waste, 30 percent is considered to form tephra; thus 30 percent of the waste in the waste packages hit by the event is, on average, contained in the tephra (range of 10 to 50 percent). Once radioactively contaminated volcanic tephra is present at the RMEI location, estimates of potential exposures can be made for three specific pathways (external exposure, ingestion, and inhalation, which include radon exposure). The volcanic eruption modeling case average annual dose is at least

100,000 times less than the regulatory dose limit for both the initial 10,000-year period and after 10,000 years (SAR Figure 2.4-18).

During the initial 10,000 years, the annual dose is dominated by Pu-239, Pu-240, and Am-241 (SAR Figure 2.4-32). For these three radionuclides, the inhalation exposure accounts for more than 98 percent of the average annual dose for the volcanic eruption modeling case, as shown in SAR Table 2.3.10-15. At very early times (i.e., the initial 500 years), there is some contribution from Sr-90 and Cs-137 (primarily from external exposure). At very long times (i.e., after 100,000 years), the annual dose is dominated by Ra-226 (SAR Figure 2.4-32). These results are partially due to the half-lives for these radionuclides. Sr-90 and Cs-137 have half-lives less than 100 years, and Am-241 has a half-life of 432 years; thus the hazard is somewhat short lived. The longer term hazard is with Pu-239 (half-life of 24,000 years), Pu-240 (half-life of 24,000 years), and Ra-226, which is a daughter product in the long-lived U-234 chain (the half-life of U-234 is 240,000 years, whereas the half-life of Ra-226 is 1,600 years).

2.2.1.4.1.3.3.2.2 NRC Staff Evaluation

(b)(5)

Comment (b)(5)

(b)(5)

Table 17-16. NRC Staff's Confirmatory Calculation Results for Pu-239 and Am-241 Annual Doses for the Volcanic Eruption Modeling Case (Inhalation Pathway)

(b)(5)

Table 17-17. NRC Staff's Confirmatory Calculation of Sr-90 and Cs-137 Annual Doses for the Volcanic Eruption Modeling Case (External Pathway)

(b)(5)

2.2.1.4.1.3.4 Average Annual Dose Limits Are Met and Statistically Stable

2.2.1.4.1.3.4.1 Summary of DOE Approach

Stability of Average Annual Dose Estimates

DOE addressed the question of the stability in SAR Section 2.4.2.2.2. The term *stability* refers to the numerical reproducibility of statistics (e.g., average annual dose) or their level of convergence as a function of model features such as size of the statistical sample and numerical approximations. Variation in the TSPA results is a function of a particular combination of uncertain and variable parameters (DOE described its treatment of epistemic and aleatory uncertainty in SAR Section 2.4.2.1.1). DOE identified aleatory parameters as those parameters with uncertainty irreducible by additional experiments or site characterization. Examples of aleatory parameters are the time of seismic and igneous events, the extent of waste package damage during a seismic or faulting event, the location of the compromised waste package in the repository, and the type of waste package (e.g., CSNF or CDSP waste packages) compromised after a disruptive event. The stability of the average annual dose will, in part, be a function of the size of the discrete sample of aleatory parameter values. DOE analyzed the effect of the size of these discrete samples by increasing the number of aleatory realizations from 30 to 90, considering more waste package damage fractions for the seismic

Table 17-18. NRC Staff's Confirmatory Calculation of Ra-226 Annual Dose for the Volcanic Eruption Modeling Case (External Pathway)

(b)(5)

and faulting modeling case, and accounting for more event times (e.g., doubling the number of event times for the seismic ground motion modeling case, increasing the number of event times from 10 to 50 for the igneous intrusion modeling case) and determined that these types of changes would have a minor effect on the magnitude of the overall average annual dose curve. DOE compared annual dose curves for a set of five realizations for all modeling cases in SAR Figures 2.4-55 to 61 and concluded, in qualitative terms, that the annual dose curve for the analyzed realizations was stable with respect to aleatory uncertainty.

DOE also examined the stability of the average annual dose curve to the treatment of the epistemic uncertainty. The epistemic parameters are generally those parameters that describe the repository components and behavior under nominal conditions (e.g., variability in hydraulic conductivity of a particular rock unit; variability in material properties over the surface of the waste package). DOE used a statistical sample size of 300 realizations for each modeling case in the SAR. To examine the stability of the annual dose curve with respect to the treatment of the epistemic uncertainty, DOE estimated dose statistics (mean, median, 5th and 95th percentiles) for the nominal modeling case considering 1,000 realizations and compared those statistics to corresponding 300-realization statistics (SAR Figure 2.4-38). DOE concluded the 300-realization and 1,000-realization annual dose statistics (mean, median, 0.05 and 0.95 percentiles) were comparable (SAR Figure 2-4-38).

Table 17-19. DOE Volcanic Eruption Modeling Case Short-Term and Long-Term Inhalation BDCFs*		
Radionuclide	BDCF Sv/yr per Bq/kg† [mrem/yr per pCi/g]	Primary Pathways
Pu-239	4.0×10^{-7} [1.5] short term‡ 6.1×10^{-7} [2.3] long term	98% of Pu-239 eruptive dose is inhalation: 39% short term 60% long term
Am-241	3.2×10^{-7} [1.2] short term‡ 5.0×10^{-7} [1.8] long term	94% of Am-241 eruptive dose is inhalation: 37% short term 57% long term
*Biosphere dose conversion factors †Sources: SAR Table 2.3.10-14 and SNL, 2007, "Biosphere Model Report," MDL-MGR-MD-000001, Rev. 02, Tables 6.12-2 and 6.12-3, Las Vegas, Nevada: Sandia National Laboratories. ‡The short-term inhalation exposure is applicable only for the initial year of the eruption.		

Table 17-20. DOE Volcanic Eruption Modeling Case Combined Ingestion, Radon, External BDCFs*		
Radionuclide	BDCF Sv/yr per Bq/m ² † [mrem/yr per pCi/m ²]	Primary Pathways
Sr-90	1.8×10^{-9} [6.7 × 10 ⁻⁶]	79% external exposure
Cs-137	7.2×10^{-9} [2.7 × 10 ⁻⁵]	99% external exposure
Ra-226	3.3×10^{-8} [1.2 × 10 ⁻⁴]	65% external exposure 33% radon decay products
*Biosphere dose conversion factors †Sources: SAR Table 2.3.10-14 and SNL, 2007, "Biosphere Model Report," MDL-MGR-MD-000001, Rev. 02, Table 6.12-4, Las Vegas, Nevada: Sandia National Laboratories.		

For all of the modeling cases, DOE considered three replicates with 300 realizations and compared statistics (mean, median, 0.05 and 0.95 percentiles) among the replicates (SAR Figures 2.4-37 to 2.4-52). Each replicate sample had the same number of realizations; however, the combination of sampled parameter values was different for each replicate. DOE qualitatively concluded that the statistics were similar for the three replicates. Also, DOE estimated 95 percent confidence bounds for the average annual dose using information from the replicates and a t-distribution with 2 degrees of freedom, as described in SNL Section J4.10 (2008ag). In all model cases, the 0.95 percentile in the average annual dose was relatively close (e.g., largest difference of 0.01 mSv/yr [1 mrem/yr] between the three replicates and generally much less for the vast majority of the 1-million-year period, as shown in SNL Figure J5-5(a) (2008ag)) to the overall average annual dose. DOE concluded the overall

average annual dose, computed using 300 realizations, to be statistically stable, as described in SAR Section 2.4.2.2.2 and SNL Section 7.3.2 (2008ag).

DOE updated its model from TSPA Model v5.000 to v5.005, with most validation and model stability analyses performed with TSPA Model v5.000, but the annual doses reported in the SAR are based on TSPA Model v5.005 (SAR p. 2.4-76 to 78). DOE compared the effect of the change from version v5.000 to v5.005 and documented those analyses in SNL Figures 7.3.1-17[a] to 7.3.3-13[a] (2008ag). Although the stability analyses were not repeated, the comparisons indicate a similar numerical behavior of versions v5.000 to v5.005, and thus the applicant stated that the same conclusions, with regard to stability, apply to version v5.005. DOE computed a range for the overall average annual dose using bootstrap analyses, compared the results of these analyses in SAR Figures 2.4-53 and 54, and concluded that 300 epistemic realizations were sufficient to estimate the average annual dose and that the results of TSPA Model v5.005 are statistically stable (SAR Section 2.4.2.2.2, p. 2.4-82).

Comparison with Annual Dose Standard

DOE presented the overall average annual dose curve over the entire compliance period in SAR Figure 2.4-10. The peak of the overall average annual dose curve is approximately 0.003 mSv/yr [0.3 mrem/yr] over the 10,000-year time period {dose limit of 0.15 mSv/yr [15 mrem/yr] for this period} and is approximately 0.02 mSv/yr [2 mrem/yr] over the 1-million-year period {dose limit of 1.0 mSv/yr [100 mrem/yr] for this period}

2.2.1.4.1.3.4.2 NRC Staff Evaluation

(b)(5)

(b)(5)

2.2.1.4.1.4 Evaluation Findings

(b)(5)

Comment	(b)(5)
(b)(5)	
Comment	(b)(5)
(b)(5)	

(b)(5)

(b)(5)

2.2.1.4.1.5 References

CNWRA. 2007aa. "Software Validation Report for Total-system Performance Assessment (TPA) Code Version 5.1." ML072840502. San Antonio, Texas: CNWRA.

CNWRA. 2004aa. "System-Level Performance Assessment of the Proposed Repository at Yucca Mountain Using the TPA Version 4.1 Code." ML041350316. San Antonio, Texas: CNWRA.

CNWRA and NRC. 2008aa. "Risk Insights Derived From Analyses of Model Updates in the Total-system Performance Assessment Version 5.1 Code." ML082240343. San Antonio, Texas: CNWRA.

CRWMS M&O. 1998aa. "Probabilistic Seismic Hazard Analyses for Fault Displacement and Vibratory Ground Motion at Yucca Mountain, Nevada." WBS 1.2.3.2.8.3.6. Las Vegas, Nevada: CRWMS M&O.

CRWMS M&O. 1996aa. "Probabilistic Volcanic Hazard Analysis for Yucca Mountain, Nevada." BA0000000-01717-2200-00082. Rev. 0. Las Vegas, Nevada: CRWMS M&O.

DOE. 2010ai. "Yucca Mountain—Supplemental Response to Request for Additional Information Regarding License Application (Safety Analysis Report Section 2.3.1), Safety Evaluation Report Vol. 3, Chapter 2.2.1.3.5, Set 1 and (Safety Analysis Report Sections 2.3.2 and 2.3.3), Safety Evaluation Report Vol. 3, Chapter 2.2.1.3.6, Set 1." Letter (February 2) J.R. Williams to J.H. Sulima (NRC). ML100340034. Washington, DC: DOE, Office of Technical Management.

DOE. 2009an. "Yucca Mountain—Response to Request for Additional Information Regarding License Application (Safety Analysis Report Section 2.1), Safety Evaluation Report Vol. 3, Chapter 2.2.1.1, Set 1." Letter (February 6) J.R. Williams to J.H. Sulima (NRC). ML090400455. Washington, DC: DOE, Office of Technical Management.

DOE. 2009bj. "Yucca Mountain—Response to Request for Additional Information Regarding License Application (Safety Analysis Report Section 2.4.4) Safety Evaluation Report Vol. 3, Chapters 2.2.1.4.1, 2.2.1.4.2, and 2.2.1.4.3, Set 1." Letter (July 29) J.R. Williams to J.H. Sulima (NRC). ML092110472. Washington, DC: DOE, Office of Technical Management.

DOE. 2009cb. "Yucca Mountain—Response to Request for Additional Information Regarding License Application (Safety Analysis Report Section 2.2, Table 2.2-5), Safety Evaluation Report Vol. 3, Chapter 2.2.1.2.1, Set 5." Letter (June 5) J.R. Williams to J.H. Sulima (NRC). ML091590581. Washington, DC: DOE, Office of Technical Management.

DOE. 2009ct. "Yucca Mountain—Response to Request for Additional Information Regarding License Application (Safety Analysis Report Sections 2.3.2, 2.3.3, and 2.3.5), Safety Evaluation Report Vol. 3, Chapter 2.2.1.3.6, Set 2." Letter (July 20) J.R. Williams to J.H. Sulima (NRC). ML0920204130 and ML0920204141. Washington, DC: DOE, Office of Technical Management.

DOE. 2009cu. "Yucca Mountain—Response to Request for Additional Information Regarding License Application (Safety Analysis Report Section 2.4.2), Safety Evaluation Report Vol. 3, Chapter 2.2.1.4.1, Set 2." Letter (October 16) J.R. Williams to J.H. Sulima (NRC). ML093030275. Washington, DC: DOE, Office of Technical Management.

DOE. 2008ab. DOE/RW-0573, "Yucca Mountain Repository License Application." Rev. 0. ML081560400. Las Vegas, Nevada: DOE, Office of Civilian Radioactive Waste Management.

NRC. 2005aa. NUREG-1762, "Integrated Issue Resolution Status Report." Rev. 1. ML051360241. Washington, DC: NRC.

NRC. 2003aa. NUREG-1804, "Yucca Mountain Review Plan—Final Report." Rev. 2. Washington, DC: NRC.

NRC and CNWRA. 2010aa. "Documentation of Analyses in Support of the Safety Review of DOE's Total System Performance Assessment Calculations for a Proposed Repository at Yucca Mountain." ML101450306. Washington, DC: NRC.

Pensado, O., and J. Mancillas. 2007aa. "Estimates of Mean Consequences and Confidence Bounds on the Mean Associated With Low-Probability Seismic Events in Total System Performance Assessments." Proceedings of the 11th International Conference on Environmental Remediation and Radioactive Waste Management, Bruges (Brugge), Belgium, September 2-6, 2007. ISBN 0-7918-3818-8. Order No. 1785CD (CD ROM). New York City, New York: ASME Press.

SNL. 2008ag. "Total System Performance Assessment Model/Analysis for the License Application." MDL-WIS-PA-000005. Rev. 00. AD 01, ERD 01, ERD 02, ERD 03, ERD 04. Las Vegas, Nevada: Sandia National Laboratories.

CHAPTER 18

2.2.1.4.2 Demonstration of Compliance With the Human Intrusion Standard

2.2.1.4.2.1 Introduction

This section of the Safety Evaluation Report (SER) provides the U.S. Nuclear Regulatory Commission (NRC) staff review of the calculation used to demonstrate compliance with the human intrusion standard, described in the following subsection on regulatory requirements. The geologic record provides a basis for evaluating the likelihood of geologic processes and events, but there is no similar record of extended duration that can be used to constrain either the probability that human intrusion could occur or the characteristics of such intrusion. Regulations specify that the potential effects of human intrusion on waste isolation must be considered when evaluating repository performance. The results of this evaluation are used to demonstrate that the repository can adequately perform if its barriers are breached by a human intrusion.

2.2.1.4.2.2 Regulatory Requirements

To evaluate human intrusion, dose limit requirements [10 CFR 63.321(b)], requirements specific to the human intrusion scenario [10 CFR 63.321(a) and 63.322], and requirements for conducting the performance assessment [10 CFR 63.113(d), 63.114, 63.303, and 63.342] must be followed. Accordingly, the U.S. Department of Energy (DOE or the applicant) must evaluate when a human intrusion might occur and the consequences of the human intrusion, following regulatory requirements. In particular, the individual protection standard for human intrusion requires the applicant to

- Determine the earliest time after disposal that the waste package would degrade sufficiently that a human intrusion could occur without the drillers recognizing it [10 CFR 63.321(a)]
- Assume for the human intrusion scenario that (i) there is a single human intrusion as a result of exploratory drilling for groundwater, (ii) the intruders drill a borehole directly through a degraded waste package into the uppermost aquifer underlying the Yucca Mountain repository, (iii) the drillers use the common techniques and practices that are currently employed in exploratory drilling for groundwater in the region surrounding Yucca Mountain, (iv) careful sealing of the borehole does not occur—instead, natural degradation processes gradually modify the borehole, (v) no particulate waste material falls into the borehole, (vi) the exposure scenario includes only those radionuclides transported to the saturated zone by water (e.g., water enters the waste package, releases radionuclides, and transports radionuclides by way of the borehole to the saturated zone), and (vii) no releases are included which are caused by unlikely natural processes [10 CFR 63.322]
- Demonstrate that there is a reasonable expectation that the reasonably maximally exposed individual (RMEI) receives, as a result of the human intrusion, no more than the following annual dose: 0.15 m [15 mrem] for 10,000 years following disposal and 1.0 mSv [100 mrem] after 10,000 years but within the period of geologic stability [10 CFR 63.321(b)]

As discussed in the Yucca Mountain Review Plan (YMRP) Section 2.2.1.2.2.2 (NRC, 2003aa), the NRC staff's review focused on the technical bases supporting the applicant's determinations of timing of the event, the representation of the human intrusion, and the peak of the average dose curve.

In addition, the staff has reviewed the applicant's description of the human intrusion event as part of its review of events that were included in the performance assessment found in SER Section 2.2.1.2.2.3. (b)(5)

(b)(5)

2.2.1.4.2.3 Technical Review

The regulations require DOE to use a performance assessment to demonstrate compliance with the dose limits for human intrusion; however, the valuation for human intrusion is subject to specific requirements regarding the determination of the timing of the human intrusion and assumptions with respect to the nature and extent of the intrusion scenario. Accordingly, the performance assessment for the human intrusion scenario is somewhat different than the performance assessment used to demonstrate compliance with individual protection. The two performance assessments are expected to differ because the performance assessment used to evaluate the human intrusion scenario includes disruption of the repository due to a postulated human intrusion as prescribed at 10 CFR 63.322. However, those portions of the performance assessment not affected by the regulatory specifications for the human intrusion scenario would be expected to be the same as the performance assessment used for demonstrating compliance with the individual protection (e.g., transport of radionuclides in the saturated alluvium, characteristics of the biosphere are not affected by the postulated human intrusion event). YMRP Acceptance Criterion 2, p. 2.2-138, includes, as part of the staff review, a determination that the total system performance assessment for human intrusion is identical to the total system performance assessment for individual protection, except that it assumes the occurrence of the postulated human intrusion scenario prescribed by regulation. As a result, the NRC staff's review of the applicant's performance assessment for the human intrusion scenario will evaluate (i) whether or not the performance assessment used for the human intrusion scenario is the same as the performance assessment used for individual protection (i.e., except for the required representation of the human intrusion scenario, there are no differences between the performance assessment used for demonstrating compliance with the individual protection dose limits and the performance assessment used for demonstrating compliance with the human intrusion dose limits that would result in a significant under-estimation of the peak dose for the human intrusion scenario) and (ii) whether or not those portions of the performance assessment for the human intrusion scenario are adequately represented in the performance assessment consistent with the specifications at 10 CFR 63.322. Those portions of the total system performance assessment for human intrusion that are identical to the total system performance assessment for individual protection (e.g., biosphere) are evaluated as part of the review of the total system performance assessment for individual protection (SER Section 2.2.1.4.1) and are not duplicated in this section.

The NRC staff's evaluation involves reviewing DOE's Safety Analysis Report (SAR), Total System Performance Assessment (TSPA) Analysis Model Report, and the TSPA model files including intermediate results provided as part of the license application.

The staff's review entails determining that

- DOE's selection of the earliest time for the human intrusion to occur is adequately supported (SER Section 2.2.1.4.2.3.1)
- The performance assessment for the human intrusion scenario provides a credible representation of the human intrusion scenario (SER Section 2.2.1.4.2.3.2)
- Dose limits are met and statistically stable [e.g., increasing the number of simulations (statistical sample size) performed with DOE's TSPA model is not expected to significantly change the calculated average dose] (SER Section 2.2.1.4.2.3.3)

2.2.1.4.2.3.1 Timing of Human Intrusion Event

Description of DOE Approach

The regulations at 10 CFR 63.321(a) specify that DOE must determine the earliest time at which a driller would penetrate a waste package without recognition (e.g., that a metal object had been contacted rather than rock), which is referred to as the human intrusion event. In SAR Section 2.4.3.2 the applicant identified general corrosion as the process that, given sufficient time, could cause significant degradation of the drip shield and waste package such that drilling performance would most likely not be affected by the presence of the drip shield and waste package. The applicant concluded that there is only a 0.0001 percent chance that the drip shield will fail by corrosion before approximately 230,000 years under nominal conditions. The applicant also concluded that the waste package has only a 5 percent chance of failure (i.e., significant degradation or thinning of the walls of the waste package) from general corrosion prior to 600,000 years. On the basis of these results, the applicant selected 200,000 years as the earliest time the waste package would degrade sufficiently that a human intrusion could occur without the drillers recognizing it. The applicant considered this a conservative approach because the waste package is estimated to have experienced limited degradation due to corrosion (i.e., waste package to be substantially intact) by that time.

The applicant also evaluated other events that might affect the timing of the human intrusion event. As specified in 10 CFR 63.322(g), the applicant need not consider unlikely natural processes and events (i.e., those events with less than 1 chance in 100,000 per year of occurring) in the evaluation of human intrusion. The applicant evaluated the likelihoods of early undetected defects, igneous events, and seismic events. For early undetected defects and igneous disruptive events, the applicant determined that the likelihood was less than the limit for likely events. For seismic events, the applicant determined that damage to either the drip shield or waste package that might compromise the structural integrity of drip shield or waste package (e.g., rupture or framework buckling of the drip shield, punctures and ruptures of the waste package) is also less than the limit for likely events (SAR Section 2.4.3.2.2, p. 2.4-303 and 304). For seismic damage that is considered likely to occur [i.e., stress corrosion cracking (SCC) of the drip shield or waste package], the applicant asserted such damage would not be sufficient to prevent the driller from recognizing it (SAR Section 2.4.3.2.2, p. 2.4-303 and 304). In summary, the applicant concluded that events such as early failures and igneous and seismic events are unlikely or would not cause enough damage to the drip shield and waste package to prevent the driller from recognizing the damage.

NRC Staff Evaluation

(b)(5)

(b)(5)

2.2.1.4.2.3.2 Representation of Intrusion Event

Description of DOE Approach

The applicant developed a separate performance assessment to evaluate the consequences of a postulated human intrusion event assumed to occur 200,000 years after permanent closure. The key elements of the postulated human intrusion event are the effects of the borehole on seepage into the waste package, release of radionuclides from the waste package, and transport of radionuclides through the unsaturated zone to the saturated zone.

The performance assessment for individual protection is used for the human intrusion analysis, including the identical sampling approach for treating uncertainty (i.e., Latin hypercube sampling). The applicant modified its performance assessment for individual protection to represent human intrusion in a manner consistent with the regulatory requirements for the human intrusion scenario in 10 CFR 63.322. Specifically, the performance assessment for human intrusion

- Does not include unlikely events (e.g., igneous activity or faulting)
- Assumes that damage to a single waste package occurs at 200,000 years and is the result of drill bit penetration with a cross-sectional area of 0.0324 m² [0.349 ft²] assumes a 20.3 cm [8-in] diameter borehole]

- Assumes that seepage water enters the waste package through the borehole
- Assumes the borehole is degraded and filled with rock debris
- Assumes that releases from the waste package are passed into a fracture pathway that is assumed to exist in the borehole all the way to the saturated zone (SAR p. 2.4-296)
- Assumes radionuclides move with the flowing water down the borehole fracture to the saturated zone and are slowed only due to matrix diffusion of dissolved radionuclides from the fracture into the rock matrix
- Considers only radionuclides transported by water from the waste package to the saturated zone by way of the borehole in the exposure scenario

The quantity of water that enters the waste package and matrix diffusion in the borehole are key aspects of the representation of the human intrusion event that affect the estimated doses (e.g., infiltration was identified as an important parameter affecting the expected dose in SAR Figure 2.4-173). The quantity of water that enters the waste package through the borehole affects the release of radionuclides that are solubility limited (e.g., the release of solubility-limited radionuclides such as Np-237 will commonly be proportional to the amount of water leaving the waste package). The applicant described how the amount of water that enters the waste package through the borehole is limited to the seepage entering the borehole (deep percolation is assumed to pass directly into the borehole opening). Other processes (e.g., drift seepage water splashing on the waste package surface and entering the waste package through the hole created by the borehole) were evaluated and determined to not significantly add to the quantity of water entering the borehole, as described in DOE Enclosure 4, Section 1.1 (2009bj). The applicant also described the basis for the process of matrix diffusion in the borehole, which can potentially delay both sorbing and nonsorbing radionuclide transport by providing a means for radionuclides to move from the relatively fast-flowing water in the borehole fracture into the slower moving water in the porous matrix of the rubble in the borehole. Although water in the borehole is estimated to take approximately 3 years to move through the unsaturated zone to the saturated zone, nonsorbing (I-129) and sorbing (Np-237) radionuclides are estimated to be delayed approximately 1,250 and 64,000 years, respectively, as outlined in DOE Enclosure 5, p. 8 (2009bj). The applicant described in DOE p. 2 (2009cp) that this effect is due to the large effective surface area for communication between the fracture and the matrix in the degraded borehole and along the borehole.

DOE also evaluated the potential effect on repository performance if the borehole penetrated a perched water zone below the repository. If radionuclides were present in a perched water zone, the borehole penetration of a perched water zone could potentially affect the transport of radionuclides from within the perched zone to the saturated zone. The applicant described that the effect of the borehole would be limited because (i) perched water zones below the repository are isolated and have limited volume, as described in DOE Enclosure 6, p. 2 (2009bj); (ii) the significance of an equivalent 20.3-cm [8-in]-diameter borehole to capture and divert any lateral flow associated with the perched water is expected to be small because the area associated with fractures in the rock is more ten-thousand times greater than the area associated with the borehole, as identified in DOE Enclosure 6, p. 5 (2009bj); and (iii) the performance assessment already includes fast transport times in fault zones, which would not be significantly influenced by another fast pathway—namely, the borehole—as outlined in DOE Enclosure 6, p. 6 (2009bj).

NRC Staff Evaluation

The NRC staff has evaluated the applicant's technical basis supporting its separate performance assessment for the postulated human intrusion event. (b)(5)

(b)(5)

(b)(5)

(b)(5)

(b)(5)

2.2.1.4.2.3.3 Annual Dose to RMEI

Description of DOE's Approach

DOE presented the dose curve for the human intrusion scenario in SAR Figure 2.4-11. The peak of the mean dose curve is approximately 0.0001 mSv/yr [0.01 mrem/yr] shortly after the time of the intrusion (i.e., 200,000 years). DOE's estimated dose is on the order of 10,000 times less than the dose limit of 1 mSv/yr [100 mrem/yr] for the period after 10,000 years.

The applicant performed tests to determine the computational stability of the average dose curve used to demonstrate compliance with the dose limit for human intrusion (SAR Section 2.4.3.3.3). The tests (i) computed three replicates to allow for different combinations of sampled values over their parameter ranges (SAR Figure 2.4-160); (ii) increased the number of aleatory samples from 30 to 90 (SAR Figure 2.4-161), and (iii) refined the timestep scheme, as shown in SNL Figures 7.3.3-10[a] and 7.3.3-11[a] (2008ag). The applicant concluded that expected doses were relatively unaffected (i.e., stable) by changes in values of sampled parameters, sample size, and timestepping.

NRC Staff's Evaluation

(b)(5)

(b)(5)

(b)(5)

2.2.1.4.2.4

Evaluation Findings

(b)(5)

2.2.1.4.2.5 References

DOE. 2009bj. "Yucca Mountain—Response to Request for Additional Information Regarding License Application (Safety Analysis Report Section 2.4.4) Safety Evaluation Report Vol. 3, Chapters 2.2.1.4.1, 2.2.1.4.2, and 2.2.1.4.3, Set 1." Letter (July 29) J.R. Williams to J.H. Sulima (NRC). ML092110472. Washington, DC: DOE, Office of Technical Management.

DOE. 2009cp. "Yucca Mountain—Supplemental Response to Request for Additional Information Regarding License Application (Safety Analysis Report Section 2.4.3), Safety Evaluation Report Vol. 3, Chapter 2.2.1.4.2, Set 1." Letter (October 20) J.R. Williams to J.H. Sulima (NRC). ML092940188. Washington, DC: DOE, Office of Technical Management.

NRC. 2003aa. NUREG-1804, "Yucca Mountain Review Plan—Final Report." Rev. 2. Washington, DC: NRC.

SNL. 2008ag. "Total System Performance Assessment Model/Analysis for the License Application." MDL-WIS-PA-000005. Rev. 00. AD 01, ERD 01, ERD 02, ERD 03, ERD 04. Las Vegas, Nevada: Sandia National Laboratories.

CHAPTER 19

2.2.1.4.3 Demonstration of Compliance With Separate Groundwater Protection Standards

2.2.1.4.3.1 Introduction

This section of the Safety Evaluation Report (SER) provides the U.S. Nuclear Regulatory Commission (NRC) staff's review of the calculation used to demonstrate compliance with the separate standards for protection of groundwater—an important source of drinking water. The NRC's regulations provide separate standards to protect the groundwater resources in the vicinity of Yucca Mountain and specify the approach to be taken to estimate the concentration of radionuclides in groundwater. Although this approach (10 CFR 63.331) is similar to that used in estimating dose to the reasonably maximally exposed individual (RMEI) for comparison with the individual protection standard (10 CFR 63.311–63.312), the standards are decidedly different. The groundwater protection standards provide for different limits depending on the radionuclide and the associated radiation. There are three distinct groups of radionuclides with the following limits: (i) radionuclides that are characterized as alpha emitters (e.g., Np-237) are grouped, and the combined concentration from radionuclides released from the repository and the natural background level of radiation presently in the groundwater must be less than 15 pCi/L (this group explicitly excludes radon and uranium); (ii) radionuclides that are characterized as beta- and photon-emitting radionuclides (e.g., I-129, Tc-99) are grouped together, and the combined concentration from radionuclides released from the repository cannot result in a dose exceeding 0.04 mSv [4 mrem] per year to the whole body or any organ, on the basis of drinking 2 L [0.53 gal] of water per day at the combined concentration; and (iii) the combined concentration of Ra-226 and Ra-228 released from the repository and the natural background levels of Ra-226 and Ra-228 in the groundwater cannot exceed a concentration of 5 pCi/L. The performance assessment used for individual protection also estimates a dose on the basis of drinking 2 L [0.53 gal] of water per day. Therefore, there are a number of similarities in the performance assessment used for demonstrating compliance with the individual protection standard and the performance assessment used to demonstrate protection with separate groundwater protection standards.

2.2.1.4.3.2 Regulatory Requirements

10 CFR 63.331 provides separate groundwater protection standards for the initial 10,000 years after closure of the repository. The regulations also specify constraints for the performance assessment used to demonstrate compliance with the groundwater protection standards and the determination of the "representative volume" of groundwater [i.e., the volume of water in which the U.S. Department of Energy (DOE) must project the concentration of radionuclides released from the Yucca Mountain disposal system]. The requirements are summarized next.

Performance Assessment for Groundwater Protection

- The performance assessment must be conducted in accordance with the general requirements for the performance assessment covering the initial 10,000 years specified at 10 CFR 63.114(a) and the limits specified at 10 CFR 63.342(a).

- The performance assessment shall exclude unlikely features, events, and processes (FEPs) that are estimated to have less than 1 chance in 100,000 per year of occurring [10 CFR 63.342(b)].
- The performance assessment shall exclude the consideration of human intrusion (i.e., representing undisturbed performance as specified at 10 CFR 63.331).
- The performance assessment's results must be weighted by their probability of occurrence (as specified at 10 CFR 63.2).

Representative Volume

- The representative volume is the volume of groundwater that would be withdrawn annually from an aquifer containing less than 10,000 mg of total dissolved solids per liter of water [10 CFR 63.332(a)].
- DOE must determine the concentration of radionuclides that will be released from the Yucca Mountain repository that will be in the representative volume of groundwater for comparison with standards [10 CFR 63.332(a)].
- DOE must determine the position and dimensions of the representative volume using average hydrologic characteristics, which must include the highest concentration level in the plume of contamination in the accessible environment [10 CFR 63.332(a)(1 and 2)].
- The representative volume contains 3,000 acre-ft of water [10 CFR 63.332(a)(3)].

Separate Standards for Groundwater Protection (10 CFR 63.331, Table 1)

- The combined concentration of Ra-226 and Ra-228 from repository releases cannot exceed 5 pCi/L (including natural background radiation presently in groundwater at Yucca Mountain).
- For gross alpha activity (including Ra-226 but excluding radon and uranium), the combined concentration from repository releases must be less than 15 pCi/L (including natural background radiation presently in groundwater at Yucca Mountain). (Np-237 is an example of an alpha-emitting radionuclide.)
- The combined concentration of beta- and photon-emitting radionuclides from repository releases cannot exceed 0.04 mSv [4 mrem] per year to the whole body or any organ (on the basis of drinking 2 L [0.53 gal] of water per day from the representative volume). (Tc-99 and I-129 are examples of beta- and photon-emitting radionuclides.)
- DOE must determine background concentrations of specific radionuclides in groundwater as identified previously for Ra-226, Ra-228, and gross alpha activity.

The performance assessment for compliance with the individual protection standard is the same performance assessment used to evaluate compliance with the groundwater protection standards (i.e., except for differences due to the regulatory requirement that unlikely events are not to be included in the performance assessment used for groundwater protection, there are no differences between the performance assessment used for demonstrating compliance with the

individual protection dose limits and the performance assessment used for demonstrating compliance with the groundwater protection limits that would result in a significant under-estimation of the concentration of radionuclides in groundwater). As a result, the NRC staff's review of the applicant's groundwater protection analysis focused on DOE's determination of the representative volume and compliance with the separate limits specified for groundwater protection. The performance assessment for individual protection is reviewed in SER Section 2.2.1.4.1.

Consistent with the Yucca Mountain Review Plan (YMRP) (NRC, 2003aa), the staff implemented the following guidance

- Determine that DOE includes the highest concentration level in the plume of contamination in the accessible environment in the representative volume
- Determine that DOE estimates the dimensions of the representative volume using one of the methods defined at 10 CFR 63.332, and explains any underlying assumptions for using the selected method
- Determine that the average concentrations in the representative volume do not exceed the separate limits

Because DOE assumed that all radionuclides which reach the compliance location in a given year are included in the annual water demand of 3,000 acre-feet, YMRP Section 2.2.1.4.3.1 states that the NRC staff may conduct a simplified review.

2.2.1.4.3.3 Technical Review

The NRC staff's review of DOE's demonstration of compliance with the separate standards for groundwater protection focused on those portions of the analysis that are distinct to the groundwater protection analysis. Specifically, the NRC staff's review focused on DOE's approach for including the highest concentration level of the plume in the representative volume, the dimensions of the representative volume, and comparison of the performance assessment results with the separate standards for groundwater protection.

2.2.1.4.3.3.1 Representative Volume Location

DOE used the same performance assessment model for evaluating groundwater protection as it used for evaluating compliance for the individual protection standards in the sense that the model abstractions for flow paths in the saturated zone and radionuclide transport in the saturated zone are the same. However, DOE has excluded the consideration of unlikely FEPs from the performance assessment used for groundwater protection (i.e., igneous activity and low probability seismic events are excluded). The location of the representative volume of groundwater was consistent with the approach used for the determining the pathway for radionuclide transport to the location of the RMEI, which is approximately 18 km [11 mi] south of the repository, as identified in the Safety Analysis Report (SAR) Volume 2, p. 2.1-1 (DOE, 2008ab). Additionally, DOE used the same approach for determining the concentration of radionuclides in groundwater for demonstrating compliance with both the groundwater protection and individual protection standards [i.e., the annual average radionuclide concentration, due to releases from the repository, was determined by assuming that all radionuclides that reach the compliance location in a given year are included in 3,000 acre-ft,

which is the annual water demand for individual protection and the representative volume for groundwater (SAR Section 2.4.4)].

Staff Evaluation

(b)(5)

2.2.1.4.3.3.2 Representative Volume Dimensions

DOE used the models and assumptions used to estimate flow and transport paths in the saturated zone for determining compliance with the individual protection standards for estimating the dimensions of the representative volume. DOE estimated, using the slice of the plume method, that dimensions of a width of 3,000 m [9,842 ft], a depth of 200 m [656 ft] and a length of 30 m [98 ft] in the direction of groundwater flow would include all the simulated flow paths of radionuclides crossing the compliance location into the accessible environment (SAR Volume 2, p. 2.4-337). DOE estimated these dimensions using average properties for hydrologic parameters such as groundwater flow rate and alluvium flow porosity (SAR Volume 2, p. 2.4-337). DOE calculated the representative volume with these dimensions yielded a volume of approximately 3,000 acre-ft.

DOE also presented a more detailed depiction of the cross section of the plume at the compliance location to further support the dimensions of the representative volume. The more detailed analysis was based on numerous particle tracks, provided in DOE Enclosure 7, Figure 1 (2009bj), representing potential release points for repository releases to the saturated zone using the saturated zone site-scale flow model. Although the cross section of the plume, based on the particle traces, is not a rectangular shape, DOE estimated that a rectangular shape of approximately 3,300 m [10,827 ft] in width (horizontally) by 220 m [722 ft] in depth (vertically) would enclose the horizontal and vertical extent of the plume cross section (an area of 726,000 m² [7.8 million ft²]). DOE estimated that approximately 40 percent of this rectangular shape did not contain any significant portion of the plume; thus DOE estimated a cross-sectional area of 435,000 m² [4.7 million ft²] given the irregularities of the shape produced by the particle

traces depicted in DOE Enclosure 7, Figure 1 (2009b)). DOE's simple rectangular approximation (i.e., 3,000 by 200 m [9,842 by 656 ft]) results in a cross-sectional area of 600,000 m² [6.4 million ft²], which provides a value between the two values calculated from the particle tracks (one a rectangular shape of 726,000 m² [7.8 million ft²] and the other an irregular shape of 435,000 m² [4.7 million ft²]). The third dimension of the representative volume was selected to obtain the volume of 3,000 acre-ft, as specified at 10 CFR 63.332(a)(3). DOE calculated the third dimension, or the length parallel to the flow direction (i.e., perpendicular to the cross section), to be approximately 34.4 m [113 ft] on the basis of the cross-sectional area of 600,000 m² [6.4 million ft²] and an average effective porosity of 0.18, as identified in DOE Enclosure 7, p. 4 (2009b)).

DOE used water quality data from the Alluvial Testing Complex (SAR Volume 2, p. 2.4-334) to determine that there were fewer than 500 mg/L of total dissolved solids in the aquifer at the compliance location. According to 10 CFR 63.332(a), the separate groundwater protection requirements only apply to aquifers containing less than 10,000 mg/L of total dissolved solids.

Staff Evaluation

The dimensions of the representative volume are required to include the highest concentration level in the plume of contamination [10 CFR 63.332(a)(1)]. DOE determined (i) the dimensions of the representative volume using the slice of the plume approach and (ii) these dimensions are sufficient to capture all the releases into the accessible environment. (b)(5)

(b)(5)

(b)(5)

(b)(5)

2.2.1.4.3.3.3 Average Concentrations

DOE determined the average concentration of radionuclides, due to repository releases, by assuming the annual releases of radionuclides were all included in the representative volume of 3,000 acre-ft and determined the dose to the whole body and individual organs for the beta- and photon-emitting radionuclides on the basis of drinking 2 L [0.53 gal] per day of water at the concentration level estimated for the representative volume (SAR Section 2.4.4.1.1.4). DOE also estimated the natural background level of radioactivity presently in the groundwater at Yucca Mountain for Ra-226, Ra-228, and the alpha-emitting radionuclides, excluding radon and uranium (SAR Section 2.4.4.1.1.3).

DOE estimated the combined concentrations for Ra-226 and Ra-228, due to releases from the repository and the natural background radiation presently in the groundwater at Yucca

Mountain, was 0.5 pCi/L with the largest contribution coming from natural background radiation (i.e., the largest annual release of Ra-226 and Ra-228 into the representative volume from the repository was estimated to be almost 1 million times less than the natural background level).

DOE estimated the concentration for the gross alpha activity, due to releases from the repository and the natural background radiation presently in the groundwater at Yucca Mountain (excluding radon and uranium), was 0.5 pCi/L with the largest contribution coming from natural background radiation (i.e., the largest annual release of the relevant alpha-emitting radionuclides into the representative volume from the repository was estimated to be more than 1,000 times less than the natural background levels).

DOE estimated the dose from beta- and photon-emitting radionuclides, due to releases from the repository, to be 0.6 μ Sv/yr [0.06 mrem/yr] for the whole body and the largest dose to any organ to be 2.6 μ Sv/yr [0.26 mrem/yr] (e.g., dose to the thyroid from I-129) as result of drinking 2 L [0.53 gal] of water per day assumed to be at a concentration level of radionuclides in the representative volume. (Natural background radiation is not considered for beta- and photon-emitting radionuclides in the separate groundwater protection standards; see 10 CFR 63.331, Table 1.)

Staff Evaluation

(b)(5)

(b)(5)

2.2.1.4.3.4 Evaluation Findings

(b)(5)

2.2.1.4.3.5 References

DOE. 2009b. "Yucca Mountain—Response to Request for Additional Information Regarding License Application (Safety Analysis Report Section 2.4.4) Safety Evaluation Report Vol. 3, Chapters 2.2.1.4.1, 2.2.1.4.2, and 2.2.1.4.3, Set 1." Letter (July 29) J.R. Williams to J.H. Sulima (NRC). Enclosures (8). Las Vegas, Nevada: DOE, Office of Civilian Radioactive Waste Management.

DOE. 2008ab. DOE/RW-0573, "Safety Analysis Report Yucca Mountain Repository License Application." Rev. 00. Las Vegas, Nevada: DOE, Office of Civilian Radioactive Waste Management.

NRC. 2003aa. NUREG-1804, "Yucca Mountain Review Plan—Final Report." Rev. 2. Washington, DC: NRC.

CHAPTER 20

2.5.4 Expert Elicitation

2.5.4.1 Introduction

This chapter of the Safety Evaluation Report (SER) evaluates the information provided in the U.S. Department of Energy (DOE) License Application for uses of expert elicitation in its license application. The applicant's uses are described in Safety Analysis Report (SAR) Section 5.4 (DOE, 2009av).

Expert elicitation is a formal, structured, and well-documented process for obtaining the judgments of multiple experts. The U.S. Nuclear Regulatory Commission (NRC) routinely accepts, for review, expert judgments applicants use to evaluate and interpret the factual bases of license applications. Throughout the period of prelicensing interactions between NRC and DOE, NRC staff has acknowledged that DOE could elect to use the subjective judgments of experts, or groups of experts, to interpret data and address technical issues and inherent uncertainties when assessing the long-term performance of a geologic repository. In its license application, DOE used the results of three formal expert elicitations to complement and supplement other sources of scientific and technical information such as data collection, analyses, and experimentation. In this context, the NRC staff has reviewed DOE's use of expert elicitation regarding the proposed geologic repository at Yucca Mountain.

In supporting its license application for the proposed repository, DOE presented the results of three expert elicitations in the areas of seismic hazard (SAR Section 2.2.2.1), igneous activity (SAR Sections 1.1.6.2, 2.2.2.2, and 2.3.11), and saturated zone flow and transport (SAR Section 2.3.9.2). SAR Section 5.4 summarized DOE's bases for its assertion that these elicitations were conducted in a manner that is generally consistent with NRC guidance. In conducting its review of DOE's use of expert elicitation, NRC staff sought to verify that DOE followed the process suggested in NUREG-1563 (NRC, 1996aa), or some other equivalent stepwise process, such as that outlined in NUREG/CR-6372 (NRC, 1997aa).

2.5.4.2 Regulatory Requirements

10 CFR Section 63.21(c)(19) specifies that the SAR must include an explanation of how expert elicitation was used. In 1996, the NRC staff published guidance for the use of expert elicitation in licensing in NUREG-1563 (NRC, 1996aa). NUREG-1563 provided general guidelines for deciding whether a formal expert elicitation would be useful, and suggested a nine-step procedure that could serve as one acceptable process to conduct an elicitation. The guidance explicitly states that the suggested procedure was not provided with the intent that it be rigidly applied. Rather, the guidance in NUREG-1563, p. 22 (NRC, 1996aa), provides that the suggested procedure "...should be viewed as a general framework for a formal elicitation that would be acceptable to the NRC staff."

Subsequent to the release of NUREG-1563, NRC staff published NUREG/CR-6372 (NRC, 1997aa). This document, referred to informally as the Senior Seismic Hazard Analysis Committee (SSHAC) report, or the SSHAC guidelines, provided a process for obtaining, communicating, and quantifying the uncertainties associated with elicitation seismic experts in the course of conducting Probabilistic Seismic Hazard Assessments (PSHAs) for commercial nuclear power plants and other critical facilities. The stepwise process for eliciting experts

described in the SSHAC guidelines for the most formal (Level 4) analysis and that recommended in NUREG-1563 are very similar. While presented in a slightly different order and structure (in seven steps as opposed to nine, respectively), the two documents recommend essentially the same approach for formally eliciting and documenting expert opinion. For example, the important content identified in NUREG-1563 as Step 4, "Assembly and Dissemination of Basic Information;" Step 6, "Elicitation of Judgments," and Step 7, "Post-Elicitation Feedback" is not treated as discrete steps in the SSHAC guidelines. Instead, the SSHAC guidelines encompass the substance of all three in a single Step 5, referred to as "Group Interaction and Individual Elicitation."

NRC staff's assessment of DOE's fulfillment of 10 CFR 63.21(c)(19) was guided by the Yucca Mountain Review Plan (YMRP) Section 2.5.4 (NRC, 2003aa). YMRP Section 2.5.4 identifies two acceptance criteria: that DOE use NUREG-1563 or equivalent procedures, and that any updated elicitation follow appropriate methods and are adequately documented. These are the only two acceptance criteria applicable to NRC staff's review of DOE's use of expert elicitation. NRC staff evaluated the techniques DOE used to conduct three expert elicitation to verify whether the elicitation either followed procedures suggested by NRC staff guidance or used equivalent procedures. DOE updated only one of the three elicitation. NRC staff evaluated the methods DOE used to update that elicitation to verify whether it was updated appropriately and adequately documented.

Note that in evaluating SAR Section 5.4, the staff recognizes that rigid adherence to the nine-step procedure outlined in NUREG-1563, or strict compliance with other NRC guidance documents, is not a regulatory requirement. As identified explicitly in NUREG-1563, p. 9, "Methods and solutions differing from those set out ... will be acceptable if they provide a sufficient basis for the findings requisite to the issuance of a permit or license by the Commission."

2.5.4.3 Technical Review

This section briefly summarizes the information provided in SAR Section 5.4 for each of the three expert elicitation the applicant used. The discussion at the end of this section provides NRC staff's evaluation on the basis of the two acceptance criteria given in the YMRP.

Probabilistic Volcanic Hazard Assessment (PVHA) Expert Elicitation

SAR Section 2.2.2.2 described the DOE approach to developing a volcanic hazard assessment for Yucca Mountain. This overall approach included an expert elicitation to develop a PVHA for Yucca Mountain. DOE conducted the expert elicitation in 1995 and published the final report in 1996 (CRWMS M&O, 1996aa). SAR Section 5.4.1 summarized the applicant's bases for how its PVHA was conducted in a manner generally consistent with the nine-step procedure suggested in NUREG-1563 (NRC, 1996aa).

For PVHA, the DOE empanelled 10 subject matter experts to assess the relevant technical issues, including a range of conceptual and probability models, associated uncertainties in model parameters, and model sensitivity to these uncertainties. The elicitation consisted of four workshops and two field trips to the Yucca Mountain area. Each panel member made an individual assessment or model of the igneous hazard on the basis of his or her interpretations of various probabilistic models. A logic tree approach was used to combine alternatives and to incorporate uncertainty. Each of the 10 experts' probability estimates was then combined with

equal weight to produce a probability distribution of the annual frequency of intersection of a basaltic dike within the proposed repository footprint.

PSHA Expert Elicitation

SAR Section 2.2.2.1 described DOE's overall approach to developing a seismic hazard assessment for Yucca Mountain, including fault displacement hazards. This approach included an expert elicitation to develop a PSHA for Yucca Mountain (CRWMS M&O, 1998aa; BSC, 2004bj). DOE conducted its PSHA in the late 1990s using a methodology that DOE claims is consistent with a Level 4 expert elicitation as described in NUREG/CR-6372 (NRC, 1997aa). SAR Section 5.4.2 summarized DOE's bases and concluded that this methodology was also generally consistent with the nine-step procedure suggested in NUREG-1563 (NRC, 1996aa).

DOE's PSHA also followed the standard framework for PSHAs in using the recurrence curve approach (e.g., Cornell, 1968aa; McGuire, 1976aa). The basic elements of this framework are (i) identification and spatial distribution of seismic sources; (ii) characterization of each source in terms of its activity, recurrence rates for various earthquake magnitudes, and maximum magnitude; (iii) description of ground motion attenuation relationships to model the distribution of the ground motions expected when a given magnitude earthquake occurs on a particular source; and (iv) incorporation of the inputs into a logic tree to integrate the seismic source characterization and ground motion attenuation relationships, along with their associated uncertainties. Each logic tree pathway is intended to represent one expert's weighted interpretations of the seismic hazard at the site. The computation of the hazard for all possible pathways results in a distribution of hazard curves that DOE considers representative of the seismic hazard at a site, including variability and uncertainty.

To accomplish the PSHA, DOE hired two panels of experts. The first expert panel consisted of six three-member teams of geologists and geophysicists (seismic source teams) who developed probabilistic distributions to characterize relevant potential seismic sources in the Yucca Mountain region. These distributions included location and activity rates for fault sources, spatial distributions and activity rates for background sources, distributions of moment magnitude and maximum magnitude, and site-to-source distances. The second panel consisted of seven seismology experts (ground motion experts) who developed probabilistic point estimates of ground motion for a suite of earthquake magnitudes, distances, fault geometries, and faulting styles. These point estimates, expressed along with estimates of their uncertainties, were specific to the regional crustal conditions of the western Basin and Range Province. The ground motion attenuation point estimates were then fitted to yield the ground motion attenuation equations used in the PSHA.

Inputs from the expert teams were combined into a logic tree and the hazard computed using a modified version of the FRISK88 computer code (Risk Engineering, Inc., 1998aa). In the integration, DOE gave equal weight to all six source teams and seven ground motion experts. The resulting ground motion hazard curves express increasing levels of ground motion as a function of the annual probability that the ground motion will be exceeded. These curves include estimates of uncertainty.

The seismic source teams also developed a Probabilistic Fault Displacement Hazard Assessment as part of the PSHA. In that aspect of the PSHA elicitation, the experts derived probabilistic fault displacement hazard curves for nine demonstration points at or near Yucca

Mountain. These demonstration points represent a range of faulting and related fault deformation conditions in the subsurface and near the sites of proposed surface facilities.

NRC staff's technical evaluation of the geological, geophysical, and seismological information used to support the expert elicitation are provided in SER Sections 2.2.1.2.2.3.2 and 2.1.1.1.3.5.2.

Saturated Zone Flow and Transport Expert Elicitation (SZEE)

SAR Section 2.3.9.2.2.6 discussed DOE's use of expert elicitation to address key issues associated with groundwater flow and transport in the saturated zone. SAR Section 5.4.3 summarized the applicant's bases for asserting that SZEE was conducted in a manner generally consistent with the nine-step procedure suggested in NUREG-1563 (NRC, 1996aa).

In 1997, the applicant carried out an expert elicitation to evaluate saturated zone flow and transport at the Yucca Mountain site (CRWMS M&O, 1998ab). The objective of SZEE was to quantify uncertainties associated with models and parameters key to modeling flow and transport in the saturated zone. A second objective was to reveal needed data collection and modeling that could reduce some of the more significant uncertainties. In this way, the expert elicitation was used to complement and guide data collection already underway, as well as to provide input to iterative performance assessment modeling by DOE.

Over six months, a panel of five experts in saturated zone hydrology was asked to address 16 technical issues related to the study of saturated zone groundwater flow and radionuclide transport at Yucca Mountain. The applicant implemented many of the panel members' recommendations in subsequent site characterization activities. In particular, the panel recommended a range of values for vertical anisotropy, dispersivity, and specific discharge that DOE later used, along with other sources of information, to characterize the uncertainty of flow and transport of radionuclides beneath and down gradient of Yucca Mountain. Written elicitation summaries, prepared by each expert, were included in an appendix to the final elicitation report (CRWMS M&O, 1998ab).

NRC staff's technical evaluation of the geological, geophysical, and hydrological information used to support the expert elicitation, as well as of that information developed as a result of it, is provided in SER Volume 3, Section 2.2.1.3.8.

Staff Evaluation

The first acceptance criterion in the YMRP for review of expert elicitation considers the nine-step procedure outlined in NUREG-1563 (NRC, 1996aa). Each of these steps will be discussed in turn, with specific examples cited from the three elicitations.

(b)(5)
(b)(5)

(b)(5)

Probability estimates for intrusive and extrusive events were not calculated separately, but were initially considered as a single probability by the experts. Because separate probability estimates needed to be developed for the DOE Total System Performance Assessment, DOE developed extrusive and intrusive probability estimates subsequent to the 1996 PVHA without re-engaging the experts to seek their opinions.

(b)(5)

(b)(5)

All of the final elicitation reports identified the participating subject matter experts, included summaries of their input to the elicitations, and provided rationales for their respective opinions. As the applicant stated in SAR Section 5.4, the experts were not asked directly to disclose potential conflicts of interest, but each expert provided sufficient information about his or her past and current affiliations (b)(5)

(b)(5)

(b)(5)

The applicant divided the PSHA into two panels of experts, each with its own set of experts. One panel focused on description and characterization of seismic sources, while the other panel focused on ground motion attenuation and modeling. Within the seismic source panel, the applicant further developed three-person elicitation teams, composed of experts with varied expertise in geology, seismology, geophysics, and Basin and Range tectonics. Among the key subissues the experts identified in the SZEE were the causes and implications of the large hydraulic gradient, spatial distribution of flow, and the range of uncertainty in groundwater specific discharge.

(b)(5)

(b)(5)

Experts received training on the elicitation process during the first workshop of each elicitation, as well as during subsequent workshops, including presentations on topics such as probability encoding, quantifying uncertainty, and identifying sources of bias.

Most of the workshops were held with sufficient advanced notice so that members of the public, affected parties, and NRC staff could directly observe the discussions among the experts and supporting technical teams. Many of the workshops included presentations by subject matter experts, both from within the teams or external to the elicitation. At later workshops, the experts presented their preliminary interpretations in a discussion format that allowed them to receive direct feedback from other experts or expert teams. Each of the elicitation projects included at

least one field trip that allowed the experts to directly observe many of the important geologic features in the Yucca Mountain region. These field trips included discussions with subject matter experts and generalists on specific field investigations carried out on behalf of the DOE in support of the site characterization. The applicant provided meeting summaries of all the workshops in the elicitation reports.

Upon completion of the workshops and field trips, facilitation teams, comprising generalists and normative experts, conducted comprehensive interviews of the experts to elicit their inputs that included discussion of how the information would be represented in the logic tree format used to calculate the results. These interviews were conducted expert by expert or, where applicable, team by team, and followed up with written documentation of the inputs.

As documented in the elicitation reports and SAR Section 5.4, the experts were provided with both informal and formal feedback at many of the workshops. At least one workshop in each elicitation was dedicated to feedback and included initial sensitivity studies provided by the facilitation team to quantify the initial expert interpretations and, through sensitivity studies, to show which inputs had the greatest impact on the overall results. (b)(5)

(b)(5) However, the applicant did not require the experts or expert teams to document the rationale for any changes made to their assessments after the feedback session. As stated in SAR Section 5.4, the applicant concluded that this requirement could anchor the experts to their initial interpretations. The applicant asserted that the experts would thus be reluctant to revise their interpretations after receiving feedback because doing so would also require them to provide full justification for the change. The applicant also stated that its approach, in this regard, is consistent with the guidance contained in NUREG/CR-6372 (NRC, 1997aa). (b)(5)

(b)(5)

For all three elicitations, equal weighting was used to aggregate the elicited results. In the case of PSHA, results were aggregated giving equal weights to the inputs from the source teams, and equal weights to the ground motion models from the individual ground motion experts. In the other cases, equal weight was assigned to the results from each expert. The elicitation reports provided summaries of each expert's (or source team's) input, including sensitivity information to demonstrate the impact each expert or each source team's interpretations had on the final result.

(b)(5)

The second acceptance criterion in the YMRP for review of expert elicitation considers documentation and methodology used in updates to an elicitation. DOE chose not to update the PSHA or the SZEE. The applicant did, however, reconvene the PVHA elicitation in 2004 to consider new information and to rely on a consistent set of event definitions and extrusive scenarios. Members of the NRC staff attended the public PVHA-Update (PVHA-U) workshops as observers. DOE published the results from the updated PVHA, or PVHA-U, after it submitted the license application (SNL, 2008ah)

(b)(5)

NRC staff's technical evaluation of the applicant's estimates of igneous event probability as they relate to the PVHA-U is given in SER Volume 3, Section 2.2.1.2.2.

2.5.4.4 Evaluation Findings

(b)(5)

2.5.4.5 References

Boyle, W.J. 2008aa. "Transmittal of Report: Probabilistic Volcanic Hazard Analysis Update (PVHA-U) for Yucca Mountain, Nevada." Letter (October 17) to Director, DHLWRS, NRC. Las Vegas, Nevada: DOE, Office of Civilian Radioactive Waste Management.

BSC. 2004bj. "Technical Basis Document No. 14: Low Probability Seismic Events." Rev. 1. MOL 20000510.0175. Las Vegas, Nevada: Bechtel SAIC Company, LLC.

Cornell, C.A. 1968aa. "Engineering Seismic Risk Analysis." *Bulletin of the Seismological Society of America*. Vol. 58. pp. 1,583–1,606.

CRWMS M&O. 1998aa. "Probabilistic Seismic Hazard Analyses for Fault Displacement and Vibratory Ground Motion at Yucca Mountain, Nevada." WBS 1.2.3.2 8.3.6. Las Vegas, Nevada: CRWMS M&O.

CRWMS M&O. 1998ab. "Synthesis of Volcanism Studies for the Yucca Mountain Site Characterization Project." 3781MR1. MOL 19981207.0393. Las Vegas, Nevada: CRWMS M&O.

CRWMS M&O. 1996aa. "Probabilistic Volcanic Hazard Analysis for Yucca Mountain, Nevada." BA00000000-01717-2200-00082. Rev. 0. Las Vegas, Nevada: CRWMS M&O.

DOE. 2009av. DOE/RW-0573, "Safety Analysis Report Yucca Mountain Repository License Application." Rev. 01. Las Vegas, Nevada: DOE, Office of Civilian Radioactive Waste Management.

McGuire, R.K. 1976aa. "FORTRAN Computer Program for Seismic Risk Analysis." USGS Open-File Report 76-67. Reston, Virginia: U.S. Geological Survey.

NRC. 2005aa. NUREG-1762, "Integrated Issue Resolution Status Report." Rev. 1. Washington, DC: NRC.

NRC. 2003aa. NUREG-1804, "Yucca Mountain Review Plan—Final Report." Rev. 2. Washington, DC: NRC.

NRC. 1997aa. NUREG/CR-6372, "Recommendations for Probabilistic Seismic Hazard Analysis: Guidance on Uncertainty and Use of Experts." Washington, DC: NRC.

NRC. 1996aa. NUREG-1563, "Branch Technical Position on the Use of Expert Elicitation in the High-Level Radioactive Waste Program." Washington, DC: NRC.

Risk Engineering, Inc. 1998aa. *FRISK88 User Manual, Version 2.0*. Boulder, Colorado: Risk Engineering, Inc.

SNL. 2008ah. "Probabilistic Volcanic Hazard Analysis Update (PVHA U) for Yucca Mountain, Nevada." Rev. 01. Las Vegas, Nevada: Sandia National Laboratories.

CHAPTER 21

Conclusions

(b)(5)

Multiple Barriers (10 CFR 63.113 and 63.115)

(b)(5)

Performance Assessments (10 CFR 63.114)

(b)(5)

Postclosure Performance Objectives (10 CFR 63.113)

(b)(5)

(b)(5)

APPENDIX B

(b)(5)

(b)(5)

